PLUG-IN HYBRID ELECTRIC VEHICLE ON-ROAD EMISSIONS CHARACTERIZATION AND DEMONSTRATION STUDY

By

Carrie M. Hohl

Submitted to the graduate degree program in Civil, Environmental and Architectural Engineering and the Graduate Faculty of the University of Kansas in partial fulfillment of the requirements for the degree of Doctor of Philosophy.

_____

Chairperson Dr. Dennis D. Lane

_____

Dr. Ray E. Carter

_____

Dr. Steven B. Case

_____

Dr. Glen A. Marotz

_____

Dr. Edward F. Peltier

_____

Dr. Laurence Weatherley

Date Defended: June 28, 2012

The Dissertation Committee for Carrie M. Hohl
Certifies that this is the approved version of the following dissertation:

Plug-In Hybrid Electric Vehicle On-Road Emissions Characterization and Demonstration Study

Chairperson Dr. Dennis D. Lane

Date approved: June 28, 2012

ABSTRACT

On-road emissions and operating data were collected from a plug-in hybrid electric vehicle (PHEV) over the course of 6months spanning August 2007 through January 2008 providing the first comprehensive on-road evaluation of the PHEV drivetrain technology. Brought to the Kansas City Area Transit Authority as part of its proof-of-concept testing, the Daimler/Chrysler PHEV was built around the Sprinter chassis and equipped with a diesel combustion engine. Using portable emissions monitoring capabilities coupled with the PHEV's proprietary data-logging-module, the University of Kansas evaluated the PHEV Sprinter's on-road behavior according to different facility types, vocations, as well as investigating the PHEV's ability to fit current vehicle specific power modal models. Even with frequent periods of electric-only, zero emissions driving, the PHEV's on-road data met the statistical criteria necessary to fit the VSP modal model. Facility or roadway type played a large role on the PHEV's emissions and operation with roadway velocity dictating the PHEV's overarching control scheme and respective use of electric versus diesel power. While the PHEV Sprinter experienced increased electric-only driving during periods with elevated battery state of charge (greater than 37%), the Kansas City-based PHEV did not achieve its anticipated electric-only range of 20miles during charge-depleting mode. The PHEV's electric-only potential resulted in increased fuel efficiency and decreased CO_2 and NOx emissions, however the transient functioning of the diesel engine during periods of frequent electric motor cycling produced high CO and hydrocarbon emissions. The PHEV was designed to optimize its plug-in potential during urban travel where slow, stop-and-go driving gained the most benefit from its electric drive capabilities. Consequently, these scenarios also promoted transient diesel engine operation and resulted in the highest CO and hydrocarbon loads of all roadways traveled.

ACKNOWLEDGMENTS

"When eating bamboo sprouts, remember the man who planted them." — Chinese Proverb

It is with an abundant heart that I acknowledge and honor those who have accompanied me throughout this entire process. While the path felt solitary at times, there was never a moment during the degree's progress where I did not benefit from the unfailing support and commitment of those around me.

First and foremost, I extend my heartfelt gratitude to my advisor, Dennis Lane, for his boundless patience, faith, and confidence in me. Your trust in my abilities, even when I questioned them myself, was a constant source of assurance. I will never forget the effort you put forth and the battles that you fought to make this project a reality. It has been as much my delight to serve as one of your graduate students as it is my deepest honor to have been accepted as one.

I thank my doctoral committee and recognize the time and commitment required of each and every one of them as they served to help me complete my doctorate. Glen Marotz, thank you for introducing me to the world of plug-in hybrids. This project has given me experiences and opportunities well beyond what I could have ever expected. Many thanks to Ray Carter and Ted Peltier. Your genuine interest in my research and your sounding board qualities helped motivate me during my endless hours of navigating the downtown Kansas City roadways. To Steve Case, throughout my graduate years, you have afforded me research opportunities well outside of the realm of engineering. Each and every one of those opportunities has given me room to grow as both a student and a person, and because of that, I leave more well-rounded and globally-sighted than I started. I most humbly thank Laurence Weatherly for graciously giving his time at short notice. Without your generosity, I might never have made it to the defense stage.

To all of the engineers and managers at Daimler and the Electric Power and Research Institute, thank you. I cannot express enough appreciation for your continual patience and never-ending willingness to answer my incessant barrage of questions. I give special thanks to Ted Stone, Wesley Biddulph, and the people at the Kansas City Area Transit Authority. I will never forget your dedication and selfless willingness to house this project and suffer all of the inconveniences that it posed.

I was fortunate to serve as a Self Fellow during the initial years of my doctoral studies. I thank Lila and Madison Self for their generosity as well as all of the people who make the fellowship program a success. Your leadership program provided me with a unique diversification that I carry with me today.

To my family and friends: thank you. Your eternal optimism continued to shine brightly month after month, year after year. Even as the finish line appeared to recede in my eyes, your encouragement remained resolute and beautifully unrelenting.

I personally thank Jim and Pam Cote, my beloved parents, whose flexibility and willingness to forgive my work responsibilities, ultimately, allowed me to complete my dissertation. Time is a sacred resource, and if you had not been so generous with yours and mine, I might still be working on Chapter 3. Thank you for giving me more trust and credit than I truly deserved.

To my dear, belated parents-in-law, George and Carol, thank you for being absent of judgment, abundant in pride (even when I did not deserve it), and for possessing an unending trust that I would, indeed, one day actually finish. I only wish I could have celebrated it with you in person.

To my husband, Chris, your steadfastness is a thing of legends. I know that when you gave your support at the start, you did not know that you were signing onto such a long and arduous process. Thank you for your mechanical expertise when my brain was not "getting it," for being present when I needed presence, and giving space when I needed space.

And last, but most certainly not least, I am forever grateful to my dear friend, Michelle; gone, but never to be forgotten. You were my strongest companion during the trials and uncertainties throughout the research journey, and your honest dose of tough love proved to be the perfect motivator when fieldwork turned to writing and my procrastinating tendencies hit their peak. Today, you are my eternal reminder to live in the moment and live each moment to its fullest. As Abraham Lincoln wisely stated, "And in the end, it's not the years in your life that count. It's the life in your years." Thank you.

TABLE OF CONTENTS

LIST OF TABLES

CHAPTER 2:

CHAPTER 3:

CHAPTER 4:

CHAPTER 5:

CHAPTER 6:

CHAPTER 7:

CHAPTER 8:

CHAPTER 9:

CHAPTER 10:

CHAPTER 11:

APPENDIX A:

APPENDIX B:

APPENDIX C:

APPENDIX D:

APPENDIX E:

APPENDIX F:

APPENDIX G:

LIST OF FIGURES

CHAPTER 2:

CHAPTER 3:

CHAPTER 5:

CHAPTER 6:

CHAPTER 8:

CHAPTER 9:

CHAPTER 10:

CHAPTER 11:

APPENDIX B:

NOMENCLATURE

A	Cross-Sectional Area of the Front of Vehicle
a	Vehicle Acceleration
A/C	Alternating Current
AC	Air Conditioning
ACEEE	American Council for an Energy Efficient Economy
AFR	Air to Fuel Mass Fraction
ANOVA	Analysis of Variance
AQMD	South Coast Air Quality Management District
bhp	Brake Horsepower
˚C	Degrees Celsius
CAN	Controller Area Network
CARB	California Air Resources Board
CD	Charge-depleting
C_D	drag coefficient
CDI	Common-Rail Direct Injection
CFFV	Clean Fuel Fleet Vehicle
CI	Compression Ignition
CO	Carbon Monoxide
CO_2	Carbon Dioxide
C_R	coefficient of rolling resistance
CS	Charge-sustaining
D	Distance Traveled
DI	Direct Injection

dICE	Diesel Internal Combustion Engine
DLM	Data Logging Module
DOC	Direct Oxidation Catalyst
ECM	Engine Control Module
EFM	Exhaust Flowmeter
EGR	Exhaust Gas Recirculation
ε_i	Mass Factor, the equivalent translational mass of rotating powertrain components
EISA	Energy Independence and Security Act of 2007
EM	Electric Motor
EM	Electric Motor
EPA	Environmental Protection Agency
EPRI	Electric Power & Research Institute
EREV	Extended Range Electric Vehicle
ϕ	Relative Humidity
FA	Factor Analysis
FedEx	Federal Express
FID	Flame-Ionization Detector
FID	Flame Ionization Detector
FTP	Federal Test Procedure
g	Gram
g	Acceleration Due to Gravity ($9.81 m/s^2$)
gal	Gallon
GHG	Greenhouse Gas
GPS	Global Positioning System

H	Altitude
H_2O	Water
HC	Hydrocarbons
HD	Heavy-Duty
HDDV	Heavy-Duty Diesel Vehicle
HEV	Hybrid Electric Vehicle
hp	Horsepower
hr	hour
Hr	Hour
HTBR	Hierarchal Tree-Based Regression Model
Hwy	Highway Roadways
I	Current (amps)
ICE	Internal Combustion Engine
IDI	Indirect Injection
IEEE	Institute of Electrical and Electronics Engineers
ILEV	Inherently Low Emission Vehicle
in	Inches
J	Joule
K	Kelvin
KCATA	Kansas City Area Transit Authority
kg	Kilogram
km	kilometer
km	Kilometer
Kph	Kilometers per Hour
KU	University of Kansas

L	Liter
l	Liter
lb	Pounds
lb	Pound
m	Meter
m	Vehicle Mass
$\dot{m}$	Mass Flow Rate
m/s	Meters per Second (unit measure for velocity)
m/s^2	Meters per Second-Squared (unit measure for acceleration)
MANOVA	Multivariate Analysis of Variance
MCS	Monte Carlo Simulation
mi	Mile
MOVES	Motor Vehicle Emissions Simulator
mph	Miles per hour
Mph	Miles per Hour
MW_x	Molecular Weight of x
N_2	Nitrogen
NDIR	Non-Dispersive Infrared
NDIR	Non-Dispersive Infrared
NDUV	Non-Dispersive Ultra-Violet
NDUV	Non-Dispersive Ultraviolet
Nm	Newton-Meter (unit measurement for torque)
NO	Nitric Oxide
NO_2	Nitrogen Dioxide
NOx	Nitrogen Oxides

NRDC	Natural Resources Defense Council
NREL	National Renewable Energy Laboratory
NY DEC	New York Department of Environmental Conservation
NYT	New York Times
O_2	Oxygen
P	Power
Pa	Pascal
PCA	Principal Component Analysis
p_d	Partial Pressure of dry air (Pa)
PEMS	Portable Emissions Monitoring Systems
PERE	Physical Emission Rate Estimator
PHEV	Plug-In Hybrid Electric Vehicle
PM	Particulate Matter
ppm	Parts Per Million
p_{sat}	Saturation Vapor Pressure
p_v	Partial Pressure of Water Vapor
R_d	Specific Gas Constant for dry air (287.058 J/(kg·K))
RPM	Revolutions per Meter
R_v	Specific Gas Constant for water vapor (461.495 J/(kg·K))
s	Second
S	Suburban Roadways
SAE	Society of Automotive Engineers
SCE	Southern California Edison
SOC	State of Charge
t	Time

T	Ambient Temperature
τ	Torque (Nm)
TAF	Toronto Atmospheric Fund
THC	Total Hydrocarbons
TRI	Transportation Research Institute
TRI	Transportation Research Institute (University of Kansas)
U	Urban Roadways
v	Vehicle Velocity
V	Voltage (volts)
VOC	Volatile Organic Compound
VSP	Vehicle Specific Power
VSP	Vehicle Specific Power
v_w	Vehicle Headwind
V_x	Volumetric Flow Rate of x
W	Watt
ω	Angular Velocity (i.e. engine speed)
WAAS	Wide Area Augmentation System
W_f	Fuel Mass Flow Rate
α	Level of Statistical Significance
π	Pi (3.1416)
ρ_x	Density of x

Chapter 1: Introduction

Vehicle emissions remain a primary cause of poor air quality in the United State's metropolitan areas. Coupled with increasing energy prices and the American consumer's growing concern regarding a heavy dependence on petroleum-based energy, alternatively fueled vehicles have become prominent features in today's mainstream automotive market. While much of the focus has been concentrated on conventional hybrid electric vehicles (HEVs), growing acceptance within the American consumer market has generated considerable interest in the next evolution of hybrid: the plug-in hybrid electric vehicle (PHEV). While rooted in hybrid drive technology, the PHEV distinguishes itself through its "plug-in" capabilities, in which vehicles are designed to provide between 20 and 30 miles of electric-only driving between grid-delivered charges before switching into hybrid mode. Supplementing the environmentally friendly hybrid design with electric-only capabilities not only increases the vehicle's energy efficiency, but also has the promise of greatly reducing its emissions potential. When applied to the public-transit sector, PHEV utilization has the potential to mitigate some of the vehicle emissions loads delivered to more congested urban areas.

In 2003 a partnership between the Electric Power Research Institute (EPRI) in Palo Alto, California and the DaimlerChrysler Corporation in Stuttgart, Germany led to the development of one of the first plug-in hybrid vehicles to reach the U.S. roadways. Designed around the Sprinter chassis, the first plug-in hybrid prototypes were designed with the option of using either petroleum or diesel internal combustion engines.

Five independent operating partners were recruited for the initial PHEV Sprinter on-road testing, the Proof-of-Concept testing Phase I. This phase of testing was

designed to provide the design and development partners with valuable on-road data relating to the PHEV's overall operation, actual on-road use, and reliability. Phase I development resulted in the production of four different Sprinter PHEVs. These vehicles were distributed to participating partners throughout the United States and Europe. The fourth PHEV Sprinter produced was delivered to the Kansas City area in September 2006. The vehicle's participating partner, the Kansas City Transit Authority (KCATA), utilized the Sprinter PHEV as a paratransit vehicle employed in their regular need-based paratransit service. In addition to its proof-of-concept testing, the Kansas City-based PHEV Sprinter prototype was selected for analogous emissions testing. The University of Kansas (KU) Civil, Environmental, and Architectural Engineering Department was contracted to work alongside the Kansas City Area Transit Authority (KCATA) in order to complete the emissions testing of the Kansas City diesel-based PHEV Sprinter.

Partner meetings in Stuttgart and Manheim, Germany determined that all emissions testing be conducted in a contiguous manner to the on-road proof-of-concept testing. At this time, the emissions portion of the PHEV Sprinter demonstration study focused all of its efforts towards on-road, continuous emissions monitoring capabilities. Using on-board emissions analyzing equipment, the emissions portion of the PHEV Sprinter's on-road campaign was initiated in August 2007 and continued for 5 months through January 2008. The emissions data were collected in conjunction with vehicle operating variables in order to produce a dataset capable of thoroughly describing the PHEV Sprinter's on-road behaviors during a multitude of different driving scenarios.

KCATA was originally brought into the project in order to add a public transit dimension to the Phase I Proof of Concept testing. As the only diesel-based PHEV

prototype created during Phase I design and development, it was deemed important to not only test the Kansas City-based PHEV Sprinter's performance as applied to transit service, but to give a comprehensive picture of the on-road implications of a diesel combustion engine-based plug-in hybrid electric vehicle. In order to achieve this, several KCATA designated routes were selected for the bulk of the on-road testing. When applicable, the routes were tested simulating both transit operations (by following a KCATA bus) and during normal, civilian driving conditions. In this manner, the Kansas City-based PHEV Sprinter was driven within the context of transit operation while still allowing for on-road operation that was not biased by the driving demands required of transit service. When necessary, additional routes outside of the KCATA network were developed in order to collect emissions data over the entire range of normal vehicle operations.

In addition to meeting the criteria of the Phase I Proof of Concept testing, several features inherent in the PHEV design piqued the interest of the participating researchers, giving dimension and direction to the demonstration study's overall goals. The ultimate goal of the developing partners and primary purpose of the proof of concept testing efforts was to bring the PHEV technology one step closer to full production and consumer-based distribution. In addition to the technological challenges presented by such a task, before any vehicle can be marketed, sold, and driven within the United States, it must meet certain baseline safety and emissions mandates. While the actual on-road emissions and operating data will give a certain picture into the PHEV Sprinter's viability regarding emissions certification, ultimately, it's on-road performance will be

applied to current emissions models in order to provide an estimation of its emissions load outside of the confines of the Kansas City-based sampling.

Current emissions models rely on and are based around the vehicle specific power construct, a proxy calculation capable of estimating a vehicle's immediate on-road power load built around various road-based, driving-based, and vehicle-based information and coefficients. With its dual drive-train capabilities, some uncertainty existed as to whether the PHEV platform would yield actual emissions and operating data able to fit current vehicle specific power models to a statistically meaningful level. Using the Kansas City-based PHEV Sprinter as the initial test subject for application to vehicle specific power models, insight can be gained into the suitability of current models as applied to alternatively fueled vehicles such as plug-in hybrid electric vehicles.

Plug-in hybrid vehicles are designed to deliver a certain amount of electric-only driving before switching to a hybrid-based operation. EPRI and Daimler estimations suggested that the PHEV Sprinter's electric-only capacity ranged from 20-30miles (driving conditions dependent). However, until the PHEV Sprinter is actually placed on-road in real driving circumstances, cited electric-only driving range remains theoretical in nature. Additionally, the Kansas City-based PHEV Sprinter was equipped with a diesel internal combustion engine, making it unique among not only the prototypes developed by Daimler, Chrysler, and EPRI, but also among the hybrid electric vehicles available to the United States market today. Part of the comprehensive demonstration study will focus on the diesel engine's performance within the PHEV framework.

A variety of dynamometer test cycles are currently used for laboratory-based simulation of a vehicle's on-road behavior and emissions. These cycles exist because a

vehicle's performance and emissions are directly dictated by its on-road experience. Whether engine power output is mandated by driver demands or road-based features, roadway type and local topography will determine the PHEV's performance as it navigates the Kansas City area both within and outside of transit service. Categorizing roadway links contained within the sampling network will give a basis from which the PHEV Sprinter's operating and emissions behaviors can be investigated. Should the PHEV platform ever be slated for transit application, an understanding of the effect that facility type and drive-scheme have on its overall performance and its ability to maximize electric-only capabilities will give transit managers the knowledge base to best place PHEVs into transit service allowing them to maximize the inherent advantages that the plug-in design delivers.

Chapter 2: Project Fundamentals and Background Information

2.1 Plug-In Hybrid Vehicles (PHEVs)

2.1.1 Introduction

By definition, a plug-in hybrid vehicle is a vehicle that possesses batteries, which can be charged by connecting, or plugging into, an electric source. Plug-in hybrids first entered mass media in 1969 when *Popular Science* published an article featuring the General Motors XP-883 PHEV (Norbye and Dunne, 1969). With six on-board 12-volt lead-acid batteries and a transverse-mounted DC electric motor powering the front wheel drive, the XP-883 could be recharged by plugging into a standard North American 12-volt AC outlet. Today, over seven automotive manufacturers have released statements regarding their intents to produce plug-in hybrid passenger vehicles in the upcoming years.

Currently, in the U.S. there is limited PHEV availability to the consumer market, with Chevrolet and luxury manufacturer Fisker, producing the only passenger-based PHEVs for sale today. Despite the limited market penetration to date, New Flyer has employed PHEV technology in their transit buses, and several automotive manufacturers have designed concept PHEVs with tentative target dates for release. This list of manufactures includes, but is not limited to, Audi, BMW, Ford, Kia, Mercedes, Mitsubishi, Suzuki, Toyota, Volkswagen, and Volvo (www.pluginamerica.org, 2011). As additional incentive, further promoting the PHEV initiative, the Energy Improvement and Extension Act of 2008 established tax incentives for the purchase of plug-in hybrid vehicles as part of the U.S. financial bailout.

The Energy Independence and Security Act of 2007 (EISA) specifically refers to plug-in electric drive vehicles (Subtitle B) where, in accordance with the act, the Secretary of Energy is to establish a competitive grants program to "encourage the use of plug-in electric drive vehicles" and appropriations were authorized for the plug-in program running from fiscal year 2008 through 2012. By EISA definition, a "plug-in electric drive vehicle" is one that draws motive power from a battery with a capacity of at least 4 kilowatt-hrs, can be recharged from an external energy source for motive power, and is a light-, medium-, or heavy-duty motor vehicle or nonroad vehicle. This definition distinguishes PHEVs from current hybrid vehicles by their ability to receive and use grid power. The Institute of Electrical and Electronics Engineers (IEEE) adds to the EISA definition for the PHEV with the caveat that PHEVs must achieve a minimum ten miles of electric-only operation with each charge.

With their increased electric-only capability, modern day plug-in hybrid vehicles possess characteristics similar to both the hybrid electric vehicles seen on the road today and true electric vehicles. As a hybrid vehicle, PHEVs possess an internal combustion engine (ICE) as well as an electric drive motor (EM). A PHEV's likeness to electric vehicles exists in its higher capacity on-board batteries, which are configured to recharge from an external power source (i.e. an AC outlet) resulting in extended electric-only range. Larger batteries give PHEV's an estimated 20-40miles of electric operation (Stephan, 2008). The fusion of electric-only capabilities with hybrid (ICE/battery) operation gives drivers the high efficient operation of a pure electric vehicle as well as the extended mileage range provided by hybrid vehicles. Plug-in hybrids are anticipated

to best meet the driving needs of short-distance commuting trips, which often occur in congested traffic conditions (Stephen, 2008).

Because of its dual operative abilities, a PHEV's configuration can be categorized into two distinct operating modes: charge-depleting mode and charge-sustaining mode. When fully charged, a PHEV will rely largely on its stored battery capacity to operate, utilizing the ICE only when on-road driving demands require additional power assist. During this time, referred to as charge-depleting mode, the PHEV will deplete its battery capacity functioning, ideally, as a pure electric vehicle, unless immediate demand requires power assist from the ICE. The PHEV enters charge-sustaining operation once its battery capacity has been reduced to a set level at which point it operates as a hybrid electric vehicle until recharged. In charge-sustaining operation, the internal combustion engine as well as additional battery capacity restored during normal on-road operation is used to power the vehicle. During hybrid function, the PHEV can switch between electric-only, electric/ICE mixed, and ICE-only operation. Like conventional hybrids, PHEVs are designed to scavenge otherwise wasted energy through regenerative braking and recuperation in order to increase the batteries' utility while the vehicle operates during normal on-road driving.

Plug-in hybrid vehicles can be designed around the same powertrain configurations used in conventional hybrid vehicles. There are three primary architectures used in today's hybrid electric vehicles: series, parallel, and series-parallel hybrids. The series configuration acts as an extended range electric vehicle (EREV) (The California Cars Initiative, 2008) using only an electric motor to actually drive the vehicle's wheels. In addition to battery storage capacity, these hybrids feature an internal

combustion engine that acts as a generator by supplying current to the electric drivetrain. Parallel hybrids possess the ability to supply two different sources of power to the drivetrain: electric drive fueled by stored battery capacity and an internal combustion engine. In these vehicles, the electric motor can provide sole power in low demand situations or it can provide supplemental power to the ICE during higher on-road demands. This allows the vehicle to fully operate with a smaller internal combustion engine than would otherwise be specified for the same conventional drive vehicle (BC Climate Exchange, 2008). Parallel-series hybrids are designed with the flexibility to operate in either series or parallel mode. Nissan, Lexus, Toyota, and Ford hybrid vehicles all utilize this design configuration (Toyota Motor Corporation, 2008).

2.1.2 Potential Fuel Savings

As of 2004, the U.S. Department of Energy reported that more than half of the 20.5million barrels of oil consumed in the United States each day was imported. While the United States consumes 25% of the world's oil supply, it only holds 3% of the global petroleum reserves (Sanna, 2005). For the United States, oil consumption and fuel usage have become both economic issues as well as national security concerns. With their increased battery capacity and ability to transform grid-sequestered electricity to on-road driving power, plug-in hybrid vehicles are anticipated to provide a greater fuel savings potential than conventional hybrid-electric vehicles (which already exceed the fuel economy achieved by most conventionally powered internal combustion engine vehicles). Increased battery capacity will also allow PHEVs to operate their internal combustion engines closer to maximum efficiency by relying on electric capacity in

driving situations that are below the ICE's peak efficiency (Gonder and Markel, 2007). Ultimately, a PHEV's energy efficiency will be dictated by the efficiency of electricity generation, electricity inversion, battery charging and discharging, the motor controller and the electric motor itself. Additionally, the PHEV's on-road duty cycle and operator behaviors (i.e. charging and driving behaviors) will impact the vehicle's real world efficiency. Based on 2004 census, the U.S. Department of Transportation determined that over 60% of daily passenger travel within the U.S. was completed by vehicles that travel fewer that 50km (31.1miles) per day (Samaras and Meisterling, 8), making the PHEV concept design particularly well-suited for travel behavior in the U.S. PHEVs are anticipated to excel, with regards to efficiency, in short-distance stop and go trips, such as daily commutes in congested traffic conditions (Stephan et al., 2008).

The EPRI Journal estimated that, based on current grid charging capabilities and expense, PHEVs can be operated on the equivalent of $0.75 per gallon (Sanna, 2005). Since more than half of the cars in the United States are driven less than 25miles per day, EPRI forecasts that a 60% reduction in petroleum consumption can be realized by using plug-in hybrid vehicles. Stephan et al. performed a comprehensive environmental assessment of plug-in hybrid vehicles in 2008. Based on EPA's 2006 average light-duty vehicle city-based fuel economy of 18.6mpg (adjusted for changes due into effect in 2008), Stephan et al. estimated that conventional vehicles yield a fleet average of 5.15MJ/km. Their calculations show that an equivalent fleet of hybrid electric vehicles (HEVs) would utilize an average energy consumption of 3.53MJ/km, and the estimated wall-to-plug energy consumption for a PHEV fleet was reported at 0.96MJ/km. Their assessment shows significant improvements in energy efficiency between PHEVs and

both conventional vehicles and HEVs. However, their energy efficiency assessment was limited to city-only driving and, therefore, assumed a very optimistic operating profile of 100% electric-only operation for the PHEV fleet. In electric-only operation, the energy saving potential for a PHEV is significant, but the increased vehicle weight resulting from a larger battery capacity will potentially reduce the overall efficiency of the PHEV's internal combustion engine.

The Society of Automotive Engineers (SAE) is currently reviewing methods to test and report the fuel economy of plug-in hybrid vehicles (U.S. Department of Energy, 2008). Daimler reported an on-road fuel efficiency of 10.1L/100km for one of their prototype PHEV Sprinter cargo vans operating with a diesel ICE (Daimler, 2007). Operated as a FedEx courier vehicle on city center routes in Paris, France, the PHEV Sprinter reported 40% reductions in fuel use over a conventional diesel Sprinter. In 2008, the Toronto Atmospheric Fund (TAF) tested ten retrofitted PHEVs (conventional hybrids fitted with plug-in capabilities). During the six-month study, TAF findings showed an average pHEV fuel efficiency of 5.8L/100km (40.6mpg). While more fuel-efficient than the pre-plug-in retrofits, the study found that the PHEVs performed below their technological potential (Hamilton, 2008).

2.1.3 Potential Emissions Reductions

It is estimated that emissions from automobiles and light-duty trucks in the United States account for 17% of the United States' greenhouse gas emissions (GHG) (Samaras and Miesterling, 2008). Despite improvements in vehicle efficiency, increases in total travel have accounted for almost 40% of recent (since 1990) rises in carbon dioxide

(CO_2) emissions (Samaras and Meisterling, 2008). In addition to their potentially improved fuel efficiency over conventional vehicles and HEVs, plug-in hybrid vehicles have garnered attention for their complimentary potential to reduce total vehicle emissions. Speculation exists regarding the extent to which a fleet of PHEVs might reduce overall fuel consumption, however, there is general consensus throughout the literature that replacing the existing U.S. vehicle fleet with equivalent PHEVs will result in *some* decrease in fleet fuel requirements. Since PHEVs transfer a significant portion of their daily power source from gasoline or diesel fuel to the electric grid, there is uncertainty whether or not adapting a PHEV fleet will result in decreased GHG emissions when evaluated on a lifecycle basis.

In effort to evaluate the potential impact that PHEV integration would have on greenhouse gas (GHG) emissions, the Electric Power Research Institute (EPRI) published two preliminary reports (EPRI, 2007 and 2008) describing PHEV implementation under an electrical system powered largely by natural gas combined cycle power plants. Assuming widespread infiltration of PHEVs from 2010 to 2050, EPRI estimated that GHG emissions would be reduced by more than 450 million metric tons in 2050. Additionally, EPRI deduced that PHEVs would improve national air quality through a reduction in criteria pollutants due to overall reductions in fuel combustion.

Samaras and Meisterling conducted a lifecycle analysis of GHG emissions attributed to PHEV production and operation. Their analysis included an assessment of PHEV battery production, power plant operation and pollution changes due to PHEV charging, and the implications of PHEV on-road use. Based on the current status of electricity generation in the U.S., they found that PHEVs had the potential to reduce

GHG emissions by 38-41% when compared to conventional vehicles. However, when compared to existing HEVs, the reductions were less significant at 7-12%. The true potential of PHEVs to reduce GHG emissions is a direct function of electricity generation in the U.S. If future power generation systems find non-carbon based fuels, or if existing carbon-based power plants begin sequestering their carbon dioxide emissions, the lifecycle operation of PHEVs will tend towards lower GHG emissions. As part of their sensitivity analysis, Samaras and Meisterling found that PHEV operation under a carbon-intensive electricity generation scenario (i.e. coal) resulted in higher GHG emissions than using HEVs (Samaras, 2008). The American Council for an Energy Efficient Economy (ACEEE) study conducted in 2005 (Kliesch and Langer, 2006) supports these findings. Similarly, driving a PHEV could result in up to 30-47% reduced GHG emissions over HEV operation if electricity generation were to follow a low-carbon scenario relying on wind, nuclear, and coal with carbon sequestering power regimes.

Under the appropriate power plant regime, PHEVs show potential to greatly reduce GHG emissions when compared to conventional vehicles and today's HEVs. Reductions in fuel combustion will also lead to reduced emissions of regulated pollutants such as volatile organic compounds, carbon monoxide, and nitrogen oxides. However, the ACEEE (Clayton, 2006) stated that, in coal-dependent areas, PHEV use would result in an increase in the net sulfur dioxide and mercury emissions due to coal combustion processes.

2.1.4 Grid Capacity

Based on the anticipated use of PHEVs (short daily drive distances, daytime operation, and operating in stop-and-go congested traffic conditions), each vehicle will undergo several hours of nightly, on-grid charging leading some industry experts to question the ability of the existing electricity grid to meet the demands of significant PHEV market penetration. The EPRI-NRDC (Natural Resources Defense Council) PHEV projection report released in 2007 found that if PHEVs represented 60% of the U.S. automotive market in 2050, only 7-8% of the grid-supplied energy would be utilized (EPRI, 2007). Consumer driving habits suggest most PHEV long charges will occur at night. Even outside of the consumer market this trend holds true; KCATA's transit PHEV service required that the vehicle be charged during the out-of-service nighttime hours. Stephan and Sullivan investigated the implications that significant PHEV use would have on the U.S. electric grid for both short- and long-term planning (Stephan and Sullivan, 2008).

Currently, utilities are sized and operate in order to meet peak electricity demands set by consumer habits and tendencies. Consumer electricity demand peaks mid-day, with the annual maximum demand occurring mid-day during the mid-summer months (i.e. July). Utilities increase capacity to meet the mid-day demand and taper production during off-peak times. Since most PHEVs will be charged during off-peak hours, utilities are not required to increase their overall capacity in order to supply the necessary energy for vehicle charging. Conversely, PHEVs will be charged using less expensive, off-peak energy while allowing the utilities to operate in a more steady-state fashion. Stephan and Sullivan (2008) found that the under-utilized spare capacity in the current grid system is

sufficient to support significant PHEV market penetration. Kitner-Meyer et al. (2007) determined that the existing grid could support 43% of the U.S. light-duty fleet for 12hours of nightly charging.

The most current and conceptual discussions relating PHEVs to the electric grid refer to a smart grid, where the PHEV becomes an integrated part of the electric grid, pulling power when needed and supplying it back to the grid when electric demands are high. For example, a PHEV owner would charge the vehicle at night during off-peak hours, but during daytime hours, the PHEV would be reconnected to the grid while parked allowing the grid to access the vehicle's excess battery capacity during high-peak demand. Sioshansi and Denhom (2010) estimated that income derived from vehicle-to-grid charging could potentially reduce the length of time required for PHEV owners to recuperate the added capital expense of purchasing a PHEV by over 20%. The true value of vehicle-to-grid charging is, ultimately, a function of the local power source. Areas serviced by non-perpetual fuel sources, such as wind power, could benefit greatly by a vehicle-assisted supplementary power supply during periods of minimal to no fuel availability (Sioshansi and Denhom, 2010).

The vehicle-to-grid concept is still in the abstract stage of infrastructure development, particularly since few PHEV production models exist in the U.S. However, Pacific Gas and Electric displayed a PHEV with vehicle-to-grid capabilities at the 2007 Silicon Valley Leadership Alternative Energy Solutions Summit.

2.1.5 PHEV Sprinter Study: Phase I

In 2003 the Electric Power and Research Instituted (EPRI) joined forces with the DaimlerChrysler organization in order to develop a plug-in hybrid vehicle based on Daimler AG's Sprinter van chassis. Sprinter PHEVs were designed with 20miles of electric drive capacity, providing the most efficient operation at low velocities. With the extended electric drive capabilities and the ability to utilize regenerative braking to recharge batteries while in use on-road, the Sprinter PHEV was expected to provide light heavy-duty vehicle service with significantly less fuel consumption and with far fewer pollutant emissions than conventional light, heavy-duty vehicles on the road today. Figure 1 displays the Sprinter PHEV's designed operating mode according to vehicle velocity (y-axis) and elapsed time (x-axis). The original Phase I Sprinter PHEVs were designed to operate solely in electric mode (no internal combustion operation) at speeds less than 10km/h.

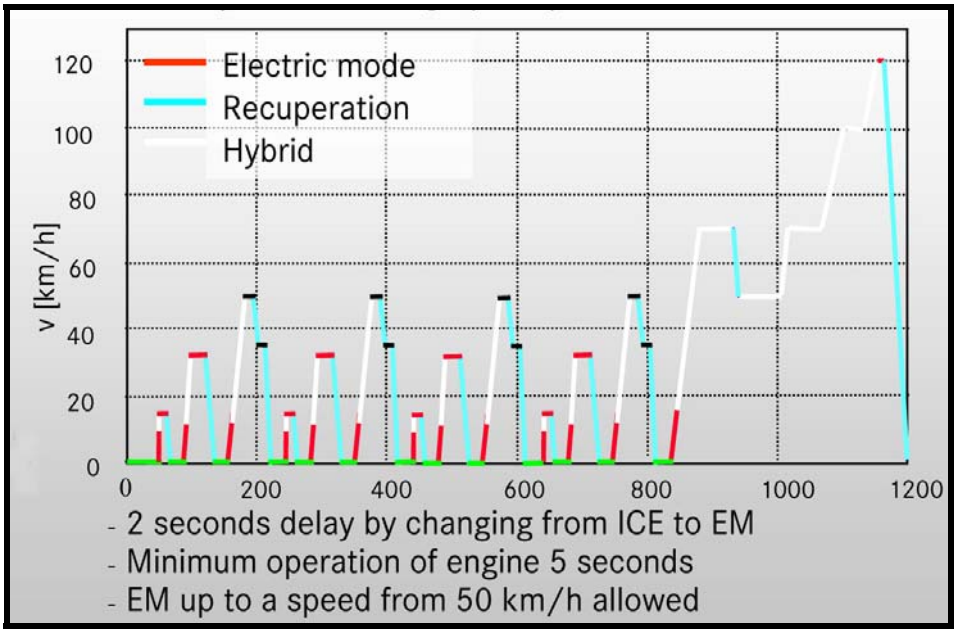

Figure 2.1: Phase I Sprinter PHEV operating mode design (Locht, 2006).

The project was introduced in multiple phases, with the first phase handling vehicle design, development, and proof-of-concept testing. Phase I goals included the development of four prototype PHEV Sprinter vans slated for on-road demonstration in the United States beginning in 2005. The initial project partners selected to demonstrate the PHEV Sprinter's on-road performance included

- South Coast Air Quality Management District (AQMD), Los Angeles, California (Prototype 1),
- Southern California Edison (SCE), Rosemead, California (Prototype 2),
- Kansas City Area Transit Authority (KCATA), Kansas City, Missouri (Prototype 3),
- Federal Express (FedEx), Paris, France (Prototype 4, first location), and
- New York Times (NYT), New York, New York (Prototype 4, second location).

Ultimately, four PHEV Sprinter prototypes were produced and tested in the United States as part of the Phase I testing. Phase I was designed with three primary goals in mind: to test the PHEVs under real world, on-road conditions for data gathering purposes, to test the Sprinter PHEV's zero emission operation in urban areas, and to test future marketability of the PHEV concept. Additional on-road emission testing was

scheduled for the KCATA Sprinter. While all PHEV Sprinters were designed as parallel-configured plug-in hybrid electric vehicles, the vehicles were developed using different internal combustion engines and battery technologies. The following table provides the design details for each of the Phase I Sprinter PHEVs.

Table 2.1: Specifications for Phase I Sprinter PHEVs (Portmann, 2008).

Prototype #	**1**	**2**	**3**	**4a**	**4b**
Demonstrating Partner	**SCE**	**AQMD**	**KCATA**	**FedEx**	**NYT**
Vocation	Cargo Van	Cargo Van	Paratransit Bus	Cargo Van	Cargo Van
Internal Combustion Engine	4-cylinder Gasoline	4-cylinder Gasoline	5-cylinder Diesel	5-cylinder Diesel	5-cylinder Diesel
Battery	Nickel Metal Hydride	Nickel Metal Hydride	Lithium-Ion	Lithium-Ion	Lithium-Ion
Gross Vehicle Weight	8550lbs	8550lbs	8550lbs	8550lbs	8550lbs
Wheelbase	140inches	140inches	158inches	140inches	140inches

Federal Express Phase I testing (as a courier vehicle) operated on a 32.4km drive cycle exhibiting an average speed of 8.7km/h (5.4mph). Under these conditions the diesel Sprinter PHEV operated in electric drive mode 62% of the time (20.1km) resulting in an average fuel consumption of 10.1L/100km (23.3 mpg). In this particular demonstration, the Sprinter PHEV provided an estimated 40% reduced fuel consumption when compared with the equivalent conventional vehicle. The New York Times also demonstrated this particular PHEV as a newspaper delivery vehicle through midtown Manhattan. The NYT typical drive cycle possessed a significantly higher average vehicle speed of 24.0km/hr (14.9mph) resulting in less overall electric drive operation (only 32% of the cycle was completed in electric-only drive mode). Fuel economy, however was improved at 7.3L/100km (32.2 mpg). When evaluated under different operating

conditions, the PHEV Sprinter performed less ideally than projected, but still exhibited the benefits of plug-in technology (Portmann, 2008).

2.1.6 PHEV Sprinter Study: Phase II

Phase II of the PHEV Sprinter project was scheduled to initiate as Phase I was in its final stages (Portmann, 2008). The Phase II vehicles were not at a production level as the Kansas City PHEV Phase I testing concluded, but several improvements had been made to the PHEV Sprinter in order to increase vehicle reliability and reduce cost through component sharing. The Li-Ion battery configuration has shifted towards a cellular design in order to improve battery cooling. The internal combustion engine for all Phase II vehicles was cited to be a 6-cylinder gasoline engine. Phase II vehicle deliveries were scheduled in the third quarter of 2008, and testing was intended to demonstrate the vehicles under a different set of operating regimes (cargo vans versus passenger shuttle vehicles) as well as different climatic distinctions. The Phase II demonstrating partners and vehicle designations are provided in Table 2.

Table 2.2: PHEV Sprinter Phase II vehicle allocations (Portmann, 2008).

Partner	Location	# Test Vehicles	Vocation
AQMD	Los Angeles, CA	3	Shuttle Service Passenger Vans
SCE	Los Angeles, CA	2	Cargo Vans
Novex	Los Angeles, CA	1	Cargo Van
ANL	Chicago, IL	1	Cargo Van
CTC	Detroit, MI	1	Passenger Van
na	Washington, DC	2	Passenger Vans

2.1.7 PHEV Sprinter Study: Kansas City Area PHEV Specifications

As mentioned previously, the PHEV Sprinter delivered to the Kansas City Area Transit Authority (KCATA) was one of the final prototype vehicles delivered to the U.S. for Phase I, proof-of-concept testing. Three additional partners contributed to the on-road PHEV Sprinter Phase I testing, but the KCATA PHEV was the only vehicle subjected to emissions testing as well as the normal on-road evaluation. The specifications dictating the emissions monitoring part of the KC PHEV proof-of-concept study were determined through a series of meetings between the University of Kansas and Daimler and EPRI representatives. The initial meetings were scheduled in Mannheim and Stuttgart, Germany in September 2004, and the final discussions occurred in Kansas City in December, 2006. The project design, timeline, goals and methodology are detailed in the University of Kansas Transportation Research Institute (TRI) proposal, "Plug-In Hybrid Emissions Characterization and Demonstration Study." The Kansas PHEV Sprinter was equipped with a 2.7L, 5-cylinder diesel engine and a Lithium-ion battery pack. Table 3, below, provides the technical details for the Kansas PHEV Sprinter.

Table 2.3: Kansas PHEV Sprinter technical specifications (Locht, 2006).

Physical Specifications:	
Wheelbase:	158inches
GVWR:	8550lbs
Curb Weight:	7620lbs
Payload:	930lbs
Combustion Engine Specifications:	
Model:	OM647 Diesel
Number of cylinders:	5
Nominal Torque:	330 Nm
Nominal output:	115 kW
Electric Engine:	
Nominal output:	72 kW
Nominal Torque:	150-180 Nm
Maximum Output:	90 kW
Maximum Torque:	275 Nm
Batteries:	
Type:	Li-ion
Capacity:	13.2 kWh
Nominal Voltage:	367 V
Maximum Output:	82 kW
Modules/Cells:	17 / 102
Weight:	160 kg

Built on the extended Sprinter van chassis, the Kansas City PHEV measured 103.6in in overall length and 76.1in in width with a total ground clearance of 8.3in. The specified curb weight of the PHEV as originally delivered to Kansas City was 5,539lb. However, in order to meet the demands of transit and paratransit service, the Kansas City PHEV required a substantial build-out. The Braun transit bus conversion added a hydraulic wheelchair lift, electrically driven side door, and additional seating to the standard Sprinter cargo-van leaving less than 1,000lbs of payload capacity. Adding the total measured weight of the on-board emissions equipment and operator at roughly 600lbs, the remaining available payload during all on-road emission testing was

estimated at just under 350lbs. Because of the limited residual payload, emission testing with different vehicle loads (representing varying passenger loading) was not part of the sampling study design.

2.2 Diesel Engine Fundamentals

2.2.1 Compression Ignition (Diesel) Engines

It is necessary to understand the fundamental operation of diesel compression ignition engines in order to appreciate the conditions and events that lead to pollutant production and emission. The primary differences between diesel and conventional petroleum or gasoline engines occur during their fuel ignition processes. Where conventional petroleum engines rely on spark-ignition of the fuel in order to initiate the combustion process, diesel engines employ compression ignition (CI).

Diesel engines are noted for their increased fuel efficiency and, hence, reduced carbon dioxide emissions. There are two fundamental differences in the combustion process between diesel and petroleum engines resulting in diesel compression ignition's increased fuel efficiency. First, diesel combustion occurs at a higher temperature than in petroleum engines, promoting more fuel-efficient combustion. Secondly, diesel fuel is more energy dense than standard gasoline, so less fuel is required to achieve the same power output from a diesel engine. These distinctions translate to significant differences in emission characteristics between diesel and gasoline engines, with NOx and particulate matter emissions being primary concerns for diesel engine operation.

The ultimate purpose of any combustion engine, diesel or gasoline, is to convert the chemical energy stored in fuel to shaft power via a set thermodynamic cycle (Heywood, 1988). In automotive applications, a reciprocating piston engine utilizing a four-stroke combustion cycle usually performs this function. With compression ignition, fuel added to the piston cylinder as a spray vaporizes and auto-ignites due to elevated

temperature and pressure conditions within the cylinder. The auto-ignition negates the need for an initial spark as used in a conventional gasoline engine.

There are two primary types of fuel delivery systems employed in diesel engines: indirect injection (IDI) and direct injection (DI). Indirect injection systems possess a pre-chamber adjacent to each cylinder where fuel and air are mixed prior to cylinder injection. Direct injection systems directly inject fuel into the combustion chamber in a way that promotes rapid mixing of the fuel and air leading to quick and uniform combustion (North, 2006). Recent developments in direct injection technologies have resulted in the development of "common rail" direct injection (CDI) systems. CDI employs a high-pressure fuel rail to supply fuel to the combustion chambers. By using electronically controlled valves instead of mechanically driven unit injectors, common rail systems are more quiet and efficient. The high-pressure delivery system results in better fuel atomization, and, hence, better combustion.

Today's diesel engines tend to be turbocharged and employ exhaust gas recirculation (EGR) designs in order to improve both power output and efficiency and to reduce emissions. Turbocharged engines compress intake air via forced induction allowing each combustion cycle to use more oxygen. The increased air mass results in increased engine power output (North, 2006). Conversely, in efforts to mitigate NOx emissions, peak combustion temperatures are mitigated through exhaust gas recirculation. EGR recycles, or retains, a portion of the exhaust gas within the combustion chamber in order to dilute the fresh fuel/air mixture (Heywood, 1988).

In addition to inherent process and operational differences, the emissions profiles for diesel and conventional gasoline engines possess some critical distinctions. Both

engine designs rely on combustion reactions in order to convert chemical energy to power using the same stoichiometric equation for complete combustion of a pure hydrocarbon fuel in excess oxygen:

$$C_xH_y + (x+y/2)O_2 \rightarrow xCO_2 + (y/2)H_2O \quad (1)$$

While compression ignition engines tend to operate in excess oxygen, lack of homogeneity in the air-fuel mixture promotes regions that tend to be fuel-rich or fuel-lean throughout the combustion chamber. The formation of localized regions with dissimilar compositions ultimately depends on the vaporization and diffusion properties of the injected mixture (Heywood, 1988). Additionally, changes in cylinder pressure and temperature during the combustion stroke perpetuate reaction chemistry deviations from the combustion equation displayed above. Vehicle certification programs regulate all carbon monoxide, hydrocarbon, and nitrogen oxides emitted by combustion engines. Unintended side reactions and incomplete combustion reactions result in production and subsequent emission of all measured pollutants. In order to evaluate a vehicle's emissions in the context of its on-road operation, it is important to investigate the chemical and physical phenomenon dictating each pollutant's formation.

Carbon monoxide (CO), an intermediate product of the hydrocarbon combustion reaction, is formed as a consequence of incomplete fuel combustion. There are multiple events that cause incomplete combustion including: insufficient oxygen required to meet the combustion reaction's stoichiometric demands, reaction inhibition due to physical changes within the cylinder (i.e. temperature or pressure), and reaction termination due to

heat loss at the cylinder's walls (Heywood, 1988). Diesel engines emit very low levels of CO when compared to gasoline engines. Atjay and Weilenmann reported difficulty measuring carbon monoxide emissions from modern diesel engines due to the inherent detection limits of the NDIR (non-dispersive infrared) analyzer being employed (Atjay and Weilenmann, 2004).

Hydrocarbon (HC) emissions refer to the vapor phase hydrocarbons (volatile organic compounds) present in a vehicle's exhaust at 190°C. Their presence is generally due to incomplete fuel combustion or oil (and some fuel) pyrolysis (Heywood, 1988). Heavier hydrocarbons condense at 190°C and associate with particulate matter in the exhaust. The heavier HC fraction and particulate matter within the PHEV's exhaust were not measured as part of the Plug-in Hybrid Vehicle Demonstration Project. Hydrocarbon emissions result from excessively rich and/or excessively lean fuel to air ratios within the combustion cylinder. Inadequate air/fuel ratios can exist throughout the entire injected mixture and in localized regions within the combustion chamber. With regards to engine operation, incorrect matching of the injection timing, fuel quantity, and EGR flow rates will result in poor air/fuel mixing (Heywood, 1988). Insufficient aur/fuel mixing is also particularly common during moments of transient operation when the engine is transitioning from one steady-state moment to another.

Nitrogen oxides (referring to the pollutants NO and NO_2) are problematic emissions for diesel engines. Unlike gasoline engines, the control catalysts used for diesel vehicles do not address NOx emissions. Additionally, the high temperatures experienced during the diesel compression ignition process foster NOx production. Unlike carbon monoxide and hydrocarbon emissions, nitrogen oxides are not formed as

part of the normal combustion reaction and are the result of auxiliary reactions occurring throughout the combustion process. Nitrogen oxidizes at high temperatures forming nitric oxide (NO). Compression stroke timing in a diesel engine is designed so that fuel is injected immediately before the end of the compression stroke, causing regions of the mixture to react early in the combustion process. Localized temperatures within these pockets increase as they are further compressed, resulting in the otherwise inert nitrogen fraction of the intake air to oxidize (Heywood, 1988). Nitrogen dioxide (NO_2) is also formed at high temperatures through the oxidation of NO. Normally, the reverse reaction occurs as temperatures cool, but the temperature drop within the cylinder happens rapidly and, in effect, "freezes" the reverse reaction. This phenomenon results in NO_2 concentrations that exceed those predicted by the chemical equilibrium (Heywood, 1988). Because diesel engines are much higher particulate matter emitters than gasoline engines, (Heywood, 1988) controlling NOx through operational parameters becomes a trade-off with compression ignition engines. Higher operating temperatures throughout the diesel ignition process that lead to the production of NOx also promote the oxidation of particulate matter to carbon dioxide (CO_2), thus lowering the overall particulate matter emissions.

Modern diesel engines do not employ the same three-way catalysts used in gasoline engines, and use, instead, a direct oxidation catalyst (DOC). While the DOC effectively oxidizes CO and unburned hydrocarbons to form CO_2, it does not reduce NOx emissions like the three-way catalyst. Additionally, the DOC does not function effectively until it reaches its minimum operating temperature (typically around 250-300°C) resulting in increased overall emissions during vehicle warm up.

While technologies such as EGR and the DOC are effective at reducing diesel emissions during established, steady state operation, transient operation can result in poor harmonization of the engine control parameters and result in peak emissions of all regulated pollutants (Heywood, 1988). Additionally, cold-start scenarios do not benefit from the use of the DOC due to insufficient operating temperature. This could have large implications for the diesel plug-in hybrid Sprinter, since hybrid operation will inherently result in transient operation due to ICE disengagement in favor of electric-only operation.

2.2.2 Plug-in Sprinter Diesel Engine Characteristics

The Kansas City PHEV Sprinter was one of two prototype PHEV Sprinters equipped with a diesel internal combustion engine (dICE). Four prototype PHEV Sprinters were distributed throughout the United States for the Phase I proof-of-concept Plug-in Hybrid Sprinter project. Two PHEV Sprinters installed with gasoline ICEs were put into field-testing in California, one PHEV Sprinter installed with a diesel ICE was initially tested in Paris, France before being transferred to New York City. The Kansas City Area Transit Authority placed the fourth PHEV Sprinter, also equipped with a diesel ICE, into field use as a paratransit bus.

The Kansas City pHEV Sprinter was equipped with a 2004 Mercedes 2.7L CDI (common rail direct injection) diesel engine including a direct oxidation catalysis (DOC) and exhaust gas recirculation (EGR). The PHEV Sprinter was certified according to the United States Environmental Protection Agency (EPA) as a Clean Fuel Fleet Vehicle (CFFV), was labeled as an Inherently Low Emission Vehicle (ILEV) according to 40CFR88, and was considered an Ultra Low Emission Vehicle by California Air

Resources Board (CARB). The Kansas City PHEV Sprinter paratransit bus was not certified for use as an urban bus as defined by 40CFR86.093-2, but as a research prototype owned by the Daimler organization in Stuttgart, Germany was allowed to participate in the proof-of-concept study as one. The EPRI/DaimlerChrysler PHEV Sprinter proof-of-concept study represents the first fleet test of diesel hybrid technology (CleanCarCongress, 2007). The following table provides all of the technical details pertaining to the diesel engine installed in the Kansas City PHEV Sprinter.

Table 2.4: Technical specifications for the 2.7L CDI Diesel Engine.

Engine Make:	Mercedes CDI
Certification Level and Agency:	CFFV (Clean Fuel Fleet Vehicle); US EPA ILEV (Inherently Low Emission Vehicle); 40CFR88 ULEV (Ultra-Low Emission Vehicle); CARB
Certification Class:	Light Heavy-Duty Diesel Engine (L HDD)
Engine Model:	OM 647 LA CID 164
Engine Family:	4MBXH2.69 DJB
Engine Code:	Code 1
Exhaust Control System:	TC.ECM.CAC.OC.EGR TC ≡ Turbocharged ECM ≡ Engine Control Module CAC ≡ Charge Air Cooler OC ≡ Oxidizing Catalyst EGR ≡ Exhaust Gas Recirculation
Date Manufactured:	2004
Advertised Output:	115KW (154HP)/3800RPM
Fuel Rate at Advertised OP:	55-63mm^3/stroke
Injection Timing:	14.5±1 degrees BTDC
Idle Speed:	680±50 RPM

2.3 Vehicle Emissions Testing

2.3.1 Vehicle Emissions Overview

Mobile emissions continue to be a major source of criteria air pollutants both in the United States and on a global level. Based on 2002 estimations (Bishop, 2008), on-road mobile sources were the single largest source of carbon monoxide (CO), volatile organic compounds (VOCs), and nitrogen oxides (NOx) to the national emission inventory. It is also estimated that on-road vehicle sources contribute 82% of the carbon monoxide, 45% of the VOCs, and up to 56% of all nitrogen oxides to national inventory levels. In addition to criteria pollutants, mobile sources have become significant greenhouse gas (GHG) emitters, specifically carbon dioxide (CO_2). United States Environmental Protection Agency (U.S. EPA) findings show that transportation accounts for 40% of the increase in total carbon dioxide emissions from 1990 through 2004. Increased total travel in the United States has offset recent advances made in vehicle efficiency (Samaras, 2008).

With the increased concern over greenhouse gas emissions, vehicle emissions are no longer *just* a localized problem for urban areas and large cities; they have become a global issue. This is particularly true in developing countries with growing transportation sectors and expanding geographic populaces (Boughedaui and Kerbachi, 2008). In China the motor vehicle numbers increase, on average, at 11% annually. By the end of 2005, an estimated 31.6million cars were on the road in mainland China (Yao, 2007). In large, densely populated cities, such as Beijing and Guangzhou, vehicle transportation has become the major source of air pollution resulting in over 80% of the carbon dioxide emitted and over 40% of the nitrogen oxides emitted. Efforts made by the Chinese

government to replace the existing vehicle fleet with newer automobiles meeting the Euro III emissions standards have failed to mitigate vehicle pollution in urban areas due to the growing number of vehicles and additional traffic congestion (Yao, 2007).

In addition to the threat of greenhouse gas emissions, vehicle emissions have been shown to cause adverse effects both environmentally and with regards to human exposures. NOx emissions have shown environmentally deleterious impacts by contributing to or causing photochemical smog, acid deposition, and visibility reduction (Shorter, 2005). Ambient pollution resulting from mobile source emissions has been causally associated with both cancer and non-cancer health effects (Zielinska and Sagebiel, 2004), with diesel engine emissions being a significant contributor. Epidemiological studies have shown increased risks of mortality associated with people living close to major roads, suggesting a causal link with exposure to ultra fine particles (Sonntag, 2008).

The 1999 EPA National Inventory estimated that 42% of on-road NOx emitted in the United States was due to diesel combustion. More recent assessments suggest that on-road diesel emissions account for as much NOx emission as gasoline mobile sources (Shorter, 2005). After the 1998 consent decree, EPA regulations mandated a 95% reduction in NOx and a 90% reduction in particulate matter associated with on-road heavy-duty diesel engines within nine years (Cocker, 2004). An abundant number of epidemiological studies indicate a causal relationship between exposure to diesel emissions and the rate of lung cancer in humans. Both diesel vapor and diesel particulate matter extracts have exhibited genotoxic reactions on mammalian cell systems, a significant biological cause of lung cancer (Lloyd and Cackette, 2001).

2.3.2 Emissions Monitoring Overview

Because of their global, environmental, and health impacts, mobile sources are subjected to substantial regulatory action. While certification efforts vary for vehicle type and class, the ultimate goal of all certification efforts is to impose emissions limits on vehicles and engines that would directly relate to their on-road operation. This mandate poses difficulties for the certification process as regulators battle with accurately simulating on-road vehicle driving while maintaining the reproducibility needed to meet the quality control and quality assurance criteria esteemed by proper laboratory practices. The juxtaposition between achieving representative yet accurate data has led to significant discussion among vehicle emission testing methodologies.

Depending on vehicle class, certification processes are conducted using either chassis or engine dynamometers under a predetermined drive cycle and simulated load. This coupling aims to show the engine or vehicle being certified under realistic on-road conditions. However, a recent review of heavy-duty vehicle emissions show that the measured on-road trends were very different than those shown in certification test data and model output. Parameters such as vehicle weight, class, age, terrain, drive cycle, vehicle maintenance and vocation, which have been shown to correlate with emissions levels, are neglected in certification tests. This absence could ultimately cause significant deviations between the certification data used for emissions inventories and models and actual on-road emissions (Shorter, 2005).

2.3.3 Emissions Monitoring Methodologies

While current U.S. EPA heavy-duty vehicle federal test procedures (FTPs) mandate engine dynamometer certification (CFR Title 40, Part 86, Subpart N), integration of both the diesel and electric motor drivetrains on the Sprinter PHEV deem an engine-only emissions investigation insufficient. In order to investigate the operating emissions and on-road characteristics of the plug-in hybrid electric Sprinter, the vehicle must be evaluated as a single, comprehensive unit using full chassis-based emission monitoring techniques. U.S. certification of light-duty vehicles is conducted on a chassis dynamometer based on a predetermined drive cycle aimed at simulating on-road operation. While this method provides laboratory-based data that can be easily reproduced, it does not fully describe the vehicle's on-road experience.

Based on meetings with project partners in 2004 and keeping with the philosophy of the proof-of-concept Phase I testing, it was unanimously determined that all emissions data be collected while the PHEV was operating on-road. Several on-road emissions sampling techniques are used today, and each presents is benefits and weaknesses. Emissions from large vehicle fleets can be efficiently measured from stationary on-road sampling systems and methodologies such as remote sensing devices and tunnel studies.

Remote sensing devices utilize a roadside setup in order to remotely measure the emissions of passing vehicles. With proper installation and setup, remote sensing devices enable researchers to quickly and efficiently measure the emissions from a large number of passing cars. Remote sensing devices are most effectively used to characterize the vehicle emissions from a vehicle fleet representing large geographical areas. Mazzoneni et al. (2004) and Bishop et al. (2008) employed remote sensing techniques to perform

large-scale, on-road emissions monitoring efforts in Las Vegas, Chicago, Denver, Los Angeles, and Phoenix. Emissions data were mapped according to vehicle owner address providing a geographically spatial representation of vehicle emissions across the studied area. Additionally, Marotz et al. (2003) used a remote sensing device to conduct a vehicle emissions campaign in Kansas City using geodemographic techniques to map vehicle emissions according to owner address and demographic designation.

Remote sensing and tunnel studies are limited by their stationary installation. While they have the capabilities to measure large numbers of vehicles, they are only able to take a snapshot picture of each particular vehicle's emissions at the time of data collection. It is impossible to fully characterize a single vehicle's emissions and operation using remote techniques.

On-board portable emissions monitoring systems (PEMS) have undergone a dramatic phase of development during the past decade. PEM systems are installed directly on the vehicle and collect data as the vehicle is driven on- or off-road under normal operating conditions. As a proof-of-concept study, the primary goal of the PHEV Sprinter's on-road existence was to demonstrate the vehicle's capabilities and tendencies while operating on-road, under normal real-world conditions. On-board, portable emissions monitoring was the only sampling method determined suitable to meet the goals and scope of work presented in the University of Kansas (KU) Transportation Research Institute's (TRI) "Plug-in Hybrid Emissions Characterization and Demonstration Study."

Two different PEMS were considered for this work: the Montana System by Clean Air Technologies and the Semtech-DS by Sensors, Inc. Both systems are highly portable and designed to collect continuous, second-by-second, on-board emissions data. The Semtech-DS system provided some superior analytical capabilities including non-dispersive ultra-violet (NDUV) determination of NO and NO_2 and portable flame-ionization detection (FID) for total hydrocarbon measurements. Prior to selecting a system, Mathew Spears and Richard Baldauf with the United States Environmental Protection Agency (U.S. EPA) and Thomas Lanni with the New York Department of Environmental Conservation (NY DEC) were consulted due to their familiarity with the operation and development of each system. Because of its ability to collect laboratory-grade data and close ties with the U.S. EPA during development, the Sensors Semtech-DS on-board emissions monitoring system was selected to monitor the PHEV Sprinter's emissions.

Chapter 3: Data Collection and Processing

3.1 On-Road Data Collection and Equipment

On-road emissions data were collected from September 2007 through January of 2008. During that time, the Kansas City PHEV experienced over 1,180miles and 81hours of on-road driving, during which second-by-second operating and emissions data were logged using on-board emissions monitoring equipment and the PHEV's data logging module. In order to meet the project's aims, set criteria were determined in order to evaluate the suitability of a given day for on-road sampling. Initially, sampling efforts were to be conducted:

- Under relatively homogeneous and moderate ambient temperatures,
- While avoiding rush hour traffic situations for all "solo" designated runs,
- In the absence of precipitation (rain, sleet, or snow) events and while road conditions were dry and safe.

Contractual delays occurring from April through July of 2007 postponed the start of the sampling timeline until August 2007. Additionally, the KC PHEV experienced a variety of unspecified service issues and was not operational during October and most of November 2007. In order to compensate for these delays, the sampling timeline was extended into spring 2008. Unfortunately, Kansas City experienced a late winter with unseasonably cold temperatures and abundant precipitation through February, March and April of 2008. In addition to cold weather conditions, the KC PHEV had an unresolved service issue during that time, further limiting viable on-road sampling opportunities. Therefore, final sampling efforts originally intended for warmer conditions were not possible. Despite this, it was determined that, due to the copious amount of on-road data

collected from September through January, sufficient data had been collected to meet the project's objectives and goals.

3.1.1 Vehicle Data Logging Module

Simultaneous on-board emissions sampling coupled with engine and position monitoring provided a comprehensive dataset capable of fully describing the PHEV Sprinter's on-road performance over the selected roadways. Proprietary data logging modules (DLMs) were installed on all four Phase I Sprinter PHEVs. The DLMs allowed project partners to collect a series of electric system, electric motor, and combustion engine parameters on a real-time basis while the vehicles were operating on-road and while receiving battery charges. EPRI designed the data logging modules in order to meet the data collection, storage, and acquisition requirements set by the Phase I proof-of-concept study. The DLMs used the existing Controller Area Network (CAN) communications buses installed in the PHEV Sprinter prototypes. The resulting communication and data collection architecture prevented a direct vehicle interface between the on-board emissions monitoring system and engine control module. Instead, the DLM data were accessed post on-road testing and merged with the emission system's data as part of the post-processing efforts.

In order to complete the goals of the emissions monitoring project, it was imperative to access the DLM data during emissions sampling periods. Prior to on-road data collection, discussions between the project partners led to consensus regarding the University of Kansas' access to DLM data. The agreed upon protocol required EPRI to transform and filter the DLM data to a format compatible with the data collected by the

on-board system. The DLM variables deemed necessary for creating a comprehensive emissions and operating dataset were agreed upon and are provided in Table 5, below. All data were filtered down to a 1point/second frequency in order to facilitate merging and time aligning the DLM data with the emissions data.

Table 3.1: Accessed DLM data.

	Unit of Measurement	Resolution
Vehicle Variables		
Vehicle Speed	km/h	na
Revolution wheels	RPM	0.5 RPM
Revolution combustion engine	RPM	1 RPM
Revolution electric motor	RPM	1 RPM
Hybrid clutch (open/closed)	%	na
Battery Data		
Battery Current (charging, discharging, recuperation)	A	0.1A
Battery voltage	V	0.1V
Battery temperature	°C	0.1°C
State of Charge (SOC)	%	1%
Operation Strategy		
Torque combustion engine	Nm	3Nm
Torque electric motor	Nm	0.1Nm
Control Auxiliary Components		
Air condition on/off	%	na
Heater on/off	%	na

3.1.2 On-board Emissions Monitoring System

All on-road emissions data were collected using the Semtech-DS, designed and manufactured by Sensors, Incorporated (Saline, Michigan). The Semtech-DS is the only commercially available on-board vehicle emissions monitoring system developed in conjunction with the U.S. EPA, and it is the only on-board system capable of providing continuous, real-time laboratory-quality measurements of CO, CO_2, NO, NO_2, and total

hydrocarbon concentrations in vehicle exhaust (Spears, 2006). By employing Sensor's electronic flowmeter (EFM) and auxiliary global positioning system (GPS) receiver, the Semtech-DS provided second-by-second mass-based emission measurements in conjunction with global positioning data (latitude, longitude, altitude, and groundspeed).

Using a heated sample line designed to maintain the exhaust sample at 200ºC, the Semtech-DS pulled a continuous 8L/min slipstream directly from the vehicle's tailpipe or electronic flowmeter (which becomes a direct extension of the vehicle's exhaust system). Ambient temperature, pressure, and relative humidity were continuously monitored and recorded via an external weather probe mounted on the outside of the vehicle. These measurements were recorded for user reference and were required for calculating, in addition to other parameters, NOx humidity correction factors. Figures 3.1 through 3.3 below provide a schematic of the on-board emissions monitoring system installation and pictures of the Semtech-DS installation on the Kansas City Sprinter PHEV.

In effort to minimize the research equipment's impact on the PHEV Sprinter's normal operation and electrical capacity, an external generator mounted to the back of the vehicle was used to power all of the equipment required for on-board emissions monitoring.

Vehicle location was tracked using an auxiliary GPS receiver that directly interfaced with the Semtech-DS. The Garmin International, Inc. model GPS 16-HVS tracked the vehicle's route, elevation, and ground speed during each test. The 16-HSV unit supports the Wide Area Augmentation System (WAAS) standard, providing significantly enhanced positional accuracy (less than three meters) when compared to standard, conventional GPS receivers.

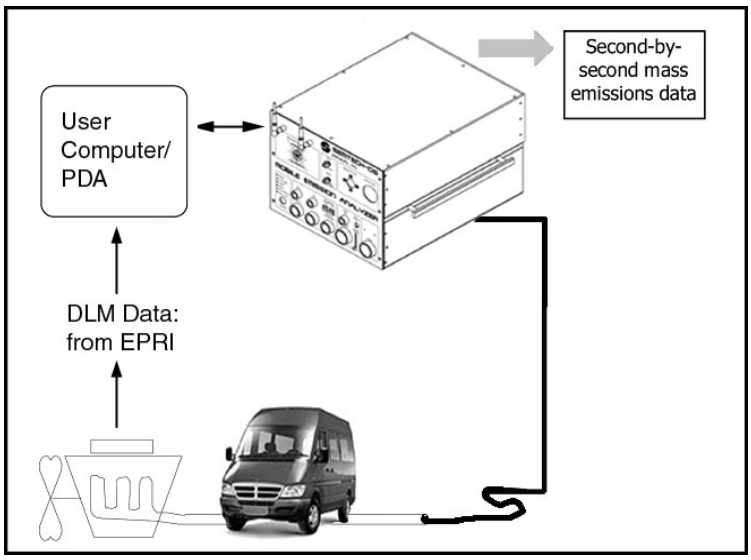

Figure 3.1: Schematic installation of on-board emissions monitoring equipment.

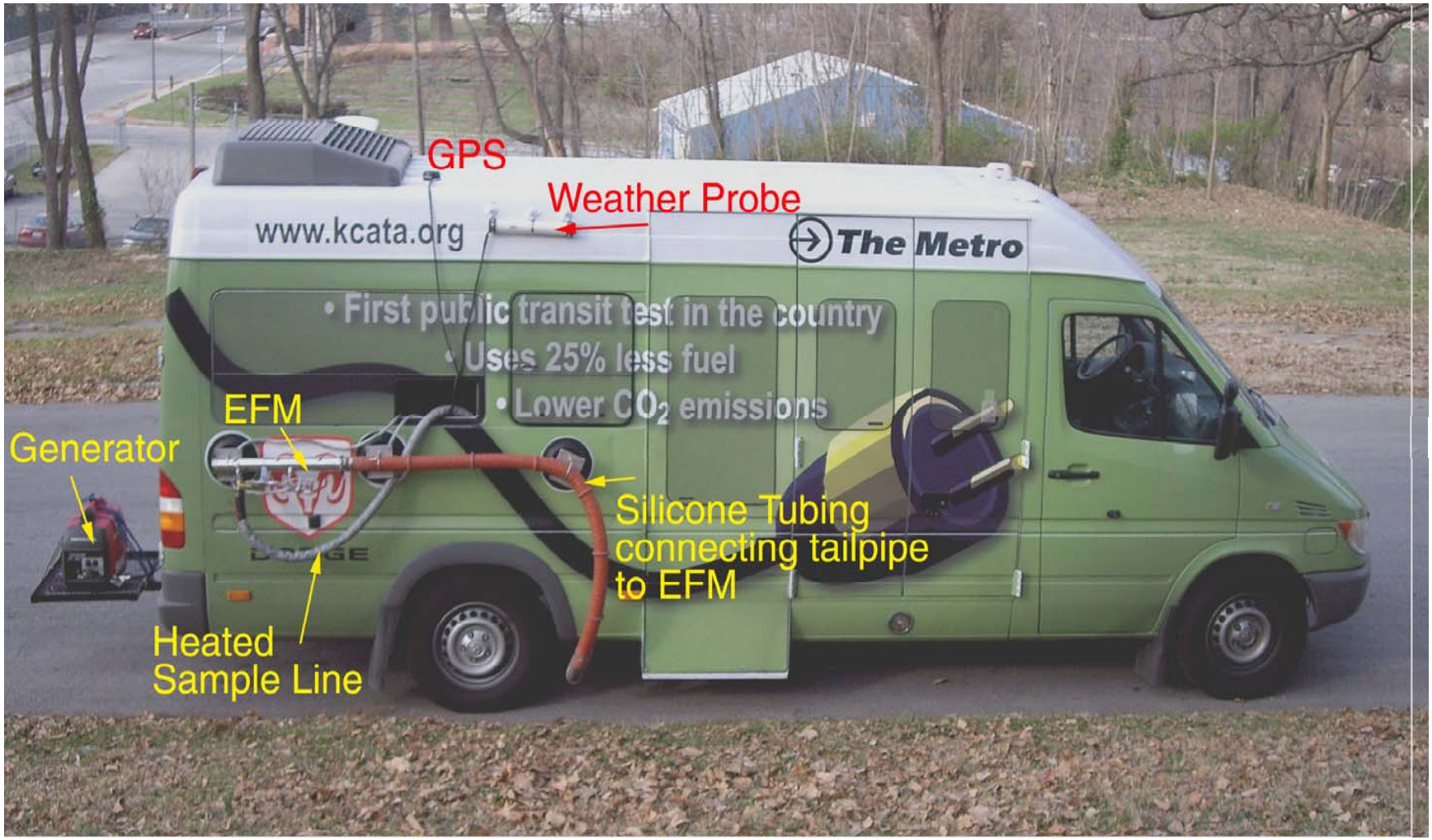

Figure 3.2: Semtech-DS installation on PHEV Sprinter.

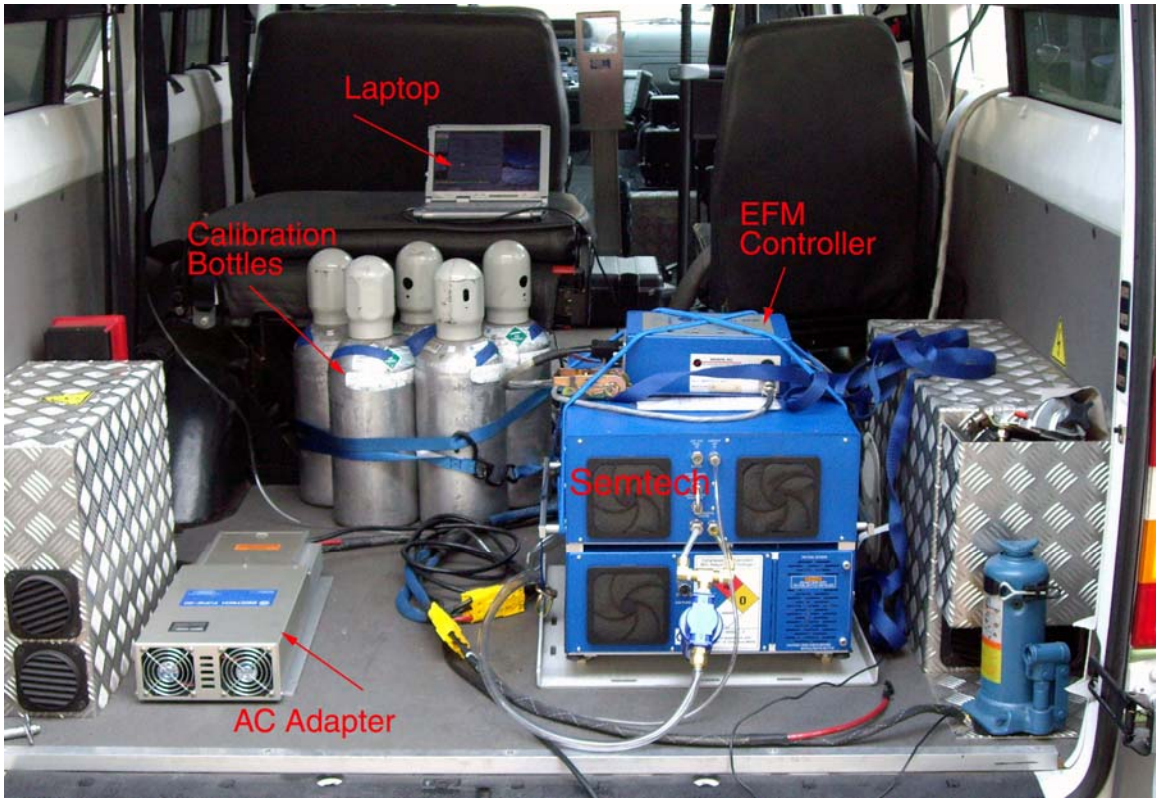

Figure 3.3: Semtech-DS set-up inside of PHEV Sprinter during data collection.

The Semtech-DS served as a mobile laboratory, measuring second-by-second concentrations of CO_2, CO, NO, NO_2, and total hydrocarbons in the sampled exhaust. The Semtech's internal design consisted of a series of modular, stand-alone analytical subsystems. Total hydrocarbons (THC or HC) were measured using a heated flame ionization detector (FID); carbon dioxide (CO_2) and carbon monoxide (CO) were measured using non-dispersive infrared (NDIR); and nitric oxide (NO) and nitrogen dioxide (NO_2) were measured using non-dispersive ultraviolet (NDUV) capabilities. In addition to the detected pollutants, an electrochemical sensor provided real-time oxygen (O_2) measurements.

The internal high-precision heated FID provided accurate total hydrocarbon measurements over a wide range of concentration classes. In order to avoid condensation, the exhaust sample was kept at 191ºC prior to entering the FID chamber. In order to maintain consistent flame operation, a bottle with a 40/60 blend of hydrogen/helium was self-contained within the Semtech housing.

Exhaust gas routed to the NDIR (for CO_2 and CO analysis) and NDUV (for NO and NO_2 analysis) was first dried using a coalescing filter followed by a thermoelectric chiller in order to avoid any hydrocarbon or water vapor contamination of the optics within each analyzer. Contact time between the condensed vapor and exhaust was minimized in order to avoid loss of the water-soluble NO_2 fraction within the exhaust sample. Table 3.2, below, provides the technical specifications and capabilities of each analyzer including measurement range, resolution, and accuracy.

Table 3.2: Measurement ranges and accuracies for the Semtech-DS analyzers (Sensors, 2006).

Pollutant	Method	Range	Resolution	Accuracy
CO_2	NDIR	0-20%	0.01%	±0.1% or ±3% of rdg
CO	NDIR	0-8%	10 ppm	50ppm or ±3% of rdg
		0-8%	0.00%	±3% or ±0.02% of rdg
THC	FID	0-100 ppm	0.1 ppm	2 ppm or ±1% of rdg
		1-1000ppm	1 ppm	±5 ppm or ±1% of rdg
		1-10,000ppm	1 ppm	±10 ppm or ±1% of rdg
NO	NDUV	0-2,500 ppm	1ppm	15 ppm or ±3% of rdg
NO_2	NDUV	0-500 ppm	1 ppm	10 ppm or ±3% of rdg

In order to ensure quality assurance of the emissions data, the Semtech was calibrated and audited at the beginning and end of each testing day. The span function checked and calibrated each analyzer to the high end of the sampling range while the audit function served as a mid-range check for each analyzer. Prior to all calibrations, the Semtech was zeroed in order to establish a baseline level zero for each of the analyzers. Since a reference zero was used during actual data collection, ambient air collected through a port placed on the far side of the PHEV away from the exhaust exit point was used for all zeroing with periodic checks using a zero-air bottle. For all calibration efforts, the PHEV was moved off-site from the KCATA bus yard. Normal bus yard

activities cause localized, higher ambient concentrations of emitted pollutants, so in order to minimize the potential of inadvertently skewing the day's data, all zeroing, calibration, and auditing functions were conducted remote from the bus yard. In order to minimize analyzer drift throughout the day, the Semtech required regular zeroing. The automatic zero option provided in the Semtech software was disabled in the interest of data continuity. In lieu of the auto-zero, the Semtech was manually zeroed at the end of each sample run (or route cycle) or every hour, whichever was shorter. The following table provides the bottle concentrations used for both the span (high calibration anchor) and audit (mid-range check) functions. The relative tolerance limits cited in Table 3.3 are the maximum variation allowed during the audit (analyzer verification) process for each pollutant in order for the Semtech to "pass" the audit procedure and be considered viable for on-road testing.

Table 3.3: Concentrations used for Span and Audit Semtech-DS functions.

Constituent	Span Gas Concentration	Audit Gas Concentration	Audit Relative Tolerance Limits
CO_2 (%)	11.90	6.05	0.182
CO (%)	0.12	0.02	0.0006
NO (ppm)	1502.0	302.0	9.06
NO_2 (ppm)	246.0	51.0	1.53
THC (ppmC)	201.70	50.44	1.513

The project was completed with minimal field personnel. A single field engineer performed daily system installation, calibration, on-road sampling, and end of day system shutdown. All on-road driving and sampling were preformed by the same driver/operator for the entire project, eliminating driver bias. The Semtech-DS proved extremely stable

and reliable, so a single person was able to complete all of the necessary fieldwork in addition to fulfilling driver/operator responsibilities.

3.1.3 Exhaust Flowrate Measurements

In order to provide a quantitative basis for calculating the PHEV's exhaust emissions as a function of mass emitted, an in-line exhaust flowmeter was required to obtain real-time exhaust flow rate measurements. Sized to the PHEV's combustion diesel engine, the Semtech-EFM (exhaust flowmeter) collected direct exhaust flow measurements for all sampling efforts.

Operating under the Bernoulli principle, the exhaust flow meter (EFM) was equipped with four differential pressure transducers, each designed for different fractions of the total flow range. In order to eliminate drift, the EFM regularly pulled individual transducers off-line for auto-zeroing. By only removing one transducer at a time for zeroing, the auto-zero was able to function without resulting in any data loss during the testing period. The EFM design also eliminated range and accuracy problems that usually arise due to pressure pulsations from the exhaust and pressure line fouling (Sensors, 2006). A schematic of the EFM tube assembly cross section is provided in Figure 3.4, and the EFM's PHEV Sprinter installation is highlighted in Figure 3.5. The 8L/min exhaust sample (grey sample line) was pulled directly from the downstream end of the EFM.

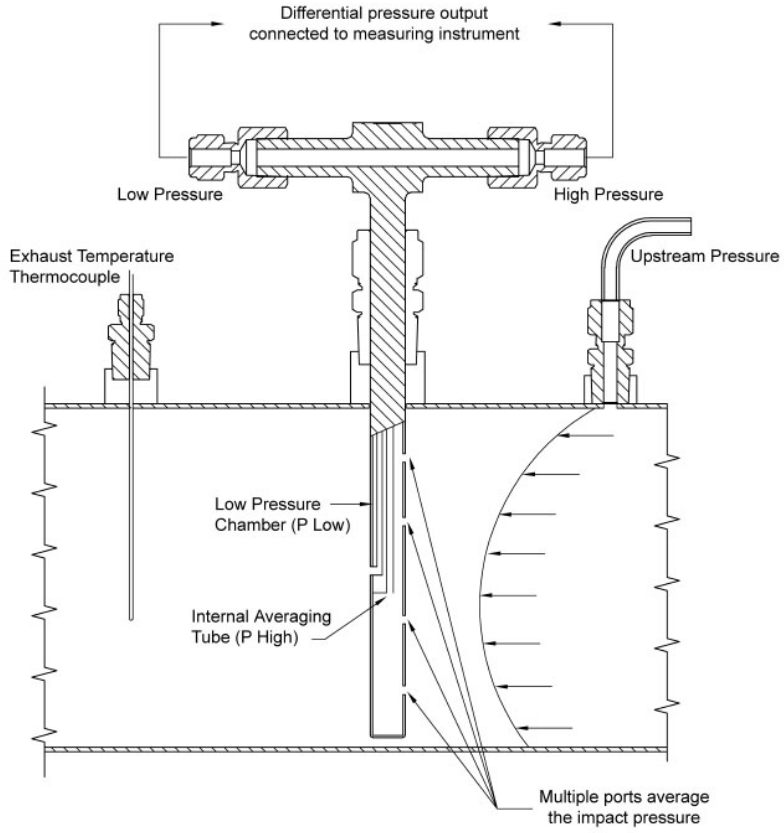

Figure 3.4: Semtech-EFM tube assembly cross-section (Sensors, EFM User's Manual, 2006).

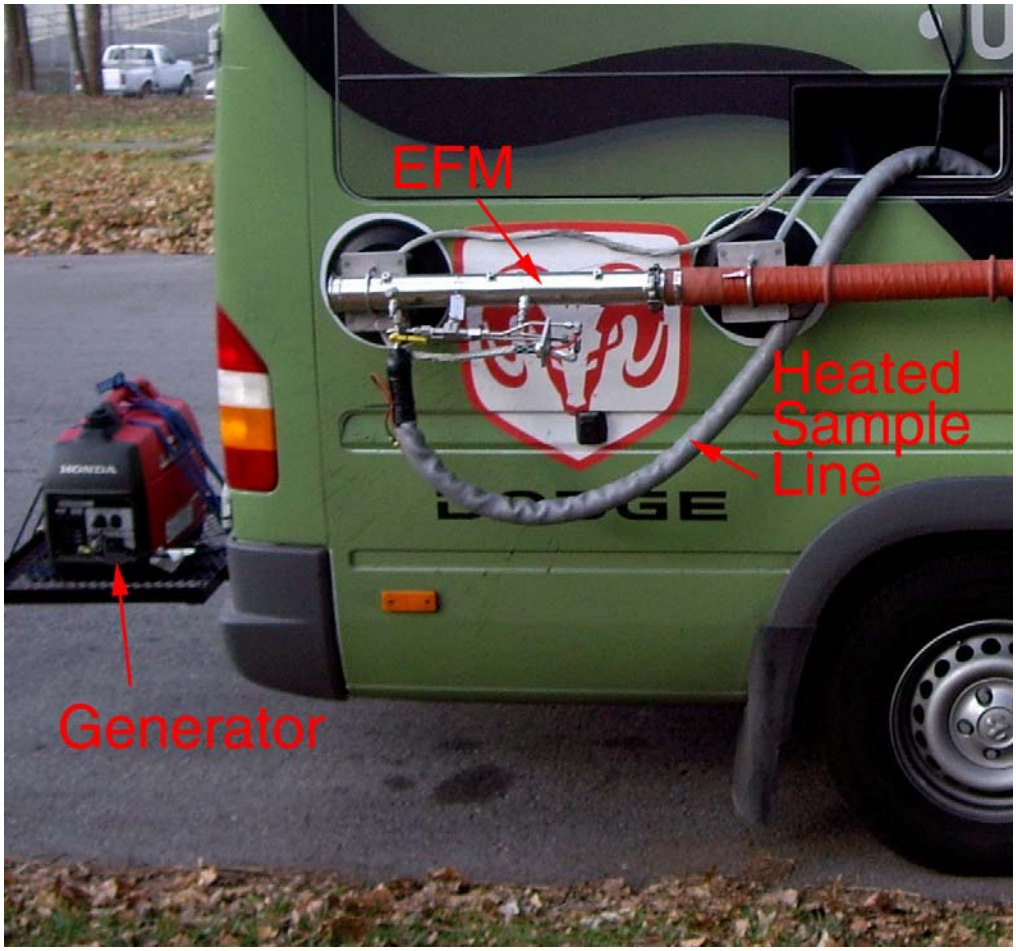

Figure 3.5: Semtech-EFM installation on the PHEV Sprinter.

3.2 Route Determination

3.2.1 Kansas City Area Transit Authority (KCATA) Operations

The Kansas City PHEV's ultimate purpose was to meet the Phase I proof-of-concept goals centered on transit operation. Since the Kansas City PHEV was configured as a paratransit vehicle, the proof-of-concept study was designed within the confines of the Kansas City Area Transit Authority's (KCATA) operations. Because of this, it was important to describe the KCATA's original intent for the Sprinter PHEV in order to articulate the rationale used when designing and Kansas City PHEV on-road emissions study.

Kansas City Area Transportation Authority (KCATA) is a transit bus operator in Kansas City, MO serving the Kansas City Metro and surrounding areas. At the time of sampling, KCATA operated 69 regular routes with an additional 7 Metroflex routes, reporting just over 51,000 in annual ridership (based on May 2007 data). KCATA was recruited as a project member in order to test the proof-of-concept PHEV Sprinter in normal paratransit operation.

Originally, the PHEV Sprinter was placed into KCATA's Metroflex service. In order to meet the needs of Metroflex operation, Braun provided the vehicle conversion necessary to accommodate the demands required of public transit buses. The conversion included adding extra seating to accommodate additional passengers, installing a hydraulic wheelchair lift, an electronic side door, KCATA radio system, and a basic, non-electronic fare box. The total conversion resulted in a total vehicle curb weight of 7620lbs with a remaining payload of 930lbs.

KCATA's Metroflex program is, by name, a "flex-service" that operates as an on-demand bus service. Due to the flexible nature of the program, KCATA's paratransit service does not adhere to a fixed-route or fixed-schedule operation, and, instead, acts more like a taxicab service that is constrained to set geographic boundaries. Large idle times are an inherent characteristic of the on-demand scheduling; therefore the PHEV's configuration did not prove suitable for the Metroflex service. Extensive time sitting at idle with auxiliary systems running depleted the PHEV's battery capacity to deleterious levels. Without the ability to regenerate electric capacity through regular driving, the Metroflex application did not permit the PHEV to operate according to its intended design.

In addition to the Metroflex's incompatibility with the plug-in hybrid concept, the service did not provide a suitable platform for conducting emissions testing. In order to most efficiently develop a dataset capable of characterizing the PHEV Sprinter's emissions, it was necessary to find realistic routes with varying drive and road conditions that could be effectively and easily reproduced. Since the Metroflex's daily (and hourly) drive requirements varied, the Metroflex routes were not selected for emissions testing simulations. Additional transit service options were discussed with KCATA officials during a July 2007 meeting, and it was decided that routes serviced by smaller transit buses with lower ridership numbers were the only suitable alternatives for PHEV implementation.

3.2.2 Route Selection Criteria

Following the decision made during the July 2007 KCATA meeting, several KCATA routes were selected to be the basis of all emission testing efforts. In order to qualify as a suitable testing platform, the selected transit routes had to meet the following criteria:

- **Actual KCATA serviced routes:** In order to best simulate transit operation, it was essential that all testing be conducted while driving actual transit routes. This also afforded the ability to shadow transit buses during actual operation;

- **Provide varying roadway scenarios:** Since one of the primary goals of the emissions demonstration study was to provide a comprehensive dataset capable of describing the PHEV's operation under a variety of different road conditions, it was important to select routes that possessed various driving scenarios, such as downtown driving near the urban core, suburban driving conditions, and highway operation;

- **Short Length:** In order to conduct the emissions evaluation study as systematically as possible, it was necessary to select routes that could be reproduced in a reasonable amount of time. Routes covering multiple geographic areas within the Kansas City Metro and outlying areas were

considered too long to allow sufficient reproducibility within the study's timeframe;

- **Near the KCATA Bus Yard:** Semtech installation and PHEV charging both occurred at the KCATA site. In order to evaluate the PHEV under a variety of different battery charge states, selected routes needed to be close enough to the KCATA home base so that the sampling site could be reached while the PHEV's state of charge was near its starting high. It was also important to remain within 10-15miles of KCATA during sampling efforts in order to address any mid-sampling service issues that arose with the PHEV Sprinter or the Semtech system;

- **Safety:** All routes were sampled in two different manners: while shadowing a KCATA bus and while driving solo (or not following a transit bus). Routes where stops were scheduled in high traffic or excessively congested areas were eliminated. Consideration was given to the PHEV's, pedestrians', and other drivers' safety when selecting sampling routes.

3.2.3 Overview of Selected Sample Routes

Four different KCATA routes were selected for emissions testing. Two of the selected routes had alternate route and stop configurations resulting in six unique routes with some inter-route roadway repetition between the different routes. In order to

evaluate the PHEV's highway operation, a 7th route outside of the KCATA serviced routes was selected to investigate the PHEV Sprinter's behavior at higher speeds. On-road operating differences were observed between transit service and normal, civilian driving during preliminary testing. Therefore, where feasible, the routes were driven in two different manners: first by shadowing or following a KCATA transit bus while in regular service, and secondly, the routes were driven solo (without following a transit bus, stopping at official bus stops, or adhering to a set bus schedule) resulting in a more conservative drive cycle representative of a normal driving scenario such as might be encountered by a standard delivery vehicle. Cadle, et al. (2006) found no statistically significant difference in the velocity and acceleration profiles between target and chase vehicles. Therefore, the act of shadowing a transit bus was accepted as a suitable simulation of actual transit operation. This dual-mode sampling method was selected in order to provide a more comprehensive view of the PHEV Sprinter's on-road operation and emissions. For the remainder of the project, the two drive scenarios will be referred to as "follow" (shadowing or following a KCATA bus) and "solo" (driving the route alone, without simulating transit operation). The selected routes are summarized in table 3.4, and all routes are mapped in Figure 3.6.

Figure 3.6: Comprehensive map with all sampled routes.

Table 3.4: Summary of the selected routes.

Route #	Description	Nominal Roundtrip Distance (mi)	Average Velocity (mi/hr)
109 Wnr	9th Street Route following the Winner Loop	7.8	16.2
109 Wnctsr	9th Street Route following the 12th/Winchester Loop	9.1	16.6
110	44th and Brooklyn Route	11.8	14.1
123	23rd Street Route	11.9	12.3
12 T/C	12th Street Route following the Truman/Crystal Loop	10.9	14.3
12 WB	12th Street Route following the West Bottoms Loop	13.4	14.0
Hwy	Derived Highway Route	13.2	35.6

All of the selected routes, aside from the 123 and Highway routes, possessed both an urban driving component and a section of suburban driving conditions. Urban driving refers to sections of the routes near Kansas City's urban core where roadways are dictated by slower allowed speed limits (less than 25mph) and increased traffic congestion. On Figure 3.6, the geographic area comprising the urban roadways for each route is marked (red circle) at the northwest side of the map bounded on the east and west by Highways 71 and I-35, respectively. Unless otherwise stated, the remainder of the sampled routes consisted primarily of suburban and transition to suburban driving (35-40mph).

Official schedules detailing the route's stops and layover points are provided in Appendix B for the routes where a transit bus was shadowed (109-both loops, 110, and 123).

3.2.4 Ninth Street (109)

The Ninth Street (109) route consisted of two different sub-routes representing different turn-around stops within the suburban portion of the route. The urban part of the route (ending at 11th and Grand) remained consistent (in both scheduled stops and

roadways traveled) regardless of which loop (Winner Road or Winchester) was being traveled. The following map provides a more close up view of the 109 Route with the Winner Loop turn-around highlighted in light green (A) and the Winchester Loop turn-around (at 12th and Winchester) highlighted in darker green (B).

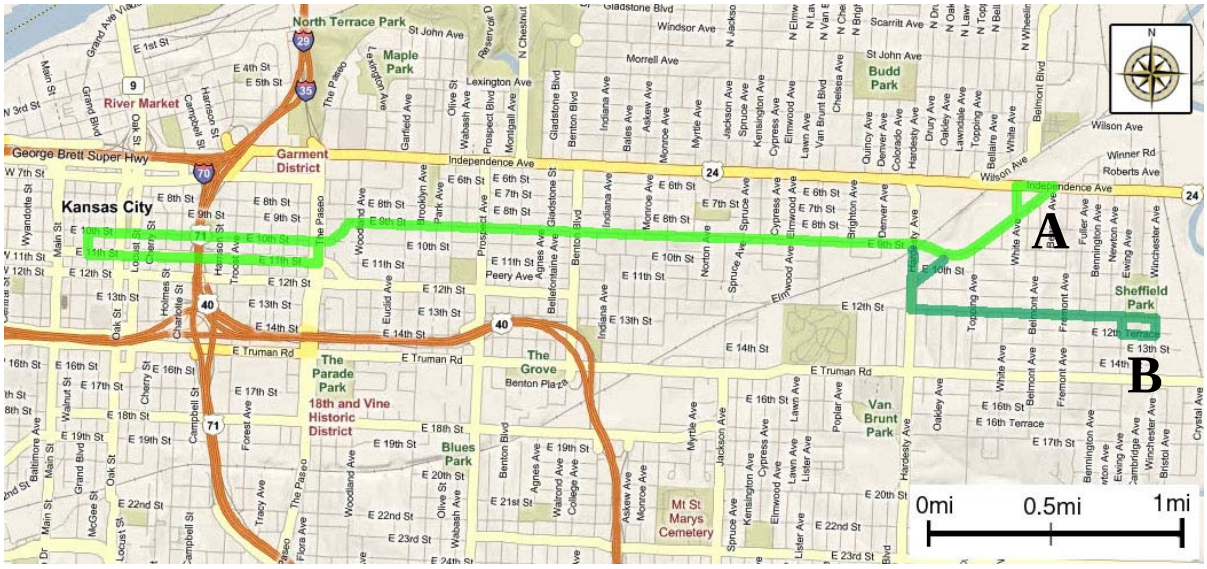

Figure 3.7: Ninth Street route with both turn-around options.

The majority of the 109 roadways were defined as suburban or transition to suburban with nominal speed limits of 35mph. The roadways located at the western edge of the route (where the route passes Highway 71 and west to Grand Street), represent urban driving conditions since this is the point where the route entered the higher traffic density roadways and slower posted speed limits (20mph) as mandated by inner-city driving near Kansas City's urban core.

Since most of the routes were selected from a limited geographic area, the overall topography was similar for all selected routes. However, road grade has been found to

have a significant impact on vehicle emissions. Krishnamurthy and Gautam (2006) found that, when sizeable, local road grade did have a statistically significant impact on vehicle emissions. Similarly, Frey, et al. (2008) determined that while road grade did not have a significant impact on vehicle emissions at the meso-scale level of analysis, micro-scale assessments of vehicle emissions did show statistically significant responses to local road grades. Therefore, in order to truly assess the PHEV's operating characteristics as a function of on-road behavior, it is important to consider the local topography for each roadway section. The topographical data for both sub-routes of the 109 (Winner Loop and Winchester Loop) are provided in Figures 9 and 10, below, according to distance traveled. The topographic chart for the Winner Loop route begins at the stop at the Winner Loop Turnaround (point A on Figure 8), continues to the urban roadways and returns to the Winner Loop Turnaround. Similarly, the topographic chart for the 109 Winchester Loop route begins at the Winchester Loop stop at 12th Street and Winchester (point B), proceeds to the urban section at Grand Street, and returns to the Winchester Loop Stop at 12th and Winchester.

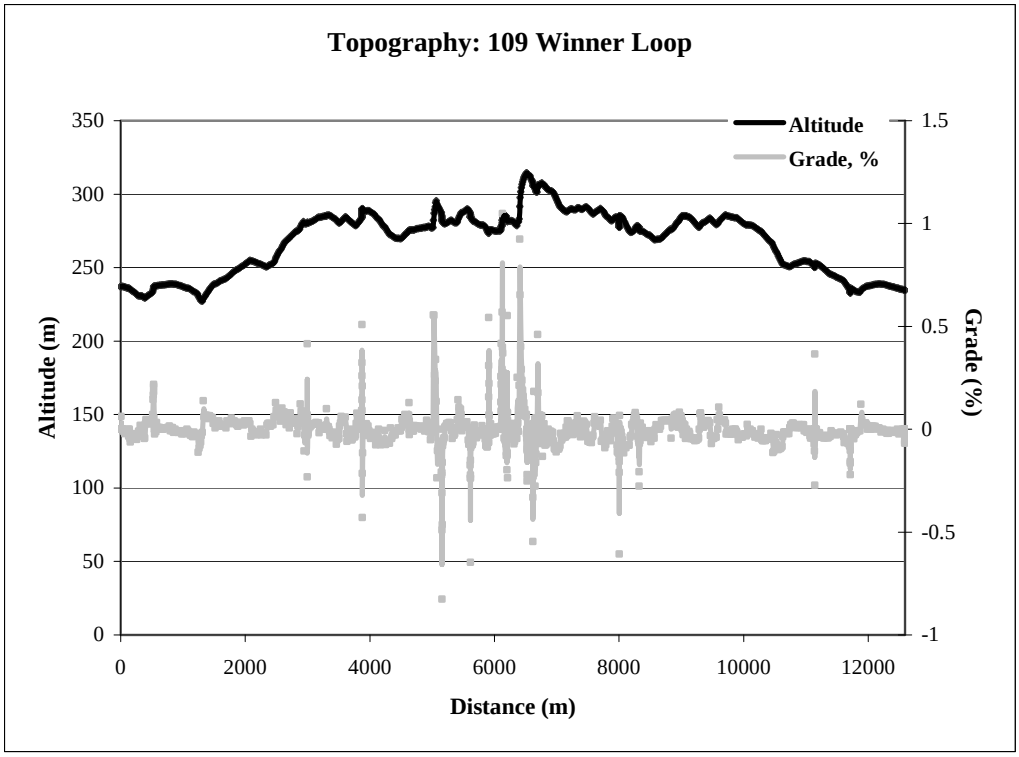

Figure 3.8: Route 109 Winner Loop topography.

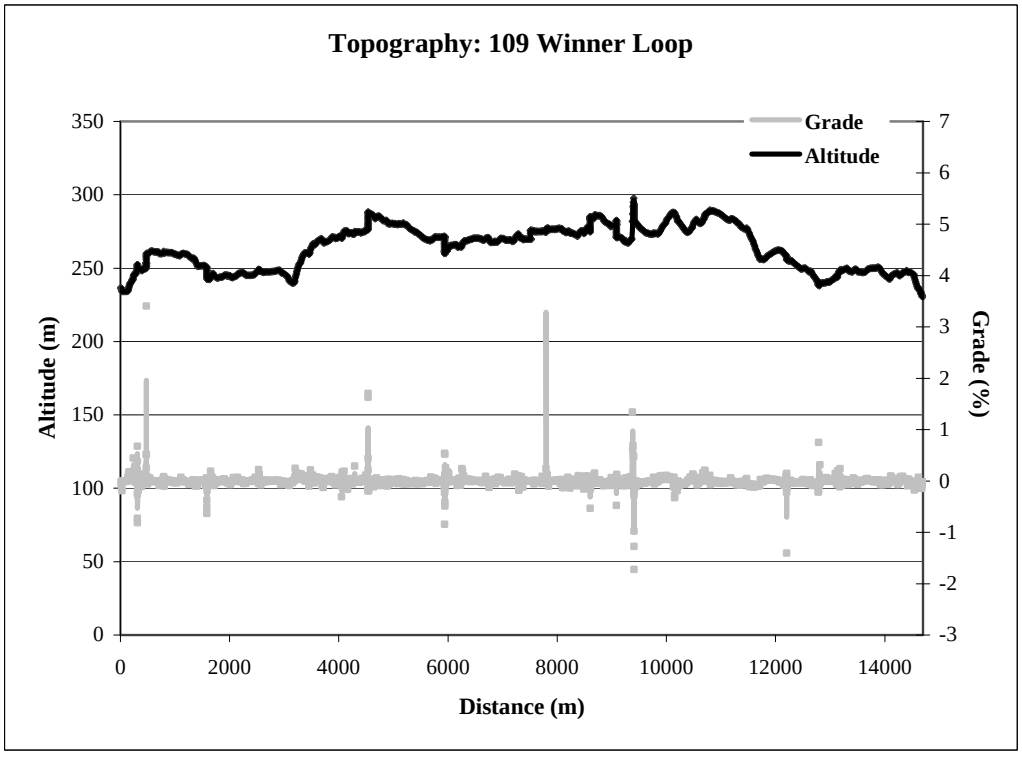

Figure 3.9: Route 109 Winchester Loop topography.

3.2.5 44th/Brooklyn (110)

Like the 109, the 110 Route consisted of primarily suburban roadways with speed limits of 35mph. The route transitioned to urban roadways at the northwestern section where it entered the urban core. At this point, the speed limits dropped to 20mph, the roadways became increasingly congested, and travel became slower and more stop-and-go in nature.

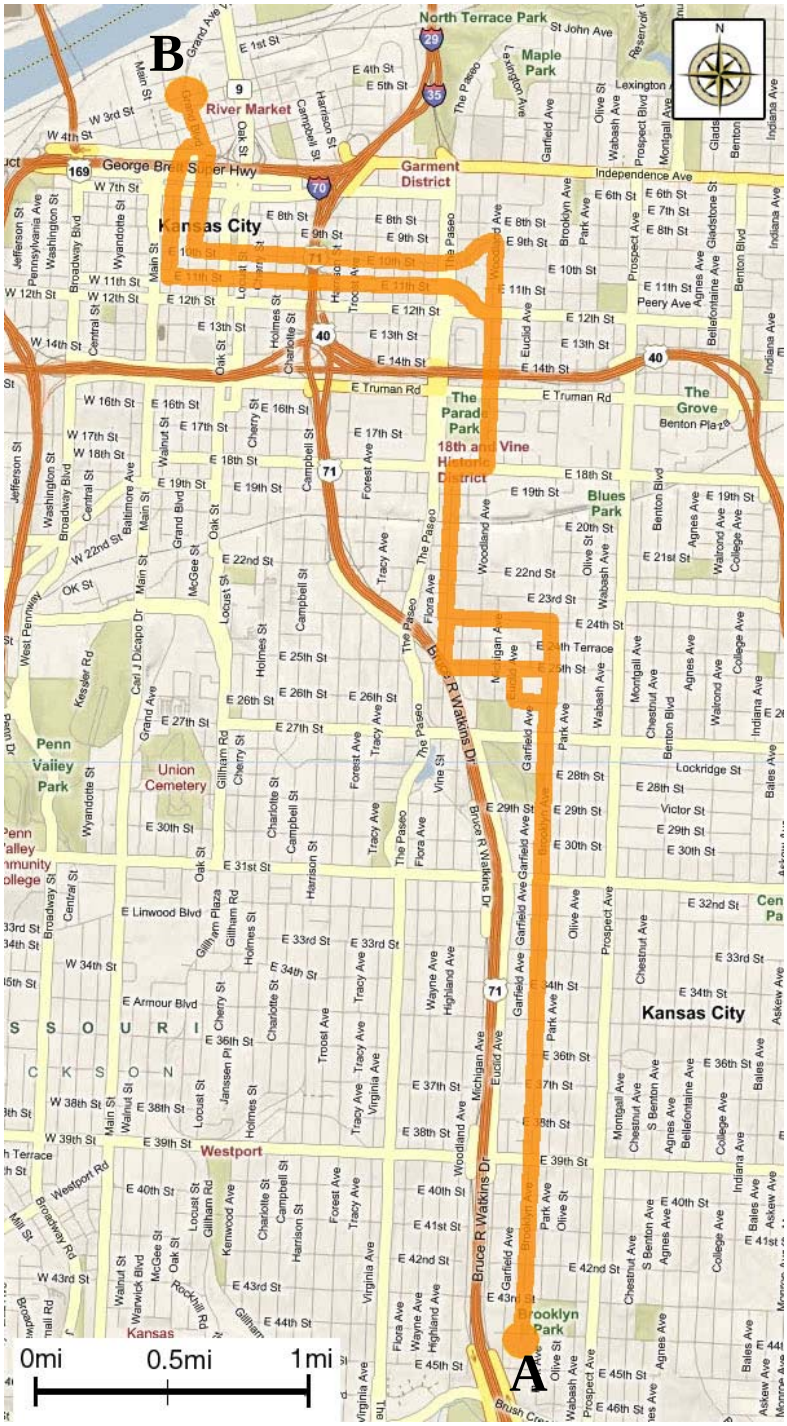

Figure 3.10: Map of 110: 44th and Brooklyn route.

The topographic chart (Figure 12) for the 110: 44th and Brooklyn route originates at the 44th/Brooklyn stop (point A), continues north to the turn-around at the urban center (point B), and then returns to 44th/Brooklyn.

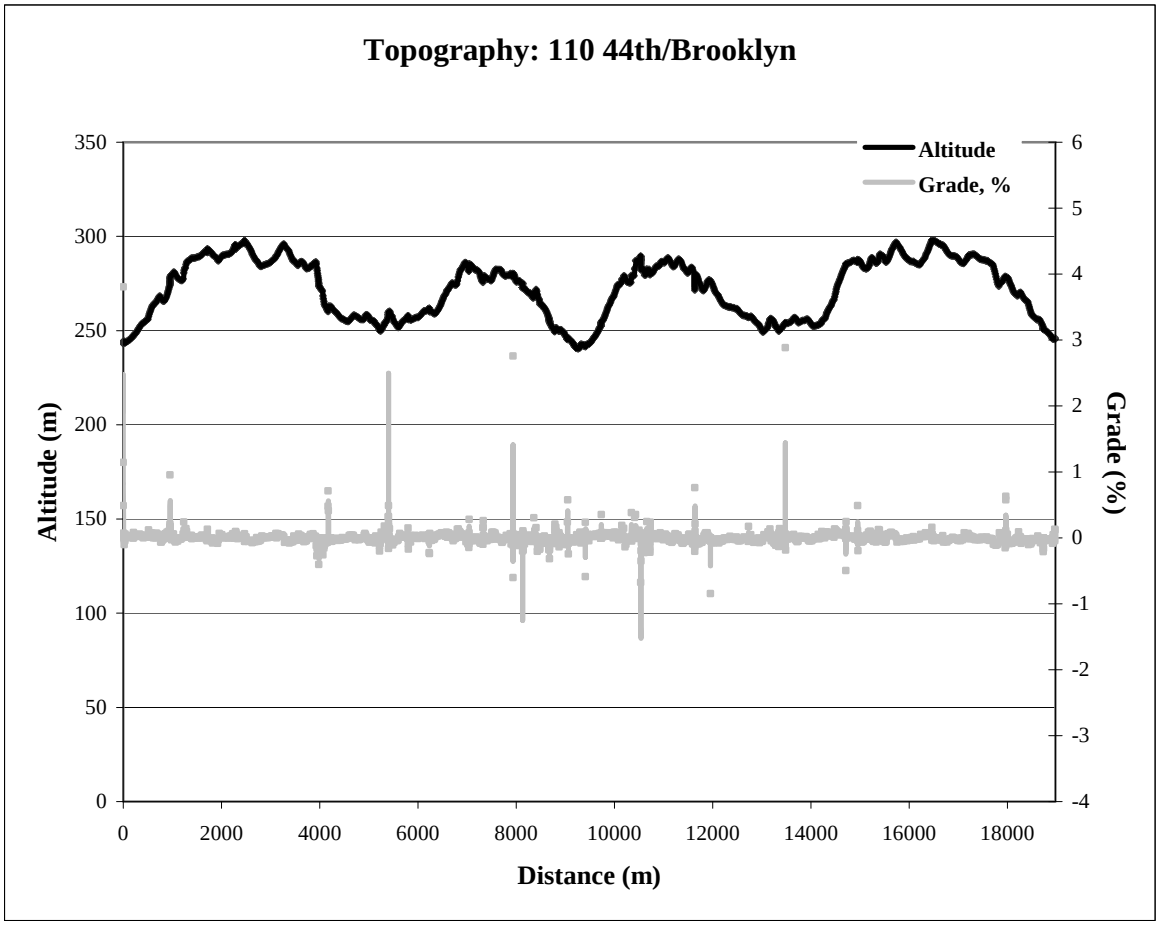

Figure 3.11: Topography for the 110-44th and Brooklyn route.

3.2.6 23rd Street (123)

The 123: 23rd Street Route included varying roadway scenarios, but did not enter the urban core of Kansas City's downtown area. Instead, this route included more transition between urban to suburban roadways with posted speed limits of 35mph

throughout its entirety. The final result was a route with a slightly lower, but more consistent average velocity across its total traveled distance. The topographic chart for this route begins at the Kansas City Union Station (point A) and continues to more remote suburbs at the turn-around stop at the Blue Valley Park (point B), then returns to the Union Station stop.

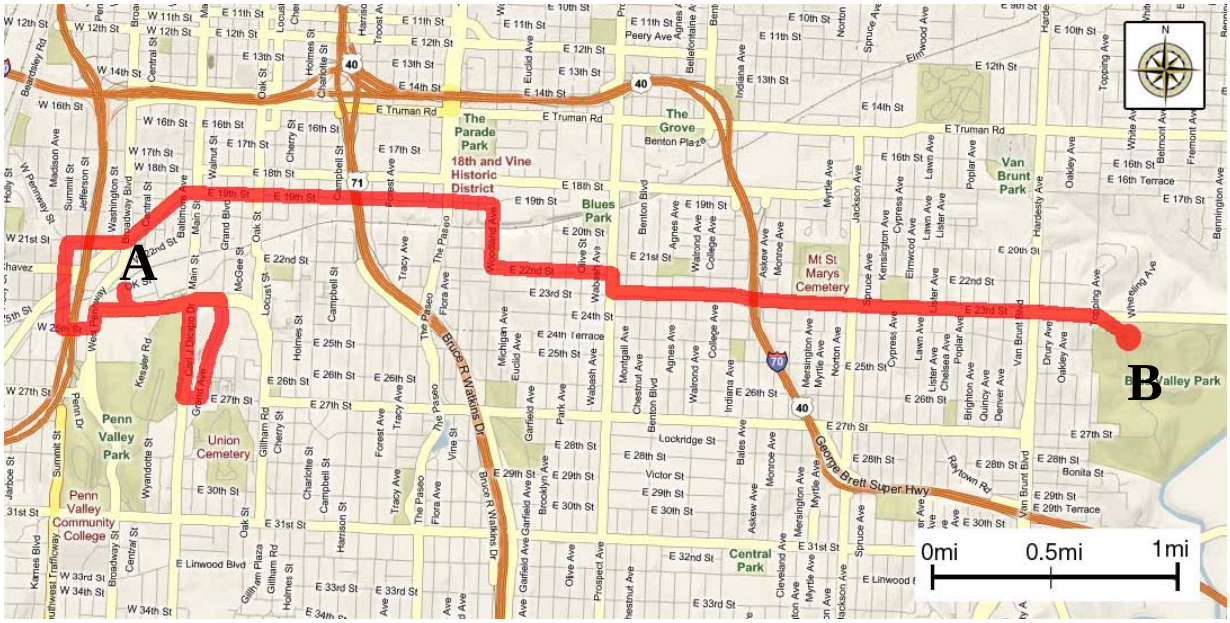

Figure 3.12: 123: 23rd Street route map.

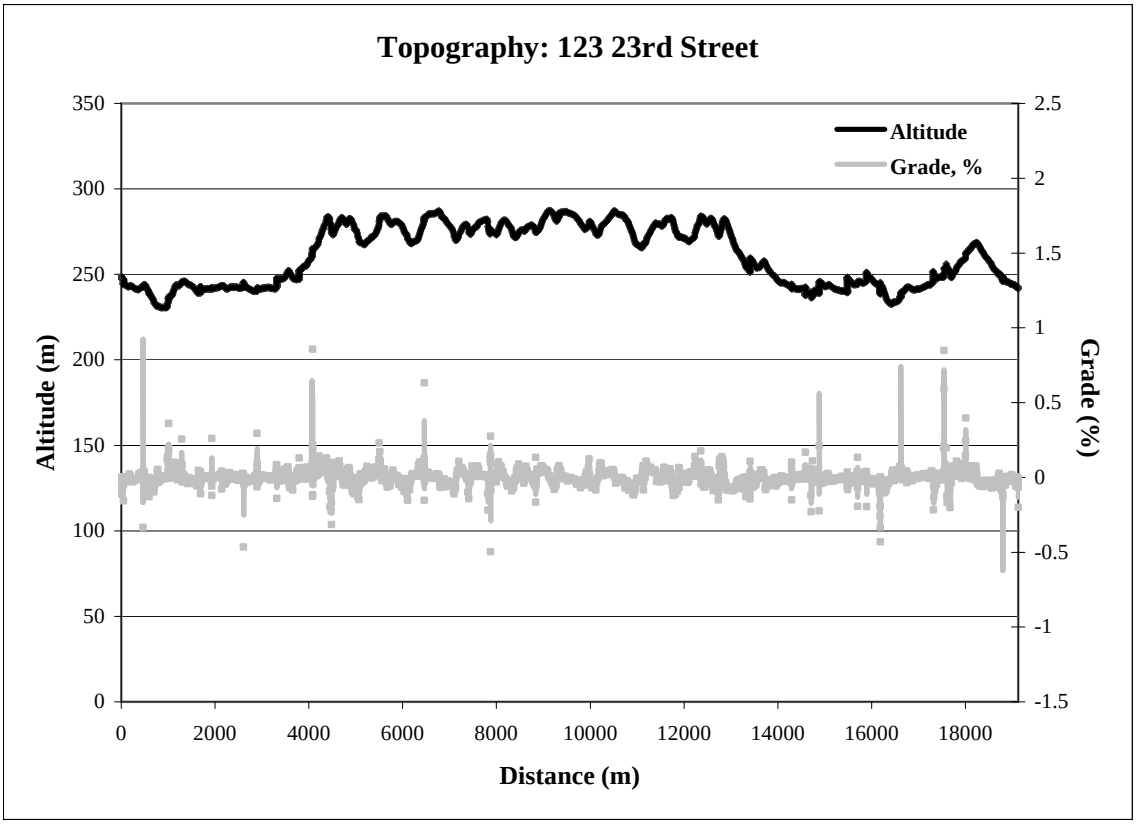

Figure 3.13: Route 123: 23rd Street topography and road grades.

3.2.7 12th Street (12)

Like the 109 Route, the 12th Street Route consisted of two different sub-routes (Truman/Crystal Loop and the West Bottoms Loop). On-board emissions data were collected for each sub-route, but sampling the West Bottoms loop was limited due to technical difficulties and PHEV service issues that arose due to excessive roadway vibration while crossing the West Bottoms Bridge. Because of this, only data from the 12th Street Truman/Crystal loop was used in the following discussions. Both 12th Street loops (Truman Crystal and West Bottoms) included an urban component as well as suburban driving conditions. The 12th Street route was generally a busier, more

congested route, serving a higher number of riders than the other selected routes. Consequently, small transit buses only drove the 12th Street routes on the Sunday schedules due to large ridership demands during the weekdays. Weather considerations limited the number of viable Sundays available for sampling. The limited access to the Sunday schedule coupled with recurring PHEV service issues during that time made shadowing the 12th Street transit bus unfeasible. Because of this, the only data available from the 12th Street routes were the result of the PHEV driving the route solo as a civilian driver. Despite this upset, over 215 miles of emissions data were collected on 12th Street. The following figures provide a more detailed map of the 12th Street Truman/Crystal route as well as the topography and road grade according to distance.

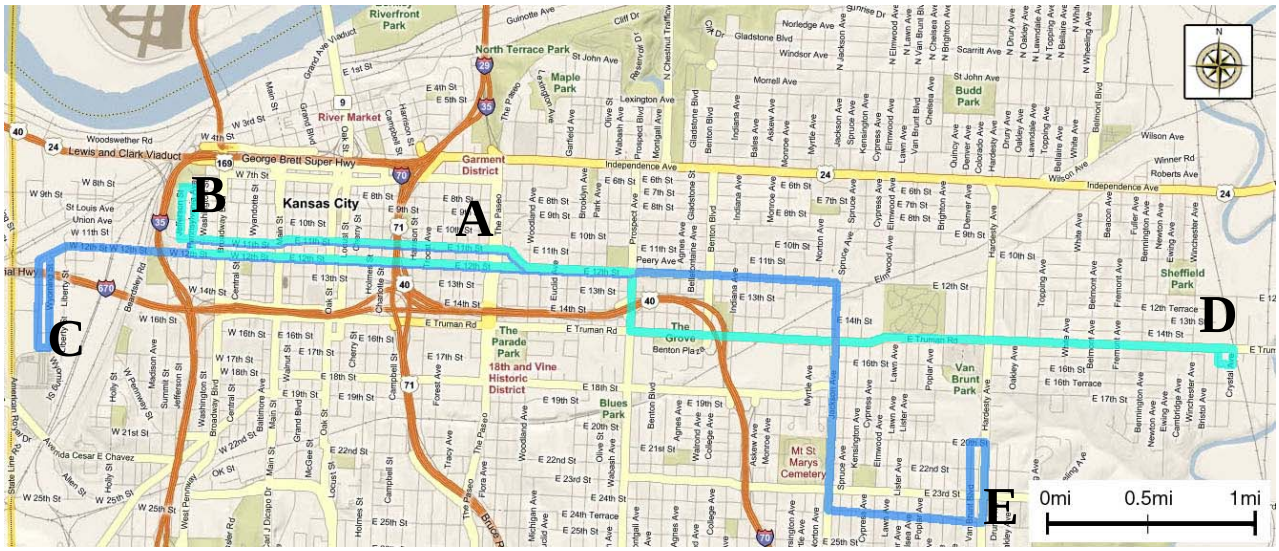

Figure 3.14: 12th Street (Truman/Crystal and West Bottoms Loops) route map.

The topographic chart for the Truman/Crystal Loop begins at point A and proceeds west towards the Kansas City downtown area. The urban turn-around loop for was located at point B, at which point the route proceeded east to point C, the

Truman/Crystal turn around loop, before returning back to point A resulting in a complete run. The followed route for the Truman/Crystal topographic chart is point A – point B – point C – point A.

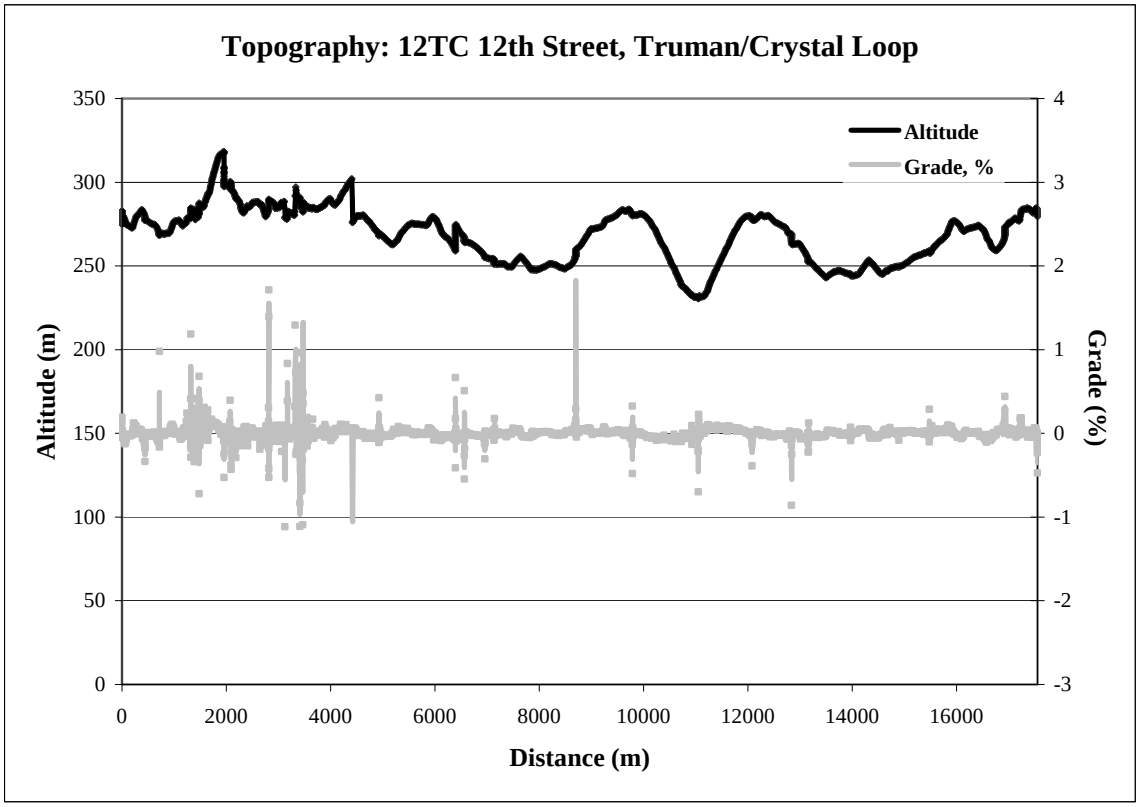

Figure 3.15: 12th Street, Truman/Crystal Loop topographic and grade chart.

3.2.8 Highway Simulation (Hwy)

None of the KCATA routes that met the route criteria listed previously possessed a suitable highway-driving component. In order to investigate the PHEV Sprinter's highway operation, a route capable of demonstrating the PHEV's function on higher velocity roadways (i.e. highways) was developed. It was important that the selected route meet all of the route selection criteria established and cited earlier. As a result of this,

Highway 71 was selected due to its proximity to KCATA, easy and safe access, 55mph maximum speed, and 45mph section with traffic lights, resulting in higher speed stop-and-go data not available from the other routes. From the initial highway access point at Paseo and Highway 71 southbound (point A), the highway maintained a 55mph constant speed limit until just north of 55th street, where the speed limit reduced to 45mph and traffic lights began regulating traffic flow until the turn-around point at 75th Street (point B). The topographic chart for the developed Highway route is provided on the following pages. The chart starts at the route's origination at point A and continues to the 75th Street Exit turn-around (point B) before returning to point A.

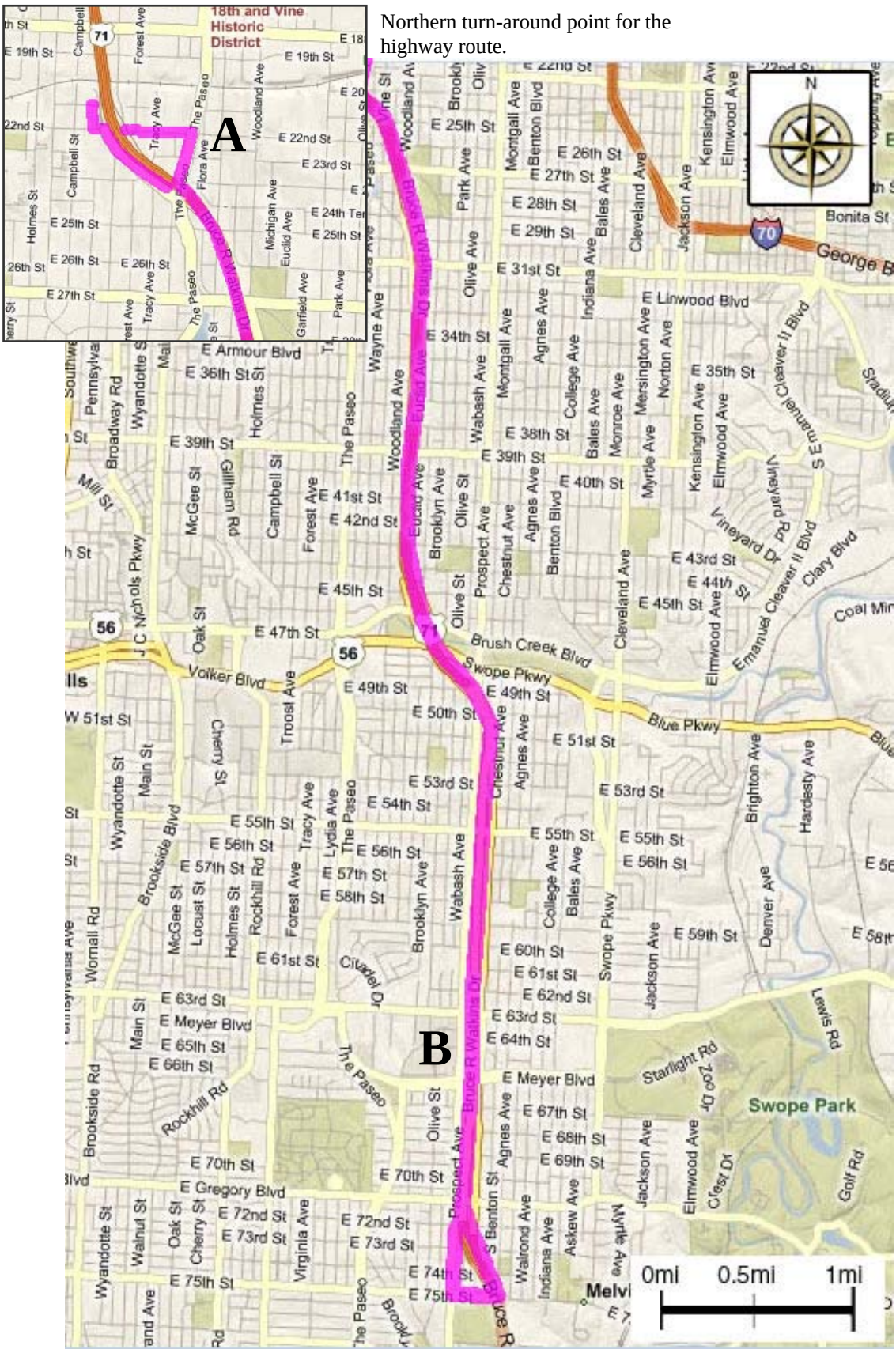

Figure 3.16: Map of the developed highway route.

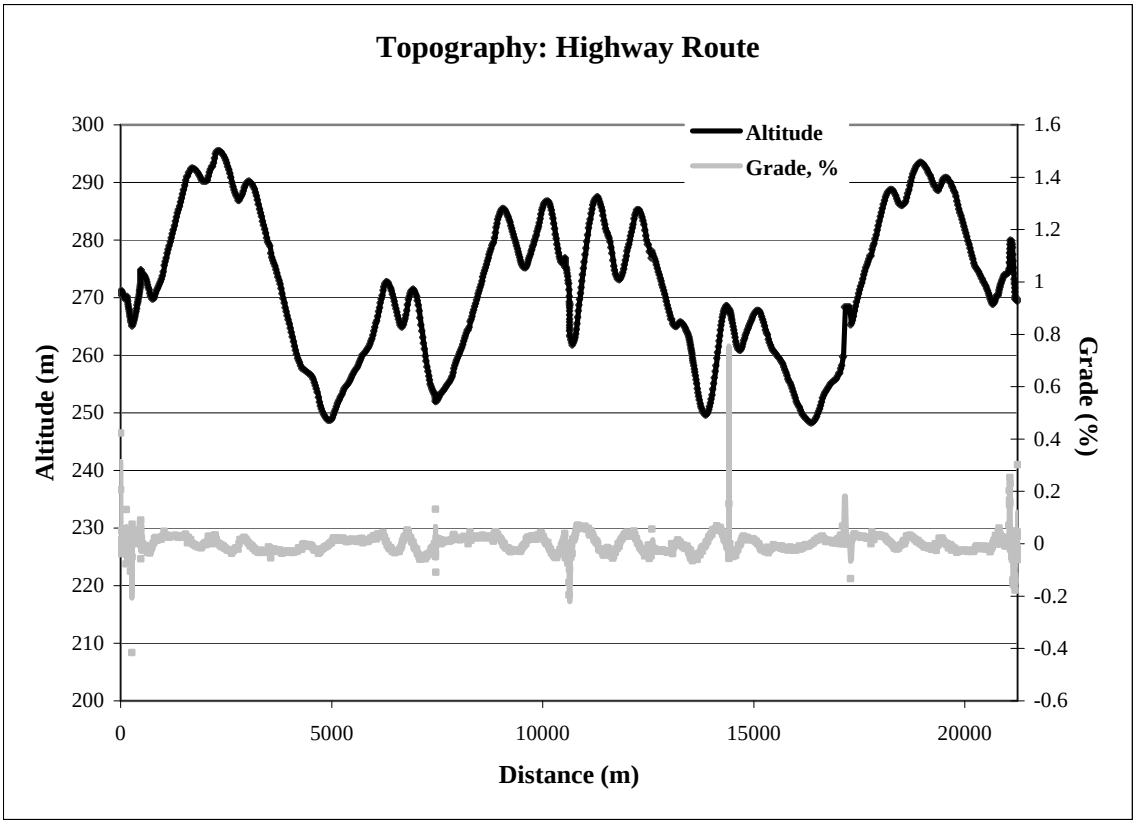

Figure 3.17: Topographic data for the Highway (HWY) route.

3.3 Data Processing

3.3.1 Time Alignment

In order to merge the DLM data with the Semtech-collected emissions data, the individual data files for each sample run had to be matched and then time-aligned to compensate for different start times in file logging. PHEV ignition start initiated the DLM data logging, whereas, the Semtech-DS did not begin recording data until prompted by the operator at the computer interface. It was not uncommon for significant time lags to occur between these two events at the start of each sample run. Additionally, exhaust transport delays between the diesel combustion engine (dICE) and the point of exhaust analysis within the Semtech system had to be accounted for. Data alignment correcting for different point-of-time references resulted in a dataset where each emissions event was aligned with and represented the exact, corresponding engine ignition event. As further quality assurance, internal time alignment checks were made on the Semtech data in order to verify the accuracy of specified transport delays occurring throughout the actual emissions monitoring system (from point of exhaust collection at the EFM to analysis at each detector).

Because the DLM data time-stamps did not directly correspond to the time-stamps in the Semtech data it was necessary to use a variable common to each dataset in order to make certain that the correct DLM data file was matched to each Semtech data file. The GPS ground speed data were matched with the DLM vehicle speed data for each test file over the entire test duration. This check was the only direct comparison that could be made between the two data files for each run. With the files confidently matched, the DLM variables for the diesel combustion engine speed (revolutions per

minute) and torque were aligned with the Semtech raw carbon dioxide concentration. Due to the transient nature of the datasets, it was important to eliminate the lag due to transport delays between the engine block and monitoring equipment to within a less than a second. When aligning data, the leading edges of the peaks between the two variables were matched. The following figures graphically detail the time-alignment process.

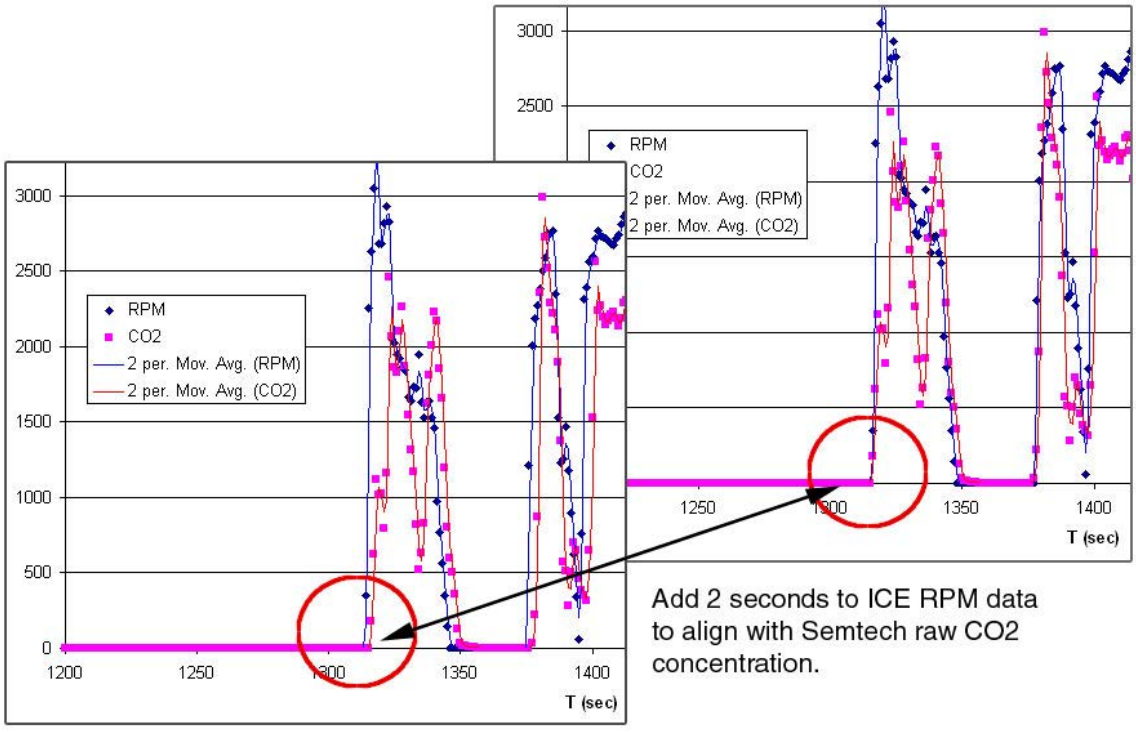

Figure 3.18: Time alignment techniques.

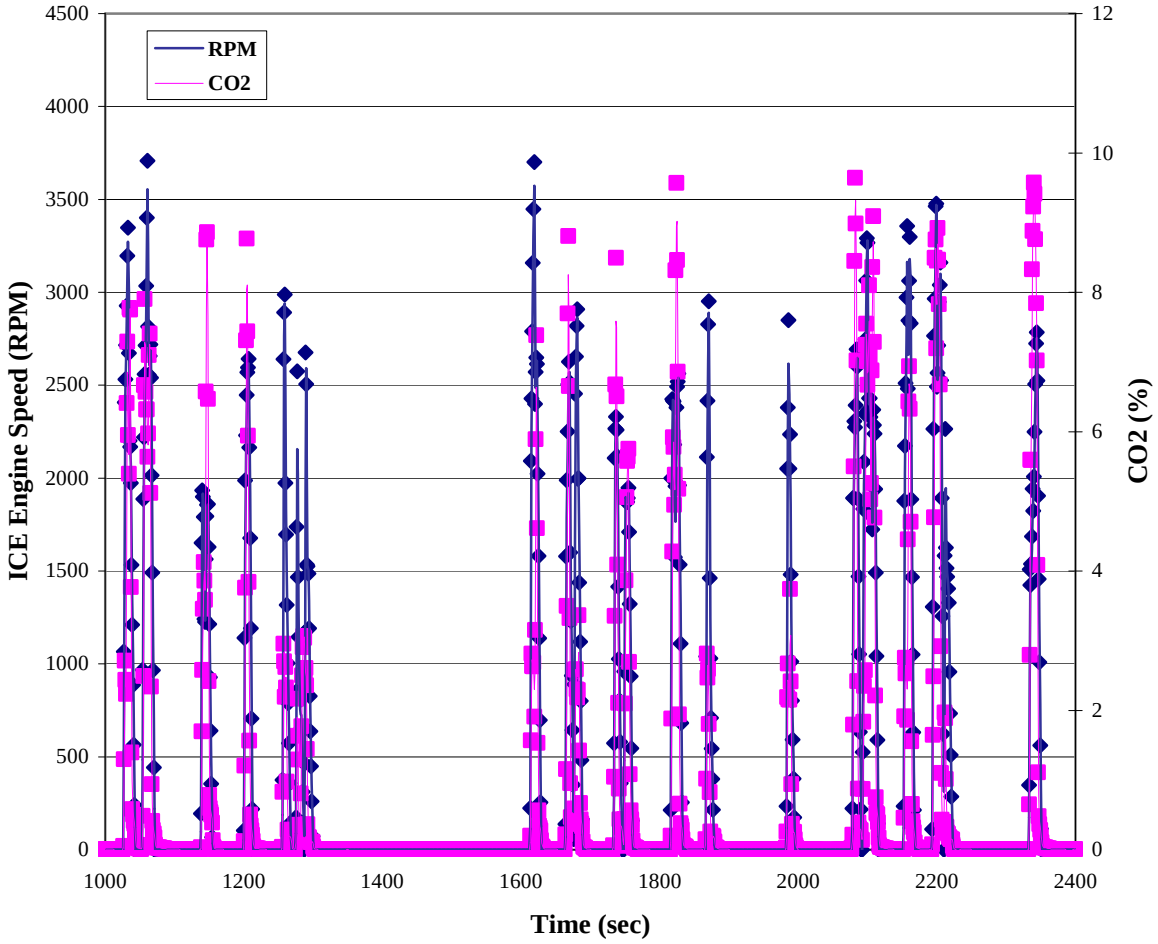

Figure 3.19: DLM and Semtech datasets aligned according to dICE revolutions/minute and raw CO_2 concentration (%).

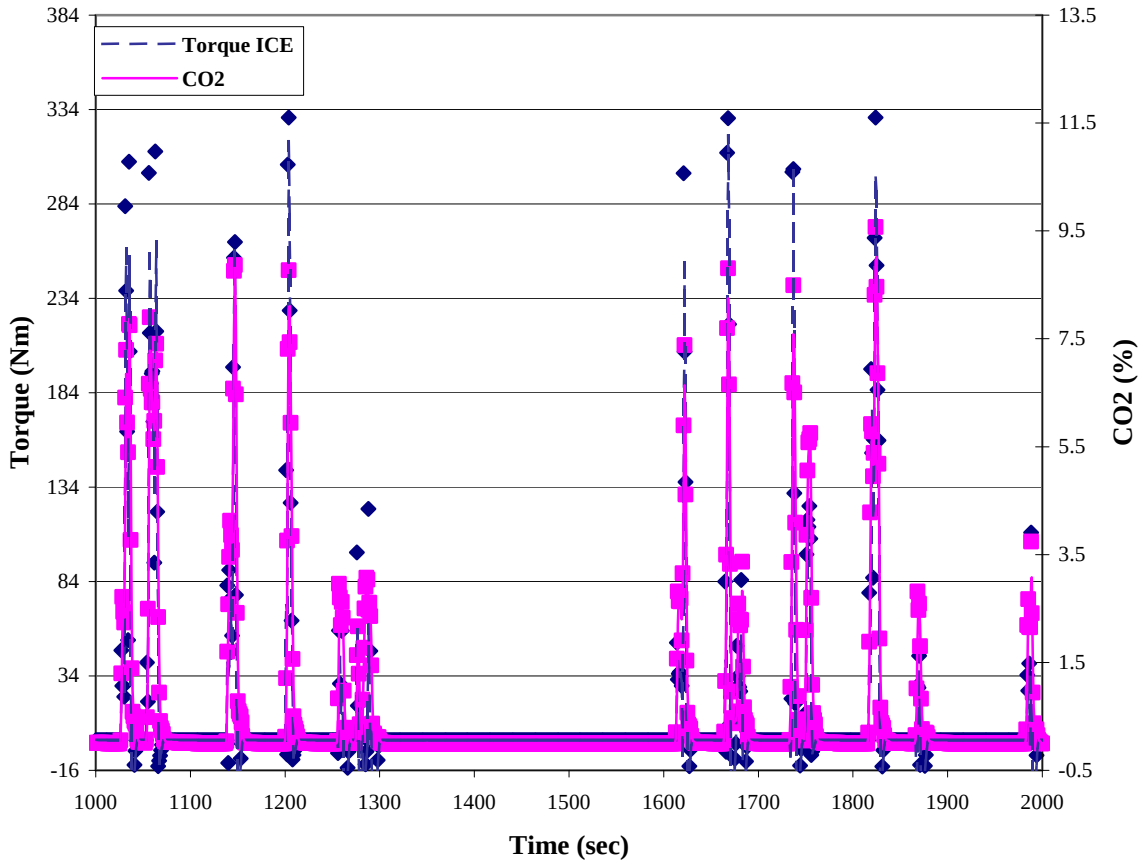

Figure 3.20: DLM and Semtech datasets aligned according to ICE Torque (Nm) and raw CO_2 concentration (%).

Semtech internal transport delays were verified by aligning raw CO_2 concentration with the Semtech computed fuel flow rate, which was derived from the exhaust flow rate measured by the EFM.

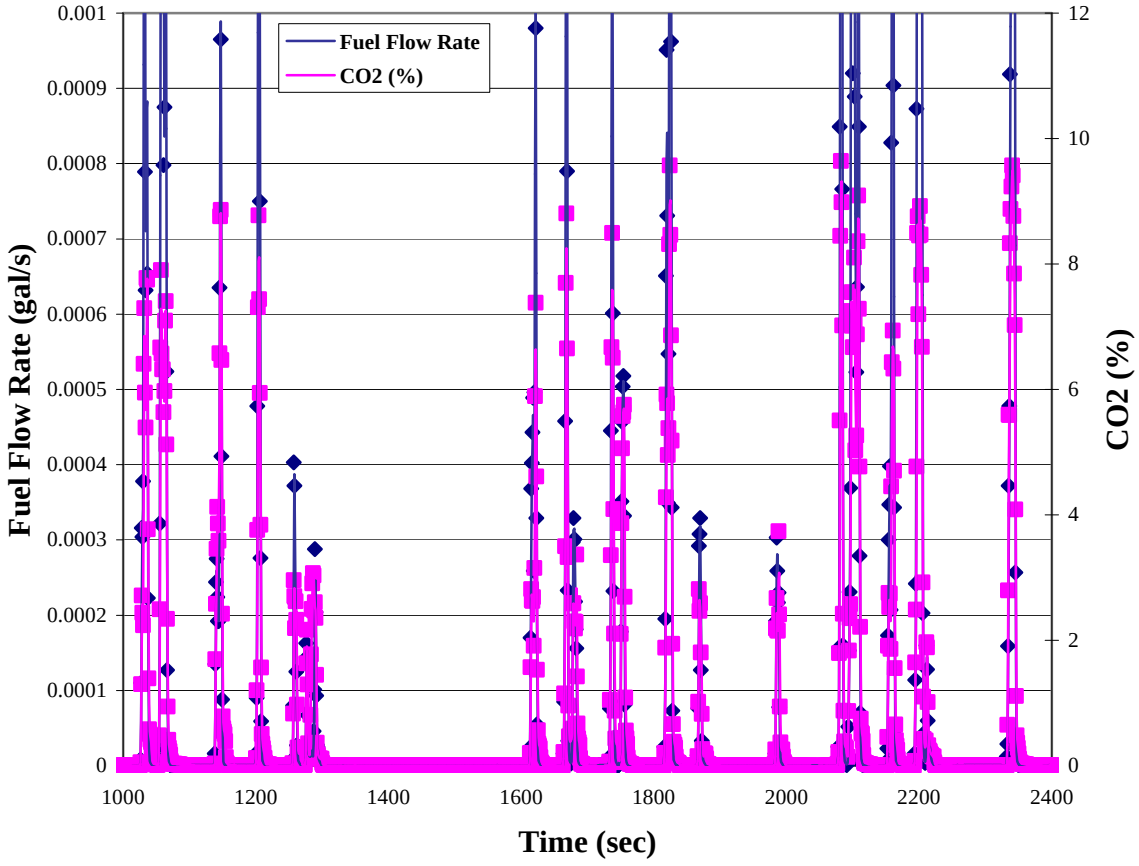

Figure 3.21: Internal aligning of Semtech data to verify post-processed inputted transport delays.

3.3.2 Semtech-DS Post-Processing

Data files collected from on-road emissions monitoring include measured parameters as well as calculated correction factors and post-processed data forms. Some of the variables (both measured and calculated) included in the Semtech output files are given below. While other parameters are provided with each output file, the following list includes the data utilized for the summarized and projected data analyses.

- **Date**, **Time**, and **Elapsed Time** are Semtech time stamps. Elapsed Time was user calculated;

- **Raw Concentrations (CO_2, CO, NO, NO_2, NOx, HC, O_2):** Raw measured concentration for each chemical constituent reported on a % or ppm basis. The raw CO_2 concentration was used primarily for time aligning the Semtech and DLM datasets;

- **Wet (CO_2, CO, NO, NO_2, NOx, kNO, kNO_2, kNOX, HC):** Wet corrected pollutant gas concentrations which have been normalized to lower bound detection limits set by the zero and corrected using Kw (dry-to-wet correction factor);

- **Relative Humidity** ambient relative humidity measured by weather probe;

- **Local Ambient Pressure:** ambient pressure measured by weather probe;

- **Local Ambient Temperature:** ambient temperature measured by weather probe;

- **Corrected Exhaust Mass Flow Rate (kg/hr):** Semtech EFM density corrected flow rate, assuming the molecular weight of air, and using a linear k value;

- **Exhaust Volumetric Flow Rate (SCFM):** Semtech EFM volumetric flow rate;

- **Exhaust Temperature:** Exhaust temperature measured at the Semtech-EFM (point of exhaust sample collection);

- **Latitude, Longitude, Altitude, Groundspeed:** GPS parameters used for all route positioning information;

- **Instantaneous Fuel Specific Emissions, g/kg-fuel (CO_2, CO, NO, NO_2, NOx, Corrected NO, Corrected NO_2, Corrected NOX, THC):** Instantaneous fuel-specific emissions for each pollutant (including wet corrected NOx factors). The mass fraction of each pollutant to the fuel in the combusted air/fuel mixture;

- **Fuel Rate (gal/s):** Calculated instantaneous fuel rate based on EFM measurements and the stiochiometry of total carbon emitted. All fuel rate calculations required No. 2 Diesel parameter assumptions;

- **Instantaneous Mass (CO_2, CO, NO, NO_2, NOx, Corrected NO, Corrected NO_2, Corrected NOX, HC):** Instantaneous g/sec emissions for all chemical constituents including wet corrected NOx factors;

- **30SW Speed, 30SW Fuel Economy:** Ground Speed and Fuel Economy integrated over a 30second moving average window;

- **Cumulative Distance (mi), Cumulative Fuel Consumption (gal), Cumulative Fuel Economy (mpg):** Calculated cumulative parameters based on moving averages updated for every second of the test;

- **Cumulative (CO_2, CO, NO, NO_2, NOx, Corrected NO, Corrected NO_2, Corrected NOX, THC), g/mi:** Calculated cumulative distance-specific mass emissions based on moving averages updated for every second of the test.

Fuel consumption, corrected raw concentrations, and all mass-based emissions data are the result of Semtech (SensorTech-PC) post-processor computations. In order to calculate fuel consumption during on-road sampling, U.S. Code of Federal Regulations' standard physical properties for number 2-diesel were used. Number 2-diesel fuel supplied by KCATA was used for all sampling efforts since this is the same fuel used for all of KCATA's operations. Chemical and physical fuel analysis was not conducted throughout the study so a fuel specific gravity of 0.850 and a fuel molar hydrogen/carbon

ratio of 1.800 were used for all calculations (CFR40 §86.1342-94). In addition to the Semtech processed computations, brake-horsepower-based emissions were calculated for each run using the DLM-recorded dICE (diesel internal combustion engine) torque and speed (RPM) data. The following paragraphs describe the computations used by the Semtech system to determine the various emissions parameters. For all analyses performed, DLM-acquired velocity was used to calculate vehicle acceleration, distance traveled, and vehicle specific power. DLM output was deemed more accurate than vehicle speeds based on GPS data used by the Semtech-DS.

3.3.3 Fuel-Specific Emissions

Several data manipulations were used by the Semtech-PC post-processor in order to provide comprehensive data output. General descriptions of the output variables were provided above, and brief overviews of the calculations used during post processing are supplied in the following paragraphs. Additional information pertaining to each can be found in the Semtech-DS user manuals (Sensors, 2006).

In order to report fuel-specific emissions data, the mass fraction of each pollutant must be determined with respect to the total fuel content of the cylinder injected fuel/air mixture. The mole fraction of the pollutant to the fuel burned is calculated and then converted to a mass basis using the molecular weights of the pollutant and fuel (equation 1). The fuel mole fraction is based on the concentrations of combustion reaction products (carbon dioxide and carbon monoxide) plus hydrocarbon breakthrough. The ambient carbon dioxide concentration must be subtracted from the molar fuel calculation to eliminate bias from non-fuel associated carbon dioxide.

The mass fraction of each pollutant to the fuel mass in the air-fuel mixture (mass pollutant/mass fuel) is reported calculated and outputted for each of the measured constituents.

$$NO_{fs}\left(\frac{g\_NO}{g\_fuel}\right)=\left(\frac{[NO]}{[CO]+[HC_1]+[CO_2]-[CO_2]_{ambient}}\right)\times\left(\frac{MW_{NO}}{MW_{fuel}}\right) \quad (1)$$

3.3.4 Instantaneous Mass Emissions

Using the measured exhaust flow rate and the normalized/humidity corrected instantaneous pollutant concentration, the instantaneous mass emission for each of the monitored constituents is calculated at each second of data collection.

3.3.5 Volumetric Exhaust Flowrate

Semtech EFM measurements provide direct mass emissions of the vehicle exhaust on a second-by-second basis. In order to determine pollutant concentration, as a function of mass emission, the EFM data must first be converted to a volumetric basis. Equations 2 and 3 convert the exhaust mass flow rate measurement obtained by the Electric Flow Meter (EFM) to standard volumetric flow rates at 20ºC and 1atm. The standard volumetric flow rate is computed by dividing the mass flow rate by the density of the exhaust at standard temperature and pressure.

$$\dot{m} = \rho V = \rho_{std} V_{std} \tag{2}$$

$$V_{std} = \frac{\dot{m}}{\rho_{std}} \tag{3}$$

The standard density must then be determined by calculating the molecular weight of the exhaust. Weighting the CO_2, N_2, O_2, and water vapor by their respective wet concentrations approximates this (equation 4).

$$MW_{exhaust} = \frac{1}{100} \sum \left[[CO_2] \cdot 44.01 + [O_2] \cdot 32.0 + [N_2] \cdot 28.013 + [H_2O] \cdot 18.015 \right] \tag{4}$$

Assuming ideality, the ideal gas constant for the exhaust is computed using the ideal gas law at 20ºC and 1atm (standard conditions). The following table (ref. CFR40 §86.1342-94) provides the standard densities for each constituent in both English and SI units.

Table 3.5: Standard densities used in instantaneous mass emission calculations (Sensors, Semtech-DS User Manual).

Chemical Component	Standard Density (g/ft^3)	Standard Density (g/l)
CO_2	51.81	1.830
CO	32.97	1.164
#2 Diesel HC ($CH_{1.80}$)	16.27	0.5746
#1 Diesel HC ($CH_{1.93}$)	16.42	0.5800
Gasoline HC ($CH_{1.85}$)	16.33	0.5768
NOx (as NO_2)	54.16	1.913

Instantaneous mass emissions (g/s basis) are calculated by multiplying the wet gas concentrations (determined by multiplying the measured dry concentrations by the Kw, the dry-to-wet conversion factor) by the standard volumetric exhaust flow rate and standard density for each constituent (equation 5).

$$CO_2(g/s) = \frac{[CO2]_{wet}}{100} \times V_{std} \times \rho_{CO2,std} \qquad (5)$$

3.3.6 Fuel Mass Flowrate

The fuel flow rate (mass basis) is calculated for each second of data collection by using the exhaust mass flow rate as measured by the EFM and the calculated air/fuel mass fraction (based on exhaust stoichiometry). Equation 6 is used by SensorTech-PC to compute the fuel mass flow rate in gal/s.

$$Wf = \frac{Exhaust\ Mass\ Flowrate}{AFR + 1} \quad (6)$$

3.3.7 NOx Humidity Correction Factor, Kh

The Semtech system applies a humidity correction factor, Kh, to the measured instantaneous NO, NO_2, and NOx concentrations. All calculations for determining Kh (applied to NO and NO_2 instantaneous measurements for determination of the wet-corrected NO, NO_2, and NOx concentrations) were done using the method cited in either CFR40 §86.1342-94 or CFR40 §86.1370-2007. Humidity corrected NO, NO_2, and NOx data were used for all subsequent analyses, although the imposed correction was minimal since the final data selected for the majority of analysis were within the ambient temperature range where humidity corrections were not imposed (55-95˚F).

3.3.8 Brake-Specific Emissions

Heavy-duty diesel engine certification is currently conducted using engine dynamometer data rather than a chassis-based method. Because of this, certification requirements for heavy-duty diesel engines are based on engine work (brake horsepower) rather than distance traveled. In order to evaluate the PHEV Sprinter's emissions in relation to certification levels, the total mass emitted per total brake horsepower (bhp) had to be determined for each sampled run. Instantaneous bhp was calculated using the DLM recorded diesel combustion engine (dICE) torque (Nm) and dICE speed (RPM) data. The appropriate unit conversion was used to convert the PHEV internal combustion torque to lb-ft from N-m.

$$hp = \frac{torque(lb \cdot ft) \times RPM}{5252} \quad (7)$$

The brake-specific mass emissions were calculated for each recorded test second and then summed for the entire test run as pollutant mass/bhp-hr. Using NOx as an example:

$$NO_x(g/hp-h) = \frac{\sum \mathrm{NO_x\ mass}}{\sum \mathrm{work}} = \frac{\sum \mathrm{NO_x\ mass}}{\sum bhp \times 1s(h/3600s)} \quad (8)$$

3.4 Vehicle Specific Power

3.4.1 Definition and Background

Vehicle specific power (VSP) is a standard proxy for estimating a vehicle's on-road power demand. Its incorporation into vehicle emissions studies has become a standard enough practice that vehicle specific power is now a functional component of current vehicle emissions models. Because of its universality and prevalence throughout modern on-road emissions research, vehicle specific power will be included in the PHEV final data submission and will be included throughout the PHEV on-road operating and emissions investigations.

Vehicle specific power (VSP) was originally introduced as Specific Power for use in remote sensing research as a surrogate for estimating the instantaneous power load on a vehicle at the time that emissions measurements were taken via a remote sensing device (Jiminez, 1999). Since this time, VSP has become a routine method for calculating a vehicle's power demand in conjunction with on-road emissions measurements. VSP has proven to be a more powerful tool for estimating and modeling vehicle emissions than individual on-road parameters such as velocity, acceleration, or fuel rate.

As presented in existing research and used here, VSP is the instantaneous power per unit mass of the vehicle. VSP is technically defined as the instantaneous power required by the engine in order to both overcome rolling resistance and aerodynamic drag as well as increases in the kinetic and potential energies of the vehicle necessary to match instantaneous on-road conditions and behaviors (Jiminez, 1999). In order to accommodate for physical forces of resistance (rolling resistance, drag resistance, and the impact of rotating powertrain components) as well as the impact of on-road driving

variables such as velocity, acceleration, and effective road grade, the VSP equation includes parameter inputs for 10 unique constants or variables. Differences in vehicle weight, operating mode, engine technology, speed, and acceleration have all been shown to have measurable effects on instantaneous vehicle emissions (Zhai, 2008), so their inclusion in VSP calculation is essential.

Jimenez's definition of specific power was a construct of "Positive Kinetic Energy" presented by Watson in 1983 (Watson, 1983; Jiminez, 1999), the "Specific Power", defined as 2*velocity*acceleration, used by the EPA in the early 1990s, and McClintocks definition of a parameter designated as "Relative Engine Load" (McClintock 1998; Jiminez 1999). "Relative Engine Load" estimated on-road power demand by incorporating driving variables such as speed and acceleration, as well as local road characteristics such as grade.

VSP's predictive ability to estimate vehicle emissions has made it a fundamental concept when developing models capable of estimating vehicle emissions for specific geographies, roadways and vehicle types (Giannelli et al., 2005). The VSP-based modal approach has been found capable of estimating fuel consumption to within ±10% of actual on-road measurements (Frey, 2007). Additionally, VSP has been used in the development of the U.S. EPA's Motor Vehicle Emissions Simulator (MOVES) model. The binning approaches to categorizing emissions according to VSP ranges has commonly been used to determine emissions factors for modeling purposes (U.S. EPA, 2003). VSP's universal acceptance in the vehicle emissions community and its prevalence in model development prompted its investigation as a tool for estimating plug-in hybrid emissions, since the PHEV's design and on-road operation is fundamentally

different than the conventional vehicles used to compile historical emissions data for model development.

Jimenez's specific power was of particular use and interest when interpreting the results from remote sensing-based vehicle emissions studies. Remote sensing devices, in the realm of vehicle emissions, capture instantaneous emissions, and velocity and acceleration snapshots of passing vehicles from a stationary point on a roadway. Using generalized values for the vehicle-specific parameters (rolling resistance, drag coefficient, etc.), measured road grade at the sampling location, and measured velocity and acceleration at the point of measured emissions event, specific power can be calculated for all passing, sampled vehicles. The ability to estimate power demand or road load at the time of an emissions event gives the experimenter vastly more interpretive potential when evaluating the final on-road emissions data.

Similarly, specific power, now commonly referred to as vehicle specific power, has found practical application in the PEMS world. While designed to collect second-by-second emissions data in addition to various on-road parameters, driving variables, and certain engine characteristics, it is not common for commercially available PEMS units to collect the comprehensive engine data required to calculate the instantaneous power load on the vehicle. When calculated for every second of on-road emissions data collection, vehicle specific power can provide a corresponding estimation of instantaneous on-road power demand.

3.4.2 Calculation

Vehicle Specific Power (VSP) is articulated in terms of power per unit mass, which translates to W/kg. The full expression of VSP is provided in equation, 9, below. All input variables and parameters are defined following equation 9.

$$VSP = v \cdot \left(a \cdot \left(1 + \varepsilon_i\right) + g \cdot grade + g \cdot C_R\right) + \frac{1}{2} \cdot \rho_a \cdot \frac{C_D \cdot A}{m} \cdot \left(v + v_w\right)^2 \cdot v \quad (9)$$

$VSP \equiv$ vehicle specific power (W/kg)

$m \equiv$ vehicle mass (3,728.5 kg)

$v \equiv$ vehicle speed (m/s)

$a \equiv$ vehicle acceleration (m/s^2)

$\varepsilon_i \equiv$ "Mass factor", the equivalent translational mass of rotating powertrain components (i.e. wheels, gears, shafts, etc.). The suffix *i* denotes that the term is transmission gear-dependent (dimensionless, 0.1)

$grade \equiv$ vertical slope of roadway (rise/run) expressed as %

$g \equiv$ acceleration due to gravity ($9.81 m/s^2$)

$C_R \equiv$ coefficient of rolling resistance (dimensionless, 0.00955)

$C_D \equiv$ drag coefficient (dimensionless, 0.34))

$A \equiv$ cross-sectional area of the front of vehicle (5.086m^2)

$\rho_a \equiv$ density of ambient air (kg/m^3), see following equation(s) for calculation

$v_w \equiv$ vehicle headwind (assumed 0m/s)

Generalized estimations of the road load parameters, C_R (coefficient of rolling resistance) and C_D (drag coefficient), are typically used for multi-vehicle emissions monitoring campaigns. However, since this study focused on a single vehicle, more specific estimations of the road load parameters were utilized. The cited drag coefficient for the model years 2005 and 2006, 3500 Dodge Sprinter Van is 0.36 (www.autos.com, www.cars.com). This value is quantitatively comparable to C_D values used for similar vehicles in the literature (Petrushov, 1997 and Giannelli et al., 2005). The cross-sectional area used for the PHEV Sprinter was calculated from height and width measurements taken from the actual vehicle. PHEV mass was measured and provided by KCATA and includes the mass of the vehicle operator, emissions sampling equipment and components, and is inclusive of all vehicle fluids as well as a full fuel tank.

The coefficient of rolling resistance accounts for the friction resulting from a round object, such as a tire, rolling on a surface at constant speed. The resulting resistance is usually caused by some degree of deformation in the rolling object, surface, or both. C_R's potential impact is, ultimately, dictated by the hysteretic and elastic properties of the rolling object. With regards to a tire rolling on pavement, the energy involved in deforming the tire is greater than that required for the tire to "recover" from the physical impact of its load. This discrepancy generates heat in the tire as it rolls. The coefficient of rolling resistance is a function of the road surface, tire type and pressure, and, to a lesser degree, vehicle velocity. The value for C_R used for the PHEV was averaged from a list of values determined for similar vehicles (in size and weight) determined by Petrushov's Coast Down Method (1997). The selected value is also quantitatively comparable to other values used for heavy-duty vehicle testing (Zhai et al., 2008).

Both the Data Logging Module (DLM) and the Semtech-DS measured vehicle velocity and elapsed time data. However, the Semtech velocity output was determined from the positioning information obtained from the WAAS GPS data. Because of the Semtech-DS's indirect method for determining velocity coupled with occasional "holes" in the GPS data within Kansas City's urban core, all DLM-obtained data was preferentially used. In order to calculate the instantaneous acceleration for each point in the dataset, elapsed time and vehicle velocity were used in equation 10, below.

$$a = \frac{\left(v_{t=i} - v_{t=i-1}\right)}{\Delta t} \qquad (10)$$

a = acceleration (m/s^2)

v = vehicle velocity (m/s)

t = time

Δt = 1 second

Power demand for a traveling vehicle is not only impacted by the physical characteristics of the vehicle and the demand of maintaining its kinetic energy on the horizontal plane, but also by the local roadway grade, as work must be done to move a vehicle against the force of gravity. For the purposes here, grade was defined as the slope of the roadway at each point in data collection time. In order to calculate instantaneous road grade, the rise and run occurring within each Δt was determined (equations 11 through 13).

$$D = \Delta x = \overline{v} \cdot t = v_o \cdot t + \left(\tfrac{1}{2}\right) \cdot a \cdot t^2 \quad (11)$$

$$\Delta H = H - H_o \quad (12)$$

$$Grade = \Delta H / D \quad (13)$$

D = distance traveled in Δt (m)

H = altitude at time t (m)

v = vehicle velocity (m/s)

a = acceleration (m/s^2)

t = time (s)

Grade was calculated from the measured GPS altitude. Data with missing or incorrect altitude readings were exempt from these calculations. In order to accurately measure distance traveled during Δt, acceleration was assumed constant across the 1Hz data collection frequency.

A more rigorous calculation of the grade would be “grade = sin(atan(grade))”, however for grades less than 14%, the relative error imposed by not using this equation is less than 1% (Jimenez, 1999). All cited references involving VSP calculations, which provided detail regarding their grade calculations, did not use the trigonometrically more accurate calculation of grade. This was initially investigated, and the relative difference was deemed negligible.

In previous vehicle emissions monitoring studies, the density of the ambient air was assumed constant over the course of the study. However, the PHEV on-road data collection spanned several months and resulted in a wide range of ambient conditions during the study period. The Semtech-DS data output includes ambient temperature and relative humidity, so, instead of assuming a constant average for air density, a value was calculated for each instantaneous VSP calculation. The following equations (14 through 17) detail the calculations and variables used to determine the density of the ambient air. Since the presence of water vapor will reduce the air density, the final equation used accounted for ambient humidity.

$$\rho = \frac{p_d}{R_d \cdot T} + \frac{p_v}{R_v \cdot T} \tag{14}$$

$$p_v = \phi \cdot p_{sat} \tag{15}$$

$$p_d = p - p_v \tag{16}$$

$$p_{sat} = 6.1078 \cdot 10^{\frac{7.5 \cdot T - 2048.625}{T - 35.85}} \tag{17}$$

$\rho \equiv$ density of humid air (kg/m^3)

$p_d \equiv$ partial pressure of dry air (Pa)

$R_d \equiv$ specific gas constant for dry air (287.058 J/(kg·K))

$T \equiv$ Ambient temperature (K)

$p_v \equiv$ pressure of water vapor (Pa)

$R_v \equiv$ specific gas constant for water vapor (461.495 J/(kg·K))

$\phi \equiv$ relative humidity (%)

$p_{sat} \equiv$ saturation vapor pressure (Pa)

The PHEV's data logging module (DLM) measured adequate engine parameters (specifically engine speed and torque for both the diesel combustion engine and electric motor) to allow a more direct calculation of second-by-second power output. Using engine-measured parameters for both the diesel internal combustion engine and the electric motor, it was possible to determine the continuous (second-by-second) power output of each powertrain. Despite the ability to calculate direct power output, vehicle specific power was still used as an analysis tool in effort to maintain consistency with technical precedence set by existing on-road, or real-time, emissions research. The continuity also provided an established categorization (binning) methodology in order to organize and analyze the on-road data and provided a reasonable quantitative basis to justify the power calculations applied to all datasets using the PHEV's engine data. Since the PHEV Sprinter was the first production-based plug-in electric hybrid to be subjected to an on-road emissions testing campaign, it was also important for to determine the suitability of VSP application to a novel drive train technology. With its zero emissions capabilities, it was uncertain if the PHEV data would provide the same statistical power of emissions estimation found with conventional vehicles, particularly if the PHEV technology were to be eventually examined and assessed using current modeling procedures.

3.4.3 Direct Power Calculation

As mentioned previously, in order to more accurately reflect the power required to move the PHEV across the designated sample routes, engine data was used to estimate the power output from both the diesel internal combustion engine and electric motor.

There was more than one point of measurement where PHEV power output could be calculated using DLM-acquired data. Diesel internal combustion engine (dICE) power output was estimated using the dICE's speed and torque data. Electric motor (EM) power output, however, could be calculated either at the battery or at the electric motor. Both were initially investigated, but in order to maintain continuity in power calculations between the dICE and EM, power calculated using engine measurements was the basis for all direct-power calculations.

Using the battery voltage and current, it was possible to calculate the power leaving the battery pack (equation 18). However, the product of this equation does not account for losses occurring in the electric motor or drivetrain. Systemic losses in the electrical powertrain were, nominally, 11% in charge sustaining mode and 19% in charge depleting operation. Because of the efficiency losses between the battery packs and the electric engine, the mechanical equation for determining power output from an engine was adopted for both the electric motor as well as the diesel internal combustion engine.

$$P = V \cdot I \qquad (18)$$

$P \equiv$ Power (Watts)

$V \equiv$ Voltage (volts)

$I \equiv$ Current (amps)

DLM-monitored engine speeds and torque were used in equation 19 in order to assess the instantaneous power demand across all sampled routes based solely on engine behavior (versus road-based data and vehicle-based constants as with VSP determination). In order to maintain consistency for quantitative comparison purposes, the units for reporting engine power output were the same as those reported by the VSP equation.

In a mechanical system, such as an internal combustion engine, the product of the engine torque and speed determines power. Individual engine make and models will have unique optimum torque maps and power curves depending on the engine design and purpose. As the force component of the power equation, torque is defined as the rotational force resulting from the piston movement during combustion within the cylinder chamber. Engine speed refers to the rate at which the pistons are firing. Equation 19, below, describes the classical method of calculating engine power output (Heywood, 1988), and was employed to calculate instantaneous power output for both the diesel internal combustion engine and electric motor.

$$P = \frac{\tau \cdot \omega \cdot \left(\frac{2 \cdot \pi}{60} \right)}{m} \qquad (19)$$

$P \equiv$ power (W/kg)

$\tau \equiv$ torque (N·m)

$\omega \equiv$ angular velocity (i.e. engine speed) (RPM, revolutions/minute)\

$m \equiv$ vehicle mass (kg)

Equation 19 was also used to determine the power input back into the battery cells during recuperation events. Unlike conventional vehicles, which convert kinetic and potential energy to heat and friction during periods of passive deceleration, deceleration due to braking, deceleration due to transmission gear shifts, coasting, or downhill travel, the PHEV Sprinter was able to "recuperate" some of that lost potential energy. Acting as an electrical generator during recuperation periods, the electric motor rotates in the opposite direction allowing electrical current to be directed back into the battery cells for storage and future use. On-road recuperation effectively extends the electric-only drive potential of the PHEV. Recuperation events were identified as periods with negative battery current, denoting current moving back into the battery pack. Actual power input from recuperation, however, was calculated using the electric motor torque and speed values instead of current and voltage readings at the battery pack in order to maintain continuity between all power calculations. Quantitatively, using data from the electric motor to determine recuperation rates over-estimates the actual amount of electrical energy returned to the battery cells due to natural efficiency losses throughout the system. In charge-sustaining mode, approximately 29.6% efficiency loss occurred between the electric motor and point of current/voltage recording at the battery cells. This efficiency loss was slightly higher during charge-depleting operation at 37.9%. Regardless of the

calculation method used to estimate periods of recuperation, the point of system determination did not affect the transient behavior of electrical recuperation. Figure 3.22, below, shows just over 8minutes of recuperation as determined by calculations at both the battery cells and electric motor. The data for this chart was selected from the 12th Street route, charge-sustaining operation.

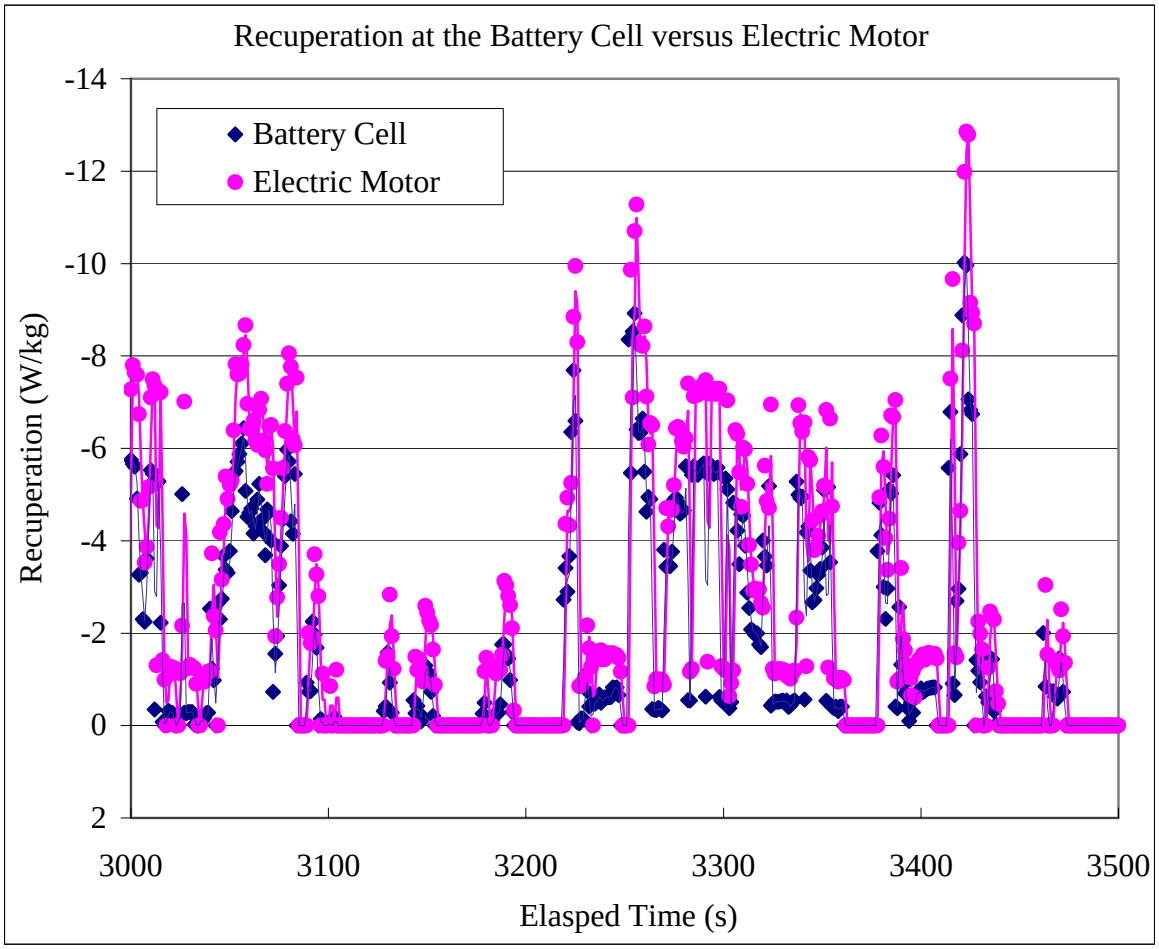

Figure 3.22: Relative magnitude of recuperation rates based on point of reference (battery cell versus the electric motor).

Certain artifacts appeared in the DLM-measured torque data, specifically negative torque readings. With respect to the electric motor, negative torque readings occur

during recuperation events, where kinetic energy that is normally lost as heat and friction in conventional vehicles is captured by the PHEV and directed back into the battery cells for storage and future use. During recuperation, the electric motor spins in the opposite direction, acting as an electric generator, hence the negative torque readings. However, the dICE also reported occasional negative torque values. These occurred at low engine speeds, and are a not uncommon artifact of internal combustion engines. Based on past precedence (Lehmann et. al., 2004), the negative torque values generated by the ICE were left unchanged in the original datasets and remained during the power calculations. Electric motor power output was set at zero during periods of recuperation (negative torque).

3.4.4 Categorizing VSP data

Instead of evaluating emissions data according to vehicle specific power (VSP) on a continuous, or second-by-second basis, binning or categorization methods have been developed in order to aggregate emissions data according to "VSP bins" based on predetermined VSP ranges. The VSP binning approach was originally developed for the U.S. EPA by the North Carolina State University (EPA, 2002) and is the basis behind current emissions models such as MOVES. The method of categorizing vehicle emissions based on VSP bin is still universally used for on-road emissions research.

There are several advantages to using a grouping method for analyzing continuous emissions data. Filtering data into groups will inherently mask some of the features within a dataset, however, despite this coarse application, VSP binning still maintains sufficient specificity to allow for meso-scale and macro-scale data analysis. If

implemented properly, modal analysis can also support a more detailed micro-scale analysis. Additionally, continuous on-road data possess a strong degree of autocorrelation. Employing a modal or binning approach to classify the data eliminates the autocorrelation innately present throughout the dataset. Modal analysis is commonly used in the vehicle emissions arena, and its use here provides a basis for comparative purposes.

Two classification systems were developed for the EPA, and both were implemented on the PHEV Sprinter data. A modal-based system specified four primary driving "modes" and established exact criteria for determining mode class for every second within a continuous, on-road dataset. The second classification scheme segregated the emissions data into concrete VSP bins based on the instantaneous vehicle specific power calculated for every second of emission data collection.

VSP bins were originally created using vehicle-based variables such as vehicle class, mileage, age, engine size, vehicle weight, and technologies present on the vehicle. Vehicle operation variables such as vehicle speed, acceleration, and vehicle specific power (used as a surrogate for power demand) were also included. Because of data availability, the researchers were also able to incorporate external parameters such as road grade, air condition usage, ambient temperature, and relative humidity into the inter-modal model. Hierarchal tree-based regression (HTBR), a forward step-wise variable selection method similar to forward stepwise regression in order to determine the end-points for each VSP bin (EPA, 2002), was used to divide the data into subsets, with each subset being more homogeneous than the amalgamation of the entire dataset. Each subset was required to be statistically unique from all other subsets, thus resulting in the

formation of discrete and unique VSP bins. HTBR was run in a partially supervised method, allowing the advantage of the inherent power in the statistical method's design while making it somewhat impervious to the impact of artifacts and variability in the data that may or may not be important from a practical and intuitive basis (the supervised part).

Explicit criteria were established for defining model categories (bins). HBTR analysis showed that vehicle specific power was the dominant explanatory variable in predicting vehicle emissions, so the binning approach was based on VSP values. NCSU researchers required that each bin should have a statistically significant different average emission rate than any other bin and that no single bin should dominate the estimate of total emissions for a typical route or trip. Based on these criteria, no bin was allowed to explain more than, approximately, 10% of the total emissions.

VSP bins created for the EPA in the 2002 NCSU report were developed for light-duty gasoline vehicles. This binning procedure, producing 14 discrete VSP bins, was initially investigated for the PHEV study; however, the PHEV data did not give sufficient weight to all VSP bins, resulting in under representation of the higher bins. Because of this, the VSP bin model developed for heavy-duty vehicle classes, and used throughout the technical literature (Zhai et al., 2008 and Frey et al., 2007) was, instead, used throughout the PHEV study. It was important that the binning approach adopted for this work fit the PHEV data to the best of its ability, primarily through sufficient data representation of all bins in the binning technique. Table 3.6 defines the 8 VSP bins used throughout the PHEV analysis.

Table 3.6: VSP bins (Frey, 2007).

VSP Mode	VSP Range (W/kg)
1	$VSP \leq 0$
2	$0 < VSP < 2$
3	$2 \leq VSP < 4$
4	$4 \leq VSP < 6$
5	$6 \leq VSP < 8$
6	$8 \leq VSP < 10$
7	$10 \leq VSP < 13$
8	$VSP \geq 13$

The second data-categorization approach was based on four distinct driving modes: idle, acceleration, cruise, and deceleration (EPA, 2002). Explicit conditions were established for designating the operating mode of the vehicle. Periods of on-road operation with zero velocity and zero acceleration were identified as idle mode. Cruising mode was defined as approximate steady-state operation with some allowable drift in velocity. In order for the vehicle to be designated as operating within acceleration and deceleration modes, several criteria were established to completely segregate acceleration and deceleration events from the oscillatory, transient operation that would naturally occur during cruise mode. First, in order for a vehicle to be designated as operating in acceleration mode, it must be identified as both moving and increasing in velocity, therefore both velocity and calculated acceleration must be greater than zero. Additionally, one of two criterion must be met in order to accurately identify acceleration mode from natural, subtle velocity fluctuations that occur during cruising: first, the vehicle must be experiencing an acceleration rate of at least two mph/sec, or the vehicle mush have established a sustained, moderate acceleration rate of one mph/sec for a minimum of three consecutive seconds. The converse (i.e. negative acceleration rates)

was required for the vehicle to meet the demands of deceleration mode. Previous research has shown that the four designated driving modes result in statistically significant differences in emission rates (Frey et al., 2001, and Frey et al., 2002).

It was further found that the predictive ability of the modal model could be improved by employing VSP modal development within the operating modes cruise and acceleration (EPA, 2002). This additional step was not included in the PHEV analysis, however, since there has been no reference of this modal development for heavy-duty vehicles, only light-duty passenger vehicles. Furthermore, the union of the two modal systems has not been used for model development. VSP binning remains the most prevalently used on-road data categorization technique to date. However, the nuances found in the VSP/drive-mode combined system are useful discussion points. For example, high VSP cruising results in higher average emissions than low VSP cruising, suggesting that emissions during cruise mode will typically be higher at higher speeds or under conditions of higher engine load (i.e. higher relative grade).

While the VSP binning approach is a more detailed and useful analysis tool, the driving mode methodology is more intuitive and easily understood. For this reason, both VSP binning and driving mode designations were used to analyze the PHEV dataset.

3.5 Statistical Methods

Univariate statistical analysis was utilized for the majority of the PHEV operating and emissions data analysis. Since most of the objectives evaluated different on-road responses to various driving, environmental, and implementation (transit versus civilian driving patterns) scenarios, basic analysis of variance (ANOVA) and the non-parametric equivalent Kruskal-Wallis tests provided the framework for the bulk of the statistical work performed for the PHEV Sprinter study.

Analysis of variance (ANOVA) examines the variance in the data in order to determine if that variance is attributable to specific sources, determining whether the means of several variables or groups are equivalent to a set degree of statistical significance (α). This test design essentially allows the experimenter to ascertain if the variation in a response variable (for example, carbon dioxide emissions) can be statistically explained by a predetermined factor variable (such as vehicle specific power bin or roadway type). ANOVA imposes the assumptions of normality, independence, and homoscedasticity.

While a number of the measured variables in the on-road dataset (both emission and operating) cannot be deemed independent due the cause-and-effect nature of the physical and chemical processes being measured during the PHEV's operation, ANOVA, and its non-parametric equivalent, Kruskal-Wallis, were suitable for investigating the relationship between route and roadway factors on both PHEV operation and emissions. Additionally, continuous, on-road data possess a degree of intrinsic autocorrelation. In time-series data, such as on-road emissions and vehicle operating data, observations close together in time have some degree of relation to one another. Without any categorization

or additional filtering, the individual measurements as a time-series cannot be considered independent from each other. Deliberate modal categorization of the on-road data, such as by VSP bin, removes the autocorrelation associated with continuous on-road data (Zhai, 2008). Additionally, filtering the second-by-second datasets down to every 5-seconds, or 5-second averages, has been found to remove essentially all autocorrelation associated with continuous on-road data (Zhai, 2008). For all analyses performed, one of the three methods of establishing independence was utilized: the data were subset into unique modes or bins according to modal models, the data were averaged over every 5seconds of data collection, and the data were aggregated into overall averages for a set link or section of road or route creating a sample or run-based value. Analyses based on aggregate sample-route data, yielding total emissions, power output, and fuel use for an entire sample route or roadway link also eliminated the impact of autocorrelation within the dataset.

Continuous on-road data is also inherently non-normal. This is particularly true with regards to the PHEV data, where a disproportionate amount of zero-valued data for a number of the measured variables exists due to its dual-mode operation (electric-only or hybrid operation). Even within individual VSP bins, the PHEV dataset proved non-normal with respect to ICE power output and carbon dioxide emissions during charge-sustaining mode due to the presence of electric-only operation within each bin. Normality, however, can be achieved by imposing a log-transformation on continuous on-road data. Unfortunately, zero-valued data recorded under electric operation continued to violate the requirements of normality for the larger datasets regardless of transformation method. Removing the electric-only data from each VSP bin resulted in

normal datasets in bins 1 through 5. With the electric-only data removed, the log-based transformation was applied to the residual charge-sustaining dataset creating a simulation of normality. However, since electric-only operation throughout charge-sustaining and charge-depleting operation is a critical feature of PHEV operation, there was no reasonable justification for removing the zero-emissions data. Since normality could not be rationally developed in the on-road PHEV data and in effort to compensate for violations of the ANOVA assumptions, all ANOVA analyses were duplicated using the non-parametric equivalent Kruskal-Wallis test. Where ANOVA evaluates population means and variance, the Kruskal-Wallis analysis tests for the equality of population medians among groups, negating the normality requirement of the parametric test.

Pearson's correlation coefficients were used to gauge the existence of linear relationships between the measured variables. While the Pearson's correlation coefficient provides a tested measure of linearity, it is not suitable for discerning non-linear relationships between variables. The nature of the on-road PHEV data suggests linear cause and effect, or co-cause and effect, relationships between variables. Pearson's correlation coefficients were used primarily to distinguish variable interactions with strong linear relationships from those with weak or no linear relationships from one another. Because correlation coefficients assume independence between observations, all data used in correlation analyses were either filtered to an every 5-second-averaged observation, or consisted of compiled summary data (i.e. on a per sample run basis), and, therefore, no longer represented a time-series dataset.

Multivariate analysis techniques were investigated for their suitability in application to the on-road continuous dataset. One of the primary requirements for

multivariate analysis is the assumption of independence between measured variables. With regards to operating and emissions data, it cannot be assumed that the variables are independent of each other since they have a direct physical or chemical cause-and-effect relationship (i.e. fuel use and carbon dioxide emissions). Additionally, the ultimate product of traditional multivariate techniques such as principal component analysis (PCA) or factor analysis (FA) did not suit the investigations of this study. The clustering and ability to subgroup data presented by PCA and FA was considered redundant given that the experimental design systematically created data subgroups such as roadway type, ambient temperature, and on-road operation scheme for use in objective design.

Multivariate analysis of variance (MANOVA), however, was employed as a justification tool for the univariate ANOVA tests performed. MANOVA is a multivariate generalization of ANOVA that safeguards against the risk of making Type I errors that exists when running a series of different, unique ANOVAs on a multivariate dataset (Johnson, 1998). Using a multivariate technique allows several populations to be compared by utilizing all of the measured variables simultaneously. By determining statistical significance with MANOVA, the researcher felt confident to rely on univariate analysis for the greater part of the data analysis.

Due to the size of the datasets being investigated (filtered or not filtered), appropriate levels of significance were determined for each test. Statistical significance for MANOVA tests was set at $\alpha<0.05$. With statistical significance found in the multivariate analysis of variance, an $\alpha<0.025$ was used to determine significance for the ANOVA and Kruskal-Wallis tests performed on the continuous datasets. Since the run-based datasets were essentially summarized compilations of the continuous on-road data,

the criteria demanded by ANOVA were no longer violated for these analyses and an $\alpha<0.05$ was accepted. The datasets were subgrouped according to investigation for all ANOVA and Kruskal-Wallis tests, so the sample sizes of the populations of interest were smaller than other tests. Correlation analysis, however, was assessed more conservatively with an $\alpha<0.025$ due to the large size of the continuous datasets.

Chapter 4: Summary and Overview of Data

4.1 Description of Complete Dataset

The PHEV Sprinter's on-road emissions were investigated from late August 2007 through January 2008. These sampling efforts resulted in over 1180miles and over 81hours of second-by-second emissions monitoring during normal on-road operation. The final dataset consists of 135 unique sample runs. In addition to the seven unique routes discussed earlier (109 Winner Loop, 109 Winchester Loop, 110, 123, 12 Truman/Crystal Loop, 12 West Bottoms Loop, and the Highway route), "transfer routes" where the PHEV was commuting between route start points and the calibration site (11^{th} and Charlotte) or between KCATA and the calibration site have also been included in the final data submission. Sample routes were selected according to a series of predetermined criteria. The sample routes were at least partially chosen for their overall travel distance, ensuring a certain degree of reproducibility in sampling efforts. Prior to initiating sampling, it was intended that all sample routes be run both solo (as a civilian driver) and follow (shadowing an in service KCATA bus), when applicable, up to 7 and 10 discrete times, providing statistically meaningful sample sizes on a per route basis. Frey et al. (2008) determined, using Monte Carlo Simulation (MCS), that for a single-vehicle analysis, a sample size of three was sufficient to ensure statistically meaningful results when evaluating additional routes. Their initial baseline was achieved using a slightly larger sample size of 14 runs, however, MCS indicated that, for subsequent routes, a much smaller n was suitable. On the basis of this work, the set study design used for the PHEV Sprinter was deemed ample.

Conceptually, the PHEV Sprinter sampling was originally planned for days with relatively consistent moderate ambient temperatures and meteorological conditions. However, the adjusted sampling schedule coupled with vehicle service issues resulted in a final total dataset collected at multitude of different ambient temperatures (ranging from 39ºC in September 2007 to -1ºC in December 2007). Between roadway and geographic commonalities among the different routes, it was possible to extract suitable subsets of on-road data permitting a preliminary investigation into the implications of ambient temperature and auxiliary system use on the PHEV Sprinter's operation and emissions. This initial evaluation gave credence to the final dataset filtering used for all planned analytical investigations. While the impact of ambient temperature on vehicle operation and emissions was not a primary objective for this study, ambient temperature has proven to be a significant factor affecting diesel vehicle emissions (Yanowitz et al., 2000) and must be considered throughout the data analysis. Given the copious amount on-road data collected, it was possible to select individual sample runs to minimize confounding effects such as seasonality, ambient temperature, and vehicle system use on the final objectives.

During on-road data collection, auxiliary systems (air conditioning and heating) were used as minimally as necessary to maintain operator comfort during normal sampling efforts. Their use was not systematically planned in order to specifically investigate cause and effect relationships between the PHEV's operation and emissions and the load imposed by the systems. Extracting specific sampling days and portions of on-road data within these days from the total data array, however, allowed a rudimentary evaluation of these relationships.

The PHEV Sprinter required 6-8hours of charging in order to achieve a state of charge nearing 100% (representing fully charged battery packs). In order to accomplish a complete charge, the PHEV was charged overnight prior to scheduled sampling days. Because of this, the first one or two runs for each day were conducted with relatively high states of charge (representing charge-depleting mode operation). Typically, several runs would be collected during a given sampling day, so the majority of the sampled runs were completed while the PHEV Sprinter's state of battery charge was in the hybrid operating range, or charge-sustaining mode (~36%).

A comprehensive summary table is provided in Appendix A. This table includes the totals and averages for the more pertinent emissions and operating variables for each sample run as provided by the Semtech-PC software output. The following pages provide a synopsis of the larger, summary table included in Appendix A. Tables 4.2 and 4.3 display operating, emissions, route, and sample day totals and averages for each of the sample routes, segregated according to whether the runs were completed as solo or follow (shadowing a KCATA in service transit bus). Table 4.1 provides a condensed summary of the overall PHEV Sprinter emissions according to each route studied.

Table 4.1: Summary of PHEV emissions by route and overall averages.

Route	S/F	CO_2 (g/mi)	CO (g/mi)	corr NOx (g/mi)	THC (g/mi)	CO_2 (g/bhp-hr)	CO (g/bhp-hr)	corr NOx (g/bhp-hr)	THC (g/bhp-hr)
109: 9th Street-Winner Loop	Solo	495.2	0.829	5.26	0.071	609.5	1.308	6.156	0.126
109: 9th Street-Winner Loop	Follow	888.2	0.751	10.34	0.045	555.4	0.469	6.441	0.027
109: 9th Street-Winchester Loop	Solo	674.7	0.768	6.59	0.014	580.0	0.907	5.604	0.023
109: 9th Street-Winchester Loop	Follow	911.3	0.927	10.85	0.042	593.8	0.604	7.032	0.027
110: 44th/Brooklyn	Solo	610.6	0.877	6.52	0.051	542.3	2.019	6.671	0.296
110: 44th/Brooklyn	Follow	653.7	1.317	6.76	0.070	600.8	1.451	6.040	0.091
123: 23rd Street	Solo	710.5	1.365	7.15	0.072	597.1	1.342	5.863	0.077
123: 23rd Street	Follow	737.5	1.758	7.07	0.105	611.1	1.648	5.738	0.109
12: 12th Street-T/C	Solo	626.8	0.917	6.79	0.041	582.4	0.903	6.277	0.039
12: 12th Street-WB	Solo	662.9	0.942	7.52	0.029	571.8	0.812	6.489	0.025
Hwy	Solo	495.3	0.357	4.60	0.068	736.5	0.593	6.641	0.105
Xfer to KCATA+	Solo	656.9	1.212	7.08	0.024	568.1	1.134	6.186	0.022
Xfer from KCATA+	Solo	1050.4	1.697	11.64	0.061	564.0	0.936	6.283	0.026
Misc Xfer	Solo	659.5	1.426	6.59	0.089	636.1	2.404	5.856	0.184
All Runs		**661.9**	**1.098**	**6.87**	**0.062**	**602.6**	**1.335**	**6.164**	**0.110**

Table 4.2: Summary table of emissions and vehicle data collected for each route run designated as solo or follow: KCATA Transit Routes.

	109: 9th Street Winner Loop		109: 9th Street Winchester Loop		110: 44th/Brooklyn		123: 23rd Street		12: 12th Street T/C	12: 12th Street WB
	Solo	Follow	Solo	Follow	Solo	Follow	Solo	Follow	Solo	Solo
Number of runs (full and partial):	**10**	**4**	**9**	**4**	**15**	**14**	**12**	**13**	**14**	**5***
Ambient Temperature (degC):										
Average:	9.65	28.62	28.75	29.10	12.06	11.36	16.88	12.78	18.24	19.48
Standard Deviation:	6.99	3.29	6.19	0.77	6.15	6.74	8.19	10.33	2.45	1.74
Maximum:	24.77	32.26	39.10	30.02	32.02	18.99	32.11	24.16	20.84	20.94
Minimum:	4.00	25.35	20.34	28.15	6.58	0.55	8.64	-1.00	13.76	16.63
Distance Traveled (mi):										
Total on all runs:	68.54	25.51	76.09	30.25	138.03	128.83	130.66	128.75	149.26	67.53
Average/run:	6.85	6.38	8.45	7.56	9.20	9.20	10.89	9.90	10.66	13.51
Maximum:	8.74	7.92	9.77	9.12	14.20	11.87	15.50	15.47	11.64	14.40
Minimum:	3.23	4.10	5.48	4.68	3.74	4.45	3.59	2.37	4.01	13.00
Fuel Consumption:										
Total Consumption all runs (gal):	3.48	1.96	4.81	2.86	8.62	8.80	9.75	9.81	9.59	0.90
Avg Fuel Economy (mpg):	26.11	11.51	19.16	10.65	18.02	16.99	15.74	14.95	18.29	15.48
Std. Dev. Fuel Economy (mpg):	16.80	2.59	14.91	1.65	6.02	6.24	6.05	4.69	9.62	NA*
Max Fuel Economy (mpg):	68.38	14.34	55.78	13.01	36.35	33.90	32.34	25.41	50.91	15.48
Min Fuel Economy (mpg):	12.85	9.26	11.48	9.22	11.67	12.93	10.56	10.50	13.58	15.48
State of Battery Charge (%):										
Average all runs:	47.45	36.18	38.26	36.14	40.28	42.26	44.77	48.66	41.26	41.52
Standard Deviation:	17.85	0.49	5.90	0.26	11.34	14.38	15.99	18.13	14.90	11.45
Maximum:	85.95	36.85	53.98	36.46	79.83	77.77	84.71	88.77	83.62	62.01
Minimum:	35.92	35.70	36.06	35.82	35.99	35.83	36.30	36.44	36.12	36.15
Emissions Data (g/mi):										
CO_2 (g/mi):										
Average:	495.2	888.2	674.7	911.3	610.6	653.7	710.5	737.5	626.8	662.9
Standard Deviation:	199.9	219.2	221.4	129.6	140.3	152.3	178.5	187.3	144.4	NA*
Maximum:	778.8	1100.4	890.2	1037.1	871.8	792.7	964.9	975.5	754.0	662.9
Minimum:	149.0	662.7	182.1	729.8	280.3	299.5	314.4	402.7	200.4	662.9
CO (g/mi):										
Average:	0.83	0.75	0.77	0.93	0.88	1.32	1.36	1.76	0.92	0.94
Standard Deviation:	0.37	0.26	0.17	0.19	0.31	0.47	0.49	0.73	0.27	NA*
Maximum:	1.73	1.04	0.99	1.12	1.71	2.44	2.82	3.64	1.62	0.94
Minimum:	0.48	0.54	0.57	0.76	0.51	0.70	0.91	1.10	0.55	0.94
NOx (g/mi):										
Average:	5.26	10.34	6.59	10.85	6.52	6.76	7.15	7.07	6.79	7.52
Standard Deviation:	2.52	2.95	2.24	1.88	1.78	2.03	2.23	2.22	1.94	NA*
Maximum:	8.59	13.41	9.22	12.87	9.15	8.52	10.03	9.56	8.56	7.52
Minimum:	1.24	7.54	1.53	8.34	2.07	2.26	2.46	3.16	1.59	7.52
THC (g/mi):										
Average:	0.07	0.04	0.01	0.04	0.05	0.07	0.07	0.11	0.04	0.03
Standard Deviation:	0.06	0.03	0.01	0.01	0.04	0.06	0.04	0.10	0.03	NA*
Maximum:	0.23	0.08	0.04	0.05	0.20	0.23	0.16	0.38	0.10	0.03
Minimum:	0.02	0.03	0.00	0.03	0.02	0.02	0.04	0.04	0.01	0.03
Total Work (bhp-hr):										
Total all runs:	60.17	43.34	95.042	48.90	162.28	151.64	170.06	168.00	128.90	72.31
Total Work/Distance (bhp-hr/mi):	0.88	1.70	1.25	1.62	1.18	1.18	1.30	1.30	0.86	1.07
Average:	6.02	10.83	10.56	12.23	10.82	10.83	14.17	12.92	12.89	14.46
Standard Deviation:	3.32	2.25	3.76	3.44	4.95	5.06	6.61	6.38	3.42	5.16
Maximum:	12.54	12.48	14.30	16.46	19.40	16.44	25.04	20.73	15.17	19.33
Minimum:	1.89	7.50	2.94	8.04	3.47	3.48	3.26	3.53	3.56	5.71

Table 4.2: continued.

	109: 9th Street Winner Loop		109: 9th Street Winchstr Lp		110: 44th/Brooklyn		123: 23rd Street		12: 12th Street T/C	12: 12th Street WB
	Solo	Follow	Solo	Follow	Solo	Follow	Solo	Follow	Solo	Solo
Emissions Data (g/bhp-hr):										
CO_2 (g/bhp-hr)										
Average:	609.5	555.4	580.0	593.8	542.3	600.8	597.1	611.1	582.4	571.8
Standard Deviation:	55.7	69.0	7.1	7.4	147.4	29.6	36.9	49.0	18.9	NA*
Maximum:	746.0	606.0	590.3	602.5	654.4	669.2	697.9	715.2	632.6	571.8
Minimum:	566.1	476.7	572.4	584.3	15.9	567.7	568.2	555.1	568.3	571.8
CO (g/bhp-hr):										
Average:	1.31	0.47	0.91	0.60	2.02	1.45	1.34	1.65	0.90	0.81
Standard Deviation:	0.96	0.11	0.93	0.08	4.08	1.17	0.92	1.04	0.38	NA*
Maximum:	3.13	0.57	3.21	0.66	16.44	4.44	3.30	3.94	1.95	0.81
Minimum:	0.45	0.35	0.39	0.49	0.49	0.58	0.69	0.73	0.64	0.81
NO (g/bhp-hr):										
Average:	6.20	5.66	4.44	6.15	6.01	5.98	5.55	5.56	5.84	6.08
Standard Deviation:	0.61	0.92	0.72	0.32	0.52	0.72	0.54	0.75	0.51	NA*
Maximum:	6.74	6.62	5.81	6.51	6.84	7.10	6.38	6.73	6.21	6.08
Minimum:	5.12	4.79	3.82	5.87	5.07	4.91	4.52	4.37	4.50	6.08
NO_2 (g/bhp-hr):										
Average:	0.30	0.62	1.05	0.71	1.65	0.34	0.53	0.46	0.63	0.75
Standard Deviation:	0.24	0.28	0.34	0.09	4.91	0.18	0.32	0.21	0.19	NA*
Maximum:	0.93	0.95	1.38	0.83	19.40	0.77	1.32	0.87	0.97	0.75
Minimum:	0.08	0.43	0.48	0.63	0.09	0.07	0.24	0.19	0.45	0.75
NOx (g/bhp-hr):										
Average:	6.51	6.28	5.49	6.86	6.70	6.32	6.08	6.02	6.48	6.83
Standard Deviation:	0.63	0.90	0.56	0.32	1.36	0.72	0.45	0.64	0.60	NA*
Maximum:	7.10	7.05	6.29	7.23	11.17	7.34	6.64	7.04	7.02	6.83
Minimum:	5.27	5.29	4.95	6.51	5.16	5.04	4.94	5.03	4.95	6.83
Corrected NO (g/bhp-hr):										
Average:	5.87	5.80	4.53	6.30	6.27	5.71	5.34	5.29	5.67	5.78
Standard Deviation:	0.48	1.03	0.65	0.33	2.28	0.59	0.42	0.57	0.54	NA*
Maximum:	6.33	6.94	5.79	6.71	14.35	6.70	5.97	6.19	6.14	5.78
Minimum:	5.01	4.91	3.96	6.01	4.76	4.60	4.52	4.34	4.27	5.78
Corrected NO_2 (g/bhp-hr):										
Average:	0.29	0.64	1.08	0.73	1.27	0.33	0.52	0.44	0.61	0.71
Standard Deviation:	0.25	0.27	0.36	0.10	3.51	0.18	0.33	0.22	0.17	NA*
Maximum:	0.93	0.95	1.44	0.86	13.96	0.76	1.32	0.87	0.92	0.71
Minimum:	0.08	0.45	0.48	0.65	0.08	0.07	0.22	0.17	0.43	0.71
Corrected NOx (g/bhp-hr):										
Average:	6.16	6.44	5.60	7.03	6.67	6.04	5.86	5.74	6.28	6.49
Standard Deviation:	0.54	0.98	0.49	0.33	2.40	0.60	0.39	0.49	0.59	NA*
Maximum:	6.68	7.38	6.27	7.44	15.18	6.99	6.22	6.47	6.67	6.49
Minimum:	5.09	5.42	4.95	6.66	4.84	4.72	4.94	4.80	4.70	6.49
THC (g/bhp-hr):										
Average:	0.13	0.03	0.02	0.03	0.30	0.09	0.08	0.11	0.04	0.03
Standard Deviation:	0.13	0.02	0.04	0.00	0.89	0.13	0.07	0.13	0.03	NA*
Maximum:	0.41	0.04	0.12	0.03	3.47	0.42	0.19	0.41	0.12	0.03
Minimum:	0.02	0.02	0.00	0.02	0.02	0.02	0.03	0.03	0.02	0.03

*EFM Data not available on 10/18/07 for 12WB runs. Computation of mass-based pollutant data and fuel consumption not possible.

**DLM Data not available on 11/1307 for 4 12T/C runs.

***Emissions data not recorded for 1 109-Winner Loop run on 9/11 and 1 109-Winchester run on 9/13.

[+]" Xfer to KCATA" is 11th/Charlotte to KCATA route. "Xfer from KCATA" is KCATA to 11th/Charlotte route.

Table 4.3: Summary table of emissions and vehicle data collected for each route run designated as solo or follow: study-developed route and transfer routes.

	Hwy Solo	Xfer to KCATA+ Solo	Xfer from Solo	Misc Xfer Solo	All Runs
Number of runs (full and partial):	**11**	**4**	**6**	**9**	**135**
Ambient Temperature (degC):					
Average:	9.58	16.77	19.35	18.06	16.24
Standard Deviation:	2.42	5.44	4.76	11.66	8.71
Maximum:	12.04	20.66	23.52	33.15	-1.00
Minimum:	7.00	9.00	10.84	0.76	39.10
Distance Traveled (mi):					
Total on all runs:	145.61	4.49	6.03	25.03	1181.6
Average/run:	13.24	1.12	1.00	2.78	8.75
Maximum:	13.52	1.17	1.04	4.55	27.01
Minimum:	13.20	1.09	0.98	1.03	0.98
Fuel Consumption:					
Total Consumption all runs (gal):	7.41	0.30	0.54	1.73	74.4
Avg Fuel Economy (mpg):	20.98	15.82	9.85	19.47	17.72
Std. Dev. Fuel Economy (mpg):	2.18	2.01	1.01	11.59	8.88
Max Fuel Economy (mpg):	24.91	17.45	11.02	44.24	68.38
Min Fuel Economy (mpg):	18.15	13.22	8.79	10.45	8.79
State of Battery Charge (%):					
Average all runs:	49.46	36.11	36.77	48.40	43.3
Standard Deviation:	13.50	0.12	1.56	21.56	14.2
Maximum:	82.71	36.23	39.45	84.42	88.77
Minimum:	41.61	36.00	35.47	35.41	35.41
Emissions Data (g/mi):					
CO_2 (g/mi):					
Average:	495.3	656.9	1050.4	659.5	661.9
Standard Deviation:	49.1	89.2	104.9	278.1	203.0
Maximum:	568.0	775.5	1166.8	982.8	1166.8
Minimum:	412.5	585.8	932.4	227.3	149.0
CO (g/mi):					
Average:	0.36	1.21	1.70	1.43	1.098
Standard Deviation:	0.11	0.52	0.60	0.70	0.579
Maximum:	0.52	1.77	2.44	2.62	3.64
Minimum:	0.19	0.52	1.13	0.59	0.19
NOx (g/mi):					
Average:	4.60	7.08	11.64	6.59	6.87
Standard Deviation:	0.74	0.90	1.09	3.33	2.52
Maximum:	5.76	8.11	12.96	10.84	13.41
Minimum:	3.46	6.30	10.33	1.26	1.24
THC (g/mi):					
Average:	0.07	0.02	0.06	0.09	0.062
Standard Deviation:	0.03	0.00	0.04	0.06	0.056
Maximum:	0.12	0.03	0.12	0.23	0.38
Minimum:	0.03	0.02	0.01	0.01	0.00
Total Work (bhp-hr):					
Total all runs:	124.20	3.85	9.21	27.07	1332
Total Work/Distance (bhp-hr/mi):	0.85	0.86	1.53	1.08	1.13
Average:	11.29	1.28	1.84	3.38	10.41
Standard Deviation:	3.07	0.12	0.39	2.14	6.13
Maximum:	14.07	1.41	2.16	6.05	39.39
Minimum:	2.96	1.17	1.18	0.28	0.28

Table 4.3: continued.

	Hwy Solo	Xfer to KCATA+ Solo	Xfer from Solo	Misc Xfer Solo	All Runs
Emissions Data (g/bhp-hr):					
CO_2 (g/bhp-hr)					
Average:	736.5	568.1	564.0	636.1	602.6
Standard Deviation:	544.9	17.4	15.8	112.9	176.9
Maximum:	2379.3	588.2	575.8	874.0	2379.3
Minimum:	561.8	557.1	541.3	556.7	15.9
CO (g/bhp-hr):					
Average:	0.59	1.13	0.94	2.40	1.335
Standard Deviation:	0.63	0.67	0.27	3.21	1.835
Maximum:	2.44	1.77	1.20	10.09	16.44
Minimum:	0.20	0.43	0.66	0.50	0.20
NO (g/bhp-hr):					
Average:	6.75	5.97	6.05	5.47	5.82
Standard Deviation:	4.25	0.22	0.27	0.96	1.45
Maximum:	19.53	6.20	6.42	6.97	19.53
Minimum:	4.87	5.75	5.78	4.12	3.82
NO_2 (g/bhp-hr):					
Average:	0.32	0.50	0.44	0.48	0.647
Standard Deviation:	0.36	0.03	0.14	0.31	1.745
Maximum:	1.37	0.53	0.55	0.94	19.40
Minimum:	0.07	0.47	0.26	0.09	0.07
NOx (g/bhp-hr):					
Average:	7.07	6.46	6.49	5.95	6.35
Standard Deviation:	4.60	0.24	0.22	0.77	1.54
Maximum:	20.90	6.73	6.68	7.23	20.90
Minimum:	5.15	6.25	6.18	4.83	4.83
Corrected NO (g/bhp-hr):					
Average:	6.34	5.71	5.86	5.37	5.68
Standard Deviation:	4.01	0.22	0.10	0.76	1.54
Maximum:	18.41	5.90	6.00	6.35	18.41
Minimum:	4.59	5.47	5.78	4.30	3.96
Corrected NO_2 (g/bhp-hr):					
Average:	0.30	0.47	0.43	0.48	0.592
Standard Deviation:	0.34	0.01	0.14	0.32	1.263
Maximum:	1.29	0.49	0.54	0.98	13.96
Minimum:	0.06	0.46	0.24	0.08	0.06
Corrected NOx (g/bhp-hr):					
Average:	6.64	6.19	6.28	5.86	6.16
Standard Deviation:	4.34	0.22	0.09	0.60	1.60
Maximum:	19.70	6.37	6.40	6.59	19.70
Minimum:	4.85	5.94	6.18	4.83	4.70
THC (g/bhp-hr):					
Average:	0.10	0.02	0.03	0.18	0.110
Standard Deviation:	0.09	0.01	0.02	0.28	0.331
Maximum:	0.35	0.03	0.04	0.87	3.47
Minimum:	0.03	0.02	0.00	0.01	0.00

*EFM Data not available on 10/18/07 for 12WB runs. Computation of mass-based pollutant data and fuel consumption not possible.

**DLM Data not available on 11/1307 for 4 12T/C runs.

***Emissions data not recorded for 1 109-Winner Loop run on 9/11 and 1 109-Winchester run on 9/13.

+" Xfer to KCATA" is 11th/Charlotte to KCATA route. "Xfer from KCATA" is t data and fuel consumption not possible.

There were three sample days with incomplete available data: DLM (data logging module) data were not recorded on November 13, 2007, the EFM (electronic flowmeter) was not operating on October 18, 2007, and two runs, one on September 11 and one on September 13 did not collect viable emissions data, although all other Semtech data were intact and feasible. Despite the unavailability of certain data recording systems on these days, the other data collection methods were intact and operational.

4.2 Summary of Analytical Objectives

Based on cumulated background knowledge surrounding plug-in hybrid vehicle development and on-road emissions testing capabilities, finding novel and unique approaches to analyzing the Sprinter PHEV on-road emissions and operating data was a relatively straightforward process. The Plug-In Hybrid Sprinter Demonstration Study funded by KU's Transportation Research Institute (TRI) is the first research endeavor focusing on on-road emissions and operation of an original equipment manufactured plug-in hybrid vehicle. Prior to this work, the only data available to the public domain concerning PHEVs was based on hybrid electric vehicles retrofitted with plug-in capabilities. The diesel configuration of the Kansas City PHEV provides an additional dimension of originality to the study. Available research surrounding hybrid electric vehicle (HEV) on-road operation and emissions is largely limited to gasoline configured HEVs. Generally speaking, diesel HEVs are not part of the regular on-road HEV fleet, so information regarding the use of a diesel internal combustion engine in hybrid electric applications is limited at best. Using the inherent novelty of the PHEV Sprinter Demonstration Study a primary focus, five primary data-analysis objectives were identified for further investigation.

4.2.1 Objective 1: Vehicle Specific Power Analysis

As a commonly used proxy for estimating a vehicle's on-road power demand, vehicle specific power (VSP) analysis often accompanies on-road emissions campaigns. Additionally, VSP has been found to better predict on-road vehicle emissions than any single drive or road-based parameter (i.e. velocity, acceleration, grade, etc.). Due to its predictive abilities, VSP categorization techniques have become the backbone to current modeling

efforts. Because the PHEV possesses the ability to operate both as an electric-only vehicle and as a conventional hybrid electric vehicle, it presented a degree of uncertainty regarding its suitability and applicability towards current emissions models. Objective 1's primary focus was to perform a comprehensive vehicle specific power analysis to the on-road PHEV data. This investigation applied VSP classification techniques to the PHEV on-road data as a means of assessing the feasibility of applying current models to the alternative-powered drivetrain.

4.2.2 Objective 2: Roadway Type Analysis (Urban/Suburban /Highway)

Where Objective 1 provides an overall investigation and assessment of the PHEV's on-road emissions and operation, Objective 2 refined its scope to evaluating the effect that roadway type has on the PHEV's operation. Frey et al. (2008) found that velocity, acceleration, and road grade were significant factors when evaluating variations in inter-vehicle emissions. The Sprinter PHEV was specifically designed to excel in urban, stop-and-go traffic by maximizing its electric drive capabilities and, thus, minimizing its total emissions. The study methodologies were purposely designed in order to showcase the PHEV's operation according to different road-types: urban, suburban, and highway. As part of this analysis, roadway-type was defined by geographic location as well as by on-road traffic profile. The PHEV Sprinter's operating characteristics (power scheme and demand, electrical recuperation, and fuel use) and emissions profiles are investigated according to roadway type.

4.2.3 Objective 3: PHEV Operating Mode Analysis

Efficient use of the internal combustion engine, effective utilization of electric drive capacity, and successful integration of the two systems define PHEV proficiency. The PHEV Sprinter was designed to function under two distinct operating modes: charge-sustaining and charge-depleting. Charge-depleting mode is defined by the PHEV's ability to store electrical capacity acquired during grid-based charging periods. The primary objective of charge-depleting operation is to efficiently use the stored battery capacity to provide a significant amount of electric-only operation. Once the battery capacity reaches a moderate state of charge, the PHEV then switches to a more conservative, charge-sustaining power scheme. During charge-sustaining mode, the PHEV functions as a conventional hybrid electric vehicle, by maintaining a nominal battery charge. Electrical recuperation provides electrical drive capacity during charge-sustaining mode, but any excess stored battery potential has already been expired during charge-depleting operation. The Phase I PHEV Sprinter's were designed to achieve 20miles of electric drive capacity with a full charge. However, initial observation of the Kansas City PHEV Sprinter led the field engineer to doubt the KC PHEV's ability to realize 20miles of electric drive during charge-depleting operation. In addition to investigating the PHEV Sprinter's electric-only range during charge-depleting mode (one of the defining features of PHEV technology), nuances in electric-only and hybrid operation between the two operating modes will be investigated in depth.

4.2.4 Objective 4: Diesel Internal Combustion Engine (dICE) as Utilized in the Plug-In Hybrid Vehicle Context

The proof-of-concept Phase I PHEV Sprinter study was one of the first studies presenting diesel hybrid electric vehicles. There are several operating characteristics regarding diesel ICE operation that may or may not be best suited to PHEV application. For example, in cold operating temperatures, it is possible that the diesel oxidation catalyst rarely reaches sufficient operating temperature to effectively control carbon monoxide and hydrocarbon emissions during high state of charge operation (when the diesel engine is only used as needed). Heywood (1988) noted that during transient diesel operation, instances of increased emissions load were likely. The on-demand use of the ICE in the PHEV context could result in an otherwise clean and efficient diesel ICE operating in a mostly transient nature. Sonntag et al. (2008) reported higher particulate matter emissions from diesel hybrid electric buses than conventional diesel buses when the direct oxidation catalyst (DOC) was the only after treatment technology utilized. The 4th objective focuses on the efficacy of using a diesel ICE in the PHEV application according to the KC PHEV Sprinter's on-road behaviors. Collins et al. (2007) reported emissions spikes from diesel engines due to both cold starts and transient events encountered during hot running conditions. Because the potential of encountering both cold starts and transient engine events is high with plug-in hybrid operation, a detailed investigation regarding the behavior of the diesel engine in the application is presented.

4.2.5 Objective 5: PHEV On-Road Vocation Analysis

Drive cycle and vehicle vocation (purpose) have been shown to be significant factors effecting on-road emissions and vehicle behaviors (Clark et al. 2002). The bulk of the studies investigating this have been primarily concerned with the ultimate impact on emissions from a meso- or macro-scale. However, the intricacies behind the differing cycles have not been fully investigated. During preliminary sampling efforts, distinct differences between transit operation (replicated by following or shadowing a transit bus) and normal, civilian driving (solo) were observed. In order to evaluate the differences between transit versus normal on-road operation, the data were investigated on two fronts: on-road behavioral differences (velocity, acceleration and deceleration profiles, and power output), and the impact on the PHEV Sprinter's operation (electric-only range during charge-depleting mode, overall hybrid operation within the two operating modes, regenerative breaking, fuel economy, and emissions loads and profiles).

Chapter 5: Temperature/Auxiliary System Analysis

5.1 Background

Because of project and development delays, the on-road PHEV Sprinter testing spanned from August 2007 through January 2008. Although the impact of ambient temperature and auxiliary system use was not one of the original points of focus for the study, in the end, the final dataset was collected while the PHEV was operated under a wide range of ambient temperature conditions and occasional auxiliary system use (i.e. air conditioning, heater). Since ambient temperature has been shown to have an impact on both the total mass of and chemical composition of vehicle emissions from both gasoline- and diesel-fueled vehicles (Zeilinshak, 2004 and Krishnamurthy and Gautam, 2006), it was deemed necessary to address the potential effect that variations in ambient temperature played on PHEV operation and emissions before the final dataset was filtered for subsequent analysis. While on-road, the PHEV Sprinter's air conditioning and heater were used as minimally as possible, and only employed in order to maintain operator comfort during sampling sessions. However, despite the intent to avoid auxiliary system use, the systems were engaged during some of the PHEV's sampling. Mitigating underlying noise or movement in the final dataset due to potentially confounding influences such as ambient conditions or auxiliary system use will improve the statistical strength of analyses for the final objectives.

A NREL study estimated that using vehicle air conditioning for in use cooling and dehumidifying results in an increased annual fuel use of 7billion gallons in the United States alone (Rugh, 2004). This additional fuel use translates to an approximately 5.5% increase in U.S. fuel demand for light-duty vehicle operation. While this increase in fuel demand may

not be measurable during an on-road emissions study, particularly when compared to uncontrolled noise and fluctuations in actual on-road driving, the demands that air conditioning place on the vehicle could be more significant when assessing auxiliary system impact on PHEV or electric vehicle (EV) operation. During the development of a test procedure to determine the impact of air conditioning use on vehicle operation, John Rugh estimated that air conditioning deployment could reduce the charge-depleting range of a PHEV by 18% to 30% depending on drive cycle (Rugh, 2010). The results in these studies were obtained using highly simulated and exceedingly controlled methods for estimating AC impact, so, while the PHEV Sprinter study, due to its on-road nature, cannot duplicate the laboratory-like results, it is worthwhile dedicating some work to evaluating the impact that air conditioning use may have had on the PHEV Sprinter's Phase I trial.

The study sampling routes had some geographic redundancy so that portions of several routes passed over the same stretch or link of roadway. In order to maximize the available data for this investigation, while attempting to homogenize the impact of roadway and traffic fluctuations, data collected while traveling on specific stretches of 11th street and 10th street were selected for this investigation. This restriction minimized natural variations in PHEV operation due to different road-types (urban, suburban, highway), topographies, and traffic disturbances.

Routes 12, 109, and 110 followed 11th street, traveling west between Paseo Blvd and the Highway 40 underpass, and routes 109 and 110 followed 10th street east from the Highway 71 overpass to Paseo Blvd. Both sections of roadway imposed a constant speed limit of 30mph and were marginally traveled with no traffic delays aside from one stoplight on 11th Street. The average distance traveled on the selected 11th Street link was, nominally,

715m, and the selected portion of 10th Street spanned 725m. Both streets run parallel to each other, separated by one city block. Aside from a single traffic light at 11th Street and Troost Road there were no traffic lights or stop signs to impede on-road progress. Traffic congestion while traveling 11th street was minimal, so the traffic signal rarely influenced the PHEV's driving patterns. With identically posted speed limits, and similar local topography, these roadway links were assumed to be the most consistent and controlled for the purposes of this analysis. Because of this, the 10th and 11th street data were compiled into a single dataset for the initial analysis in order to increase the statistical power of the investigation. Figures 5.1 and 5.2, below provide a map of the 10th and 11th street links as well as each link's topography for the distance being evaluated.

Figure 5.1: Map of 10th and 11th Street links.

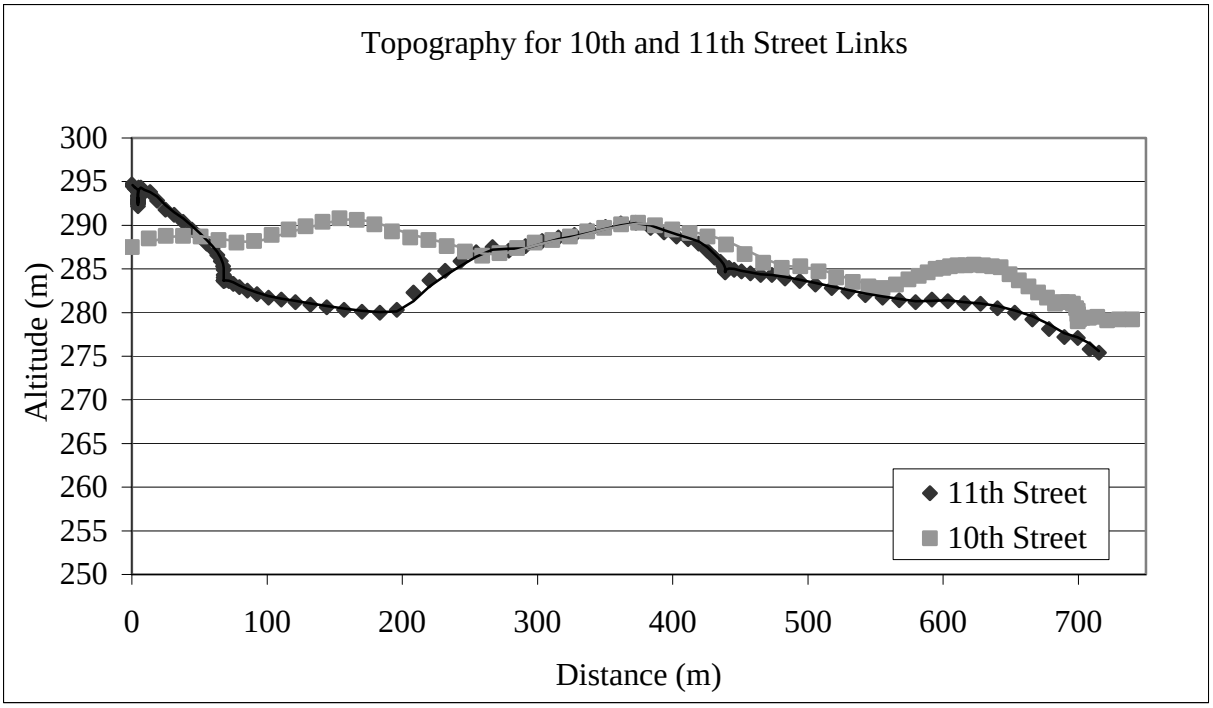

Figure 5.2: Topography for 10th an 11th Street links.

The impact of ambient temperature and auxiliary system use was evaluated while the PHEV was operating in charge-sustaining (hybrid) mode. Insufficient data was collected during charge-depleting operation to be able to expand this analysis to both PHEV operating modes. The datasets selected for this analysis were categorized according to auxiliary system use: air conditioning use during the entire run, heater use during the entire run, or no system in use during the entire run. Datasets presenting link travel with partial system use were not included in this analysis. Since auxiliary system use was dependent on operator comfort, a definite link exists between system use and auxiliary temperature. Table 5.3 in the following section details the temperature range for each system use as employed by the PHEV operator.

5.2 Ambient Temperature/Auxiliary System Impact Analysis

The continuous on-road emissions and operating data collected by the Semtech-DS and PHEV Sprinter's data-logging module (DLM) were categorized and aggregated for the sections of roadway being considered. By compiling the continuous, second-by-second data into calculated averages for specific roadway links, any autocorrelation and lack of normality apparent in the continuous dataset was negated, and parametric statistical tests deemed acceptable.

Analysis of variance (ANOVA) conducted on the data (compiled from both 10^{th} and 11^{th} street links) shows that auxiliary system use is a statistically significant factor ($\alpha<0.05$) for the diesel internal combustion engine (dICE) power output, normalized for distance traveled, W/kg·km, ($p=0.044$), with air conditioning employment resulting in higher power demands from the ICE. The same analysis on the electric motor (EM) did not yield statistically significant differences between EM power output according to auxiliary system use (air conditioning, heater, or no system). However, since the PHEV Sprinter was operating in charge-sustaining mode (hybrid operation), it is likely that the dICE was preferentially employed to handle overages in power demand due to AC use.

Table 5.1: Power output according to auxiliary system use for compiled dataset of both links 10th street and 11th street.

	ICE Power (W/kg×km)			
System	**N**	**Mean**	**St. Dev.**	**P**
AC	24	526.7	296.5	0.044
Heater	6	258.0	291.9	
None	18	353.1	239.0	
	EM Power (W/kg×km)			
System	**N**	**Mean**	**St. Dev.**	**P**
AC	24	147.3	150.4	0.300
Heater	6	233.2	136.6	
None	18	204.9	146.4	
	Total Power (W/kg×km)			
System	**N**	**Mean**	**St. Dev.**	**P**
AC	24	674.0	214.6	0.115
Heater	6	491.2	272.3	
None	18	558.7	223.5	

While originally expected to be similar, significant differences appeared between the power output (on a per kilometer basis) required to travel 10th street versus 11th street, with 11th street requiring an average of 731.1W/kg·km total power output while 10th street only required an average of 402.6W/kg·km. Power output proved to be a statistically significant response to traveled street when the analysis of ICE and EM power output were performed separately ($p=0.000$, $p=0.018$, and $p=0.007$ for Total Power, EM Power, and ICE Power, respectively). Despite having similarly distributed traffic schemes and identically imposed speed limits, ANOVA analysis shows a statistically significant difference between the average velocity traveled along 10th and 11th streets ($p=0.045$), with 10th street travel resulting in an average velocities more than 15% greater than 11th street (mean velocities of 35.5km/h and 30.3km/h for 10th and 11th street links, respectively). Some of the components of the PHEV's exhaust emissions also demonstrated a statistically significant response to

roadway link with carbon dioxide, carbon monoxide, and total hydrocarbon emissions varying between the 10^{th} street and 11^{th} street links (Table 5.2).

Similar to power output and velocity, some of the measured emissions did show a statistically significant ($\alpha<0.05$) response to link traveled. Based on ANOVA analysis, carbon dioxide, carbon monoxide, and total hydrocarbon emissions are significant responses to the specific link being traveled (10^{th} Street versus 11^{th} Street). Despite roadway similarity as determined by link characteristics (speed limit, topography, traffic signals) and operator observation (traffic density and behavior), substantial differences emerged between the links traveled. It is likely that differences in link topography and/or the impact of vehicle operation according to the point in the "sample run" that the on-road data was extracted from (i.e. at the very beginning versus in the middle of the sample run) resulted in the discrepancy in PHEV operation between two seemingly similar links.

Table 5.2: ANOVA results showing the response of emissions to link.

	CO_2 (g/m)			
Link	**N**	**Mean**	**St. Dev.**	**P**
10th	17	0.244	0.251	0.049
11th	30	0.393	0.239	
	CO (g/m)			
Link	**N**	**Mean**	**St. Dev.**	**P**
10th	17	1.477E-04	1.810E-04	0.043
11th	30	4.696E-04	6.199E-04	
	NO (g/m)			
Link	**N**	**Mean**	**St. Dev.**	**P**
10th	17	2.242E-03	2.295E-03	0.090
11th	30	3.372E-03	2.062E-03	
	NO_2 (g/m)			
Link	**N**	**Mean**	**St. Dev.**	**P**
10th	17	3.950E-04	5.634E-04	0.916
11th	30	3.769E-04	5.563E-04	
	NOx (g/m)			
Link	**N**	**Mean**	**St. Dev.**	**P**
10th	17	2.638E-03	2.729E-03	0.155
11th	30	3.749E-03	2.412E-03	
	HC (g/m)			
Link	**N**	**Mean**	**St. Dev.**	**P**
10th	17	6.600E-06	8.780E-06	0.015
11th	30	3.235E-05	4.141E-05	

Logistically, the data collected on the 10th and 11th streets were systematically different due to how and when the PHEV traveled each roadway. Tenth street data were collected as a continuous part of a larger sampling route as the vehicle was traveling east out of and away from Kansas City's urban core, whereas the 11th street data were always collected at the beginning of a sampling run, immediately after a short respite for Semtech zeroing or start of the day calibration. Short periods of vehicle shutdown could result in significantly different use of the internal combustion engine versus the electric motor.

Because of the discrepancy between PHEV power output when traveling 10th street versus 11th street, the "ambient temperature and auxiliary system use" investigation was conducted evaluating data from each street independent from the other.

ANOVA analysis of 10th street data does not reveal a statistically significant difference, at $\alpha<0.05$, between ICE, EM, and total power output under different auxiliary system configurations (the air conditioning on, heater on, or no system use). However, loosening the alpha requirement slightly ($\alpha<0.10$) yields a statistically significant difference in ICE power output and total power output according to auxiliary system use. Despite the lack of statistical significance at $\alpha<0.05$, qualitative differences are apparent between the power output required to travel 10th street under the use of different auxiliary systems. Air conditioning use required more power output from the internal combustion engine than using the heater or no system at all.

The same analysis for the 11th street data showed no difference between the power outputs required for different auxiliary system use ($p=0.797$ for total power, $p=0.551$ for dICE power, and $p=0.459$ for EM power output). ANOVA analysis limited to evaluating the impact of only heater use (versus no system use) did not yield statistically significant differences between power requirements with or without the PHEV's heater. Since little to no difference was apparent between the power demands for no system use and heater use, the ANOVA tests were restructured to evaluate air conditioning use versus no air conditioning use.

Table 5.3: Temperature ranges over which different auxiliary system configurations occurred.

System use	Temperature Range	Mean Ambient Temperature
No System	44-61°F	49.6°F
Air Conditioning	65-102°F	82.5°F
Heater	49-51°F	50.3°F

Table 5.4: 10th street ANOVA results.

10th Street

	ICE Power (W/km)			
System	**N**	**Mean**	**St. Dev.**	**P**
AC	8	454.0	296.9	
Heater	3	73.6	127.5	0.054
None	7	186.1	207.6	
	EM Power (W/km)			
System	**N**	**Mean**	**St. Dev.**	**P**
AC	8	74.1	104.0	
Heater	3	196.4	78.3	0.216
None	7	128.0	102.4	
	Total Power (W/km)			
System	**N**	**Mean**	**St. Dev.**	**P**
AC	8	528.1	251.6	
Heater	3	270.1	56.4	0.071
None	7	316.0	127.4	

Table 5.5: 11th Street ANOVA results.

11th Street

System	ICE Power (W/km) N	Mean	St. Dev.	P
AC	16	563.0	299.1	
Heater	3	442.3	307.9	0.551
None	11	459.4	198.2	
System	**EM Power (W/km) N**	**Mean**	**St. Dev.**	**P**
AC	16	184.0	159.0	
Heater	3	270.0	190.9	0.459
None	11	253.8	152.9	
System	**Total Power (W/km) N**	**Mean**	**St. Dev.**	**P**
AC	16	747.0	155.1	
Heater	3	712.3	188.6	0.797
None	11	713.2	87.8	

The resulting emissions for each link were investigated in a similar manner as the power output. ANOVA analysis indicated that both carbon dioxide (CO_2) and nitrogen dioxide (NO_2) emissions, evaluated as gram emitted per kilometer traveled, were statistically significant responses to auxiliary system utilization, with air conditioning usage resulting higher overall average emissions. Similarly, Broderick et al., 1995, reported significantly higher vehicle emissions of CO_2, NOx, and HC during periods of air conditioning employment. All other pollutants (carbon monoxide, CO, nitric oxide, NO, and total hydrocarbon, HC) did not demonstrate a significant relationship to auxiliary system use, although more lenient criteria for alpha ($\alpha<0.10$) would result in statistical significance with carbon dioxide emissions as well. Regardless of statistical significance, aside from hydrocarbon emissions, quantitatively, AC use resulted in higher average emission of measured pollutants. As a result of transient dICE operation, HC emissions are a function of

PHEV dominant control scheme. It is likely that the PHEV's dICE utilization is a larger dictator of HC emissions than auxiliary system use.

Table 5.6: Compiled 10th and 11th street link ANOVA results specifying emissions (g/m) as a response to auxiliary system use (factor).

	CO_2 (g/m)			
System	**N**	**Mean**	**St. Dev.**	**P**
AC	23	0.422	0.268	
Heater	6	0.204	0.236	0.066
None	18	0.277	0.204	
	CO (g/m)			
System	**N**	**Mean**	**St. Dev.**	**P**
AC	23	4.247E-04	6.251E-04	
Heater	6	1.059E-04	1.530E-04	0.426
None	18	3.420E-04	4.597E-04	
	NO (g/m)			
System	**N**	**Mean**	**St. Dev.**	**P**
AC	23	3.455E-03	2.243E-03	
Heater	6	1.978E-03	2.148E-03	0.264
None	18	2.664E-03	2.096E-03	
	NO_2 (g/m)			
System	**N**	**Mean**	**St. Dev.**	**P**
AC	23	6.497E-04	6.944E-04	
Heater	6	1.465E-04	1.611E-04	0.003
None	18	1.223E-04	8.550E-05	
	NOx (g/m)			
System	**N**	**Mean**	**St. Dev.**	**P**
AC	23	4.105E-03	2.759E-03	
Heater	6	2.124E-03	2.307E-03	0.118
None	18	2.786E-03	2.160E-03	
	HC (g/m)			
System	**N**	**Mean**	**St. Dev.**	**P**
AC	23	1.735E-05	2.123E-05	
Heater	6	1.200E-05	1.605E-05	0.242
None	18	3.398E-05	5.049E-05	

When the roadway links were analyzed independently from one another, NO_2 emissions showed a statistically significant response to auxiliary system use for the 10th street data, but no pollutants were statistically significant responses to system use when traveling along the 11th street link ($\alpha<0.05$). If, however, the p-value constraints dictating statistical significance were relaxed so that statistical significance were established with a more liberal $\alpha<0.10$, then carbon dioxide, carbon monoxide, and nitrogen dioxide emissions would also be significant responses to auxiliary system use for the 10th street link. However, except for nitrogen dioxide, no pollutant emissions would demonstrate statistical significance according to auxiliary system use for the 11th street link.

Table 5.7: ANOVA results for pollutant emissions according to auxiliary system use for each link.

	10th Street Link				11th Street Link			
	CO_2 (g/m)				CO_2 (g/m)			
System	N	Mean	St. Dev.	P	N	Mean	St. Dev.	P
AC	7	0.404	0.283	0.064	16	0.430	0.270	0.672
Heater	3	0.060	0.105		3	0.347	0.259	
None	7	0.162	0.171		11	0.351	0.194	
	CO (g/m)				CO (g/m)			
System	N	Mean	St. Dev.	P	N	Mean	St. Dev.	P
AC	7	2.562E-04	2.352E-04	0.092	16	4.984E-04	7.293E-04	0.728
Heater	3	2.050E-05	3.490E-05		3	1.913E-04	1.882E-04	
None	7	9.370E-05	8.010E-05		11	5.036E-04	5.352E-04	
	NO (g/m)				NO (g/m)			
System	N	Mean	St. Dev.	P	N	Mean	St. Dev.	P
AC	7	3.341E-03	2.573E-03	0.209	16	3.505E-03	2.174E-03	0.935
Heater	3	7.070E-04	1.225E-03		3	3.249E-03	2.277E-03	
None	7	1.802E-03	2.028E-03		11	3.212E-03	2.036E-03	
	NO_2 (g/m)				NO_2 (g/m)			
System	N	Mean	St. Dev.	P	N	Mean	St. Dev.	P
AC	7	8.196E-04	6.898E-04	0.021	16	5.754E-04	7.054E-04	0.104
Heater	3	4.910E-05	8.430E-05		3	2.439E-04	1.712E-04	
None	7	1.187E-04	9.420E-05		11	1.246E-04	8.420E-05	
	NOx (g/m)				NOx (g/m)			
System	N	Mean	St. Dev.	P	N	Mean	St. Dev.	P
AC	7	4.160E-03	3.126E-03	0.127	16	4.081E-03	2.693E-03	0.733
Heater	3	7.560E-04	1.309E-03		3	3.492E-03	2.446E-03	
None	7	1.921E-03	2.108E-03		11	3.336E-03	2.100E-03	
	HC (g/m)				HC (g/m)			
System	N	Mean	St. Dev.	P	N	Mean	St. Dev.	P
AC	7	7.842E-06	1.017E-05	0.685	16	2.152E-05	2.364E-05	0.172
Heater	3	2.440E-06	4.227E-06		3	2.156E-05	1.876E-05	
None	7	7.138E-06	9.225E-06		11	5.106E-05	5.800E-06	

Because the PHEV's air conditioning and heater were only used to maintain operator comfort throughout the study period, their use was directly dictated by ambient temperature. It is not possible to truly discern between the effect of ambient temperature versus auxiliary system employment with regards to the PHEV's operation and emissions. Hybrid electric vehicle (HEV) fuel economy has been shown to be a function of ambient weather conditions, demonstrating a proportional relationship between fuel economy and ambient temperature

(Fontaras, 2008). Smokers, et al. found that a minute increase in ambient temperature (from 23˚C to 27˚C) resulted in a 7% fuel economy increase. However, when coupled with the decrease in fuel economy associated with air conditioning use, the true effect of ambient temperature on HEV fuel economy is more difficult to discern in real world, on-road studies where air conditioning use naturally occurs with increased ambient temperature. To some degree, the impacts of each phenomenon negate each other. In the case of the PHEV Sprinter's limited on-road dataset, it is impossible to completely separate the effect of ambient temperature versus auxiliary system use.

Correlations performed on engine power output (ICE, EM, and Total), as well as on emissions were used as a final statistical method to evaluate the impact of ambient temperature. While system use is definitely related to temperature (air conditioning use occurred at temperatures between 65-102°F, with a mean of 82.5°F, and heater use occurred at temperatures between 49-51°F, with a mean of 50.3°F, while the temperature range when no system was required was 44-61°F, with a mean of 49.6°F), investigating the impact of ambient temperature provides a more continuous scale rather than the three discrete auxiliary-system categories. While on-road sampling throughout the study occurred at a much wider range of temperatures than evaluated here, this analysis was limited to charge-sustaining operation when the PHEV was traveling the selected 10^{th} and 11^{th} street links.

Ambient temperature is weakly positively correlated with ICE operation and less so with total power output ($\alpha<0.05$). Electric motor use did not provide a statistically significant correlation with ambient temperature. Even if the alpha restrictions were lessened to allowing significance at alpha<0.10, the Pearson's correlation coefficient between EM power output and ambient temperature is very weak at best.

Table 5.8: Correlation between ICE, EM, and Total power (on a per km basis), and ambient temperature.

		ICE Total (W/kg/km)	EM Total (W/kg/km)	Total Power (W/kg/km)
EM Total (W/kg/km)	Pearson Correlation	-0.623		
	P-Value	0.000		
Total Power (W/kg/km)	Pearson Correlation	0.867	-0.151	
	P-Value	0.000	0.311	
Ambient Temperature (˚F)	Pearson Correlation	0.418	-0.251	0.367
	P-Value	0.003	0.089	0.011

As intuitively expected, power (ICE, EM, and total) correlated with all emissions (except for total hydrocarbon emissions). The correlations presented here were performed on data collected only on the specified links during charge-sustaining operation, and are, thus, not necessarily equivalent to similar correlation analysis of the entire PHEV on-road dataset. Unlike a conventional vehicle, the PHEV can operate using its electric motor alone, its internal combustion engine alone, or a hybridization of both engines. Because of this, the diesel engine routinely turns on and off during normal operation. The presence of several "cold-starts" during a normal operating cycle has emissions implications for the PHEV that are not at issue with a conventional vehicle. This phenomenon is of interest and will be investigated in future analyses.

Ambient temperature is significantly positively correlated with CO and less significantly with HC emissions, however, no statistical significance was present in the correlation results between ambient temperature and the other measured pollutants for the dataset evaluated here.

Table 5.9: Correlation between emissions (on a per km basis), and ambient temperature.

		CO_2 (g/km)	CO (g/km)	NO (g/km)	NO_2 (g/km)	NOx (g/km)	HC (g/km)
CO (g/km)	Pearson Correlation	0.321					
	P-Value	0.194					
NO (g/km)	Pearson Correlation	0.978	0.166				
	P-Value	0.000	0.509				
NO2 (g/km)	Pearson Correlation	0.722	-0.066	0.748			
	P-Value	0.001	0.794	0.000			
NOx (g/km)	Pearson Correlation	0.977	0.159	1.000	0.765		
	P-Value	0.000	0.529	0.000	0.000		
HC (g/km)	Pearson Correlation	0.397	0.939	0.262	-0.006	0.254	
	P-Value	0.103	0.000	0.293	0.980	0.309	
Ambient Temp (˚F)	Pearson Correlation	-0.248	0.583	-0.377	-0.382	-0.381	0.458
	P-Value	0.322	0.011	0.123	0.118	0.119	0.056

5.3 Conclusions

While PHEV emissions and power output were not universally impacted (in a statistically significant manner) by temperature or auxiliary system operation, some of the measured variables did show a statistically significant response to ambient temperature and auxiliary system use. Because of this potentially confounding issue, all subsequent analyses are conducted using on-road data collected when no auxiliary system was in operation, and the ambient temperature range was, consequently, more moderate. Appendix C provides the comprehensive tables detailing the PHEV Sprinter's emissions and power output during different auxiliary system employment used in the previous discussion.

Chapter 6: Vehicle Specific Power Modal Analysis

6.1 Background and Introduction

Vehicle specific power (VSP) has become a prevalent tool for both analyzing and modeling on-road and on-road simulated vehicle emissions and operation. As a proxy calculation for estimating instantaneous road load, VSP is an important factor for intuitively evaluating a vehicle's on-road behavior. Inclusive of both on-road driving variables (such as velocity and acceleration) as well as physical characteristics impacting the vehicle's movement through space (i.e. road grade, drag, rolling resistance, etc.), VSP has proven to be more powerful at predicting vehicle emissions than using measured velocity and acceleration alone (Frey et al., 2007). Since the U.S. EPA has incorporated VSP into mobile model development, it was important that the initial investigation into the Sprinter PHEV's on-road behavior be focused on VSP. A basic VSP exploration will give insight into the suitability of plug-in hybrid technology as applied to current modeling techniques.

The VSP calculation requires an assessment of grade, which in this case was garnered from local altitude measured by the GPS unit. Holes in the GPS data where satellite signal was lost, largely due to building obstruction in Kansas City's downtown district, were present on the 109 and 12T/C routes. For this initial vehicle specific power (VSP) analysis, lost values were removed from the dataset. Additionally, all idle data at the beginning and end of each run were removed from the selected datasets. Superfluous data that was inadvertently collected before and after the PHEV Sprinter began its sample routes are the result of the operator's documentation practices at the start and end of each route, and are, therefore, not pertinent to the PHEV's normal on-road operation

Although not statistically conclusive for all measured emissions pollutants and all power schemes, there exists at least a small role between ambient temperature (and/or auxiliary system use) and the PHEV's operation and emissions. While the results from the PHEV on-road dataset are statistically fragmented, past research has conclusively shown that vehicle fuel use and emissions fluctuate according to both changes in ambient temperature and air conditioning use (Frey et al, 2003, Zhai and Frey, 2008, Krishnamurthy and Gautam, 2006, and Rugh, 2010). For this reason, the datasets used for the VSP analysis were limited to those that were collected while the PHEV was operating during marginal (40˚F to 66˚F) ambient temperatures and while no auxiliary system was in use. Basic initial analysis shows that the PHEV fuel use and emissions were significantly impacted by the on-road drive scheme (shadowing an in-service transit bus or civilian driving according to normal traffic flow), so only data collected during civilian (solo) driving was selected for use here. A thorough investigation into the effect that drive-scheme or vocation had on PHEV operation and emissions will be presented in subsequent chapters. Ultimately, forty-five data files from routes 12T/C, 109, 123, 110, and Highway met the set criteria and served as the basis for the VSP analysis. These files represent over 21hours and more than 540km of on-road data collection.

PHEV operation occurs within one of two distinct operating modes (charge-depleting or charge-sustaining), with two different control schemes dictating power output for each. Because of the significant differences in diesel internal combustion engine (dICE) versus electric motor (EM) utilization between charge-depleting and charge-sustaining modes, the selected data files were segregated according to mode and analyzed independently.

Using the calculation methods presented earlier in Chapter 3, instantaneous VSP was determined for every second of data collection on the selected routes. Continuous VSP data were categorized into 8 unique VSP bins and four distinct driving modes (idle, acceleration, deceleration, cruise) for independent analysis. The VSP binning approach was developed for heavy-duty vehicles, and the VSP range criteria for binning are presented in Table 6.1 below (Frey, 2008).

The data were also subjected to a secondary categorization technique based on the PHEV's active drive-mode at of every second of data measurement. Developed by the North Carolina State University for the U.S. EPA, the drive-mode categorization defines a vehicle's on-road behavior according to four distinct behaviors: cruising, acceleration, deceleration, and periods of idling (EPA, 2002). The requirements for defining the different driving modes were determined by the North Carolina State University for the U.S. EPA, and are supplied in Table 6.2 (EPA, 2002).

Table 6.1: VSP Bin definitions.

VSP Mode	VSP Range (W/kg)
1	$VSP \leq 0$
2	$0 < VSP < 2$
3	$2 \leq VSP < 4$
4	$4 \leq VSP < 6$
5	$6 \leq VSP < 8$
6	$8 \leq VSP < 10$
7	$10 \leq VSP < 13$
8	$VSP \geq 13$

Table 6.2: Driving mode criteria.

Driving Mode	Velocity and Acceleration Criteria
Idle	Velocity = 0m/s Acceleration=0m/s^2
Cruise	All else
Acceleration	Velocity > 0m/s **&** Acceleration > 0m/s^2 **AND** Acceleration > 2 m/s^2 **OR** Acceleration > 1 m/s^2 for 3consecutive seconds
Deceleration	Velocity > 0m/s **&** Acceleration < 0m/s^2 **AND** Acceleration < -2 m/s^2 **OR** Acceleration < -1 m/s^2 for 3consecutive seconds

6.2 VSP Bin and Drive Mode Distribution of On-Road PHEV Data

Five routes were selected for this analysis: 12T/C, 109, 110, 123, and Highway. The PHEV Sprinter dataset showed significantly better representation using the 8-bin VSP model developed for heavy-duty vehicles than the 14-bin light-duty model developed by NCSU in 2002. When segregated according to the 14-bin model, the PHEV data severely under-represented the top three VSP bins, so the 8-bin categorization was selected in the interest of more evenly distributed data representation across all bins. Despite this, the majority of the PHEV's on-road time was spent in VSP bin 1 for all routes evaluated. Bar charts showing the bin and mode distribution for each route each are located below. The charts were compiled for the entire on-road dataset (both charge-sustaining and charge-depleting operation) selected according to temperature and auxiliary system mandates.

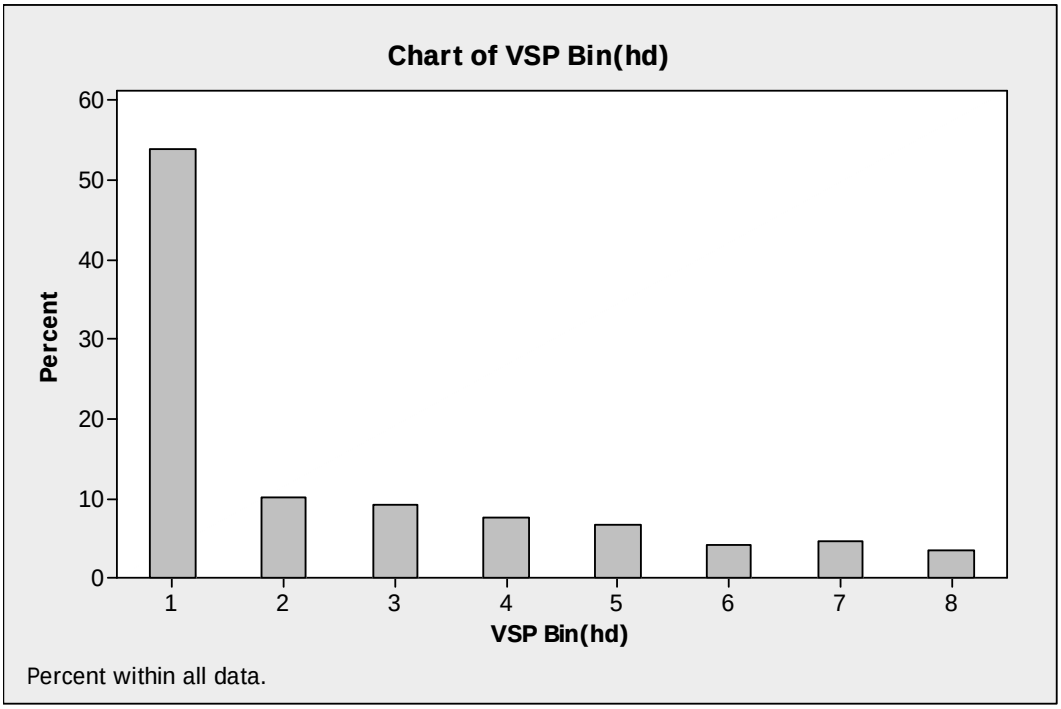

Figure 6.1: VSP bin distribution on 12T/C route.

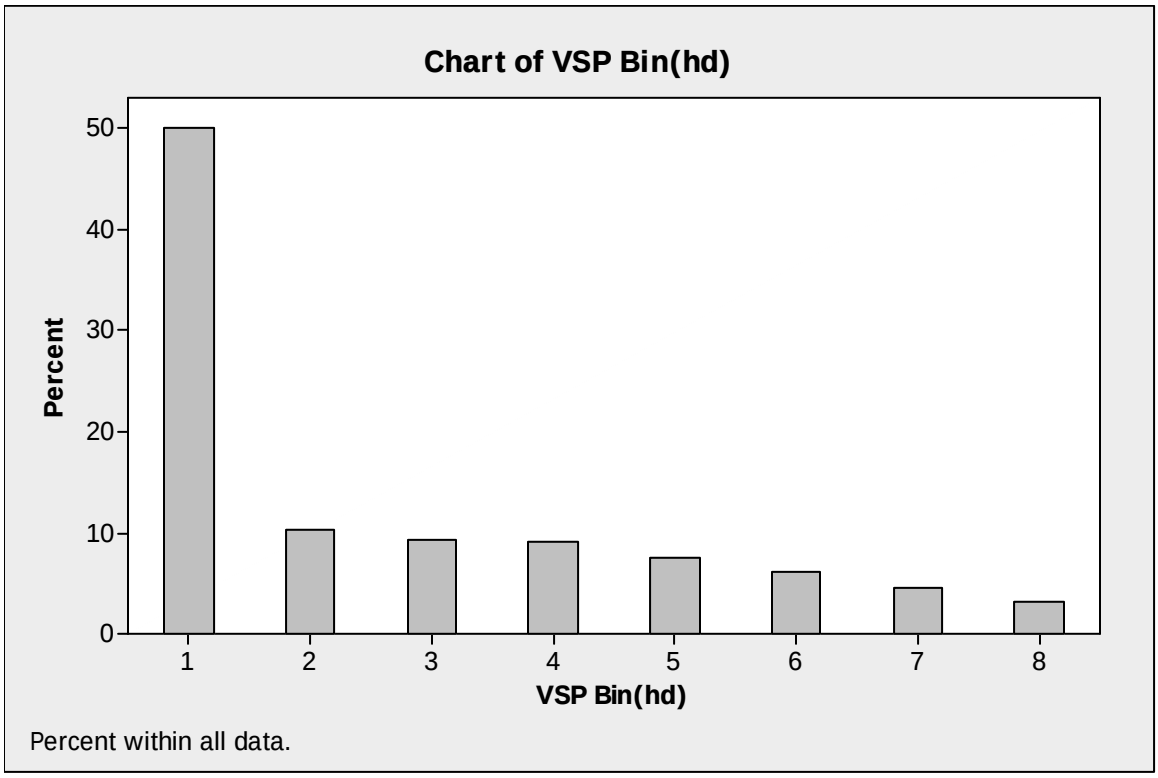

Figure 6.2: VSP bin distribution on route 109.

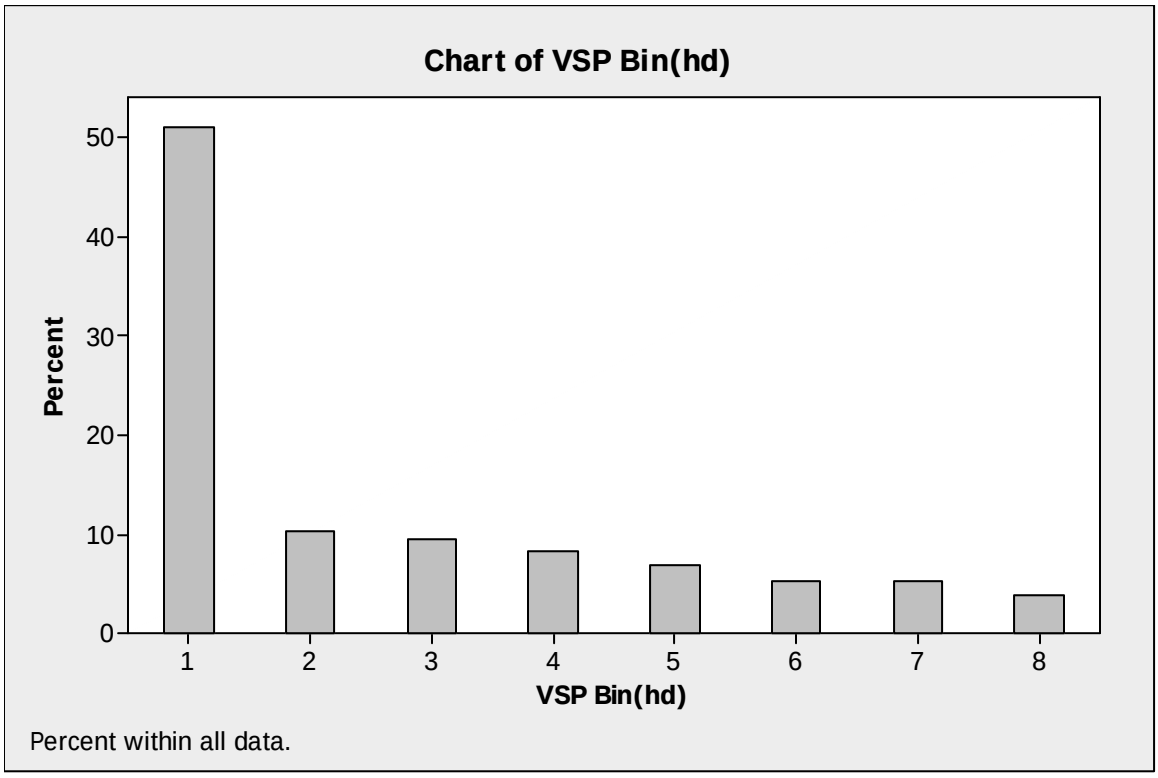

Figure 6.3: VSP Bin distribution for route 110.

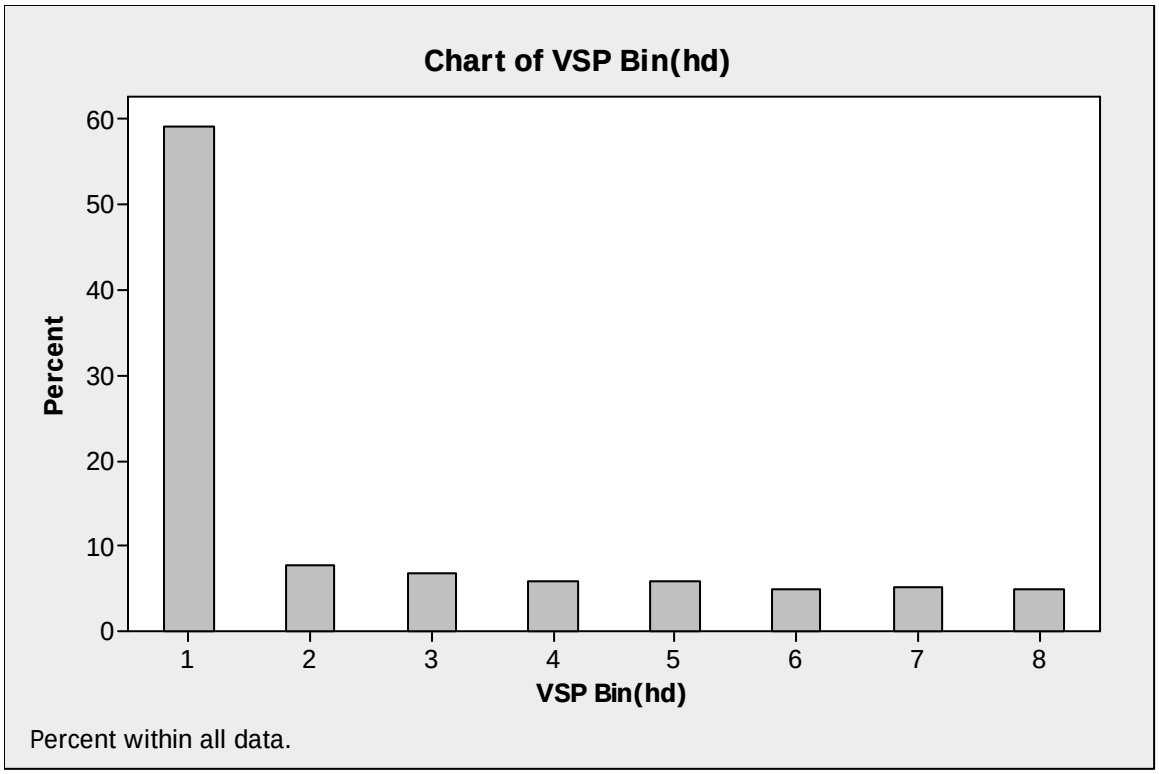

Figure 6.4: VSP Bin Distribution for route 123.

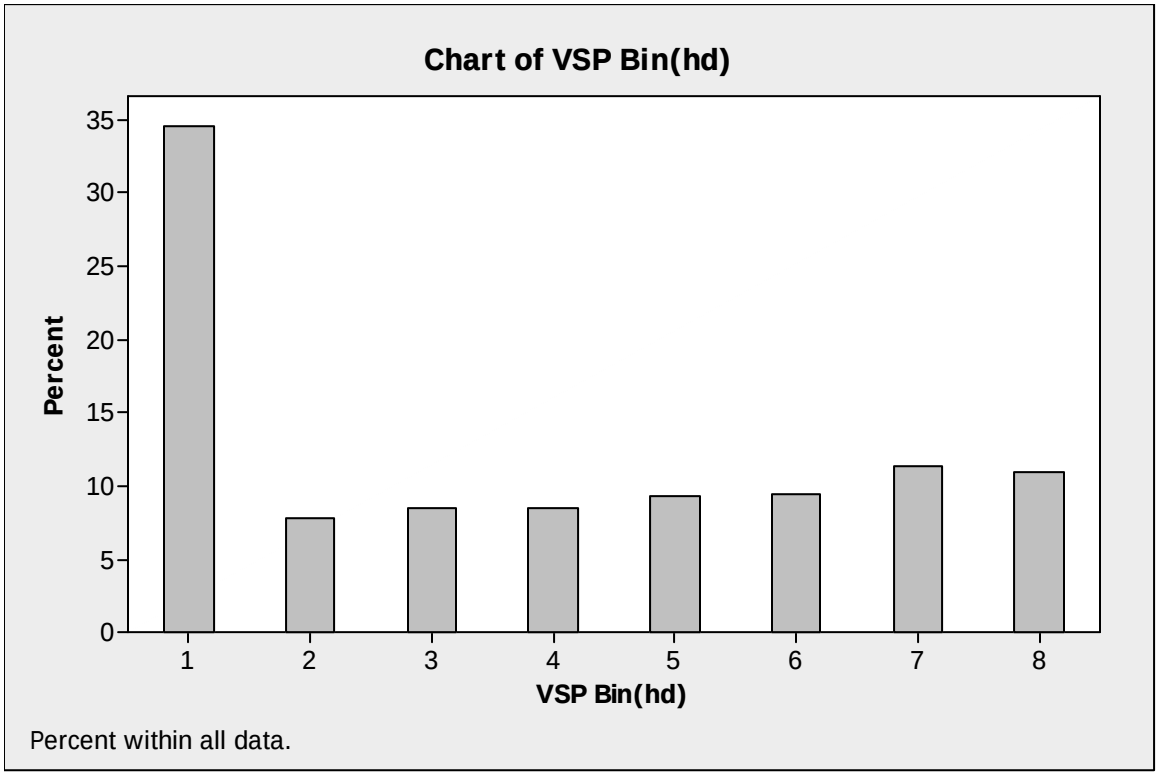

Figure 6.5: VSP Bin distribution for the Highway route.

VSP bin distribution was similar for all sampled routes. The majority of the on-road time occurred in the first VSP bin, with a relatively even distribution of on-road driving occurring through the remaining 7 bins. Aside from a heavy presence of VSP Bin 1 throughout the data (over 50% of the time on-road for routes 12, 109, 110, and 123, and almost 35% of the sample time on the Highway route), all bins were sufficiently represented in order to accept the 8-bin, Heavy-Duty Vehicle VSP Binning methodology.

Driving mode distribution demonstrated a similar profile across the driven routes as well. The PHEV Sprinter operated in cruise mode for the majority of the sampling period for all routes. This is likely attributable to the disproportionate amount of suburban roadway (versus urban) traveled in each designated route. Time spent in periods of acceleration and deceleration were similar for each route (nominally, 10-20% each), while the amount of idle time fluctuated across the routes, with the highly suburban-based 123 route possessing the largest percentage of idle time (25%). The highway route, as expected, traveled in cruising mode 75% of the time, with the remainder of the time evenly divided between periods of acceleration (8.5%), deceleration (8.3%), and idle (8.2%).

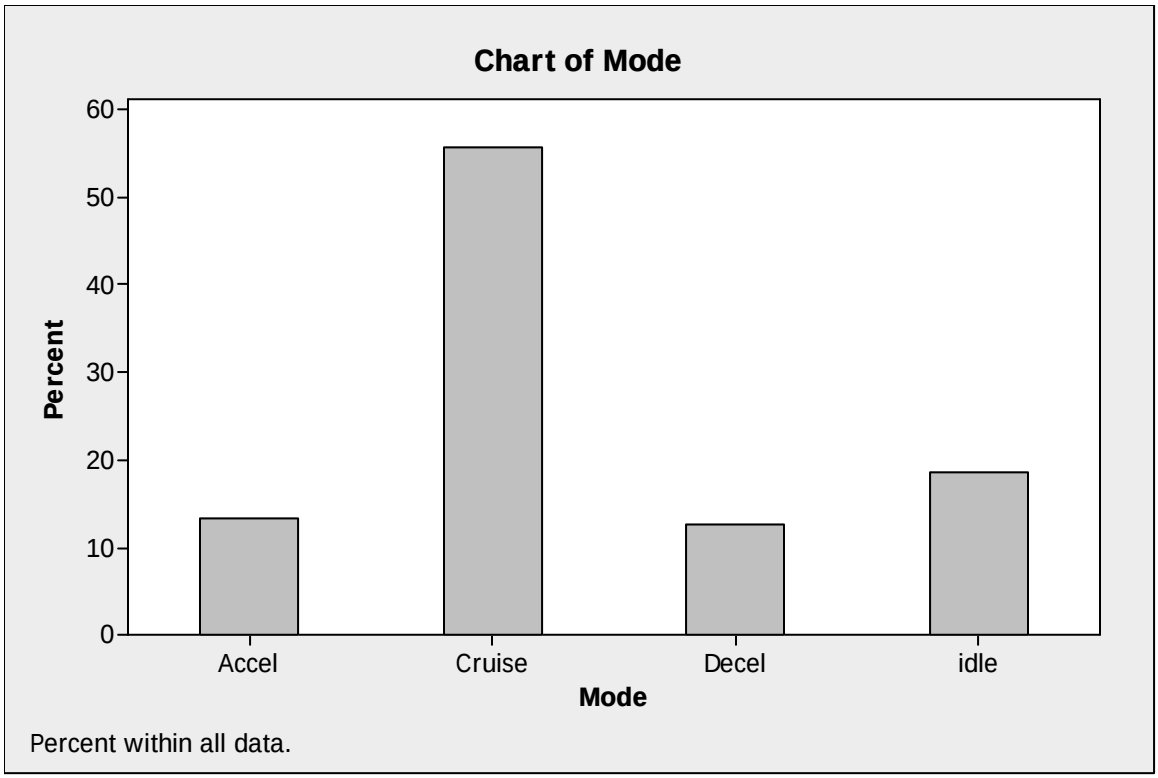

Figure 6.6: Modal distribution for 12T/C route.

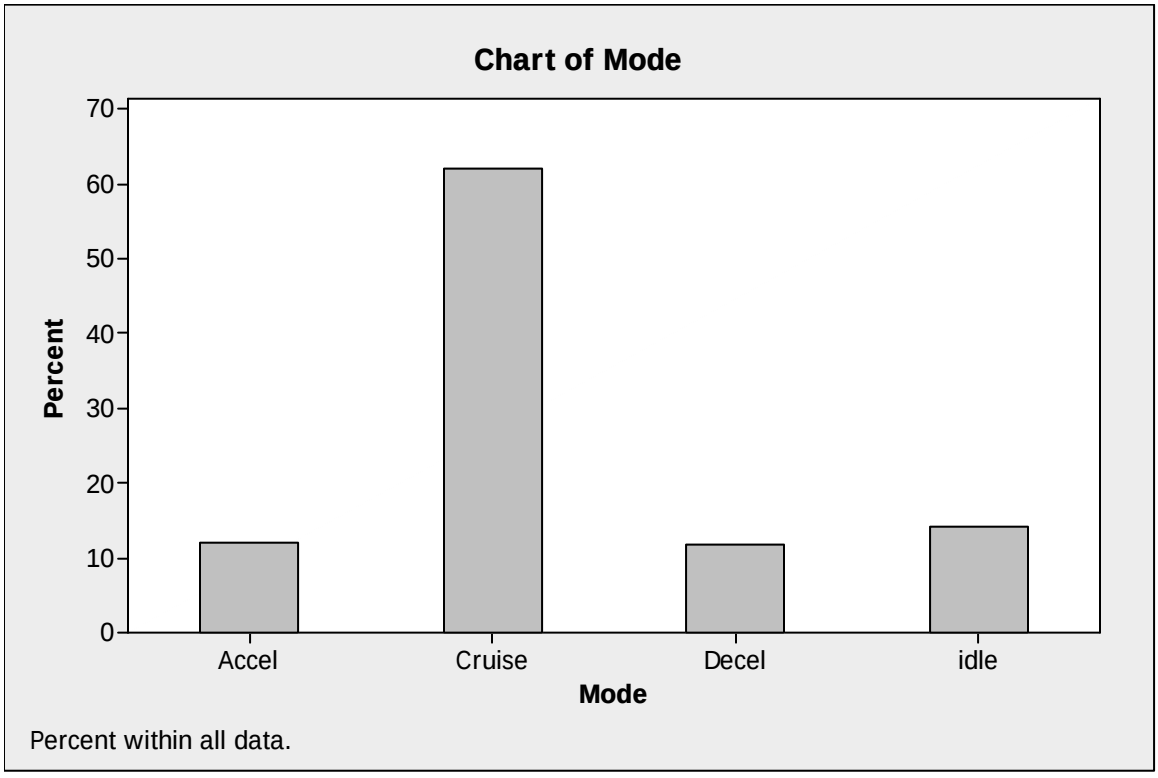

Figure 6.7: Modal distribution for the 109 route.

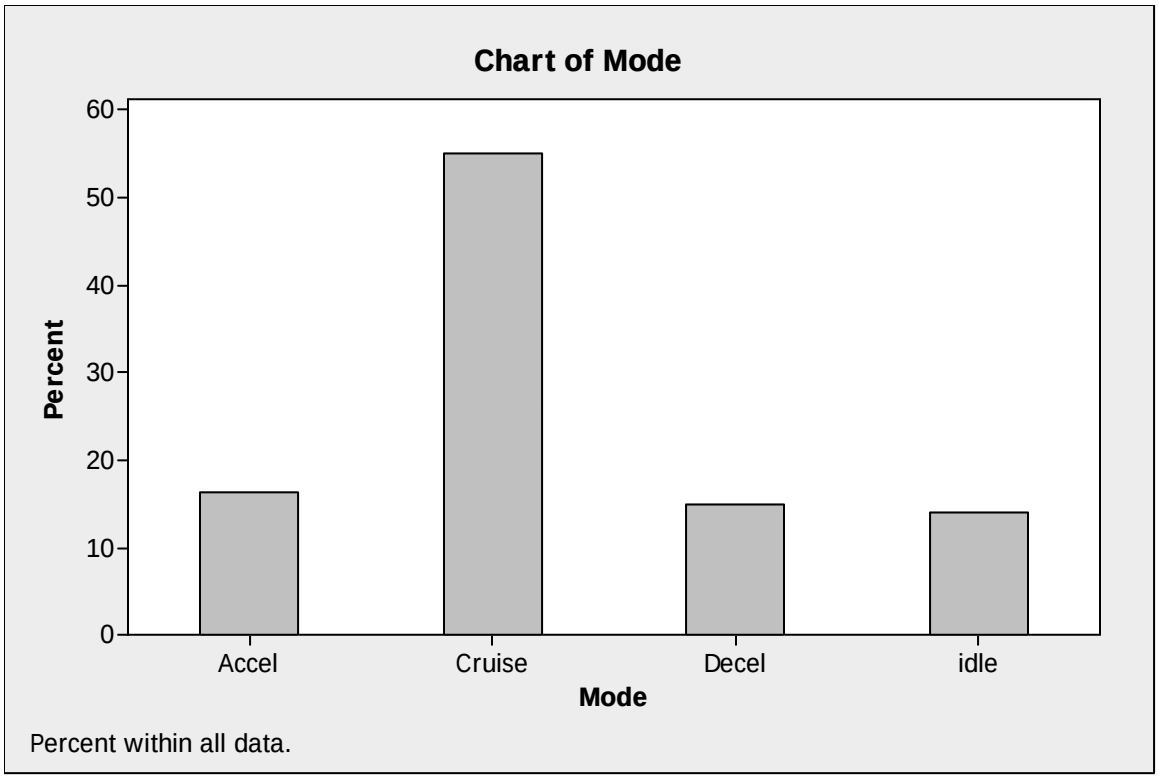

Figure 6.8: Modal distribution for route 110.

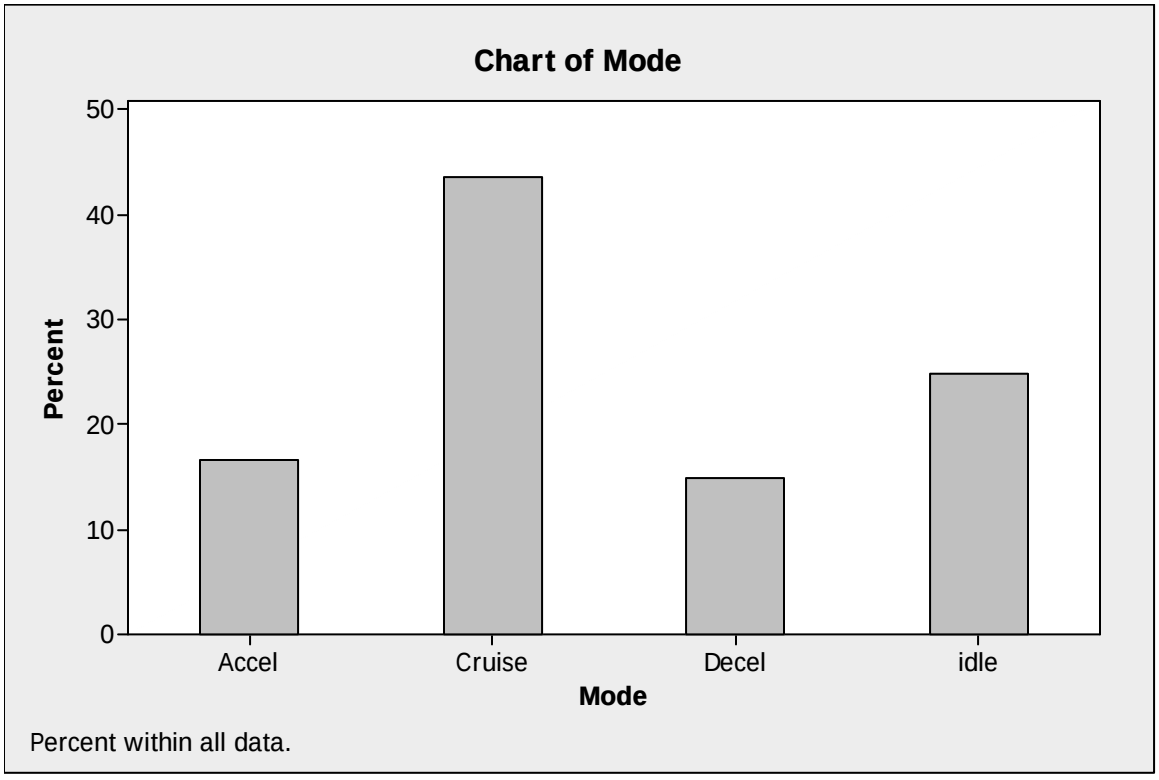

Figure 6.9: Modal distribution for route 123.

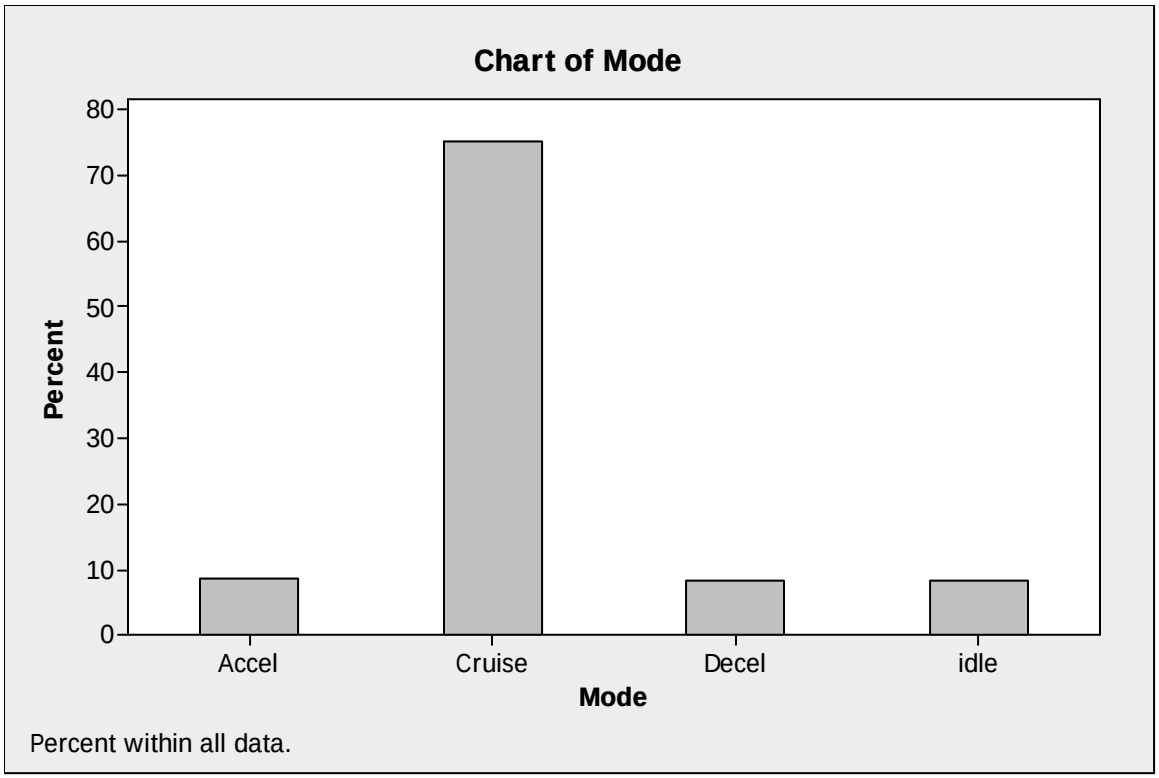

Figure 6.10: Modal distribution for the Highway route.

Comparable patterns in VSP Bin and driving mode were also present when assessed on a distance-traveled basis. The following table details the percentage of distance traveled within each VSP bin for the period of time that the PHEV was operating in charge-sustaining mode. Routes 109, 110, and 12T/C had similar geographic and roadway profiles, possessing similar distances of urban and suburban travel. Similar percent-traveled profiles across all 8-VSP bins are evidence of the comparable nature of these routes. Route 123, however, traveled exclusively on what is defined by this study as suburban roadways, with no presence near the Kansas City urban core. As a consequence of this, the PHEV traveled proportionally longer distances while operating in the upper VSP bins due to this route's higher posted speed limit. The Highway route was specifically selected to demonstrate the PHEV Sprinter's operation at higher speeds during highway operation, resulting in a VSP bin distribution (based on time and

distance) that is very different than the other selected routes. Between the freeway travel and occasional traffic lights at high-posted speed limits (45mph), traveling the Highway route resulted in much higher representation of VSP bins 4 through 8.

Table 6.3: Distance-traveled distribution according to VSP bin for all routes.

	Route: 109		Route: 110		Route: 12T/C		Route: 123		Route: Highway	
VSP Bin	Distance (km)	%	Distance (km)	%	Distance (km)	%	Distance (km)	%	Distance (km)	%
1	22.25	38.9%	64.37	39.3%	25.24	39.4%	40.82	42.2%	34.04	22.9%
2	7.02	12.3%	19.43	11.9%	7.94	12.4%	9.78	10.1%	12.43	8.4%
3	6.60	11.6%	20.20	12.3%	7.89	12.3%	9.00	9.3%	15.06	10.1%
4	6.84	12.0%	17.31	10.6%	6.87	10.7%	7.94	8.2%	15.23	10.2%
5	5.25	9.2%	14.03	8.6%	5.85	9.1%	7.85	8.1%	16.84	11.3%
6	4.02	7.0%	10.53	6.4%	3.48	5.4%	6.73	7.0%	16.55	11.1%
7	3.08	5.4%	9.96	6.1%	3.82	6.0%	6.98	7.2%	19.60	13.2%
8	2.09	3.7%	7.94	4.8%	3.03	4.7%	7.55	7.8%	19.09	12.8%
TOTAL:	**57.14**		**163.76**		**64.11**		**96.65**		**148.82**	

6.3 On-Road Power Demand

Given the nature of the PHEV's design and its ability to operate in three different power scenarios (electric motor only, diesel engine only, and hybridization of electric and diesel power), it was uncertain whether the PHEV's power output for each engine would correspond to VSP, a calculated proxy for on-road power demands. It was also uncertain if the PHEV's operating scenarios would prove consistent enough within each of the different VSP bins to afford statistically significant differences in power and emissions between the bins. VSP has historically been utilized to develop on-road emission models capable of translating roadway power demands to emissions loads. In order for alternative-fueled vehicles to be amenable to current models, they must provide meaningful consistency within each of the designated VSP bins and operating modes. Based on the PHEV Sprinter's on-road data, instantaneous VSP calculations correspond well with total power output as determined by the dICE (diesel internal combustion engine) and EM (electric motor). Figure 6.11 provides a trace of both total power output and instantaneous VSP with time for a segment of data collected on the 12T/C route. Generally, total power output and instantaneous VSP correspond well with each other. Since VSP is only a proxy for power demand, whereas the total power output was determined by the PHEV's internal combustion engine and electric motor, the agreement between the arguments exceeded expectations. The most common point of departure between the two power estimations was during periods of negative acceleration and negative grade (downhill travel). During these moments of PHEV operation, the dICE and EM do not exhibit power demands, so the total power output calculated by the PHEV's DLM is effectively zero (since periods of recuperation were isolated from the

power calculations). However, the VSP equation produces negative outputs when acceleration and grade are sufficiently negative to overcome the power requirements of the basic vehicle load (due to vehicle drag, mass, and air resistance).

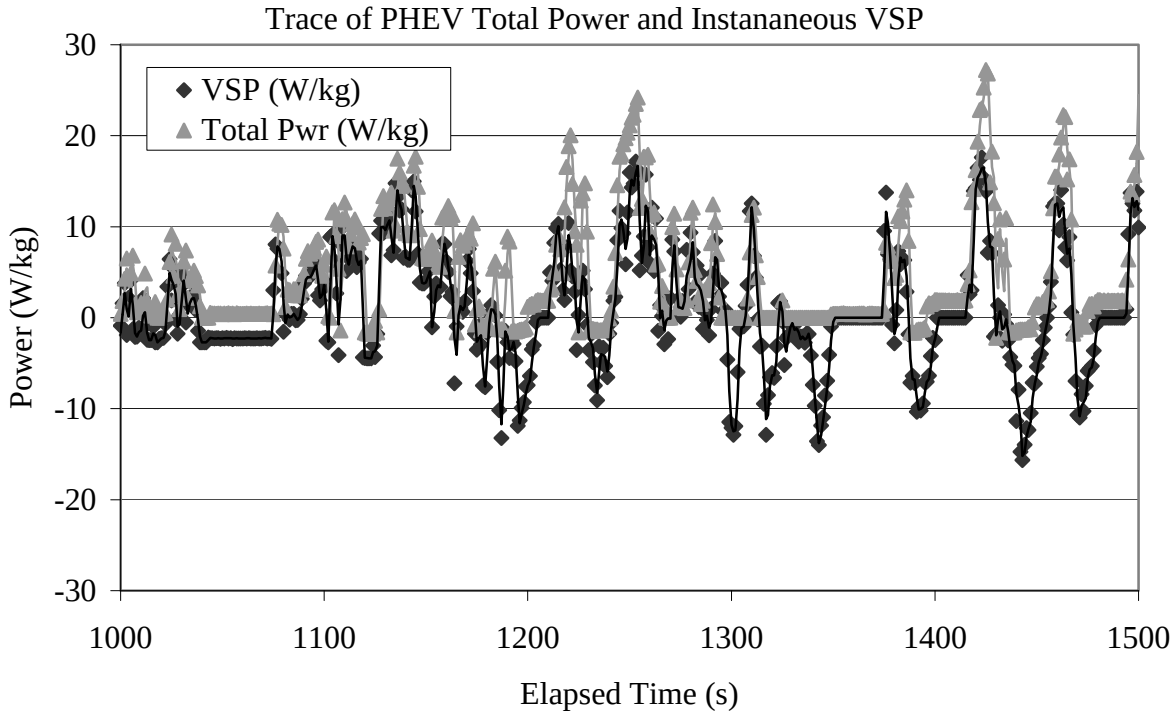

Figure 6.11: Power as determined by dICE and EM measurements versus instantaneous VSP calculations.

While total power output and instantaneous VSP calculations correspond strongly with each other, this does not guarantee that the PHEV, and other alternatively fueled vehicles, will provide a strong fit to VSP-based models. Electric motor operation reduces the total power output of the dICE, thus increasing the PHEV's fuel efficiency and reducing its emissions. For any given VSP bin, the electric motor will provide a portion of the power output either through electric-only operation or hybrid-electric operation.

Periods of zero, or greatly reduced, fuel use and emissions have the potential to reduce the statistical consistency of the emissions and operating data within the individual VSP bins, potentially eliminating the possibility of statistical significance within the modal analysis. Like Figure 6.11, above, Figure 6.12, below, provides PHEV total power output and instantaneous VSP for a short duration of 12T/C travel. However, PHEV total power output in Figure 6.12 has been broken down according to dICE power output and EM power output. Periods of measurable EM power output correspond with zero dICE power output, indicating electric-only operation at these instances. Despite the presence of electric-only operation, calculated instantaneous VSP still corresponds to dICE power output, since the diesel engine provided a majority of the PHEV Sprinter's power output.

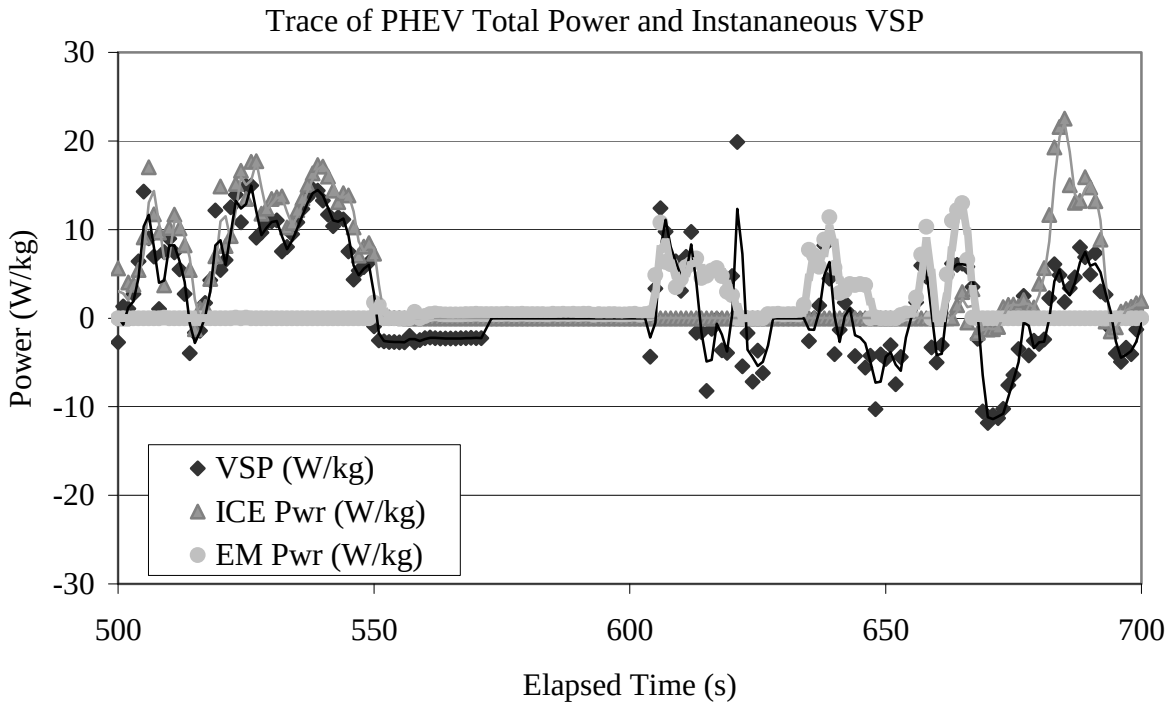

Figure 6.12: Trace of VSP Power, EM Power, and dICE Power with time (s).

Total power and dICE power both increase with VSP bin, however, where total power exhibits a straight line regression with VSP bin (R=0.9928), dICE power output shows a more rapid increase with increasing VSP bin with regression yielding a best-fit 4th order convex polynomial, R=0.9993. The electric motor (EM) power output increases with VSP from bins one through six, but demonstrates a concave decrease during bins seven and eight (3rd order concave polynomial, R=0.9875), suggesting that power demands at high VSP bins are best met by the dICE versus the EM (as dictated by the PHEV's electronic control module). These results are for charge-sustaining operation. Figure 6.13, below, provides a bar chart detailing total, ICE, and EM power output across the 8 VSP bins.

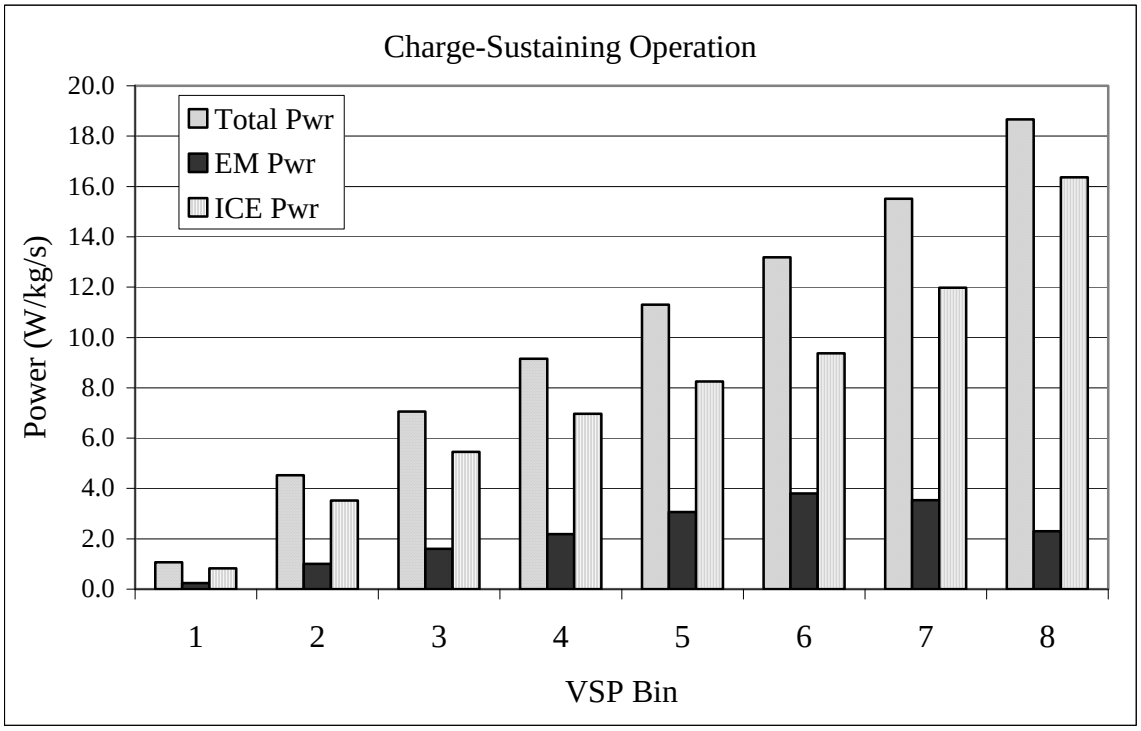

Figure 6.13: Power demands across VSP bins during charge-sustaining operation.

Similar trends are displayed during charge-depleting operation, with total power proportionally increasing with VSP bin, and dICE power output increasing (at an increasing rate) with VSP bin as the EM power output drops off in the higher VSP bins (seven and eight). However, with the additional grid-provided electrical reserve power available during charge-depleting operation, the total amount of power output provided by the dICE within each VSP bin is greatly reduced compared with charge-sustaining operation. Conversely, the amount of power output per kilometer provided by the EM is significantly higher in all VSP bins during charge-depleting operation versus charge-sustaining operation. Since charge-depleting operation was intended to be a primarily electric-only period of the PHEV's on-road operation, the large recruitment of the dICE during this time is contrary to original expectations. However, unlike charge-sustaining mode, during charge-depleting operation the EM supplied more motive power than the dICE in bins one and two. This phenomenon exists for all routes except the highway route. Highway operation resulted in a higher average state of battery charge than the other tested routes when operating in charge-sustaining operation. This maintained higher average state of battery charge suggests that highway operation did not fully utilize the PHEV's electric potential.

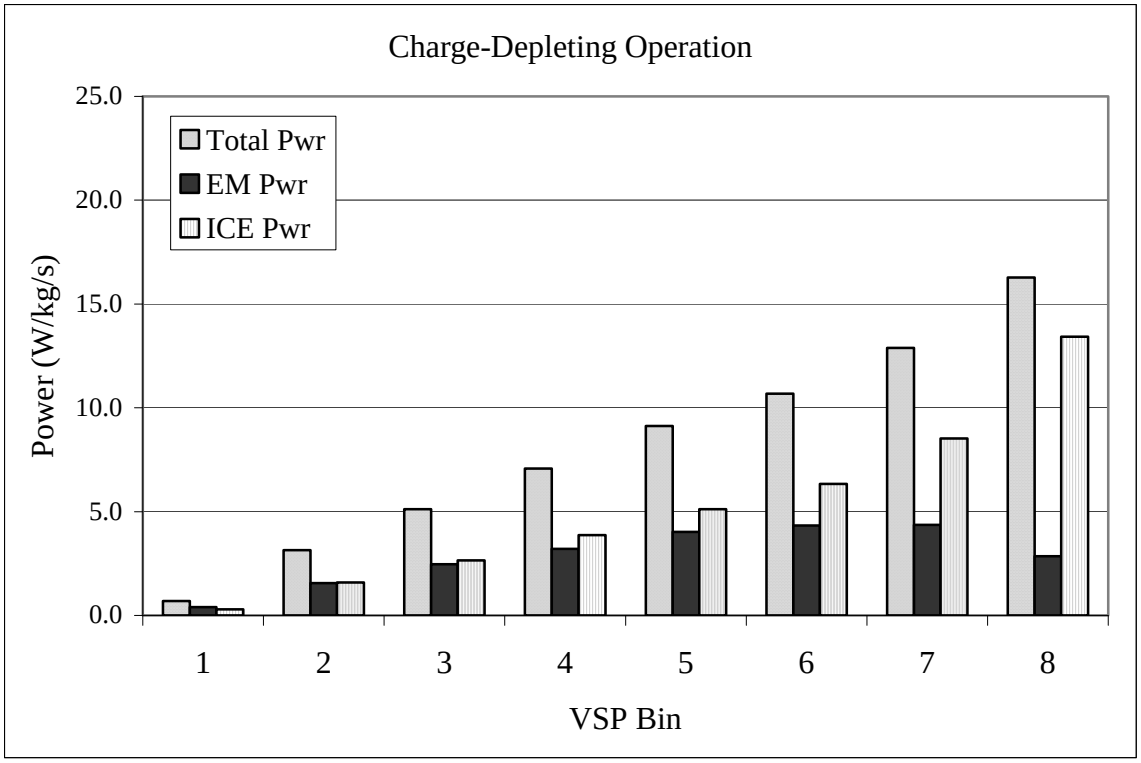

Figure 6.14: Power demands across VSP bins during charge-depleting operation.

Both analysis of variance (ANOVA) and the nonparametric equivalent, Kruskal-Wallis, tests were run on the PHEV Sprinter's power output as a response to designated VSP bin. The statistical tests were performed on the complete datasets, segregated according to charge-sustaining and charge-depleting operation. The larger, compiled datasets were an amalgamation of all sample runs selected for this analysis (i.e. meeting the ambient temperature and auxiliary system use requirements). Total power, dICE power, and EM power all showed statistically significant responses to VSP bin ($\alpha<0.05$) for the entire charge-sustaining and charge-depleting datasets with P values equal to 0.000 for all analyses. The following tables provide the ANOVA and Kruskal-Wallis results for the compiled dataset, for both charge-sustaining and charge-depleting operation.

Table 6.4: ANOVA results of power output for the compiled, charge-sustaining dataset.

Charge-Sustaining Mode

ANOVA Results

		ICE Power (W/kg/s)		EM Power (W/kg/s)		Total Power (W/kg/s)	
VSP Bin	**N**	**Mean**	**St Dev**	**Mean**	**St Dev**	**Mean**	**St Dev**
1	29028	0.832	2.720	0.240	1.023	1.071	2.839
2	5406	3.528	4.938	1.000	2.275	4.528	4.744
3	5071	5.452	5.784	1.602	3.033	7.054	5.026
4	4563	6.968	6.318	2.187	3.808	9.155	4.935
5	4149	8.246	7.087	3.062	4.753	11.309	4.867
6	3408	9.376	7.771	3.803	5.541	13.179	4.833
7	3434	11.972	8.196	3.539	6.008	15.512	4.943
8	2956	16.367	8.473	2.302	5.571	18.669	5.831
F-value		6262.13		1297.56		15950.39	
p-value		0.000		0.000		0.000	

Table 6.5: Kruskal-Wallis results for power output for the compiled charge-sustaining dataset.

Charge-Sustaining Mode

Kruskal-Wallis Results

		ICE Power (W/kg/s)		EM Power (W/kg/s)		Total Power (W/kg/s)	
VSP Bin	**N**	**Median**	**Z-Score**	**Median**	**Z-Score**	**Median**	**Z-Score**
1	29028	0.0000	-109.25	0.000	-26.51	0.3387	-161.01
2	5406	0.0000	-5.46	0.000	0.36	3.6930	-6.24
3	5071	5.3668	14.92	0.000	6.39	7.5870	23.53
4	4563	8.2816	27.44	0.000	8.73	9.5628	41.95
5	4149	9.5972	34.41	0.000	13.49	11.1849	56.95
6	3408	10.9938	37.15	0.000	16.39	12.9485	62.87
7	3434	13.8778	52.38	0.000	9.51	15.2459	74.97
8	2956	18.2833	66.61	0.000	-2.64	18.9834	78.36
H-Statistic		16078.32		972.37		32962.40	
p-value		0.000		0.000		0.000	

Table 6.6: ANOVA results for power output for the compiled charge-depleting dataset.

Charge-Depleting Mode

ANOVA Results

		ICE Power (W/kg/s)		EM Power (W/kg/s)		Total Power (W/kg/s)	
VSP Bin	**N**	**Mean**	**St Dev**	**Mean**	**St Dev**	**Mean**	**St Dev**
1	9399	0.291	1.722	0.402	1.245	0.693	2.080
2	1597	1.587	3.111	1.552	2.730	3.139	3.522
3	1478	2.651	4.032	2.459	3.591	5.110	4.071
4	1318	3.874	4.738	3.208	4.239	7.082	4.031
5	1254	5.113	5.574	4.017	5.108	9.131	4.265
6	1152	6.342	6.027	4.335	5.621	10.676	3.955
7	1217	8.520	6.675	4.367	6.528	12.887	4.672
8	1061	13.429	7.984	2.848	6.025	16.278	5.669
F-value		2149.07		513.20		5739.15	
p-value		0.000		0.000		0.000	

Table 6.7: Kruskal-Wallis results for power output for the compiled charge-depleting dataset.

Charge-Depleting Mode

Kruskal-Wallis Results

		ICE Power (W/kg/s)		EM Power (W/kg/s)		Total Power (W/kg/s)	
VSP Bin	**N**	**Median**	**Z-Score**	**Median**	**Z-Score**	**Median**	**Z-Score**
1	9399	0.0000	-56.22	0.000	-25.89	0.3637	-94.27
2	1597	0.0000	-3.06	0.021	3.24	2.3636	-2.95
3	1478	0.0000	4.14	0.041	8.31	4.7220	12.11
4	1318	1.9372	10.70	0.048	10.40	6.9164	23.34
5	1254	4.3484	15.30	0.049	11.82	9.4085	31.46
6	1152	7.0882	19.79	0.047	11.80	10.9233	36.77
7	1217	10.3079	29.17	0.028	7.73	12.8145	43.96
8	1061	15.0547	39.62	0.000	-2.76	16.1645	47.09
H-Statistic		4542.86		826.60		11099.72	
p-value		0.000		0.000		0.000	

VSP bin proved to be a statistically significant factor for predicting both dICE and EM power output. At the highest VSP bins, the diesel engine becomes the dominant power source when compared with the lower bins during both charge-sustaining and charge-depleting modes of operation. Except for the first one or two bins, the EM is a

secondary source of on-road power for the PHEV Sprinter in both charge-depleting and charge-sustaining (predominantly hybrid) operation.

In order to ensure that the results found for the continuous charge-sustaining or charge-depleting datasets were also prevalent on a smaller, per sample-run basis, ANOVA and Kruskal-Wallis analyses were also performed on a condensed dataset comprised of individual sample runs. It was important to verify that statistical trends present on the smaller scale not be masked (Type I error) by the analysis of the larger, second-by-second dataset. Equally important, it was necessary to verify that statistical significance found within each VSP bin on the large, compiled datasets pervade on a smaller, per-run scale. The probability of producing a Type I error by using univariate analysis methods on a large multivariate dataset is significant enough to justify the additional effort. Tables 6.8 through 6.13 detail the results achieved for the statistical analyses performed for the sample run-based datasets (CD and CS).

As a result of the per-sample run analysis, it was determined that total power, dICE power, and EM power outputs were also statistically significant responses to VSP bin designation ($\alpha<0.05$), negating the possibility of having performed a Type I error on the analyses of the larger, second-by-second datasets. However, with respect to power output, some inter-route discrepancies in power demand at each VSP bin were noticed. While VSP profiles were expected to vary based on the different routes, and possibly sample runs, the corresponding power output at each VSP range (within each bin) was expected to be similar for all routes. As a proxy for on-road load, VSP should remain impervious to the actual roadway that its calculation is being applied to. Despite this, definite differences in power output exist within each VSP bin between highway

operation and the in-town routes. Small variations in power output between the in-town routes (109, 110, 12T/C, 123) were also observed. Tables 6.8 through 6.13 provide power outputs for each route aggregated according to VSP bin. The following discussions are based on observation of the power/km data for each route, and were not subjected to statistical analysis in order to determine if the observations were statistically meaningful at this time. Inter-route investigations are presented later in this section.

Table 6.8: Total Power demand according to VSP bin per route in charge-sustaining operation.

	Charge-Sustaining Mode				
VSP Bin	Route: 109 Total Power (W/kg/km)	Route: 110 Total Power (W/kg/km)	Route: 12T/C Total Power (W/kg/km)	Route: 123 Total Power (W/kg/km)	Route: Highway Total Power (W/kg/km)
1	188.8	177.3	214.2	189.3	69.1
2	420.2	481.3	471.4	469.9	308.8
3	617.4	659.6	691.5	758.8	404.2
4	814.1	894.2	831.4	969.5	480.2
5	982.4	1137.6	1076.4	1251.0	576.2
6	1195.1	1379.4	1279.0	1517.5	660.2
7	1418.2	1656.2	1548.1	1714.3	741.3
8	1619.6	1715.9	1777.3	1922.5	957.4

Table 6.9: Total Power demand according to VSP bin per route in charge-depleting operation.

	Charge-Depleting Mode				
VSP Bin	Route: 109 Total Power (W/kg/km)	Route: 110 Total Power (W/kg/km)	Route: 12T/C Total Power (W/kg/km)	Route: 123 Total Power (W/kg/km)	Route: Highway Total Power (W/kg/km)
1	84.0	121.6	153.5	208.7	49.2
2	226.9	300.4	403.7	406.2	219.5
3	415.9	488.3	746.8	603.1	302.6
4	599.9	699.2	1162.1	766.1	396.3
5	766.3	1006.5	1185.5	1047.5	475.9
6	907.2	1173.6	1123.8	1208.7	575.5
7	966.2	1356.6	1584.1	1449.1	662.4
8	1075.7	1454.8	1489.8	1622.8	864.0

With respect to total power output, highway operation consistently required less power than in-town operation for each VSP bin. Despite similar VSP ratings, more consistent operation at higher average velocities results in higher PHEV efficiencies. This trend proved consistent for both charge-sustaining and charge-depleting operations. Amongst the in-town routes, total power output was similar for each VSP bin for routes 109, 110, and 12T/C. Route 123 generally appeared to require more power output per km in VSP bins 3 through 8. Of the 4 in-town routes sampled, the 123 was the most dissimilar to the other in-town routes being based solely on suburban roadways.

Table 6.10: ICE power demand according to VSP bin per route in charge-sustaining operation.

Charge-Sustaining Mode:

VSP Bin	Route: 109 ICE Power (W/kg/km)	Route: 110 ICE Power (W/kg/km)	Route: 12T/C ICE Power (W/kg/km)	Route: 123 ICE Power (W/kg/km)	Route: Highway ICE Power (W/kg/km)
1	151.3	136.8	160.7	152.1	50.2
2	337.7	360.5	357.8	361.5	267.3
3	464.1	487.2	568.5	545.9	355.0
4	596.4	656.5	628.6	717.2	416.0
5	675.2	800.6	777.1	869.8	479.7
6	772.3	916.3	879.7	1055.7	546.1
7	1033.1	1183.5	1124.5	1343.2	636.6
8	1410.6	1382.8	1474.8	1744.9	880.5

Table 6.11: ICE power demand according to VSP bin per route in charge-depleting operation.

Charge-Depleting Mode:

VSP Bin	Route: 109 ICE Power (W/kg/km)	Route: 110 ICE Power (W/kg/km)	Route: 12T/C ICE Power (W/kg/km)	Route: 123 ICE Power (W/kg/km)	Route: Highway ICE Power (W/kg/km)
1	9.2	35.2	42.9	114.6	29.0
2	110.6	56.8	181.0	190.1	172.7
3	167.0	129.6	213.3	313.0	245.4
4	249.3	204.4	642.7	402.2	318.3
5	345.2	272.3	646.7	496.2	400.6
6	396.3	412.5	748.0	559.2	467.2
7	473.0	565.2	1376.3	730.1	552.0
8	682.5	884.1	1207.2	1247.2	793.7

Similar to total power output, dICE power output across all 8 VSP bins was less during highway operation than in-town driving for charge-sustaining operation. Route 109 required less dICE power per km than the other in-town routes (charge-sustaining operation), suggesting that the 109 was more apt at utilizing the electric motor than the other in-town routes across all 8 VSP bins. Trends in dICE power demand between the sampled routes across the VSP bins were less apparent in charge-depleting operation. While perceptible differences between the routes exist within each VSP bin, no single route required consistently lower or higher dICE power output across all VSP bins.

Table 6.12: EM power demand according to VSP bin per route in charge-sustaining operation.

	Charge-Sustaining Mode				
VSP Bin	Route: 109 EM Power (W/kg/km)	Route: 110 EM Power (W/kg/km)	Route: 12T/C EM Power (W/kg/km)	Route: 123 EM Power (W/kg/km)	Route: Highway EM Power (W/kg/km)
1	37.5	40.5	53.5	37.2	18.9
2	82.5	120.9	113.6	108.4	41.5
3	153.4	172.4	123.1	212.9	49.2
4	217.7	237.7	202.8	252.3	64.2
5	307.2	337.0	299.3	381.2	96.6
6	422.9	463.1	399.4	461.7	114.1
7	385.2	472.7	423.6	371.1	104.7
8	209.0	333.1	302.5	177.6	76.8

Table 6.13: EM power demand according to VSP bin per route in charge-depleting operation.

	Charge-Depleting Mode				
VSP Bin	Route: 109 EM Power (W/kg/km)	Route: 110 EM Power (W/kg/km)	Route: 12T/C EM Power (W/kg/km)	Route: 123 EM Power (W/kg/km)	Route: Highway EM Power (W/kg/km)
1	74.8	86.5	110.6	94.1	20.2
2	116.4	243.5	222.7	216.1	46.9
3	248.9	358.7	533.5	290.1	57.2
4	350.6	494.8	519.4	363.9	78.0
5	421.1	734.2	538.8	551.2	75.3
6	510.9	761.1	375.8	649.5	108.2
7	493.3	791.4	207.8	719.0	110.4
8	393.2	570.8	282.6	375.6	70.3

Consistent with total and dICE power output, highway operation required less EM power output than in-town driving for all 8 VSP bins. This trend exists for both charge-sustaining and charge-depleting operation. EM operation within each VSP bin was generally the same for in-town driving, regardless of the actual route being traveled.

During charge-depleting operation, highway driving still required the least amount of EM power for all VSP bins. While no obvious distinctions exist between the in-town routes across all VSP bins, different in-town routes appeared to benefit the most from the EM at different VSP ranges. During the upper VSP bins (5 through 8) the 110 route utilized the EM more than the other in-town routes, whereas the 12T/C route had the highest EM power output while operating in the lower range of VSP bins (1 through 4). Again, the discussion regarding tables 6.8 through 6.13 is largely observational and was not verified with statistical analysis. An investigation regarding inter-route variability within each VSP bin is provided later in this section.

The PHEV on-road dataset was also categorized according to driving mode as defined by NCSU (EPA, 2002). Using cruise, idle, acceleration, and deceleration as discrete categories for segregating the PHEV Sprinter's operating and emissions data resulted in a more coarse analysis than VSP binning since the NCSU model only specifies four modal divisions. Unlike the VSP binning approach, the driving-based modal analysis provides a stronger basis for intuitive evaluation since each category pertains to a distinct mode of vehicle driving. Figures 6.15 and 6.16 display the total, dICE, and EM power output for each mode. During charge-sustaining operation, the dICE provided the majority of the power compared with the electric motor. This is particularly true during the cruise mode, where the dICE was the dominant power source.

During periods of acceleration, however, the EM was more heavily utilized when compared to the other driving modes. Periods of deceleration did not utilize EM power output since deceleration is one of the primary sources of electrical recuperation.

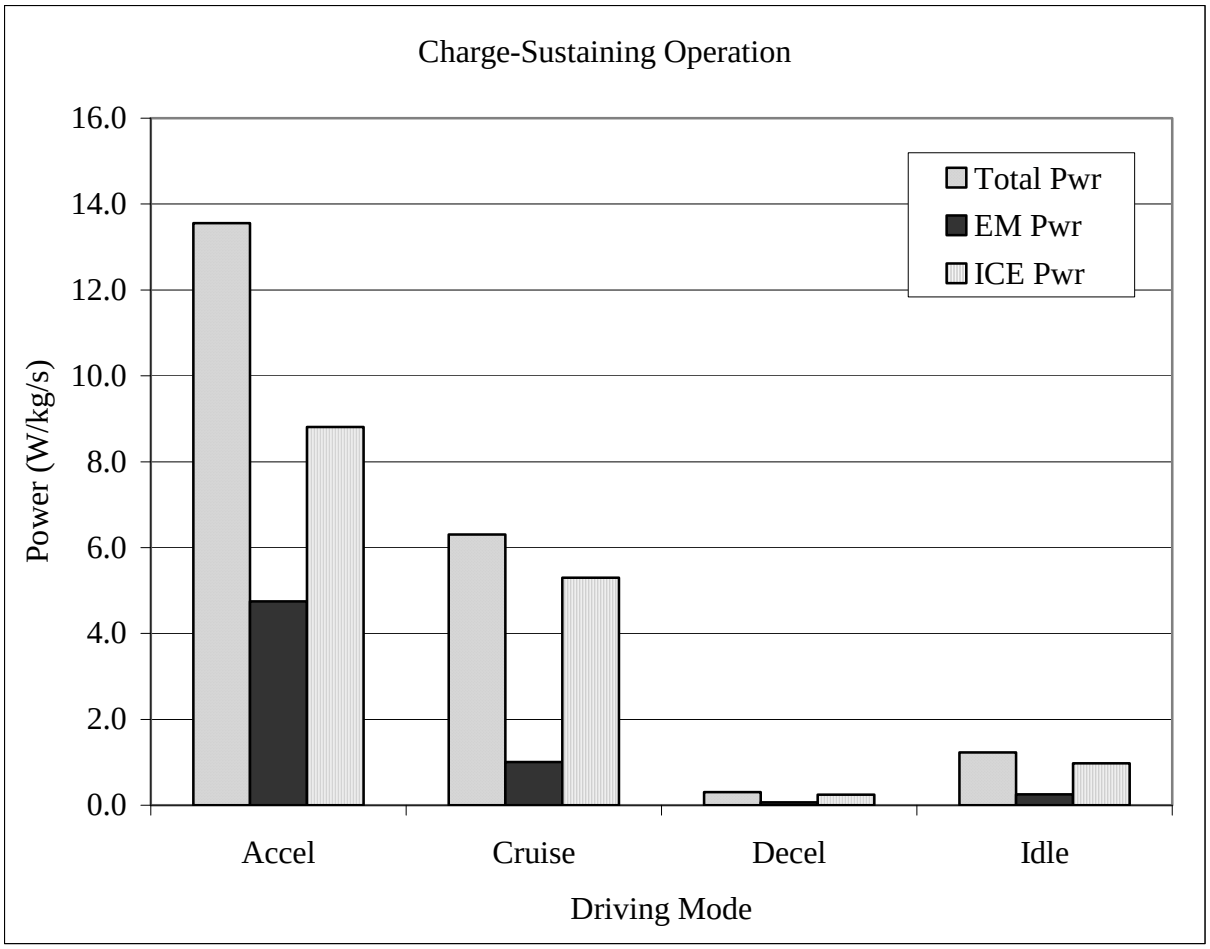

Figure 6.15: ICE versus EM power output during charge-sustaining operation according to NCSU defined driving modes.

During charge-depleting operation, the electric motor is a more prevalent power source compared to charge-sustaining operation. The EM was the dominant power source during acceleration events and provided an equal share of the work output during periods of idling. However, even during charge-depleting operation, the diesel engine

was the primary source of motive power during cruise mode. These figures are based on data obtained from all sampled routes including highway driving. Using only one category to define cruising, particularly for the PHEV Sprinter study where cruising occurred at either low to moderate velocities or relatively high speeds (55mph+ for highway operation), may prove to be an oversimplification depending on how the PHEV's control scheme was designed to handle vastly different velocity scenarios.

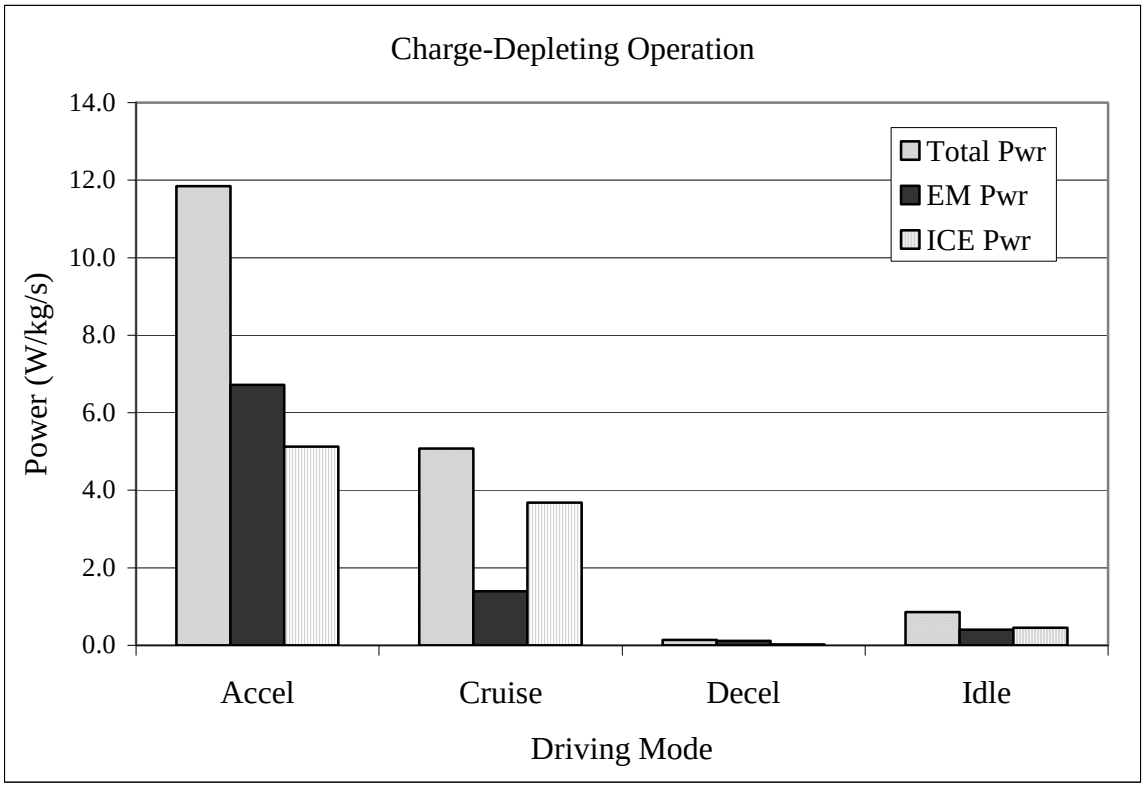

Figure 6.16: ICE versus EM power output during charge-depleting operation according to NCSU defined driving modes.

ANOVA and Kruskal-Wallis tests were conducted on the drive mode-categorized dataset. Similarly to the VSP bin analysis, each statistical test was run on the compiled, continuous dataset as well as on the dataset based around each individual sampling run.

In all cases, the PHEV's power output, whether electric, diesel, or total was a statistically significant factor according to driving mode ($\alpha<0.05$). ANOVA and Kruskal-Wallis output for the compiled datasets (charge-sustaining and charge-depleting) are provided in Tables 6.14 through 6.17.

Table 6.14: ANOVA results for power output as a response to driving mode, charge-sustaining operation.

Charge-Sustaining Mode

ANOVA Results

		ICE Power (W/kg/s)		EM Power (W/kg/s)		Total Power (W/kg/s)	
Mode	**N**	**Mean**	**St Dev**	**Mean**	**St Dev**	**Mean**	**St Dev**
Accel	8232	8.809	9.19	4.746	6.044	13.555	6.591
Cruise	33028	5.301	6.928	1.006	2.746	6.307	6.722
Decel	7715	0.246	1.247	0.063	0.257	0.309	1.26
Idle	9040	0.977	1.166	0.253	0.675	1.23	1.149
p-value<		0.000		0.000		0.000	

Table 6.15: Kruskal-Wallis results for power output as a response to driving mode, charge-sustaining operation.

Charge-Sustaining Mode

Kruskal-Wallis Results

		ICE Power (W/kg/s)		EM Power (W/kg/s)		Total Power (W/kg/s)	
Mode	**N**	**Median**	**Z-Score**	**Median**	**Z-Score**	**Median**	**Z-Score**
Accel	8232	5.4998	46.62	0.02799	50.78	13.24860	99.51
Cruise	33028	0.5882	14.32	0.00000	-39.90	5.84534	12.44
Decel	7715	0.0000	-53.33	0.00000	-23.56	0.00000	-78.98
Idle	9040	0.0000	-14.47	0.06949	27.68	1.40743	-38.79
p-value<		0.000		0.000		0.000	

Table 6.16: ANOVA results for power output as a response to driving mode, charge-depleting operation.

Charge-Depleting Mode

ANOVA Results

		ICE Power (W/kg/s)		EM Power (W/kg/s)		Total Power (W/kg/s)	
Mode	**N**	**Mean**	**St Dev**	**Mean**	**St Dev**	**Mean**	**St Dev**
Accel	2417	5.124	7.563	6.719	6.202	11.843	5.982
Cruise	10500	3.684	5.722	1.394	3.170	5.078	5.758
Decel	2212	0.025	0.963	0.112	0.313	0.137	1.01
Idle	3347	0.452	0.868	0.405	0.642	0.857	0.893
p-value		0.000		0.000		0.000	

Table 6.17: Kruskal-Wallis results for power output as a response to driving mode, charge-depleting operation.

Charge-Depleting Mode

Kruskal-Wallis Results

		ICE Power (W/kg/s)		EM Power (W/kg/s)		Total Power (W/kg/s)	
Mode	**N**	**Median**	**Z-Score**	**Median**	**Z-Score**	**Median**	**Z-Score**
Accel	2417	0.0000	13.74	6.88922	40.11	11.45090	56.55
Cruise	10500	0.0000	18.85	0.00000	-28.27	3.63051	12.08
Decel	2212	0.0000	-26.44	0.00000	-23.77	0.00000	-47.24
Idle	3347	0.0000	-13.99	0.38742	21.28	0.48023	-25.23
p-value		0.000		0.000		0.000	

As expected, the electric motor provided substantially more power output in charge-depleting mode than charge-sustaining. In charge-depleting operation, the electric motor supplied 57%, 27%, 82%, and 45% of the work for the acceleration, cruise, deceleration, and idle driving modes, respectively, whereas only 35%, 16%, 20%, and 21% of the total power output in acceleration, cruise, deceleration, and idle driving modes, respectively, was electrically generated during charge-sustaining operation.

The intuitive nature of the driving-mode model makes it more qualitatively valuable for assessing variations in the power output for individual routes. The power requirements and sources varied with each route for the different driving modes. Unlike VSP-binning, where each VSP bin is associated with a predetermined range of estimated power demand, the driving-based modal model only segregates data according to defined on-road driving behaviors, which were based solely on velocity and acceleration criteria. In order for a vehicle to meet the demands of the acceleration mode, it only had to maintain a set level of acceleration for a specified period of time. Whether the acceleration occurred at low velocity or high velocity cannot be ascertained. Likewise, cruise mode only requires that the vehicle maintain a constant velocity with only moderate and transient periods of acceleration or deceleration. The actual velocity at

which the vehicle achieves cruise mode does not factor into its classification. Because of this, certain divergences between the routes for each driving mode cannot be assessed based on the bulk figures provided and discussed above. In order to assess the nuances within each driving mode, the individual sample routes need to analyzed separately.

Route 110 required the lowest total power output for the two primary, power-inducing driving modes, cruise and acceleration. Figures 6.17 and 6.18 show relative total power requirements for each of the sample routes according to driving mode (Accel, Decel, Cruise, or Idle). Routes 109 and 110, each containing a suburban and urban section, demonstrated similar total power demand in both cruise (within 7% of each other) and acceleration (0.05% difference) driving modes. While Highway operation only required slightly higher power output during acceleration events than the 109 or 110, highway cruising resulted in an over 65% increased total power demand compared to the in-town routes. Highway cruising occurs at significantly higher average velocities than in-town suburban or urban driving. While technically meeting the criteria for cruise operation, cruise velocity had a significant effect on the PHEV Sprinter's total power demand.

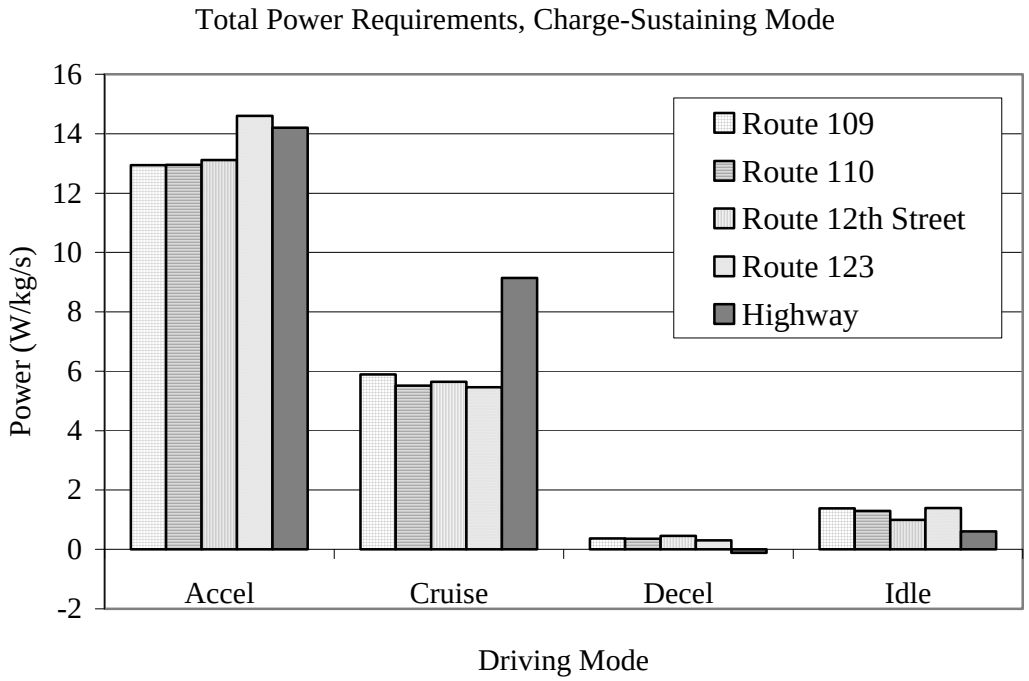

Figure 6.17: Total power demand by route in charge-sustaining operation for each driving mode.

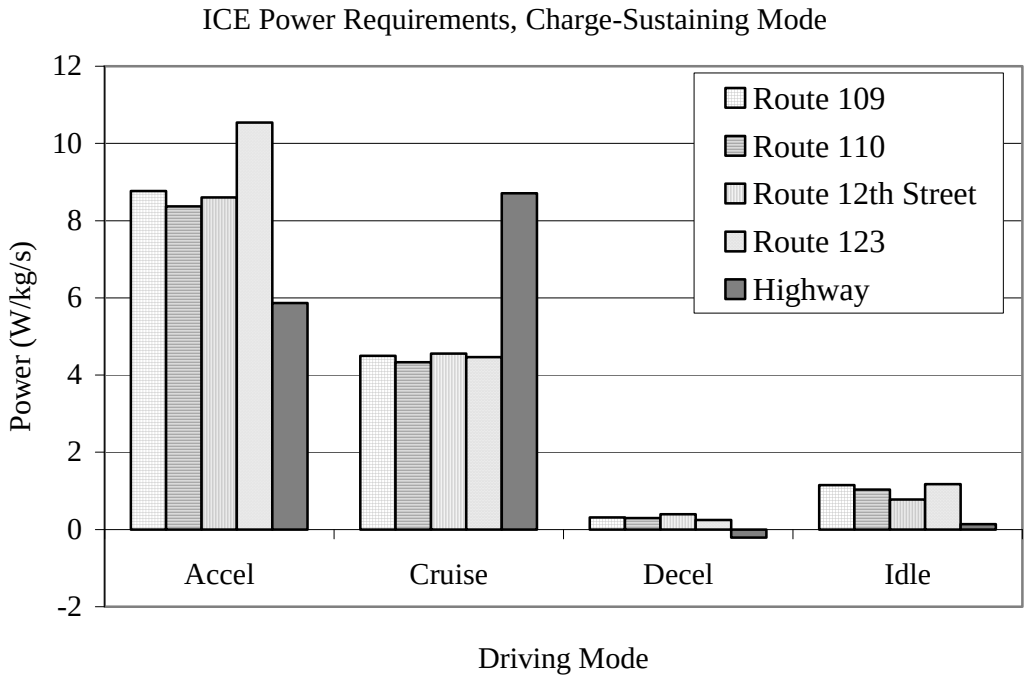

Figure 6.18: ICE power demand by route in charge-sustaining operation for each driving mode.

Since the ultimate goal of the PHEV design is to reduce the load on the internal combustion engine, and, hence, reduce the on-road emissions and petroleum fuel requirements, a shift from ICE-supplied to EM-supplied power for a particular route shows that the PHEV is being better used to its potential as an electric-vehicle. The 109 and 110 routes proved relatively consistent with regards to the amount of the total power demand for each driving mode. Additionally, these routes showed similar dICE use across all four driving modes. During charge-sustaining operation, the dICE supplied the majority of the work for all driving modes while traveling these routes. However, highway operation, which represents considerably different driving conditions within the acceleration and cruise modes, required very different dICE output than the more conventional, in-town transit routes (109 and 110). The dICE provided 95% of the motive work required during cruise mode on the highway routes. At high speeds, PHEV's electronic control module is not programmed to supply a significant amount of the power output from the electric motor, since the dICE is expected to operate more efficiently during highway driving. An additional consequence of proportionally higher dICE utilization during highway driving was that the PHEV Sprinter maintained a consistently higher average state of battery charge for the remaining three modes, since recuperation still occurred during highway cruising events, even if the EM wasn't being heavily recruited.

6.4 Electric Recuperation

Similar to other hybrid-electric vehicles on the road today, one of the PHEV Sprinter's design features is the ability to recover normally lost potential and kinetic energy through electrical recuperation. By redirecting current back into the on-board batteries during periods of deceleration, braking, and transmission downshifting, the PHEV is able to extend the work output of the electric motor. For the purposes of this analysis, recuperation was considered to be occurring during periods of negative battery current, and was quantified as negative power calculated at the electric motor measured in W/kg/km or W/kg/s, depending on the analysis. Recuperation periods (with negative measured battery current) coincided with negative electric motor torque readings.

Similar to power output, ANOVA and Kruskal-Wallis analyses showed that the PHEV Sprinter's electric recuperation rates were a statistically significant ($\alpha<0.05$) factor as a response to both VSP bin and driving mode (acceleration, cruising, deceleration, and idle) during both charge-sustaining and charge-depleting operation for all routes analyzed. ANOVA and Kruskal-Wallis tests were applied to all individual sample runs selected for this discussion; recuperation rates were a statistically significant response to both VSP-bin and driving mode (acceleration, cruise, deceleration, idle) for all statistical tests conducted. Consistent statistical results were found when applied to the entire charge-sustaining and charge-depleting datasets independently. The following tables provide a summary of the recuperation rates according to VSP bin and driving mode for each evaluated route.

Figures 6.19 and 6.20 display the absolute value of the recuperation rates during both charge-sustaining and charge-depleting operation for both modal analysis

techniques. Absolute values of recuperation are displayed for ease of visualization. Recuperation rates were calculated from negative electric motor torque measurements, and are reported as negative power. Periods of time with the smallest (most negative) reported recuperation rates reflect moments when the PHEV was sequestering the highest amount of electrical energy, redirecting it back into the battery packs.

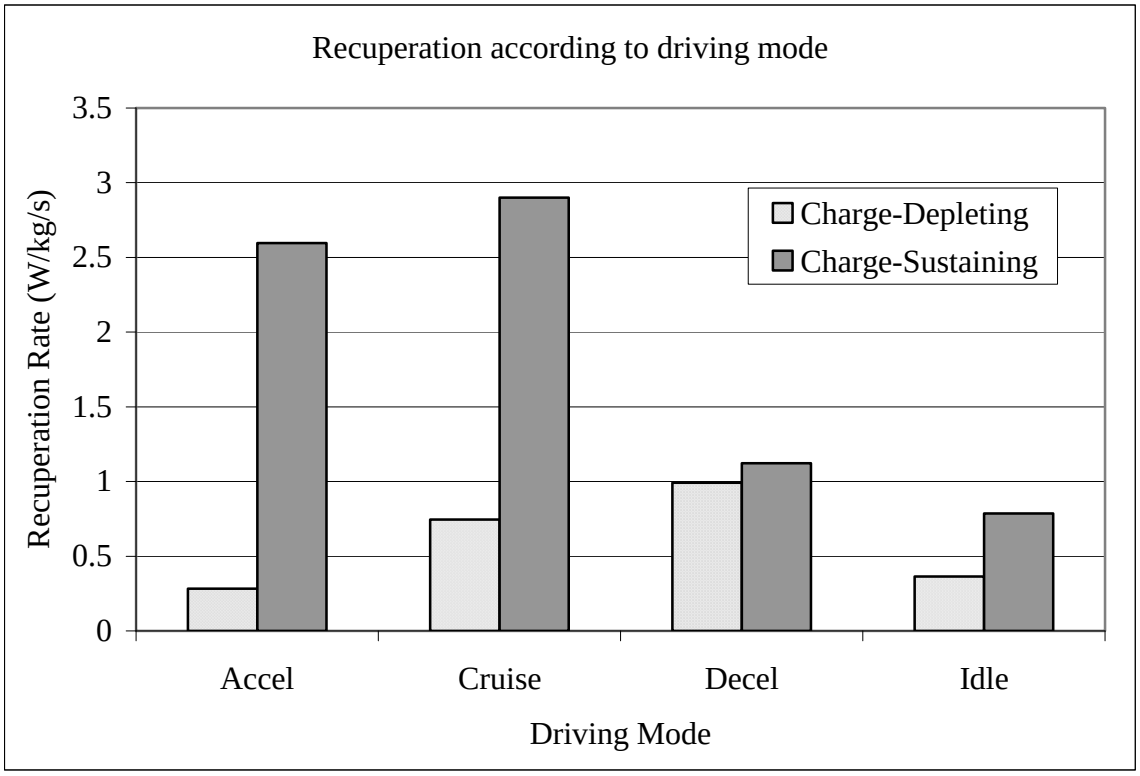

Figure 6.19: Absolute value of recuperation rates according to driving mode.

The highest levels of electrical recuperation occurred while the PHEV was operating in charge-sustaining mode. During cruise and acceleration driving, charge-sustaining operation resulted in a 74% and 89%, respectively, higher average recuperation rates (W/kg/s) than charge-depleting mode. Based on the driving mode analysis, cruise mode resulted in the highest average recuperation rate, with the

acceleration mode creating the second highest average recuperation rate. Deceleration events did not contribute as significantly as originally expected to electrical recuperation. During periods of moderate to strong deceleration, regenerative braking is minimized in the interest of safety, as the friction brakes become the dominant source of deceleration. While the exact control scheme dictating the PHEV Sprinter's recuperation remains proprietary knowledge of the PHEV Sprinter developers, it was somewhat unexpected that the majority of recuperative benefit occurred during cruise and acceleration modes. Slight fluctuations in vehicle velocity during cruise mode, that are not extreme enough to qualify as acceleration or deceleration events, give significant opportunity for the PHEV to utilize electrical recuperation as the mechanical transmission downshifts. Brief investigation into the relationship between recuperation rates and vehicle acceleration, during acceleration mode, showed that PHEV recuperation occurred while the vehicle was accelerating at a low to moderate rates (from $0.5 m/s^2$ to $1.5 m/s^2$), and was completely absent at acceleration rates greater than $1.7 m/s^2$. Based on this, recuperation remains a function not only of vehicle control system design, but of driver behavior as well.

Based on Figure 6.20, the PHEV's ability to reclaim lost energy increased with increasing VSP bin during charge-sustaining operation. Conversely, during charge-depleting operation, VSP bin 1 afforded the highest rates of recuperation, with the remaining 7 VSP bins providing little to no meaningful recuperative energy to the PHEV system. Similar to the driving mode analysis, charge-sustaining mode consistently attained 80-90% higher recuperation rates than charge-depleting operation for the same VSP bin (except for bin 1).

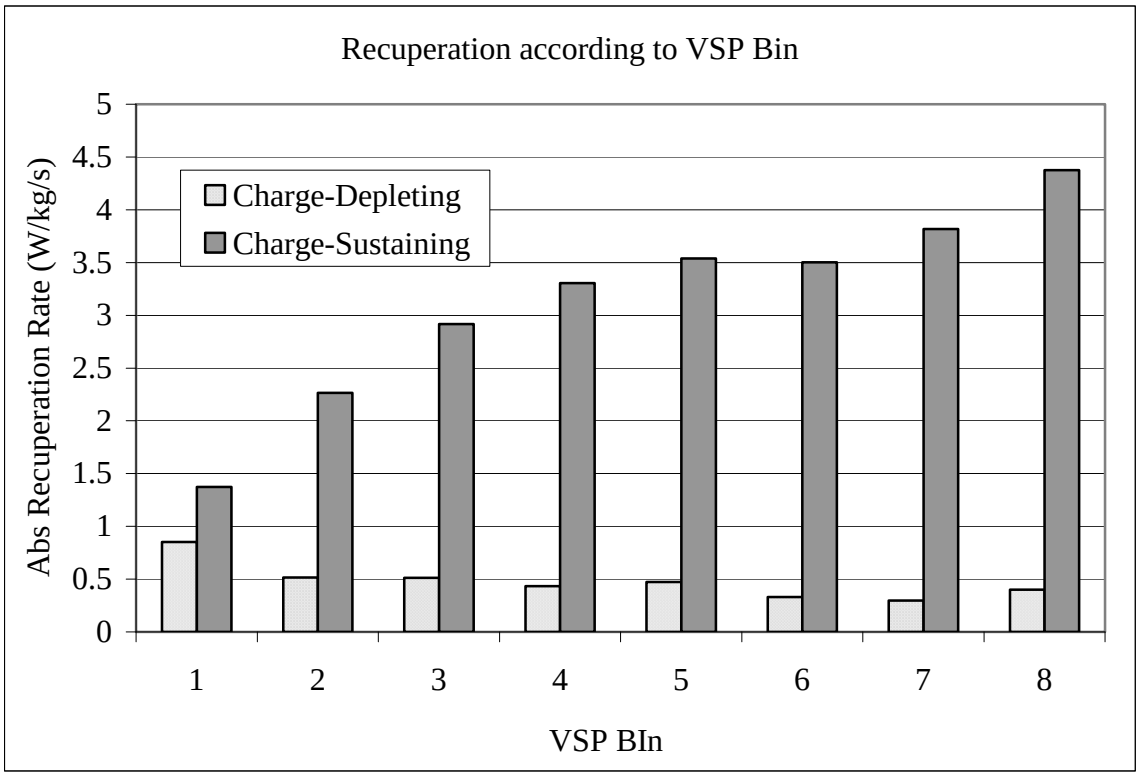

Figure 6.20: Absolute value of recuperation rates according to VSP bin.

Recuperation rates were evaluated on a per-route basis in order to first verify statistical significance at different levels of analysis (operating mode-based, route-based, and sample run-based) and to investigate the possibility of route influences on recuperation within each VSP bin. Tables 6.18 and 6.19 provide recuperation rates according to route for all 8 VSP bins during charge-sustaining and charge-depleting operation. During charge-sustaining operation, good agreement exists among the in-town routes across all 8 VSP bins. Highway operation, however, yielded the lowest recuperation rates resulting in 30-50% lower average recuperation rates in bins 1 through 4, and 60-85% lower average recuperation rates in bins 5 through 8.

Table 6.18: Recuperation rates by route in charge-sustaining mode.

Charge-Sustaining Mode: Recuperation Rates					
VSP Bin	109 W/kg/km	110 W/kg/km	12 T/C W/kg/km	123 W/kg/km	Highway W/kg/km
1	-215.1	-216.1	-234.9	-271.3	-137.9
2	-231.7	-241.7	-249.7	-244.9	-166.2
3	-275.2	-279.8	-316.7	-283.7	-171.9
4	-304.6	-318.8	-317.9	-341.8	-164.1
5	-319.6	-366.6	-329.8	-361.1	-139.4
6	-330.2	-365.0	-345.4	-379.8	-124.9
7	-389.4	-389.1	-373.2	-401.9	-106.0
8	-449.2	-421.5	-458.9	-404.5	-68.0

The consistency in average recuperation rate across the bins observed during charge-sustaining operation on the in-town routes was lost during charge-depleting operation. Generally, the 109 and 12T/C routes benefited least from the PHEV's recuperative abilities, while routes 110 and 123 still maintained low to moderate levels of recuperation.

Table 6.19: Recuperation rates by route in charge-depleting mode.

Charge-Depleting Mode: Recuperation Rates					
VSP Bin	109 W/kg/km	110 W/kg/km	12 T/C W/kg/km	123 W/kg/km	Highway W/kg/km
1	-106.5	-142.7	-153.2	-220.9	-89.3
2	-29.4	-53.2	-46.1	-93.6	-28.0
3	-15.6	-55.1	-13.6	-109.3	-23.8
4	-6.1	-57.2	-7.8	-75.7	-23.6
5	-7.9	-61.0	-1.6	-88.8	-23.5
6	-2.0	-68.2	-3.6	-47.6	-15.9
7	-3.6	-55.6	0.0	-54.6	-10.3
8	-13.2	-90.5	0.0	-92.1	-6.2

While recuperation rates demonstrated statistical significance according to VSP-bin and driving mode on a run-, route-, and compiled dataset-basis for both charge-sustaining and charge-depleting operation, qualitative investigation suggests that there are

noteworthy differences in the amount of electrical recuperation achieved while on the highway route compared to the more urban- and suburban-based routes. The route-based investigation provided later in this section will discuss this phenomenon further and determine the level of statistical merit behind the observations.

6.5 Fuel consumption

Using instantaneous exhaust flow rate measurements and the stoichiometry of emitted carbon, the Semtech software calculated instantaneous fuel consumption on a gal/s basis. With an electric reserve capacity allowing for electric-only operation, the PHEV Sprinter only uses petroleum fuel while the diesel internal combustion engine is actively running. Measurements used to calculate power output from the diesel internal combustion engine (dICE) were collected from the PHEV's data-logging module (DLM), whereas the Semtech took the measurements used to calculate fuel consumption from the vehicle's exhaust. Intuitively, it is expected that the instantaneous fuel consumption directly track with the dICE's power output. The following figure displays the fuel consumption and dICE power output versus elapsed time. Additionally, correlation analysis (Chapter 7) showed a strong relationship between fuel consumption and dICE power output exhibiting a Pearson's correlation coefficient of 0.945 between the two calculated variables. The parallel behavior between the two calculated constructs not only follows intuitive expectations, but also further shows that the two separate monitoring systems (DLM and Semtech-DS) were in direct alignment with each other.

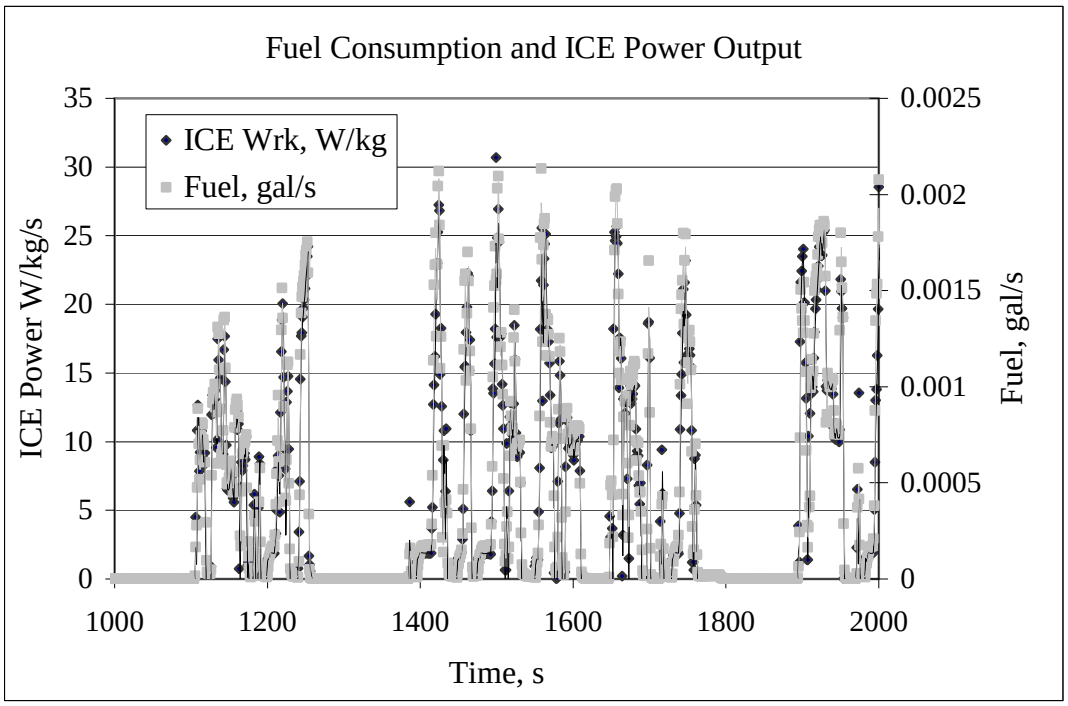

Figure 6.21: 12th St TC route (12TCs1), collected October 19 while PHEV in charge-sustaining mode.

Analogous with dICE power output, fuel consumption increased with increasing VSP bin in both charge-sustaining and charge-depleting modes of operation, although fuel consumption in charge-depleting operation was consistently lower than that required for charge-sustaining operation. The difference in fuel consumption between the two operating scenarios diminished as VSP bin increased, with charge-depleting operation requiring 49% less fuel per second in bins 1 and 2, and 42%, 38%, 31%, 26%, 23%, and 15% less fuel per second in bins 3 through 8, respectively. This trend was also evident when evaluating the compiled datasets according to drive mode (acceleration, deceleration, idle, and cruise) with charge-depleting operation requiring less fuel than charge-sustaining operation in all four driving modes. Trending consistently with dICE power output, the majority of the PHEV's fuel consumption occurred during acceleration

events, with cruise mode fuel consumption following second. Fuel use during periods of deceleration and idle was minimal.

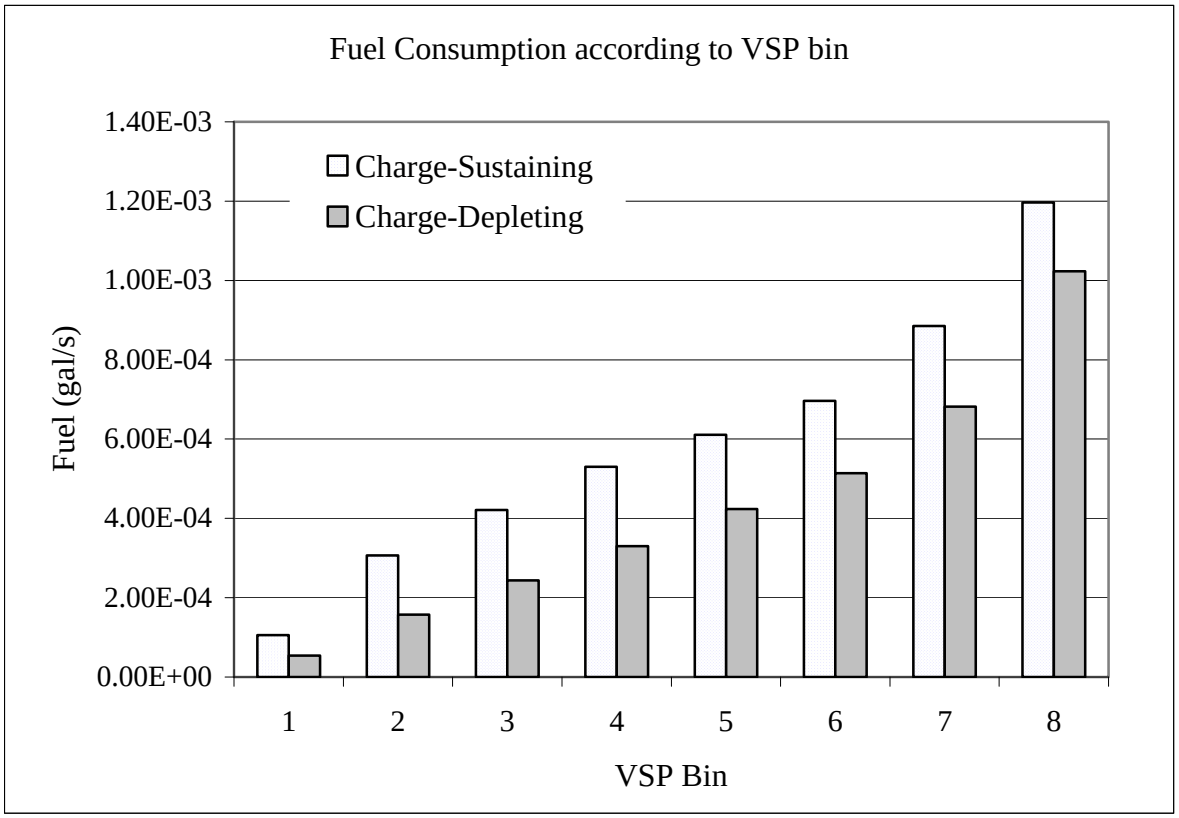

Figure 6.22: PHEV Sprinter fuel consumption according to VSP bin.

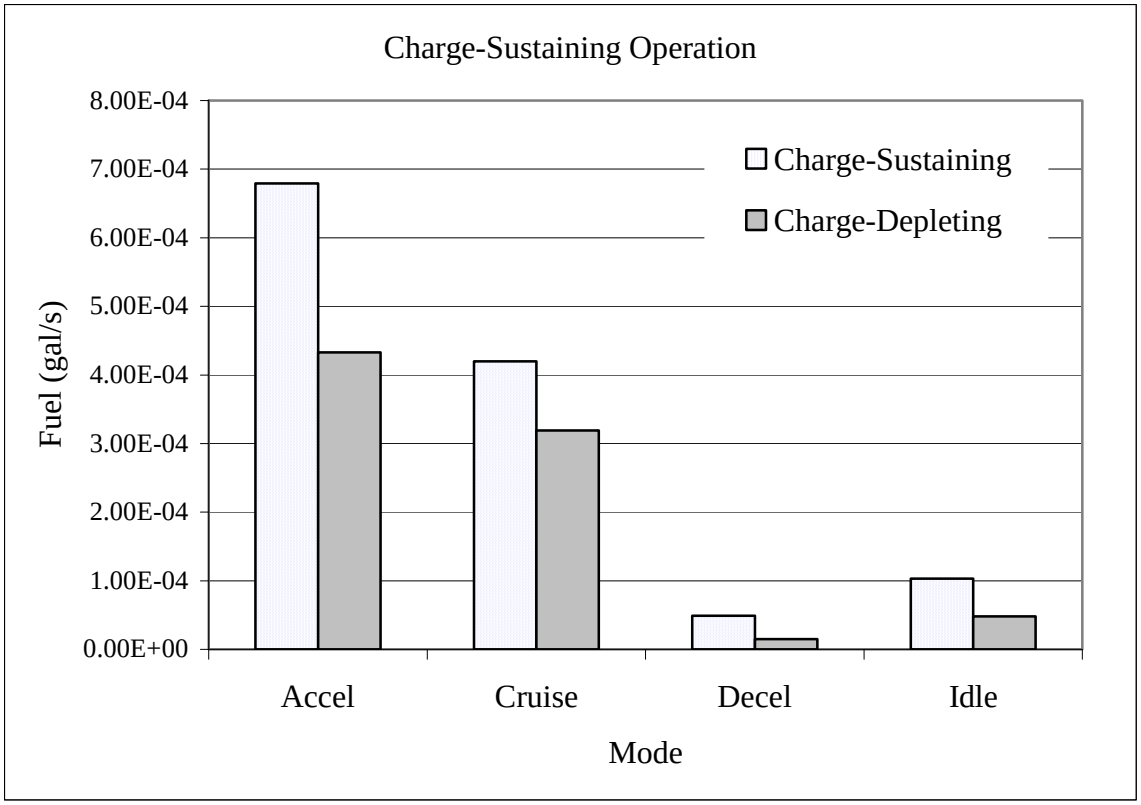

Figure 6.23: PHEV Sprinter fuel consumption according to driving mode.

There appears to be good continuity in fuel consumption across the VSP bins for all of the in-town routes while the PHEV was running in charge-sustaining operation (109, 110, 12T/C, and 123), however the 123 route, which was based on suburban roadways and did not enter the Kansas City urban core, used 12-20% more fuel in VSP bins 4 through 8 than the other in-town routes. This trend is consistent with the 123 route's relatively high dICE power outputs during the upper VSP bins. Contrary to the PHEV Sprinter's fuel requirements for in-town driving, the Highway route used appreciably less fuel than all other routes across all VSP bins during charge-sustaining operation. The observed difference in fuel requirements between in-town and highway driving during charge-sustaining operation were less apparent during charge-depleting

mode, where the EM supplied a larger proportion of the PHEV Sprinter's power output during in-town driving, but was still relatively unused on the highway.

Table 6.20: Fuel use for each route according to VSP bin during charge-sustaining operation.

	Charge-Sustaining Mode				
VSP Bin	Route: 109 Fuel (gal/km)	Route: 110 Fuel (gal/km)	Route: 12T/C Fuel (gal/km)	Route: 123 Fuel (gal/km)	Route: Highway Fuel (gal/km)
1	0.016	0.016	0.024	0.019	0.009
2	0.028	0.032	0.031	0.033	0.022
3	0.036	0.038	0.040	0.044	0.027
4	0.046	0.050	0.046	0.055	0.032
5	0.051	0.059	0.055	0.064	0.037
6	0.059	0.068	0.059	0.079	0.041
7	0.079	0.088	0.073	0.100	0.048
8	0.107	0.103	0.095	0.129	0.065

Table 6.21: Fuel use for each route according to VSP bin during charge-depleting operation.

	Charge-Depleting Mode				
VSP Bin	Route: 109 Fuel (gal/km)	Route: 110 Fuel (gal/km)	Route: 12T/C Fuel (gal/km)	Route: 123 Fuel (gal/km)	Route: Highway Fuel (gal/km)
1	0.005	0.006	0.009	0.016	0.007
2	0.013	0.007	0.021	0.018	0.016
3	0.017	0.012	0.028	0.030	0.021
4	0.022	0.019	0.053	0.035	0.026
5	0.031	0.023	0.048	0.043	0.032
6	0.035	0.033	0.052	0.047	0.037
7	0.043	0.048	0.086	0.061	0.043
8	0.059	0.071	0.085	0.101	0.058

6.6 Emissions

6.6.1 Carbon Dioxide Emissions

During both charge-sustaining and charge-depleting operation, the PHEV's carbon dioxide emissions increased with increasing VSP bin. Operating in charge-sustaining mode resulted in approximately 50% higher CO_2 production during bins 1 and 2, 40% higher CO_2 production in bins 3 and 4, between 25 and 30% increased production in bins 5 and 6, and 15-23% increased CO_2 emissions in bins 7 and 8 when compared to charge-depleting operation. The difference in CO_2 emissions between the operating modes decreased with increasing VSP bin, as the internal combustion engine became the dominant power source when the PHEV experienced higher on-road power loads. Proportionally, the largest increase in CO_2 emissions occurred between Bins 1 and 2, with an almost 200% increase CO_2 production. The rate of increase in CO_2 emissions with VSP bin, generally, corresponds to the increase in dICE power output with increasing VSP bin. When evaluated according to drive mode (periods of acceleration, cruise, deceleration, and idle), CO_2 emissions remained higher during charge-sustaining operation versus charge-depleting operation for all designated driving modes, with periods of acceleration resulting in the highest levels of CO_2 emissions. Cruise mode was the second highest producer of CO_2. Both ANOVA and Kruskal-Wallis analysis of carbon dioxide emissions showed a statistically significant relationship between carbon dioxide emissions and both VSP bin and driving mode ($\alpha<0.05$). Statistical significance prevailed for each operating mode (charge-sustaining and charge-depleting) on a sample-run, route, and overall compiled dataset (continuous, second-by-second) level.

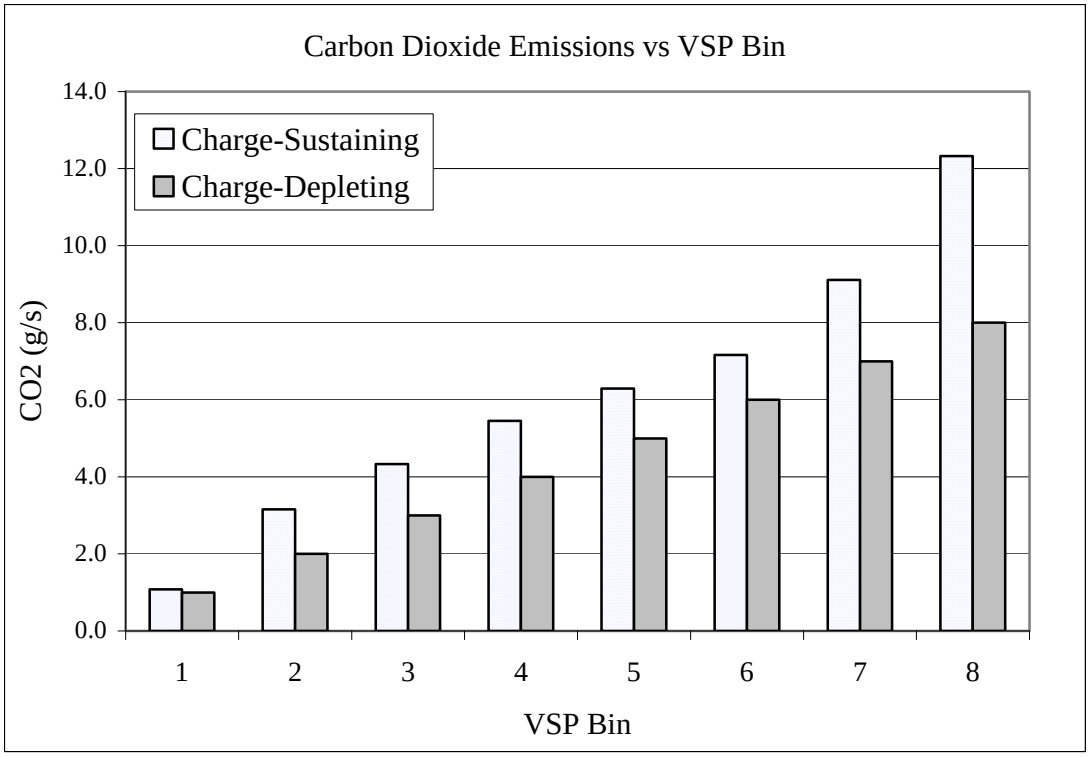

Figure 6.24: Carbon dioxide emissions according to VSP bin.

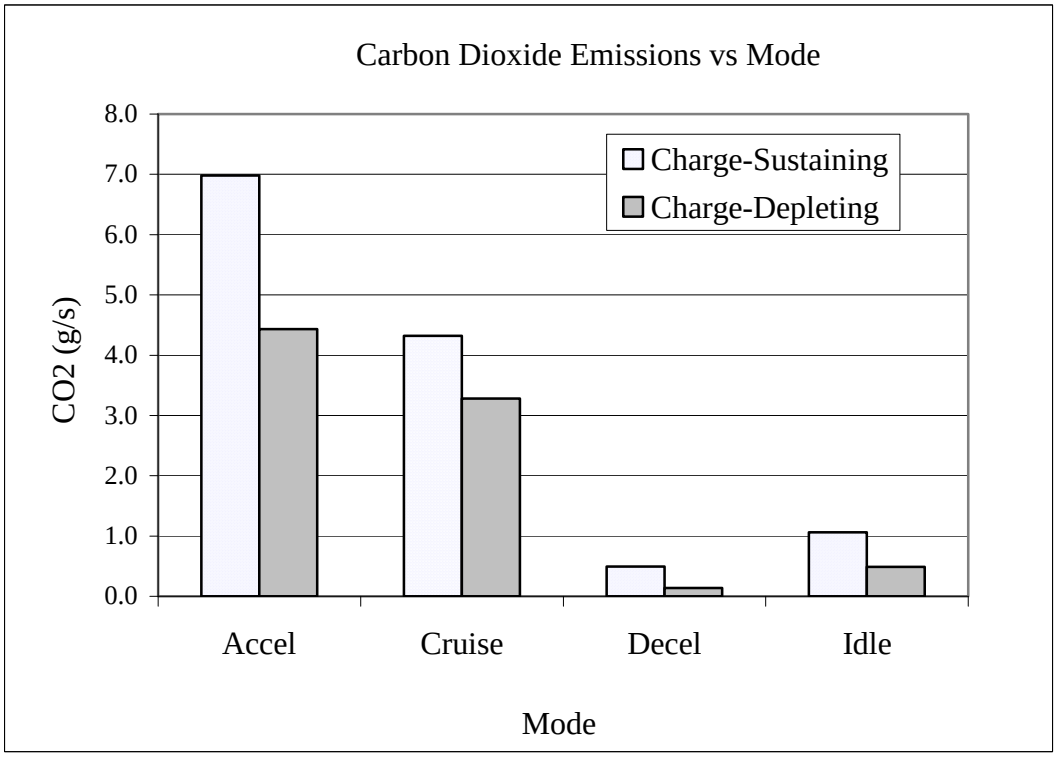

Figure 6.25: Carbon dioxide emissions according to driving mode.

Similar to power output, recuperation, and fuel use, some discrepancy exists between the carbon dioxide emissions for individual VSP bins according to the route being sampled. Given the nature of the VSP equation, this phenomenon is unexpected and contrary to the inherent purpose and merit of the VSP's intent. Carbon dioxide emissions were the lowest on the highway route across all 8 VSP bins compared to the in-town routes. Regarding CO_2 emissions during in-town driving, no obvious trends are present between the different in-town routes (109, 110, 12T/C, and 123) during charge-sustaining operation.

Table 6.22: Carbon dioxide emissions between sample routes in charge-sustaining operation.

	Charge-Sustaining Mode				
VSP Bin	**Route: 109 CO_2 (g/km)**	**Route: 110 CO_2 (g/km)**	**Route: 12T/C CO_2 (g/km)**	**Route: 123 CO_2 (g/km)**	**Route: Highway CO_2 (g/km)**
1	166.7	164.8	243.0	190.3	93.8
2	284.5	324.1	322.9	343.2	229.5
3	369.9	392.3	407.7	455.7	283.1
4	474.3	515.6	468.9	565.7	328.4
5	522.1	605.7	567.0	662.5	377.0
6	603.1	697.0	609.0	818.6	424.4
7	818.6	907.8	754.1	1035.3	491.8
8	1106.6	1056.5	978.9	1331.6	665.9

Carbon dioxide emissions during charge-depleting operation show considerable variability between sample route for each VSP bin. Based on cursory analysis, no pervading trends emerge between routes across all VSP bins. Highway operation resulted in the lowest levels of CO_2 emission at higher VSP levels, but during bins 1 through 4, highway driving was not extraordinary compared to the in-town routes. The 12T/C route presented the significantly higher CO_2 emissions in VSP bins 4, 6, and 7

than all other measured routes, while the 123 had the highest emissions during low VSP operation (bins 1 through 3). Routes 109 and 110 had the lowest CO_2 emissions of all in-town routes throughout all 8 VSP bins.

Table 6.23: Carbon dioxide emissions between sample routes in charge-depleting operation.

	Charge-Depleting Mode				
VSP Bin	Route: 109 CO_2 (g/km)	Route: 110 CO_2 (g/km)	Route: 12T/C CO_2 (g/km)	Route: 123 CO_2 (g/km)	Route: Highway CO_2 (g/km)
1	54.6	59.6	91.2	162.8	70.7
2	131.1	74.7	219.6	182.1	161.0
3	171.7	124.7	283.3	307.8	217.0
4	229.2	190.3	547.0	360.6	269.1
5	314.4	239.9	492.8	443.5	330.0
6	361.3	343.2	536.4	481.6	381.6
7	437.4	487.0	879.8	628.1	444.1
8	601.7	731.9	872.1	1039.6	600.8

6.6.2 Carbon Monoxide Emissions

Carbon monoxide's (CO) production as an emission pollutant is associated with incomplete or improper combustion within the combustion cylinder of the diesel internal combustion engine. Since carbon monoxide emissions are indicative of transient dICE operation, they do not directly correlate with the dICE work output or fuel use even though CO emissions are a direct cause of dICE's operation. Because of this, the CO emissions demonstrate a significantly different profile across VSP bins than observed with CO_2 or fuel-use data. During charge-sustaining operation, carbon monoxide emissions increased significantly between VSP bins 1 and 2 (from 0.00172g/s to 0.00642g/s), however, during operation in bins 2 through 7, carbon monoxide emissions, for the most part, plateaued until VSP bin 8, where they rose slightly. Unlike dICE

power output, fuel consumption, or CO_2 emissions, CO emission was lowest during charge-sustaining, or hybrid, operation where the diesel internal combustion engine's involvement in PHEV operation was maximized. During VSP bins 4 through 8, charge-depleting operation resulted in higher CO emissions than charge-sustaining operation, even though dICE work output was lowest during charge-depleting operation throughout these bins. This suggests that the diesel ICE, when engaged, was operating in a more transient nature during charge-depleting operation. The diesel ICE's application as a plug-in hybrid is investigated in more detail in Chapter 10. This phenomenon was also apparent when assessing CO emissions on a modal basis, with acceleration and cruise modes resulting in the highest CO emissions while the PHEV Sprinter was in charge-depleting operation.

During charge-sustaining mode CO emissions increased substantially (almost 275%) between VSP bins 1 and 2 and (on a g/s basis) plateaued in bins 2 through 7. Despite the appearance of leveled CO emissions in VSP bins 2 through 7, there was still enough distinction in CO emissions between the different bins to yield a statistically significant response between CO emissions and VSP bin as determined by ANOVA and Kruskal-Wallis analyses ($\alpha<0.05$). Carbon monoxide emissions also proved to be a statistically significant response to both VSP bin and driving mode during charge-depleting operation according to both ANOVA and Kruskal-Wallis analysis.

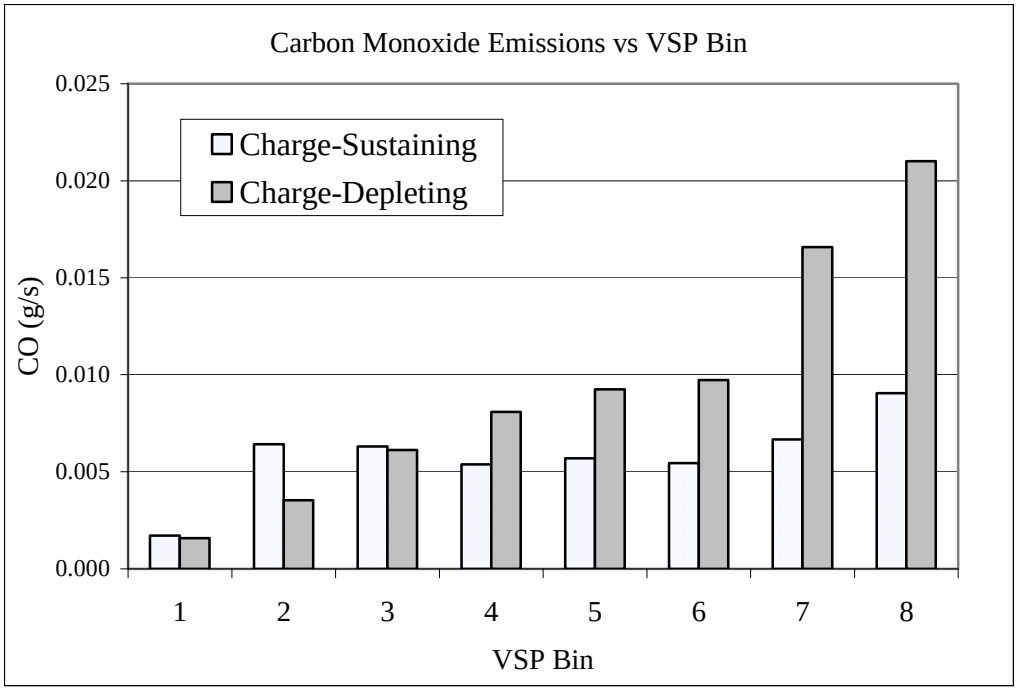

Figure 6.26: Carbon monoxide emissions according to VSP bin for both modes of operation.

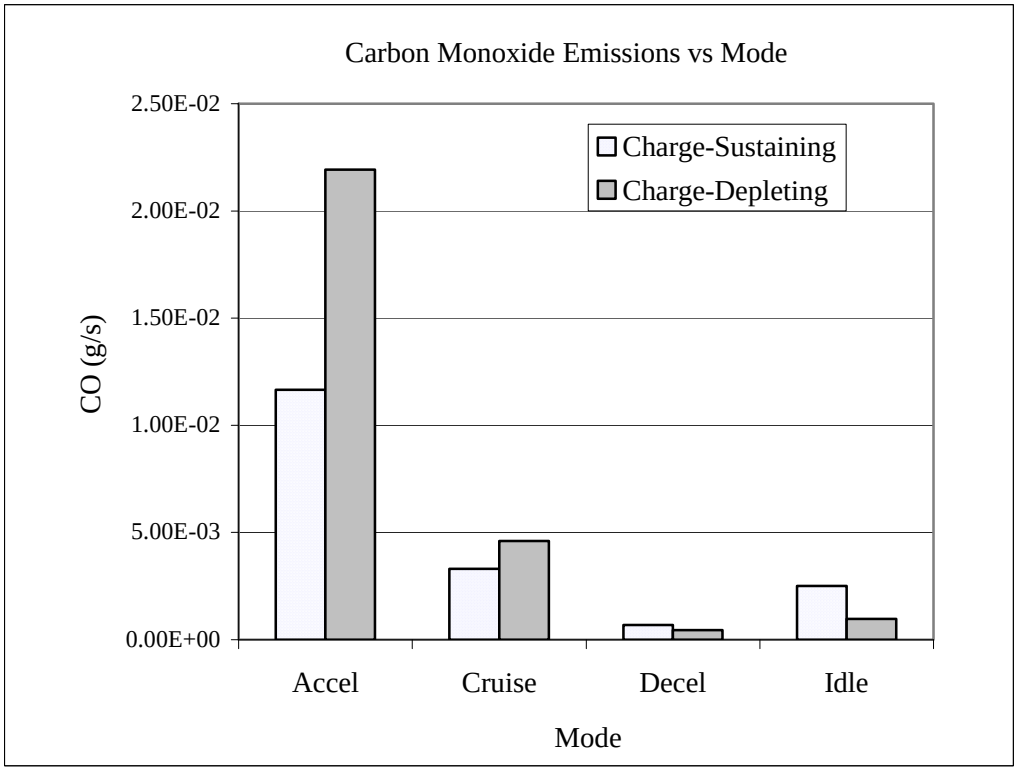

Figure 6.27: Carbon monoxide emissions according to driving mode for both charge-sustaining and charge-depleting operation.

Similar to CO_2 emissions and fuel use, discrepancies in carbon monoxide emissions according to VSP bin between the sample routes are apparent. During VSP bins 1 through 7, during charge-sustaining operation, the highway route yielded the lowest measured CO emissions of all routes sampled. Even though highway-based CO emissions remained lower than measured in-town emissions for VSP bin 8, the difference in highway versus in-town CO emissions in bin 8 was substantially diminished, and not guaranteed meaningful without statistical analysis (see Chapter 8). Route 123, the only exclusively suburban-based route, experienced the highest CO emissions during VSP bins 2 through 7. Similar results were found during charge-depleting operation, with the highway route yielding the lowest carbon monoxide emissions across all eight VSP bins.

Table 6.24: Carbon monoxide emissions, by sample route, across all VSP bins for charge-sustaining operation.

	Charge-Sustaining Mode				
VSP Bin	**Route: 109 CO (g/km)**	**Route: 110 CO (g/km)**	**Route: 12T/C CO (g/km)**	**Route: 123 CO (g/km)**	**Route: Highway CO (g/km)**
1	0.216	0.314	0.259	0.402	0.058
2	0.374	0.778	0.626	1.091	0.105
3	0.434	0.571	0.538	1.282	0.122
4	0.448	0.531	0.489	0.895	0.118
5	0.549	0.480	0.505	1.014	0.187
6	0.639	0.632	0.489	0.713	0.172
7	0.580	0.712	0.588	0.898	0.282
8	0.703	0.651	0.925	0.753	0.608

Table 6.25: Carbon monoxide emissions, by sample route, across all VSP bins for charge-depleting operation.

	Charge-Depleting Mode				
VSP Bin	Route: 109 CO (g/km)	Route: 110 CO (g/km)	Route: 12T/C CO (g/km)	Route: 123 CO (g/km)	Route: Highway CO (g/km)
1	0.277	0.214	0.222	0.555	0.085
2	0.480	0.317	0.663	0.502	0.130
3	0.473	0.632	1.125	0.999	0.234
4	0.692	0.719	2.473	1.406	0.253
5	0.992	1.049	1.256	1.665	0.235
6	1.066	1.291	0.794	1.762	0.278
7	2.163	2.190	2.836	3.134	0.426
8	1.664	3.245	1.517	2.983	0.744

6.6.3 Hydrocarbon emissions

Hydrocarbon emissions are the result of fuel (and sometimes oil) pass-through into the exhaust from the engine's combustion chambers due to incomplete combustion processes. High hydrocarbon (HC) emissions are indicative of transient ICE operation and most likely attributable to improper air/fuel ratios within the combustion chamber or poor injection timing. Since they are not an expected product of the ideal combustion reaction, hydrocarbon emissions, like carbon monoxide emissions, will not necessarily correspond in a direct manner with the diesel ICE power output even though they are a product of ICE operation.

Similar to CO emissions, charge-depleting operation, versus charge-sustaining operation, consistently resulted in the highest HC emissions for all 8 VSP bins. Hydrocarbon exhaust levels remained consistently 50% to 60% higher during CD mode even as the on-road calculated power load increased to the upper bounds of Bin 8. Regardless of prevalent operating mode, HC emissions consistently and continuously

increased with increasing power demand, with the largest increases in HC emissions occurring between bins 1 and 2 (58% and 53% increase for charge-depleting and charge-sustaining modes, respectively) and between bins 7 and 8 in charge-depleting mode (48% increase in emissions). Additionally, HC production experienced significant increases between bins 6 and 7 and between bins 7 and 8 during charge-sustaining operation (nominal 40% increase in emissions in both instances). For both modes of operation, hydrocarbon emissions increase at a faster rate as power demand approaches its maximum.

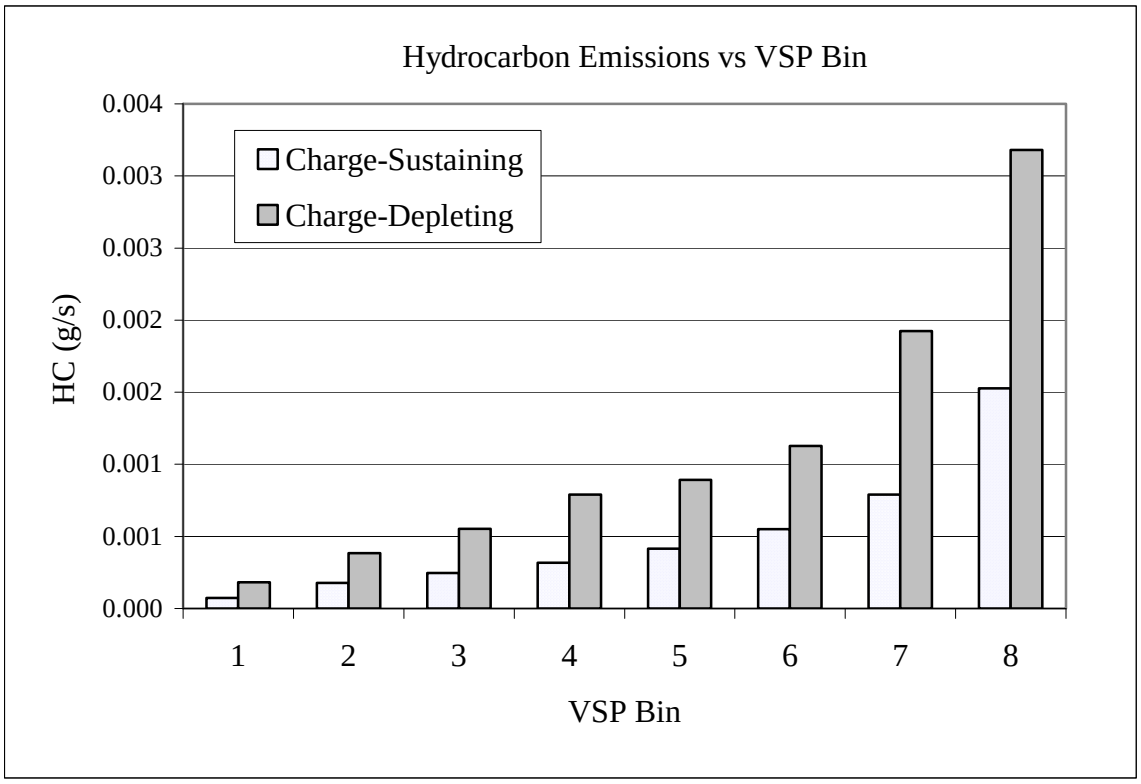

Figure 6.28: Hydrocarbon emissions during both charge-sustaining and charge-depleting mode across 8 VSP bins.

When classified according to driving mode, charge-depleting operation continued to demonstrate the highest levels of hydrocarbon production, resulting in a 64% increase in emissions during periods of acceleration and a 55% increase in emissions during cruise mode when compared to charge-sustaining operation. Acceleration events resulted in peak HC emissions followed by cruise mode, with acceleration events producing 58% and 48% more HC output than cruise mode during charge-sustaining and charge-depleting operation, respectively. Both deceleration and idle modes represented almost negligible HC exhaust levels.

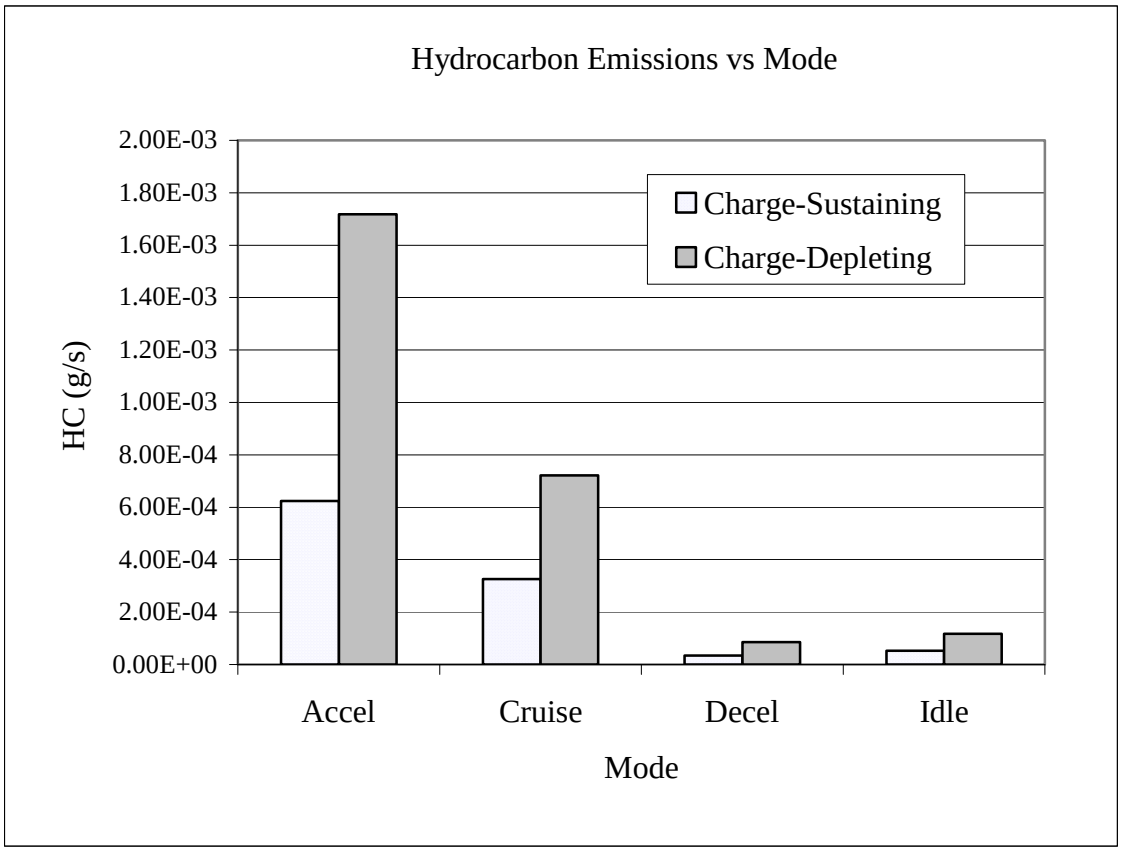

Figure 6.29: Hydrocarbon emissions during charge-sustaining and charge-depleting operation according to driving mode.

Generally, variations in hydrocarbon emissions between the different sample routes were not as significant as other pollutants or measured variables (power output), particularly at lower VSP levels such as bins 1 through 4. As VSP increased, divergent behavior in HC emissions (at each VSP bin greater than 5) appeared between the different sample routes. While all routes demonstrated increasing HC emissions with progressive VSP bin, HC emissions during highway operation accelerated the fastest. The relation of (average) HC emissions according to route for each VSP bin during charge-sustaining operation is shown in Table 6.26 and Figure 6.30 below.

Table 6.26: Hydrocarbon emissions according to sample route for each VSP bin during charge-sustaining operation.

	Charge-Sustaining Mode				
VSP Bin	**Route: 109 HC (g/km)**	**Route: 110 HC (g/km)**	**Route: 12T/C HC (g/km)**	**Route: 123 HC (g/km)**	**Route: Highway HC (g/km)**
1	0.017	0.007	0.014	0.014	0.011
2	0.020	0.013	0.017	0.021	0.018
3	0.028	0.017	0.020	0.028	0.021
4	0.034	0.024	0.023	0.036	0.024
5	0.041	0.034	0.028	0.046	0.029
6	0.047	0.051	0.027	0.061	0.039
7	0.060	0.071	0.033	0.082	0.057
8	0.077	0.079	0.062	0.108	0.143

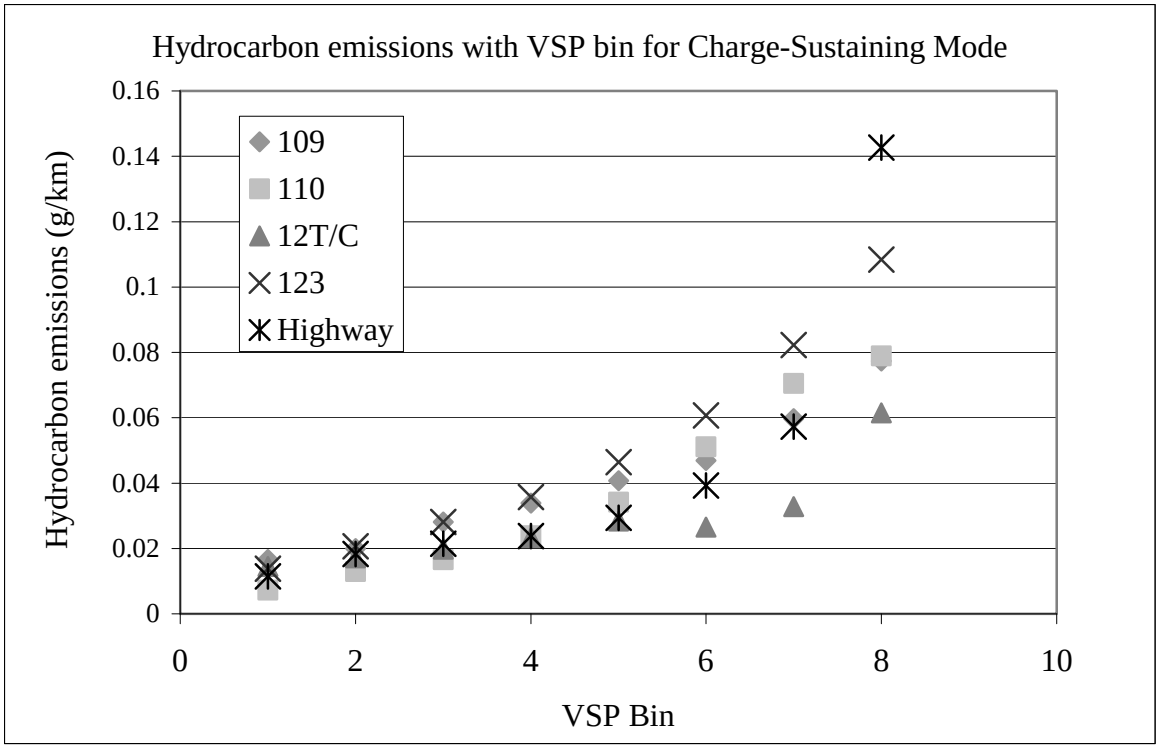

Figure 6.30: Hydrocarbon emissions according to VSP bin for each sample route, during charge-sustaining operation.

Where the highway, 123 and 12T/C routes showed the fastest rates of increasing HC emissions with progressive VSP bin from bins 5 through 8 in charge-sustaining operation, route behaviors changed during charge-depleting operation. The highway route was the least electrically active route during charge-depleting operation. However, despite the relative increase in dICE dependence, the highway route demonstrated the lowest hydrocarbon emissions during charge-depleting mode. Where the 110 route showed, comparatively, moderate HC emissions with a relatively steady (i.e. not accelerating) increase in HC production with increasing VSP bin in during charge-sustaining mode, it became the highest HC emitting route during charge-depleting operation when on-road power demand resided in the upper VSP bins.

Table 6.27: Hydrocarbon emissions according to VSP bin for each sample route during charge-depleting operation.

	Charge-Depleting Mode				
VSP Bin	**Route: 109 HC (g/km)**	**Route: 110 HC (g/km)**	**Route: 12T/C HC (g/km)**	**Route: 123 HC (g/km)**	**Route: Highway HC (g/km)**
1	0.040	0.028	0.022	0.047	0.014
2	0.063	0.030	0.044	0.039	0.021
3	0.080	0.043	0.052	0.061	0.027
4	0.105	0.081	0.082	0.088	0.033
5	0.112	0.090	0.050	0.126	0.034
6	0.131	0.137	0.064	0.161	0.044
7	0.235	0.269	0.167	0.255	0.070
8	0.201	0.403	0.237	0.337	0.149

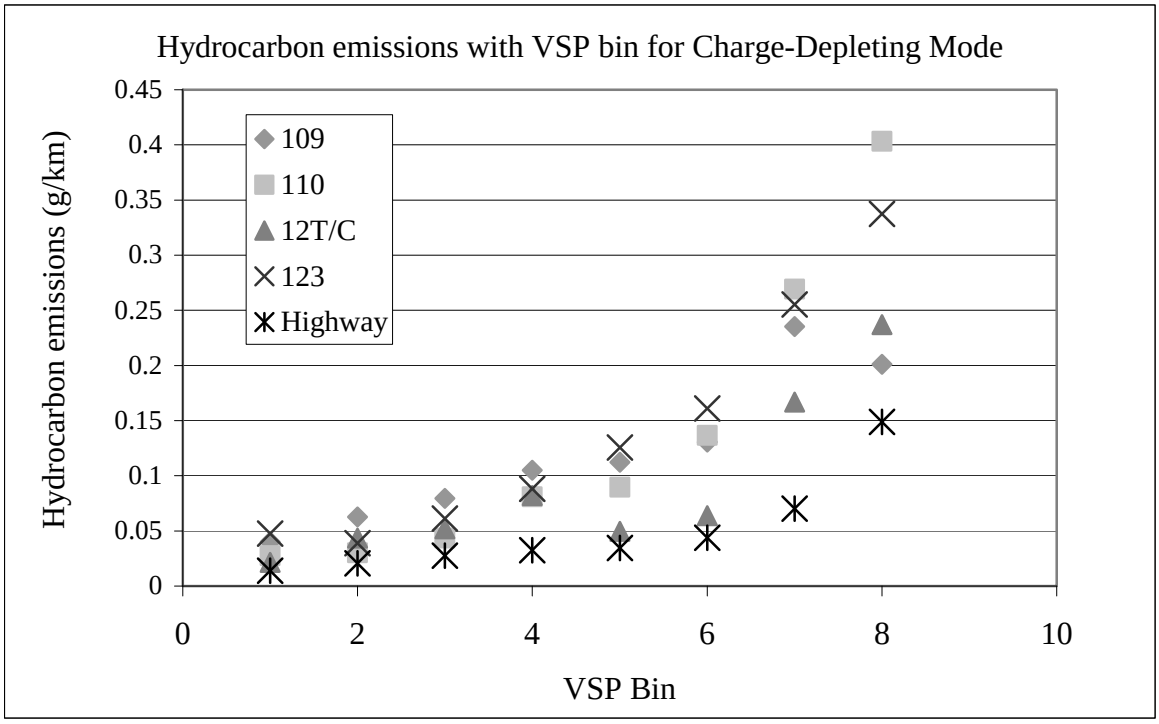

Figure 6.31: Hydrocarbon emissions according to VSP bin during charge-depleting operation.

6.6.4 Nitrogen Oxides Emissions

Nitrogen oxides (NOx), a combination of nitric oxide (NO) and nitrogen dioxide (NO_2), are a regulated compilation of pollutants in the transportation sector. In the case of the PHEV Sprinter's emissions, NOx emissions are dominated by the presence of NO compared with NO_2. Therefore, the quantitative differences and trends observed with NOx emissions between the operating modes (charge-sustaining versus charge-depleting) and sample routes are similar to those reported in the NO emissions discussion. For this reason, discussion of NOx emissions will be succinct in favor of the more detailed investigation into NO and NO_2 production independently.

NOx emissions increased with increasing VSP bin for both charge-sustaining and charge-depleting operation, with charge-sustaining operation resulting in the highest levels of NOx formation. With regards to driving mode-based analysis, acceleration mode produced significantly higher levels of NOx than cruise mode, with deceleration and idle modes showing low-levels of NOx emissions. The variation between acceleration and cruise mode was much less pronounced during charge-depleting operation. ANOVA and Kruskal-Wallis analyses of NOx emissions according to modal categorization showed that NOx emissions were a statistically significant response ($\alpha<0.05$) to driving mode and VSP bin for both modes of operation on a compiled dataset level, route-based level, and sample run scale.

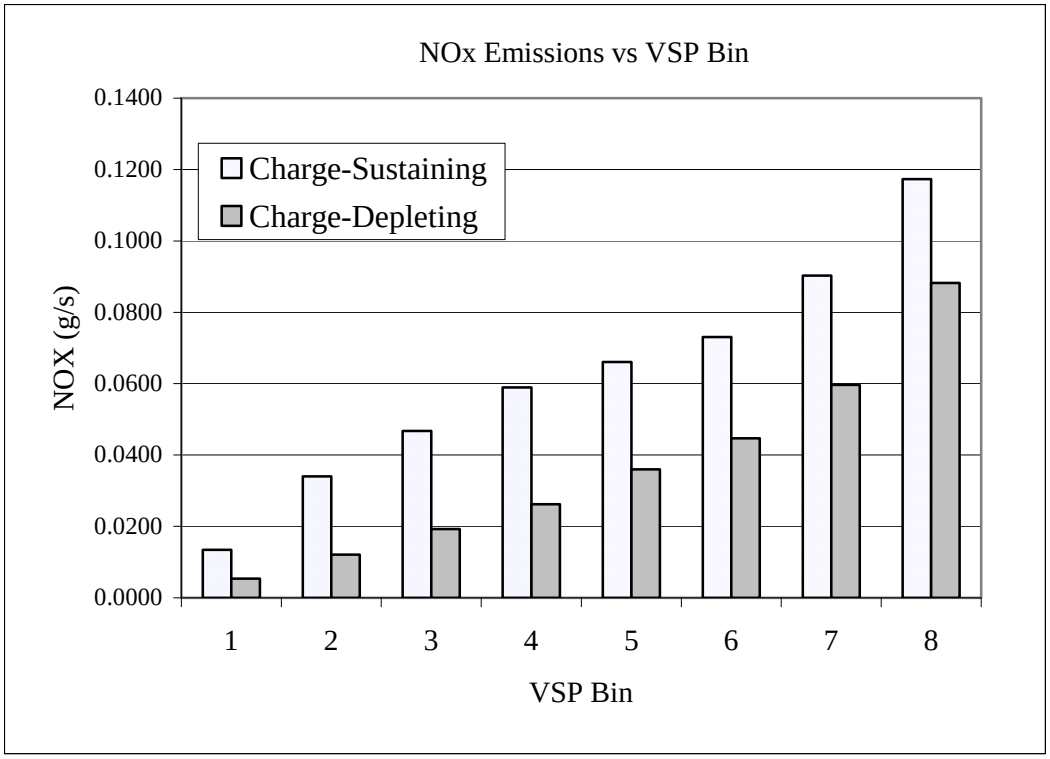

Figure 6.32: NOx emissions according to VSP for both PHEV operating modes.

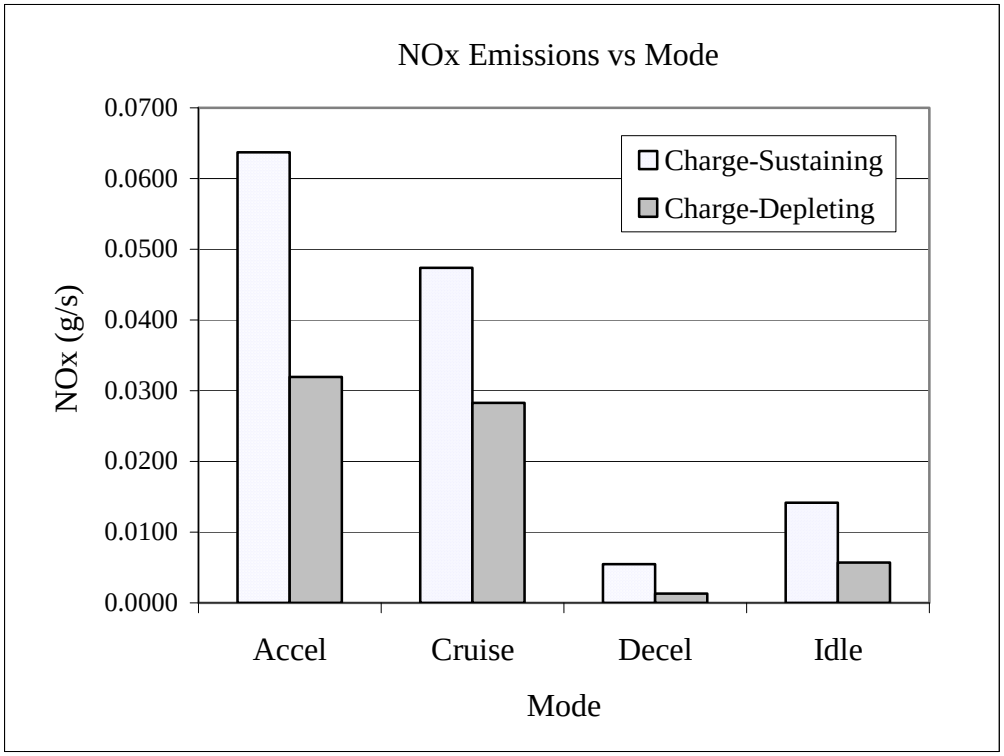

Figure 6.33: NOx emissions according to driving mode for both PHEV operating schemes.

6.6.5 Nitric Oxide and Nitrogen Dioxide Emissions

The Semtech-DS directly measured nitrogen oxide (NO) and nitrogen dioxide (NO_2) in the PHEV's exhaust. General trends relating to NO and NO_2 emissions were discernable by evaluating the NOx data, however, nuances in NO and NO_2 formation within the plug-in hybrid design are not apparent by looking at the NOx emissions alone.

Nitrogen oxide (NO) and NO_2 emissions increased with increasing VSP bin. However, in charge-sustaining operation, where NO emissions consistently and constantly increased from VSP bins 1 through 8, NO_2 emissions demonstrated a plateau during VSP bins 4, 5, and 6 before showing an increase in bins 7 and 8. Nitrogen dioxide is a secondary pollutant whose formation occurs in the presence of excessive heat and pressure and is not the result of the normal combustion reaction. Periods of plateau in NO_2 formation are indicative of stable ICE operation, so the tapering of NO_2 emissions in the mid-VSP range suggests comparatively stable ICE function providing more homogeneous combustion conditions. More detailed distinctions in ICE operation and power demand during different VSP bins are investigated in Chapter 10.

Nitrogen oxide and nitrogen dioxide emissions during charge-depleting operation also showed an increase in pollutant formation with increasing VSP bin, although charge-depleting operation resulted in overall lower emissions for all 8 VSP bins. Nitrogen dioxide emissions showed a straight-line increase through all 8 VSP bins during charge-depleting operation, and did not demonstrate the leveling during the midrange VSP bins (4, 5, and 6) that was observed during charge-sustaining mode.

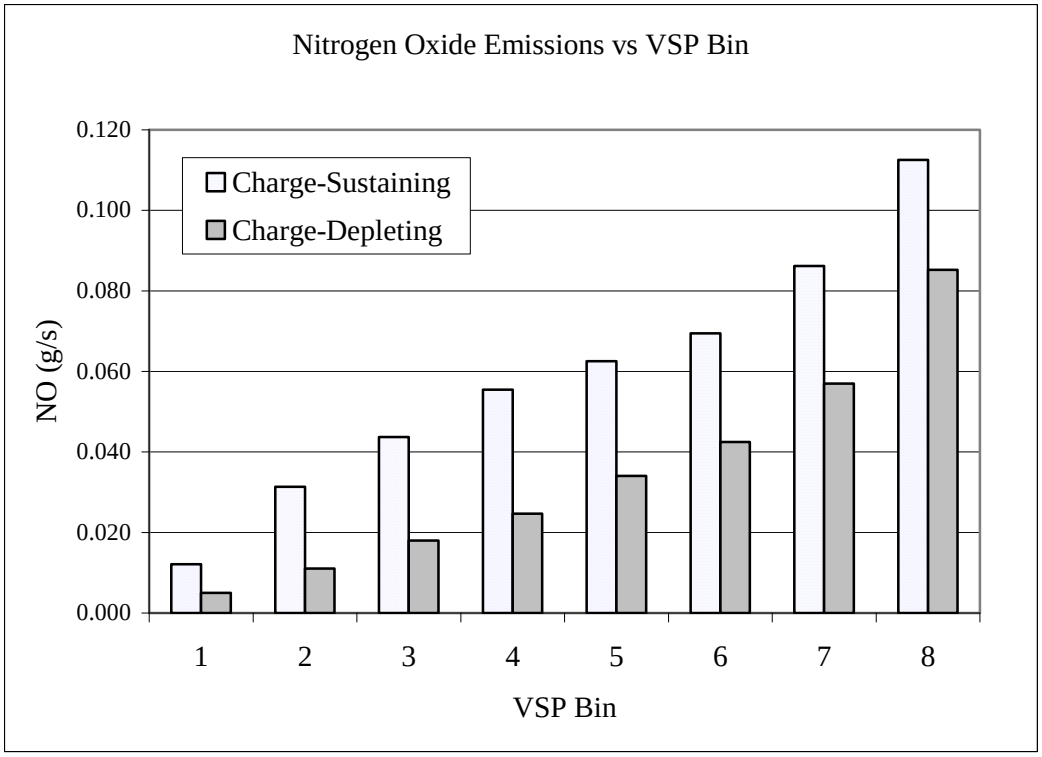

Figure 6.34: NO emissions according to VSP bin.

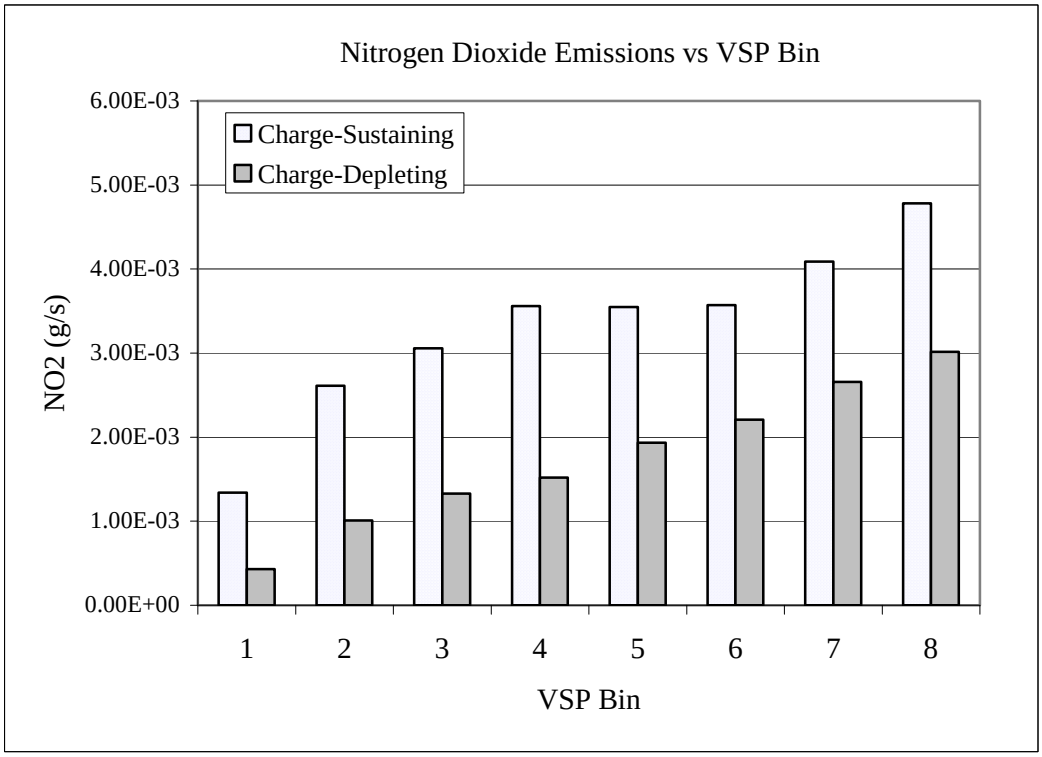

Figure 6.35: NO_2 emissions according to VSP bin.

Modal analysis shows that periods of acceleration resulted in the highest NO and NO_2 emissions during charge-sustaining operation, where cruise mode resulted in the second highest levels of NO and NO_2 production. This trend was less apparent during charge-depleting operation, where moments of acceleration only resulted in a slight increase in NO emissions, and an actual decrease in NO_2 emissions when compared to cruise mode. Charge-sustaining idling resulted in a not-insignificant production of NO and NO_2, particularly when compared to deceleration events, whereas idling during charge-depleting operation resulted in NO and NO_2 emissions that were considerably closer to those witnessed during periods of deceleration. Nitrogen oxide and nitrogen dioxide emissions were statistically significant responses to both VSP bin and driving mode ($\alpha<0.05$) according to analysis of variance and its non-parametric equivalent, Kruskal-Wallis analysis.

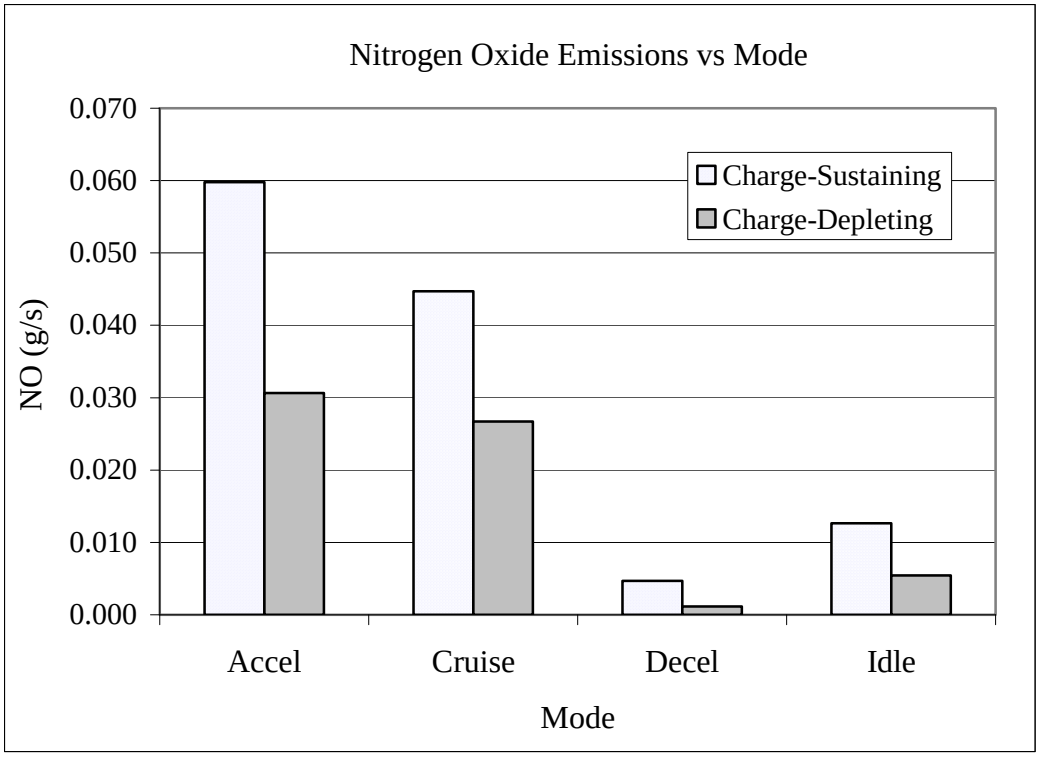

Figure 6.36: NO emissions according to driving mode.

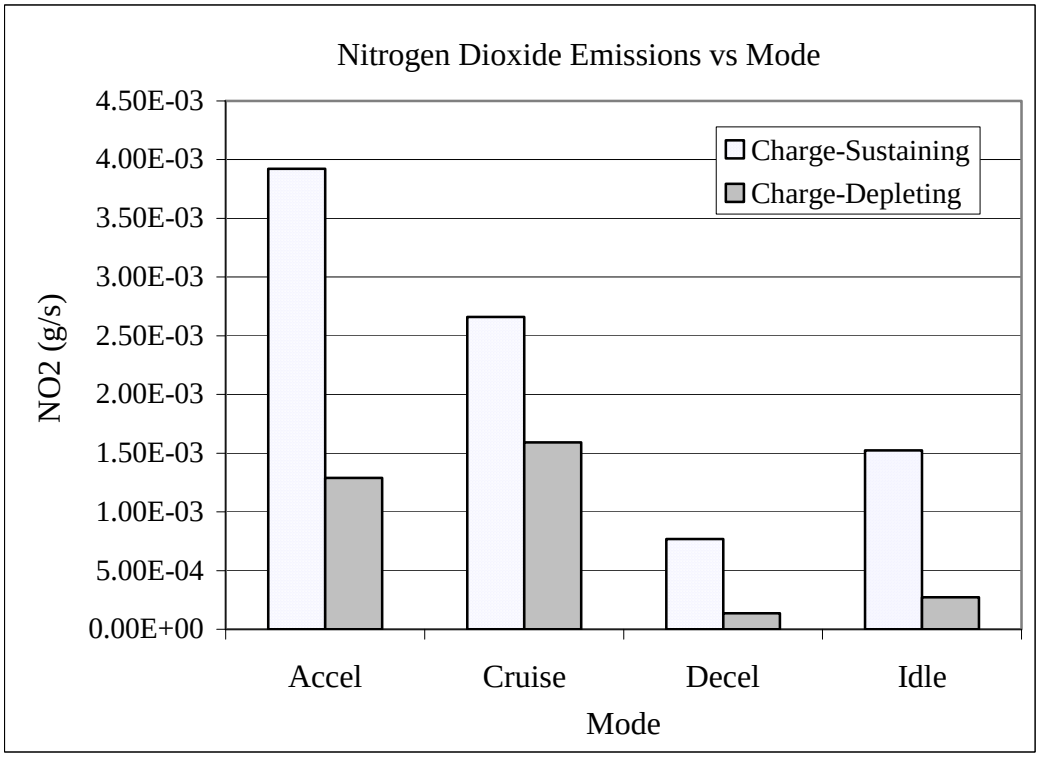

Figure 6.37: NO_2 emissions according to driving mode.

With regards to charge-sustaining operation, highway driving resulted in the lowest levels of both NO and NO_2 emissions across all 8 VSP bins. Nitrogen oxide production during highway operation was almost half of what was emitted during in-town driving during the first six VSP bins. Slight convergence between roadways was observed during the highest load VSP bins (7 and 8), but the highway route still maintained the lowest levels of NO formation. Similar to NO, highway driving produced a fraction of the NO_2 emissions that the in-town routes did, on average.

Some variation in NO emissions may exist between the in-town routes, but charge-sustaining operation yielded no obvious trends between the different routes. The 123 route resulted in the highest levels of NO emissions while the PHEV was operating under higher loads, but statistical significance can not be determined based on cursory observation alone. Nitrogen dioxide emissions, however, did demonstrate consistent variability between the in-town routes with the 109 route producing the lowest NO_2 emissions and the 12T/C resulting in the highest (between 59% and 68% higher emissions, VSP bin dependent) NO_2 production across all 8 VSP bins.

Table 6.28: NO emissions according to route during charge-sustaining operation.

	Charge-Sustaining Mode				
VSP Bin	**Route: 109 NO (g/km)**	**Route: 110 NO (g/km)**	**Route: 12T/C NO (g/km)**	**Route: 123 NO (g/km)**	**Route: Highway NO (g/km)**
1	2.094	1.853	2.538	2.266	0.833
2	3.188	3.419	3.086	3.431	1.823
3	4.108	4.280	4.127	4.387	2.390
4	5.409	5.446	4.718	5.586	2.948
5	5.574	6.349	5.420	6.455	3.493
6	6.145	6.829	5.677	7.730	4.138
7	7.896	8.395	6.785	9.419	4.913
8	9.932	9.637	8.537	11.571	6.391

Table 6.29: NO_2 emissions according to route during charge-sustaining operation.

Charge-Sustaining Mode					
VSP Bin	Route: 109 NO_2 (g/km)	Route: 110 NO_2 (g/km)	Route: 12T/C NO_2 (g/km)	Route: 123 NO_2 (g/km)	Route: Highway NO_2 (g/km)
1	0.140	0.206	0.437	0.236	0.056
2	0.160	0.258	0.521	0.276	0.092
3	0.174	0.274	0.562	0.303	0.110
4	0.219	0.322	0.655	0.367	0.116
5	0.210	0.320	0.698	0.375	0.125
6	0.247	0.346	0.670	0.459	0.128
7	0.280	0.416	0.815	0.524	0.115
8	0.366	0.499	0.889	0.621	0.106

Unlike charge-sustaining operation, no obvious trends emerged between the different sample routes with regards to NO and NO_2 emissions while the PHEV was in charge-depleting mode. Sizeable differences in NO and NO_2 emissions between the sample routes exist within each VSP bin, however, the statistical significance of these differences cannot be assessed based on the information presented here. This is presented in more detail in Section 6.8.

Table 6.30: NO emissions according to route during charge-depleting operation.

Charge-Depleting Mode					
VSP Bin	Route: 109 NO (g/km)	Route: 110 NO (g/km)	Route: 12T/C NO (g/km)	Route: 123 NO (g/km)	Route: Highway NO (g/km)
1	0.480	0.593	0.681	1.686	0.529
2	0.891	0.605	1.312	1.546	0.947
3	1.261	1.088	1.722	2.357	1.413
4	1.725	1.603	2.519	2.563	1.953
5	2.717	1.859	2.825	3.312	2.602
6	3.046	2.750	3.791	3.333	3.172
7	3.472	3.584	5.231	4.450	3.845
8	4.440	5.321	6.099	7.434	5.170

Table 6.31: NO_2 emissions according to route during charge-depleting operation.

Charge-Depleting Mode					
VSP Bin	**Route: 109 NO_2 (g/km)**	**Route: 110 NO_2 (g/km)**	**Route: 12T/C NO_2 (g/km)**	**Route: 123 NO_2 (g/km)**	**Route: Highway NO_2 (g/km)**
1	0.011	0.018	0.065	0.149	0.079
2	0.021	0.025	0.187	0.156	0.116
3	0.025	0.033	0.207	0.209	0.134
4	0.030	0.037	0.312	0.191	0.150
5	0.036	0.050	0.417	0.236	0.172
6	0.043	0.072	0.449	0.230	0.186
7	0.057	0.086	0.589	0.254	0.193
8	0.065	0.125	0.486	0.356	0.182

6.7 PHEV Sprinter Emissions Compared to Literature Findings

High anticipation of the emerging plug-in hybrid market is primarily based on the technology's potential to reduce petroleum demand as well as minimize on-road vehicle emissions. Despite regular media mention, the PHEV market has yet to truly emerge on a production level. Researchers have been testing the plug-in hybrid concept on retrofitted hybrid vehicles for the past five to six years (Carlson et al, 2007), however, these studies have been limited in scope and design based on vehicle availability and research focus. The Kansas City PHEV Sprinter was truly unique in vehicle class, engine designation, and its on-road, in-use use testing. Because of this, it is not possible to find direct comparative vehicle emissions or fuel use data from which to assess the Sprinter PHEV's emission-reduction potential and efficiency gains.

Using on-board data collected from 12 different in-use transit buses, Zhai, et al, evaluated on-road emissions from heavy-duty (HD) diesel transit buses (Zhai, 2008), reporting fleet averaged emissions data for the 8-bin VSP modal distribution. Unlike the lighter-duty PHEV, the transit buses were heavy-duty, 12-ton vehicles, equipped with 8.5L engines. Despite the obvious physical differences in vehicles, Zhai's work represents the most analogous comparison of on-road emissions data available to date.

6.7.1 Carbon dioxide: Comparative discussion of the PHEV Sprinter versus conventional vehicles

Like the PHEV, the transit buses showed increasing CO_2 emissions with increasing VSP bin, however, where the PHEV's CO_2 emissions exhibited only a slight rate of increase with higher VSP bins, heavy-duty diesel buses showed a fairly straight-

line increase in CO_2 emissions with increasing vehicle load, exhibiting a profile more consistent with the PHEV's charge-depleting operation. However, compared with the heavy-duty diesel transit buses, the PHEV Sprinter quantitatively demonstrated significantly lower carbon dioxide emissions. PHEV on-road operation resulted in a nominal decrease in carbon dioxide emissions of between 55% and 70% in charge-sustaining operation, and between 64% and 80% in charge-depleting operation. Again, this comparison favors the PHEV Sprinter since it is of a lower vehicle class and weight.

Table 6.32: Carbon dioxide emissions compared with heavy-duty transit buses.

VSP Bin	HD Transit Buses	Charge-Sustaining		Charge-Depleting	
	CO_2 (g/s)	CO_2 (g/s)	% Reduction	CO_2 (g/s)	% Reduction
1	2.4	1.08	55%	0.54	77%
2	7.8	3.16	60%	1.62	79%
3	12.5	4.33	65%	2.51	80%
4	17.1	5.45	68%	3.39	80%
5	21.2	6.29	70%	4.36	79%
6	24.8	7.16	71%	5.29	79%
7	27.6	9.12	67%	7.01	75%
8	29.5	12.33	58%	10.52	64%

6.7.2 Carbon Monoxide: Comparative discussion of the PHEV Sprinter versus conventional vehicles

Carbon monoxide emissions profiles varied considerably between the transit buses and the PHEV Sprinter. In-use transit buses showed a peak CO emission rate at VSP bin 6, with declining emissions during VSP bins 7 and 8. Conversely, the PHEV Sprinter demonstrated continuously increasing CO emissions with increasing VSP bin. VSP bins 7 and 8 exhibited the fastest rate of increasing CO emissions during charge-sustaining operation. When the PHEV Sprinter was operating during charge-depleting

operation, however, it did not show any significant trend in CO emissions with increasing VSP bin, resulting in steadily increasing emissions during VSP bins 2 through 7. In addition to obvious differences in the trend of CO emissions with increasing power demand between the conventional transit buses and PHEV Sprinter, the PHEV provided substantial reductions in CO emissions across all VSP bins for both charge-sustaining and charge-depleting operation, Table 6.33.

Table 6.33: Carbon monoxide emissions compared with heavy-duty transit buses.

VSP Bin	HD Transit Buses	Charge-Sustaining		Charge-Depleting	
	CO (g/s)	CO (g/s)	% Reduction	CO (g/s)	% Reduction
1	0.009	0.002	81%	0.002	82%
2	0.036	0.006	82%	0.004	90%
3	0.045	0.006	86%	0.006	86%
4	0.072	0.005	93%	0.008	89%
5	0.085	0.006	93%	0.009	89%
6	0.091	0.005	94%	0.010	89%
7	0.084	0.007	92%	0.017	80%
8	0.062	0.009	85%	0.021	66%

6.7.3 Hydrocarbons: Comparative discussion of the PHEV Sprinter versus conventional vehicles

Unlike the PHEV's accelerating increase in hydrocarbon emissions with increasing VSP bin, the HD transit buses exhibited a relatively flat trend in HC emissions across the 8 VSP bin categories, with the only marked change in emissions occurring between bins 1 and 2. Additionally, the PHEV Sprinter's on-road use resulted in an almost order of magnitude decrease in HC emissions compared with the HDDV transit buses for the first 6 VSP bins during charge-sustaining mode, and first 5 VSP bins during charge-depleting operation. At the highest VSP ranges, PHEV hydrocarbon emissions

neared those of the transit buses during charge-sustaining operation, and exceeded the conventional transit buses during charge-depleting operation.

Table 6.34: Hydrocarbon emissions compared with heavy-duty transit buses.

VSP Bin	HD Transit Buses	Charge-Sustaining		Charge-Depleting	
	HC (mg/s)	HC (mg/s)	% Reduction	HC (mg/s)	% Reduction
1	1.23	0.074	94%	0.181	85%
2	1.70	0.177	90%	0.383	77%
3	1.75	0.247	86%	0.552	68%
4	1.84	0.318	83%	0.791	57%
5	1.94	0.414	79%	0.892	54%
6	2.05	0.551	73%	1.127	45%
7	2.08	0.789	62%	1.925	7%
8	2.15	1.528	29%	3.181	-48%

6.7.4 Nitrogen Oxides (NOx): Comparative discussion of PHEV versus conventional vehicles

Similar to the other measured and regulated pollutants, the PHEV Sprinter exhibited significantly lower NOx emissions compared to the transit buses, particularly during charge-depleting operation.

Table 6.35: NOx emissions compared with heavy-duty transit buses.

VSP Bin	HD Transit Buses	Charge-Sustaining		Charge-Depleting	
	NOx (g/s)	NOx (g/s)	% Reduction	NOx (g/s)	% Reduction
1	0.04	0.013	66%	0.005	86%
2	0.13	0.034	74%	0.012	91%
3	0.18	0.047	74%	0.019	89%
4	0.22	0.059	73%	0.026	88%
5	0.24	0.066	72%	0.036	85%
6	0.26	0.073	72%	0.045	83%
7	0.28	0.090	68%	0.060	79%
8	0.31	0.117	62%	0.088	72%

While notable differences in the trends and extent of pollutant emissions were apparent between the PHEV Sprinter and on-road diesel transit buses, care must be interjected into the above comparisons, since the PHEV Sprinter and transit buses are of different vehicle class, age, and designated purpose (transit versus civilian driving, as was the case in the PHEV data used here). All three differences have been found to be significant factors in on-road emissions measurements (Clark and Kern, 2002 and Frey et al., 2008).

The PHEV Sprinter's emissions were quantitatively inline with the reported on-road emissions from a large, passenger, gasoline-powered, 5.3L Tahoe (Zhang, 2006). The PHEV Sprinter produced consistently lower carbon dioxide emissions across the VSP ranges in consideration during both charge-sustaining and charge-depleting operation. The PHEV did report slightly higher CO emissions, particularly in the upper VSP range in charge-sustaining operation, with PHEV emissions well exceeding the passenger vehicle in charge-depleting operation. However, the charge-sustaining hydrocarbon PHEV emissions remained lower than Tahoe's until the highest VSP levels.

As expected, NOx emissions from the PHEV were several orders of magnitude higher than the gasoline-powered vehicle.

6.8 Differences between routes within VSP Bins

Distinct differences in the PHEV Sprinter's operation (power output and fuel use) and pollutant emissions were noticed between the sample routes within each VSP bin. Variations in PHEV operation and emissions within the 8 VSP bins were contradictory to experimenter expectation. The reaction of the measured response variables to estimated power demand was anticipated to be similar within a set power range regardless of traveled roadway. Other than basic observation and noting obvious trends between sample routes, the possibility that PHEV on-road operation possessed a degree of route dependency, even within normalized VSP bins, was previously not subjected to a more rigorous statistical analysis. In the interest of delivering a well-rounded narrative of the PHEV Sprinter's on-road experience, this section will dedicate itself to delivering a more statistically robust analysis of the potential differences between the sample routes.

Both ANOVA and the non-parametric equivalent, Kruskal-Wallis, tests were employed in the following investigation. However, unlike the VSP analysis on the prior pages, statistical significance was set at $\alpha<0.025$ for both ANOVA and Kruskal-Wallis analyses. Due to the size of the datasets and concern for attributing statistical significance where none existed, the statistical analyses were interpreted in a conservative manner. Failure of either analysis to meet the set alpha was considered sufficient grounds to regard the comparison void of statistical significance.

Prior to conducting a series of univariate analyses on the different operating, driving, and emissions variables according to route at the VSP bin level, multivariate analyses of variance (MANOVA) were performed on the compiled charge-sustaining and charge-depleting datasets. It was important to establish statistical validity at the

multivariate level before proceeding to a series of independent univariate analyses in order to avoid making Type I errors due to the sheer size of the datasets.

For both the charge-sustaining and the charge-depleting dataset, MANOVA was conducted on the dataset comprised of all sample routes and on a separate dataset based on the in-town sample routes only (109, 123, 110, and 12T/C), exclusive of the highway route. Since the largest discrepancy between routes was observed between highway and in-town driving, there was concern that the PHEV Sprinter's noticeable difference in operation and emissions during highway driving would suggest statistically significant differences between all of the routes, when, in actuality, the only meaningful difference occurred between highway and in-town sampling. In all four MANOVAs, selected emissions (CO_2, CO, NO, NO_2, NOx, and HC), operating (dICE power output and EM power output), and driving (velocity, acceleration, and grade) variables were modeled as responses to the factors VSP Bin and Sample Route. For all tests reported, statistical significance was verified on both the VSP Bin and Route levels. Verifying statistical significance using MANOVA provides validity to proceed with univariate analysis in order to investigate the effect of route on PHEV operation and emissions within each VSP bin.

6.8.1 Driving Variables

Before investigating the PHEV's dependent operating and emissions variables, driving and roadway effects were evaluated, focusing the initial univariate analysis on vehicle velocity, acceleration, and roadway grade. Highway driving presented the most unique on-road characteristics when compared to the in-town routes, so all ANOVA and

Kruskal-Wallis tests were run on the data inclusive of all routes, and again on the in-town (109, 110, 123, 12T/C) routes alone. There was some concern that the exceptional nature of the highway driving could force statistical significance when all routes are analyzed together that might not hold true when considering the in-town (urban/suburban) routes alone. Tables 6.36 and 6.37 provide synopsis of the statistical tests conducted on the roadway-based variables.

Table 6.36: Statistical results for road-based variables, for all routes.*

VSP BIN	1	2	3	4	5	6	7	8
Velocity (km/h)	y	y	y	y	y	y	y	y
Acceleration (m/s^2)	y	y	y	y	y	y	y	y
Grade (%)	y	Inc2	y	y	y	y	y	y

Table 6.37: Statistical results for road-based variables, for in-town routes only.*

VSP BIN	1	2	3	4	5	6	7	8
Velocity (km/h)	y	y	y	y	y	y	y	y
Acceleration (m/s^2)	Inc2	y	y	y	y	y	y	y
Grade (%)	y	n	Inc2	Inc2	y	Inc2	Inc2	y

*y≡Valid for both ANOVA and Kruskal-Wallis
n≡Invalid for both ANOVA and Kruskal-Wallis
Inc1≡Valid for ANOVA, invalid for Kruskal-Wallis
Inc2≡Invalid for ANOVA, valid for Kruskal-Wallis

The highway route, across all 8 bins, had a consistently higher average velocity than all other routes. However, even the analyses of the in-town routes demonstrated statistically significant variations in velocity across all 8 VSP Bins with routes 109 resulting in the highest average vehicle velocity while route 123 held the lowest average velocity in bins 1 through 6. Since the population tests used rely on calculated mean and

determined median of each sample tested, excessive time at zero velocity within each bin had the potential to skew the statistical results to some extent.

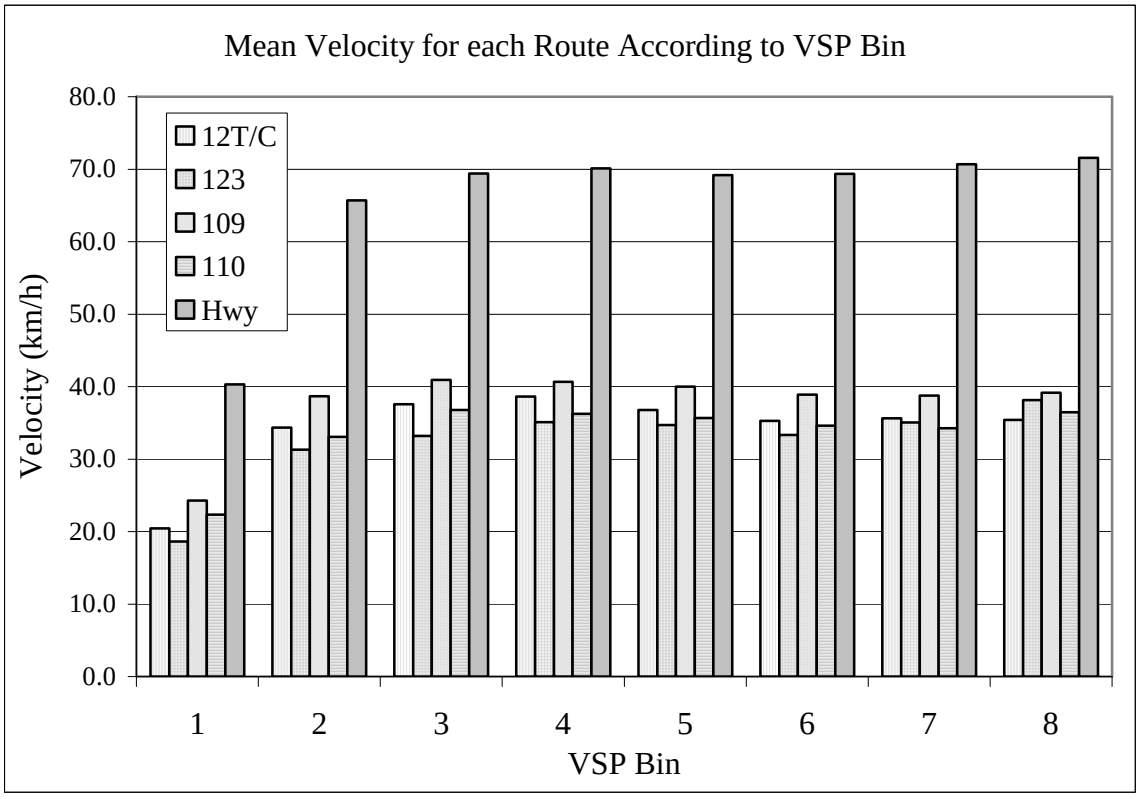

Figure 6.38: Average velocity according to route for 8 VSP bins.

Acceleration rate was also statistically significant between routes for all VSP bins except for bin 1 when the in-town routes were analyzed together. Highway driving resulted in consistently, and markedly, lower acceleration rates than all in-town driving for all VSP bins. Aside from bin 1, where no statistical significance in acceleration rate according to route was found, the 123 and 110 routes demonstrated the largest acceleration rates for all remaining VSP bins, with the general pattern distribution of acceleration rates for each route pervading across bins 2 through 8.

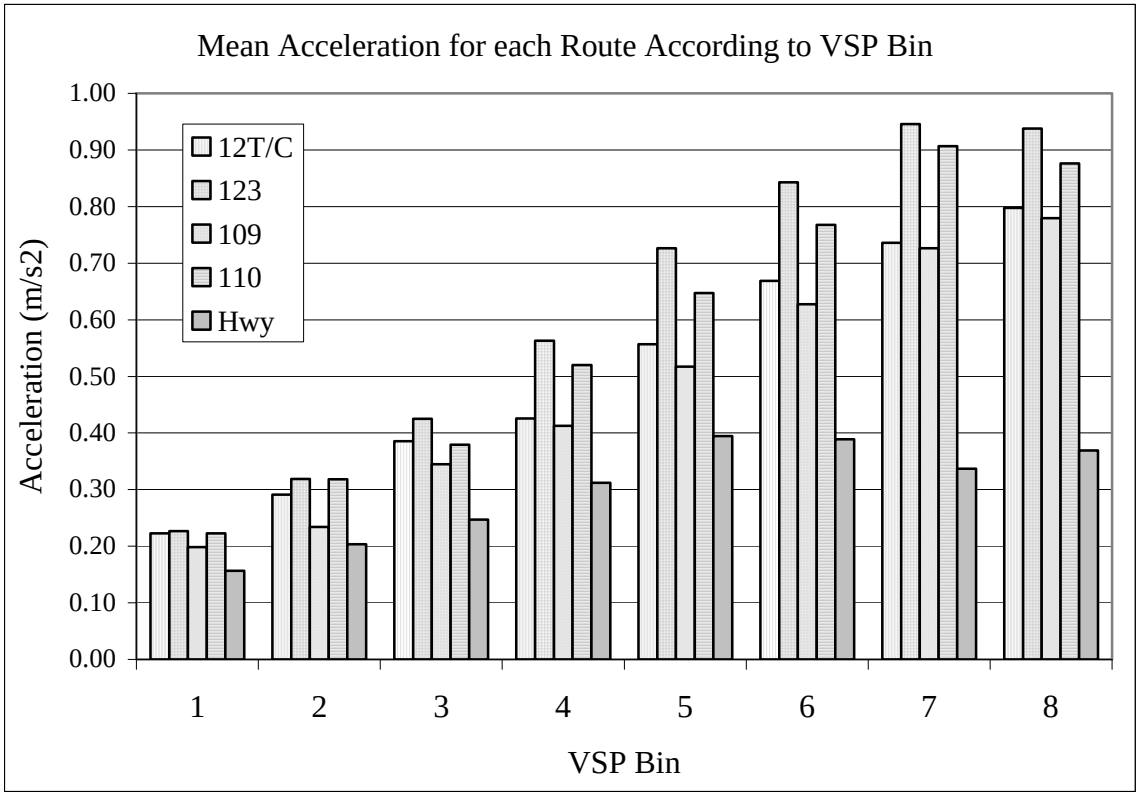

Figure 6.39: Average acceleration rates according to sample route for all VSP bins.

Unlike velocity and acceleration rate, grade did not prove to be a strong response to route for each VSP bin. In order to provide a meaningful estimation of the demand that grade places on the PHEV's operation, only data with grades of zero or greater were included in this analysis. The initial analysis, inclusive of the highway route, did show statistically significant differences between average grades for each route for all VSP bins except bin 2. Geographically, the highway route was the most distant and removed route from those sampled. All other routes tended to span the same general geographic area (see Figure 3.6). However, when the in-town, or suburban/urban routes were analyzed exclusive of the highway route, the statistical significance of grade in each VSP bin dropped considerably, with only bins 1, 5, and 8 showing statistical significance according to grade. Unlike, velocity and acceleration, both of which showed some

patterned consistency between routes across VSP bins; no pattern emerges between the routes with regards to grade across the VSP bins.

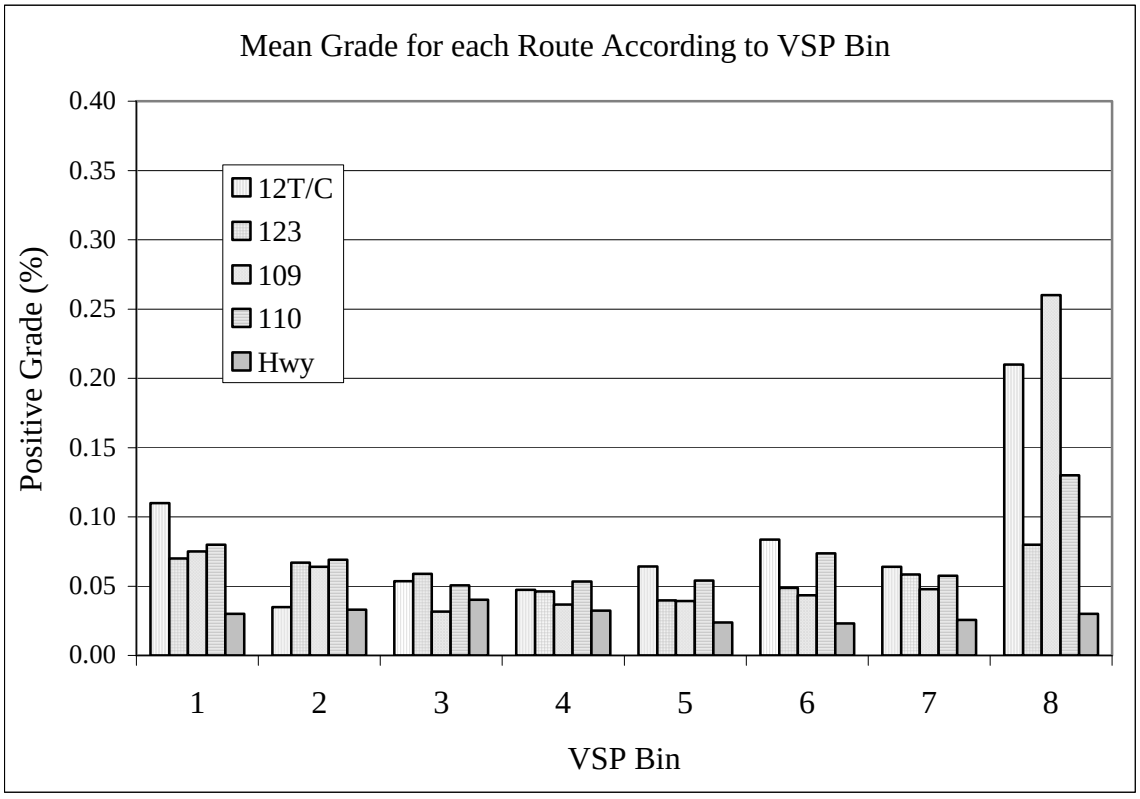

Figure 6.40: Positive grade according to each route for all VSP Bins.

6.8.2 Dependent Variables by Route, VSP Bin

6.8.2.1 Charge-Sustaining Operation: Power Output

As noted earlier, there is a statistically strong relationship between PHEV total power output and VSP bin. However, embedded within the VSP bin categorization, some variation in power output between routes was noted. VSP bins 1, 2, 5, 7, and 8 exhibited a statistically significant relationship between sample route and total power, however, no discernable pattern emerged between the routes across the VSP bins. The

difference in total power output across the different sampled routes within each bin is very small compared to the overall trend in total power output across the 8 different VSP bins. Any statistically significant association between the different routes and the diesel internal combustion engine (dICE) power output across the 8 VSP bins was limited to bins 1-5 and 8. However, similar to total power output, no apparent trends or patterns between the different routes and dICE power output were noticeable across the bins. Tables 6.38 and 6.39 give a synopsis of the statistical results attained for the all-routes analysis and the in-town routes only analysis.

Table 6.38: Statistical results for all routes during charge-sustaining operation, in each VSP bin.*

VSP BIN	**1**	**2**	**3**	**4**	**5**	**6**	**7**	**8**
Fuel, gal/s	y	y	y	y	y	y	y	y
CO_2, g/s	y	y	y	y	y	y	y	y
CO, g/s	y	y	y	y	y	y	Inc1	y
NOx, g/s	y	Inc2	Inc2	Inc2	no	y	y	y
NO, g/s	y	Inc2	y	y	y	y	y	y
NO_2, g/s	y	y	y	y	y	y	y	y
HC, g/s	y	y	y	y	y	y	y	y
ICE Power, W/kg/s	y	y	y	y	y	y	y	y
EM Power, W/kg/s	y	y	y	y	y	y	y	y
Total Pwr, W/kg/s	y	y	y	no	y	y	y	y
Recup, W/kg/s	y	y	y	Inc2	Inc1	Inc1	y	y

*y≡Valid for both ANOVA and Kruskal-Wallis
n≡Invalid for both ANOVA and Kruskal-Wallis
Inc1≡Valid for ANOVA, invalid for Kruskal-Wallis
Inc2≡Invalid for ANOVA, valid for Kruskal-Wallis

Table 6.39: Statistical results for the in-town routes during charge-sustaining operation in each VSP bin.*

VSP BIN	1	2	3	4	5	6	7	8
Fuel, gal/s	y	y	y	y	y	y	Inc2	Inc2
CO_2, g/s	y	y	y	y	y	y	Inc2	Inc2
CO, g/s	y	y	y	y	y	y	y	y
NOx, g/s	y	Inc2	Inc2	Inc2	y	Inc2	y	y
NO, g/s	y	y	y	y	y	y	y	y
NO_2, g/s	y	y	y	y	y	y	y	y
HC, g/s	y	y	y	y	y	y	y	y
ICE Power, W/kg/s	y	y	y	y	y	Inc2	Inc2	y
EM Power, W/kg/s	y	y	y	y	y	y	y	y
Total Pwr, W/kg/s	y	y	no	y	y	Inc2	y	y
Recup, W/kg/s	y	y	y	y	y	y	y	y

*y≡Valid for both ANOVA and Kruskal-Wallis
n≡Invalid for both ANOVA and Kruskal-Wallis
Inc1≡Valid for ANOVA, invalid for Kruskal-Wallis
Inc2≡Invalid for ANOVA, valid for Kruskal-Wallis

Electrical motor (EM) power output across the VSP bins showed more variability between routes in each bin than either total or dICE power output. This variability was found to be statistically significant across all 8 VSP bins, although no visible pattern between the routes was apparent. Other than highway driving resulting in the least amount of EM recruitment across all bins, no single suburban/urban route stood out as consistently requiring the most or least EM usage across the VSP range. EM power output fluctuated the most among the different routes in the higher VSP bins (7 and, particularly, 8). Similar with dICE power output across the range of 8 VSP bins, the variation, on average, in EM power output between the different VSP bins exceeded any differences in EM power output between the different sample routes within each bin. Inter-route variability in power output within each VSP bin is not as significant as the power output across the different VSP bins.

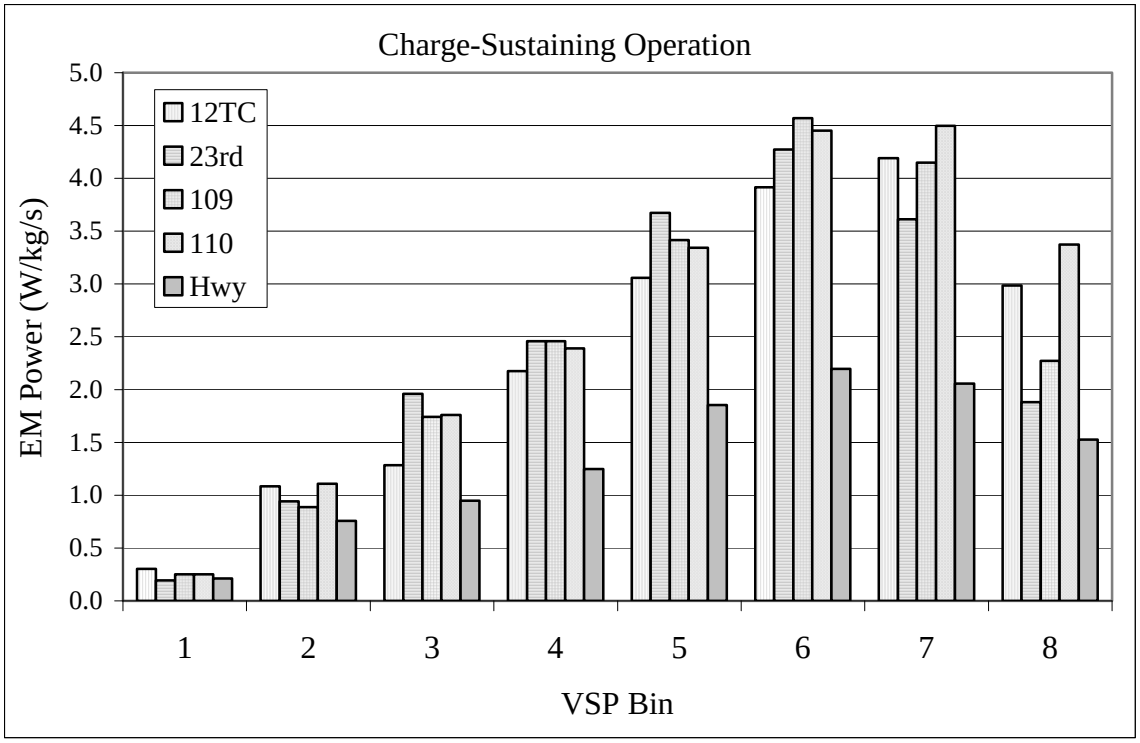

Figure 6.41: Electric motor power output for all sample routes across VSP bins during charge-sustaining operation.

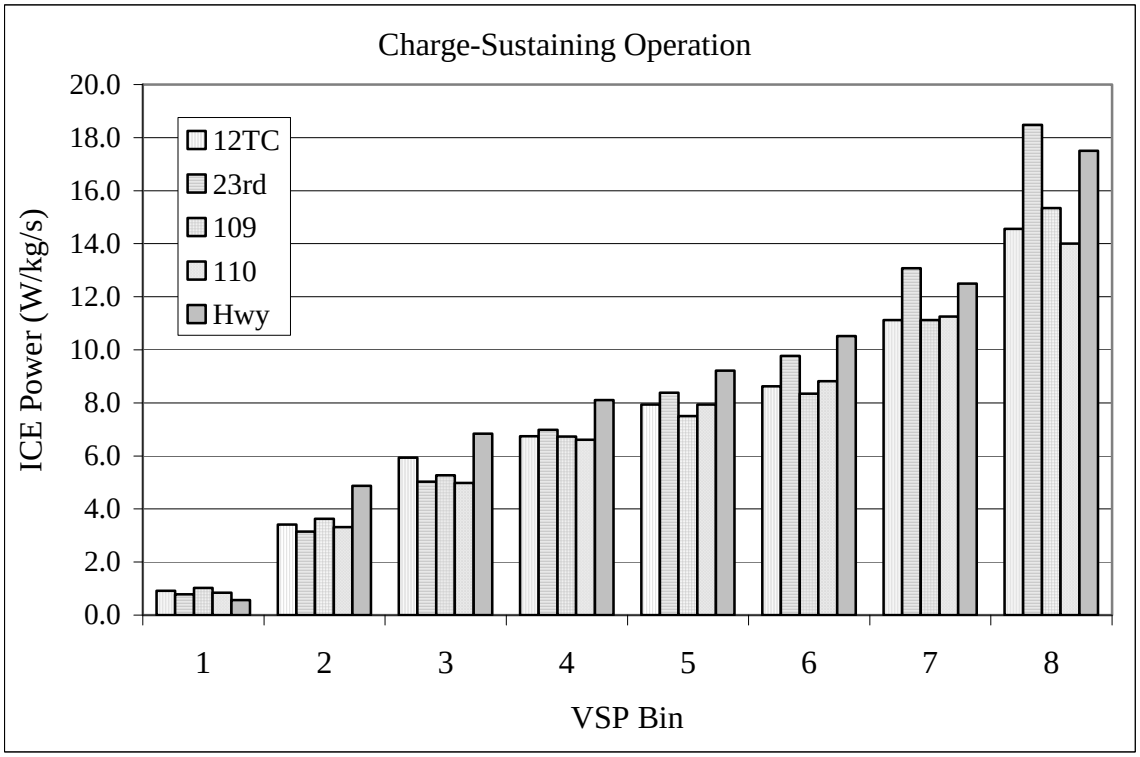

Figure 6.42: Diesel ICE power output for all sample routes across all VSP bins during charge-sustaining operation.

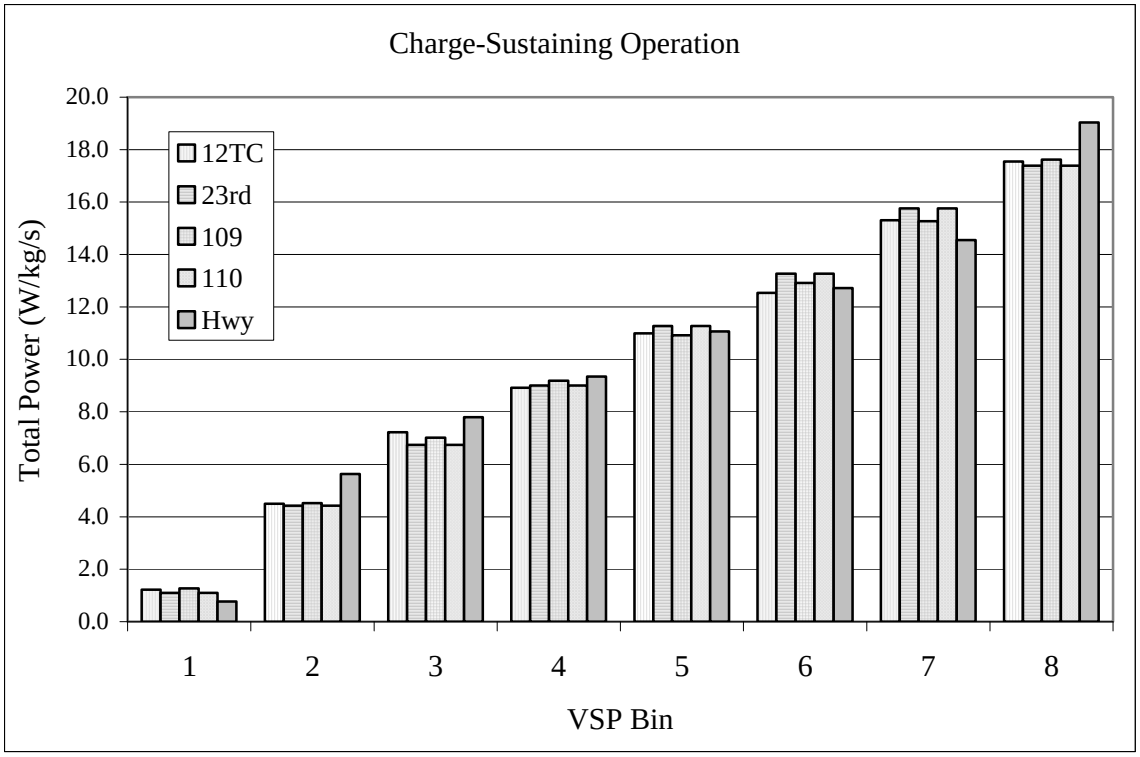

Figure 6.43: Total power output for all sample routes across all 8 VSP bins during charge-sustaining operation.

6.8.2.2 Charge-Sustaining Operation: Emissions

Overall, the PHEV's fuel use increased with increasing VSP bin ($\alpha<0.05$) however, within VSP bins one through six, both ANOVA and Kruskal-Wallis analysis found statistically significant differences in fuel use between each of the sample routes. Other than the highway route requiring more fuel per second than the urban/suburban routes, no obvious pattern emerges between the sampled in-town routes across VSP bins 1 through 6. Route 123 used more fuel while the 12th Street T/C loop used the least amount of fuel compared to the other in-town routes while operating in the upper VSP bins (bin 4 and greater). Even though fuel use from the individual sample routes was found to be from statistically different populations in VSP bins 1 through 6, the variation between the routes was the smallest during the lower VSP bins, suggesting that the

PHEV Sprinter operated in a more consistent manner during periods of lower imposed vehicle load.

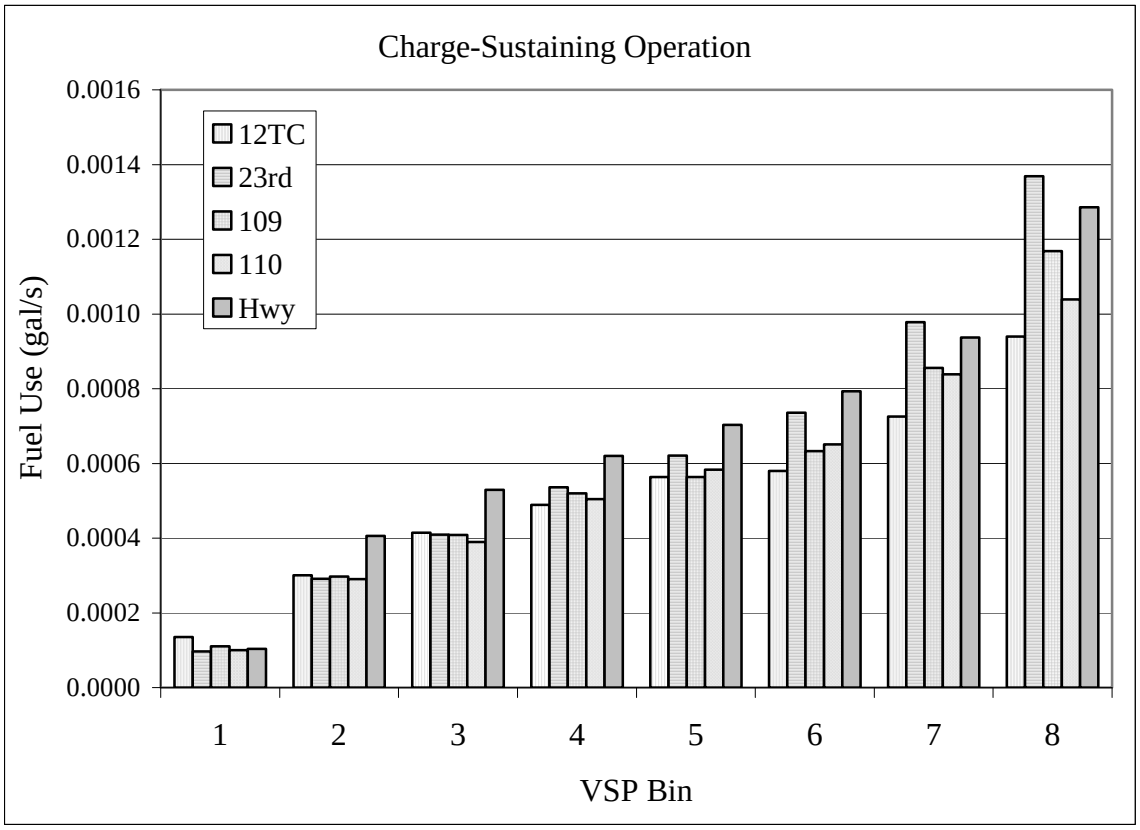

Figure 6.44: Fuel use for each sample route, according to VSP bin during charge-sustaining operation.

Carbon dioxide emission correlates directly with fuel use. Slight changes to carbon dioxide emissions during transient operation where, stoichiometrically, carbon monoxide production would utilize a portion of the available carbon, were not noticeable due to the three order of magnitude difference in CO_2 versus CO emissions. Carbon monoxide emission made no quantitative impact on measured CO_2 in the PHEV's exhaust. Because of this, any trends or observations in fuel use according to sampled route across the range of VSP bins are applicable to CO_2 emissions. In bins 4 and

greater, the 123 route emerged as the highest CO_2 producer, where the 12th Street T/C route resulted in the lowest CO_2 emissions. While statistical significance between the routes was found at all VSP bins, when the analysis was inclusive of all sampled routes analysis of the in-town routes alone did not yield route as a statistically significant factor to CO_2 emissions in VSP bins 7 and 8. Corresponding to the highway route's proportionally larger utilization of the dICE across most VSP bins and resulting increased fuel use in bins 2 through 8, highway operation resulted in the highest CO_2 emissions compared with in-town driving for all VSP bins except bin 1.

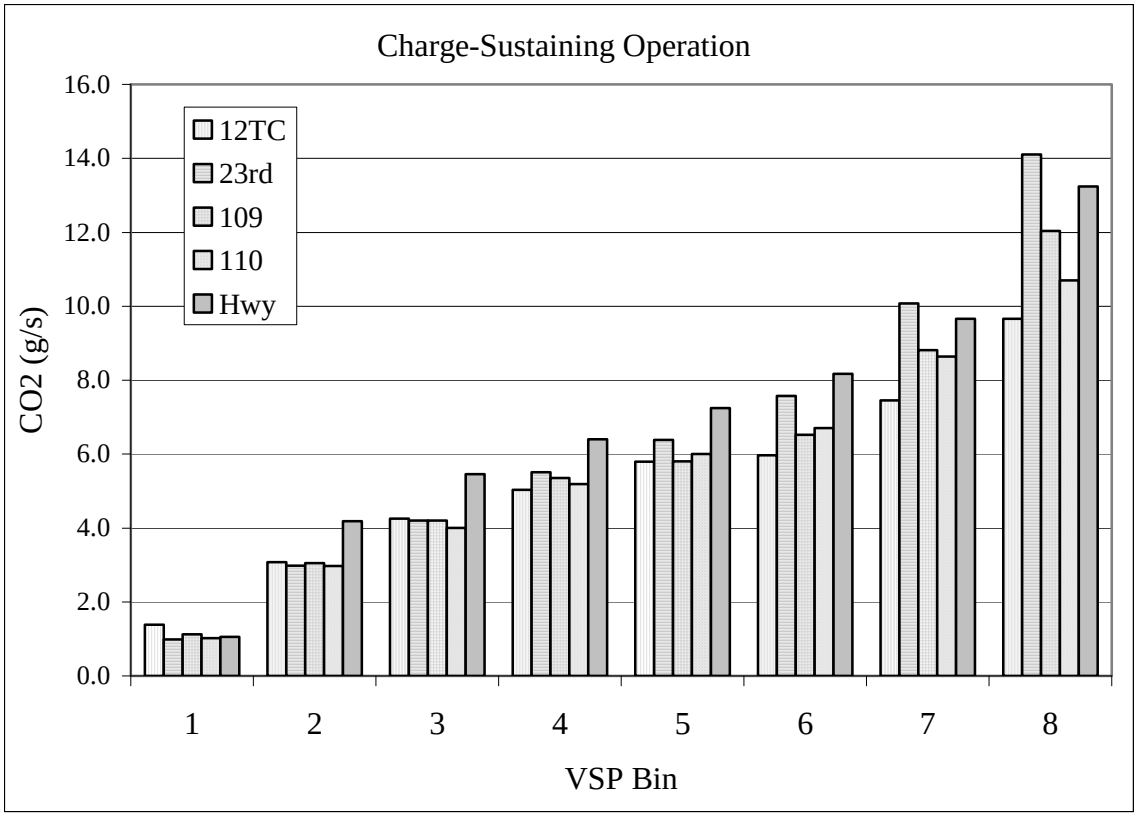

Figure 6.45: Carbon dioxide emissions for each route according to VSP bin during charge-sustaining operation.

Nitrogen oxide (NO) emissions also correlate highly with the diesel ICE use and, consequently, fuel use. However, unlike fuel use and carbon dioxide emissions, NO emissions remained a statistically significant response to route across all VSP bins, except for the "all routes" analysis of bin 2 (in-town only routes proved to be statistically significant factors to NO emissions at bin 2). The spread in NO emissions between routes increased with increasing VSP bin. While highway operation generally produced higher NO emissions in all VSP bins except 1, for in-town driving, the 123 route produced the highest NO emissions in bins 6 through 8, with the 9th street route producing slightly higher NO emissions in bins 2 through 4. Nitrogen oxide was positively, weakly, correlated with both vehicle velocity and acceleration. It is not unlikely that driving characteristics dominated NO production, with the in-town route resulting in the highest acceleration, route 123, dominating NO production during the higher VSP bins (where acceleration rates were the most dramatic), and the in-town route with the higher average velocity, route 109, resulting in the highest NO emissions (along with highway operation) during the lower VSP bins.

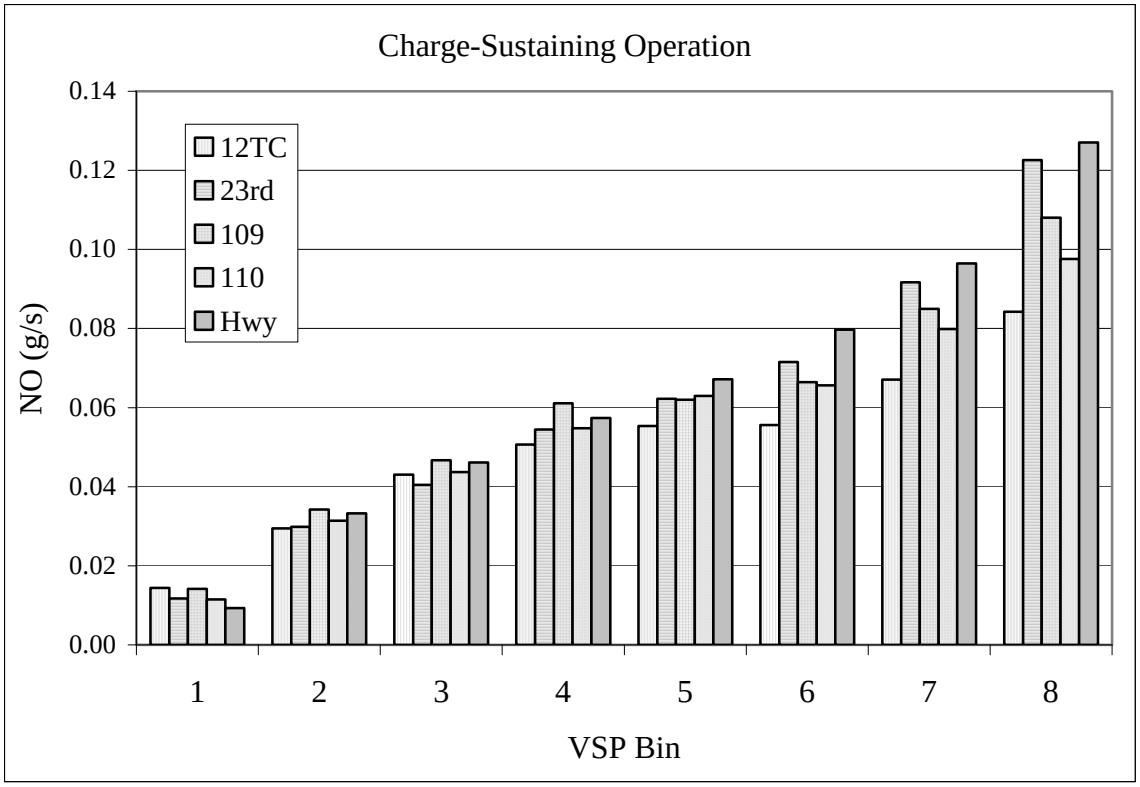

Figure 6.46: Nitrogen oxide emissions for all sample routes according to VSP bin during charge-sustaining operation.

Nitrogen dioxide emissions are not *direct* products of the combustion reaction, but are, instead, the by-product of the oxidation of nitrogen at high temperatures. Because of this, nitrogen dioxide emissions were not expected to correlate as highly with dICE operation parameters (dICE power output and fuel use) as more direct emission products such as carbon dioxide. Nitrogen dioxide emissions were found to be a statistically significant response to sample route across all VSP bins for both the all-route inclusive analysis as well as the in-town route only analysis. Comparatively, the relative production of NO_2 for each route remained consistent across all 8 VSP bins, with the 12th street T/C route resulting in the highest NO_2 emissions, and the highway route producing the lowest levels of NO_2. Quick analysis of exhaust temperatures across the different sample routes for each VSP bin indicated that the exhaust temperatures were statistically

significantly different for each of the sample routes across all 8 VSP bins, however, where highway operation resulted in the lowest NO_2 production on a g/s basis, the highway operation actually resulted in consistently higher exhaust temperatures than in-town sampling across all 8 VSP bins. The highest NO_2-emitting in-town route, 12th T/C, produced consistently lower exhaust temperatures than either highway operation or 123 route sampling. Gross analysis of the sampled routes across the VSP bin categories does not provide an intuitive basis for explaining NO_2 emissions, suggesting that transient events embedded within the individual VSP bins are likely a better explanation of NO_2 emissions. Such an investigation is beyond the scope of the VSP analysis, but will be better addressed in subsequent chapters.

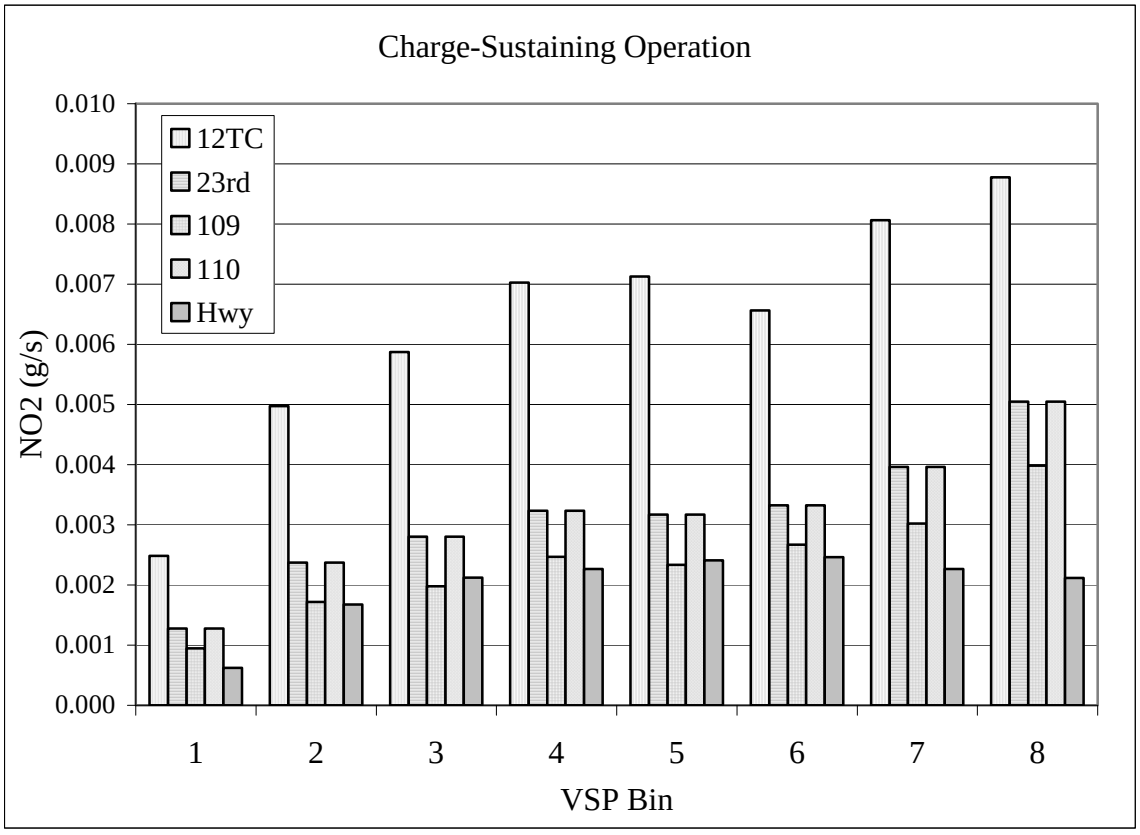

Figure 6.47: Nitrogen dioxide emissions for each sample route according to VSP bin during charge-sustaining operation.

Carbon monoxide emissions demonstrated little to no correlation with the other measured variables and pollutants. However, carbon monoxide emission did prove to be a statistically significant response to sample route across all VSP bins, except bin 7, for both the all-routes inclusive analysis and in-town only analysis. Route 123 was the largest CO producer during bins 2 through 5 (CO emissions, while still significantly different according to route, were comparatively the closest for all routes in bin 1). Highway operation produced the lowest CO emissions during the bins 1 through 7 until bin 8 where highway operation produced the highest levels of CO emissions on a g/s basis. Aside from bins 2 and 3, there is little comparative consistency in CO emissions across the different sample routes in each bin.

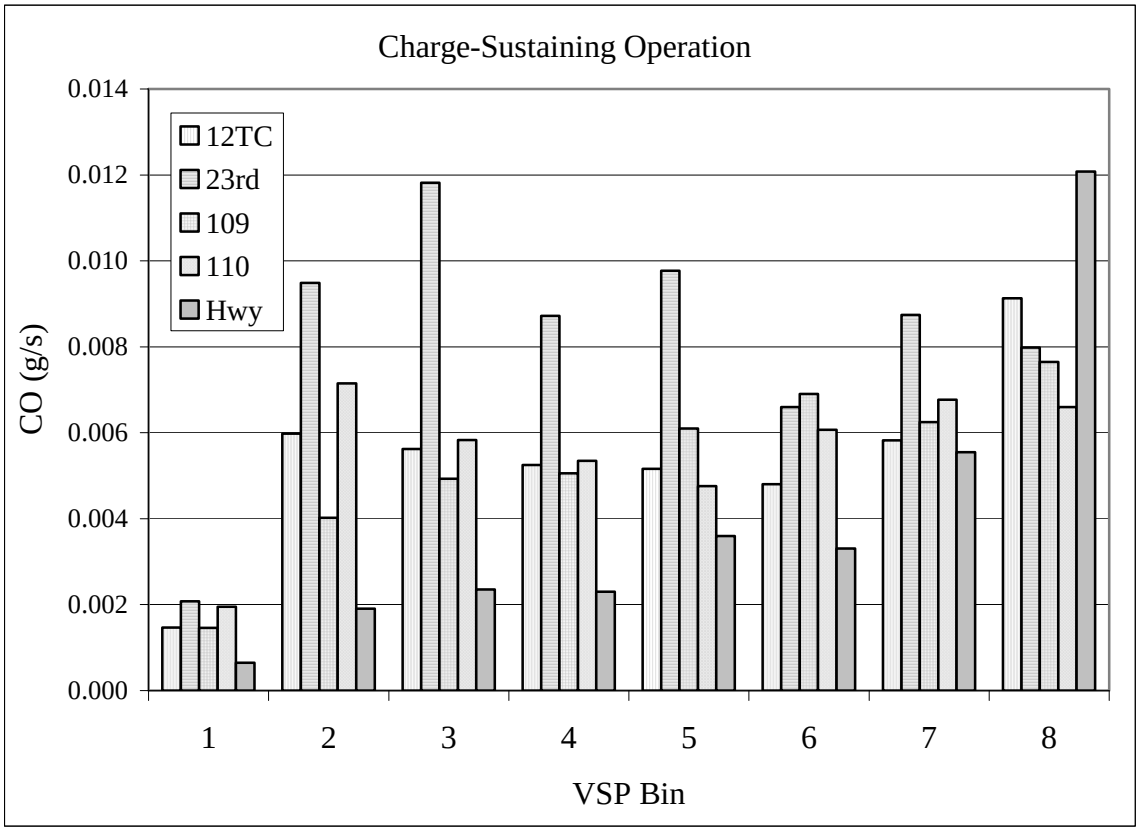

Figure 6.48: Carbon monoxide emissions for all routes according to VSP bin during charge-sustaining operation.

Hydrocarbon emissions increased with increasing VSP bin on an overall basis as well as for each individual route. Within the different VSP bins, hydrocarbon emissions were found to vary with route to a statistically significant degree, with highway operation resulting in the highest levels of hydrocarbon emissions and in-town route 12th T/C producing the lowest level of hydrocarbon emissions in the upper VSP bins. During the lower VSP bins, 1 through 4, route 110 yielded the lowest HC emissions of all routes. The relative emissions of each route with respect to one another held consistent during VSP bins 1 through 5, at which point the pattern of hydrocarbon emissions across the routes shifted slightly showing a relative increase in 23rd street emissions with increasing VSP bin.

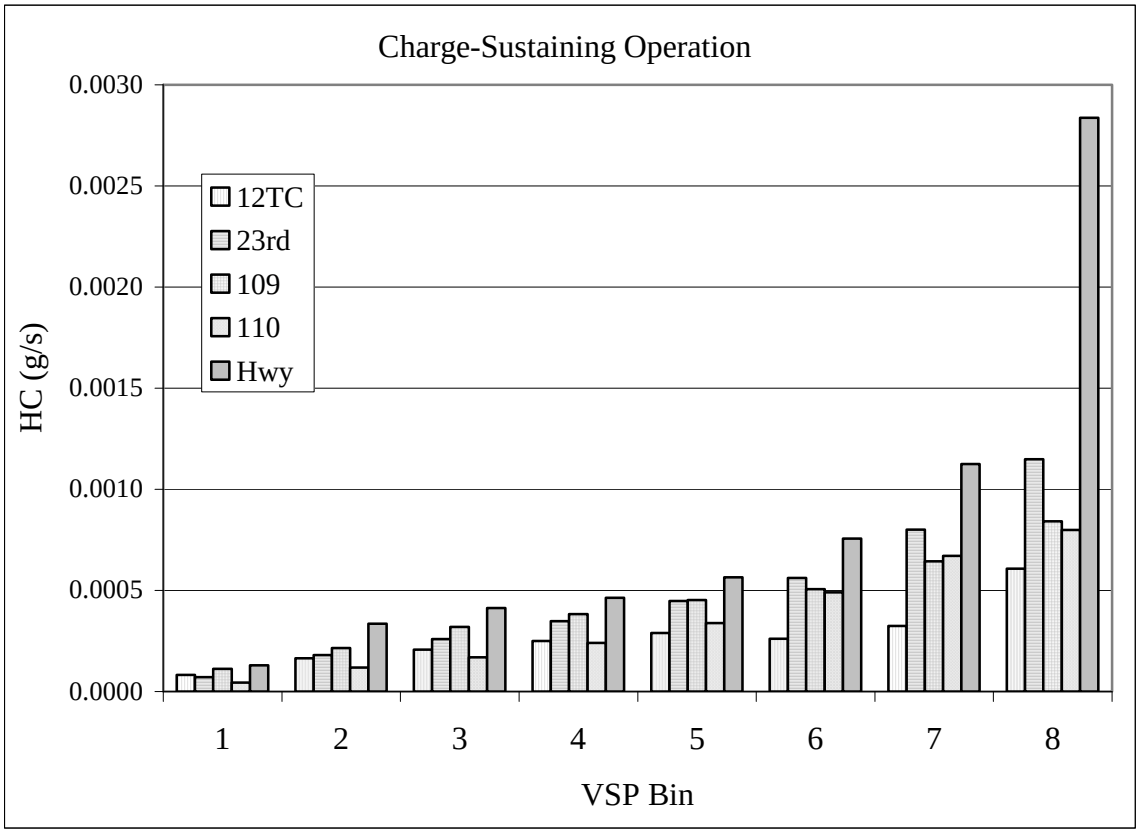

Figure 6.49: Hydrocarbon emissions for all routes according to VSP bin during charge-sustaining operation.

6.8.2.3 Charge-Depleting Operation: Power Demand

In the previous section, VSP bin analyses of the charge-depleting dataset proved that both dICE and EM power output were statistically significant responses to bin categorization ($\alpha<0.05$). However, based on this analysis, subtle differences in power demand between the sample routes became apparent. Remembering that charge-depleting mode represented the "plug-in" capability of the PHEV Sprinter, charge-depleting mode was cited to occur primarily under electric-only operation with dICE assist and recruitment occurring only as necessary to meet immediate on-road power demands. In this manner, charge-depleting mode represents a fundamentally different operating scheme than the hybrid-based charge-sustaining mode discussed previously.

ANOVA and Kruskal-Wallis analyses of the dICE, EM, and total power outputs during charge-depleting operation conclusively showed that the differences between the routes within each bin were statistically significant ($\alpha<0.025$) when all routes are analyzed together. Highway driving resulted in the lowest EM power output across all VSP bins, likely due to the higher average velocity required during highway operation compared with in-town driving. Additionally, analysis of the in-town routes also yielded statistically significant differences in both ICE and EM utilization across all 8 VSP bins (except for bin 6 on the ICE analysis and bin 8 on the EM analysis). Tables 6.40 and 6.41, below, provide highlights of the ANOVA and Kruskal-Wallis results for the intra-route analysis.

Table 6.40: Results for statistical tests conducted on all-routes during charge-depleting operation according to VSP bin.*

VSP BIN	1	2	3	4	5	6	7	8
Fuel, gal/s	y	y	y	y	y	y	y	y
CO_2, g/s	y	y	y	y	y	y	y	y
CO, g/s	y	y	Inc2	y	y	y	Inc1	y
NOx, g/s	y	y	y	y	y	y	y	y
NO, g/s	y	y	y	y	y	y	y	y
NO_2, g/s	y	y	y	y	y	y	y	y
HC, g/s	y	y	y	y	y	y	y	Inc2
ICE Power, W/kg/s	y	y	y	y	y	y	y	y
EM Power, W/kg/s	y	y	y	y	y	y	y	y
Total Power, W/kg/s	y	y	y	y	y	y	y	y
Recup, W/kg/s	y	y	y	y	Inc2	Inc2	Inc2	y

Table 6.41: Results for statistical tests conducted on in-town routes only during charge-depleting operation according to VSP bin.*

VSP BIN	1	2	3	4	5	6	7	8
Fuel, gal/s	y	y	y	y	y	y	y	y
CO_2, g/s	y	y	y	y	y	y	y	y
CO, g/s	Inc2	Inc2	Inc2	y	Inc2	Inc2	Inc2	y
NOx, g/s	y	y	y	y	y	Inc2	Inc2	y
NO, g/s	y	y	y	y	y	Inc2	Inc2	y
NO_2, g/s	y	y	y	y	y	y	y	y
HC, g/s	y	y	y	y	y	n	n	y
ICE Power, W/kg/s	y	y	y	y	y	Inc1	y	y
EM Power, W/kg/s	y	y	y	y	y	y	y	Inc1
Total Power, W/kg/s	Inc2	Inc1	Inc1	Inc1	y	Inc2	y	y
Recup, W/kg/s	Inc2	y	y	y	Inc1	Inc1	Inc1	Inc1

*y≡Valid for both ANOVA and Kruskal-Wallis
n≡Invalid for both ANOVA and Kruskal-Wallis
Inc1≡Valid for ANOVA, invalid for Kruskal-Wallis
Inc2≡Invalid for ANOVA, valid for Kruskal-Wallis

No overall transcending pattern in the routes' power requirements was presented across the VSP bins for either dICE or EM use, but some trends were apparent across certain, smaller VSP ranges with regards to dICE utilization. For example, the 123 route resulted in the highest dICE power output in bins 2 and 3, with a similar distribution of

power output from the other routes throughout these two bins. Likewise, bins 4 through 6 showed consistent relative dICE power output for all routes. No apparent pattern in dICE power output between the different sample routes was present during operation within the highest VSP bins, 7 and 8, when the PHEV Sprinter was experiencing its highest on-road power demand.

Unlike dICE power output, no distinct or persistent patterns in relative EM power requirement across the routes were obvious during charge-depleting operation. Route 110 consistently utilized the EM more than all other routes in VSP bins 4 through 8, and highway operation used the least amount of electrical power in all 8 VSP bins. Despite these two consistencies, the relative electrical power output in all other routes, while different among each other to the set degree of statistical significance, did not show any intra-route uniformity. Aside from the high average velocity maintained by the highway route across for all 8 VSP bins, fluctuations in driving characteristics (i.e. velocity and acceleration) between the different routes and across the 8 VSP bins do not, based on the analyses performed here, give reason for explaining the different power requirements of each route throughout the VSP bins utilized in this study. The only trend common to all routes, with the exception of the 12^{th} T/C loop, was that EM recruitment increased with increasing VSP bin until a maximum electric-only power output was achieved (around bins 5, 6 or 7, route depending), at which point EM power output decreased significantly as power demands increased.

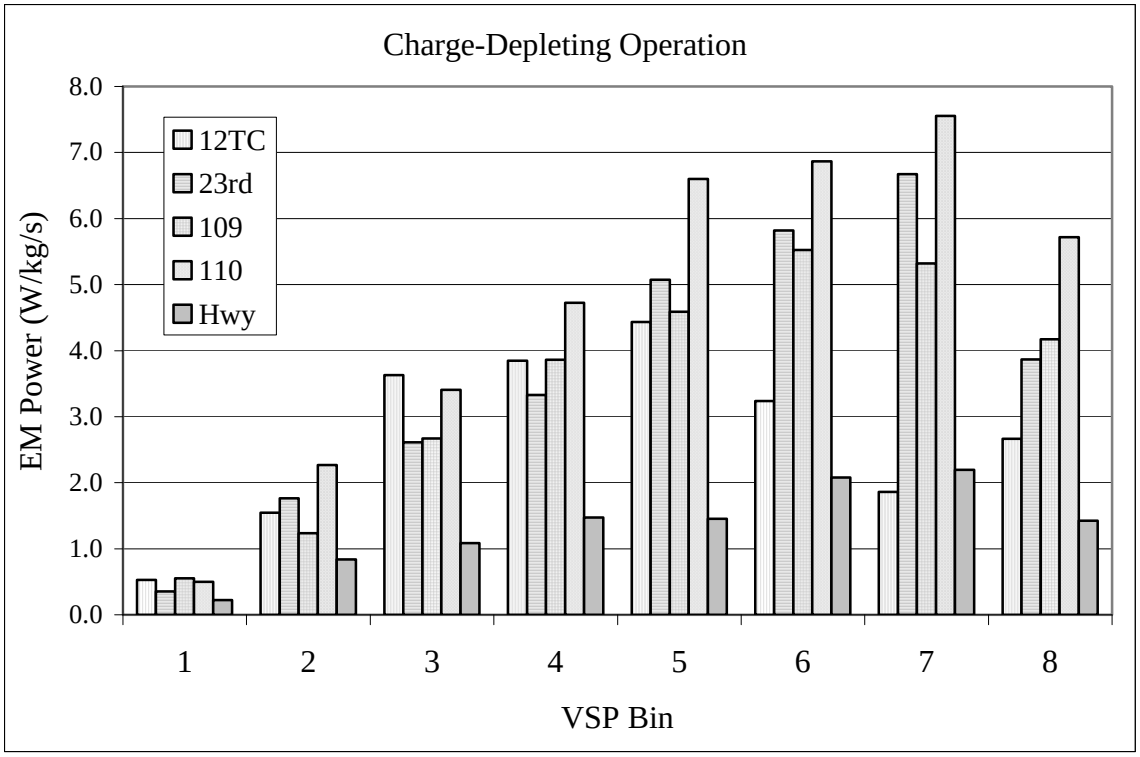

Figure 6.50: EM Power output according to sample route across all VSP bins during charge-depleting operation.

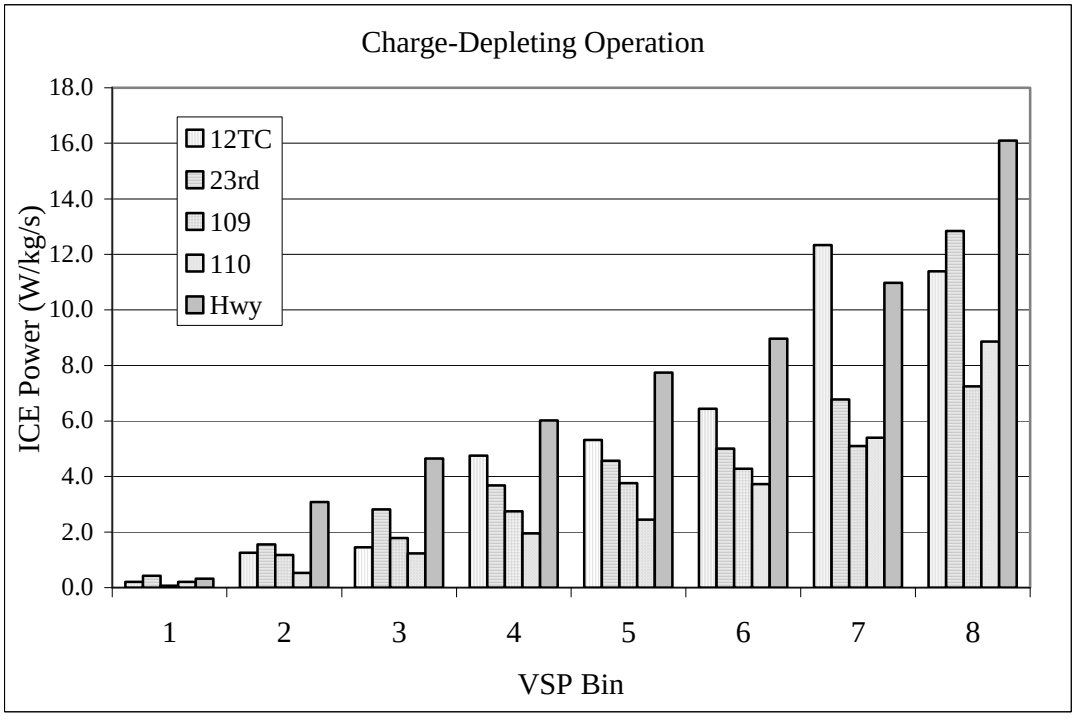

Figure 6.51: ICE Power output according to sample route across all VSP bins during charge-depleting operation.

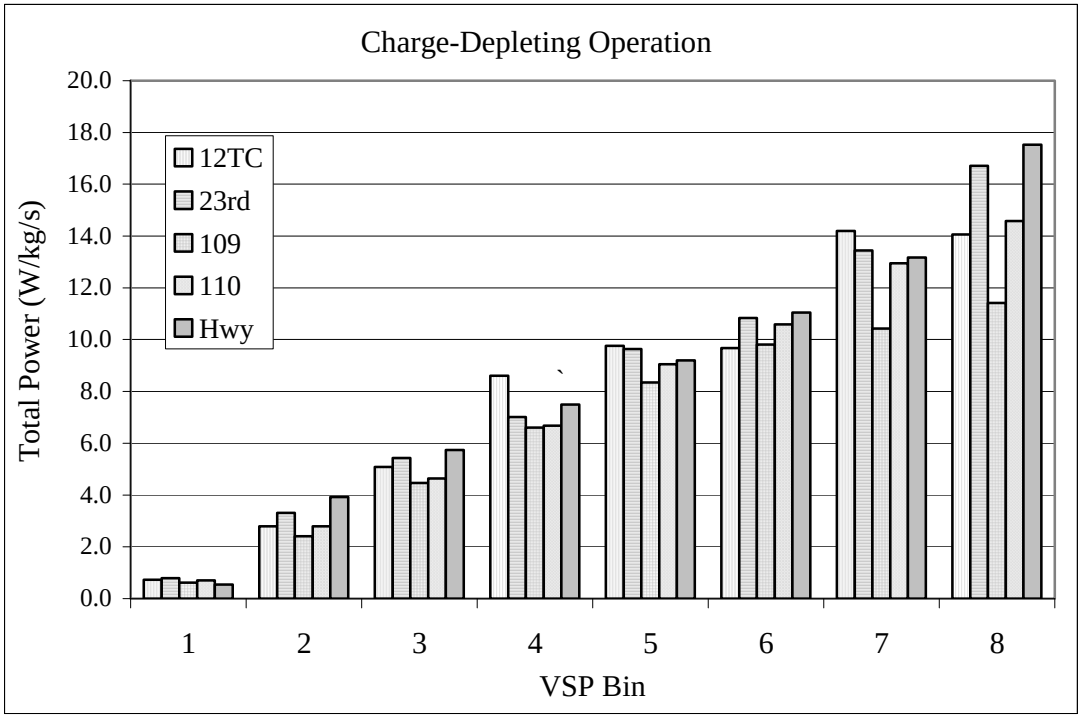

Figure 6.52: Total power output for each sample route across all VSP bins during charge-depleting operation.

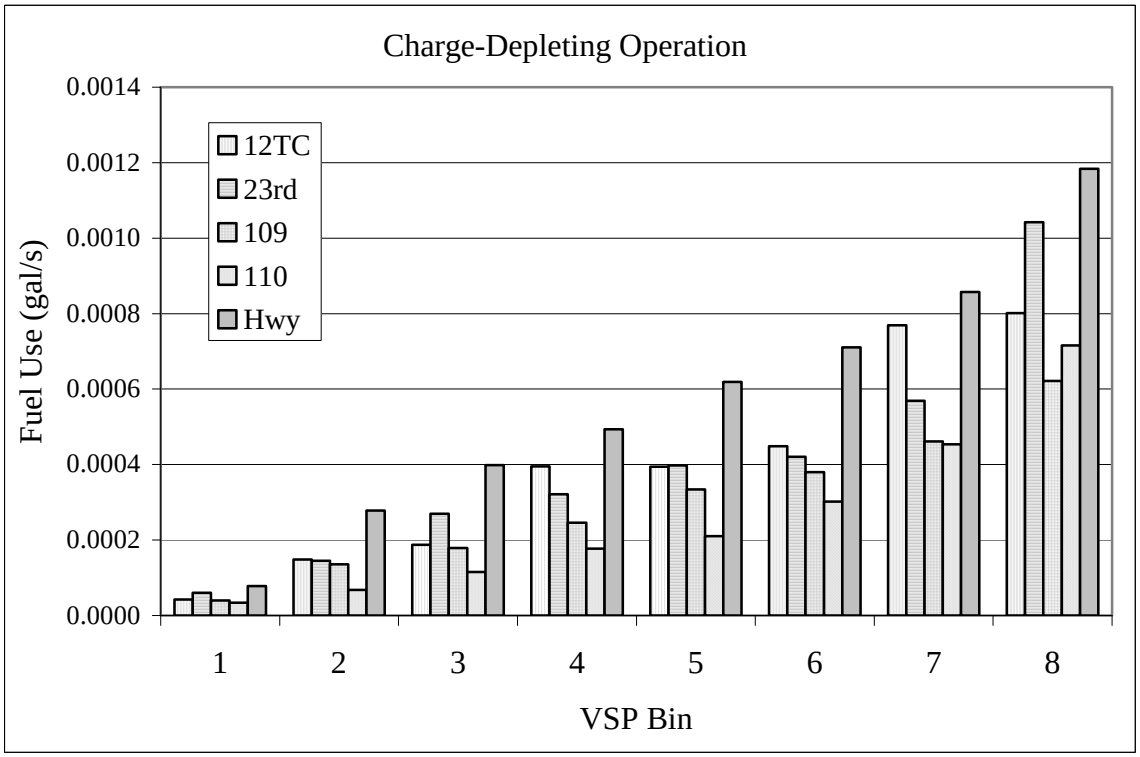

Figure 6.53: Fuel use for each sampled route during charge-depleting operation according to VSP bin.

6.8.2.4 Charge-Depleting Operation: Emissions

Like charge-sustaining operation, fuel use and carbon dioxide emissions during charge-depleting operation were directly correlated with dICE power output, demonstrating the same intra-route variability and trends within and across all VSP bins.

Nitrogen oxide emissions during charge-depleting operation showed statistically significant variation with sample route throughout all 8 VSP bins for the all-route analysis, and for bins 1 through 5 and 8 for the in-route only analysis. Highway driving resulted in higher NO emissions, which is consistent with the positive correlation found between vehicle velocity and NO emissions. However, when limiting the investigation to in-town routes only, route 123 (the in-town route with the lowest mean velocity across VSP bins 1 through 6) exhibited slightly to moderately higher NO emissions than the other 3 in-town routes. When evaluated according to VSP bin, the in-town route with the highest mean acceleration rate across all 8 VSP bins (route 123) produced the highest NO emissions, suggesting a stronger correlation between NO emission and vehicle acceleration when analyzed according to VSP bin rather than as a filtered, but still relatively continuous, dataset of all-routes data compiled.

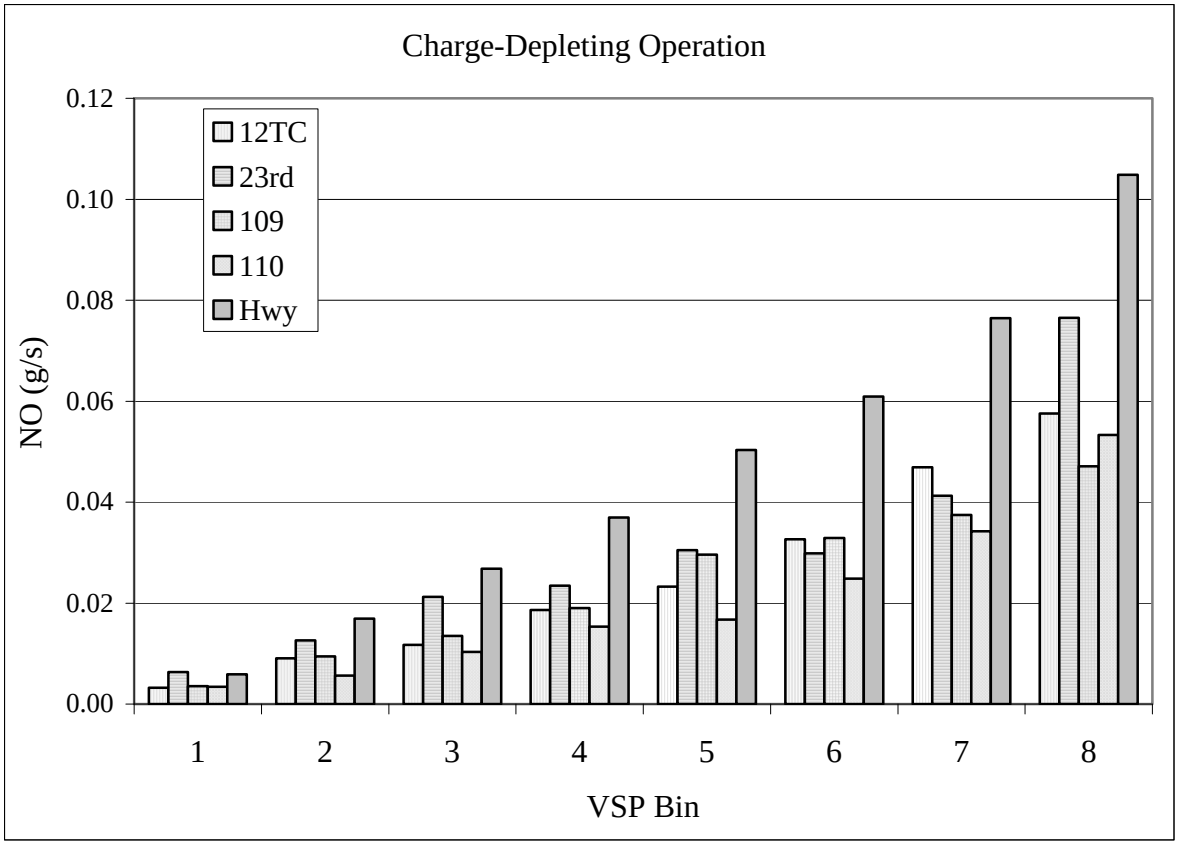

Figure 6.54: Nitrogen oxide emissions for all sample routes according to VSP bin during charge-depleting operation.

As with charge-sustaining mode, nitrogen dioxide (NO_2) emissions exhibited statistically significant differences between the sampled routes in all 8 VSP bins. In-town routes 12T/C and 123 as well as the highway route produced the highest levels of NO_2 emissions, with the 109 and 110 routes producing, on average, 81% lower NO_2 emissions than the average of the highest emitting in-town routes (12T/C and 123). While NO_2 emissions correlated most strongly with velocity compared with the other on-road driving characteristics considered, the variation in NO_2 emissions between the routes does not reflect a strong influence on any particular on-road variable when evaluated according to VSP bin. Because the PHEV's charge-depleting mode utilizes electric-only operation

more than charge-sustaining mode, the dICE experiences more transient and less consistent operation. The presence of transient events in dICE operation will greatly contribute to the PHEV's NO and NO_2 emissions.

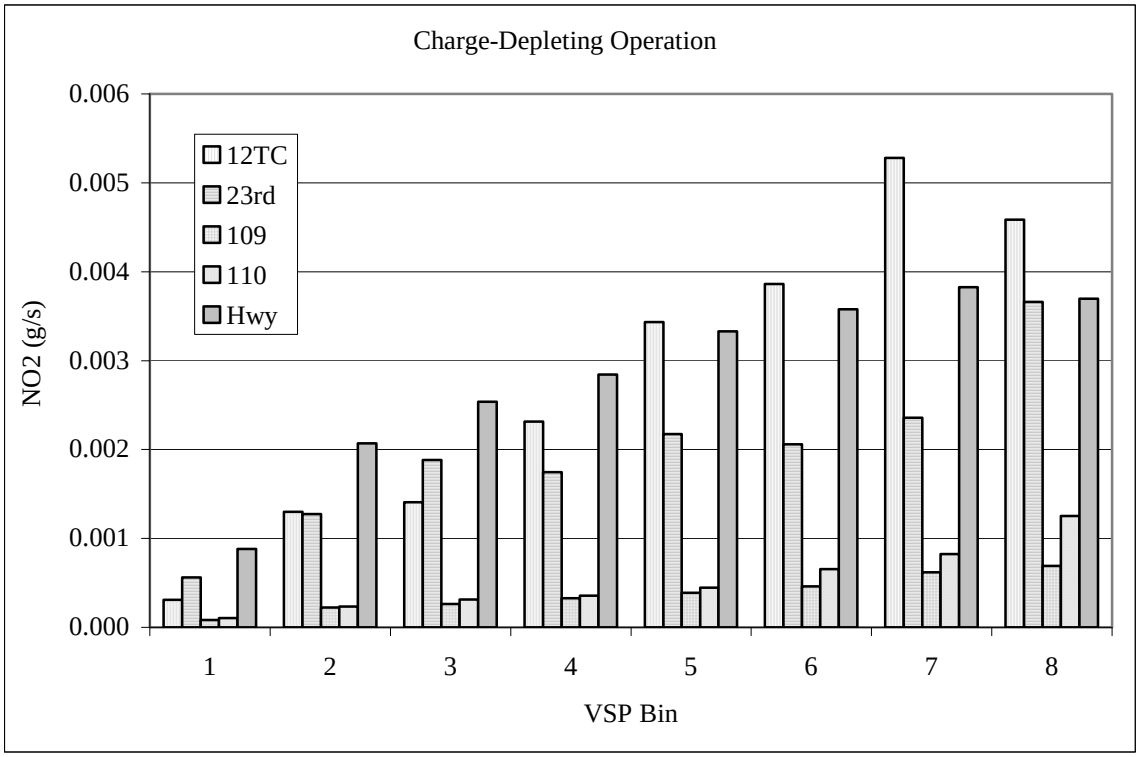

Figure 6.55: Nitrogen dioxide emissions for all sampled routes during charge-depleting operation according to VSP bin.

Carbon monoxide (CO) emissions were lowest for highway driving across all 8 VSP bins, however, the statistical results for in-town only analysis were inconclusive across all eight VSP bins except for 4 and 8, showing no meaningful difference in CO emissions between in-town routes. The same analysis of charge-sustaining operation yielded statistically significant differences between the routes for all VSP bins except for bin 7. It is likely that the transient operation of the ICE during charge-depleting

operation resulted in a wide range of CO emissions regardless of route within each VSP bin making statistical significance difficult to establish.

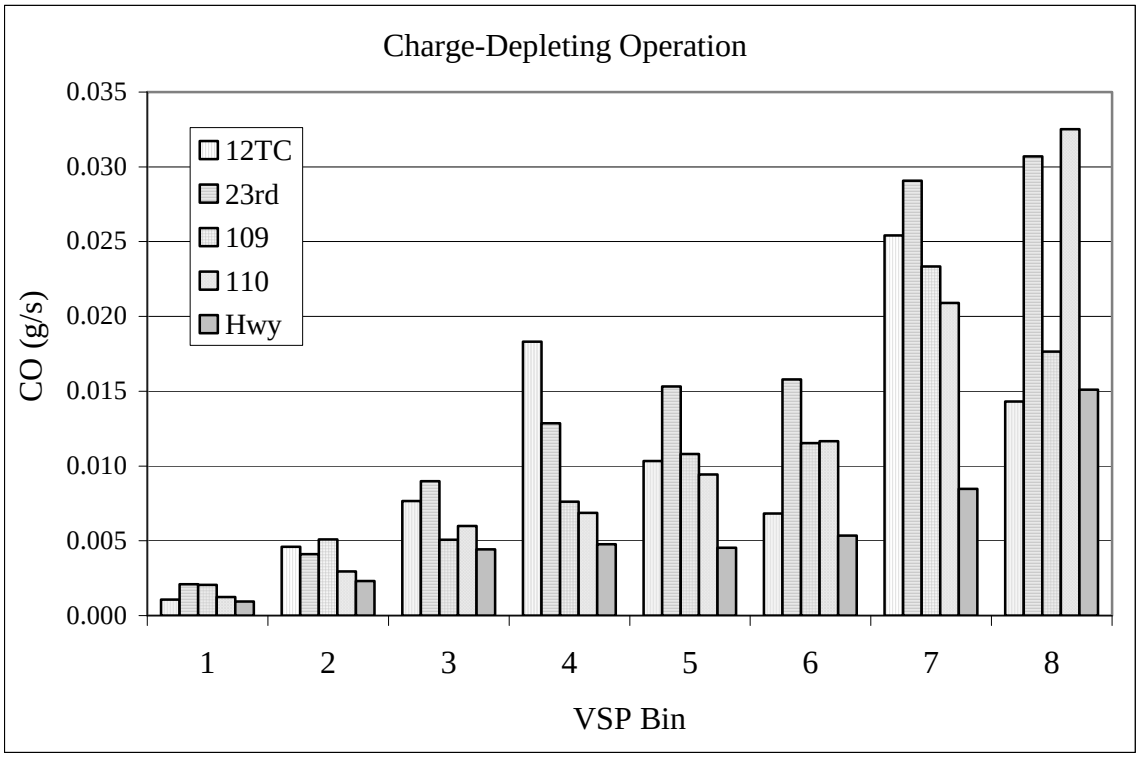

Figure 6.56: Carbon monoxide emissions for all sample routes during charge-depleting operation according to VSP bin.

As noted earlier, hydrocarbon (HC) emissions increased with increasing VSP bin. Analysis of the variation in emissions between routes showed that HC emissions, when investigated for all routes, had a statistically significant difference between the sample routes for all VSP bins except 8, with highway driving resulting in the lowest HC emissions of all sampled routes. When the dataset was limited to in-town routes only, statistical significance indicating meaningful difference between the in-town routes was lost during the higher VSP bins, 6 through 8. However, in the earlier bins, route 109 yielded the highest HC emissions compared to the other sampled routes. Based on the

correlation analysis of the entire 5-second average filtered dataset, HC emissions did not correlate significantly with any of the driving variables. Despite this, the 109 route did have the highest mean velocity across VSP bins 1 through 6 (except for highway).

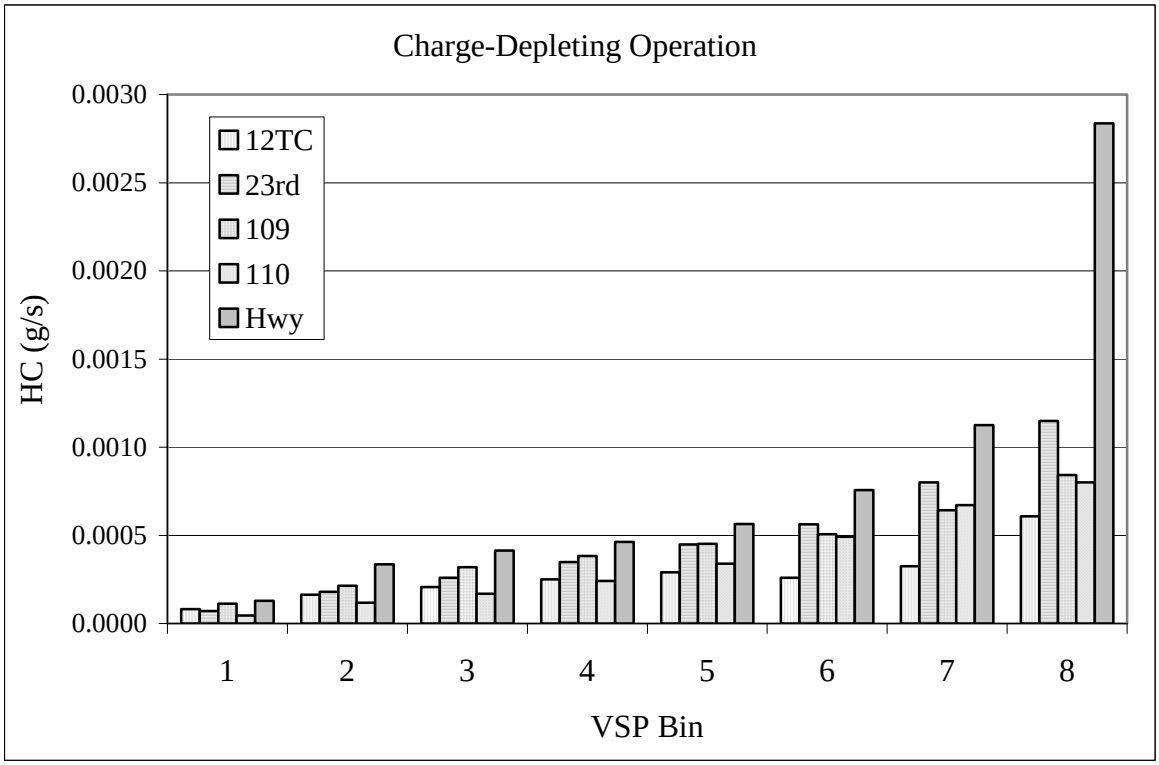

Figure 6.57: Hydrocarbon emissions for all sample routes during charge-depleting operation according to VSP bin.

While routes were consistently found to be a statistically significant response to pollutant emissions and power demand across the eight designated VSP bins, aside from the highway route, only small trends could be discerned between the in-town routes. No overall intra-route (in-town) trends in emissions or power train use consistently transcended all VSP bins. It is possible that the statistical significance found was, at least partially, a function of the sheer sizes of the charge-sustaining and charge-depleting datasets. Equally possible is that subtle phenomenon not available for observation

occurring within the PHEV's operation could result in one route producing different emissions than another. This phenomenon also gives suggestion that the PHEV's active power scheme (electric-only, dICE-only, or varying degrees of hybridization) at any point during data collection could have been a function of something other than instantaneous power demand. If the ECM dictated the PHEV's power scheme based on historical road demand and driver behaviors, then instantaneous power demand would not be the only motivator dictating the PHEV's power usage. Generally speaking, however, the differences in the routes between the VSP bins, while statistically significant on an inter-route scale, were not significant enough to overreach the differences found in emissions and power train operation between the different, discrete VSP bins.

It was noted on several occasions that the inter-routes output appears to vary according to VSP bin range, with bins 1 through 4 or 5 showing different patterns than the upper bins, 5 or 6 through 8. Patterns that emerged during lower power demands did not often hold up during periods of high on-road power requirements. Literature sources did not report standard deviations within VSP bins for on-road emissions, so it is not possible to compare the variation in the PHEV's output with other on-road studies. In the bar charts presented, only variable means are displayed; no indication of the variance within the datasets is reported. Although the means between the routes appear to be more disperse during the upper VSP bins, statistical significance was often lost due to the very fluctuant and variant operation while the PHEV is under high on-road load demands.

Ultimately, differences is emissions and power demand between the routes exist, but the lack of pattern and the fact that the magnitude of the differences is small

compared to inter-VSP bin analysis suggest that the unexpected reality of inter-route variations within each VSP bin is not as significant as originally thought.

6.9 Conclusions

Vehicle Specific Power modal models are commonly used methods of reporting and modeling vehicle emissions for use in both emissions inventories and as a method for discussing on-road emissions data. As a proxy calculation for estimating a vehicle's immediate on-road power demand, vehicle specific power is based on the vehicle's physical parameters (size, cross-sectional area), on-road resistances (rolling and drag resistances, road grade, etc), and immediate driving behaviors (velocity and acceleration). With generally accepted values readily available for most coefficients and classes of vehicles, VSP is an easily accessible method of estimating a vehicle's on-road power load without the requirement of directly measuring engine data.

VSP modal models categorize emissions data according to bins based on defined VSP ranges developed for various classes of vehicles (i.e. light-duty versus heavy-duty). Models have been developed for conventional vehicles and were created with the assumption that emissions within each bin be relatively homogeneous while remaining statistically unique to the other bins in the model. However, plug-in hybrid technology presents a very different on-road reality compared to conventional vehicles. The potential for electric-only driving within any given VSP bin raises the possibility of interjecting zero-valued emissions and fuel use data for unknown durations of time. Because of this, it was uncertain whether the PHEV Sprinter data would prove statistically viable for the widely accepted VSP modal models.

Using the VSP binning approach developed for heavy-duty vehicles, the PHEV Sprinter's on-road data was statistically robust enough to meet the criteria of modal analysis. ANOVA and Kruskal-Wallis analyses of the PHEV Sprinter's power, fuel, and

emissions data proved that the VSP bins created from PHEV data were statistically unique from one another. With statistical significance established between the VSP bins, VSP modal discussion concerning the PHEV Sprinter's on-road data was viable.

Both total power and dICE power output increased with increasing VSP bin, however EM power output reached a peak in bin 6 and continued to decrease during bins 7 through 8. During heavy on-road power loads, the PHEV's dICE became the more dominantly recruited power source. These trends were consistent regardless of operating mode, although the relative portion of power output from the EM was significantly higher during charge-depleting operation.

There was a noticeable difference in power output, fuel use, and emissions between the different sample routes even within the same VSP bin, which was contrary to expectation given the general purpose and nature of the VSP equation. While the inter-route variability was statistically significant in certain instances, the variability in measured variables between the different routes was small compared to the inter-VSP bin variability of the final modal model.

A second modal model based on active driving mode was employed for the purpose of discussion. Since this model anchors emissions data to actual driving scenarios, it is somewhat more intuitive for overall discussion purposes. The cruise and acceleration driving modes were the most work intensive (versus idle periods or moments of deceleration) and gave the strongest basis for discussion. While the dICE provided the majority of the power during charge-sustaining operation, the EM was more heavily recruited during acceleration events. During charge-depleting mode the EM provided the majority of the PHEV's on-road power during periods of acceleration, however the dICE

remained the dominant power source during periods of cruise (or steady-state driving). In all instances, both fuel use and CO_2 emissions tracked with dICE power output, showing a general increase with increasing VSP power load.

Charge-depleting operation followed similar trends as charge-sustaining operation, but with overall reduced CO_2 emissions and greater fuel efficiency. This applied until the higher VSP bins, where the difference in charge-sustaining and charge-depleting CO_2 emissions became much more pronounced. It is suspected that the increasingly high levels of CO emissions with increasing VSP bin during charge-depleting operation accounted for this phenomenon as CO_2 was reduced to CO during moments of dICE transient operation.

Similar to CO emissions, charge-depleting mode resulted in higher levels of HC formation and emission than charge-sustaining operation at comparable power demands. The potential for CO and HC formation during periods of transient dICE operation will be discussed in more detail in Chapters 9 and 10.

The VSP modal analysis gave basis for comparing the PHEV Sprinter's emissions with other conventional vehicles. Unfortunately, the data from an equivalent class of vehicle were not available, so the PHEV Sprinter was discussed in contrast to heavy-duty diesel transit buses and conventional gasoline-powered passenger cars. When compared to HDD transit buses, the PHEV Sprinter exhibited significantly lower levels of emissions for all pollutants except hydrocarbon emissions during charge-depleting operation. While comparison of heavy-duty vehicles to a light-heavy-duty vehicle may be slightly incongruous it is also important to consider the physical load that the PHEV Sprinter carried throughout its on-road sampling campaign. Zhai and Frey (2008)

reported that for a 100% increase in passenger load (20 passengers to 40 passengers), buses exhibited a more than 33% increase in emissions. The PHEV Sprinter was placed into proof of concept testing at near payload capacity.

Chapter 7: Overall Correlation Analysis

In the preceding section, the PHEV Sprinter's operation and emissions were subjected to an in-depth modal analysis utilizing two unique categorization models: VSP Binning and Driving Mode Analysis. Strong trends in the PHEV's operation and resulting emissions became apparent through both analyses. While a useful tool for investigating the PHEV's overall reaction to on-road power demands and driving mode, the modal analysis did not provide in-depth insight regarding relationships between the PHEV Sprinter's measured operating variables, on-road driving variables, and exhaust emissions.

Pearson correlations were run on the bulk of the dataset including measured pollutant emissions, engine power output, on-road variables such as velocity, acceleration, grade, and calculated vehicle specific power, and electrical system data (battery recuperation, battery state of charge, and electric motor power output). Analysis of variance (ANOVA) and its non-parametric equivalent, Kruskal-Wallis, have been utilized for a bulk of the statistical work presented thus far, however, other than determining if a statistical relationship exists between two variables, ANOVA does not provide information concerning the direction and magnitude of the relationship between select variables. Continuous emissions and vehicle operating data have been shown to demonstrate high levels of autocorrelation, so that independence between subsequent observations cannot be automatically assumed. While this phenomenon was mitigated by VSP-bin categorization in Chapter 6, it was necessary to filter the continuous data prior to running any correlation tests. Zhai, Frey and Rouphail (2008) found that autocorrelation in continuous data was reduced by filtering the dataset to observations

collected every 3 seconds, and virtually eliminated using a 5 second filtering technique. For the correlation results presented here, both complete charge-depleting and charge-sustaining datasets used for all VSP analyses in Chapter 6 were reduced to 5-second consecutive averaged observations. Because correlations remain highly susceptible to the presence of outliers within the data, each filtered dataset was investigated for outliers in the calculated variables acceleration, grade, and vehicle specific power. No obvious outliers were present in either dataset, so no observations were removed.

Tables 7.2 and 7.3 provide the comprehensive results for the Pearson's Correlations conducted on the charge-sustaining and charge-depleting data, respectively. For ease of discussion, the following criteria (Table 7.1) were implemented to categorize the variables' relationships to one another. Due to the large size of the datasets, the required p-value for determining statistical significance was set to a more conservative $\alpha<0.025$ rather than the conventionally accepted $\alpha<0.050$. Pairs of variables with "very high" or "good" correlations are listed in bold type while pairs of variables with "moderate" correlations are labeled in bold, italicized type in Tables 7.2 and 7.3. Additionally, pairs of variables whose Pearson's correlation not meet the $\alpha<0.025$ criteria required for determining statistical significance have been crossed out with an "x."

Table 7.1: Criteria for assessing correlation results.

	Pearson Correlation Coefficient Range	**Corresponding R^2 Range**
Very High Positive Correlation	0.90 - 1.00	0.81 - 1.00
Good Positive Correlation	0.70 - 0.89	0.49 - 0.80
Moderate Positive Correlation	0.50 - 0.69	0.25 - 0.48
Weak Positive Correlation	0.30 - 0.49	0.09 - 0.24
Negligible Correlation	-0.29 - 0.29	0.00 - 0.08
Weak Negative Correlation	-0.30 - -0.49	0.09 - 0.24
Moderate Negative Correlation	-0.5 - -0.69	0.25 - 0.48
Good Negative Correlation	-0.70 - -0.89	0.49 - 0.80
Very High Negative Correlation	-0.90 - -1.00	0.81 - 1.00

Table 7.2: Pearson's Correlation results for Charge-Sustaining operation.

	Fuel (gal/s)	Exhaust Temp (C)	CO_2 (g/s)	CO (g/s)	NO (g/s)	NO_2 (g/s)	NOx (g/s)	HC (g/s)	ICE Pwr (W/kg/s)	EM Pwr (W/kg/s)	Tot Pwr (W/kg/s)	VSP Inst (W/kg/s)	Recup (W/kg/s)	Grade (%)	Accel (m/s^2)	Velocity (m/s)
Exhaust Temp (C)	***0.540***															
	0.000															
CO_2 (g/s)	**1.000**	***0.540***														
	0.000	***0.000***														
CO (g/s)	0.327	0.057	0.322													
	0.000	0.000	0.000													
NO (g/s)	**0.955**	***0.552***	**0.955**	0.244												
	0.000	***0.000***	**0.000**	0.000												
NO_2 (g/s)	***0.643***	0.478	***0.643***	0.262	***0.654***											
	0.000	0.000	***0.000***	0.000	***0.000***											
NOx (g/s)	**0.955**	***0.560***	**0.955**	0.251	**0.999**	***0.694***										
	0.000	***0.000***	**0.000**	0.000	**0.000**	***0.000***										
HC (g/s)	0.330	0.140	0.329	0.360	0.263	0.078	0.255									
	0.000	0.000	0.000	0.000	0.000	0.000	0.000									
ICE Pwr (W/kg/s)	**0.945**	0.493	**0.946**	0.243	**0.912**	***0.544***	**0.907**	0.308								
	0.000	0.000	**0.000**	0.000	**0.000**	***0.000***	**0.000**	0.000								
EM Pwr (W/kg/s)	-0.227	-0.315	-0.226	-0.013	-0.272	-0.217	-0.275	0.071	-0.233							
	0.000	0.000	0.000	0.162	0.000	0.000	0.000	0.000	0.000							
Total Pwr (W/kg/s)	**0.830**	0.338	**0.831**	0.235	**0.775**	0.436	**0.769**	0.341	**0.882**	0.254						
	0.000	0.000	**0.000**	0.000	**0.000**	0.000	**0.000**	0.000	**0.000**	0.000						
VSP Inst (W/kg/s)	***0.644***	0.201	***0.645***	0.185	***0.606***	0.331	***0.601***	0.289	***0.670***	0.326	**0.825**					
	0.000	0.000	***0.000***	0.000	***0.000***	0.000	***0.000***	0.000	***0.000***	0.000	**0.000**					
Recup (W/kg/s)	***-0.651***	-0.480	***-0.651***	-0.041	***-0.673***	-0.430	***-0.671***	-0.146	**-0.721**	0.338	***-0.553***	-0.250				
	0.000	0.000	***0.000***	0.000	***0.000***	0.000	***0.000***	0.000	**0.000**	0.000	***0.000***	0.000				
Grade (%)	-0.002	0.003	-0.002	0.001	0.000	-0.001	0.000	-0.001	-0.003	-0.004	-0.005	0.017	0.004			
	0.867	0.789	0.868	0.882	0.995	0.913	0.999	0.931	0.767	0.691	0.626	0.065	0.697			
Accel (m/s^2)	0.384	-0.026	0.384	0.268	0.321	0.256	0.324	0.151	0.383	0.410	***0.580***	***0.674***	-0.106	0.000		
	0.000	0.007	0.000	0.000	0.000	0.000	0.000	0.000	0.000	0.000	***0.000***	***0.000***	0.000	0.987		
Velocity (km/hr)	0.389	***0.500***	0.389	-0.082	0.391	0.120	0.381	0.168	0.403	-0.036	0.383	0.248	-0.404	-0.014	0.044	
	0.000	***0.000***	0.000	0.000	0.000	0.000	0.000	0.000	0.000	0.000	0.000	0.000	0.000	0.135	0.000	
SOC (%)	0.051	0.170	0.051	-0.041	0.025	-0.098	0.047	0.099	0.044	0.089	0.048	0.091	0.107	-0.002	-0.024	0.340
	0.000	0.000	0.000	0.000	0.008	0.000	0.073	0.000	0.000	0.340	0.000	0.000	0.000	0.847	0.008	0.000

Table 7.3: Pearson's Correlation results for Charge-Depleting operation.

	Fuel (gal/s)	Exhaust Temp (C)	CO_2 (g/s)	CO (g/s)	NO (g/s)	NO_2 (g/s)	NOx (g/s)	HC (g/s)	ICE Pwr (W/kg/s)	EM Pwr (W/kg/s)	Tot Pwr (W/kg/s)	VSP Inst (W/kg/s)	Recup (W/kg/s)	Grade (%)	Accel (m/s^2)	Velocity (m/s)
Exhaust Temp (C)	***0.588***															
	0.000															
CO_2 (g/s)	**1.000**	***0.589***														
	0.000	***0.000***														
CO (g/s)	0.405	0.050	0.398													
	0.000	0.002	0.000													
NO (g/s)	**0.954**	***0.576***	**0.955**	0.302												
	0.000	***0.000***	**0.000**	0.000												
NO_2 (g/s)	***0.683***	***0.680***	***0.684***	0.135	***0.679***											
	0.000	***0.000***	***0.000***	0.000	***0.000***											
NOx (g/s)	**0.955**	***0.592***	**0.956**	0.298	**0.999**	**0.710**										
	0.000	***0.000***	**0.000**	0.000	**0.000**	**0.000**										
HC (g/s)	0.415	0.121	0.410	***0.691***	0.307	0.102	0.300									
	0.000	0.000	0.000	***0.000***	0.000	0.000	0.000									
ICE Pwr (W/kg/s)	**0.983**	***0.564***	**0.983**	0.339	**0.941**	***0.672***	**0.942**	0.377								
	0.000	***0.000***	**0.000**	0.000	**0.000**	***0.000***	**0.000**	0.000								
EM Pwr (W/kg/s)	-0.213	-0.282	-0.214	0.122	-0.254	-0.235	-0.258	0.095	-0.196							
	0.000	0.000	0.000	0.000	0.000	0.000	0.000	0.000	0.000							
Total Pwr (W/kg/s)	**0.765**	0.339	**0.765**	0.386	**0.700**	0.466	**0.699**	0.404	**0.791**	0.445						
	0.000	0.000	**0.000**	0.000	**0.000**	0.000	**0.000**	0.000	**0.000**	0.000						
VSP Inst (W/kg/s)	***0.657***	0.270	***0.657***	0.292	***0.622***	0.404	***0.620***	0.339	***0.674***	0.354	**0.837**					
	0.000	0.000	***0.000***	0.000	***0.000***	0.000	***0.000***	0.000	***0.000***	0.000	**0.000**					
Recup (W/kg/s)	-0.061	-0.189	-0.060	0.035	-0.117	-0.179	-0.123	0.031	-0.056	0.253	0.107	0.286				
	0.000	0.000	0.000	0.031	0.000	0.000	0.000	0.064	0.000	0.000	0.000	0.000				
Grade (%)	0.050	0.011	0.049	0.144	0.046	0.014	0.045	0.020	0.035	0.008	0.037	0.075	0.008			
	0.002	0.488	0.003	0.000	0.005	0.389	0.006	0.249	0.032	0.642	0.023	0.000	0.649			
Accel (m/s^2)	0.301	-0.023	0.301	0.325	0.243	0.152	0.242	0.210	0.292	0.490	***0.572***	***0.640***	0.229	0.031		
	0.000	0.170	0.000	0.000	0.000	0.000	0.000	0.000	0.000	0.000	***0.000***	***0.000***	0.000	0.063		
Velocity (km/hr)	***0.506***	***0.680***	***0.507***	0.012	0.479	***0.498***	0.488	0.134	0.487	-0.082	0.394	0.313	-0.072	-0.008	0.033	
	0.000	***0.000***	***0.000***	0.476	0.000	***0.000***	0.000	0.000	0.000	0.000	0.000	0.000	0.000	0.642	0.046	
SOC (%)	-0.033	-0.153	-0.034	-0.065	-0.061	-0.135	-0.067	0.055	-0.062	-0.084	-0.109	-0.051	0.254	0.048	0.007	-0.138
	0.042	0.000	0.039	0.000	0.000	0.000	0.000	0.001	0.000	0.000	0.000	0.002	0.000	0.278	0.654	0.000

The following discussion pertains to charge-sustaining operation during which the PHEV Sprinter behaved in a manner more consistent with conventional hybrid vehicles. During the PHEV's hybrid operation, the diesel internal combustion engine provided the majority of the PHEV's on-road power, with electric motor recruitment occurring only as excess battery capacity was present. Akin to its name, the ultimate purpose of charge-sustaining operation was to maintain a consistent level of battery charge. With its electrical recuperation abilities, even charge-sustaining, or hybrid, driving resulted in periodic instances of electric-only operation. As intuitively expected, fuel use (gal/s) and the internal combustion engine power output (W/kg/s) were highly correlated. With carbon dioxide production and emission directly related to the combustion process, it makes intuitive sense that carbon dioxide was also highly correlated with both dICE power output and fuel use. Additionally, nitric oxide (NO) emissions were highly positively correlated with dICE power output and fuel use.

Pollutant emissions whose formation was the result of secondary reactions and not directly attributable to the combustion process did not yield strong associations with the PHEV Sprinter's power demand or fuel use. Hydrocarbon presence in the exhaust was largely due to fuel pass-through and incomplete combustion most commonly associated with transient dICE operation. Because of this, hydrocarbon emissions were only weakly (positively) correlated with fuel use and dICE power output. Likewise, nitrogen dioxide (NO_2) formation occurs as a secondary reaction to the combustion process where NO, in the presence of excessively high temperatures and a stoichiometric excess of oxygen, is converted to NO_2. As a result, nitrogen dioxide emissions were only moderately, positively correlated with fuel use, carbon dioxide (CO_2) emissions, and nitrogen oxide (NO)

emissions. The Pearson correlation coefficient between exhaust emissions of NO_2 and O_2 was only weakly positive at 0.444. As the primary component comprising NOx emissions, nitric oxide's high positive correlation with NOx makes intuitive sense. Carbon monoxide emissions, a product of incomplete combustion, did not significantly correlate with any of the measured emissions, vehicle data, or driving variables.

While strong positive correlations exist between some of the measured pollutants (CO_2, NO, and, consequently, NOx) and variables relating to dICE use (fuel use and dICE and total power output), variables indicative of the PHEV's on-road behavior (calculated instantaneous vehicle specific power (VSP), velocity, acceleration, and grade) did not exhibit correlations as strong as those exhibited between CO_2, fuel use, NO, NOx, and dICE and total power output. Instantaneous VSP calculations did show moderate, positive correlations with fuel use, dICE power**,** acceleration, NOx, NO, and CO_2 with a good positive correlation between VSP and total power. Driving behavior variables velocity and acceleration only demonstrated moderate correlations with other measured variables. While acceleration showed a moderately positive correlation with total power output and calculated VSP, velocity appeared less integrated with the other variables, possessing only a moderately positive correlation with exhaust temperature. Noted correlations between velocity and other measured variables are weak at best. Based on the results from the correlation analysis, road grade was the least explanatory or related road-based variable, showing no statistically significant correlation with any measured or calculated variables. Available literature remains divided regarding the correlative relationship between road grade and a vehicle's emissions. Frey and Unal (2003) originally found no relationship between road grade and vehicle emissions, but subsequent work (Frey et al., 2007 and 2008) conducted on diesel-

powered transit buses showed some degree of correlation between road grade and emissions, however, the degree of correlation was based on the geographic scale of the data analysis with micro-scale analysis showing a correlation that was then lost on the meso-scale level. Additionally, Krishnamurthy and Gautam (2006) found that road grade did not have an impact on heavy-duty diesel emissions within the geographic context of their study. Based on available literature, the extent of correlation that might present between emissions and on-road variables such as velocity, acceleration, and road grade remains a function of the study area and roadway matrix evaluated.

Since the calculations for determining battery recuperation were relative to the prevalent flow of electrical energy out of the PHEV, recuperation rates are negative, with the most negatively reported recuperation rates indicating periods of highest electrical recovery. Battery recuperation demonstrated a moderate correlation with total power output, and emissions of NOx, NO, and CO_2. Recuperation was most strongly correlated with ICE power output (Pearson correlation coefficient =-0.721) suggesting that recuperation was not only more prevalent during ICE operation, but that the rate of recuperation (on a per second basis) increased with increasing power output of the diesel internal combustion engine. Conversely, recuperation rates were only weakly inversely correlated with the electrical motor power output. Part of this difference could be explained by electrical recuperation achieved with transmission downshifting during dICE operation that is absent during EM operation.

The categorization of Pearson's correlations (very high, good, moderate, or weak) for charge-depleting mode did not, generally, vary from the results found during charge-sustaining operation. During charge-depleting operation, the electric motor provided a

proportionally larger percentage of the total power output than during charge-sustaining operation. Consequently, a larger proportion of the vehicle's acceleration occurred under electric-only operation thus diluting the magnitude of the correlations between emissions and acceleration in most cases. The proportionally increased road-time occurring under electric-only operation also resulted in larger correlation coefficients between dICE power output, fuel use and all emissions except for CO and HC. However, despite more extensive and frequent periods of zero emissions and no fuel use during charge-depleting operation, the correlations of measured variables with the electric-motor power output remained weak (positively or negatively) at best. Recuperation rates during electric-only operation are minimal compared to when the dICE is running, so no meaningful correlations exist between recuperation rate and all measured and calculated variables during charge-depleting operation. When compared to charge-sustaining operation, even the weak correlations between recuperation rates and the other measured and calculated variables were significantly less when the PHEV was in charge-depleting operation. The following table provides the relative change in Pearson's correlation coefficients for PHEV operation in charge-depleting versus charge-sustaining operation. The relative changes were calculated using absolute values of the correlation coefficients, so negative percentages indicate smaller correlation coefficients in charge-depleting operation. Correlations between road grade and the other variables were not included in Table 7.4, since grade did not statistically correlate with any other variables during charge-sustaining operation. Cells listed with "NA" denote lack a of statistical significance in the calculated charge-sustaining or charge-depleting Pearson's correlation coefficient.

Table 7.4: Relative change in Pearson's correlation coefficient between charge-depleting and charge-sustaining operation.

	Fuel (gal/s)	Exhaust Temp (C)	CO_2 (g/s)	CO (g/s)	NO (g/s)	NO_2 (g/s)	NOx (g/s)	HC (g/s)	ICE Pwr (W/kg/s)	EM Pwr (W/kg/s)	Total Power	VSP Inst (W/kg/s)	Recup (W/kg/s)	Accel (m/s^2)	Velocity (m/s)
Exhaust Temp (C)	9%														
CO_2 (g/s)	0%	9%													
CO (g/s)	21%	-13%	21%												
NO (g/s)	0%	4%	0%	21%											
NO_2 (g/s)	6%	35%	6%	-64%	4%										
NOx (g/s)	0%	6%	0%	17%	0%	2%									
HC (g/s)	23%	-15%	22%	63%	15%	27%	16%								
ICE Pwr (W/kg/s)	4%	13%	4%	33%	3%	21%	4%	20%							
EM Pwr (W/kg/s)	-6%	-11%	-5%	NA	-7%	8%	-6%	29%	-17%						
Total Pwr	-8%	0%	-8%	49%	-10%	7%	-10%	17%	-11%	55%					
VSP Inst (W/kg/s)	2%	29%	2%	45%	3%	20%	3%	16%	1%	8%	1%				
Recup (W/kg/s)	-166%	-87%	-166%	NA	-141%	-82%	-138%	NA	-171%	-29%	-135%	13%			
Accel (m/s^2)	-24%	NA	-24%	19%	-28%	-51%	-29%	33%	-27%	18%	-1%	-5%	73%		
Velocity (km/hr)	26%	31%	26%	NA	20%	122%	25%	-23%	19%	78%	3%	23%	-139%	NA	
State of Charge (%)	NA	-11%	NA	45%	84%	32%	NA	-57%	34%	NA	78%	-56%	81%	NA	-85%

*Relative change calculated: % Change = (absCD – absCS)/((absCD + absCS)/2).

Chapter 8: Roadway-Type Analysis

8.1 Introduction: Initial Roadway Definition and Data Processing

During the modal analysis, the PHEV Sprinter's on-road behaviors, operation, and emissions were investigated according to calculated power demand and driving mode. In all cases, the PHEV's actual power demand and emissions were found to be statistically significant responses to modal segregation. This trend was consistent regardless of active operating mode: charge-sustaining and charge-depleting. Additionally, the modal analysis gave elucidation into the distinct differences between the PHEV Sprinter's functioning between its two power schemes. Phase I of the PHEV Sprinter study required that the PHEV be evaluated under a variety of different roadway scenarios. While the VSP/Driving Mode modal analysis gave insight into the vehicle's reaction to various on-road power demands, the modal analysis was not designed to specifically address the PHEV's operation on distinctly different roadway types.

One of the primary objectives of the original study was to assess the PHEV Sprinter's operation both during general on-road driving and as a metropolitan-based transit bus. Because of the large diversity of roadways covered by the Kansas City Area Transit Authority (KCATA), one of the priorities used for selecting sample routes was the ability to evaluate the PHEV's operation and emissions as a function of roadway, or facility, type. In order to help accomplish this goal, routes were selected that operated within and near the Kansas City urban core as well as on surrounding and transitioning roadways traveling between the urban core and midtown neighborhoods and communities. As detailed in the Chapter 3, four routes servicing moderate ridership were selected from the KCATA index of active routes. Additionally, a highway-based "route"

was developed in order to evaluate the PHEV Sprinter's operation at higher and more consistent velocities. Based on the route selection and knowledge of the Kansas City area, three distinct roadway types were selected for investigation: urban, suburban, and highway. No formal method existed for geographically determining which roadway links should be considered urban or suburban, so the initial boundaries used for roadway-type designation were established based solely on operator observation and on-road experience. Figure 8.1, below, displays a map of all of selected routes. The highway route followed Highway 71 on a north and south trajectory. Roadways near and within Kansas City's urban core are highlighted and given more detail in subsequent Figure 8.2. All highlighted routes outside of the urban bubble and exclusive of Highway 71 were transition roads and considered suburban driving.

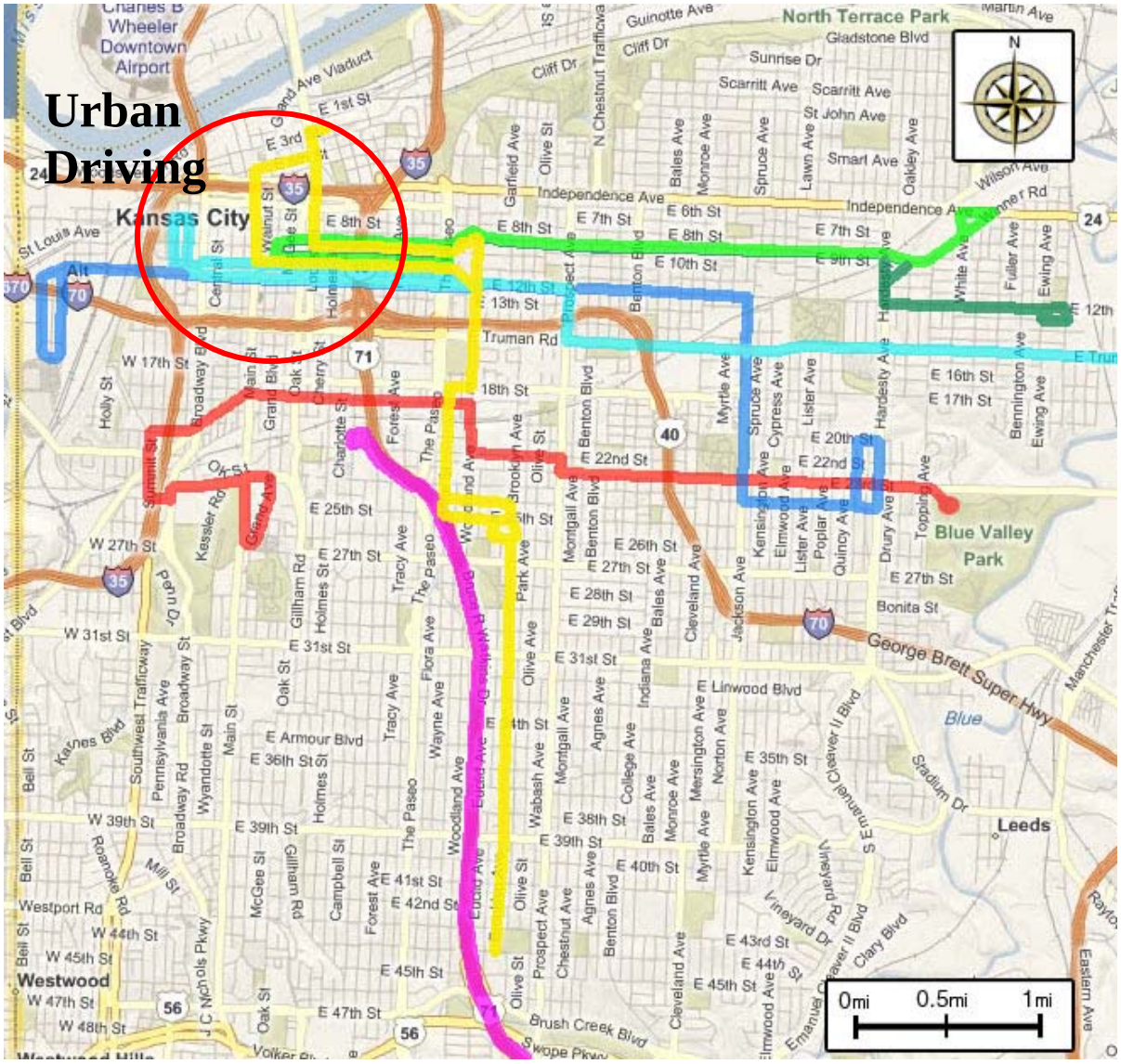

Figure 8.1: Overall map detailing selected routes throughout the Kansas City metropolitan area.

Figure 8.2: Close-in view of urban roadways around the Kansas City urban core.

Because of the difference in geography and service between the selected roadway types, several distinctions were noted between the urban, suburban, and highway roadways. These are detailed below according to roadway designation:

Urban:

- Roads within the Kansas City downtown area,
- Nominal posted speed limits (20mph or 32.2kph),
- Heavier presence of stop and go traffic with higher traffic density than surrounding, transition roads, and
- Stop lights or signs at all major and minor intersections.

Suburban:

- Moderate speed limits, in this case 35mph or 56.3kph,
- Transition roads between communities and surrounding areas outside of urban core,
- More thoroughfare roadways with less stop and go traffic, and
- Traffic lights present at major intersections only, so frequency of traffic lights was significantly less than on urban roads.

Highway:

- Highest posted speed limits of all traveled sample routes (55mph or 88.5kph),
- Total absence of traffic lights, so there was no stop and go traffic during highway operation, and
- Moderate traffic density, but consistent flow did not impede or impact the PHEV's on-road behaviors.

All of the collected data were individually tagged according to the roadway type being navigated at each point of data collection. The original highway route was comprised of a section of true highway traveling at a consistent 55mph posted speed limit and a section of 45mph travel that was regulated by occasional traffic lights. In order to maintain continuity when assessing the PHEV's operation at higher travel velocities, the highway data were reduced so that all travel at posted speeds less than 55mph was removed from the highway datasets. Additionally, data collected during the transition

between the Semtech calibration location (in a nearby neighborhood) and the highway on and off ramps were removed from the final datasets.

Urban roadways resulted in the smallest travel distances of all three roadway designations. In order to maximize the amount of urban roadway data available for analysis, data that were removed from the VSP analysis due to GPS failure in the urban core were reinserted into the final datasets for this investigation. Travel around the urban core was spatially congested due to the close proximity of high-rise buildings; this resulted in occasional periods where satellite acquisition was not possible and GPS data not available. While only 4.4% of the on-road data did not have accompanying GPS data, this percentage translates to almost 31% of the data collected during urban travel being void of GPS information. Since velocity and acceleration were taken from the PHEV's Data Logging Module (DLM) and, therefore, not dependent on GPS operation, the only impact that vacant GPS data had was on the calculation of Vehicle Specific Power (VSP) as road grade was calculated from GPS-derived altitude readings. Since total power output (as calculated from diesel internal combustion engine, dICE, and electric motor, EM, speeds and torque readings) proved to track directly with VSP calculations, the PHEV power data were used to back-calculate VSP during periods of GPS failure. The average difference between baseline positive VSP calculations and power output (since VSP could be calculated as negative, but power output was only negative as an artifact of torque measurements) was accounted for, and VSP was set equivalent to total power output. From the pseudo-VSP data, altitude and, subsequently, road grade were determined. The impact of simulating VSP from actual power output during GPS failure was further verified through graphical analysis. Using the route's

topography, visual investigation of charted altitude was used to ensure that the altitude proxies fell consistent with the available GPS data.

8.2 Roadway Type Verification: Initial Statistical Analysis

In order to verify that the selected boundaries used to define roadway-type were justifiable, variables defined by local roadway characteristics and traffic patterns were initially subjected to statistical investigations in order to determine that unique and meaningful differences exist between the designated roadway classifications.

Because of the small, but still present, impact that ambient temperature and auxiliary system use had on PHEV Sprinter emissions, this analysis proceeds with the filtered set of data files used for the vehicle specific power (VSP) analysis in Chapter 6. As with the VSP analysis, all statistical tests presented here were performed in duplicate. The initial round of analyses was conducted comparing all three roadway designations (highway, suburban, and urban). However, the large differences between highway and in-town driving created concern that basing all roadway comparisons on analyses from all three roadway types could result in determining statistical significance between all roadways, when, in actuality, no statistical difference exists between urban and suburban travel. Therefore, the same statistical tests were also conducted as a comparison between urban and suburban travel only (labeled as in-town). Similar to the VSP investigation, statistical tests designed to discern whether sets of data are from the same or different populations based on central tendency were used for the bulk of the roadway analysis. In efforts to account for the inherent non-normality present in the continuous, on-road data, all tests were conducted in duplicate using both the parametric Analysis of Variance (ANOVA) test as well as the non-parametric Kruskal-Wallis test. Unless otherwise specified, statistical significance was accepted at an alpha<0.025 for all analyses of the

continuous data and an alpha<0.05 was used for analyzing datasets created from compiled means of individual sample runs.

The tests were also conducted on three separate scales, as defined by collection frequency. ANOVA and Kruskal-Wallis tests were performed on the compiled dataset of all continuous data (collected second-by-second) and continuous data averaged for every 5^{th} second as well as on the dataset generated from mean values obtained from the individual sample runs. Autocorrelation always remains a concern when assessing continuous datasets, so redundant statistical analysis using the dataset filtered to the 5-second average of all variables of interest was deemed prudent and not superfluous. It was important to verify that the statistical trends and behaviors were consistent regardless of how the data were processed prior to analysis.

8.3 Defining Roadway Types

8.3.1 On-Road Variable Evaluation

The following tables provide a synopsis of the ANOVA and Kruskal-Wallis results for road and driving-based responses as a function of roadway type. Acceleration and grade measurements contain both positive and negative values. In order to eliminate any confusion in the evaluation of means calculated from a single variable (for example acceleration) that encompasses two different and unique occurrences (both acceleration and deceleration events), both grade and acceleration data were each subdivided into two variables more able to describe the PHEV Sprinter's on-road experience and driving situation. Data with positive and zero acceleration rates were kept under the label "acceleration" whereas data where the PHEV was slowing down and experiencing a quantitatively negative acceleration were segregated into separate deceleration column. Likewise, periods where the PHEV Sprinter was operating on a flat surface or driving uphill (zero value or positive grade) were labeled positive grade, and data collected while the PHEV was driving downhill were segregated and labeled as negative grade. In the following, and subsequent similar, tables, "y" denotes that the statistical investigation proved to be statistically significant ($\alpha<0.025$ for continuous data and $\alpha<0.05$ for run-based datasets) for both ANOVA and Kruskal-Wallis analyses. Likewise, "n" denotes that the investigation failed both statistical tests conducted. Statistical inquiries that met the criteria for one test but failed the criteria for the second test were deemed inconclusive according to criteria 1 (Inc1: passing the parametrical, ANOVA test, but failing the non-parametrical, Kruskal-Wallis statistical test) or criteria 2 (Inc2: failing the ANOVA test, but passing the Kruskal-Wallis).

Table 8.1: Synopsis of statistical results for road and driving-based variables according to roadway-type.

Continuous Datasets, second-by-second and 5th sec averaged

Variable:	All Roadways	Suburban/Urban only
Velocity (km/h)	y	y
Acceleration (m/s^2)*	y	y
Deceleration (m/s^2)*	y	Inc2
Positive Grade (%)**	y	y
Negative Grade (%)**	y	y

*Acceleration: $a \geq 0$, Deceleration $a < 0$.
**Positive Grade: $g \geq 0$, Negative Grade, $g < 0$.

Table 8.2: Synopsis of statistical results for road and driving-based variables according to roadway-type, applied to the run-based dataset.

Variable:	All Roadways	Suburban/Urban only
Velocity (km/h)	y	y
Acceleration (m/s^2)*	y	y
Deceleration (m/s^2)*	y	n
Positive Grade (%)**	y	y
Negative Grade (%)**	y	y

*Acceleration: $a \geq 0$, Deceleration $a < 0$.
**Positive Grade: $g \geq 0$, Negative Grade, $g < 0$.

When ANOVA and Kruskal-Wallis analysis was applied to the dataset inclusive of all roadway distinctions, all investigated road and driving-based variables were found to be statistically significant ($\alpha < 0.025$ and $\alpha < 0.05$, dataset dependent). Statistical significance was present regardless of the dataset resolution being investigated (i.e. second-by-second continuous (Table 8.1), averaged for every 5^{th} data point (Table 8.1), or averaged for each sample run (Table 8.2)). Tables 8.1 and 8.2 provide a synopsis of the statistical analyses performed, however, they are void of information regarding the

different behaviors and relative magnitudes of each driving and road variable with respect to road-type. Table 8.3 and Figure 8.3 provide the mean values of all road and driving-based variables for each roadway type. As intuitively expected, vehicle velocity was highest during highway travel and the lowest while navigating more urban areas. Highway travel resulted in the slowest acceleration and deceleration rates, which is not unexpected given the lack of traffic influence and signal presence during highway travel. In-town acceleration rates were more inline with each other, however, urban driving resulted in slightly, but still statistically significant, higher acceleration rates than suburban travel. The subtle difference in deceleration rates reported between urban and suburban roadways were not statistically meaningful, suggesting that driver tendencies when braking were consistent regardless of the type of roadway being navigated.

Table 8.3: Mean values of on-road variables by roadway type for entire dataset.

Roadway Type	Velocity (km/h)	Acceleration (m/s^2)	Deceleration (m/s^2)	Grade, Positive (%)	Grade, Negative (%)
Highway	73.2	0.212	0.239	0.020	-0.022
Suburban	29.5	0.290	0.559	0.037	-0.050
Urban	17.7	0.315	0.561	0.642	-0.086

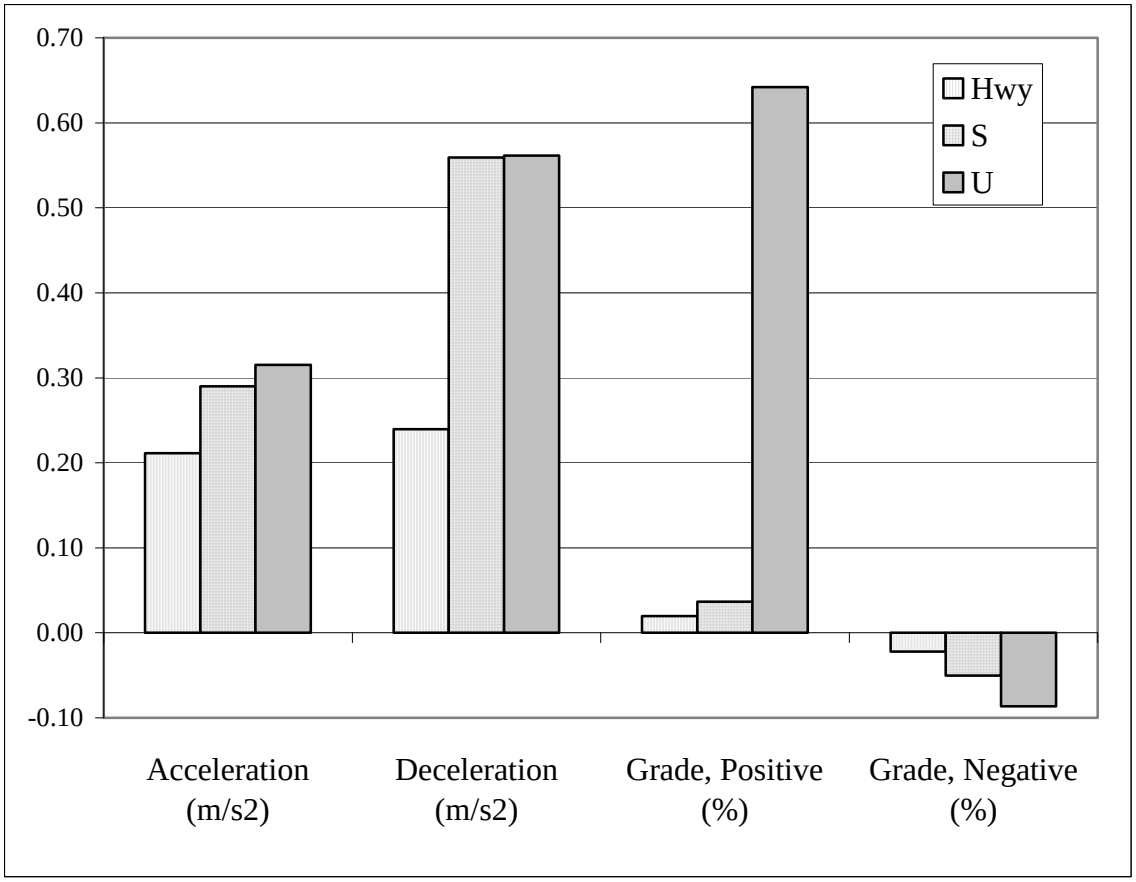

Figure 8.3: Mean acceleration, deceleration, grade (positive and negative) for each roadway-type investigated.

The individually selected roadway-types were located in different geographical pockets around the Kansas City metropolitan area. As mentioned earlier in this chapter and detailed more specifically in Chapter 3, all urban roadways were located within and around the Kansas City urban core; suburban or transition roadways were located in the area more aptly described as mid-town, branching out from the urban periphery towards the east and south. A north and south traveling, 3-mile stretch of Highway 71 was selected for all highway investigations. Geographic continuity exists within each of the roadway-types. Conversely, each designated roadway-type was geographical separate from the others leading to subtle, but distinctly different, variations in local topographies

between the three roadway types. Both positive and negative grade were found to be statistically significant responses to roadway type for all analyses (Tables 8.1 and 8.2). Highway driving provided the most level surface, while the Kansas City urban core possessed the largest elevation changes of the entire sample route system.

8.3.2 Traffic Pattern and Behavior Assessment

The initial statistical investigation proved that the selected roadway designations were, indeed, different from one another on the basis of mean velocity, acceleration, deceleration (for the all roadways comparison), and grade. Driver observation noted that traffic conditions as well as stoplight frequency and duration varied with roadway type. In order to quantify and assess potential differences in traffic conditions between the selected roadways, the number of stops (to zero velocity) and the amount of time spent at zero velocity was totaled for each roadway type for each sample run selected for the roadway-type analysis. Travel distance per roadway type per sample run was used as a basis for normalizing the traffic-related information, so that the final dataset yielded the average amount of time per stop, number of stops per distance traveled, the amount of time at zero velocity per distance traveled, and the percent of sample time that was spent at zero velocity for each sample run and roadway type traveled.

Table 8.4: Averaged number of stops and stopped time for each roadway type.

	Highway	Suburban	Urban
# Sample Runs	10	34	20
Time/Stop (s)	na	16.2	19.5
# Stops/Distance Traveled	0.0	1.3	3.0
Time stopped/Distance Traveled (s/km)	1.5	22.9	59.1
% Time at Zero Velocity	3.0%	16.5%	27.3%

Similar with the original road-based variables, the parameters calculated to assess the number of stops and time at zero velocity were subjected to ANOVA and Kruskal-Wallis analyses in order to investigate stop patterns as a response to roadway type. Since Highway driving did not result in stops, its traffic patterns were vastly different than all in-town driving. Because of this, the in-town-based roadways were analyzed separately as well. Based on the statistical tests, all stop-based parameters proved to be statistically significant ($\alpha<0.05$) responses to roadway type, except the average amount of time per stop, which remained similar for both urban and suburban roadway travel.

Table 8.5: Synopsis of statistical results for traffic pattern evaluation.

Variable:	All Roadways	Suburban/Urban Roadways
Time/Stop (s)	y	n
# Stops/Distance	y	y
Time at V=0km/h / Distance (s)	y	y
% Time Stopped (V=0km/h)	y	y

Urban driving resulted in twice the frequency of stops per kilometer traveled compared with suburban travel (3.0stops/km versus 1.3stops/km). Additionally, driving urban roads resulted in the most amount of time at zero velocity, which makes intuitive sense since the amount of time per stop was comparable for both urban and suburban travel (Figure 8.4).

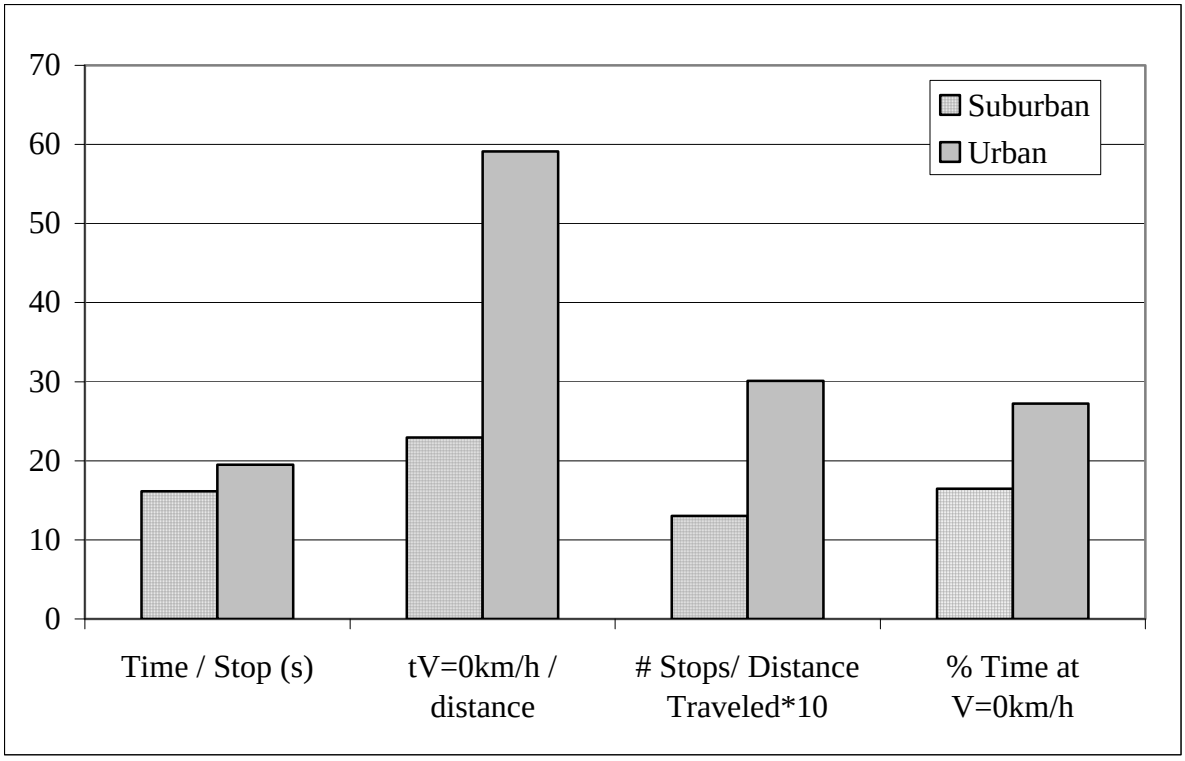

Figure 8.4: Bar chart of stopped parameters for urban and suburban travel.

8.3.3 Potential Influence of Street-Based Noise within Roadway Distinctions

While each in-town sample route presented either a mix of urban and suburban driving or all suburban travel, there was minimal direct street overlap between the different routes. Obvious and significant differences exist between the roadway types, but inherent differences between the streets of the individual sample routes were not discernable from the previous analyses. From a project planning perspective, being able to estimate the natural variation possible between different streets of the same roadway designation holds certain value.

The following evaluations were conducted using mean values obtained from each sample run, so the utilized dataset contained a single value for each sample run that was part of the originally selected group of runs. Comprehensive tables for the dataset used in these analyses can be found in Appendix E.

8.3.4 Suburban Driving: Intra-route variations

For suburban travel, both the number of stops per distance as well as the time spent at zero velocity (on a distance traveled basis) were statistically significant responses to the suburban street being traveled. Traveling East/West along 12th street and Truman Avenue on the 12T/C route resulted in the lowest number of stops per distance traveled, whereas East/West travel along 19th and 23rd Streets on the 123 route incurred the highest number of stops per distance traveled as well as the longest average amount of time per stop, and, consequently, the longest amount of stop time per distance traveled than all other suburban roadways traveled. Aside from the 123 route, no statistically significant difference in average velocity existed between the different suburban streets. The suburban-based 123 route resulted in the lowest average calculated velocity, however, travel along 123 did incur the highest frequency and duration of vehicle stops, which would negatively impact the calculated average velocity for this route.

Slight, but still statistically significant ($\alpha<0.05$), differences did exist in the acceleration and deceleration rates between the different suburban streets. The suburban routes were split in their acceleration profiles with routes 110 and 123 exhibiting the fastest, but quantitatively similar, rates of acceleration. Conversely, both 109 and 12T/C routes had similar average acceleration rates that were statistically slower than those

witnessed on the 110 and 123 routes. Where 109 and 12T/C routes were slower accelerators during suburban travel, they also represented the streets with the mildest rates of deceleration. This suggests that the streets comprising the suburban component of the 109 and 12T/C routes represented areas where travel was less aggressive.

8.3.5 Urban Driving: intra-route variations

Three of the selected routes for the PHEV on-road characterization study contained street travel that fell within the geographic and speed restriction criteria set for urban roadways. However, despite the close proximity of all of the urban roadways selected for this study, there was little overlap in the actual streets traveled between the routes containing a component of urban travel. Therefore, a similar, inter-route analysis was performed on the urban roadways as well.

The number of stops per distance was not a statistically significant response to urban route or street with the 109, 110, and 12T/C urban sections all resulting in similar frequencies of moments where the PHEV Sprinter was completely stopped. However, the amount of time spent at zero velocity per distance traveled did vary significantly ($\alpha<0.05$) between the urban routes being sampled. Both the 109 and 110 exhibited similar periods of stop time, however, travel along the 12T/C urban component experienced almost twice as much time at zero velocity than the 109 and 110 routes (53s/km for 109 route, 42s/km for 110 route, and 97s/km for the 12T/C route). This trend persisted when the data were analyzed on a time basis as well, with 12T/C travel spending almost 36% of its on-road urban component stopped (versus 27% for the 109 route and 23% for the 110 route).

Regardless of the statistically different times at zero velocity between the different urban routes, the average velocity between the routes did not vary to a significant degree. Acceleration and deceleration rates did show a statistically significant response to route traveled within the Kansas City urban core, however, with the 110 route exhibiting significantly higher acceleration rates (0.38m/s^2 on average versus 0.29m/s^2 and 0.26m/s^2 for the 109 and 12T/C routes, respectively). Deceleration rates did not vary significantly with route, suggesting that within more close-knit traffic scenarios, inherent driver patterns of behavior dominate deceleration events.

Similar to findings from the VPS analysis, definite differences existed between individual streets of the selected routes even when assessed according to roadway type. However, as found with the VPS investigation, the differences between the routes, while still statistically significant, were of a much smaller magnitude than the differences between the roadway types.

8.3.6 Defining Roadway Types: Summary

On the basis of velocity, acceleration, deceleration, and parameters calculated to assess traffic behavior, statistically significant ($\alpha<0.025$ or $\alpha<0.05$ depending on dataset resolution) differences exist between the roadways denoted as urban, suburban, and highway. These statistical differences were persistent regardless of whether the analysis was conducted on all roadways together or the analyses limited to the more in-town urban and suburban roadways only. Based on the previous investigation, it was determined that the criteria established for defining different roadway types in the Kansas City metropolitan area for the purpose of the PHEV Sprinter on-road characterization study

were sufficient for showcasing the PHEV Sprinter's on-road operation of different roadway types. Therefore, the sampling routes selected successfully yielded the collection of on-road operating and emissions data pertaining to the three defined and discrete roadway types. These types are indicative of the various modes of on-road travel commonly encountered in mid- to large- sized cities. While the statistically determined differences in individual streets within each roadway class were present in the sample run-based variables, the extent of these differences are marginal and not anticipated to contribute any meaningful information to the following PHEV-specific roadway analysis. However, for the purpose of defining and selecting sites for on-road vehicle emissions campaigns, the possibility of encountering statistically significant variations in on-road behavior for different streets within the same roadway type should be considered and accounted for if necessary.

8.4 Vehicle specific power, PHEV power output and recuperation rates

8.4.1 Charge-Sustaining Mode

With the initial roadway analysis proving that a statistical difference ($\alpha<0.025$ for all statistical tests using continuous data and $\alpha<0.05$ for all statistical tests conducted on the run or sample-based compiled data) exists between the designated roadway types according to road-based and driving-characteristic-based variables, the following investigation will focus on the PHEV Sprinter's operation and power requirements for the three roadway types: urban, suburban, and highway. The implications that roadway type has on Vehicle Specific Power (VSP), a calculated proxy for instantaneous on-road power demand, will be evaluated alongside the PHEV's DLM-derived power demand. VSP was proven in previous chapters to proportionally and directly track with the PHEV's total power demand, as calculated from electric motor and internal combustion engine outputs. It was included in this analysis not as a source of statistical and analytical redundancy, but because of its independence from the engine-sequestered data. As a calculated surrogate for power demand, VSP can be determined for a specific route or roadway type without reference to a specific vehicle by using accepted averages for vehicle parameters based on a particular class of vehicle. Any trends or correlations between instantaneously calculated VSP for a particular roadway type or between roadway types are translatable to other roadways of similar type and other geographies.

Because the PHEV Sprinter possesses two distinct operating modes: charge-sustaining, and charge-depleting, the analysis has been broken into two subsets according to operating mode. While total power demand and VSP will not be affected by PHEV operating mode, the respective use of the diesel internal combustion engine (dICE) versus

the electric motor (EM) will vary greatly depending on whether the PHEV is operating to deplete excess stored battery capacity (charge-depleting) or as a more conventional hybrid using the EM as an assist to the dICE (charge-sustaining).

ANOVA and Kruskal-Wallis tests were run on the charge-sustaining and charge-depleting datasets using the previously mentioned levels of statistical significance. For both modes of operation, the datasets were compiled from means of variables for individual sample runs. All statistical tests were performed on the compiled, per-sample dataset as well as on the continuous data (both second-by-second and on the continuous datasets averaged for every 5^{th} second). While autocorrelation should not impact the results from a statistical test assessing the variance and central tendency equivalence of different sample populations, the 5^{th}-second averaged dataset was still run alongside the continuous, second-by-second dataset for all analyses. Since highway operation was very different than in-town driving, all analyses were run twice: once on all three roadway types compared together, and again on the in-town roadway types (urban and suburban) alone. Tables 8.6 and 8.7 display the results of the ANOVA and Kruskal-Wallis tests. The presence of a "y" denotes that the criteria for establishing statistical significance was met for both tests, a "n" shows that neither tests were passed, and an inconclusive result, labeled "inc", was assessed when only one of the two tests passed. While tight criteria were maintained for establishing acceptable levels of statistical significance ($\alpha<0.025$) for all analyses on the continuous data, instances where statistical significance was not met generally resulted in p-values well in excess of even lax levels of significance (i.e. $p>0.10$). Because of the data's tendency to either meet significance with p-values nearing or equaling to zero or void statistical significance with p-values well beyond that

which would be acceptable in even the most lenient statistical analyses, the possibility of creating a Type II error was considered negligible.

Table 8.6: Statistical results for tests conducted on complete, charge-sustaining dataset for both continuous, second-by-second data and continuous data averaged every 5th second.

Variable:	All Routes	In-town routes only
VSP Ins, W/kg/s	y	y
VSP Bin (1-8)	y	y
ICE, W/kg/s	y	y
EM, W/kg/s	y	y
Total Pwr, W/kg/s	y	y
Recup, W/kg/s	y	y

Inc 1: yes ANOVA, no Kruskal-Wallis
Inc 2: no ANOVA, yes Kruskal-Wallis

Table 8.7: Statistical results for Charge-Sustaining data; analysis conducted on a sample run basis.

Variable:	All Routes	In-town routes only
VSP Ins, W/kg/s		
VSP Bin (1-8)		
ICE, W/kg/s	y	y
EM, W/kg/s	y	Inc2
Total Pwr, W/kg/s	y	y
Recup, W/kg/s	y	y

Inc 1: yes ANOVA, no Kruskal-Wallis
Inc 2: no ANOVA, yes Kruskal-Wallis

Table 8.8: PHEV power requirements by sample route for each roadway type, charge-sustaining operation.*

Road Code	Route	N	ICE Power (W/kg/s)		EM Power (W/kg/s)		Tot. Power (W/kg/s)		Recuperation (W/kg/s)	
			Mean	StDev	Mean	StDev	Mean	StDev	Mean	StDev
Hwy	Highway	851	8.07	6.51	0.78	3.02	8.86	6.32	-2.16	2.22
Hwy	Highway	832	7.53	6.86	0.77	3.00	8.30	6.82	-2.52	2.64
Hwy	Highway	876	8.39	7.23	0.70	2.82	9.09	7.07	-2.61	2.67
Hwy	Highway	791	9.74	6.93	0.39	2.21	10.13	6.78	-3.06	2.95
Hwy	Highway	693	9.70	6.83	0.41	2.15	10.12	6.59	-3.53	3.07
Hwy	Highway	1246	9.77	6.98	0.51	2.52	10.28	6.77	-2.89	2.42
S	109	522	3.60	5.71	1.09	3.11	4.69	5.88	-2.63	2.89
S	109	1015	4.07	6.58	1.66	3.73	5.73	6.65	-2.57	3.06
S	109	1137	4.05	6.36	1.40	3.42	5.46	6.42	-2.40	2.87
S	109	866	4.38	6.82	1.24	3.15	5.62	6.80	-2.46	3.13
S	109	1325	3.98	6.41	1.17	3.19	5.14	6.51	-2.38	3.00
S	109	775	4.15	6.41	1.55	3.44	5.70	6.43	-2.31	2.99
S	110	924	3.61	6.46	1.32	3.40	4.94	6.68	-2.23	2.88
S	110	1181	3.97	6.42	1.44	3.51	5.41	6.52	-2.32	2.97
S	110	1094	3.81	6.88	1.58	3.56	5.39	7.02	-2.31	3.05
S	110	1982	4.05	6.71	1.22	3.14	5.27	6.76	-2.24	3.01
S	110	1899	3.72	6.17	1.29	3.25	5.01	6.29	-2.17	2.88
S	110	882	4.76	6.99	1.30	3.31	6.06	6.93	-2.61	3.24
S	110	678	4.71	6.97	1.61	3.94	6.31	7.10	-2.67	3.17
S	110	742	4.25	6.95	1.21	3.05	5.45	6.99	-2.19	3.11
S	110	1154	3.96	6.64	1.43	3.79	5.39	6.98	-2.40	2.92
S	110	1101	4.37	6.99	1.41	3.42	5.78	7.04	-2.41	3.18
S	110	1779	4.26	6.84	1.58	3.82	5.84	6.98	-2.52	3.15
S	110	1782	4.18	6.59	1.48	3.67	5.66	6.72	-2.51	3.11
S	110	1902	4.19	6.75	1.61	3.74	5.80	6.84	-2.46	3.17
S	123	2721	4.16	7.06	1.22	3.40	5.38	7.25	-2.14	2.83
S	123	2666	4.24	7.13	1.17	3.32	5.41	7.26	-2.23	2.86
S	123	2759	4.05	7.05	1.17	3.26	5.22	7.22	-2.09	2.83
S	123	924	3.33	5.87	1.11	3.16	4.44	6.15	-2.03	2.65
S	123	2029	4.26	7.52	1.35	3.63	5.61	7.79	-2.27	3.11
S	12T/C	1568	4.02	6.56	1.45	3.72	5.47	6.78	-2.51	3.03
S	12T/C	1551	4.52	6.91	1.46	3.72	5.98	7.01	-2.61	3.06
S	12T/C	1503	4.38	6.66	1.14	3.05	5.51	6.65	-2.46	2.92
S	12T/C	1736	4.09	7.12	1.47	3.67	5.56	7.31	-2.26	3.08
U	109	61	0.00	0.00	4.71	3.94	4.71	3.94	-0.29	0.64
U	109	313	3.33	5.73	1.17	3.18	4.51	6.10	-1.83	2.99
U	109	283	3.60	5.78	1.11	3.27	4.70	6.13	-2.06	2.63
U	109	280	2.92	5.09	1.38	3.04	4.30	5.21	-1.69	2.74
U	109	269	2.49	4.29	1.39	2.91	3.87	4.51	-1.26	1.69
U	110	321	4.24	6.96	1.83	4.18	6.07	7.24	-2.04	3.05
U	110	658	3.71	5.92	0.92	2.77	4.64	6.05	-2.06	2.60
U	110	743	3.07	5.38	1.07	2.77	4.14	5.51	-1.67	2.47
U	110	709	3.14	5.62	0.98	2.88	4.11	5.85	-1.70	2.51
U	110	739	3.11	5.34	0.98	2.84	4.10	5.51	-1.90	2.49
U	110	582	3.71	6.08	1.09	2.66	4.80	5.99	-1.97	2.77
U	110	592	4.15	6.61	0.90	2.43	5.05	6.52	-2.17	2.93
U	12T/C	1150	1.44	3.80	1.14	2.94	2.59	4.50	-0.85	1.50
U	12T/C	855	3.16	5.76	0.88	2.68	4.03	5.91	-1.78	2.50
U	12T/C	877	2.56	5.07	0.78	2.36	3.35	5.22	-1.51	2.44
U	12T/C	893	2.90	4.76	0.65	1.92	3.55	4.77	-1.64	2.28

*In table, above, Hwy=highway roads, S=suburban roadways, and U=urban roadways.

During charge-sustaining operation, all of the power-based variables proved to be statistically significant responses to navigated roadway-type, with the only exception being EM power output assessed on a sample run-basis. For the analysis of the compiled, run- or sample-based dataset, EM power output did not meet the criteria set for determining statistical significance for the ANOVA test performed comparing in-town roadways ($p=0.786$).

Since VSP is calculated from road- and driving-based information as well as coefficients relating to the PHEV Sprinter's physical size and inherent on-road resistances, reported VSP will not depend on the PHEV's active operating mode. According to accepted modeling practices, instantaneous VSP data were categorized into discrete bins developed for heavy-duty on-road vehicles (Zhai and Frey, 2008). Figure 8.5 shows the relative VSP-bin distribution for each roadway-type investigated. As presented earlier, VSP, and consequently, VSP-bin, proved to be statistically significant responses to roadway-type regardless of the level of analysis performed.

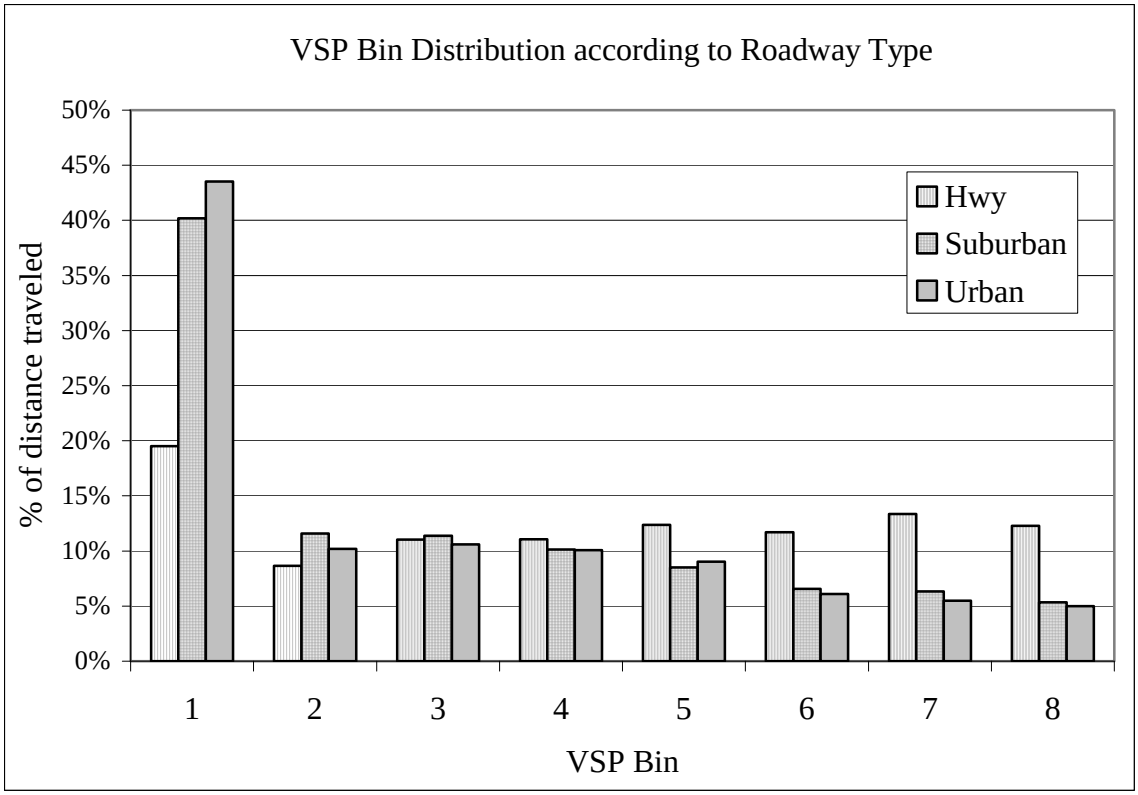

Figure 8.5: VSP bin distribution for the three roadway-types investigated.

The general trend in VSP-bin distribution was similar for all roadway types, with the majority of the on-road time occurring in VSP-bin 1 and a relatively even distribution of the remaining data occupying VSP bins 2 through 8. Despite the general continuity between highway, suburban, and urban travel in VSP-bin distribution, certain differences do present between the roadway types. Highway travel resulted in the least amount of time in VSP-bin 1, instead requiring significantly higher power requirements than the other more in-town roadways, as demonstrated by the high representation of data collected in bins 5 through 8. Suburban and urban travel resulted in, comparatively, more similar VSP bin profiles across all 8 VSP bins. For both urban and suburban travel, a disproportionate amount of the distance traveled occurred in VSP bin 1 (43.5% for urban travel and 40.2% for suburban). Distance was used instead of time in order to avoid

artificially inflating the differences between roadways due to inherent differences in the amount of time at zero velocity between the assessed roadway types. However, where urban travel resulted in the most amount of time in VSP bin 1, operating near the urban core produced slightly lower representation of VSP bins 2 through 8 compared with suburban travel, suggesting that, based on VSP, urban travel required the least amount of on-road power (on a time basis as the units for VSP are W/kg/s).

Aside from the in-town analysis of the compiled, sample-run-based dataset of electric motor power output as a response to urban/suburban roadway-type, power demand and utilization (both into and out of the PHEV drive train) proved to be a statistically significant response to the type of roadway being traveled. Figure 8.6, below, provides a summary of the PHEV's power output and recuperation according to roadway-type. Not unexpectedly, the largest divergence in PHEV power utilization occurred during highway travel. The highway's higher average velocities required more power, on a per second basis, than in-town driving. Because the PHEV was designed to optimize its electric-only range during slower, more stop-and-go traffic scenarios, a majority of the power used to operate the PHEV Sprinter during charge-sustaining, highway travel was derived from the dICE. Surprisingly, however, highway driving resulted in the highest rates of electrical recuperation. Because recuperation can only safely occur during more moderate moments of deceleration, the subtle oscillations in vehicle velocity that occur during a long distance, more constant speed scenario, such as highway driving, may be more suited to electrical recuperation.

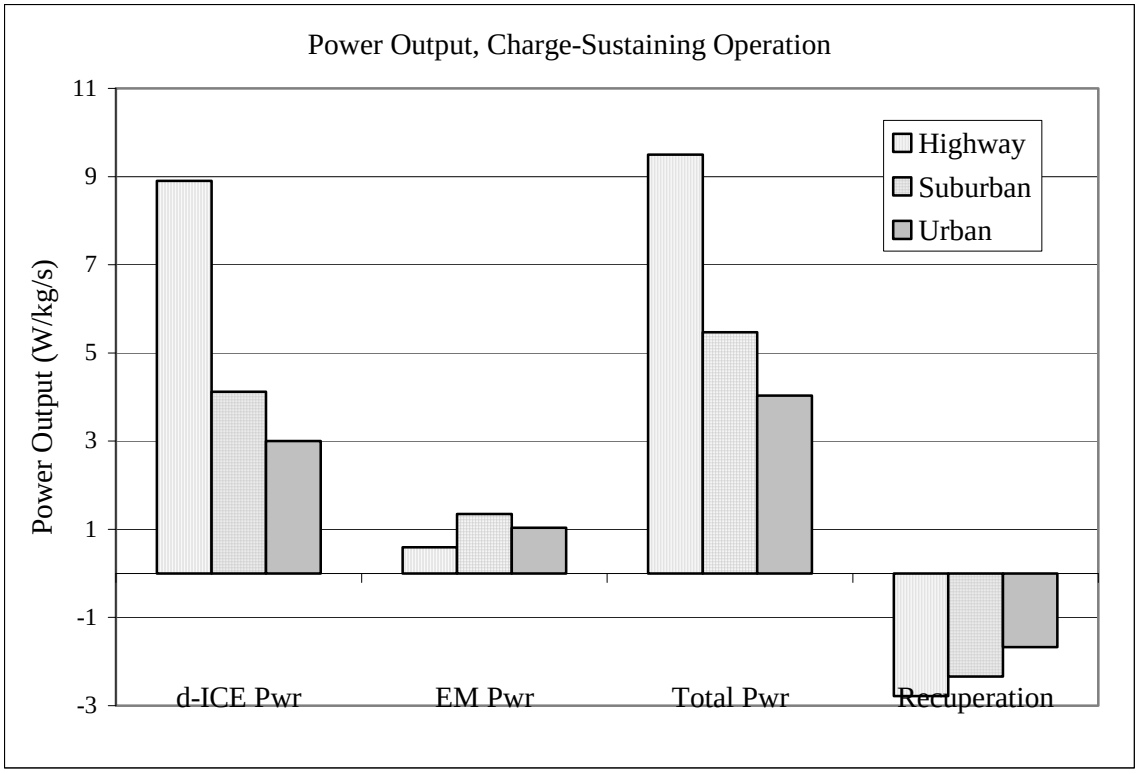

Figure 8.6: Power output and electrical recuperation according to roadway-type during charge-sustaining operation.

Vehicle emissions and operating data, when collected in a continuous manner, are conventionally reported on a basis of time (per second) (Frey, 2007, Younglove and Scora, 2004, Yu et al., 2008, Zhai, 2008). This convention lends itself to continuous on-road sampling efforts where measured observations are standardized to every second. However, when assessing roadways with significantly different velocity and traffic profiles, considering the data on a distance basis is equally useful, and can provide additional insight into the true emissions load imposed by vehicle presence in specific geographic areas within and around a metropolitan area. Figure 8.7, below, displays the power demand and output of the PHEV subsystems and overall use on a distance-traveled basis.

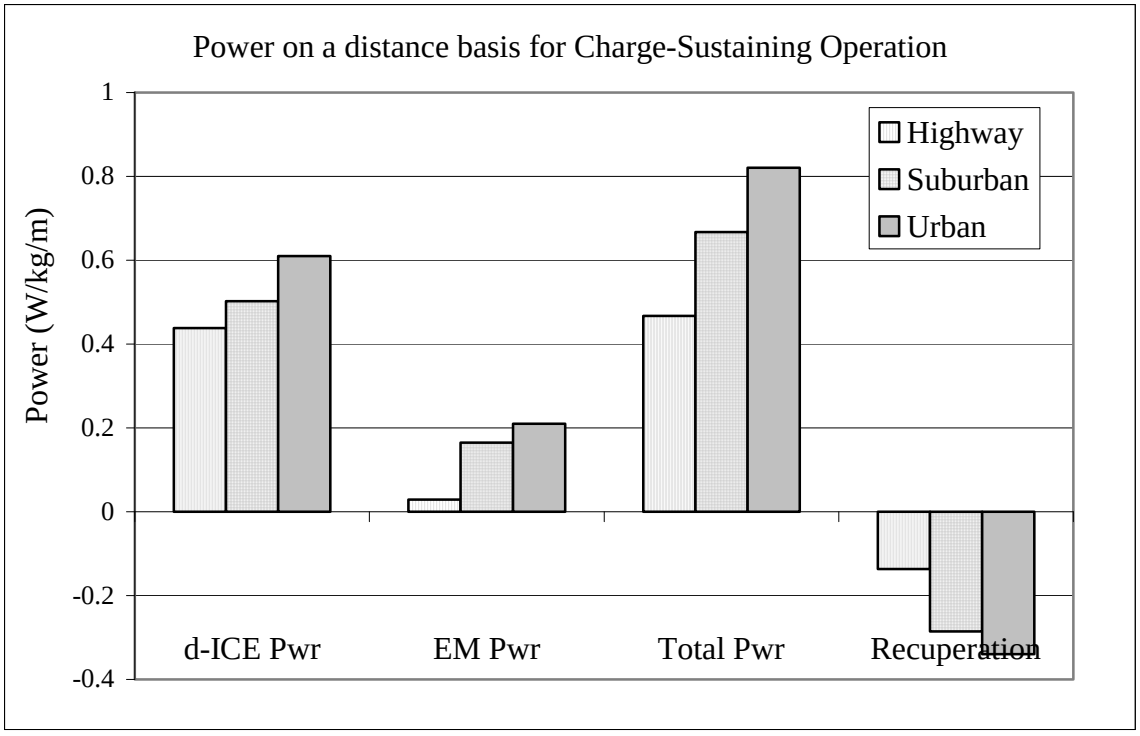

Figure 8.7: Power demand and output on a distance basis for Charge-Sustaining operation.

Highway travel occurs at a significantly higher average velocity than either of the designated in-town roadways. Because of this, for a given second of highway driving, the PHEV Sprinter traveled a considerably longer distance compared with either urban or suburban driving resulting in a relatively higher power demand when assessed on a per time basis. In reality, however, highway driving resulted in the most efficient method of PHEV operation. Highway operation required the least amount of power output on a per distance basis with regards to total power, dICE power demand, and EM power output. As mentioned earlier, the PHEV Sprinter's electrical drive capabilities were designed to be maximized during slower, more congested traffic when vehicle operation is inherently inefficient, so the minimal EM use during highway travel is in accordance to the PHEV's design and intent. With regards to the in-town roadways, as the average velocity

decreased, the amount of power demand per distance traveled showed a corresponding increase. Where urban travel proved to be the most efficient on a time basis, urban travel required the highest amount of energy and work for every meter of roadway covered. The actual difference between suburban and urban travel is magnified by the large amount of stop time incurred when driving more congested, urban roadways. For the purpose of continuity with existing research, the majority of the statistical evaluation will be focused on time-based data. However, distance-based results will be provided alongside the time-based in order to provide a balanced basis for evaluation.

Table 8.9: Compiled power demand per second of data collection for all roadway types, charge-sustaining operation.

	d-ICE Pwr (W/kg/s)	EM Pwr (W/kg/s)	Total Pwr (W/kg/s)	Recuperation (W/kg/s)
Highway	8.90	0.60	9.50	-2.78
Suburban	4.12	1.35	5.47	-2.34
Urban	3.00	1.03	4.03	-1.67
% decrease of Urban vs Suburban	27.2%	23.4%	26.3%	28.7%

Table 8.10: Compiled power demand per meter of distance traveled for all roadway types, charge-sustaining operation.

	d-ICE Pwr (W/kg/m)	EM Pwr (W/kg/m)	Total Pwr (W/kg/m)	Recuperation (W/kg/m)
Highway	0.438	0.029	0.467	-0.137
Suburban	0.503	0.165	0.667	-0.286
Urban	0.610	0.210	0.820	-0.340
% decrease of Urban vs Suburban	-21.4%	-27.7%	-22.9%	-18.9%

8.4.2 Charge-Depleting Mode

The previous discussion pertained to charge-sustaining operation only. While a more comparative discussion regarding the differences between charge-sustaining and charge-depleting operation will be presented in Chapter 9, as part of a comprehensive operating mode analysis, it is important to assess the roadway-types for both modes of PHEV operation. The general trend in power demand between roadway types reported for charge-sustaining operation persists in charge-depleting mode as well.

Statistical results achieved for the charge-depleting datasets were considerably less conclusive than the results found for charge-sustaining operation. Analyses performed on the continuous charge-depleting dataset (both second-by-second and data averaged for every 5^{th} second) showed that all manifestations of the PHEV Sprinter's power output (both DLM-derived and calculated VSP) and recuperation were statistically significant responses to roadway type when the analyses were executed on all three roadways. However, when the analysis was limited to evaluating the differences between suburban and urban roadways (in-town), neither EM nor dICE power output proved to be statistically conclusive responses to roadway type. The goal of charge-depleting operation is to maximize the vehicle's electric-only range while maintaining on-road performance standards. Because of this, localized on-road demands such as moments of more intense acceleration or significant road grade will demand more dICE assist than normal operation would require.

The statistical results were slightly different for the analysis performed on the compiled sample-run means. Analysis of the three roadway types together proved to be statistically significant for all power-related variables, however, when the same statistical

tests were run on the suburban and urban roadways alone, both EM power output and electrical recuperation lost their statistical significance resulting in p-values of 0.529(ANOVA) and 0.346(Kruskal-Wallis) for the electric motor power output and 0.066(ANOVA) and 0.157(Kruskal-Wallis) for recuperation rates.

Table 8.11: Statistical results for ANOVA and Kruskal-Wallis analysis on the charge-depleting, continuous dataset run on both second-by-second data and 5-second averaged.

Variable:	All Routes	In-town routes only
VSP Ins, W/kg/s	y	y
VSP Bin (1-8)	y	y
ICE, W/kg/s	y	Inc1
EM, W/kg/s	y	Inc1
Total Pwr, W/kg/s	y	y
Recup, W/kg/s	y	y

Inc 1: yes ANOVA, no Kruskal-Wallis
Inc 2: no ANOVA, yes Kruskal-Wallis

Table 8.12: Statistical results for analysis on a sample run basis, charge-depleting mode.

Variable:	All Routes	In-town routes only
VSP Ins, W/kg/s		
VSP Bin (1-8)		
ICE, W/kg/s	y	y
EM, W/kg/s	y	n
Total Pwr, W/kg/s	y	y
Recup, W/kg/s	n	n

Table 8.13: PHEV power requirements by sample route for each roadway type, charge-depleting operation.*

Charge-Depleting Mode: Synopsis of all routes by sample run.

Road Code	Route	N	ICE Power (W/kg/s)		EM Power (W/kg/s)		Tot. Power (W/kg/s)		Recuperation (W/kg/s)	
			Mean	StDev	Mean	StDev	Mean	StDev	Mean	StDev
Hwy	Highway	815	8.01	6.43	0.38	2.15	8.39	6.37	-1.32	1.75
Hwy	Highway	827	7.23	6.39	0.16	1.28	7.39	6.43	-0.30	0.82
Hwy	Highway	747	7.11	6.86	0.73	2.88	7.84	6.79	-0.27	0.67
Hwy	Highway	615	7.47	6.04	0.78	3.42	8.25	6.21	-0.26	0.78
S	109	479	2.39	4.08	0.96	2.82	3.35	4.50	-0.49	0.81
S	109	1183	1.81	4.14	2.20	3.96	4.01	5.11	-0.47	1.01
S	109	614	1.76	3.71	2.87	4.83	4.63	5.27	-0.52	1.08
S	110	1014	1.06	3.56	2.59	4.46	3.66	5.52	-0.55	1.00
S	110	868	1.38	4.19	3.12	4.55	4.50	5.57	-0.58	1.26
S	110	1085	1.80	5.02	3.00	4.60	4.80	6.07	-1.06	2.27
S	123	1294	1.62	4.20	0.88	2.35	2.50	4.55	-0.44	0.85
S	123	3992	2.03	4.92	1.85	4.02	3.87	5.90	-0.92	1.62
S	12T/C	344	2.01	4.94	2.18	3.88	4.19	5.64	-0.74	1.28
U	109	301	0.94	3.07	2.05	3.55	2.99	4.25	-0.24	0.59
U	109	185	0.00	0.00	2.89	4.24	2.89	4.24	-0.24	0.63
U	110	793	1.49	3.76	1.81	3.74	3.30	4.99	-0.64	0.93
U	110	341	0.31	1.84	1.69	3.28	2.00	3.66	-0.49	0.95
U	110	663	1.27	3.45	1.90	3.60	3.16	4.46	-0.59	0.93
U	12T/C	1009	1.66	4.15	1.26	2.92	2.92	4.75	-0.35	0.66

*In table z, above, Hwy=highway roads, S=suburban roadways, and U=urban roadways.

On a per-second basis, highway travel required significantly more power than either in-town roadway type. Because the PHEV was not designed to maximize its electric-potential at higher velocities, electric motor utilization still remains markedly low during highway travel, despite the excess stored battery capacity of charge-depleting operation.

Similar to the results found for charge-sustaining operation, suburban roadways imposed a higher power demand on the PHEV Sprinter compared with urban travel, on a time reported basis. However, in charge-depleting operation, excess battery capacity resulted in more than 50% of the total PHEV power output being provided by the electric motor for both urban and suburban travel. As reported previously, the statistical results between suburban and urban travel were inconclusive for both the ICE and EM power output during charge-depleting operation. When assessed on a per sample-run basis, EM

power output was not a statistically significant response to in-town roadway type. Charge-depleting operation was inherently transient, and much less homogeneous than charge-sustaining mode. In order to maximize the PHEV Sprinter's electric-only operation while still maintaining performance standards, the PHEV frequently oscillated between zero-emissions operation (electric-only) to significant dICE assist.

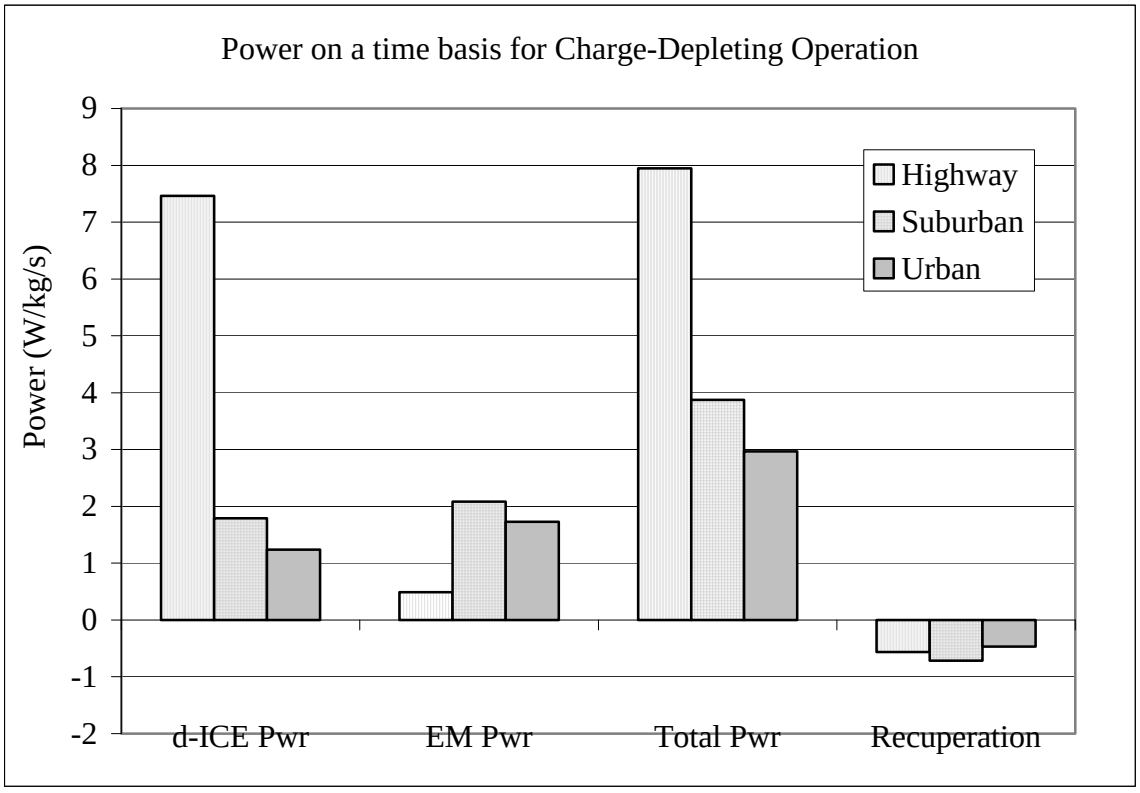

Figure 8.8: Power demand according to roadway-type for charge-depleting operation.

The charge-depleting data were also assessed on a distance basis. Similar to highway operation during charge-sustaining mode, when the data were rearranged according to distance traveled, highway driving proved to be the most efficient of the designated roadway-types, requiring the lowest total power output per meter traveled. The general trend found during charge-sustaining operation for total power output

remained for urban and suburban travel as well, with urban driving requiring more vehicle work and energy per meter than suburban travel. However, compared with in-town driving, during charge-depleting mode, highway operation required the most use of the dICE, since the in-town roads better monopolized the PHEV's excess battery capacity, providing more electric-only operation on slower, more congested roads. Where urban travel required less energy than suburban travel on a time basis, due to the slower average velocity and increased stop time of urban travel, on a per meter basis driving near Kansas City's urban core required more power from both the dICE and EM than navigating the more suburban, transition roads.

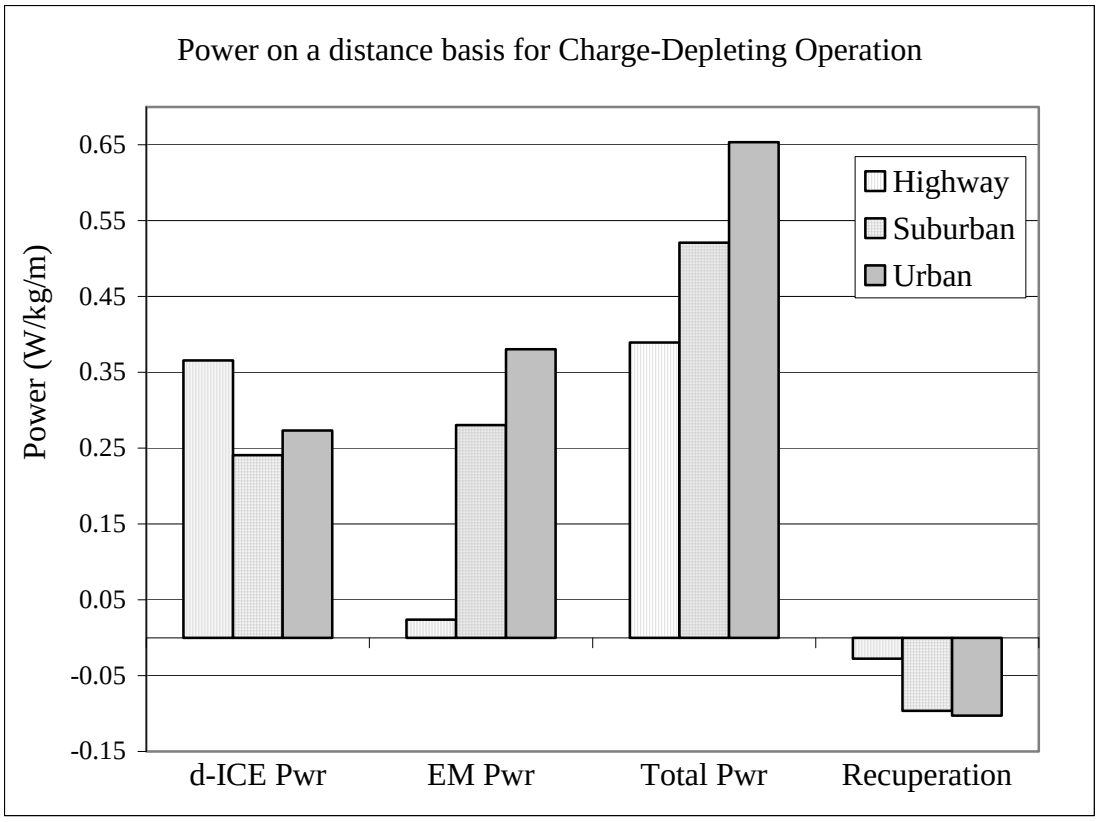

Figure 8.9: Power demand on a distance basis for charge-depleting operation, according to roadway type.

Tables 8.15 and 8.16, below, provide the total power output for the PHEV and its various subsystems on a time- and distance-basis. On a per second basis, urban travel is significantly more efficient than suburban travel, showing an over 30% reduction in power output from the diesel engine (dICE), and a 17% reduction in electric power from the EM. However, when assessed on a distance basis, urban travel requires considerably more energy for every meter of roadway. Conversely, recuperation rates, judged by distance, are maximized by urban travel compared with either suburban or highway data. The slower velocity ranges and more dynamic topography of urban travel in Kansas City yield themselves to increased recuperative benefit.

Table 8.14: Compiled power demand according to roadway-type for charge-depleting operation on a per second basis.

	d-ICE Pwr (W/kg/s)	EM Pwr (W/kg/s)	Total Pwr (W/kg/s)	Recuperation (W/kg/s)
Highway	7.46	0.49	7.95	-0.56
Suburban	1.79	2.09	3.88	-0.72
Urban	1.24	1.73	2.97	-0.47
% decrease of Urban vs Suburban	30.7%	17.1%	23.4%	35.1%

Table 8.15: Compiled power demand according to roadway-type for charge-depleting operation on a per second basis.

	d-ICE Pwr (W/kg/m)	EM Pwr (W/kg/m)	Total Pwr (W/kg/m)	Recuperation (W/kg/m)
Highway	0.366	0.024	0.390	-0.028
Suburban	0.241	0.280	0.521	-0.096
Urban	0.273	0.381	0.654	-0.103
% decrease of Urban vs Suburban	-13.4%	-35.7%	-25.4%	-6.3%

8.5 Correlation Analysis of Power Output and Usage

8.5.1 Charge-Sustaining Mode

Correlation analysis was employed here to discern any additional influences that the road-based variables had on the PHEV Sprinter's actual power demand for each different roadway-type. Similar to earlier correlation analyses, Pearson's correlations were performed on the power and road-based variables in order to elucidate any potential relationships between the PHEV's power demands and the road- and driving-based variables. In order to mitigate the presence of autocorrelation in the continuous, second-by-second dataset, all variables of interest were averaged over a 5-second time span. Zhai, et al. (2008) determined that averaging second-by-second observations over a set averaging time could diminish the degree of autocorrelation inherent in continuous on-road data. It was determined that increasing the averaging time from 3 seconds to 5 seconds continued to drop the autocorrelation by a factor of more than two. For the purposes of this study, a 5-second averaging time was selected in order to allay autocorrelation within the PHEV Sprinter dataset without excessive risk of loosing any descriptive or explanatory features present within the original dataset. Due to the large size of the on-road datasets, an alpha<0.025 criteria was used to establish statistical significance.

The same standards used in preceding correlation discussions were used to provide guidance for assessing the extent of correlation between variables were implemented here.

Table 8.16: Criteria used to assess strength of correlation analysis.

	Pearson Correlation Coefficient Range	Corresponding R^2 Range
Very High Positive Correlation	0.90 - 1.00	0.81 - 1.00
Good Positive Correlation	0.70 - 0.89	0.49 - 0.80
Moderate Positive Correlation	0.50 - 0.69	0.25 - 0.48
Weak Positive Correlation	0.30 - 0.49	0.09 - 0.24
Negligible Correlation	-0.29 - 0.29	0.00 - 0.08
Weak Negative Correlation	-0.30 - -0.49	0.09 - 0.24
Moderate Negative Correlation	-0.5 - -0.69	0.25 - 0.48
Good Negative Correlation	-0.70 - -0.89	0.49 - 0.80
Very High Negative Correlation	-0.90 - -1.00	0.81 - 1.00

Variables that were deemed at least moderately correlated (Pearson correlation coefficient > abs0.50) are formatted in bold type in the following tables. Similarly, variables whose correlation did not meet the set level for statistical significance (p-value>0.025) are crossed out. Some correlation exists between the road-based variables (velocity, acceleration, grade) and PHEV power output, however, those that are present are weak at best (Pearson correlation coefficient < abs0.490).

During highway operation, grade proved to be weakly, positively correlated with both total power and dICE power output (Pearson Coefficients of 0.434 and 0.416, respectively). Frey et al. (2008) found that road grade had a significant effect on a vehicle's fuel use and emissions, however, the scale of that assessment dictated the ultimate impact that was found. At the micro-scale level, grade proved to be significant, but as the analysis expanded in geographic scope, meso-scale analyses did not yield a

statistically significant impact between road grade and fuel use or emissions. Since the bulk of this analysis occurs on the meso-scale, it is understood that certain nuances in the data that may present at the micro-scale might be lost.

Highway acceleration was also weakly positively correlated with total PHEV Sprinter power output (Pearson's correlation coefficient=0.490), however, acceleration was a stronger influence on EM power demand (Pearson's correlation coefficient =0.445) than dICE power demand (Pearson's correlation coefficient =0.308). Because of its limited use during highway driving, variables that impact EM utilization will tend to show stronger correlations than with dICE power output, since the dICE was employed during most of the highway driving. Based on the positive correlation between PHEV acceleration and EM utilization, it is surmised that when the vehicle was operating had higher velocities the electric capabilities of the PHEV were more consistently used as a power assist during periods of slight acceleration. Vehicle velocity at the highway level demonstrated a slightly weak positive correlation with dICE power and a weak, negative correlation with EM power output. As the PHEV Sprinter increased its cruising velocity, the combustion engine disproportionately provided the increased workload as the electric motor was pulled off line. Recuperation did not correlate with any driving-based variables except for velocity, indicating that at higher velocities, when the EM was being under-utilized, the electrical potential was being redirected into the battery packs as stored capacity instead.

Table 8.17: Correlation analysis of power-based data with road- and driving-based variables for highway operation.

Charge-Sustaining, Highway Roadway Operation

	Velocity (km/hr)	Accel (m/s^2)	Grade (%)	VSP Inst (W/kg/s)	ICE Pwr (W/kg/s)	EM Pwr (W/kg/s)	Total Pwr (W/kg/s)	Recup (W/kg/s)
Accel (m/s^2)	0.020							
	0.525							
Grade (%)	-0.039	-0.091						
	0.200	0.003						
VSP Inst (W/kg/s)	0.260	**0.601**	**0.529**					
	0.000	**0.000**	**0.000**					
ICE Pwr (W/kg/s)	0.468	0.308	0.434	**0.785**				
	0.000	0.000	0.000	**0.000**				
EM Pwr (W/kg/s)	-0.376	0.445	-0.078	0.130	-0.260			
	0.000	0.000	0.011	0.000	0.000			
Total Pwr (W/kg/s)	0.335	0.490	0.416	**0.857**	**0.927**	0.122		
	0.000	0.000	0.000	**0.000**	**0.000**	0.000		
Recup (W/kg/s)	-0.380	0.036	0.211	0.088	-0.322	0.254	-0.232	
	0.000	0.239	0.000	0.004	0.000	0.000	0.000	
SOC (%)	-0.028	-0.370	-0.071	-0.339	**-0.510**	-0.172	**-0.591**	**0.511**
	0.355	0.000	0.021	0.000	**0.000**	0.000	**0.000**	**0.000**

Pearson's Coefficient: top number; P-Value: bottom number

Compared with highway travel, in-town driving of either suburban or urban roadways was an inherently more dynamic process, given the stop-and-go nature of adhering to local traffic signals and increased traffic congestion. Because of the presence of frequent acceleration/deceleration events and varying velocities during in-town

driving, the effect of grade on suburban travel did not correlate with PHEV power demand or usage. Acceleration, however, did prove to be positively, moderately correlated with total PHEV Sprinter power output (correlation coefficient=0.607). Its correlation with both dICE and EM power output was still positively correlated, but to a lesser degree (Pearson's correlation coefficients of 0.415 and 0.396, respectively). Velocity was less predictive than acceleration, showing only a weak positive correlation with total PHEV power output (correlation coefficient=0.306). Electrical recuperation during suburban travel was more strongly related to PHEV velocity than with acceleration (deceleration included). The PHEV Sprinter's electrical recuperation often occurred during moderate deceleration events. Deceleration rates were significantly higher during both urban and suburban travel compared with highway driving. During the driving mode analysis of the previous section, recuperation during deceleration events strong enough to meet the deceleration mode's criteria did not result in significant electrical recuperation. Since, in the interest of safety, regenerative braking systems give way to more conventional, friction-based braking during times of aggressive deceleration, it was not surprising to find limited recuperation during the specified deceleration mode. However, for the roadway-type analysis, deceleration was not limited to the definition provided by the driving mode model. All periods of negative acceleration (regardless of magnitude or period of duration) are considered deceleration. By the deceleration definition used in this analysis, it is not surprising to find a stronger correlation between deceleration and recuperation than previously cited.

Table 8.18: Correlation analysis of power-based data with road- and driving-based variables for suburban operation.

Charge-Sustaining, Suburban Roadway Operation

	Velocity (km/hr)	Accel (m/s^2)	Grade (%)	VSP Inst (W/kg/s)	ICE Pwr (W/kg/s)	EM Pwr (W/kg/s)	Total Pwr (W/kg/s)	Recup (W/kg/s)
Accel (m/s^2)	0.056							
	0.000							
Grade (%)	-0.033	0.005						
	0.003	0.644						
VSP Inst (W/kg/s)	0.134	**0.711**	0.124					
	0.000	**0.000**	0.000					
ICE Pwr (W/kg/s)	0.286	0.415	0.052	**0.633**				
	0.000	0.000	0.000	**0.000**				
EM Pwr (W/kg/s)	0.048	0.396	0.008	0.372	-0.225			
	0.000	0.000	0.451	0.000	0.000			
Total Pwr (W/kg/s)	0.306	**0.607**	0.055	**0.810**	**0.874**	0.277		
	0.000	**0.000**	0.000	**0.000**	**0.000**	0.000		
Recup (W/kg/s)	-0.466	-0.138	-0.013	-0.325	**-0.807**	0.348	**-0.622**	
	0.000	0.000	0.241	0.000	**0.000**	0.000	**0.000**	
SOC (%)	0.025	-0.060	-0.006	-0.029	-0.005	-0.070	-0.040	0.004
	0.023	0.000	0.606	0.009	0.627	0.000	0.000	0.725

Pearson's Coefficient: top number; P-Value: bottom number

When evaluating urban travel, acceleration was still somewhat predictive, but velocity was more strongly related to PHEV power demand and usage during travel on urban roads compared with suburban travel. A lot of this could be due to the excessive stop time on urban roads, resulting in a significant amount of data being collected while the PHEV was sitting idle. Recuperation was only very slightly correlated with velocity, demonstrating increased recuperation rates with increased velocity. Road grade did not

provide a statistically significant correlation ($\alpha<0.025$) with any of the measured or calculated variables, which is somewhat unexpected since Kansas City's urban core provided the most drastic topographical changes of all roadways evaluated.

Table 8.19: Correlation analysis of power-based data with road- and driving-based variables for urban roadways.

Charge-Sustaining, Urban Roadway Operation

	Velocity (km/hr)	Accel (m/s^2)	Grade (%)	VSP Inst (W/kg/s)	ICE Pwr (W/kg/s)	EM Pwr (W/kg/s)	Total Pwr (W/kg/s)	Recup (W/kg/s)
Accel (m/s^2)	0.074							
	0.001							
Grade (%)	-0.028	0.000						
	0.223	0.994						
VSP Inst (W/kg/s)	0.230	0.489	0.043					
	0.000	0.000	0.061					
ICE Pwr (W/kg/s)	0.359	0.394	-0.006	**0.504**				
	0.000	0.000	0.812	**0.000**				
EM Pwr (W/kg/s)	0.168	0.354	-0.010	0.250	-0.217			
	0.000	0.000	0.674	0.000	0.000			
Total Pwr (W/kg/s)	0.436	**0.562**	-0.010	**0.620**	**0.876**	0.281		
	0.000	**0.000**	0.659	**0.000**	**0.000**	0.000		
Recup (W/kg/s)	-0.491	-0.067	0.004	-0.309	**-0.792**	0.289	**-0.636**	
	0.000	0.004	0.851	0.000	**0.000**	0.000	**0.000**	
SOC (%)	-0.166	-0.031	0.006	-0.081	-0.116	-0.061	-0.144	0.143
	0.000	0.177	0.788	0.000	0.000	0.008	0.000	0.000

Pearson's Coefficient: top number; P-Value: bottom number

8.5.2 Charge-Depleting Mode

Due to the excess stored battery capacity, the PHEV Sprinter utilizes its electric motor more fully during charge-depleting operation. As a result of this, the PHEV Sprinter operated electric-only for a higher percentage of the drive time and distance than during charge-sustaining operation.

Correlation analysis of highway driving during charge-depleting mode proves that on-road variables such as velocity and acceleration were, statistically, slightly more predictive than found during the charge-sustaining correlation analysis. Acceleration was the strongest indicator of the PHEV Sprinter's power demand, demonstrating moderate to good correlation with both total power output and EM power output. Weak, but still positive correlation exists between PHEV acceleration and dICE power (Pearson's correlation coefficient of 0.378) and recuperation rates (Pearson's correlation coefficient of 0.306). On-road charge-depleting data also showed slightly increased responsiveness to local road grade, with total and dICE power output demonstrating moderate, positive correlations with road grade (Pearson's correlation coefficients of 0.536 and 0.567, respectively). Total power did not yield even a weak correlation with velocity; however dICE power output showed a weak but positive correlation with vehicle velocity (Pearson's correlation coefficient=0.353) where EM power output was weakly negatively correlated with on-road velocity (Pearson's correlation coefficient= -0.354).

Table 8.20: Correlation analysis of power-based data with road- and driving-based variables for highway driving during charge-depleting operation.

Charge-Depleting, Highway Operation

	Velocity (km/hr)	Accel (m/s^2)	Grade (%)	VSP Inst (W/kg/s)	ICE Pwr (W/kg/s)	EM Pwr (W/kg/s)	Total Pwr (W/kg/s)	Recup (W/kg/s)
Accel (m/s^2)	0.041 0.320							
Grade (%)	0.068 0.095	0.007 0.871						
VSP Inst (W/kg/s)	0.255 0.000	**0.606** **0.000**	**0.619** **0.000**					
ICE Pwr (W/kg/s)	0.353 0.000	0.378 0.000	**0.567** **0.000**	**0.858** **0.000**				
EM Pwr (W/kg/s)	-0.354 0.000	**0.498** **0.000**	-0.067 0.098	0.140 0.001	-0.161 0.000			
Total Pwr (W/kg/s)	0.217 0.000	**0.562** **0.000**	**0.536** **0.000**	**0.901** **0.000**	**0.929** **0.000**	0.216 0.000		
Recup (W/kg/s)	0.066 0.107	0.306 0.000	0.204 0.000	0.451 0.000	0.276 0.000	0.104 0.011	0.312 0.000	
SOC (%)	-0.129 0.002	-0.037 0.371	-0.004 0.921	-0.053 0.192	-0.038 0.348	-0.033 0.422	-0.050 0.219	0.316 0.000

Pearson's Coefficient: top number; P-Value: bottom number

The correlation results for in-town driving did not vary significantly between charge-sustaining and charge-depleting modes of operation. During charge-depleting mode, acceleration remained a good predictor of total PHEV Sprinter power output resulting in decently strong, positive Pearson's correlation coefficients for both urban and suburban travel (0.685 and 0.638, respectively). However, where the power output for subsystems dICE and EM remained moderately correlated with acceleration during charge-sustaining mode, the same correlations calculated for charge-depleting operation were positive, but only weakly so. The transient nature of charge-depleting operation and frequent alternating between zero-emissions (electric) and hybrid operation diminishes

the explanatory power that a one-dimensional correlation analysis, such as acceleration and power, can provide. Road grade did not affect PHEV power output to a meaningful degree. Neither urban nor suburban travel resulted in a statistically significant correlation analysis of road grade on power distribution and output.

The recuperation scheme between charge-sustaining and charge-depleting modes shifted slightly. Since charge-depleting operation is significantly more electric-only intensive than charge-sustaining operation, the periods of measurable recuperation are fewer. As a consequence of the inherently different control and power strategies between the modes of operation, recuperation proved to be more strongly correlated with acceleration during charge-depleting operation, whereas recuperation rates were more strongly associated with vehicle velocity during charge-sustaining operation. This observation is for urban roadways only; electrical recuperation did not result in even a weak correlation with on-road variables during suburban travel.

Table 8.21: Correlation analysis of power-based data with road- and driving-based variables for suburban roadways during charge-depleting operation.

Charge-Depleting, Suburban Roadway Operation

	Velocity (km/hr)	Accel (m/s^2)	Grade (%)	VSP Inst (W/kg/s)	ICE Pwr (W/kg/s)	EM Pwr (W/kg/s)	Total Pwr (W/kg/s)	Recup (W/kg/s)
Accel (m/s^2)	0.050							
	0.020							
Grade (%)	-0.022	0.012						
	0.304	0.585						
VSP Inst (W/kg/s)	0.148	**0.723**	0.062					
	0.000	**0.000**	0.004					
ICE Pwr (W/kg/s)	0.179	0.352	0.026	**0.549**				
	0.000	0.000	0.226	**0.000**				
EM Pwr (W/kg/s)	0.158	0.490	0.000	**0.495**	-0.146			
	0.000	0.000	0.987	**0.000**	0.000			
Total Pwr (W/kg/s)	0.259	**0.638**	0.021	**0.800**	**0.698**	**0.607**		
	0.000	**0.000**	0.337	**0.000**	**0.000**	**0.000**		
Recup (W/kg/s)	-0.160	0.188	-0.004	0.211	-0.267	0.292	-0.003	
	0.000	0.000	0.853	0.000	0.000	0.000	0.895	
SOC (%)	-0.131	0.007	0.024	-0.046	-0.073	-0.111	-0.139	0.271
	0.000	0.742	0.256	0.033	0.001	0.000	0.000	0.000

Pearson's Coefficient: top number; P-Value: bottom number

Table 8.22: Correlation analysis of power-based data with road- and driving-based variables for Urban Roadways during charge-depleting operation.

Charge-Depleting, Urban Roadway Operation

	Velocity (km/hr)	Accel (m/s^2)	Grade (%)	VSP Inst (W/kg/s)	ICE Pwr (W/kg/s)	EM Pwr (W/kg/s)	Total Pwr (W/kg/s)	Recup (W/kg/s)
Accel (m/s^2)	0.078							
	0.046							
Grade (%)	0.039	0.052						
	0.324	0.179						
VSP Inst (W/kg/s)	0.198	**0.581**	0.201					
	0.000	**0.000**	0.000					
ICE Pwr (W/kg/s)	0.134	0.432	0.029	0.400				
	0.001	0.000	0.450	0.000				
EM Pwr (W/kg/s)	0.195	0.486	0.086	0.479	-0.103			
	0.000	0.000	0.027	0.000	0.008			
Total Pwr (W/kg/s)	0.245	**0.685**	0.086	**0.656**	**0.679**	**0.661**		
	0.000	**0.000**	0.028	**0.000**	**0.000**	**0.000**		
Recup (W/kg/s)	-0.156	0.333	0.091	0.300	0.087	0.335	0.314	
	0.000	0.000	0.019	0.000	0.025	0.000	0.000	
SOC (%)	-0.116	-0.002	0.024	-0.037	0.162	-0.113	0.038	-0.069
	0.003	0.969	0.535	0.340	0.000	0.004	0.326	0.079

Pearson's Coefficient: top number; P-Value: bottom number

The driving- and road-based differences between roadway types translated to statistically significant differences in PHEV Sprinter power usage and output according to traveled roadway. The reported results for PHEV power output depended on the basis for normalization: time versus distance. Because of this, subsequent discussion regarding pollutant emissions and fuel usage will be presented on per second and per meter basis. Slight differences were observed between charge-sustaining mode and charge-depleting

mode power output. While noted here, these differences will be discussed in greater detail in the following chapter.

8.6 Emissions and Fuel Usage

8.6.1 Charge-Sustaining Mode

Statistical analysis of the PHEV Sprinter's road-collected data was extended to include an assessment of the PHEV's exhaust emissions and fuel usage. Similar to the analysis of road-based variables and PHEV power output, ANOVA and Kruskal-Wallis tests were employed in order to verify that the PHEV's emissions profiles collected from different roadway types were from different or the same populations to the set degree of statistical significance. The emissions and fuel data were analyzed in duplicate, on two different dataset types: the continuous dataset of second-by-second data, and the condensed dataset of compiled means of observations from the discrete sample runs (per run-basis). The continuous data were analyzed in both the full form with one observation per second, and in the slightly filtered format where observations were averaged over every 5-seconds of data collection. In order to give added assurance to the reported results, the in-town roadways (suburban and urban) were, again, analyzed together, exclusive of highway driving.

As reported with the PHEV Sprinter power output, exhaust emissions generally proved to be a statistically significant response to roadway-type (Tables 8.23 and 8.24, below). Aside from hydrocarbon emissions when analyzed as a function of in-town driving, all other measured pollutants varied to a statistically significant degree according to the roadway being driven. These results were somewhat less conclusive for the compiled, run-based analysis, where nitrogen dioxide and hydrocarbon emissions were not statistically significant responses to roadway designation for all levels of analysis. The origination and chemical and physical formation of the measured pollutants are very

diverse, with some chemical formations (i.e. carbon dioxide) being direct products of the combustion processes or airflow through the engine and others (i.e. NO_2, CO, and HC) being the result of transient dICE operation. Because of this, some pollutants will directly correlate with fuel use and power output, while others will appear independent of the PHEV's work output.

Table 8.23: Synopsis of statistical tests conducted on emissions data according to roadway type, based on continuous charge-sustaining data.

Variable:	All Routes	In-town routes only
Fuel, gal/s	y	y
CO_2, g/s	y	y
CO, g/s	y	y
NOx, g/s	y	y
NO, g/s	y	y
NO_2, g/s	y	y
HC, g/s	y	Inc2

Inc1: y ANOVA, n KW
Inc2: n ANOVA, y KW

Table 8.24: Synopsis of statistical tests conducted on emissions data according to roadway type, based on charge-sustaining dataset of compiled run-based means.

Variable:	All Routes	In-town routes only
Fuel, gal/s	y	y
CO_2, g/s	y	y
CO, g/s	y	y
NOx, g/s	y	y
NO, g/s	y	y
NO_2, g/s	n	n
HC, g/s	y	n

Inc1: y ANOVA, n KW
Inc2: n ANOVA, y KW

As with the PHEV's power output analysis, exhaust emissions are reported as a function of time (per second) and distance (per km). Since average roadway velocity will result in different conclusions regarding roadway efficiency depending on the basis of measurement, all analyses that involved roadway categorization will be performed on both a time basis and a distance basis. Figures 8.10 and 8.11 provide a visual assessment of the PHEV's exhaust emissions and fuel usage. In order to allow all measured variables to exist on comparable scales, certain variables were scaled up or down according to a specified power of 10 (denoted on x-axis labels).

On a time basis, highway travel resulted in, nominally, twice the exhaust emissions of in-town driving for all measured pollutants except CO and NO_2. Additionally, every second of highway operation required twice the fuel compared with each second of in-town driving. The two-fold increase in emissions and fuel consumption for highway driving are quantitatively consistent with the increased power output for highway travel that was reported earlier. Carbon monoxide (CO) formation occurs as an unintended by-product of the combustion process. Its presence in vehicle exhaust is a symptom of transient dICE operation. Likewise, nitrogen dioxide (NO_2) formation is not part of the fundamental combustion reaction. Its formation occurs as a function of excessive temperature and pressure conditions within the exhaust causing NO, in the presence of excess oxygen, to react, forming NO_2. Neither of these pollutants is directly traceable to fuel use, or even power output. They are, instead, an indication of overall dICE operation, becoming components of the vehicle exhaust during periods of time in which the dICE is operating in a more transient manner (not steady-state). Since the dICE provides 93.7% of the work during highway travel, its operation is the most

steady state during highway driving. Conversely, in-town (urban and suburban roadways) travel results in considerably higher utilization of the EM (24.7% for suburban travel and 25.6% during urban driving), and, consequently, sees the highest frequency of zero-emissions operation (100% EM-powered driving). In order to provide this, the dICE is continually being started and stopped causing more transient conditions within the ICE combustion chambers and exhaust system. While this discussion will go into more detail in the proceeding section (Chapter 9: Operating Mode Analysis), from a roadway-type investigation, the fundamental differences in PHEV Sprinter operation between the roadway designations need to be highlighted here. Carbon monoxide emissions are low during suburban travel, but exceptionally high during urban driving possibly due to the increased frequency that the dICE is pulled on and offline during urban travel. Nitrogen dioxide emissions, however, remain high during suburban travel (on a time basis). The more aggressive acceleration rates and overall faster velocities that occur during suburban travel lead to higher exhaust temperatures promoting NO_2 formation.

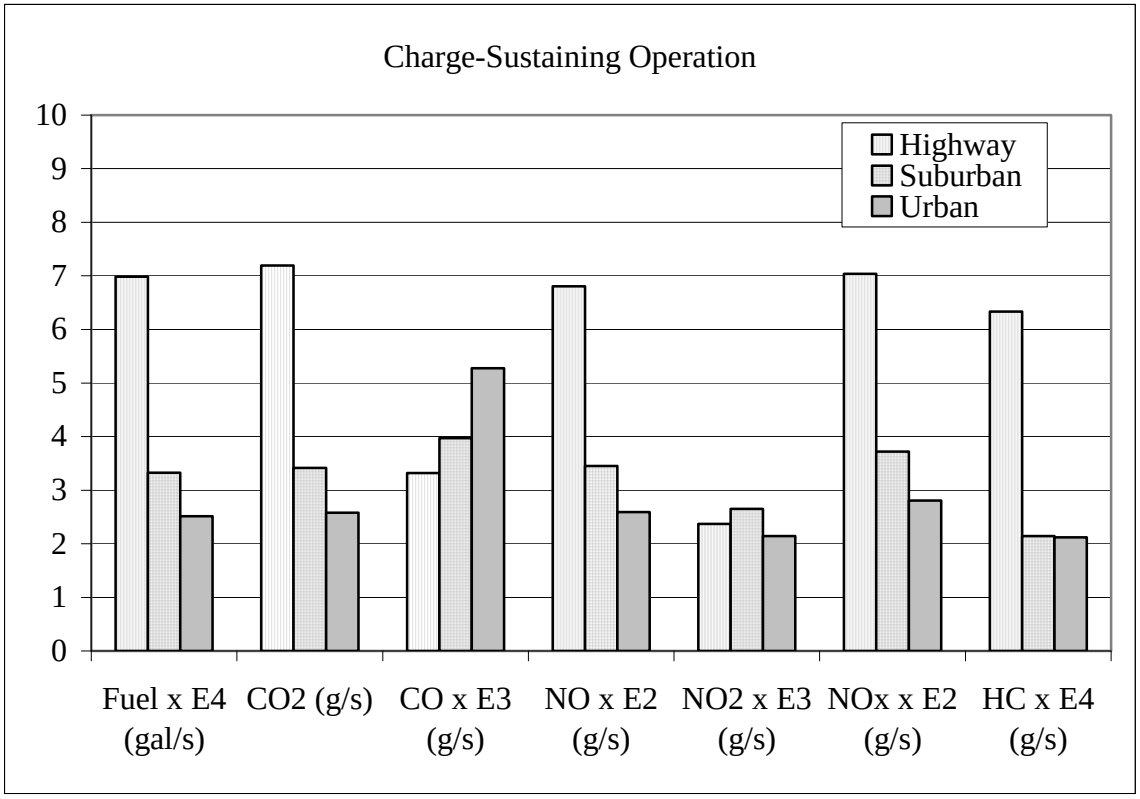

Figure 8.10: Fuel use and emissions output (reported on a time basis) during charge-sustaining operation according to roadway type.

Comparable to power output findings, when investigated on a distance basis, highway driving proved to be the more fuel efficient and cleaner traveling of the roadways evaluated. With the exception of hydrocarbon emissions (HC), the highway produced lower amounts (on a mass basis) of all measured pollutants. Conversely, urban travel resulted in the least efficient, highest emitting roadways within the sampling area. Comparatively, carbon monoxide production during urban driving was, on average, over 121% greater than suburban driving and more than 6.5times greater than highway travel.

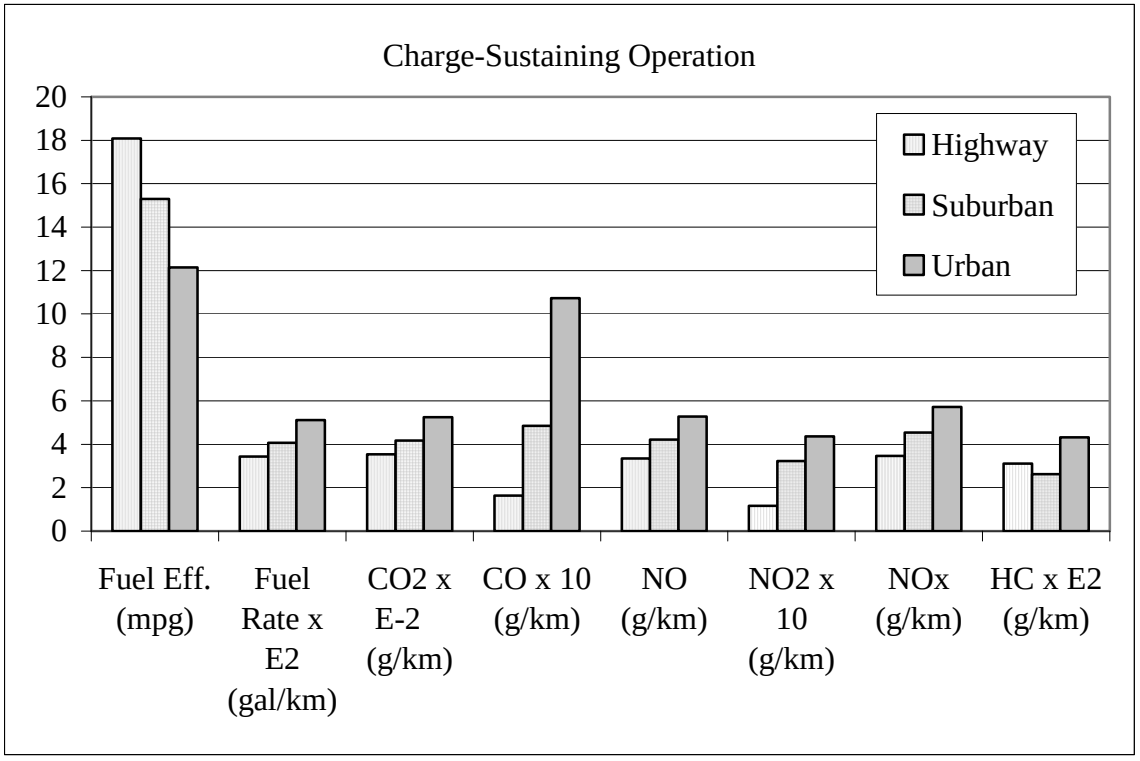

Figure 8.11: Fuel use and emissions output (reported on a distance basis) during charge-sustaining operation according to roadway type.

Tables 8.25 and 8.26 provide mean fuel use and pollutant exhaust emissions for each roadway type according to a time-basis and distance-basis. The large discrepancy between the bases of normalization can be seen by the comparison between the differences in exhaust emissions between suburban and urban driving. When decision makers are attempting to determine the true load that a transit system or new type of transit vehicle will have on specific areas within and around a metropolitan area, the method of normalizing the data will have a direct effect on the intra-roadway evaluation.

Table 8.25: Mean fuel use and exhaust emissions on a time basis for all roadway-types.

	Fuel Rate (gal/s)	CO_2 (g/s)	CO (g/s)	NO (g/s)	NO_2 (g/s)	NOx (g/s)	HC (g/s)
Highway	0.000698	7.19	0.00332	0.0680	0.00237	0.070	0.000633
Suburban	0.000333	3.42	0.00397	0.0345	0.00265	0.037	0.000215
Urban	0.000251	2.58	0.00527	0.0259	0.00214	0.028	0.000212
% decrease of Urban vs Suburban	24.5%	24.5%	-32.9%	24.9%	19.2%	24.5%	1.2%

Table 8.26: Mean fuel use and exhaust emissions on a distance basis for all roadway-types.

	Fuel Eff. (mpg)	Fuel Rate x E2 (gal/km)	CO_2xE-2 (g/km)	CO x 10 (g/km)	NO (g/km)	NO_2 x 10 (g/km)	NOx (g/km)	HC x E2 (g/km)
Highway	18.1	3.4353	3.54	1.63	3.35	1.168	3.46	3.1142
Suburban	15.3	4.0609	4.17	4.84	4.21	3.235	4.54	2.6184
Urban	12.2	5.1140	5.25	10.73	5.28	4.359	5.71	4.3146

Based on the modal analysis portion of the Vehicle Specific Power investigation, normal, on-road driving can be described by four discrete operating modes: idle, cruise, acceleration, and deceleration (EPA, 2002). It was determined earlier that the acceleration and traffic profiles for each roadway varied to a degree of statistical significance. As a final step in the charge-sustaining, roadway analysis, variations in roadway types during the idle and acceleration driving modes will be investigated. The extremely high level of carbon monoxide emissions during urban driving drew question regarding which factors and components of urban travel would promote seemingly high instances of transient ICE operation.

Both the number of stops and amount of time at zero velocity were statistically significant responses to the type of roadway being traveled. The amount of idle time for

urban and suburban travel was a relatively substantial portion of the on-road time with 26.8% and 15.8% of the on-road time being spent at zero velocity for urban and suburban driving, respectively. Urban travel experienced over twice as many stops per kilometer travel as suburban driving. Additionally, the amount of stop time near the urban core resulted in over twice as much time at zero velocity than traveling the more transitioning, suburban roads due to the longer idle periods on urban roadways. Even though idle periods are relatively low producers of exhaust pollutants and generally consume marginal amounts of fuel when compared to the more dynamic driving modes (cruise and acceleration), the amount of time at zero velocity has the potential to artificially inflate the implications of the distance-based emissions analysis,

ANOVA and Kruskal-Wallis analyses were performed on the idle data, investigating fuel use, power output, and exhaust emissions according to roadway type. All analyses were conducted in duplicate: once on the second-by-second data and again on the averaged every 5^{th} second dataset. The results varied considerably based on the level of dataset filter. Since the second-by-second data had not been smoothed by a time-based averaging technique, every moment of zero velocity was represented in the analyses performed on this dataset. However, in order for moments of zero velocity to mathematically register as a stop event in the 5^{th} second averaged dataset, the PHEV must have been stopped for a minimum of 5 consecutive seconds. Because of this, the 5^{th} second averaged idle results are more likely related to extended stops at traffic signals, and, therefore more homeostatic in nature. Because highway travel did not result in stop periods, the following discussion pertains to suburban and urban travel only. Table 8.27 provides a synopsis of the ANOVA and Kruskal-Wallis tests conducted on stopped data

during charge-sustaining operation. Consistent with previous analysis of the continuous dataset (versus the sample-based dataset) a rigorous $\alpha<0.025$ was mandated for determining statistical significance.

Table 8.27: Synopsis of statistical tests conducted for idle data according to in-town roadway type.

VSP BIN	Second-by-Second	Avg Every 5th Sec
Fuel, gal/s	Inc1	n
CO_2, g/s	y	n
CO, g/s	Inc2*	n
NOx, g/s	y	Inc2
NO, g/s	y	n
NO_2, g/s	Inc1**	n
HC, g/s	y	Inc1
Ambient Temp, degC	y	
Exhaust Temp, degC	y	y
Exhaust Flow, SCFM	y	
ICE, W/kg/s	n	n
EM, W/kg/s	Inc2	Inc2
Total Power, W/kg/s	Inc2	Inc2

Inc1: y ANOVA, n KW
Inc2: n ANOVA, y KW

Ambient temperature and exhaust flow rate were not included in the filtering process used to produce 5th second averaged on-road data, so these variables were not available for idle analysis of the averaged dataset. As expected, the 5th second averaged data were more consistent between the roadway types. Since this data required longer stop times before the velocity data were mathematically defined as idle, transient periods of PHEV operation as the vehicle entered idle operation had, generally, passed. As a result of this, the statistical significance of the response that on-road observations had according to roadway type was markedly lower than the same analysis performed on the

second-by-second data. The second-by-second dataset contained every instance of stop time within the charge-sustaining mode of operation. Because of this, periods of more transient operation at the start of every stopped instance were present in the second-by-second analysis. As a result, on-road operation and emissions observations proved to be much more statistically significant responses to roadway-type. The carbon monoxide and nitrogen dioxide analyses, marked as Inc2* and Inc1**, respectively, are conditionally inconclusive. The failed ANOVA test for the carbon monoxide analysis still had a relatively low p-value of 0.049 and a p-value of 0.000 for the Kruskal-Wallis test. Similarly, p-value for the failed nitrogen dioxide-based Kruskal-Wallis test was 0.045, with an ANOVA-generated p-value of 0.000. If a more common level ($\alpha<0.05$) of significance had been implemented for these analyses, these tests would have been universally conclusive.

Table 8.28 displays the means and standard deviations of the assessed variables for idle periods during each roadway type. Reported values were obtained from the second-by-second dataset, and are, consequently, more representative of actual charge-sustaining operation. Because idle is defined by zero velocity, time was the basis of normalizing the data for this analysis. Rows with italicized print were statistically inconclusive for both ANOVA and Kruskal-Wallis analyses.

Table 8.28 Summarized data for idling periods during charge-sustaining operation, separated according to roadway type.

	Road Code	Total Count	Mean	Standard Deviation
Ambient Temp. (degC)	Suburban	6779	10.7	2.8
	Urban	2642	11.8	3.3
Exhaust Temp. (degC)	Suburban	6779	88.5	39.2
	Urban	2642	77.4	38.1
Exhaust Flowrate	Suburban	6779	17.4	24.1
	Urban	2642	15.9	20.3
Fuel (gal/s)	*Suburban*	*6779*	*1.13E-04*	*1.72E-04*
	Urban	*2642*	*1.03E-04*	*1.41E-04*
CO_2 (g/s)	Suburban	6779	1.15	1.76
	Urban	2642	1.05	1.44
CO (g/s)	Suburban	6779	2.89E-03	2.09E-02
	Urban	2642	2.00E-03	1.60E-02
NO (g/s)	Suburban	6779	0.0136	0.0188
	Urban	2642	0.0121	0.0153
NO_2 (g/s)	Suburban	6779	1.71E-03	2.77E-03
	Urban	2642	1.43E-03	1.97E-03
NOx (g/s)	Suburban	6779	0.0154	0.0212
	Urban	2642	0.0135	0.0169
Hydrocarbon (g/s)	Suburban	6779	5.60E-05	1.05E-04
	Urban	2642	7.70E-05	1.37E-04
d-ICE Power (W/kg/s)	Suburban	6779	1.05	1.17
	Urban	2642	1.03	1.11
EM Power (W/kg/s)	*Suburban*	*6779*	*0.234*	*0.673*
	Urban	*2642*	*0.208*	*0.463*
Total Power (W/kg/s)	*Suburban*	*6779*	*1.28*	*1.16*
	Urban	*2642*	*1.23*	*1.01*

Inconclusive statistical results between ANOVA and Kruskal-Wallis analyses.

Aside from hydrocarbon emissions, idling periods on suburban roadways were more taxing on the PHEV's operation. Suburban roadways resulted in idle periods with higher exhaust flow rates and temperatures, increased power output, and higher exhaust emissions loads when compared to urban travel. Idle operation does not explain the relatively high carbon monoxide emissions witnessed on urban roadways.

The roadway-based modal analysis was expanded to the acceleration and cruising modes as well. A continuous analysis using distance-based data is unviable due to the nature of on-road monitoring data. Periods where the PHEV was stationary, but the dICE was operational are mathematically indefinable (dividing by zero). Forcing data during stationary periods to zero values results in underestimation of the PHEV's emissions, fuel use, and work. Because of this, unless suitable for sample run-based analysis, discussions pertaining to continuous data will remain limited to a time-basis (per second), as time remains constant regardless of the PHEV's behavior or characteristics.

During periods of acceleration, the PHEV's power output, exhaust emissions, and fuel use all remained statistically significant responses to roadway type (Table 8.29). The only exceptions to this were nitrogen dioxide and hydrocarbon emissions during the suburban/urban roadway analysis, suggesting that exhaust and dICE conditions were similar enough during both suburban and urban travel to result in comparable levels of production and emission of these pollutants.

Table 8.29: Statistical synopsis of roadway analysis for acceleration driving mode during charge-sustaining operation.

VSP BIN	All Roadways	In-Town
Fuel, gal/s	y	y
CO_2, g/s	y	y
CO, g/s	y	y
NOx, g/s	y	y
NO, g/s	y	y
NO_2, g/s	y	n
HC, g/s	y	n
Exhaust Temp, degC	y	y
Exhaust Flow, SCFM	y	y
ICE, W/kg/s	y	y
EM, W/kg/s	y	y
Total Power, W/kg/s	y	y

Inc1: y ANOVA, n KW
Inc2: n ANOVA, y KW

While Table 8.29 provides a synopsis of the statistical results, it does not give any indication regarding the relative nature of the PHEV Sprinter's operation on urban versus suburban roadways. Table 8.30 displays mean and standard deviation values for the observed variables of interest for each roadway designation. Acceleration events significant enough to qualify as "Accel" driving mode accounted for 4.9% of the time during highway travel, 15.3% of the time on-road during suburban travel, and 13.3% of the time spent during urban travel. Regarding dICE operation, suburban driving resulted in the most aggressive acceleration events, exhibiting high exhaust flow rates compared with urban travel, high exhaust temperatures, and the highest dICE power output of all three roadway designations. Correspondingly, suburban acceleration had the highest fuel usage of all other roadway accelerations. These conditions translate to comparatively high emissions of carbon dioxide, nitrogen oxides, and hydrocarbons during suburban travel.

Highway travel was designed to occur at a constant velocity. Acceleration events during highway operation were simply corrections to velocity undulations resulting from occasional coasting and accounting for locally slower areas of highway traffic, and therefore, rarely met the criteria of the "Accel" driving mode. Highway travel began at the start of the entrance ramp and ended when the vehicle left the highway, so the majority of the qualifying acceleration events occurred as the PHEV was entering the highway. As such, the amount of positive acceleration data that met the "Accel" criteria according to the driving mode model (accelerating greater than 2.0m/s^2 or sustained acceleration of 1.0m/s^2 or greater for more than 3 consecutive seconds) (EPA, 2002) was very limited (4.9% of the highway drive time). These accelerations were moderate and generally began after the engine had been sitting for several minutes for Semtech calibration and zeroing. While accelerating at high velocities resulted in the highest average measured exhaust flow rates for all roadway types, the exhaust temperature while driving the highway route was moderate since the PHEV had been sitting prior to acceleration.

Acceleration events during urban travel were limited by the low-posted speed limits (20mph or 32.2kph). The low upper velocity bound of urban driving resulted in acceleration events that were both shorter in duration and less aggressive than suburban driving acceleration. As a result of this, urban accelerations resulted in lower exhaust flow rates and temperatures than other roadways. Urban accelerations also required the least amount of power output per second (dICE, EM, and total power). Compared with suburban roads, urban acceleration resulted in fewer exhaust emissions for all pollutants except for carbon monoxide. Based on the PHEV Sprinter operating data presented

previously, no clear reason exists capable of explaining the significantly higher carbon monoxide emissions during urban travel. Because the information presented so far details mean values, it cannot describe features within the emissions and operating profile. Despite this, it can be conclusively stated that acceleration events are a contributing factor to the relatively high urban CO emissions compared with the other roadways. The operating mode analysis in the following chapter will investigate features of the PHEV Sprinter operation that could lead to excessive CO emissions near the urban core (for example, the timing of dICE engagement after being off).

During the Modal Analysis of the Chapter 6, acceleration events proved to be the largest contributors to the PHEV Sprinter's exhaust emissions, with carbon monoxide formation being significantly impacted by acceleration events. Only 13.3% of the time on urban roadways occurred during acceleration events. Despite the relatively short amount of time that the PHEV spent in Acceleration mode, acceleration is viable explanation of the high urban-based CO emissions. Given the significantly high formation of CO emissions during acceleration events (every second of acceleration produced 3.5times as much CO as an equivalent second in cruise mode), coupled with the fact that CO emissions were, nominally, 50% greater during urban acceleration compared with suburban acceleration, acceleration is a plausible cause of high CO emissions measured during urban travel.

Table 8.30: Summary of PHEV operation and exhaust emissions variables according to roadway type during acceleration events during charge-sustaining operation.

	Road Code	Total Count (N)	Mean	Standard Deviation
Exhaust Flowrate (SCFM)	Highway	261	131.3	123.3
	Suburban	6160	122.3	104.5
	Urban	1242	98.2	85.5
Exhaust Temp. (degC)	Highway	261	95.0	34.9
	Suburban	6160	109.5	48.5
	Urban	1242	91.6	44.7
Fuel (gal/s)	Highway	261	6.61E-04	7.64E-04
	Suburban	6160	7.18E-04	6.97E-04
	Urban	1242	5.83E-04	5.69E-04
CO_2 (g/s)	Highway	261	6.79	7.86
	Suburban	6160	7.38	7.18
	Urban	1242	5.99	5.85
CO (g/s)	Highway	261	0.0193	0.0456
	Suburban	6160	0.0108	0.0315
	Urban	1242	0.0151	0.0395
NO (g/s)	Highway	261	0.0516	0.0712
	Suburban	6160	0.0639	0.0653
	Urban	1242	0.0542	0.0536
NO_2 (g/s)	Highway	261	0.00067	0.00156
	Suburban	6160	0.00436	0.00556
	Urban	1242	0.00425	0.00517
NOx (g/s)	Highway	261	0.0523	0.0722
	Suburban	6160	0.0683	0.0691
	Urban	1242	0.0584	0.0569
Hydrocarbon (g/s)	Highway	261	2.13E-03	4.71E-03
	Suburban	6160	5.16E-04	1.18E-03
	Urban	1242	5.03E-04	1.11E-03
d-ICE Power (W/kg/s)	Highway	261	8.38	10.48
	Suburban	6160	9.36	9.28
	Urban	1242	7.39	7.39
EM Power (W/kg/s)	Highway	261	7.37	6.89
	Suburban	6160	4.45	5.95
	Urban	1242	3.33	5.09
Total Power (W/kg/s)	Highway	261	15.76	6.94
	Suburban	6160	13.81	6.59
	Urban	1242	10.71	5.86

Regardless of roadway type, the majority of the PHEV's on-road time occurred in the "cruise" driving mode as defined by the NCSU Driving Mode model introduced in Chapter 3 and implemented in Chapter 6 (EPA, 2002). Almost 90% of highway travel time occurred within cruise mode, and while the proportional amount of cruise time was less during in-town driving, cruise remained the dominant driving mode with 54.7% of the on-road time during suburban travel and 47.8% of the on-road time near the Kansas City urban core.

Table 8.31: Statistical synopsis for roadway-type analysis of cruise driving mode during charge-sustaining mode.

VSP BIN	All Roadways	In-Town
Fuel, gal/s	y	y
CO_2, g/s	y	y
CO, g/s	y	y
NOx, g/s	y	y
NO, g/s	y	y
NO_2, g/s	y	y
HC, g/s	y	Inc2*
Exhaust Temp, degC	y	y
Exhaust Flow, SCFM	y	y
ICE, W/kg/s	y	y
EM, W/kg/s	y	Inc1
Total Power, W/kg/s	y	y

Inc1: y ANOVA, n KW
Inc2: n ANOVA, y KW

Similar to the other modes, the PHEV Sprinter's exhaust emissions and operating variables during cruise mode proved to be statistically significant responses to roadway type. This phenomenon held true for analyses of all three roadways and for in-town driving only. While EM power output was not conclusively responsive to in-town roadway type, the p-value for the Kruskal-Wallis hydrocarbon in-town analysis was

relatively low at 0.045*. This exceeds the set level of significance selected for this study, but is within limits for most statistical work.

Table 8.32: Mean values according to roadway type for cruise driving mode during charge-sustaining operation.

	Road Code	Total Count (N)	Mean	Standard Deviation
Exhaust Flowrate (SCFM)	Highway	4647	147.4	55.0
	Suburban	21982	69.4	66.1
	Urban	4458	54.1	62.3
Exhaust Temp. (degC)	Highway	4647	172.9	23.5
	Suburban	21982	118.0	47.2
	Urban	4458	92.7	46.5
Fuel (gal/s)	Highway	4647	7.57E-04	4.31E-04
	Suburban	21982	3.61E-04	4.62E-04
	Urban	4458	2.88E-04	4.25E-04
CO_2 (g/s)	Highway	4647	7.80	4.45
	Suburban	21982	3.71	4.76
	Urban	4458	2.96	4.37
CO (g/s)	Highway	4647	0.0027	0.0025
	Suburban	21982	0.0032	0.0165
	Urban	4458	0.0053	0.0237
NO (g/s)	Highway	4647	0.0745	0.0497
	Suburban	21982	0.0400	0.0509
	Urban	4458	0.0307	0.0452
NO_2 (g/s)	Highway	4647	0.00266	0.00254
	Suburban	21982	0.00292	0.00412
	Urban	4458	0.00223	0.00352
NOx (g/s)	Highway	4647	0.0771	0.0508
	Suburban	21982	0.0429	0.0537
	Urban	4458	0.0329	0.0476
Hydrocarbon (g/s)	Highway	4647	6.00E-04	5.92E-04
	Suburban	21982	2.23E-04	5.98E-04
	Urban	4458	2.44E-04	8.66E-04
d-ICE Power (W/kg/s)	Highway	4647	9.68	6.44
	Suburban	21982	4.54	6.69
	Urban	4458	3.51	6.02
EM Power (W/kg/s)	Highway	4647	0.25	1.62
	Suburban	21982	1.14	2.89
	Urban	4458	1.10	2.65
Total Power (W/kg/s)	Highway	4647	9.92	6.30
	Suburban	21982	5.67	6.56
	Urban	4458	4.61	5.97

Highway driving's high average velocity resulted in significantly higher exhaust flow rates and significantly higher exhaust temperatures. The dICE was operational for almost all of the highway operation, which contributed to high mean exhaust parameters. Exhaust emissions during highway travel fell in accordance with the high level of dICE operation and, consequent, elevated fuel use. Since most of the highway operation occurred during cruise mode, the original discussion of exhaust emissions during highway operation is pertinent here.

Exhaust flow rate and temperatures fell in trend with roadway average velocity with suburban travel resulting in higher exhaust flows and temperatures compared with urban travel. Again, except for carbon monoxide emissions, this translated to fuel use and all other exhaust emissions, with suburban travel demonstrating, on a time basis, higher emissions and fuel consumption than urban travel. Similar to acceleration mode urban travel resulted in the highest levels of carbon monoxide emissions of all designated roadways, regardless of normalizing basis.

8.6.2 Charge-Depleting Mode

The following tables display the results from the ANOVA and Kruskal-Wallis statistical tests performed on the PHEV's charge-depleting dataset. These results are for the comprehensive dataset and have not been evaluated according to driving mode. The continuous dataset was evaluated on both a per-second basis and on the 5^{th} second averaged level. The italic font in Table 8.33 for carbon monoxide and nitrogen dioxide emissions shows the results for the analysis of both levels of the continuous dataset. Where second-by-second data proved to be statistically significant, the averaged 5^{th}

second data were inconclusive, passing the criteria for the Kruskal-Wallis test but failing the ANOVA tests for CO, and, on an in-town level analysis of NO_2 emissions, passing ANOVA but failing the 5^{th} second averaged Kruskal-Wallis application.

Table 8.33: Summary of statistical results from continuous dataset, during charge-depleting operation, according to roadway type.

Variable:	All Routes	In-town routes only
Fuel, gal/s	y	y
CO_2, g/s	y	y
CO, g/s	*y, Inc2*	*y, Inc2*
NOx, g/s	y	y
NO, g/s	y	y
NO_2, g/s	y	*y, Inc1*
HC, g/s	y	y

Inc1: y ANOVA, n KW
Inc2: n ANOVA, y KW

While the CO and in-town based NO_2 analyses were statistically inconclusive when associated with the 5^{th} second averaged dataset, these particular tests were statistically insignificant when applied to the compiled, run-based dataset.

Table 8.34: Synopsis of statistical results for charge-depleting operation of sample-run based dataset according to roadway type.

Variable:	All Routes	In-town routes only
Fuel, gal/s	y	y
CO_2, g/s	y	y
CO, g/s	n	n
NOx, g/s	y	y
NO, g/s	y	y
NO_2, g/s	y	n
HC, g/s	Inc2	y

Inc1: y ANOVA, n KW
Inc2: n ANOVA, y KW

Exhaust emissions of pollutants whose formation is most directly tied with the combustion process remained universally high during charge-depleting highway travel compared with in-town driving, since the dICE was the primary power source at high velocities, regardless of operating mode. However, HC emissions during urban and suburban travel were proportionally higher than CO_2 or NO_2 emissions, and during in-town operation, carbon monoxide emissions exceeded those reported for highway driving. Disproportionately elevated emissions of transient pollutants during in-town driving, despite the reduced dICE recruitment, suggests that the on- and off-nature of ICE use during plug-in hybrid applications has a deleterious impact on the formation of certain exhaust emissions. Similar to the other time-based analysis, roadways with faster average velocities exhibited larger power requirements and subsequent exhaust emissions when assessed on a time basis.

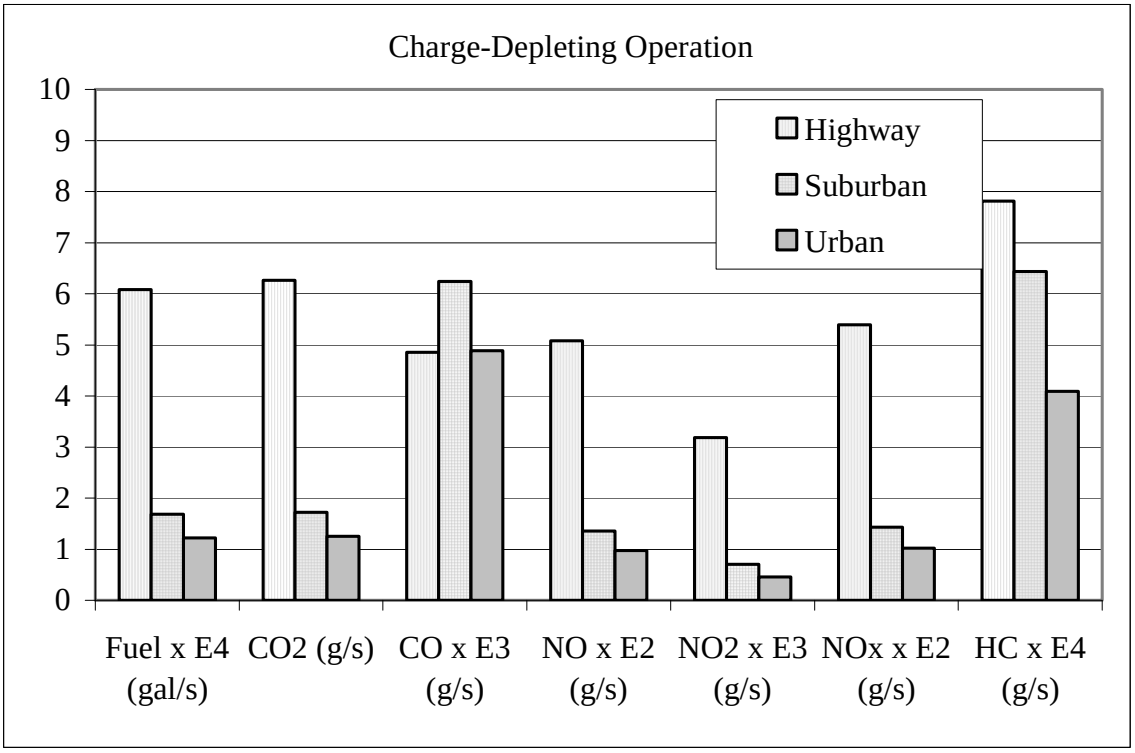

Figure 8.12: Fuel use and exhaust emissions during charge-depleting operation, according to roadway-type.

When looking at the per-distance data, highway emissions become more inline, quantitatively, with in-town driving. However, unlike the previous analyses of the charge-sustaining dataset, the highway emissions do not actually drop below the in-town emissions on a distance basis, largely due to the much stronger dICE recruitment during charge-depleting highway travel. Similar to all other analyses, on a distance-basis, urban travel becomes the least fuel-efficient, highest emitting of the roadway types evaluated.

In charge-depleting mode, carbon monoxide emissions did not prove to be a statistically significant response to roadway type, regardless of level of analysis. While the charts above give the visual impression that there is a strong discrepancy between carbon monoxide emissions according to roadway type, they do not give any indication into the variance within the datasets. By failing the statistical tests, carbon monoxide

emissions must have demonstrated a strong level of variance within the individual datasets. This volatility seems particular to CO emissions since the other measured pollutants variables (except NO_2 when assessed for in-town driving) were significant responses to road type.

On a distance basis, highway driving used more fuel in accordance with its heavy dICE reliance, and, consequently emitted more CO_2 and NO. As natural products of the combustion process and internal combustion engine operation, this phenomenon is consistent with expectations. However, due to its more consistent dICE use, highway travel proved to be cleaner with regards to the transient pollutants.

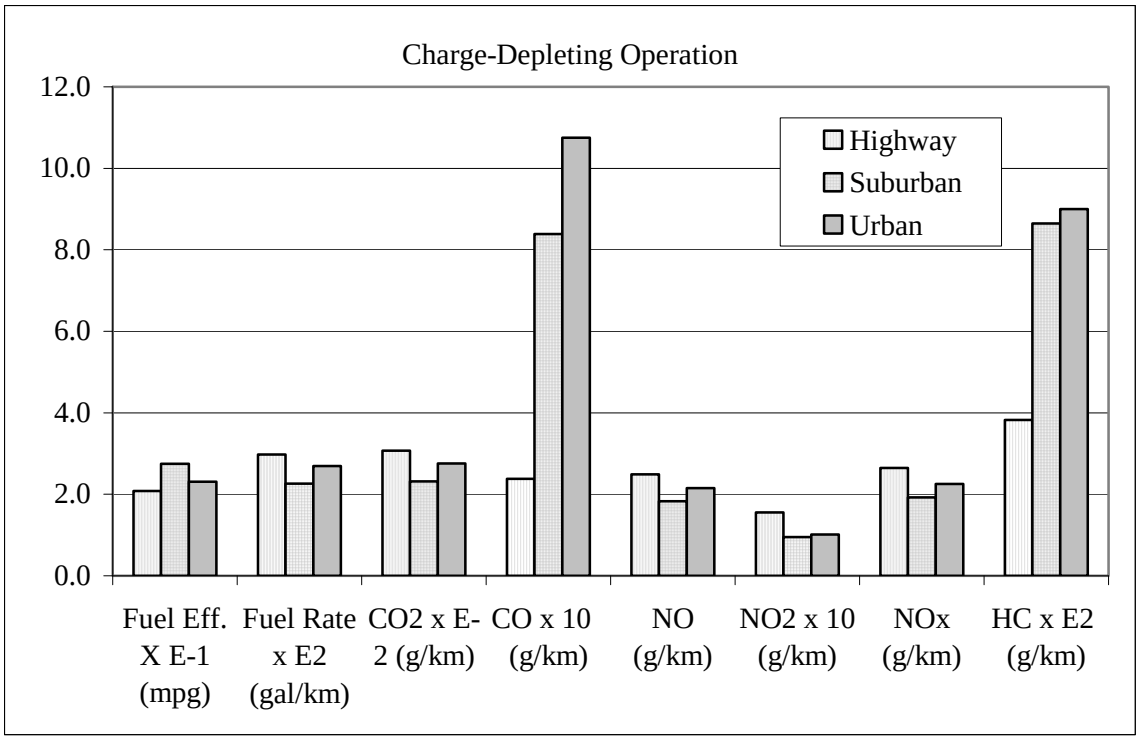

Figure 8.13: Fuel use and exhaust emissions according to roadway-type for charge-depleting operation, on a distance basis.

Table 8.35: Time-based fuel and emissions averages according to roadway-type for charge-depleting operation.

	Fuel Rate (gal/s)	CO_2 (g/s)	CO (g/s)	NO (g/s)	NO_2 (g/s)	NOx (g/s)	HC (g/s)
Highway	0.000608	6.26	0.00485	0.0508	0.00318	0.0539	0.000781
Suburban	0.000168	1.73	0.00624	0.0136	0.00071	0.0143	0.000643
Urban	0.000122	1.25	0.00488	0.0098	0.00046	0.0102	0.000409
% decrease of Urban vs Suburban	27.3%	27.4%	21.7%	28.2%	34.9%	28.5%	36.4%

Table 8.36: Distance-based fuel and emissions averages according to roadway-type for charge-depleting operation.

	Fuel Eff. (mpg)	Fuel Rate (gal/km)	CO_2 (g/km)	CO (g/km)	NO (g/km)	NO_2 (g/km)	NOx (g/km)	HC (g/km)
Highway	20.8	0.0298	307	0.24	2.49	0.156	2.64	0.0383
Suburban	27.4	0.0226	232	0.84	1.83	0.095	1.92	0.0865
Urban	23.1	0.0269	276	1.08	2.15	0.101	2.25	0.0900
% decrease of Urban vs Suburban	16.0%	-19.0%	-18.9%	-28.2%	-17.6%	-6.6%	-17.1%	-4.1%

Charge-depleting data were also subjected to a driving mode-based analysis, in order to provide more definition regarding distinctions in the PHEV's emissions according to roadway type. Within the charge-depleting dataset, which is considerably smaller than the charge-sustaining dataset, acceleration rate did not prove to be a statistically significant response to roadway type, and will, therefore, be excluded from this modal analysis.

Highway operation, due to its lack of idle data, was excluded from the following discussion. Generally, idling during charge-depleting operation did not result in meaningful differences in exhaust emissions according to roadway type (urban versus

suburban). Table 8.37, below, provides the results from the ANOVA and Kruskal-Wallis analyses of the charge-depleting idle data. While ambient and exhaust temperatures and electric and total power demonstrated a statistically significant response to roadway type during idle periods, the suite of measured pollutants did not provide any, conclusive statistically significant responses according to roadway type.

Table 8.37: Statistical synopsis for charge-depleting idle data according to roadway type.

VSP BIN	Second-by-Second	Avg Every 5th Sec
Fuel, gal/s	n	n
CO_2, g/s	n	n
CO, g/s	Inc2	n
NOx, g/s	n	n
NO, g/s	n	n
NO_2, g/s	Inc1	n
HC, g/s	n	n
Ambient Temp, degC	y	
Exhaust Temp, degC	y	Inc2
Exhaust Flow, SCFM	Inc1	
ICE, W/kg/s	n	n
EM, W/kg/s	y	y
Total Power, W/kg/s	y	n

Inc1: y ANOVA, n KW
Inc2: n ANOVA, y KW

Charge-depleting operation results in higher utilization of the electric motor, and, consequently, more zero-emissions on-road operation. With the abundance of zero valued data for all emissions, fuel use, and dICE-derived data, statistical relevance and meaning in the resulting data is elusive at best. Table 8.38 provides a synopsis of the mean values for the investigated variables during idle operation. Italicized print denotes variables that did not show a statistically meaningful response to roadway-type.

Generally speaking, urban travel resulted in higher EM utilization, using more electric-based power per second than suburban travel, indicating that urban travel, during charge-depleting operation, was more suited to take advantage of the PHEV Sprinter's electric-only design and intent.

Table 8.38: Mean values for measured variables during idling periods of charge-depleting operation, segregated according to roadway-type.

	Road Code	Total Count (N)	Mean	Standard Deviation
Ambient Temp. (degC)	Suburban	2504	10.1	3.0
	Urban	980	9.6	3.7
Exhaust Temp. (degC)	Suburban	2504	38.8	30.7
	Urban	980	42.8	21.8
Exhaust Flowrate (SCFM)	*Suburban*	*2504*	*8.2*	*13.0*
	Urban	*980*	*9.5*	*16.0*
Fuel (gal/s)	*Suburban*	*2504*	*5.20E-05*	*9.10E-05*
	Urban	*980*	*5.70E-05*	*1.09E-04*
CO_2 (g/s)	*Suburban*	*2504*	*0.54*	*0.94*
	Urban	*980*	*0.59*	*1.12*
CO (g/s)	*Suburban*	*2504*	*9.16E-04*	*7.41E-03*
	Urban	*980*	*1.28E-03*	*1.19E-02*
NO (g/s)	*Suburban*	*2504*	*0.0059*	*0.0103*
	Urban	*980*	*0.0064*	*0.0117*
NO_2 (g/s)	*Suburban*	*2504*	*3.53E-04*	*9.06E-04*
	Urban	*980*	*2.67E-04*	*7.06E-04*
NOx (g/s)	*Suburban*	*2504*	*0.0063*	*0.0109*
	Urban	*980*	*0.0066*	*0.0120*
Hydrocarbon (g/s)	*Suburban*	*2504*	*1.21E-04*	*2.77E-04*
	Urban	*980*	*1.29E-04*	*2.76E-04*
d-ICE Power (W/kg/s)	*Suburban*	*2504*	*0.50*	*0.88*
	Urban	*980*	*0.53*	*0.93*
EM Power (W/kg/s)	Suburban	2504	0.362	0.521
	Urban	980	0.509	1.053
Total Power (W/kg/s)	Suburban	2504	0.86	0.82
	Urban	980	1.04	1.20

In the previous modal-analysis, even during charge-depleting operation, the dICE provided the majority of the power output during cruising events. The relatively disproportionate utilization of the electric motor during cruise mode (when compared to the other driving modes) resulted in fuel consumption during cruise mode that was only slightly less than that found during acceleration events. This trend corresponded to CO_2, NO, and NOx emissions as well. However, due to the less transient nature of the PHEV's power scheme during cruise mode, CO emissions were significantly less compared with periods of acceleration, with acceleration accounting for 82% of the total carbon monoxide emissions occurring between the two modes. Similarly, while hydrocarbon emissions were significant during cruise mode, the majority of them occurred during periods of acceleration. An anomaly to the general cruise versus acceleration trend, NO_2 emissions were significantly higher during cruise mode compared with acceleration.

When analyzed according to roadway type, the charge-depleting data show a strong response to roadway designation for both emissions and PHEV operating variables. Table 8.39 provides a synopsis for all of the charge-depleting data analyzed according to roadway type during cruise operation. Except for EM power output when assessed for in-town driving, all tests run were conclusively statistically significant ($\alpha<0.025$).

Table 8.39: Statistical synopsis of charge-depleting, cruise operation according to roadway type.

VSP BIN	All Roadways	In-Town
Fuel, gal/s	y	y
CO_2, g/s	y	y
CO, g/s	y	y
NOx, g/s	y	y
NO, g/s	y	y
NO_2, g/s	y	y
HC, g/s	y	y
Exhaust Temp, degC	y	y
Exhaust Flow, SCFM	y	y
ICE, W/kg/s	y	y
EM, W/kg/s	y	n
Total Power, W/kg/s	y	y

Inc1: y ANOVA, n KW
Inc2: n ANOVA, y KW

Table 8.40: Summary of results for charge-depleting cruise operation according to roadway type.

	Road Code	Total Count (N)	Mean	Standard Deviation
Exhaust Flowrate (SCFM)	Highway	2629	138.9	51.4
	Suburban	5389	44.8	61.4
	Urban	1466	30.2	49.8
Exhaust Temp. (degC)	Highway	2629	152.4	22.7
	Suburban	5389	58.0	41.6
	Urban	1466	45.4	28.6
Fuel (gal/s)	Highway	2629	6.48E-04	4.06E-04
	Suburban	5389	1.82E-04	3.29E-04
	Urban	1466	1.16E-04	2.60E-04
CO_2 (g/s)	Highway	2629	6.68	4.19
	Suburban	5389	1.86	3.39
	Urban	1466	1.19	2.66
CO (g/s)	Highway	2629	0.0037	0.0050
	Suburban	5389	0.0051	0.0144
	Urban	1466	0.0042	0.0136
NO (g/s)	Highway	2629	0.0549	0.0427
	Suburban	5389	0.0150	0.0292
	Urban	1466	0.0085	0.0182
NO_2 (g/s)	Highway	2629	0.00356	0.00212
	Suburban	5389	0.00078	0.00188
	Urban	1466	0.00045	0.00146
NOx (g/s)	Highway	2629	0.0585	0.0437
	Suburban	5389	0.0157	0.0304
	Urban	1466	0.0089	0.0189
Hydrocarbon (g/s)	Highway	2629	6.76E-04	7.36E-04
	Suburban	5389	7.20E-04	1.77E-03
	Urban	1466	4.70E-04	1.50E-03
d-ICE Power (W/kg/s)	Highway	2629	7.96	5.95
	Suburban	5389	1.86	4.49
	Urban	1466	1.02	3.25
EM Power (W/kg/s)	Highway	2629	0.12	1.02
	Suburban	5389	1.98	3.57
	Urban	1466	1.76	3.29
Total Power (W/kg/s)	Highway	2629	8.08	5.90
	Suburban	5389	3.85	5.12
	Urban	1466	2.78	4.25

As with all other time-based analyses, highway operation required the greatest level of power output per second of drive time. Despite having excess battery capacity, the high velocities mandated by highway operation resulted in disproportionate use of the dICE and virtually no EM use. Essentially, the highway power scheme remained largely unchanged between charge-sustaining and charge-depleting operation. For the in-town roadways, power output remained relative to average velocity, with the faster traveling suburban roadways requiring more power output than the slower urban roads. The trend in total power output translated to both ICE and EM power use. As mentioned previously, power use and exhaust emissions during cruise mode were generally less than those observed during acceleration events, even though the majority of the PHEV's time was spent in cruise operation.

With regards to roadway type, suburban driving required more power, fuel, and resulted in higher exhaust emissions of all pollutants than urban travel. It should be noted that the standard deviations are sometimes an order of magnitude larger than the actual mean value for the data, indicating a lot of zero-valued data during charge-depleting cruise operation. This is particularly true of NO_2, HC, and CO emissions. For all of the other reported variables, the standard deviations are as large as mean values. For every second of electric-only operation, every measured variable except for EM power output and total power output will report as zero values. Despite high variances inherent to the charge-depleting dataset, both ANOVA and Kruskal-Wallis tests proved statistically significant for all variables.

8.7 Correlation Discussion: Emissions

As the final component to the roadway analysis, Pearson's correlations were performed on the individual roadway data. By using correlation analysis, any varying responses between on-road, operating, and emissions variables can be easily investigated according to roadway-type involvement. Complete results from the correlation analyses are provided in Appendix E; the generalized results are synopsized according to operating mode (charge-sustaining versus charge-depleting) in the following pages. The same criteria for ranking the strength of the Pearson's correlation coefficients in all previous correlation analyses were employed here.

8.7.1 Charge-Sustaining Mode

During charge-sustaining operation, the driving variables did not exhibit very strong correlations with either the PHEV Sprinter's operating or emissions variables for any of the roadway types analyzed. However, some variables did show a moderate degree of correlation with acceleration rates. Only the instantaneous vehicle specific power (VSP Inst) showed a moderate correlation with acceleration during highway driving. This correlation was slightly higher for suburban travel and not significant during urban driving. Any correlation between Instantaneous VSP values and either acceleration or velocity is somewhat redundant since both velocity and acceleration were direct inputs into the VSP equation. Acceleration did, however, show moderate positive correlation with total power output for in-town driving, regardless of whether it was on suburban or urban roadways. Since the acceleration rates between the in-town roadways were similar, this continuity was not unexpected. During charge-sustaining operation,

velocity was considerably less correlated with the PHEV's on-road experience than acceleration, which only demonstrated meaningful correlation during highway travel. During highway driving, exhaust temperature exhibited a good correlation with velocity, and both fuel use and carbon dioxide emissions proved to be positively, moderately correlated with velocity during highway travel.

Exhaust temperature was not a highly predictive variable, only demonstrating a moderate correlation with exhaust emissions and power output. During highway operation, exhaust temperature showed a moderately negative correlation with EM power output that did not translate to in-town driving. This is partly due to the fact that exhaust temperature during in-town driving remained moderately low compared with highway operation. Nitrogen oxides, and the nitrogen dioxide and nitrogen oxide that comprise it, were moderately correlated with exhaust temperature for both in-town roadways. Nitrogen dioxide's correlation makes intuitive sense as its formation is due to a secondary reaction occurring within the exhaust system under high temperatures and pressures.

Exhaust emissions of carbon dioxide, nitrogen oxide, and NOx (because it quantitatively based on NO emissions) were the direct result of dICE operation. Consequently, these pollutants remained highly correlated (very high or good) with both fuel use and dICE power output for all roadway types. However, the quantitative magnitude of these correlations lessened as the average velocity decreased and stop time increased for each roadway type.

Exhaust pollutants more strongly associated with transient dICE operation (CO, NO_2, and HC) did not demonstrate the strong correlations with power output and fuel use

as discussed above. Carbon monoxide formation was only moderately correlated with hydrocarbon emissions during highway operation. Beyond this relationship, carbon monoxide emission did not result in a statistically meaningful correlation with any other pollutants, on-road data, or PHEV operating variables for in-town driving. Conversely, other than a moderate correlation with CO emissions during highway operation, hydrocarbon formation did not result in any statistically meaningful correlations with the other measured variables.

Nitrogen dioxide emissions demonstrated a moderately positive correlation with exhaust temperature (which was intuitively expected) for all roadway types. A moderate correlation between NO emissions and dICE power output exists for suburban and urban roadways, but not for highway travel. This may be a mathematical artifact due to the fact that the dICE operated continuously during highway operation, but experienced periods of shut down during in-town operation. Table 8.41 provides a synopsis of the correlation results for each roadway type during charge-sustaining operation.

Table 8.41: Correlation results for PHEV Sprinter emissions and exhaust conditions during charge-sustaining operation.

Variable	Level of Sign	Highway		Suburban		Urban	
		Exhaust Emissions	Operating Variables	Exhaust Emissions	Operating Variables	Exhaust Emissions	Operating Variables
CO_2 (g/s)	V. High	NO	Fuel	NO	Fuel	NO	Fuel
		NOx	ICE Power	NOx	ICE Power	NOx	
			Total Power				
	Good		VSP Inst	NO_2	Total Power	NO_2	ICE Power
					Recup (-)		Total Power
							Recup (-)
	Moderate		Velocity		VSP Inst		
			SOC (-)				
NO (g/s)	V. High	CO_2	Fuel	CO_2	Fuel	CO_2	Fuel
		NOx	ICE Power	NOx	ICE Power	NOx	
	Good		Total Power	NO_2	Total Power		ICE Power
			VSP Inst		Recup (-)		Total Power
							Recup (-)
	Moderate		SOC (-)		Exhaust Temp	NO_2	Exhaust Temp
					VSP Inst		
NOx (g/s)	V. High	CO_2	Fuel	CO_2	Fuel	CO_2	Fuel
		NO	ICE Power	NO	ICE Power	NO	
	Good		Total Power	NO_2	Total Power	NO_2	ICE Power
			VSP Inst		Recup (-)		Total Power
	Moderate		SOC (-)		Exhaust Temp		Exhaust Temp
					VSP Inst		Recup (-)
CO (g/s)	V. High						
	Good						
	Moderate	HC					
NO_2 (g/s)	V. High						
	Good			CO_2	Fuel	CO_2	Fuel
				NO		NOx	
				NOx			
	Moderate		Exhaust Temp		Exhaust Temp	NO	ICE Power
					ICE Power		Exhaust Temp
Hydrocarbon (g/s)	V. High						
	Good						
	Moderate	CO					
Velocity (kph)	V. High						
	Good		Exhaust Temp				
	Moderate	CO_2	Fuel				
Acceleration (m/s^2)	V. High						
	Good				VSP Inst		
	Moderate		VSP Inst		Total Power		Total Power
Exhaust Temperature (deg C)	V. High						
	Good						
	Moderate		EM Power (-)	NO		NO	
				NOx		NO_2	
				NO_2		NOx	
State of Charge (%)	V. High						
	Good						
	Moderate	CO_2 (-)	ICE Power (-)				
		NO (-)	Total Power (-)				
		NOx (-)	Recup (+)				

8.7.2 Charge-Depleting Mode

Compared with charge-sustaining operation, the measured driving variables acceleration and velocity showed slightly higher correlation associations with power output for all roadway types during charge-depleting operation. While only moderate in strength, total power was positively correlated with acceleration for all designated roadway types. Since velocity did not hold any significant correlation strength with any of the power measures, acceleration is comparatively the more predictive measure of total on-road power requirements while the PHEV Sprinter was operating in charge-depleting mode. During highway operation, excessive battery capacity remained largely underutilized, however, the moderate, positive correlation with EM power output suggests that the EM assist was most prevalent during acceleration periods. Similar with charge-sustaining operation during highway driving continued dICE use resulted in a good positive correlation between exhaust temperature and velocity during charge-depleting operation.

Exhaust emissions of CO_2, NOx, and NO were strongly correlated with each other as well as with the PHEV Sprinter's fuel use and dICE power output for all designated roadway types. During highway operation, the EM provided very little of the PHEV's power output, so the strong correlation between CO_2 and dICE power output corresponds to a strong correlation between carbon dioxide emissions and total power output as well. The shift in power scheme between charge-sustaining and charge-depleting mode also resulted in a slight increase in the correlative significance (through moderate, positive correlation) of road grade on the PHEV's CO_2, NO, and NOx emissions during highway operation.

Charge-depleting operation's increased electrical capacity results in more electrical-only operation during in-town driving. This leads to the potential of increased transient operation and load on the dICE as the PHEV Sprinter will employ the combustion engine when in need of additional power assist. This inherent distinction from charge-sustaining operation is exhibited in the increased correlation between the secondary pollutant emissions and PHEV operating variables. During charge-depleting operation, carbon monoxide emissions have a good correlation with hydrocarbon emissions during highway and suburban travel, and to a lesser degree with urban travel. Fuel use and dICE power output become positively correlated with carbon monoxide emissions on urban roadways.

Nitrogen dioxide emissions show a moderate positive correlation with exhaust temperature during both highway and suburban operation; which follows intuitive reasoning given the conditions that promote NO_2 formation. Compared with charge-sustaining operation, dICE power becomes more predictive of NO_2 emissions during charge-depleting operation, and fuel use consistently provides a moderate, positive correlation with NO_2 emissions for all roadway types.

Hydrocarbons also experience a slight increase in correlative properties throughout the charge-depleting analysis, showing positive correlation with CO for all roadway types. Where HC emissions did not associate with any PHEV operation variables during charge-sustaining operation, during charge-depleting operation of in-town roadways, HC emissions are moderately, positively correlated with both fuel use and dICE power output.

Table 8.42: Correlation results for PHEV Sprinter emissions and exhaust conditions during charge-depleting operation.

Variable	Level of Sign	Highway		Suburban		Urban	
		Exhaust Emissions	Operating Variables	Exhaust Emissions	Operating Variables	Exhaust Emissions	Operating Variables
CO_2 (g/s)	V. High	NO	Fuel	NO	Fuel	NO	Fuel
		NOx	ICE Power	NOx	ICE Power	NOx	ICE Power
			Total Power				
	Good		VSP Inst			CO	
	Moderate	NO_2	Grade	CO	Total Power	NO_2	Total Power
				NOx	VSP Inst	HC	
				HC			
NO (g/s)	V. High	CO_2	Fuel	CO_2	Fuel	CO_2	Fuel
		NOx	ICE Power	NOx	ICe Power	NOx	
	Good		Total Power				ICE Power
			VSP Inst				
	Moderate		Grade	NO_2	Exhaust Temp	CO	Total Power
					Total Power	NO_2	
						HC	
NOx (g/s)	V. High	CO_2	Fuel	CO_2	Fuel	CO_2	Fuel
		NO	ICE Power	NO	ICE	NO	ICE Power
	Good		Total Power				
			VSP Inst				
	Moderate	NO_2	Grade	NO_2	Exhaust Temp	CO	Total Power
					Total Power	NOx	
						HC	
CO (g/s)	V. High						
	Good	HC		HC		CO_2	Fuel
	Moderate			CO_2	Fuel	NO	ICE Power
						NOx	
						HC	
NO_2 (g/s)	V. High						
	Good						
	Moderate	CO_2	Exhaust Temp	CO_2	Exhaust Temp	CO_2	Fuel
		NOx	Fuel	NO	Fuel	NO	ICE Power
			Velocity	NOx	ICE Power	NOx	
Hydrocarbon (g/s)	V. High						
	Good	CO		CO			
	Moderate			CO_2	Fuel	CO_2	Fuel
					ICE Power	CO	ICE Power
						NO	
						NOx	
Velocity (kph)	Good		Exhaust Temp				
	Moderate	NO_2					
Acceleration (m/s^2)	V. High						
	Good				VSP Inst		
	Moderate		EM Power		Total Power		Total Power
			Total Power				VSP Inst
			VSP Inst				
Exhaust Temperature (deg C)	V. High						
	Good		Velocity				
	Moderate	NO_2	EM Power (-)	NO			SOC
				NO_2			

8.8 Concluding Remarks

In accordance with the objectives set during the planning and development phases of the PHEV Sprinter on-road evaluation study, sample routes were selected in order to investigate the PHEV's operation on a multitude of different roadway scenarios. From the selected sample routes, three primary roadway types were designated: urban, suburban, and highway. Initial statistical analysis was conducted in order to verify that the designated roadways were, indeed, unique and represented different roadway classifications. All statistical tests were performed in triplicate: first on the continuous dataset, second on the every 5^{th} second average of the continuous dataset, and third on the sample run-based dataset consisting of an observation for every full sample run. This redundancy was employed to avoid the potential of committing a Type I error, deeming statistical significance where none existed. Based on velocity and acceleration profiles coupled with traffic-based measures, statistical analysis gave conclusive indication that the roadway designations characterized three distinct and different on-road scenarios.

The PHEV Sprinter's power output was a statistically significant response to roadway type during charge-sustaining mode; however, statistical significance was lost with respect to the electric motor's power output during charge-depleting operation when the in-town routes were tested against one another. When comparing the three roadway designations against each other, the unit basis of normalization played a significant role on the final conclusions. When evaluated on a per time basis, the slower roadways appeared to be more energy efficient, however, when the same data were transformed to a per distance basis, highway travel (the fastest of the three roadways) proved to require the

least amount of power. Ultimately, the basis of normalization will depend upon the purpose of the assessment.

Aside from a few specific instances, emissions and fuel use demonstrated statistically significant responses to roadway type. Exceptions include the sample run-based analysis of NO_2 and the in-town roadways' evaluation of NO_2 and HC, where both NO_2 and HC emissions were independent of suburban versus urban travel. On a time basis, highway travel generally resulted in significantly (over twice as high) higher emissions and fuel consumption than in-town driving on either urban or suburban roadways for all pollutants except NO_2 and CO. On-road velocity was also a decent predictor of pollutant emissions during in-town driving, where the faster traveled suburban roadway resulted in higher emissions than urban driving for all pollutants except for CO, which was consistently an urban-generated pollutant. While these results may, in part, be an artifact of the time basis of normalization, there are instances where time, rather than distance would be the preferable measure of assessment. For example, city planners might be more concerned regarding the amount of time that a vehicle is emitting to the urban core rather than the amount of distance that the vehicle traveled. In this case, time would be a better assessment of human exposure. However, the same analysis performed on the basis of distance, showcased highway driving as the cleanest, most fuel-efficient method of travel in all cases aside from HC emissions, which were still lowest during suburban travel. Conversely, urban driving, on a distance basis, was the least fuel-efficient, highest polluting roadway evaluated. Carbon monoxide emissions, in particular, were exceedingly high during urban travel.

In efforts to give some clarification to the high levels of CO emissions observed during urban driving, the roadway analysis was expanded to incorporate the driving modal model presented in Chapter 6, where cruise, acceleration, and idle operation were investigated according to roadway designation. Cruise mode emissions and fuel use corresponded to the PHEV's average velocity for each roadway, with the fastest traveled roadway type (highway) producing the highest level of exhaust emissions and fuel use. Urban travel demonstrated the lowest levels of emissions and fuel use for all pollutants except for CO. Acceleration rate proved to be a statistically significant response to roadway type with suburban travel resulting in, on average, the fastest acceleration rates of all measured roadways. This translated to higher emissions of all pollutants, except CO (which remained highest during urban travel) and higher dICE power output for suburban travel compared to the other roadways. Roadway and driving mode analysis failed to provide reasonable explanation regarding the high CO levels measured during urban travel. Chapters 9 and 10 will give more focus to this question.

Chapter 9: Operating Mode Analysis

9.1 Charge-Sustaining versus Charge-Depleting Overview

One of the most powerful benefits that the PHEV Sprinter offers in the way of emissions reductions and increased fuel efficiency is through its electric-only capacity. Plug-in hybrid vehicles are marketed as providing the best of both worlds spanning the chasm between conventional and electric-only vehicles. With their ability to store grid-sequestered electrical energy, plug-in hybrid vehicles possess the capability to provide a finite range of zero-emissions operation. However, where the electric-only vehicle must be recharged or fitted with fresh battery packs once its stored electrical capacity is utilized, the plug-in hybrid can act as an extended-range vehicle by transitioning to hybrid operation, where it utilizes the combustion engine as its primary power source while still employing the electrical drivetrain for power assist and on-road electrical recuperation. The facility to charge the PHEV from the grid during off hours provides the potential to greatly ease the on-road burden of the combustion engine. Literature distributed during the Kansas City-based PHEV Sprinter training indicated that the PHEV Sprinter had the ability to gain 20 to 30miles of electric-only operation before switching to its conventional hybrid mode (Locht, 2006).

Due to the PHEV Sprinter's novel design and unique drivetrain, an in-depth assessment of its operating modes and on-road electric-only range was immediately placed as one of the principal objectives for the on-road emissions and characterization study. A preliminary investigation into Objective 3, the operating mode analysis, showed that the KC PHEV Sprinter's electric-only drive range was considerably lower than original expectations. In order to investigate the PHEV's electric-only capacity achieved

during normal operating conditions (driving on KCATA designated routes), six specific sampling days were selected for preliminary investigation. The sample days were selected according to two primary criteria:

- First, the PHEV Sprinter started the sample day with a full battery charge (as obtained from overnight charging). Enough mileage had to have been logged during the sample day in order to fully exhaust the excess battery charge transitioning the PHEV Sprinter into charge-sustaining mode. This ensured that the states of charge where electric-only operation was most prominent (between 100% and 40%) were fully exhausted, and

- Second, that the PHEV was operated long enough to collect ample hybrid mode operation data. It was important that sampling occurred while the PHEV was functioning at the charge-sustaining mode representative of the vehicle's longer-range hybrid operation for comparative purposes.

Plug-in hybrid vehicles operate according to one of two modes of electric capacity utilization. On-road operation immediately following a full charging session is expected to primarily be electric-only or zero emissions operation. The PHEV Sprinter is able to most fully utilize its electric motor while the battery system holds excess capacity. More conventional operation will occur only during periods when immediate, transient demand requires internal combustion engine (ICE) power assist. This initial, electric-drive intensive mode of operation is referred to charge-depleting (CD) mode since stored

battery capacity will be preferentially used while available. When the battery capacity (state of charge) falls to a predetermined "safe" level, the PHEV switches its drive mode to a control scheme more reflective of conventional hybrid electric vehicle (HEV) operation. This mode is referred to as "charge-sustaining." Once entering charge-sustaining (CS) operation, the PHEV is designed so that the ICE becomes a more prominent motive source in efforts to maintain a safe state of battery charge. As the battery capacity increases due to regenerative breaking during charge-sustaining operation, the PHEV will preferentially use the electric motor in effort to minimize ICE operation. Figure 9.1 displays the state of battery charge as a function of distance traveled for the KC PHEV Sprinter while driving the 123 route. Charge-depleting mode occurs during the initial 18miles of on-road operation. Once the PHEV Sprinter reachs a 35% state of charge, it transitions into hybrid operation where the battery capacity is used as available, but never drops below a set minimum of 34%. This is done to protect and preserve the battery's lifespan.

Initial analysis of Figure 9.1 suggests that the PHEV Sprinter achieves 18miles of electric-only drive range in while operating in charge-depleting mode. However, during normal driving conditions, the diesel engine was periodically required as an assist during the electric-only range of this mode. Consequently, preliminary analysis shows that the PHEV Sprinter did not achieve the anticipated 20miles of electric-only operation during the charge-depleting mode.

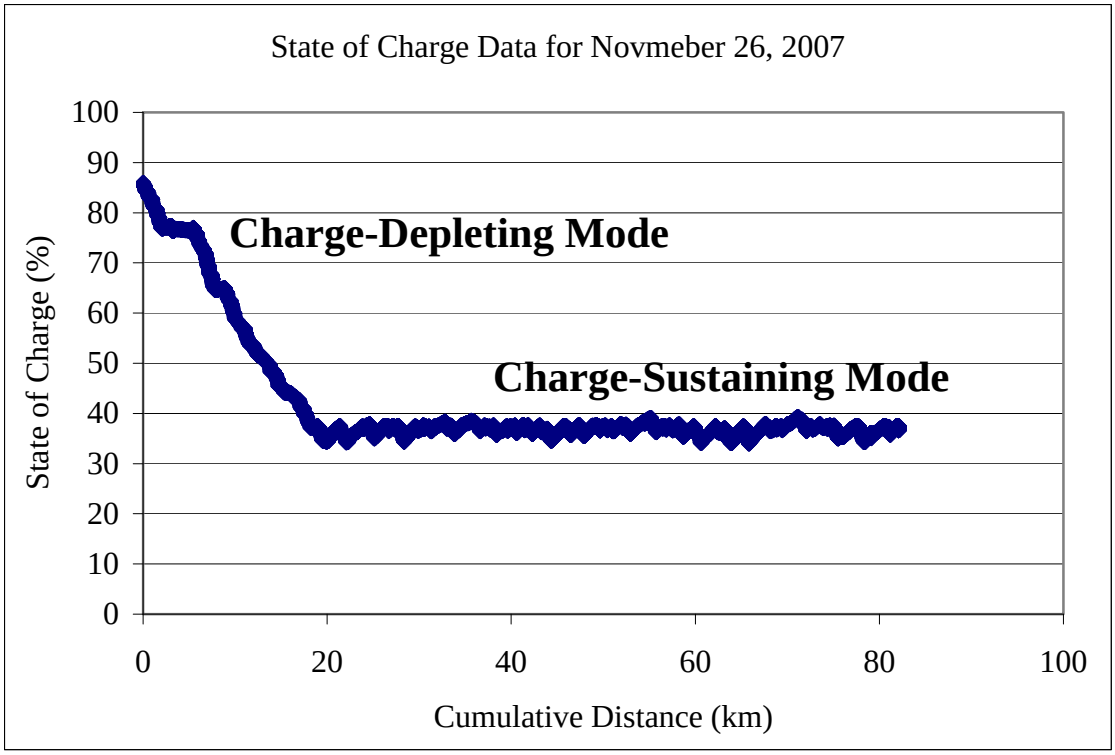

Figure 9.1: State of Charge versus distance for the 23rd Street route driven on November 26, 2007.

Six sampling days meeting the previously set criteria were selected for the preliminary investigation of this objective: September 10, September 12, November 20, November 26, and December 20, and December 21. Additional details about the actual runs that comprised each of these sampling days can be found in the summary table in Appendix F. Details specific to each sample day are listed below:

- **September 10:** Start charge was 89.4%. Route 109 was run 3.5 times with two additional KCATA transfer runs occurring midday. The total day's mileage was 37.8miles.

- **September 12:** Start charge was 85.3%. Route 109 was run twice with two additional KCATA transfer runs occurring midday. The day's total mileage was 18miles.
- **November 20:** Start charge exceeded 90%. KCATA transit bus was shadowed on the 123 route resulting in 58.8miles of recorded on-road operation.
- **November 26:** Start charge was 85.0%. Route 123 was run "solo" resulting in a total recorded distance of 51.0miles.
- **December 20:** Start charge was over 90%. Route 110 was tested while driving "solo" resulting in 61.7miles of recorded distance traveled.
- **December 21:** Start charge exceeded 90%. Route 110 was tested under "solo" operation and while shadowing a KCATA transit bus. Total recorded distance for the day was 60.7miles.

For the purpose of this analysis, the data were segregated into two discrete categories according to the PHEV's state of charge:

- **Category 1:** state of charge from 100% to the first recorded 37% (charge-depleting mode), and

- **Category 2:** the remainder of the run where the state of charge fluctuated between 34% and 38% (charge-sustaining mode).

Historically, the first section of the SOC plot, where the state of charge uniformly drops from a high charge (in Figure 9.1, 85%) to a plateau level (the level that the PHEV will oscillate within for the remainder of its hybrid operation, nominally 36-39%), has been described to as electric-only range. In order to quantify the PHEV Sprinter's electric-only operation, the data for each sample day were divided into two different datasets (data representing charge-depleting operation and data representing charge-sustaining operation). For the purpose of this discussion, electric-only operation was considered active when the hybrid-clutch was open (100%), signifying that the diesel engine was not running. Data collected when the hybrid clutch was closed or transitioning from open to close (<100%) occurred while the PHEV was operating either with complete dICE function or with a combination of dICE and electric motor (EM) derived power. Carbon dioxide emissions and diesel engine speed were used to verify that the combustion engine was not running while the hybrid clutch was open but that it was operational whenever the clutch was closed. Table 9.1 displays the number of miles obtained when in electric-only operation and with the diesel engine running for each mode of operation. "Electric Motor" refers solely to electric-only or zero emissions operation, whereas "Diesel Engine" refers to PHEV Sprinter operation with the internal combustion engine running (with or without electric motor power assist). The term "Diesel Engine" may be a slight misnomer as it would imply diesel engine-only operation, when, in fact, the PHEV might be deriving its power from both the diesel ICE and EM at this time. All labeling conventions aside, the "Diesel Engine" data refer to miles when the diesel engine was actually running, whether or not it was the sole power source.

Table 9.1: Driving distances achieved in electric only operation categorized according to state of charge.

	Sept. 10 109: 9th St Solo		Sept. 12 109: 9th St Solo		Nov. 20 123: 23rd St. Follow		Nov. 26 123: 23rd St. Solo		Dec. 20 110: 44th/Brkln Solo		Dec. 21 110: 44th/Brkln Follow and Solo	
	km	mi	km	mi	km	mi	km	mi	km	mi	km	mi
Battery State of Charge from 100% to 37%:												
Diesel Engine	2.9	1.8	3.6	2.2	5.5	3.4	6.8	4.2	5.6	3.5	5.3	3.3
Electric Motor	13.8	8.6	10.9	6.7	11.2	6.9	12.6	7.8	17.3	10.7	14.0	8.7
% Distance EM:	**82.6%**		**75.0%**		**67.0%**		**65.0%**		**75.5%**		**72.4%**	
Total Distance:	16.7	10.4	14.5	9.0	16.7	10.3	19.4	12.1	22.9	14.2	19.3	12.0
Battery State of Charge 37% plateau and on:												
Diesel Engine	34.4	21.4	10.5	6.5	61.1	38.0	43.5	27.0	45.6	28.3	49.7	30.9
Electric Motor	9.8	6.1	3.7	2.3	16.9	10.5	19.2	12.0	30.8	19.2	28.7	17.8
% Distance EM:	**22.2%**		**26.2%**		**21.7%**		**30.7%**		**40.4%**		**36.6%**	
Total Distance:	44.2	27.5	14.2	8.8	78.0	48.5	62.7	39.0	76.4	47.5	78.3	48.7
All Battery States of Charge (the entire day's sum):												
Diesel Engine	37.3	23.2	14.1	8.8	65.9	41.0	50.2	31.2	51.2	31.8	55.0	34.2
Electric Motor	23.6	14.7	14.6	9.1	28.7	17.8	31.8	19.8	48.1	29.9	42.7	26.5
% Distance EM:	**38.8%**		**50.8%**		**30.3%**		**38.8%**		**48.5%**		**43.7%**	
Total Distance:	60.9	37.8	28.7	17.8	94.6	58.8	82.1	51.0	99.3	61.7	97.6	60.7

Preliminary analysis of charge-depleting mode (category I) shows, as expected, that the majority of the PHEV's operation is in electric-only operation. Additionally, Category 2 (charge-sustaining operation, more akin to hybrid operation) still sees a benefit from the vehicle's electric-only capabilities, resulting in between 21% and 40% of charge-sustaining operation being powered solely by the electric engine. However, as mentioned earlier, the Kansas PHEV Sprinter did not yield 20-30miles of electric-only capacity while operating in charge-depleting mode as indicated in the literature. The discrepancies of the electric-only drive capacities seen between the selected sampling days (total distance achieved and percent of electric-only operation) were not analyzed as

part of this preliminary investigation and need to be addressed. The selected sample days were completed on different routes, under different driving configurations (solo versus follow), and at different ambient temperatures (September 10 and September 12 had ambient temperatures ranging from 20ºC to 26ºC, whereas, sampling conducted in December occurred at considerably colder conditions with average ambient temperatures ranging from 8ºC to 13ºC). It is likely that underlying confounding factors such as driving configuration or ambient temperature are influencing the results reported in Table 9.1. The remainder of the operating mode analysis will be conducted using the specific sample runs selected for the VSP and Roadway Type investigations. The resulting dataset comprises sufficient data representation for both operating modes controlled for ambient temperature, auxiliary system use, and on-road driving designation (solo or following an in-service transit bus).

All of the data reported in the summary table in Chapter 4 are for the PHEV Sprinter system as a whole, however, if the emissions output and fuel economy are calculated with reference to the diesel engine alone (removing all of the electric-only capacity), the Kansas City PHEV Sprinter's fuel efficiency would be almost half of what is cited above, and the mass/distance emissions would be almost double what is reported in the summary table.

Table 9.2: Fuel efficiency calculations from the selected datasets according to aux system use and ambient temperature.

Overall CS mpg:	15.45
Overall CD mpg:	24.04
Overall mpg of selected datasets:	16.94

The overall fuel efficiency (mpg) based on the entire collected dataset is 15.13mpg. This figure possesses a small amount of error due to the percentage of the on-road data collection time when the GPS was unable to record the vehicle's traveled distance due to loss of satellite signal. At these times, the resulting calculated travel distance was artificially set at zero even though the PHEV was using fuel. The 15.13mpg is a slight underestimation of the PHEV Sprinter's actual on-road fuel efficiency and based on Semtech-PC calculations, not the PHEV's data-logging module (DLM) recorded values.

Table 9.2 highlights the fuel efficiency calculated for the selected data used in Chapters 6, 7, and 8. The dataset filtered for ambient temperature and auxiliary system effects and limited to normal civilian driving not under the influence of transit operation resulted in a slightly improved fuel efficiency compared to that reported for the PHEV on-road dataset in its entirety.

9.2 Drive Time/Distance Distribution between Operating Modes

While the preliminary operating mode analysis was conducted using a finite number of sample runs selected according to state of charge range (starting near or over 90% and ending well within charge-sustaining operation), the remainder of this discussion will pertain to the sample runs selected for the VSP and Roadway analysis. Possible confounding influences of auxiliary system use and ambient temperature are significant enough to warrant limiting this discussion to the aforementioned sample runs. Rugh (2010), through simulation, estimated that a PHEV had the potential to lose up to 18% of its electric-only drive distance if the air conditioning system was being utilized.

The preliminary analysis gave some indication regarding the PHEV's actual electric-only range during charge-sustaining and charge-depleting modes. While the reported results show that the PHEV did not actually achieve the proposed electric-only range suggested during early meetings with the PHEV Sprinter developers, the results do slightly underestimate the electric-only range during charge-depleting operation. Theoretically, charge-depleting operation occurs from a state of charge of 100% (immediately off of the charging station) to 36%. However, due to the sampling constraints of the KC PHEV Sprinter Demonstration Study, on-road sampling rarely occurred during states of charge exceeding 90%. By the time the PHEV Sprinter was removed from the charging station, repositioned throughout the KCATA bus yard, moved for Semtech installation, and driven off-site for initial Semtech calibration the highest state-of-battery-charge range (from 100% to 90%) was largely expired and unavailable for on-road monitoring. Preserving integrity in the sampling protocol was considered of utmost importance, so in order to provide a meaningful discussion of operating mode

while still using data collected with the same scrutiny as that applied to all on-road sampling data collected from the PHEV Sprinter, the charge-depleting and charge-sustaining data were normalized according to distance traveled or travel time for the remainder of this investigation. This also compensates for the fact that the majority of the on-road data collection occurred during charge-sustaining operation, as charge-depleting mode was only possible at the start of each sampling day, and could not be achieved again until a full night's charging was available.

Electric-only range according to operating mode was investigated on a per distance and per travel-time basis. Previous analyses have shown that the PHEV Sprinter's operation and exhaust emissions proved to be statistically significant responses to Vehicle Specific Power (VSP), Driving Mode designation (Acceleration, Deceleration, Cruise, and Idle), and Roadway type. In order to most thoroughly investigate the PHEV Sprinter's two operating modes, the data are presented in bulk (overall) according to VSP-bin and by roadway-type. The Driving Mode model of categorizing data was excluded from this analysis, since only two of the four driving modes (Cruise and Acceleration) represented power-demand-based scenarios. The descriptive capacity of expanding this analysis to include the Driving Mode model was not deemed sufficient enough to justify the additional effort of reporting.

Similar to the preliminary analysis, electric-only operation was assessed according to the PHEV Sprinter's hybrid clutch position. When the hybrid clutch was open (reported 100%), the PHEV was powered solely by its electric motor. During this time the diesel internal combustion engine (dICE) was turned off. However, when the hybrid clutch was closed (reported as 0%) or in the state of closing (recorded as 0% <

100%), the PHEV's motive power was, at least partially, provided by the diesel ICE. These periods are referred to as hybrid operation, where, although the diesel ICE was always operational, it was receiving some amount of power assist from the electric motor (EM) most of the on-road time. Table 9.3 shows the relative distances of on-road travel achieved during charge-depleting and charge-sustaining operation as well as the amount of those distances that occurred under electric-only operation. For comparative purposes the percentage of electric-only operation is provided for each level of reporting (the overall dataset consisting of all selected sample runs, according to roadway-type, and by VSP-bin).

As expected, the electric-only operation was proportionally higher during charge-depleting mode, when the PHEV Sprinter possessed excess battery capacity. However, when the PHEV was under higher road-load scenarios (either due to increased velocity or higher overall VSP), the percentage of electric-only operation was reduced in each operating mode. During the driving scenarios with the highest velocity (highway driving) and during the highest imposed on-road load (VSP bins 7 and 8) the amount of electric-only driving distance between the different operating modes started to converge. Regardless of battery state of charge, the diesel ICE became the dominant power source during high operating-load scenarios.

Table 9.3: Summary of percentage of distance spent during electric-only operation.

	Charge-Depleting Mode			Charge-Sustaining Mode		
	Distance of All Operation (km)	Distance EM-Only Operation (km)	% Electric-Only Operation	Distance of All Operation (km)	Distance EM-Only Operation (km)	% Electric-Only Operation
Overall	157.10	60.03	38.2%	482.88	132.76	27.5%
Roadway Type:						
Urban	14.95	9.55	63.9%	45.84	17.37	37.9%
Suburban	80.86	48.11	59.5%	329.46	110.74	33.6%
Highway	61.29	2.37	3.9%	107.53	4.64	4.3%
VSP Bins:						
1	53.20	27.89	52.4%	172.94	57.99	33.5%
2	16.65	7.16	43.0%	52.41	16.19	30.9%
3	16.59	6.22	37.5%	54.47	14.53	26.7%
4	14.97	5.31	35.5%	50.05	12.38	24.7%
5	14.19	4.77	33.7%	45.41	10.99	24.2%
6	12.55	3.58	28.5%	36.84	9.15	24.8%
7	14.79	3.24	21.9%	37.68	7.52	19.9%
8	14.16	1.86	13.1%	33.07	3.99	12.1%

For comparative visualization between the operating modes, the electric-only operation according to roadway-type and VSP-bin is displayed in Figures 9.2 and 9.3. The convergence of electric-only distance between the operating modes with increased power demand is observed in VSP bins 6 through 8.

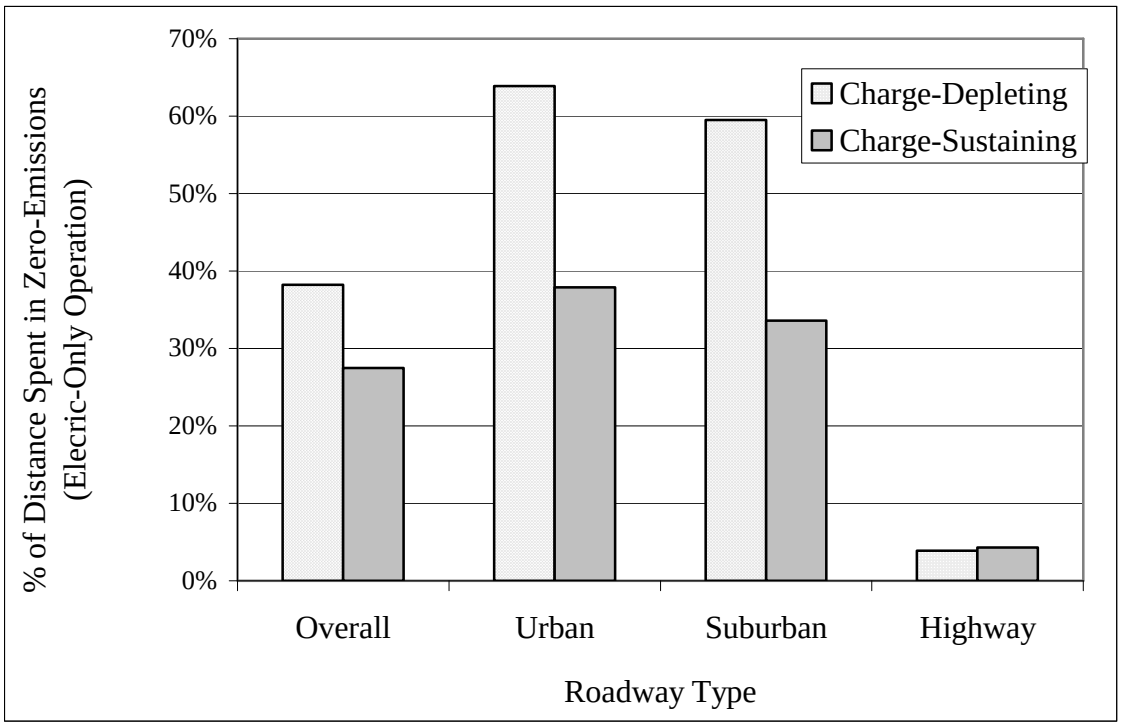

Figure 9.2: Roadway bar chart, electric-only distance for each operating mode.

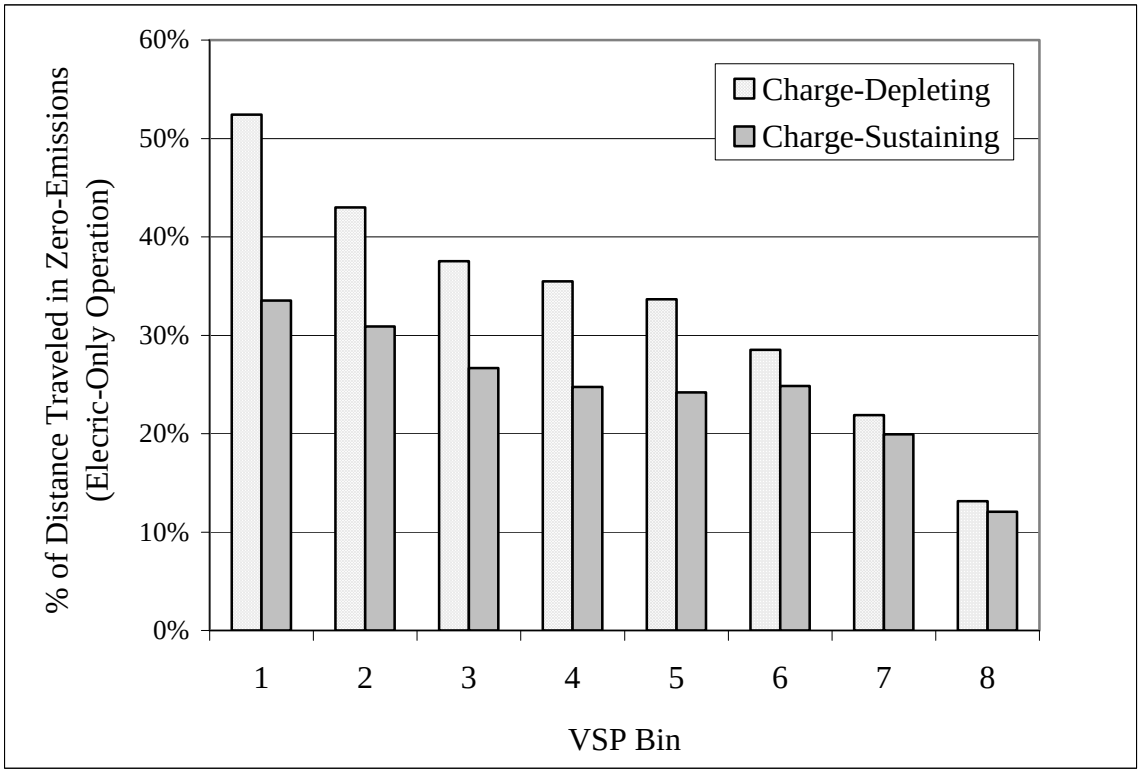

Figure 9.3: VSP-bin bar chart, electric only distance for each operating mode.

During the roadway analysis investigation (Chapter 8), distinct quantitative differences in PHEV power output and exhaust emissions were witnessed between the two bases of data normalization (time versus distance) due to the significantly different average velocities between the designated roadway types. Because of this, the electric-only data were normalized according to road-time as well as distance traveled. While on-road data is most commonly reported on a per time basis, in order to truly assess the PHEV's impact to the local area and communities it is important to evaluate its operation according to both distance traveled and travel time.

The general trends in electric-only operation between the two operating modes that were observed during the distance-based analysis promulgated to the time-based data. Charge-depleting mode resulted in the highest percentage of electric-only (zero emissions) on-road time, with the difference in electric-only time between the operating modes diminishing as the on-road power demand and/or travel velocity increased (Table 9.4, Figures 9.4 and 9.5).

Table 9.4: Summary of the percentage of time spent in electric-only operation between operating modes according to both roadway type and VSP bin.

	Charge-Depleting Mode			Charge-Sustaining Mode		
	Time of all Operation (s)	Only Operation (s)	% Distance, EM only	Time of all Operation (s)	Time EM-Only Operation (s)	% Distance, EM only
Overall	17169	9589	55.9%	54815	20268	37.0%
Roadway Type:						
Urban	3292	2215	67.3%	9325	3952	42.4%
Suburban	10873	7041	64.8%	40197	15680	39.0%
Highway	3004	333	11.1%	5289	636	12.0%
VSP Bins:						
1	9015	5995	66.5%	28054	11987	42.7%
2	1483	823	55.5%	5112	1873	36.6%
3	1380	692	50.1%	4776	1595	33.4%
4	1216	580	47.7%	4289	1353	31.5%
5	1160	555	47.8%	3851	1233	32.0%
6	961	405	42.1%	3098	1016	32.8%
7	1038	346	33.3%	3080	804	26.1%
8	916	193	21.1%	2555	407	15.9%

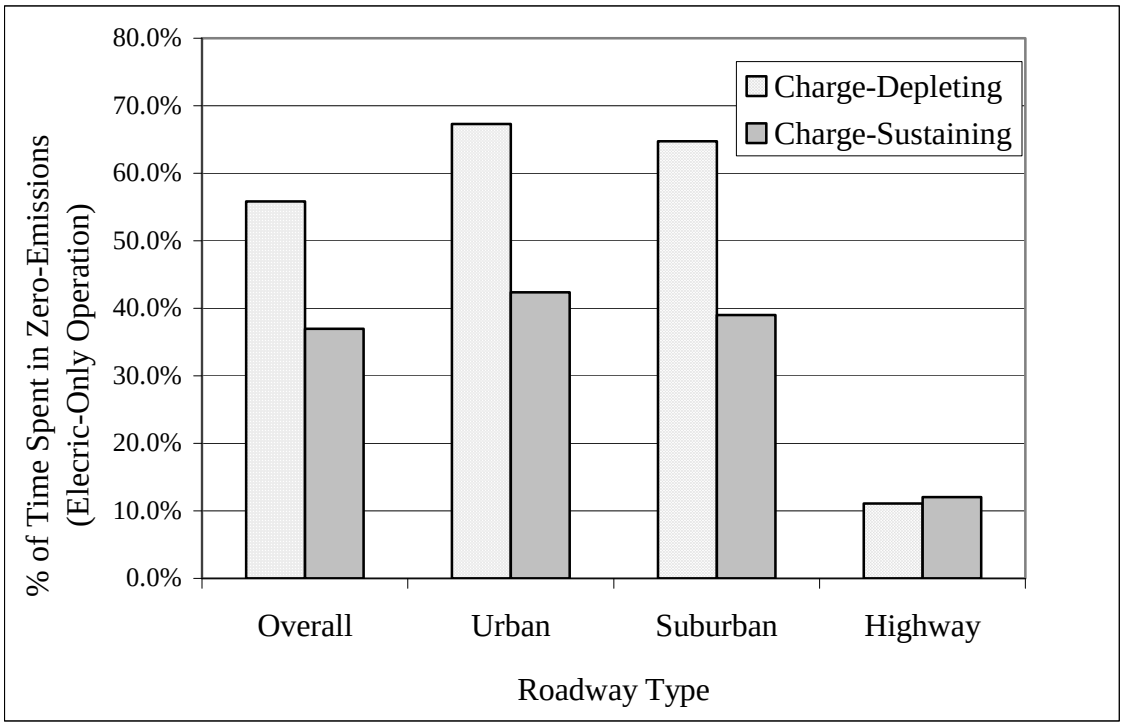

Figure 9.4: Electric-only operation based on time, according to roadway type.

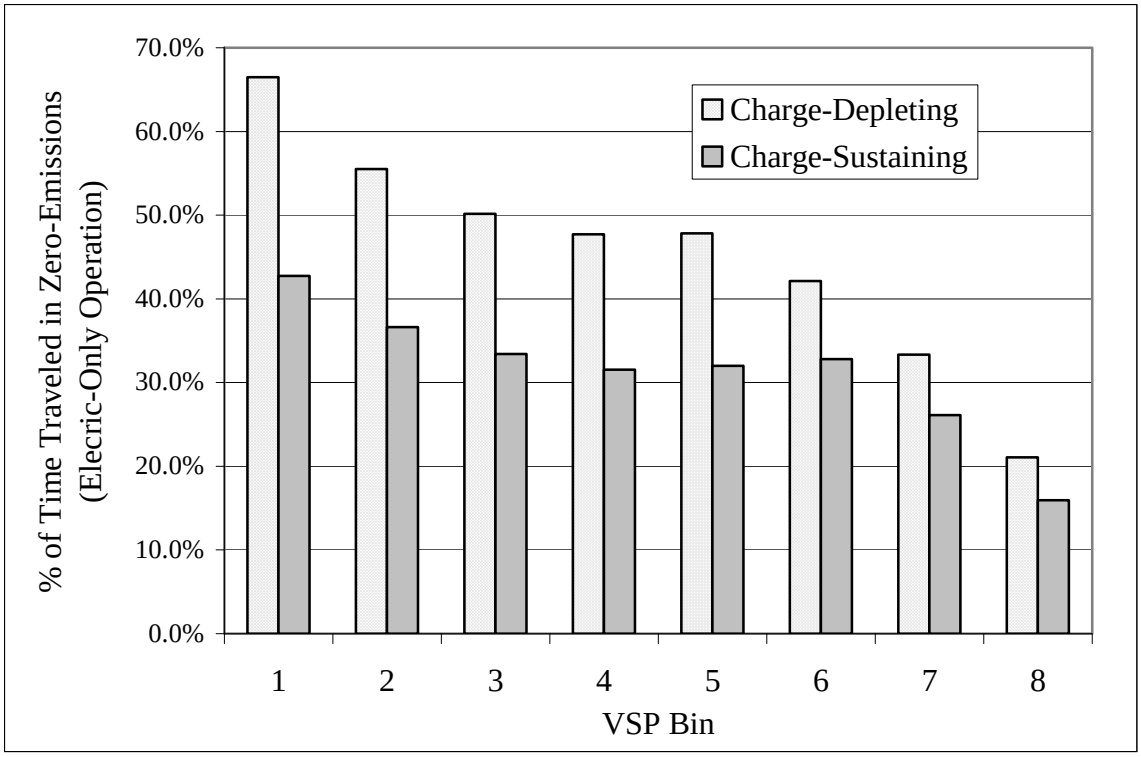

Figure 9.5: Electric-only operation, based on road time, according to VSP bin.

While the amount of electric-only operation was consistently higher during charge-depleting mode compared with charge-sustaining mode, the amount of electric-only operation (whether time or distance based) during charge-depleting operation was significantly less than 100%. The diesel ICE still provided a significant amount of the power output during charge-depleting mode, which is somewhat contrary to the general, broad-based description of the PHEV Sprinter that was originally presented to the public. Periods of low power demand driving and roadways with the lowest relative velocity best utilized the PHEV Sprinter's electric-only capacity in both operating modes, although this trend was more prominent during charge-depleting operation.

9.3 Power Output According to Operating Mode

9.3.1 Statistical Results

Analysis of Variance (ANOVA) and its non-parametric equivalent, Kruskal-Wallis, tests were performed on the PHEV Sprinter's on-road data in order to evaluate the differences in the PHEV's on-road experience between the two operating modes (CD versus CS) to a degree of statistical significance. All analyses were conducted on the continuous, second-by-second dataset, and again on the condensed dataset consisting of the run-based compilation of the continuous dataset. Due to the size of the continuous dataset, more conservative criteria were enforced for determining statistical significance with an $\alpha<0.025$ in efforts to minimize the risk of performing Type I error. However, analyses of the sample run-based dataset were assessed under a less stringent $\alpha<0.05$.

Prior to initiating the univariate analysis of the continuous dataset, Multivariate Analyses of Variance (MANOVA) were performed on the power data in order to safeguard against performing a Type I error during the subsequent univariate analyses. Because total power output is not independent of electric motor power and diesel ICE power, each power constituent was assessed separately. Six MANOVAs were conducted in the initial investigation, assessing the statistical significance of each power component as a response to either VSP bin and operating mode or Roadway Type and operating mode. In all cases, power output remained a highly statistically significant response to the combination of operating mode and either VSP bin or Roadway Type factors (p-values=0.000). With conclusive results established on a multivariate level, the investigation proceeded to univariate analyses.

The data were evaluated as a single unit (overall), according to roadway type (urban, suburban, and highway, as defined in Chapter 8), and based on VSP-bin (1 through 8 as modeled for heavy-duty vehicles and discussed in Chapter 6). The PHEV's exhaust temperature, dICE power output, total power output, and recuperation rate all proved to be statistically significant responses to operating mode for all facets of analysis (roadway type and VSP-bin). Electric motor power output was also a statistically significant response to operating mode, however, during highway operation, the statistical tests were not conclusive, failing to meet the criteria established for determining statistical significance for the ANOVA test.

Table 9.5: ANOVA and Kruskal-Wallis results for power output according to operating mode based on VSP bin, for the continuous dataset.

VSP BIN	1	2	3	4	5	6	7	8
ICE Power, W/kg/s	y	y	y	y	y	y	y	y
EM Power, W/kg/s	y	y	y	y	y	y	y	y
Total Power, W/kg/s	y	y	y	y	y	y	y	y
Recup, W/kg/s	y	y	y	y	y	y	y	y

Inc1: y anova, n kw

Inc2: n anova, y kw

Table 9.6: ANOVA and Kruskal-Wallis results for power output according to operating mode based on Roadway Type, for the continuous dataset.

Roadway Type	Overall	Urban	Suburban	Highway
ICE Power, W/kg/s	y	y	y	y
EM Power, W/kg/s	y	y	y	Inc2
Total Power, W/kg/s	y	y	y	y
Recuperation, W/kg/s	y	y	y	y

Inc1: y anova, n kw

Inc2: n anova, y kw

As mentioned earlier, the roadway-segregated data were tested in duplicate with the second iteration focusing on the compiled dataset of mean values for each sample run. Given the nature of the compiled dataset, VSP bin analysis was not viable. Additionally, exhaust temperature information was not included in the compiled dataset, and is, therefore, not assessed on a per-sample run basis. Table 9.7 provides a synopsis of the results from the ANOVA and Kruskal-Wallis analyses conducted on the compiled dataset. Total power output and the dICE power output were statistically significant responses to all categories of analysis (entire dataset, and urban, suburban, and highway roadways). Additionally, recuperation rate proved to be a statistically significant response to operating mode for the sample-run level analysis. The electric motor (EM) power output was the least statistically conclusive power-related variable assessed. For the entire dataset, EM power output was a statistically significant response to operating mode, however, the results were less definitive as the analyses were carried out according to the different roadway types. As discussed earlier, as the PHEV Sprinter was operated at higher velocities and higher overall road-loads, the difference in EM power output between the operating modes became less significant as the PHEV's power control scheme increased the dICE's recruitment. As a consequence of this, highway travel did not prove to provide a statistically significant response of EM power output according to operating mode for either statistical test performed. Statistical significance in the EM results was maintained during suburban travel, but became inconclusive during the slower, more stop-and-go urban travel. Despite having quantitatively different EM power output means between the two operating modes, the large standard deviation and variance of urban EM power output voided statistical significance of the ANOVA test.

Table 9.7: Statistical synopsis of power usage according to operating mode, segregated based on roadway type for the compiled dataset.

Variable	Overall	Urban	Suburban	Highway
ICE Power, W/kg/s	y	y	y	y
EM Power, W/kg/s	y	Inc2	y	n
Total Power, W/kg/s	y	y	y	y
Recuperation, W/kg/s	y	y	y	y

Inc1: y anova, n kw
Inc2: n anova, y kw

The initial data file selection performed during the VSP analysis (Chapter 6) alleviated any confounding effects on the PHEV Sprinter's operation and emissions due to auxiliary system use and the impact of ambient temperature changes. In order to verify that the differences in power usage between the roadway types were, indeed, the result of the PHEV's active operating mode rather than the result of embedded differences in on-road driving behaviors, statistical analysis was extended to the primary on-road variables responsible for the PHEV Sprinter's power output: vehicle velocity and acceleration (defined by positive acceleration, where acceleration rates were greater than or equal to zero). This additional quality assurance work was limited to the compiled, sample-run based dataset. All ANOVA and Kruskal-Wallis analyses of the PHEV's average velocity and average acceleration demonstrated no differences in the driving variables between the operating modes for all roadway types assessed, just verifying that the roadway differences observed were due to the different roadways and not driver bias.

9.3.2 EM vs. dICE Use Between Operating Modes

While the statistical summaries proved that statistically significant and meaningful differences exist between the operating modes with regards to the PHEV Sprinter's power usage and control scheme (according to dICE versus EM use), the direction of the relative differences in power usage and recuperation was not discernable from the previous tables and discussion. The PHEV's power usage will be presented as a time-basis from this point on, maintaining continuity with existing research and protocol. It is important to remember that the results reported as a function of travel time will present differently than those reported as a function of travel distance, particularly when comparing high-speed roadways such as highway driving to much slower stop-and-go traffic scenarios (urban and suburban). Because vehicle specific power is a calculated proxy for on-road vehicle load, it is not only a function of travel velocity but also of acceleration, grade, and the PHEV Sprinter's physical characteristics.

As expected, the PHEV Sprinter required less power output from the dICE during charge-depleting operation, when the PHEV possessed excess stored battery capacity. The PHEV consistently required more power output from the dICE during charge-sustaining mode through all 8 VSP bins (Figure 9.6), particularly during higher road-load situations (VSP bins 7 and 8). This relative trend in dICE power recruitment was also apparent, and statistically significant for the different roadway types evaluated (Figure 9.7). The largest difference in dICE power use between operating modes occurred during the slower, more stop-and-go, in-town roadways (urban and suburban). While a statistically significant difference was demonstrated during highway driving, the quantitative difference in dICE power output between the operating modes was smallest

during highway travel. Just as the difference in dICE power output between the operating modes diminished with increasing velocity, this difference also decreased with increasing VSP bin or road-load.

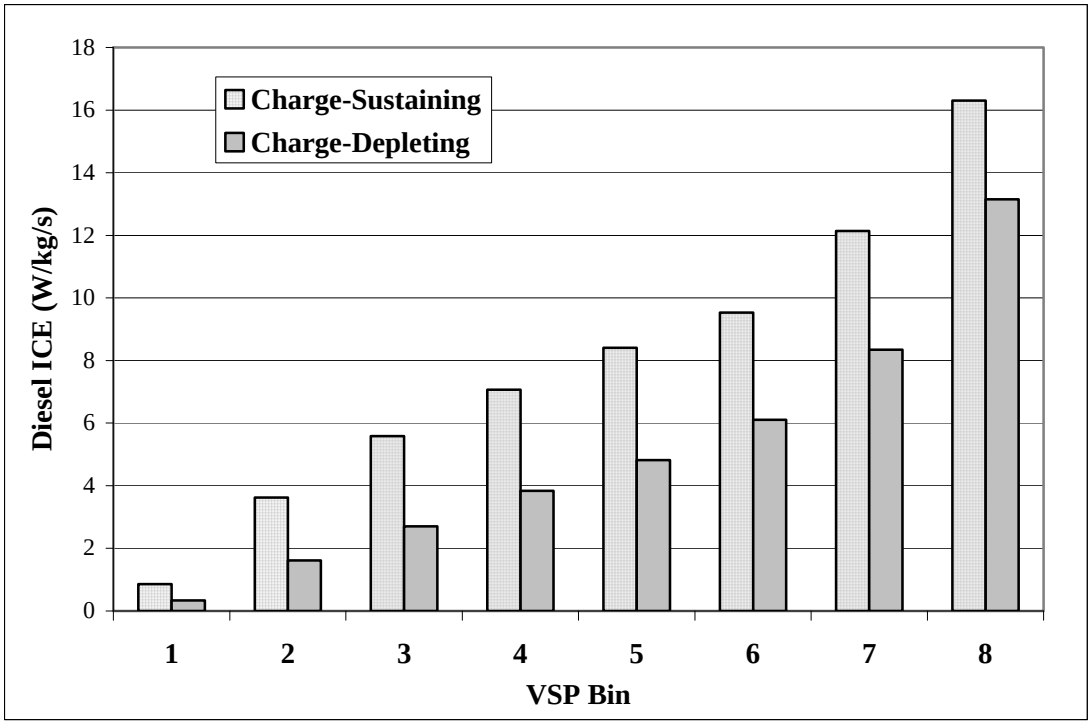

Figure 9.6: Diesel ICE power output between charge-depleting and charge-sustaining mode according to VSP bin.

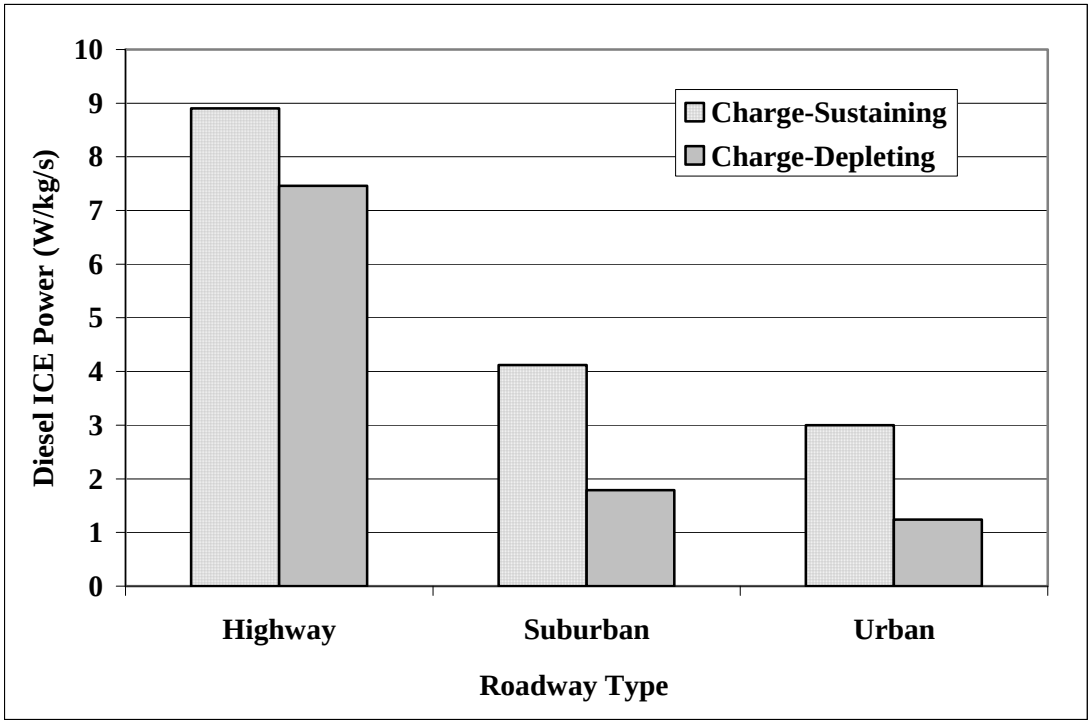

Figure 9.7: Diesel ICE power output between charge-depleting and charge-sustaining mode according to roadway type.

While charge-depleting mode required less power output from the dICE compared with charge-sustaining mode through all 8 VSP bins, the rate of dICE recruitment with increasing VSP bin was highest during charge-depleting mode (Table 9.8). This trend is particularly true during the highest VSP bins, when the PHEV Sprinter was experiencing its largest on-road workloads.

Table 9.8: Relative rates of increased diesel combustion engine (dICE) demand in charge-sustaining versus charge-depleting modes according to VSP bin.

VSP Bins	% Change ICE Power	
	CS	CD
1-2	123%	132%
2-3	43%	50%
3-4	24%	35%
4-5	17%	23%
5-6	13%	24%
6-7	24%	31%
7-8	29%	45%

As discussed in the Vehicle Specific Power analysis (Chapter 6), electric motor use reached its maximum recruitment during VSP bin 6 with a subsequent reduction in power output in bins 7 and 8. As the overall road load requirements increased during VSP bins 7 and 8, the dICE became a more prominent source of power output due to immediate on-road performance demands that were most likely a function of periods with high rates of acceleration or velocity. This trend was persistent regardless of the PHEV's operating mode. Despite available excess battery capacity, EM recruitment during charge-depleting mode also dropped off in VSP bins 7 and 8. While the PHEV was operating under low to moderate road-load demands, the EM supplied a consistently increasing amount of the PHEV's motive work during both charge-sustaining and charge-depleting modes. As expected, because of its grid-sequestered battery capacity, charge-depleting operation resulted in higher recruitment of the EM than charge-sustaining operation for all VSP bins. EM power output during charge-depleting mode plateaued during VSP bins 5, 6, and 7, suggesting that the EM might have been at its peak power output during these VSP bins.

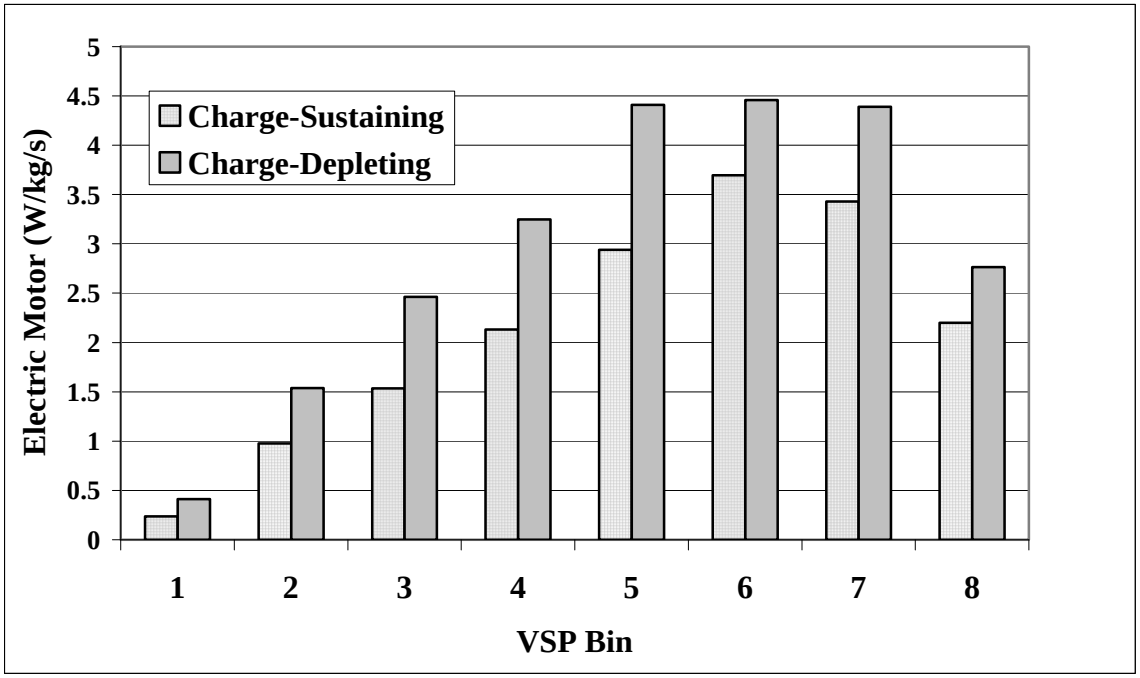

Figure 9.8: Electric motor power output between charge-depleting and charge-sustaining mode according to VSP bin.

Similar to what was reported during the VSP bin analysis, the charge-depleting operating mode better utilized the EM to meet the PHEV's immediate on-road work demands. This trend is particularly noticeable during slower, stop-and-go, in-town driving, as seen with both suburban and urban driving. During highway operation, high vehicle velocities resulted in a proportionally larger amount of the work output from the dICE compared to the EM for both modes of operation. As a consequence of the convergence of the two operating modes, conclusive statistical significance was not achieved during the ANOVA and Kruskal-Wallis analyses of EM power output as a response to operating mode during highway travel.

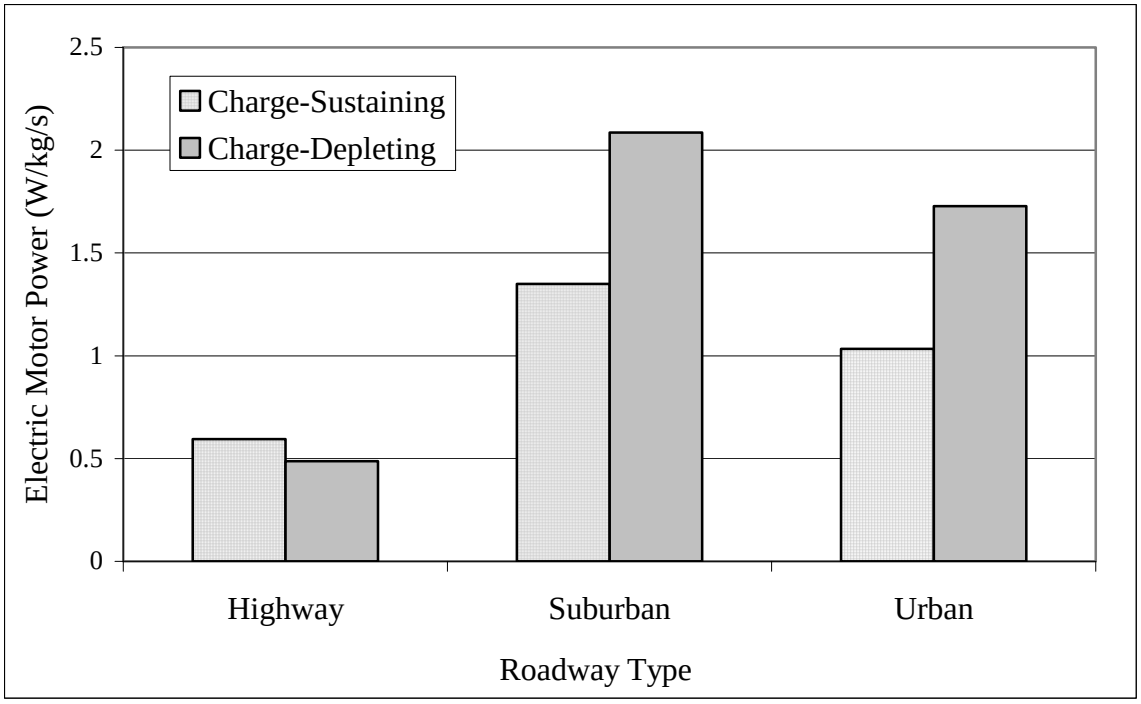

Figure 9.9: Electric motor power output between charge-depleting and charge-sustaining mode according to roadway type.

Where the relative changes in the rates of dICE recruitment through VSP bin varied according to operating mode, the rates of increased EM use with progressive VSP bin did not demonstrate significant differences between the operating modes. Except for the rates of change between VSP bins 5 and 6, the rate of increasing EM use remained consistent between charge-depleting and charge-sustaining operation. As referenced in Figure 9.8, EM power output hits its maximum during charge-depleting operation under VSP bins 5, 6, and 7. The discrepancy in the rate of change of EM power usage between charge-depleting and charge-sustaining modes observed during the transition from VSP bins 5-6 is largely due to the plateau in EM power output exhibited during charge-depleting operation.

Table 9.9: Relative rates of increased EM demand in charge-sustaining versus charge-depleting modes according to VSP bin.

VSP Bins	% Change EM Power	
	CS	CD
1-2	122%	115%
2-3	44%	46%
3-4	33%	27%
4-5	32%	30%
5-6	23%	1%
6-7	-7%	-2%
7-8	-44%	-45%

Total power output appears to trend in a similar manner as dICE power output with VSP bin, showing a steady increase with higher calculated on-road loads. Because the dICE supplies a majority of the PHEV's on-road power, regardless of operating mode or VSP bin, this phenomenon makes quantitative sense. However, where the recruitment of the individual power sources was projected to vary according to operating mode and, hence, prominent control scheme, the total power output was expected to remain consistent regardless of operating mode. Contrary to expectation, the overall total power output reported during charge-depleting mode was significantly ($\alpha<0.025$) less than that required for charge-sustaining operation. This trend holds steady throughout all 8 VSP bins and roadway types. As mentioned previously, velocity and acceleration rates for each roadway type were scrutinized using ANOVA and Kruskal-Wallis tests in order to verify that the primary driving variables affecting on-road power demand were statistically the same regardless of the PHEV Sprinter's effective mode of operation. These results coupled with the control of ambient temperature and auxiliary system use through sample-run selection, indicate that the PHEV's on-road experience was the same

for each mode. Figures 9.10 and 9.11 illustrate the PHEV's total power demand according to operating mode for both the VSP bin categorization and roadway type.

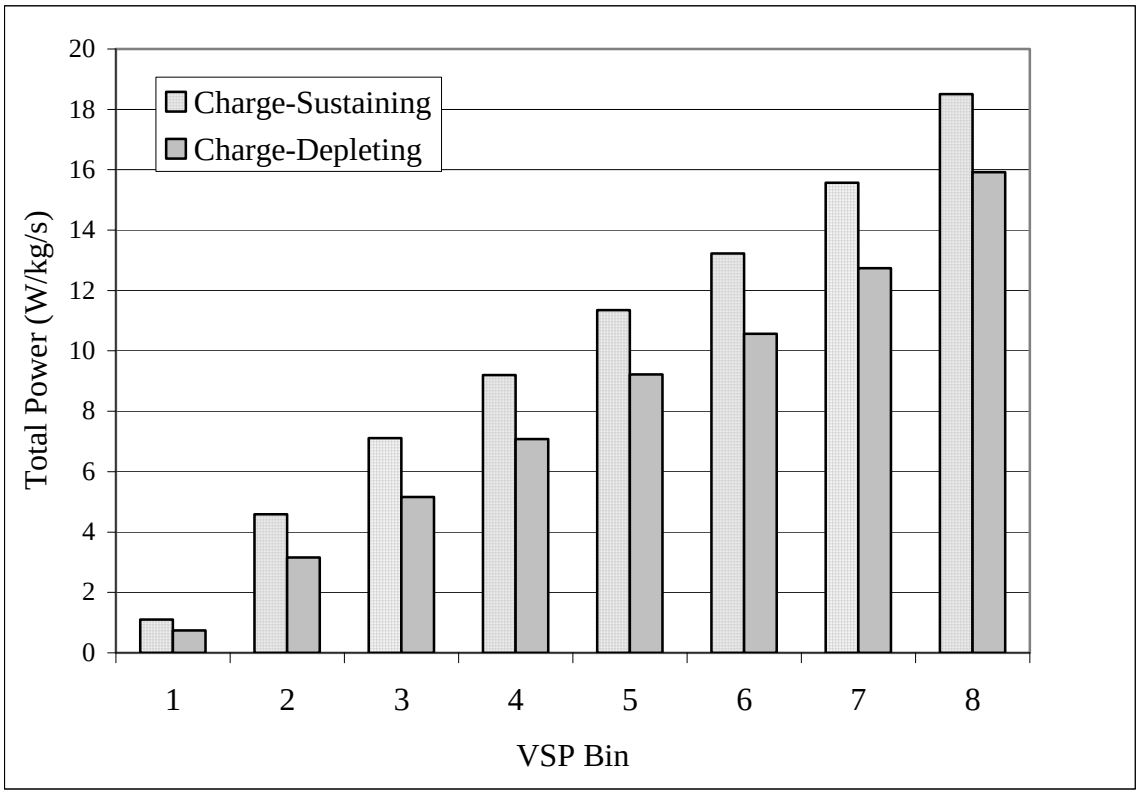

Figure 9.10: Total power output between charge-depleting and charge-sustaining mode according to VSP bin.

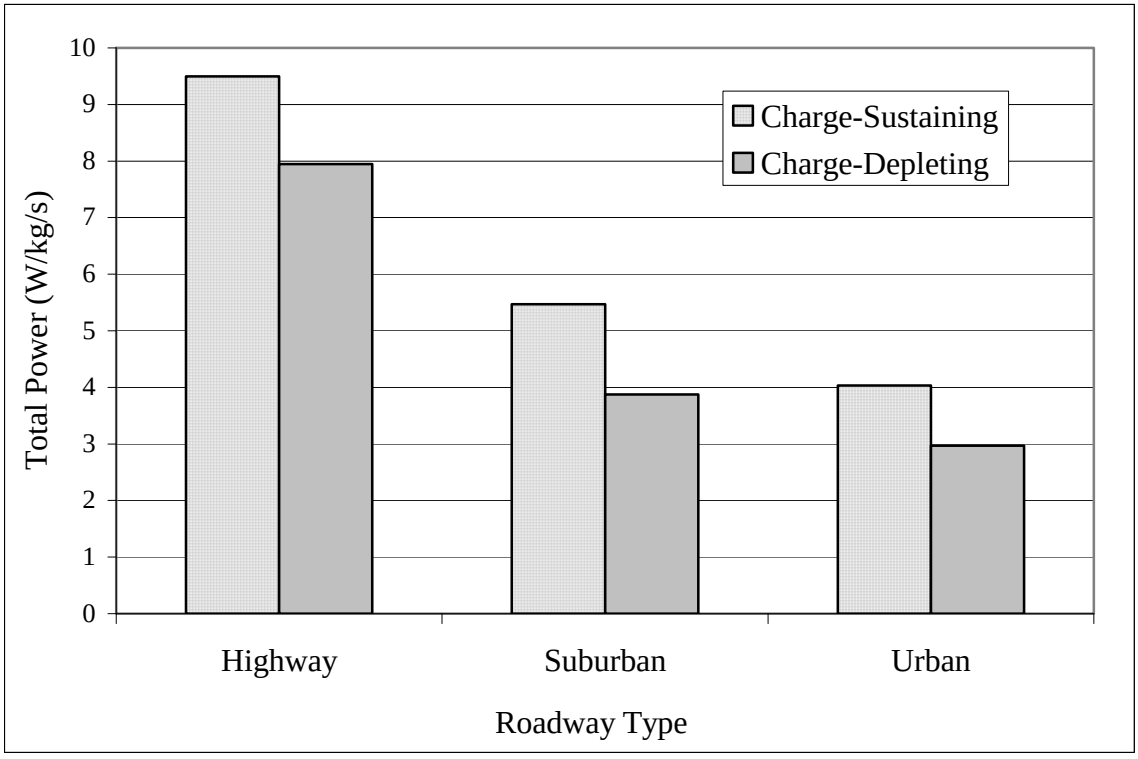

Figure 9.11: Total power output between charge-depleting and charge-sustaining mode according to roadway type.

Electric motors are inherently more efficient than internal combustion engines. The internal combustion engine is essentially a thermal engine converting the chemical energy of the fuel to energy released as pressure and temperature. It is estimated that the typical ICE loses 70-72% of its efficiency through heat alone (Baglione, et. al.). While the combustion process in the engine cylinders produces enough pressure to turn the engine's crankshaft, the majority of the energy created during the combustion process leaves the vehicle as heat in the exhaust system. Additional efficiency losses in the ICE process include parasitic losses (approximately 5-6%) due to system components such as the water pump and alternator, drivetrain losses (estimated at 5-6%), and power-to-wheels losses due to rolling resistances, aerodynamic drag, and braking heat losses (Department of Energy, 2011). While some of these losses are common to electric

vehicles (power-to-wheels and certain parasitic losses), electric vehicles have a tank-to-wheels efficiency that is a factor of three higher than internal combustion engines (European Commission Mobility & Transport, 2011).

Despite the inherent noise from uncontrollable factors embedded in on-road emissions and operating data, the increased efficiency gained from EM employment translated to an overall reduced PHEV Sprinter power output regardless of the roadway being navigated or the VSP bin being operated within. The percent differences in total power output between charge-sustaining and charge-depleting modes according to both VSP bin and roadway type are provided in Tables 9.10 and 9.11.

Table 9.10: Percent differences in total power between the PHEV Sprinter's operating modes according to VSP bin.

VSP Bin	% Difference CS vs CD
1	38.3%
2	37.1%
3	31.8%
4	26.0%
5	20.7%
6	22.4%
7	20.0%
8	15.0%

Table 9.11: Percent differences between the PHEV Sprinter's operating modes according to roadway type.

Roadway Type	% Difference CS vs CD
Highway	17.8%
Suburban	34.1%
Urban	30.4%

Based on total power output, charge-depleting mode was more efficient than charge-sustaining mode. This phenomenon was particularly noticeable under low road load scenarios, when the EM provided a proportionally larger amount of the PHEV Sprinter's power. With increased power demands, the PHEV's control scheme naturally migrated to more dICE-dependent operation, regardless of acting operating mode. This shift in the PHEV's power scenario translates to the relative power demands of each operating mode. As VSP bin increased, the difference in total power output between the operating modes diminished, so much so that during VSP bin 8 only a 15% difference in work output was exhibited between charge-depleting and charge-sustaining mode. Similarly, the roadways with the lowest power demands resulted in the largest deviation between total work required between charge-sustaining and charge-depleting operation. High load roadways, in this case highway travel, still benefited with increased overall efficiency from charge-depleting operation, but the benefit was reduced due to increased dICE involvement.

Electrical recuperation proved to be extremely sensitive to operating mode. Since the primary intent of charge-depleting operation is to maximize the electric-only drive capacity of the PHEV's design by best utilizing excess battery capacity, electrical recuperation during this mode was at a minimum. Most of the PHEV's ability to sequester energy potential inherent in on-road driving was presented during more conventional operation, which corresponds to charge-sustaining mode. Periods of transmission downshifting and subtle braking result in electrical-recuperation, so dICE functioning is a direct link to recuperation rates. Figures 9.12 and 9.13 display the PHEV

Sprinter's recuperation rates according to operating mode for both methods of categorization: VSP bin and roadway type.

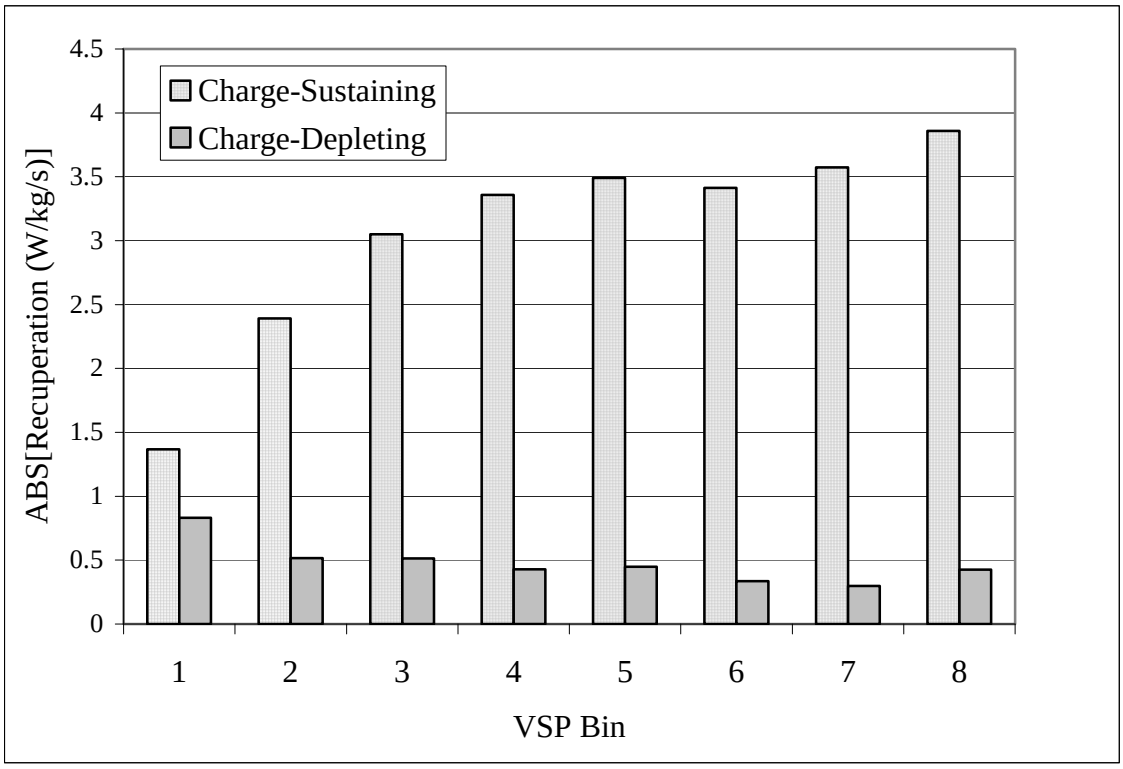

Figure 9.12: Recuperation rates according to operating mode by VSP bin.

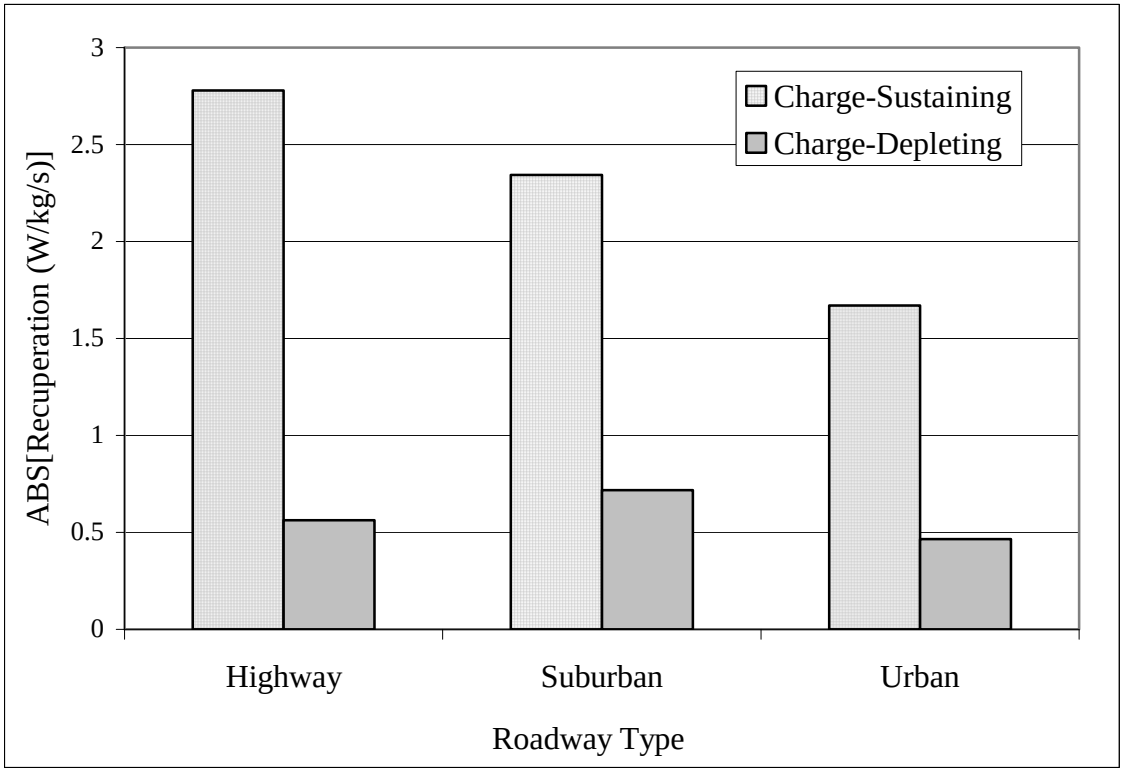

Figure 9.13: Recuperation rates according to operating mode by roadway type.

9.4 Pollutant Emissions

Most of the exhaust component emissions and fuel use trended with ICE use. The overall correlation analysis presented earlier showed that during both charge-sustaining and charge-depleting operation, exhaust emissions of carbon dioxide, nitrogen oxide, and, consequently, NOx, correlated very strongly with dICE power output. Nitrogen dioxide proved to be less, but still moderately correlated with dICE power output regardless of operating mode. In accordance with the correlation analysis, pollutant emissions whose production is most directly related to the dICE operation and combustion processes within the engine behave in a similar manner to dICE power output when compared between the operating modes across VSP bins or roadway types. Appendix E provides tables comparing the correlation results from each operating mode against each other segregated according to roadway type. While differences exist between the operating modes with regards to power output and use, exhaust emissions, and fuel use, the relative behaviors of the variables as responses to one another, as determined by Pearson's correlation coefficients, was not impacted by the PHEV Sprinter's operating mode.

MANOVA tests were performed on the fuel and emissions data as a function of operating mode and either VSP bin or roadway type on the continuous dataset. In all cases, the dependent variables (component exhaust emissions and fuel use) proved to be statistically significant responses to both VSP bin and operating mode and roadway type and operating mode ($\alpha<0.05$). Multivariate analyses were used as a precursor analysis prior to all univariate testing in order to establish at least a baseline level of statistical significance within the continuous dataset.

Univariate statistical analysis of the PHEV Sprinter's fuel use and exhaust emissions according to VSP bin and roadway type showed statistically significant response of all variables to operating mode, for both ANOVA and Kruskal-Wallis testing. Stringent levels of significance ($\alpha<0.025$ for analysis of the continuous dataset and $\alpha<0.05$ for sample-run compiled dataset) were maintained for all analyses.

Table 9.12: Summary of statistical analyses for PHEV emissions and fuel use according to operating mode, by VSP bin for the continuous dataset.

VSP Bin	1	2	3	4	5	6	7	8
Fuel, gal/s	y	y	y	y	y	y	y	y
CO_2, g/s	y	y	y	y	y	y	y	y
CO, g/s	n	Inc1	Inc2	y	y	y	y	y
NOx, g/s	y	y	y	y	y	y	y	y
NO, g/s	y	y	y	y	y	y	y	y
NO_2, g/s	y	y	y	y	y	y	y	y
HC, g/s	y	Inc1	y	y	Inc1*	y	y	y
Exhaust Temp (deg C)	y	y	y	y	y	y	y	y

Inc1: y anova, n kw

Inc2: n anova, y kw

Table 9.13: Summary of statistical analyses for PHEV emissions and fuel use according to operating mode, by roadway type, for the continuous dataset.

	Overall	Urban	Suburban	Highway
Fuel, gal/s	y	y	y	y
CO_2, g/s	y	y	y	y
CO, g/s	y	Inc2	y	y
NOx, g/s	y	y	y	y
NO, g/s	y	y	y	y
NO_2, g/s	y	y	y	y
HC, g/s	y	y	y	y
Exhaust Temp (deg C)	y	y	y	y

Inc1: y anova, n kw

Inc2: n anova, y kw

Table 9.14: Summary of statistical analyses for PHEV emissions and fuel use according to operating mode, by roadway type, for the compiled, sample-run based dataset.

VSP BIN	Overall	Urban	Suburban	Highway
Fuel, gal/s	y	y	y	n
CO_2, g/s	y	y	y	n
CO, g/s	y	n	y	y
NOx, g/s	y	y	y	y
NO, g/s	y	y	y	y
NO_2, g/s	y	y	y	n
HC, g/s	y	n	y	n

Inc1: y anova, n kw
Inc2: n anova, y kw

Exhaust temperature was included with the emissions' analytical efforts. Deviations in the PHEV Sprinter's measured exhaust temperatures are an indication of the dICE's operation, giving insight into the amount of time that the dICE was operational as well as the extent to which the dICE was warmed up. For the following analyses, exhaust temperature will be used as a possible indicator of transient dICE operation. While specific pollutant emissions that are a direct product of the combustion reaction, such as carbon dioxide, will remain tied with fuel use regardless of the state of dICE warm-up, by-products of internal combustion engine operation such as carbon monoxide, hydrocarbons, and nitrogen dioxide are generally formed during more transient, non-steady-state dICE operation. A precursory investigation into the PHEV Sprinter's exhaust temperatures may give some explanatory weight to the nature of the transient pollutants' formation and emissions.

As shown in summary tables 9.12 and 9.13, exhaust temperature proved to be a statistically significant response to operating mode when applied to the continuous dataset. As mentioned above, exhaust temperature was not included in the compiled,

sample-run based dataset, and was, therefore, not available for analysis on this level. While this discussion is limited to the overall dataset, inclusive of both hybrid and electric-only operation within each operating mode, the general trends reported here apply to the exhaust temperature investigation when limited to dICE-operation only (hybrid) as will be presented in the following chapter focusing on the diesel ICE's operation within the plug-in hybrid matrix. Consistent with the dICE's relative power output in each operating mode, charge-depleting operation resulted in statistically significantly lower exhaust temperatures than charge-sustaining mode.

The difference in exhaust temperature is particularly noticeable during lower on-road power demands, which represent periods of time when electric-only operation was highest, regardless of operating mode, and the dICE power demand was minimized. As on-road power demand increased, exhaust temperature increased for both operating modes, however, this change is more marked during charge-depleting operation. The average exhaust temperature between bins 1 and 8 increased only 41ºC during charge-sustaining operation, but during charge-depleting mode, the mean exhaust temperature between VSP bins 1 and 8 increased by 54ºC.

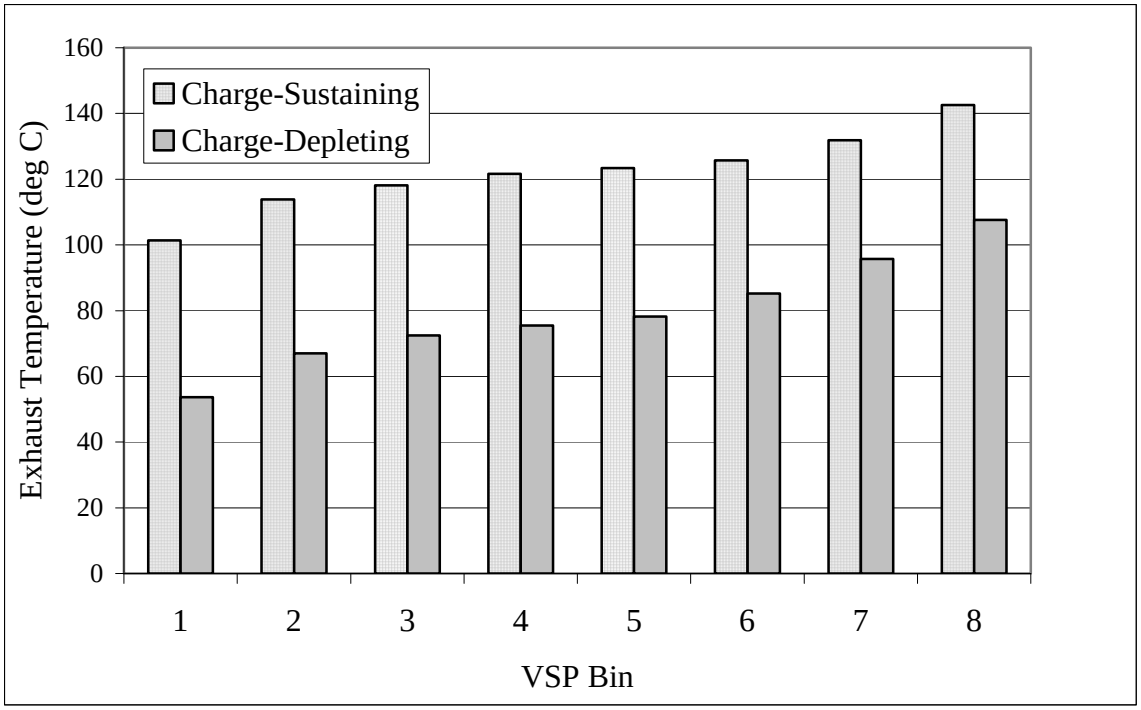

Figure 9.14: PHEV's exhaust temperature according to operating mode by VSP bin.

Similarly, the PHEV's exhaust temperature was significantly lower during charge-depleting mode according to the different roadway types (Figure 9.15). The deviation between charge-sustaining and charge-depleting mode was largest during in-town driving, when electric-only operation was more fully utilized during charge-depleting operation. The difference between the operating modes became less expansive during highway travel, when dICE use became a stronger function of travel velocity than active operating mode.

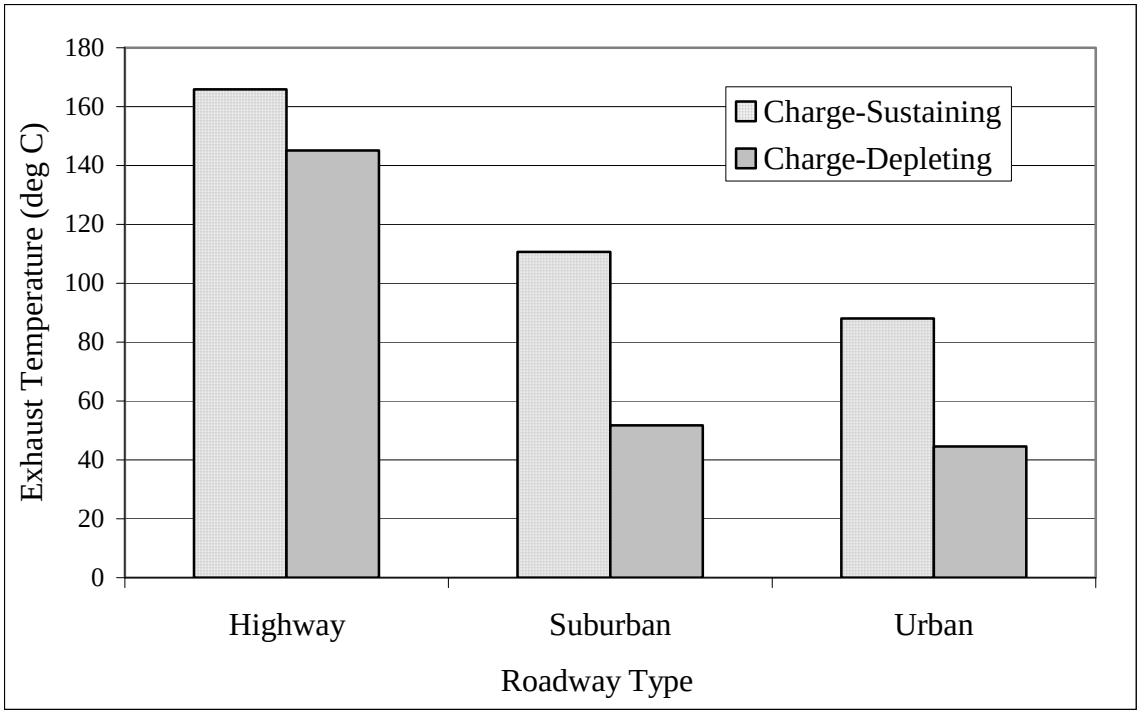

Figure 9.15: PHEV's exhaust temperature according to operating mode by roadway type.

Fuel use was consistently higher during charge-sustaining mode, regardless of VSP bin or the roadway type being navigated. Consistent with dICE power output, the PHEV Sprinter's fuel use increased with increasing VSP bin (and, consequently, on-road power load) throughout the entire VSP range. In accordance with relative dICE power output, charge-depleting operation was reliably more fuel-efficient than charge-sustaining mode. While charge-sustaining mode consistently resulted in higher rates of fuel use for all VSP bins and roadway types, the percent difference in fuel use between the operating modes decreased as on-road power load increased. This is particularly prevalent when assessing the roadway types. Diesel ICE utilization during charge-depleting mode was most prominent during highway operation when the on-road velocities reached a level that mandated higher dICE recruitment. As a result of this increased dICE power use, the

relative fuel use between charge-sustaining and charge-depleting modes is the closest during highway travel when compared with in-town driving.

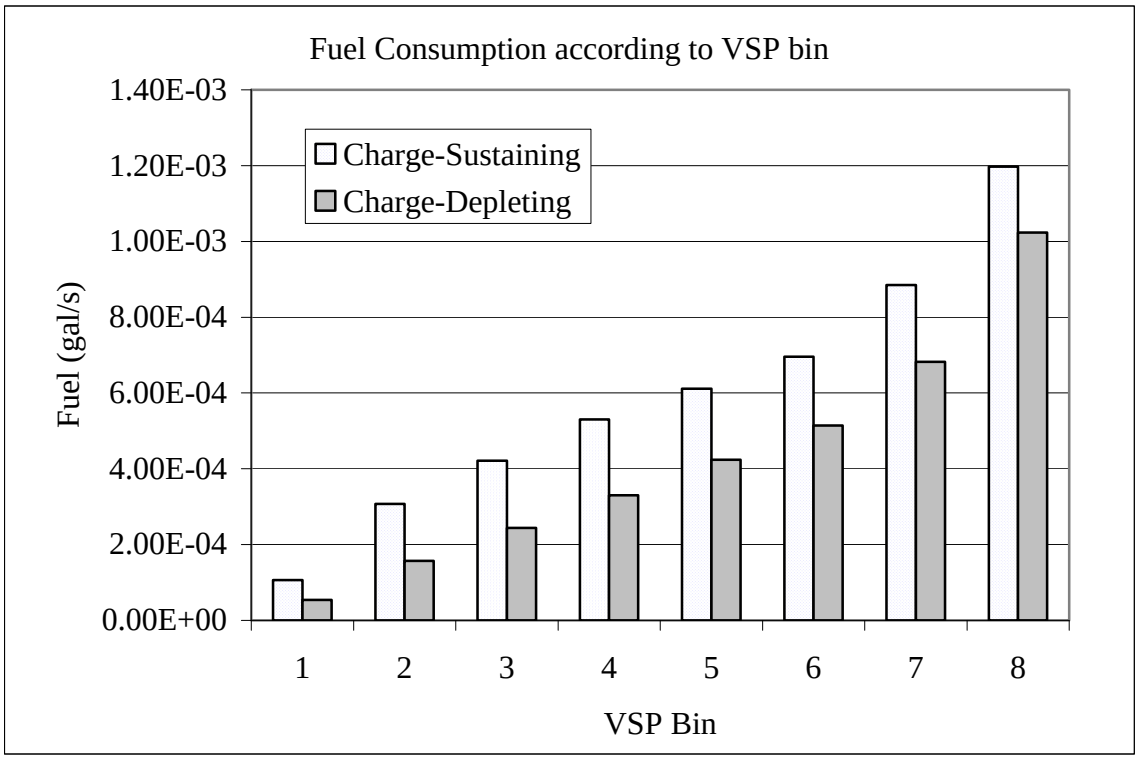

Figure 9.16: Fuel use according to operating mode, segregated by VSP bin.

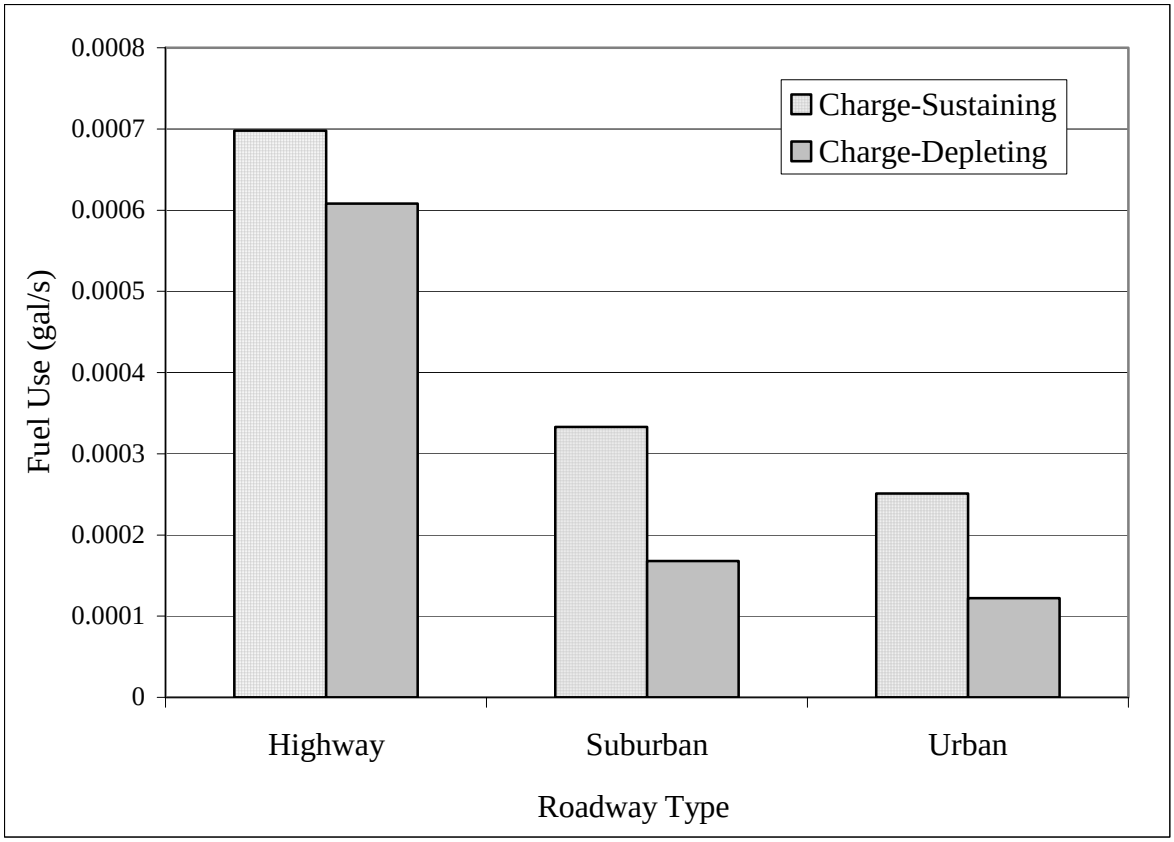

Figure 9.17: Fuel use according to operating mode, segregated by roadway.

Similar to fuel use, carbon dioxide (CO_2) emissions fell in strong accordance with dICE power output. As a direct product of the combustion reaction, CO_2 emissions proved to directly track with dICE power output to a statistically significant level during the overall correlation analysis, the VSP investigation, and the roadway-type evaluation. As a result of this, the general trend in CO_2 emissions with increasing road load and with differing roadway type was a direct translation of dICE power output both in overall magnitude and in the relative difference between the two operating modes. Both operating modes experienced increasing CO_2 emissions with increased VSP bin, with charge-sustaining mode resulting in higher CO_2 emissions overall than the more electric-intensive charge-depleting mode.

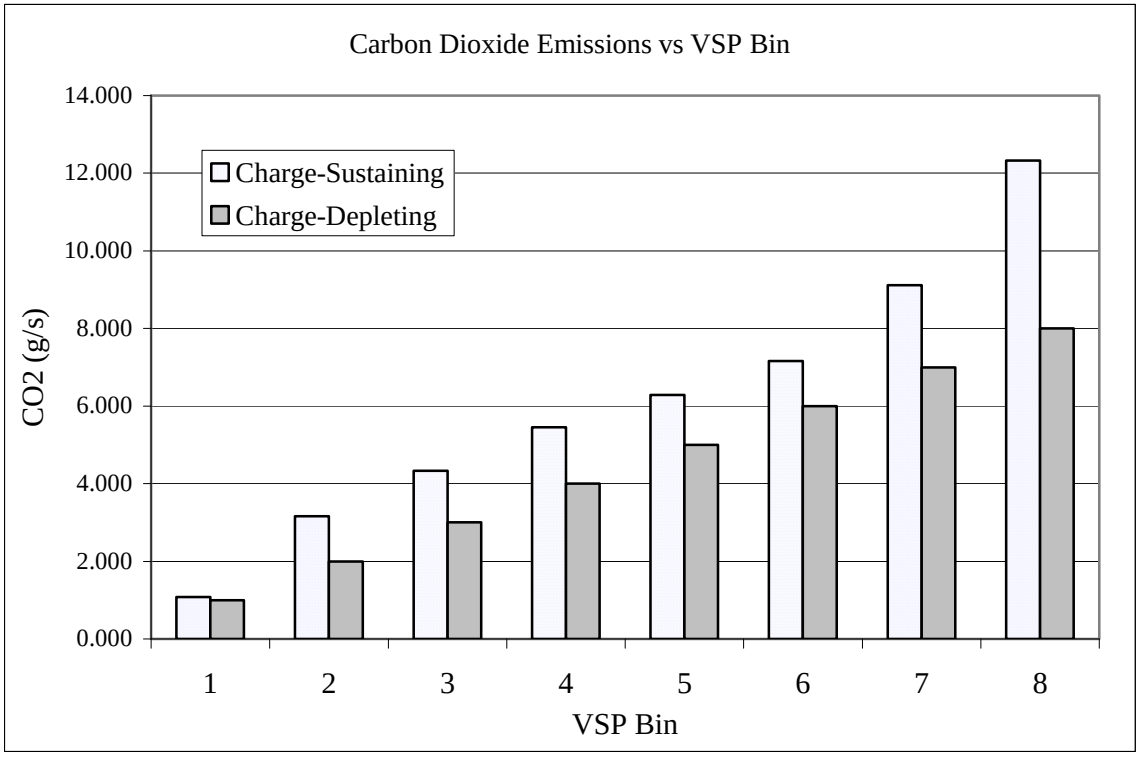

Figure 9.18: Carbon dioxide emissions according to operating mode, by VSP bin.

Carbon dioxide emissions also proved to be a statistically significant response to operating mode when the data were segregated according to roadway type. For all designated roadways, charge-depleting operation resulted in lower overall CO_2 emissions than charge-sustaining mode, in accordance with dICE power output. This difference dropped considerably as the PHEV traveled on the highway route, where high vehicle velocities became a more dominant function of control scheme, resulting in increased dICE recruitment regardless of battery state of charge. The highway results were somewhat inconclusive, as statistical significance was found at the $\alpha<0.025$ level for the continuous dataset, but not at the $\alpha<0.05$ level for the equivalent analysis of the sample-run compiled dataset.

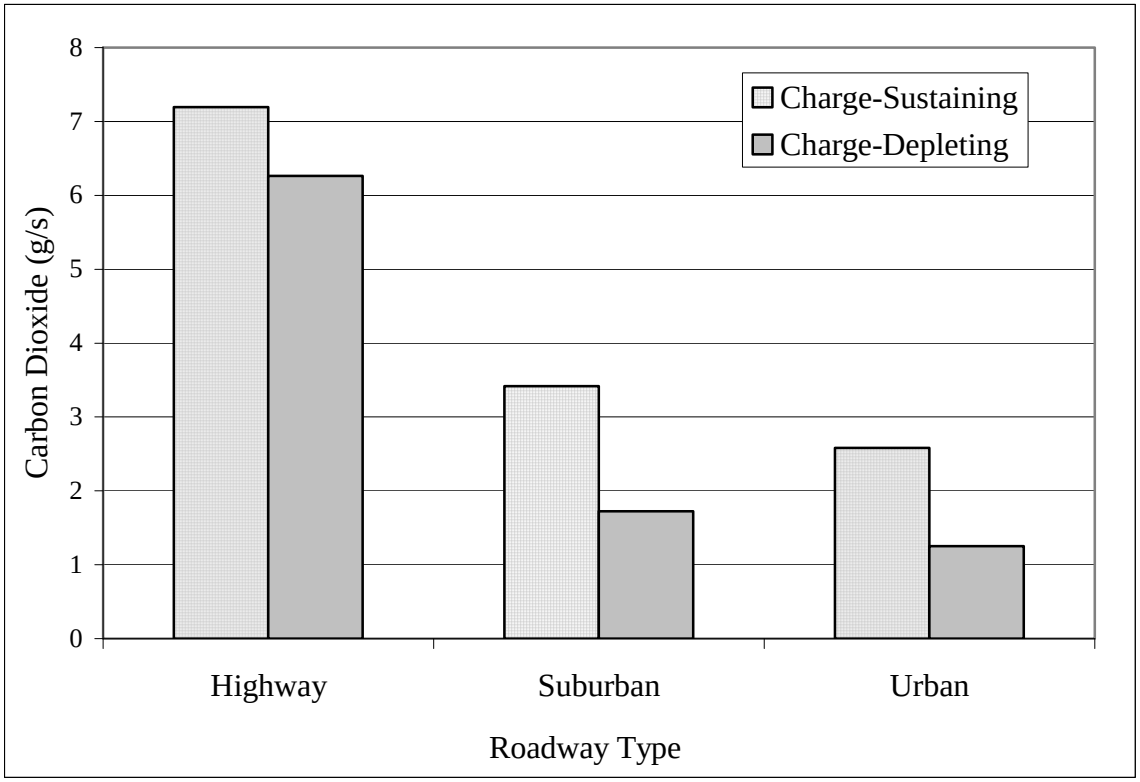

Figure 9.19: Carbon dioxide emissions according to operating mode, by roadway type.

While not a direct product of the combustion reaction, the nature of nitrogen monoxide (NO), or nitric oxide, formation in a vehicle's exhaust tends to correlate with the dICE's operation, so that as power output and fuel demands increase, so does the level of NO in the vehicle's exhaust. With increased power output, the vehicle's overall air flow through the engine, and resulting exhaust temperature increases, leading to conditions favorable for the formation of NO (when relatively inert nitrogen pass-through from the combustion chamber reacts with excess, un-reacted oxygen to form NO in the exhaust during periods of sufficiently high temperature and pressure). As a consequence of this, the PHEV Sprinter's NO exhaust emissions have followed the same general trends as dICE power output. Nitrogen monoxide emissions not only increased with

increasing dICE power output, but they were consistently and meaningfully higher during charge-sustaining mode compared to charge-depleting mode. While the overall trend and relative behavior of NO emissions was similar to dICE power output, fuel use, and CO_2 emissions, the proportional difference in NO emissions between the operating modes was more significant, with NO emissions during charge-sustaining mode being considerably higher than charge-depleting mode (between 80%-100% higher during VSP bins 1 through 4, gradually tapering to 32% higher by VSP bin 8). Acting exhaust temperatures may have played an additional role in NO formation. The statistically lower exhaust temperatures observed during charge-depleting operation may have inhibited the NO formation pathway during this operating mode resulting in larger differences in NO emissions between the operating modes than witnessed with CO_2 emissions or fuel use.

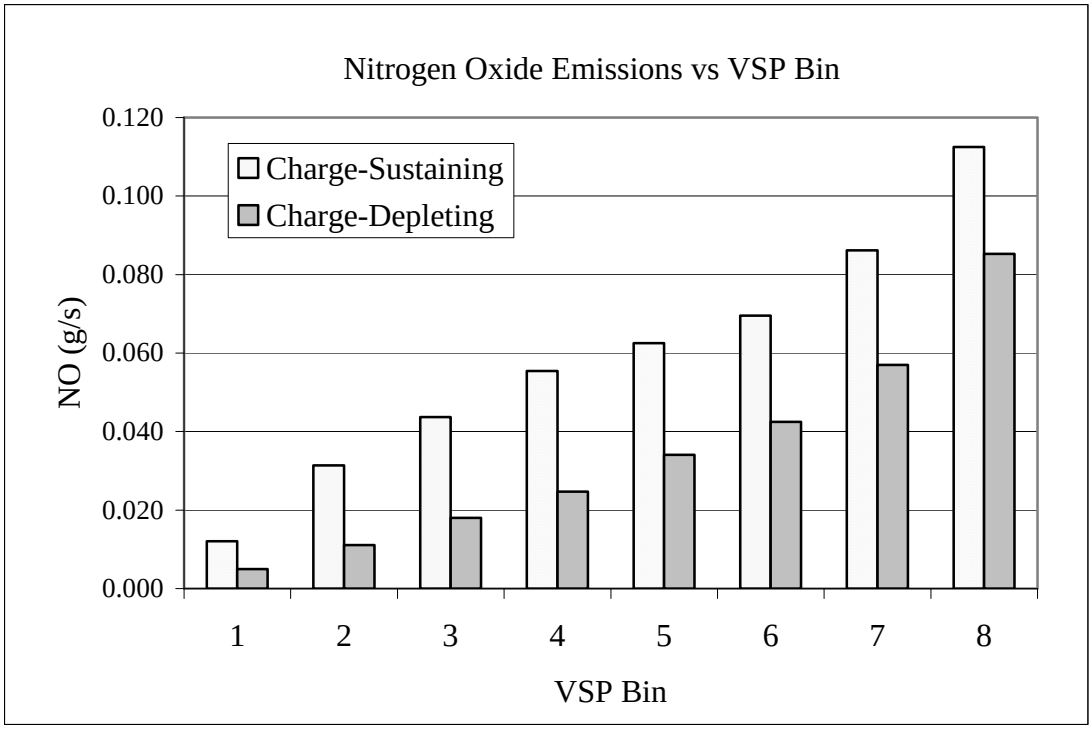

Figure 9.20: Nitrogen monoxide emissions according to operating mode, by VSP bin.

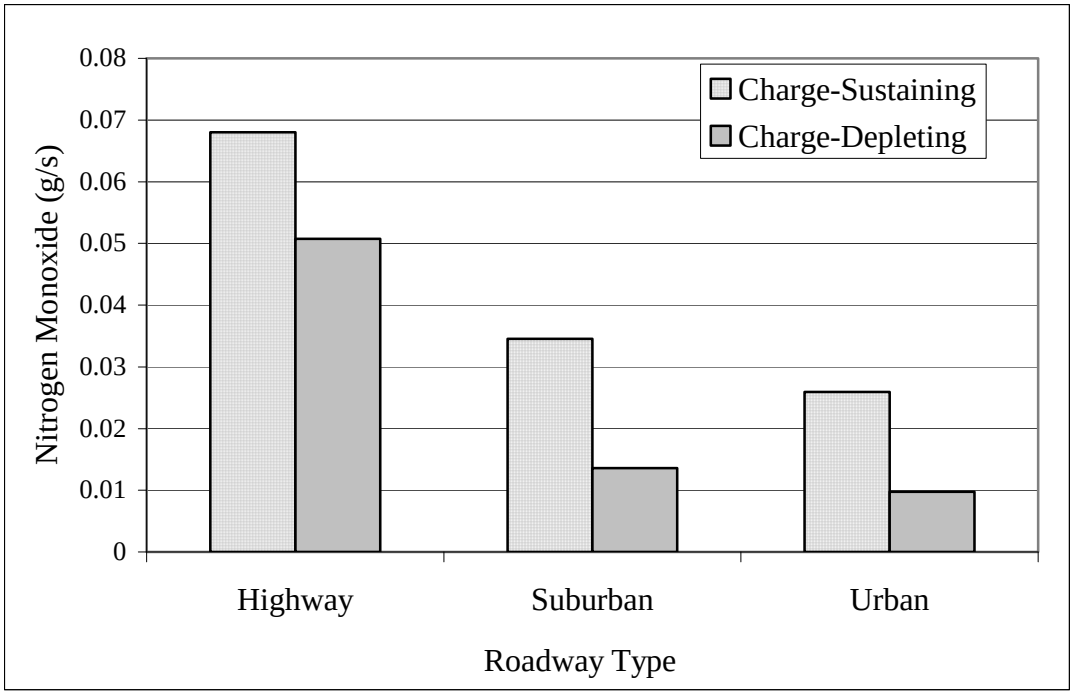

Figure 9.21: Nitrogen monoxide emissions according to operating mode, by roadway type.

Nitrogen dioxide (NO_2) emissions also demonstrated a statistically significant response to operating mode for both the VSP bin and roadway analyses. Nitrogen dioxide emissions were consistently higher during charge-sustaining mode across all 8 VSP bins with the largest deviation between modes occurring in bins 2, 3, and 4. Where charge-sustaining NO_2 emissions demonstrated a period of plateaued growth with increasing VSP bin during bins 4, 5, and 6, charge-depleting NO_2 emissions continued to increase with increasing VSP bin (on-road power demand). This relative difference in NO_2 behavior between the operating modes does not correspond to dICE power output, as dICE power output showed a constant increase with VSP bin for both operating modes. With the available PHEV operating data limited to power output and exhaust conditions (temperature and flow rate), there is not enough information available to

discern why the operating modes exhibit different growth in NO_2 emissions with increasing on-road power demand.

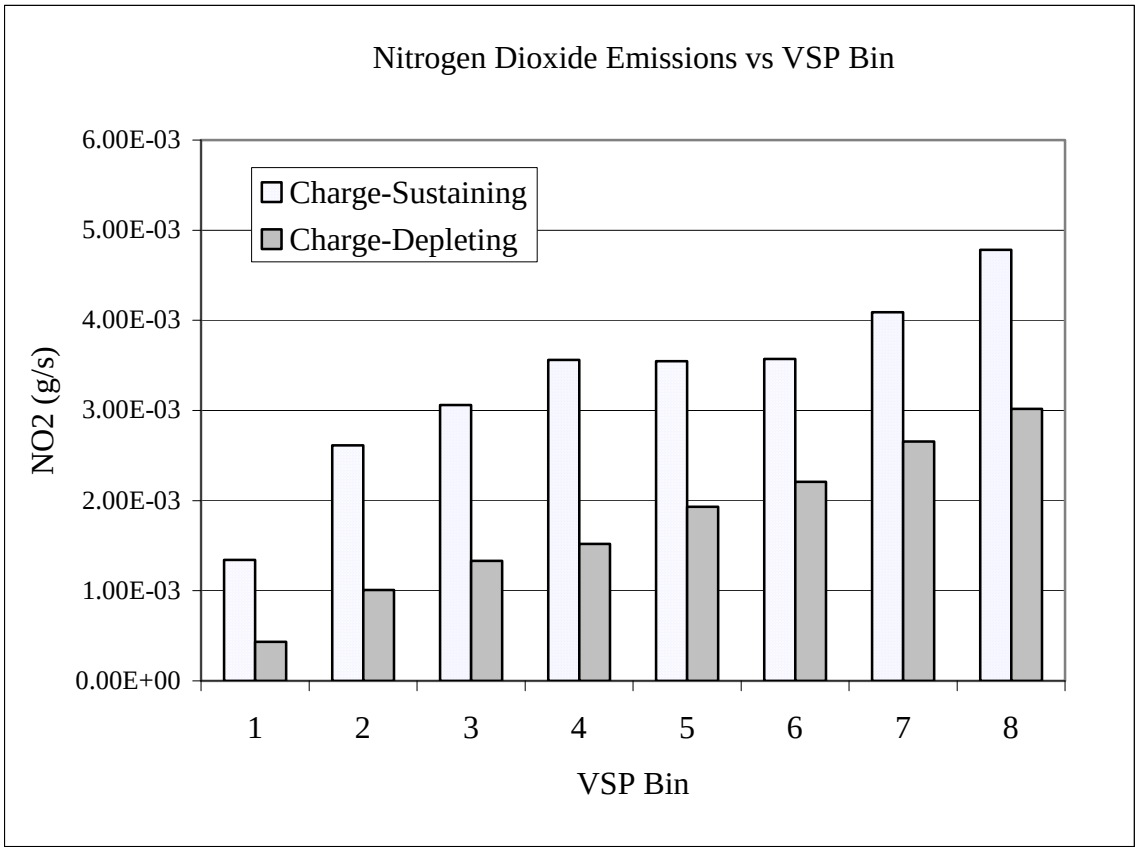

Figure 9.22: Nitrogen dioxide emissions according to operating mode by VSP bin.

Similar to the VSP investigation, NO_2 emissions were consistently lower during charge-depleting operation during all in-town travel, where the electric-only operation was maximized. This trend reversed during highway travel, at which point charge-depleting operation became the prominent NO_2 producer. Statistical analysis of highway travel was somewhat inconclusive, showing statistical significance at the $\alpha<0.025$ level for the continuous dataset, but failing at the $\alpha<0.05$ level for the analyses on the compiled, run-based dataset. Despite this, it can still be concluded that internal

conditions within the dICE and PHEV's exhaust system became much more conducive to NO_2 formation during charge-depleting highway travel than the slower, more stop-and-go in-town roadways.

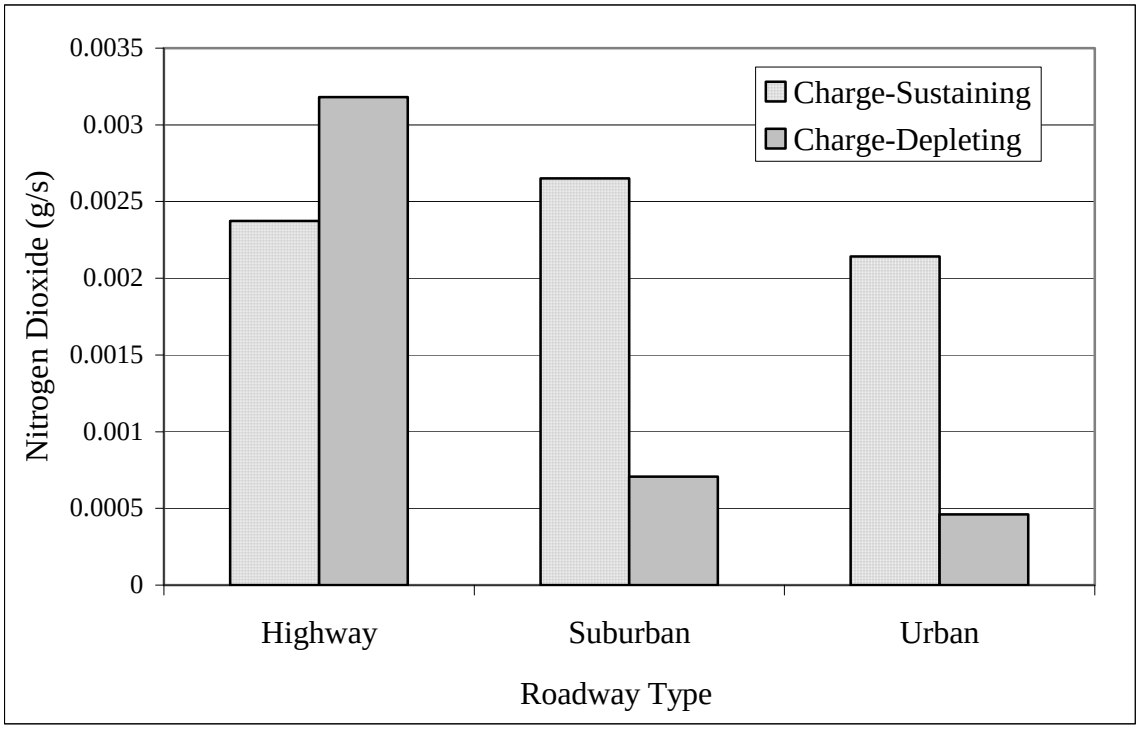

Figure 9.23: Nitrogen Dioxide emissions according to operating mode, by roadway type.

Quantitatively, NOx emissions (a product of NO and NO_2 formation), tended to reflect NO emissions most strongly, due to the shear magnitude of NO formation compared with NO_2 formation (generally an order of magnitude higher on average across the 8 VSP bins). Because of this, the graphical representation of NOx emissions between the operating modes according to either VSP bin or roadway type is very similar to that reported earlier for NO emissions.

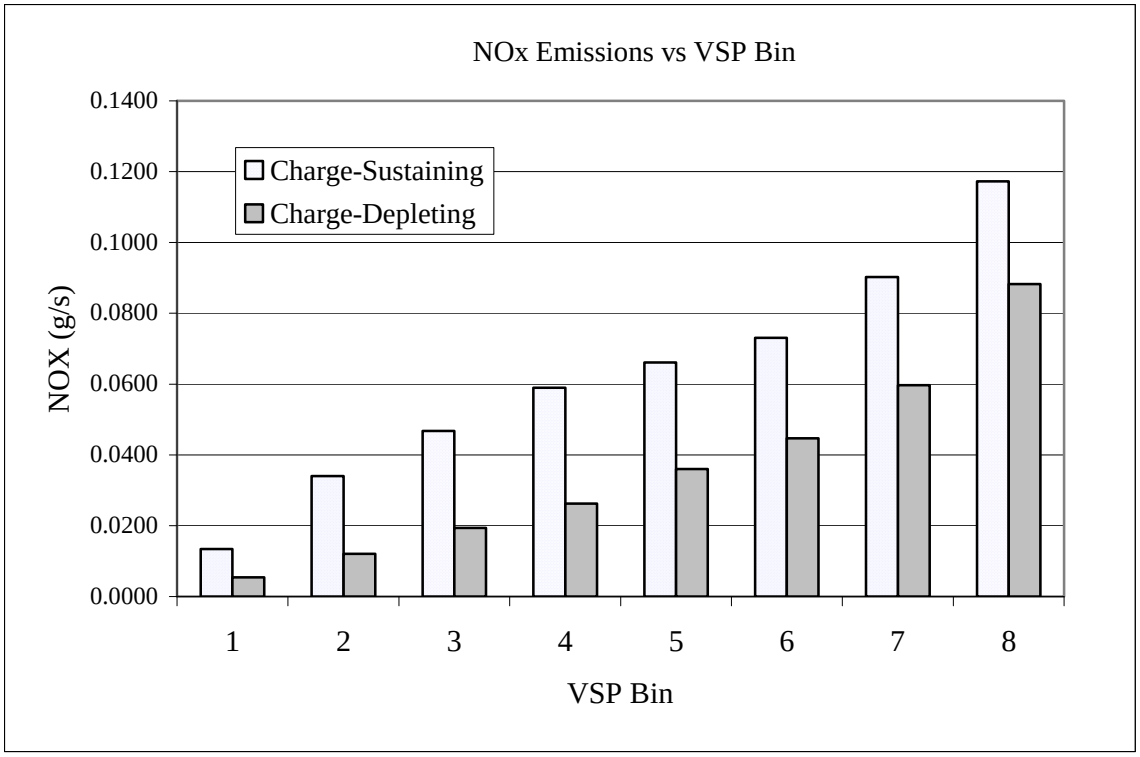

Figure 9.24: NOx emissions according to operating mode, by VSP bin.

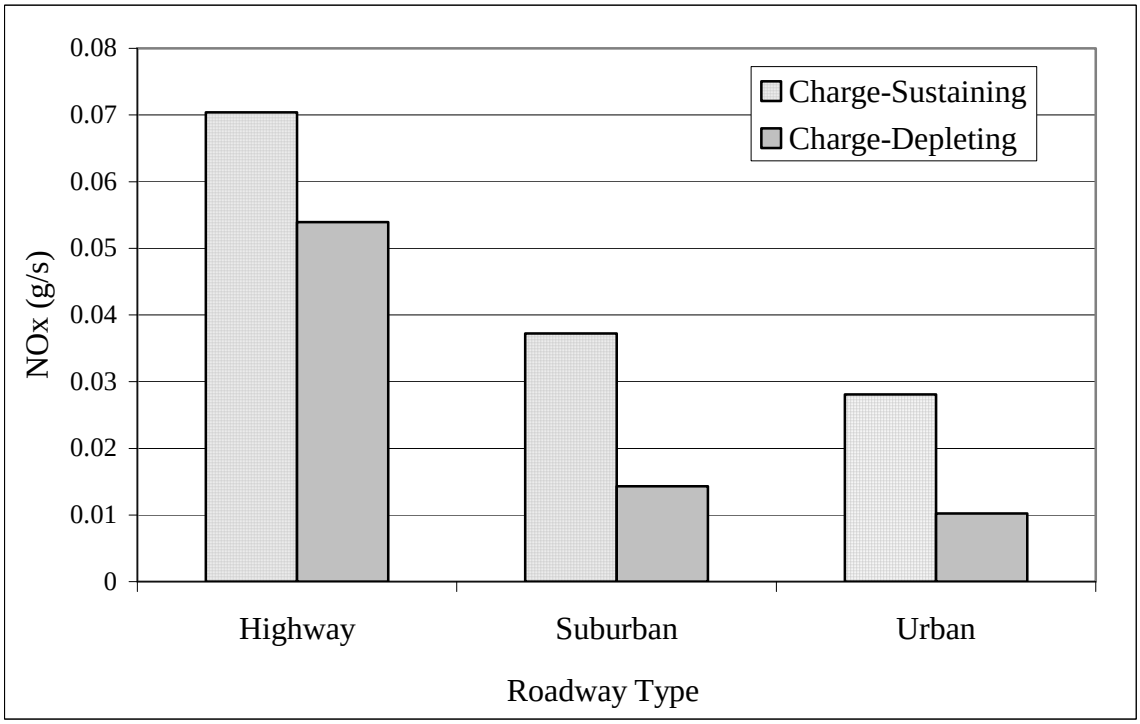

Figure 9.25: NOx emission according to operating mode, by roadway type.

Contrary to the general trend found with CO_2 and NOx emissions, carbon monoxide and hydrocarbon emissions did not correspond to dICE power output between the two operating modes. Both CO and HC emissions are unintended by products of the combustion reaction and ICE operation. Because of this, more transient ICE operation will promote CO formation and HC pass-through and emissions due to the ICE's deviation from its normal, ideal, steady state operation. Periods of immediate, intense increases in on-road power demand, as well as cold-starts will produce more transient ICE operation, and, consequently, result in higher CO and HC emissions. Because of this, these emissions are best discussed in the context of ICE operation rather than just ICE power output.

Charge-depleting operation generally resulted in higher CO emissions. Statistical significance in CO emissions between the operating modes was not achieved in VSP bin 1, and the statistical results were inconclusive for VSP bins 2 and 3, failing the Kruskal-Wallis test for the analysis of Bin 2 and failing the ANOVA for the analysis of bin 3. However, statistical analysis of VSP bins 4 through 8 conclusively (passing both the ANOVA and Kruskal-Wallis tests) showed that CO emissions were a significant response to operating mode, with the highest CO emissions occurring during charge-depleting operation. As the PHEV Sprinter attempts to maximize its electric-only operation during charge-depleting mode, it still requires dICE power assist during periods of high on-road load. Employing the dICE in an assisting fashion like this results in more occurrences where the dICE is cycled on and off. Conversely, during charge-sustaining operation, the amount of electric-only operation is greatly limited by the low state of battery charge, and the dICE on/off cycling occurs less frequently as the PHEV operates

in a more consistent, hybrid manner with the dICE providing a majority of the power output and the EM supplying power assist where appropriate and available. While the exact nature of the dICE's on/off cycling will be investigated in more detail in the following chapter, the increased transient dICE operation during charge-depleting operation is clearly witnessed in the heightened CO emissions that occur during the PHEV's "cleaner and more efficient" method of operation. Figure 9.26 displays CO emissions according to operating mode for each VSP bin. As on-road loads increased (increasing bin) the relative difference in CO emissions between the operating modes increased proportionally. Table 9.15 provides the percent increase in CO emissions of charge-depleting mode over charge-sustaining mode across the VSP bins.

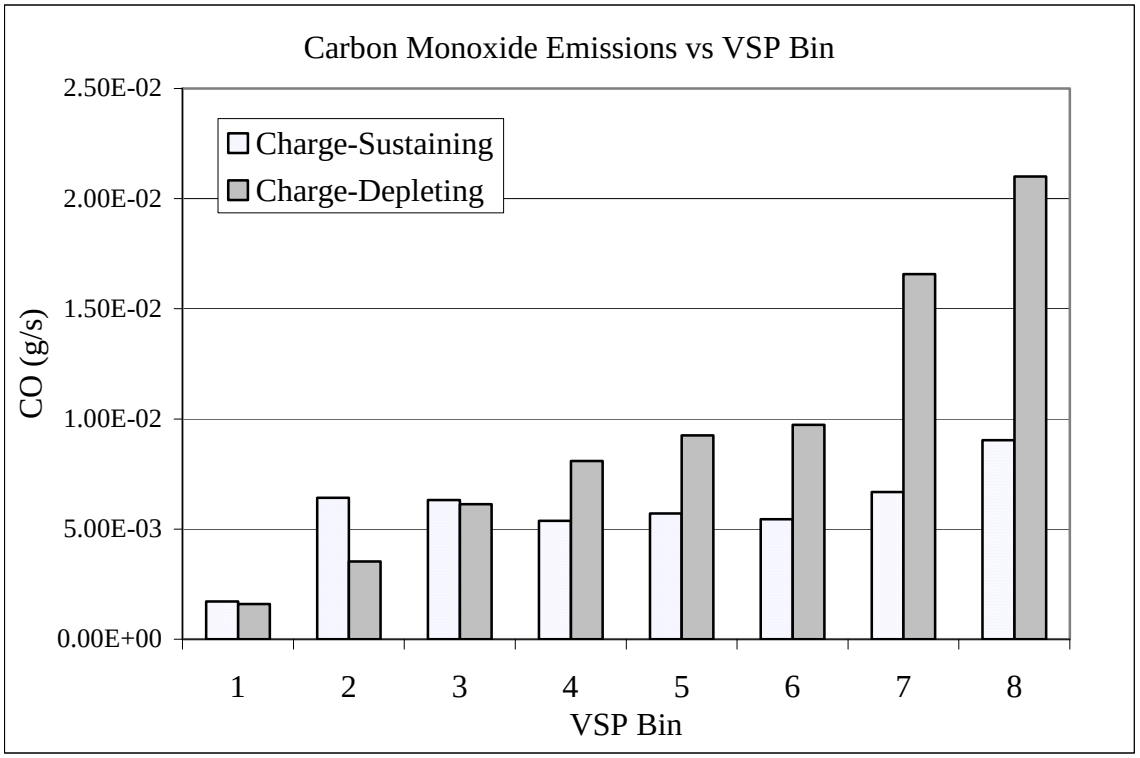

Figure 9.26: Carbon monoxide emissions according to operating mode by VSP bin.

Table 9.15: Percent increase in CO emissions between operating modes across VSP bins.

VSP Bin	% Difference CD vs CS
1	-7.5%
2	-45.0%
3	-2.8%
4	50.5%
5	62.2%
6	78.7%
7	148.4%
8	132.2%

With respect to roadway types, carbon monoxide emissions were also higher during charge-depleting mode. This phenomenon was found to be statistically significant for all analyses of highway and suburban roadway travel. Analyses, however, of the urban roadways were inconclusive. Both ANOVA and Kruskal-Wallis tests failed to demonstrate statistical significance at the $\alpha<0.05$ level when evaluating CO emissions as a response to operating mode when applied to the compiled, run-based dataset. Additionally, statistical results investigating CO emissions according to operating mode for the continuous urban-based dataset remained inconclusive, failing the ANOVA but passing the Kruskal-Wallis test ($\alpha<0.025$). The power investigation conducted earlier did not suggest that the overall power distribution during urban travel was significantly different than that observed during suburban or highway travel for each operating mode. However, an investigation of overall power output does not give any insight into the actual instances in which and how the individual power sources are being utilized. These phenomenons will be given more attention in the following section.

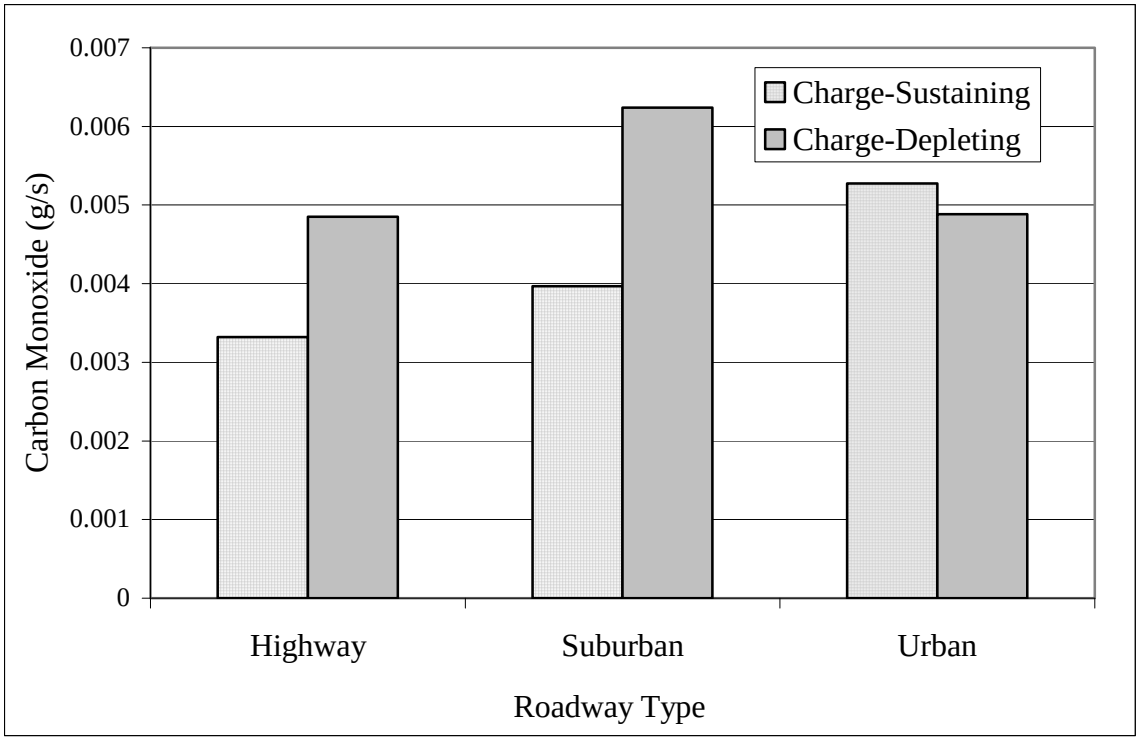

Figure 9.27: Carbon monoxide emissions according to operating mode by roadway type.

Similar to carbon monoxide emissions, the PHEV's hydrocarbon emissions did not directly correspond to the dICE power output. While the overall increase in dICE power output with increased on-road load is reflected in the observed hydrocarbon emissions, the relative amount of hydrocarbons in the PHEV's exhaust between operating modes did not correspond to the relative difference in dICE power output required for each operating mode. Hydrocarbon presence in a vehicle's exhaust can be due to a multitude of factors, however, when intact hydrocarbon fractions from a vehicle's fuel source present in the exhaust stream, they are the result of nonreacted fuel from the exhaust chamber. This can be due to excessively lean conditions resulting in inadequate oxygen for complete combustion, and, when present in a properly tuned vehicle, is often

observed during periods of transient ICE operation. In the case of the PHEV Sprinter, the more transient dICE operation during charge-depleting mode resulted in increased emissions of incomplete combustion products such as hydrocarbons and carbon monoxide. The following chapter will give specific attention to the diesel ICE's behavior in each operating mode, but the general trend in hydrocarbon emissions will be discussed here.

Hydrocarbon emissions increased with increased road-load for both operating modes, however, charge-depleting operation resulted in significantly higher hydrocarbon emissions despite this operating mode's reduced reliance on dICE power output. Hydrocarbon emissions proved to be statistically significant responses to active operating mode for all VSP bins except bins 2 and 5. Both bins were statistically inconclusive passing the ANOVA test but failing the level of significance established for the Kruskal-Wallis test. VSP bin 5 did not lie far outside of the statistical bounds set for the continuous dataset with the resulting p-value for the failed Kruskal-Wallis test at 0.030. The relative difference in hydrocarbon emissions between operating mode with increasing VSP bin was relatively consistent with charge-depleting mode resulting in between 69% to 84% higher hydrocarbon emissions than charge-sustaining operation.

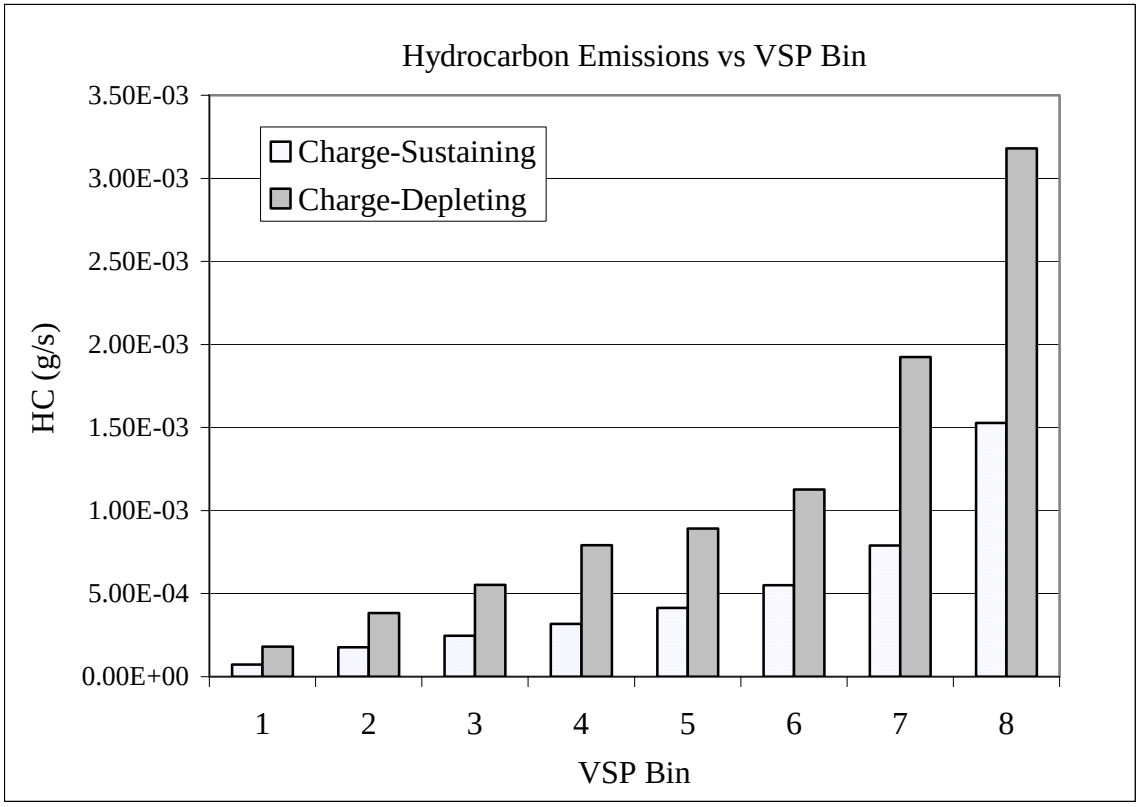

Figure 9.28: Hydrocarbon emissions according to operating mode by VSP bin.

Analysis of the continuous dataset indicated that hydrocarbon emissions were a statistically significant response to operating mode according to VSP bin as well as for all designated roadway types ($\alpha<0.025$). Figure 9.29 highlights the significant difference in hydrocarbon emissions for the three roadway designations, with charge-depleting operation resulting in dramatically higher levels of hydrocarbon emissions during in-town driving (63.4% higher on urban roadways, 99.8% greater during suburban travel, and only 20.9% greater on the highway). However, when the same statistical methods were applied to the compiled, run-based dataset, statistical significance fell apart, with only suburban travel meeting the established criteria of $\alpha<0.05$.

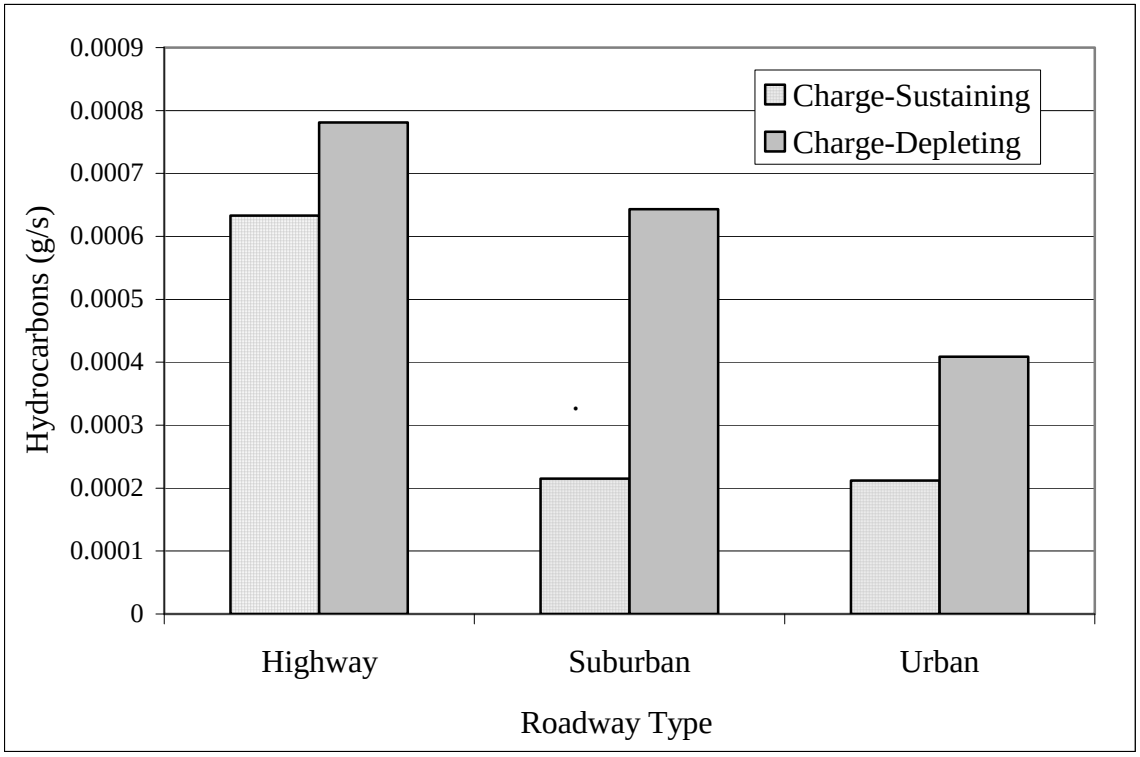

Figure 9.29: Hydrocarbon emissions according to operating mode by roadway type.

The following chapter will give more focused attention to the intricacies of the diesel ICE's behavior and operation in the different operating modes. In addition to significant differences in dICE and EM power output between the operating modes, statistically significant differences were found in the exhaust temperatures between the modes. Observed exhaust temperatures will fluctuate according to ICE use. During each operating mode, higher average reported exhaust temperatures is an indication of two possibilities: first, the diesel ICE was operational a larger proportion of the time, and secondly, the diesel ICE experienced longer periods of run time allowing it to fully warm-up between periods of electric-only operation. The PHEV Sprinter was equipped with a direct-oxidation catalyst (DOC) employed to reduce the amount of carbon monoxide and hydrocarbons in the PHEV's exhaust. No data pertaining to the DOC was

provided by the DLM, so the only feedback available concerning the DOC's operation is based on CO and HC exhaust emissions and exhaust temperature. Direct oxidation catalysts function when fully warmed up. Since these catalysts are generally heated via passive exhaust flow, periods where the diesel ICE is routinely cycled on and off line may not allow the DOC to fully reach its optimum temperature, resulting in excessive breakthrough of both carbon monoxide and hydrocarbon compounds. Based on the data available, it is not possible to discern whether excessive CO and HC emissions during charge-depleting mode are due to transient dICE operation or ineffective DOC utilization.

9.5 Concluding Remarks

Operating mode proved to be a statistically significant factor when assessing the PHEV Sprinter's power output, recuperation rates, and exhaust pollutants. Statistical significance at the $\alpha<0.025$ was consistent regardless of level of analysis, and was found for the overall dataset as well as when the data were segregated according to VSP bin and roadway type. Generally speaking, the excess battery capacity that defines charge-depleting operation resulted in lower power output from the diesel-ICE, which translated to higher average fuel efficiency. Charge-depleting mode's enhanced fuel efficiency waned with increasing road load demands as the diesel ICE was more strongly employed in order to meet the performance demands of high VSP and high velocity (highway travel) operation. At high loads and velocities the respective control schemes between the operating modes began to converge despite the different states of battery charge (stored electric capacity).

Pollutant emissions whose formation is most closely tied with the combustion process and internal combustion engine operation demonstrated trends that were consistent with dICE power output. Charge-depleting operation resulted in lower exhaust emissions of carbon dioxide, nitrogen oxide, and nitrogen dioxide compared with charge-sustaining operation, and the relative emission of each exhaust component increased with increasing road-load (evaluated by VSP bin). Paralleling dICE power output, the difference in carbon dioxide and NOx emissions diminished with increasing road load as dICE recruitment during charge-depleting mode became more in line with its utilization during charge-sustaining operation.

While a specific, more in depth analysis of the diesel ICE's role within each operating mode was not addressed here, a perfunctory investigation using exhaust temperature was performed. Exhaust temperature provides a limited degree of insight into the dICE's operation. Lower average exhaust temperatures are indications of periods when the dICE is off-line for large periods of time, or when the dICE is not running for sufficiently long periods of time to allow a proper warm up. Exhaust temperature proved to be a statistically significant response to operating mode, with charge-depleting operation resulting in the lowest average exhaust temperatures. Carbon monoxide and hydrocarbons both had higher emissions during charge-depleting mode, even though the dICE (the cause of all emissions) was used less. Higher carbon monoxide and hydrocarbon emissions that occurred during charge-depleting operation suggest more frequent transient dICE operation during this mode. Both carbon monoxide and hydrocarbons are by-products of the normal combustion processes, and their formation occurs during periods when the dICE's functioning has deviated from normal steady state resulting in lower than normal operating efficiencies.

Despite all of the reported nuances between the operating modes, electric motors are inherently, on a thermodynamic level, more efficient than internal combustion engines. Total power output was actually less during charge-depleting than charge-sustaining operation, indicating that the higher EM recruitment and use in charge-depleting mode resulted in lower overall power output to travel the same roads. A velocity and acceleration analysis between the roadways was conducted in order to verify that the on-road profiles during each operating mode were statistically the same. This work coupled with the effort to remove confounding impacts from ambient temperature

and auxiliary system use through sample run selection, ensured that the driving parameters during each operating mode were the same, so observed differences between modes was due to the actual differences between the modes.

Chapter 10: Diesel Internal Combustion Engine Use in PHEV Concept

10.1 Introduction

As a plug-in-hybrid vehicle employing a diesel internal combustion engine (dICE), the Kansas City-based PHEV Sprinter was truly a novel vehicle. The available research to date concerning hybrid-electric vehicles (HEVs) has focused primarily on gasoline-fueled HEVs. While several light-duty HEVs are for sale in the United States with additional model releases each year, none of the production based hybrid electric vehicles are based on a diesel-fueled platform. As light-duty diesel-fueled vehicles begin their reemergence into the U.S. market, interest and awareness into the efficiency advantages of diesel-based transportation for the general populace has grown markedly over the past several years. However, despite public acceptance of the hybrid-electric vehicle and the growing number of passenger-based diesel cars, the concept of a diesel-HEV is still in its infancy, and, until the Daimler/Chrysler PHEV efforts, a diesel-based plug-in hybrid electric vehicle was nonexistent.

Hybrid-electric vehicles feature very different drivetrains and control schemes than conventional ICE-propelled cars and trucks. The purpose of the HEV platform is to increase the vehicle's efficiency by employing electrical assist and allowing the vehicle to sequester what was once lost potential energy for the purposes of running vehicle systems and providing motive power. Plug-in hybrid technologies advance the HEV concept through on-board storage of grid-derived electrical capacity, giving the PHEV the ability to both operate as an electric vehicle, a hybrid-electric vehicle simultaneously using energy from the electric motor and internal combustion engine, and a conventional vehicle operating solely on the energy output of the internal combustion engine. The

PHEV context, novel in its advanced technology as an alternatively fueled vehicle, is also novel in its employment of the diesel-based internal combustion engine. Continuous on and off cycling of the ICE during PHEV operation imposes additional stresses on the ICE that are rarely encountered during conventional vehicle, or even HEV, operation.

Because the On-Road Emissions and Characterization PHEV Sprinter study was focused on a single vehicle, no additional Sprinter vans based on other drivetrains were available for comparative study. It is not possible to truly discern whether the diesel internal combustion engine of the Kansas City PHEV Sprinter was operating more or less efficiently in the PHEV framework than a more conventional diesel-based Sprinter or one of the gasoline-powered PHEV Sprinters developed as part of the Phase I proof of concept study.

Original expectations for the Kansas City PHEV Sprinter were that it would be not just a superior vehicle regarding overall efficiency, but that it would be a superior plug-in hybrid vehicle due to the increased fuel efficiency of the diesel engine compared to the gasoline combustion engines employed in the other PHEV Sprinter prototypes. As shown previously, this expectation was not realized during the on-road study where the KC PHEV actually reported lower overall fuel efficiencies than that cited for the gasoline-based PHEV Sprinters. On-road payload and operation are highly influencing factors regarding a vehicle's efficiency and resulting emissions. Because of this, it is not justifiable to judge the diesel PHEV based on a single, and independently garnered, measure of efficiency. This discrepancy, however, did promote interest in the nuances behind the diesel ICE's employment in the PHEV setting.

The previous section provided an in-depth assessment of the PHEV Sprinter's two operating modes: charge-depleting and charge-sustaining. While the following investigation is still comparatively based on the charge-sustaining versus charge-depleting question, the PHEV's power scenario within each operating mode is further dissected. Each operating mode possessed periods of on-road travel in electric-only or zero-emissions operation, where 100% of the PHEV's motive power was provided by the electric motor and the diesel-ICE was completely shutdown. Additionally, each mode had periods of ICE-dominant or "hybrid" operation (as defined by the experimenter) where the PHEV was being powered by the diesel-ICE with or without the assist of the electric motor (EM). For each designated operating mode, the PHEV's electric-only and hybrid operation will be investigated.

10.2 Electric Drivetrain

Similar to previous investigations, ANOVA and Kruskal-Wallis statistical tests provided the basis for the determining statistical significance in the emissions and operating data between the different modes of operation (charge-depleting and charge-sustaining). Evaluating the diesel ICE's behaviors between the operating modes was not conducive to the sample-run based analysis which has, prior to this investigation, been performed contiguously with the analyses of the continuous datasets. Only the second-by-second continuous data was utilized for the following discussions. In order to minimize the risk of performing a Type I error and inadvertently establishing statistical significance where none exists, stringent criteria put into place ($\alpha<0.025$) for basing statistical significance.

Electric-only operation was determined by the position of the hybrid clutch. When the clutch was open (100%), the electric motor (EM) was the sole source of power and the dICE was turned off. The dICE came on-line when the hybrid clutch was closed (<100%). Using these criteria, the full dataset used for the VSP, Roadway Type, and Operating Mode investigations was segregated according to the PHEV Sprinter's primary power source. ANOVA and Kruskal-Wallis tests were performed on the electric-only and hybrid data, evaluating the effect that operating mode (charge-depleting versus charge-sustaining) had on system (power) performance. Three primary scenarios were assessed: EM operation during electric-only operation, EM operation during hybrid mode, and dICE operation during hybrid mode.

The PHEV Sprinter's data-logging module (DLM) collected operating and on-road data directly from the PHEV's on-board computer. For each power source, engine

speed and torque were recorded. Additionally, current, voltage, and state of charge (SOC) were recorded from the battery subsystem. Regardless of the level of analysis (VSP bin, driving mode, or roadway type), the electric motor's operation during zero-emission driving was not a statistically significant response to operating mode (charge-depleting versus charge-sustaining).

Battery voltage is directly related to the battery's state of charge, so regardless of the level of analysis, battery voltage was a significant response to operating mode, as intuitively expected since battery state of charge was the criteria for defining operating mode for each second of on-road data collection.

Each respective engine's data were analyzed according to the two modal models presented in Chapter 6: vehicle specific power (VSP) binning, and driving mode. Additionally, the data were evaluated according to roadway type (urban, suburban, or highway) being traveled.

Table 10.1: Statistical summary of the EM during electric-only operation according to operating mode by VSP bin.

VSP BIN	1	2	3	4	5	6	7	8
EM Speed (RPM)	n	n	n	n	n	n	n	n
Battery Current (A)	Inc2	n	n	n	n	Inc1	n	n
Battery Voltage (V)	y	y	y	y	y	y	y	y
EM Torque (Nm)	y	n	n	n	n	y	n	n
EM Power (W/kg/s)	Inc2	n	n	n	n	y	n	n

Inc1: y anova, n kw
Inc2: n anova, y kw

Table 10.2: Statistical summary of the EM during electric-only operation according to operating mode by drive mode designation.

Driving Mode	Idle	Decel	Accel	Cruise
EM Speed (RPM)	n	n	n	n
Battery Current (A)	y	Inc2	n	n
Battery Voltage (V)	y	y	y	y
EM Torque (Nm)	y	y	n	n
EM Power (W/kg/s)	y	Inc2	n	n

Inc1: y anova, n kw
Inc2: n anova, y kw

Table 10.3: Statistical summary of the EM during electric-only operation according to operating mode by roadway type.

Roadway Type	Overall	Urban	Suburban	Highway
EM Speed (RPM)	y	n	y	n
Battery Current (A)	Inc1	n	Inc1	n
Battery Voltage (V)	y	y	y	y
EM Torque (Nm)	y	Inc2	Inc1	n
EM Power (W/kg/s)	y	Inc2	Inc1	n

Inc1: y anova, n kw
Inc2: n anova, y kw

During electric-only or zero-emissions driving, as the sole power source, the EM's behavior and power output were dictated entirely by the on-road load, not by the PHEV Sprinter's control scheme. Because of this, zero-emissions operation should be independent of operating mode.

Similarly, ANOVA and Kruskal-Wallis analyses were applied to the subset of data collected during the period of time that the PHEV Sprinter was operating in hybrid (as defined by hybrid clutch <100%) mode. Diesel ICE and EM responses are provided separately from one another, and, since they are a direct response of dICE operation,

exhaust emissions were assessed in conjunction with the dICE-specific data according to roadway type.

Contrary to zero-emissions driving, which resulted in similar EM operation regardless of active operating mode, during hybrid operation, the electric motor's operation did vary significantly according to charge-sustaining versus charge-depleting operation. Generally speaking, charge-depleting operation resulted in higher EM speeds, torque, and power output, suggesting that excess battery capacity affected the relative control strategies of the two power sources when utilized in conjunction with each other as a HEV.

Table 10.4: Statistical summary of electric motor behavior during hybrid operation according to operating mode (CD versus CS) operation by VSP bin.

VSP BIN	1	2	3	4	5	6	7	8
EM Speed (RPM)	y	y	y	y	y	n	y	n
Battery Current (A)	y	y	y	y	y	y	y	y
Battery Voltage (V)	y	y	y	y	y	y	y	y
EM Torque (Nm)	y	y	y	y	y	y	y	y
EM Power (W/kg/s)	Inc2	Inc2	y	y	y	Inc2	Inc2	y

Inc1: y anova, n kw
Inc2: n anova, y kw

Table 10.5: Statistical summary of electric motor behavior during hybrid operation according to charge-depleting versus charge-sustaining operation by drive mode.

Driving Mode	Idle	Decel	Accel	Cruise
EM Speed (RPM)	Inc1	Inc2	n	y
Battery Current (A)	y	Inc2	y	y
Battery Voltage (V)	y	n	y	y
EM Torque (Nm)	Inc1	n	y	y
EM Power (W/kg/s)	n	n	y	y

Inc1: y anova, n kw
Inc2: n anova, y kw

Table 10.6: Statistical summary of electric motor behavior during hybrid operation according to charge-depleting versus charge-sustaining operation by roadway type.

Roadway Type	Overall	Urban	Suburban	Highway
EM Speed (RPM)	y	n	y	Inc2
Battery Current (A)	y	y	y	y
Battery Voltage (V)	y	y	y	y
EM Torque (Nm)	y	y	y	y
EM Power (W/kg/s)	y	y	y	Inc2

Inc1: y anova, n kw
Inc2: n anova, y kw

Electric motor use during hybrid operation was consistently higher during charge-depleting mode across all 8 VSP bins. The EM's utilization between the VSP bins followed a less distinct trend when the battery capacity was high, indicating that specific road-based variables dictating on-road load were strong influences on the PHEV Sprinter's power designation. While the VSP equation was designed to provide a calculation method of accurately approximating a vehicle's on-road load, it is likely that the PHEV Sprinter responded to different road factors in different manners. For example, localized areas of immediate acceleration likely played a larger influence on the PHEV's relative power scheme than other on-road variables deemed influential by the VSP calculation (such as velocity or grade). Periods of immediate, transient fluctuations in road-based factors will result in dramatic changes in the PHEV's established power usage as the vehicle's control scheme attempts to maintain vehicle performance over all road conditions and operator requests. The EM's trend in power output across the VSP bins was somewhat less erratic during charge-sustaining mode, where the EM provided proportionally less of the PHEV Sprinter's total power output. Similar to the analysis of the entire dataset (electric-only and hybrid operation inclusive), EM power output peaked

around VSP bins 6 and 7 and then dropped off during VSP bin 8. This trend is consistent for both operating modes.

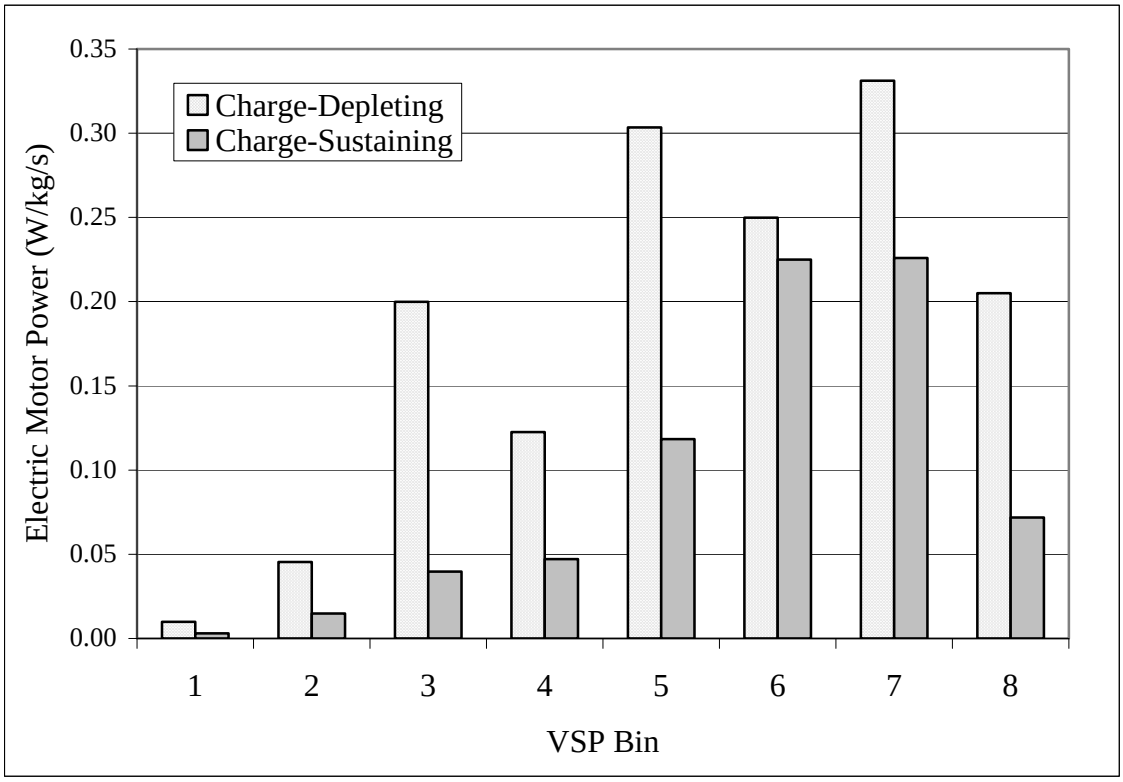

Figure 10.1: Electric motor power output during hybrid operation according to operating mode by VSP bin.

Significant differences exist between the operating modes when the EM power output during hybrid operation was assessed according to the designated roadway types. The PHEV's efforts to maximize its electric potential during periods of excess battery capacity are most significantly observed during urban operation, where the EM provides almost six times more power per second during charge-depleting mode compared with charge-sustaining mode.

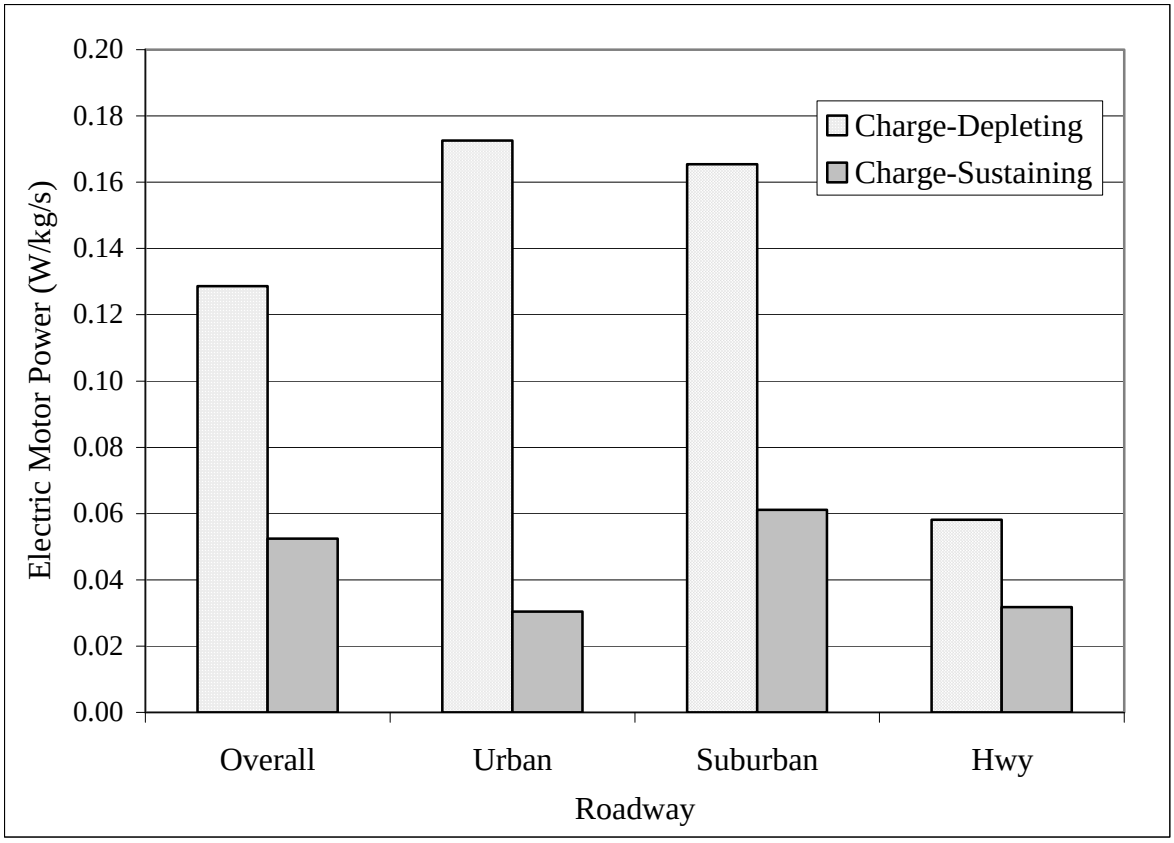

Figure 10.2: Electric motor power output during hybrid operation according to operating mode by roadway type.

10.3 Diesel Internal Combustion Engine

10.3.1 Power scheme

The diesel ICE was only employed during hybrid operation. With the hybrid clutch closed, the dICE functioned at some level of output during every second of hybrid driving, regardless of the PHEV Sprinter's active operating mode. The presence of the electric-only data will only serve to magnify the difference in the dICE's output between the operating modes (charge-sustaining versus charge-depleting), regardless of whether the PHEV was using the dICE differently during its active periods between the operating modes. Analyzing the dICE's operation in the absence of the electric-only data truly shows the differences in the dICE's utilization between operating modes. Statistical synopses of the dICE's behavior and power output according to operating mode are provided in Tables 10.7 through 10.9. Except for engine speed, all of the dICE's operating data (torque and power output) were conclusively statistically significant responses to operating mode, regardless of data categorization. Coupled with the EM results reported above, it is obvious that the control scheme used during hybrid operation was different according to the active driving mode, and was, therefore, strongly influenced by the PHEV Sprinter's battery capacity.

Table 10.7: Statistical summary of dICE behavior during hybrid operation according to charge-depleting versus charge-sustaining mode by VSP bin.

VSP BIN	1	2	3	4	5	6	7	8
dICE Power, W/kg/s	y	y	y	y	y	y	y	y
dICE Speed (RPM)	y	y	y	y	y	n	y	n
dICE Torque (Nm)	y	y	y	y	y	y	y	y
Exhaust Temp (degC)	y	y	y	y	y	y	y	y

Inc1: y anova, n kw
Inc2: n anova, y kw

Table 10.8: Statistical summary of dICE behavior during hybrid operation according to charge-depleting versus charge-sustaining mode by drive mode.

Driving Mode	Idle	Decel	Accel	Cruise
dICE Power, W/kg/s	y	y	y	y
dICE Speed (RPM)	Inc1	Inc1*	n	y
dICE Torque (Nm)	y	y	y	y
Exhaust Temp (degC)	y	y	y	y

Inc1: y anova, n kw
Inc2: n anova, y kw
*ANOVA P-Value: 0.021, KW P-Value: 0.028

Table 10.9: Statistical summary of dICE behavior during hybrid operation according to charge-depleting versus charge-sustaining mode by roadway type.

Roadway Type	Overall	Urban	Suburban	Highway
CO_2, g/s	y	Inc1	Inc1	y
CO, g/s	y	y	y	y
NOx, g/s	y	y	y	y
NO, g/s	y	y	y	y
NO_2, g/s	y	y	y	y
HC, g/s	y	y	y	y
dICE Power, W/kg/s	y	y	y	y
dICE Speed (RPM)	y	n	y	Inc2
dICE Torque (Nm)	y	y	y	y
Exhaust Temp (degC)	y	y	y	y
Recup, W/kg/s	y	y	y	y

Inc1: y anova, n kw
Inc2: n anova, y kw

For all VSP bins and roadway types assessed, the diesel ICE provided a higher power output during charge-sustaining mode compared with charge-depleting mode. The relative difference in dICE power output between the modes during hyrid driving was quantitatively consistent at all levels of analysis with charge-sustaining operation requiring between 15% and 30% more dICE power than charge-depleting operation for

all roadways evaluated. Regardless of operating mode, the dICE was the dominant power source during all hybrid operation, supplying, on average, 47 times more power than the EM during charge-depleting mode and 132 times more power than the EM during charge-sustaining mode. Quantitatively, the EM's power output during charge-sustaining mode, when the PHEV Sprinter did not hold excess battery capacity, was negligible.

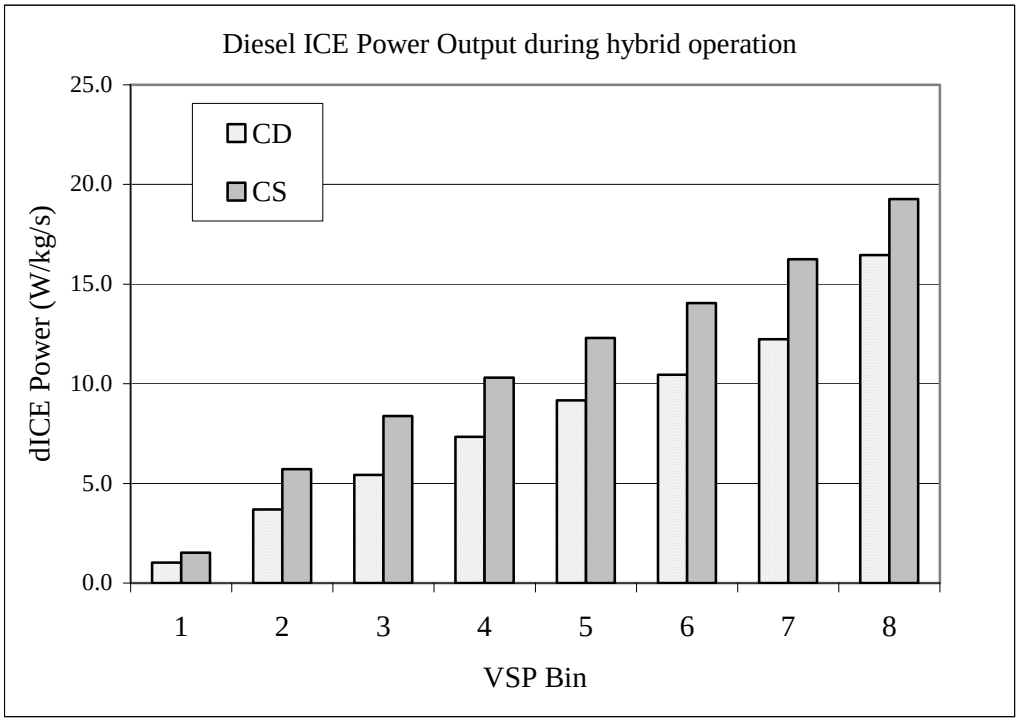

Figure 10.3: Diesel ICE power output during hybrid operation according to operating mode by VSP bin.

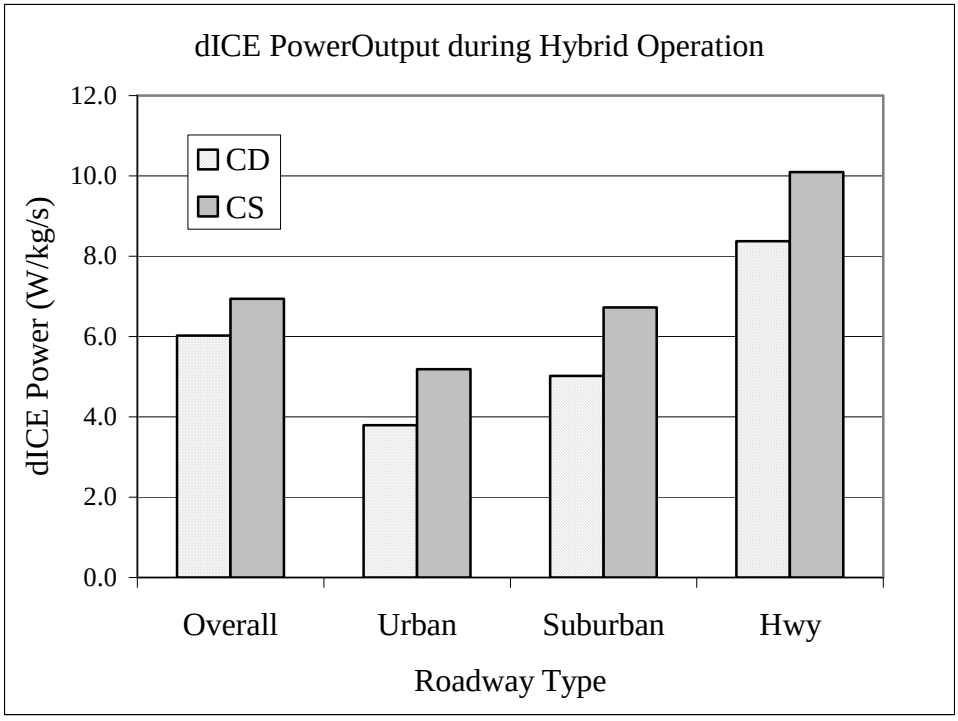

Figure 10.4: Diesel ICE power output during hybrid operation according to operating mode by roadway type.

As discussed in the Chapter 9, the PHEV Sprinter's total power output was a statistically significant response to operating mode, contrary to original expectations, since total power, as a function of immediate on-road load, was predicted to be equivalent between the two operating modes. It was deduced earlier that the enhanced efficiency inherent in the electric motor over the thermally-based dICE was responsible for the reduced total power output during charge-depleting mode, when the EM was a more significant source of the PHEV Sprinter's overall power scheme. Comparable analysis of the PHEV's total power output limited to hybrid operation also demonstrated a statistically significant response to operating mode ($\alpha<0.025$), with charge-depleting hybrid operation requiring less total power output than charge-sustaining hybrid operation. Despite the EM's markedly lower power contribution during hybrid operation,

its increased participation during charge-depleting mode was still sufficient enough to result in an overall increased on-road efficiency for the PHEV Sprinter regardless of navigated roadway.

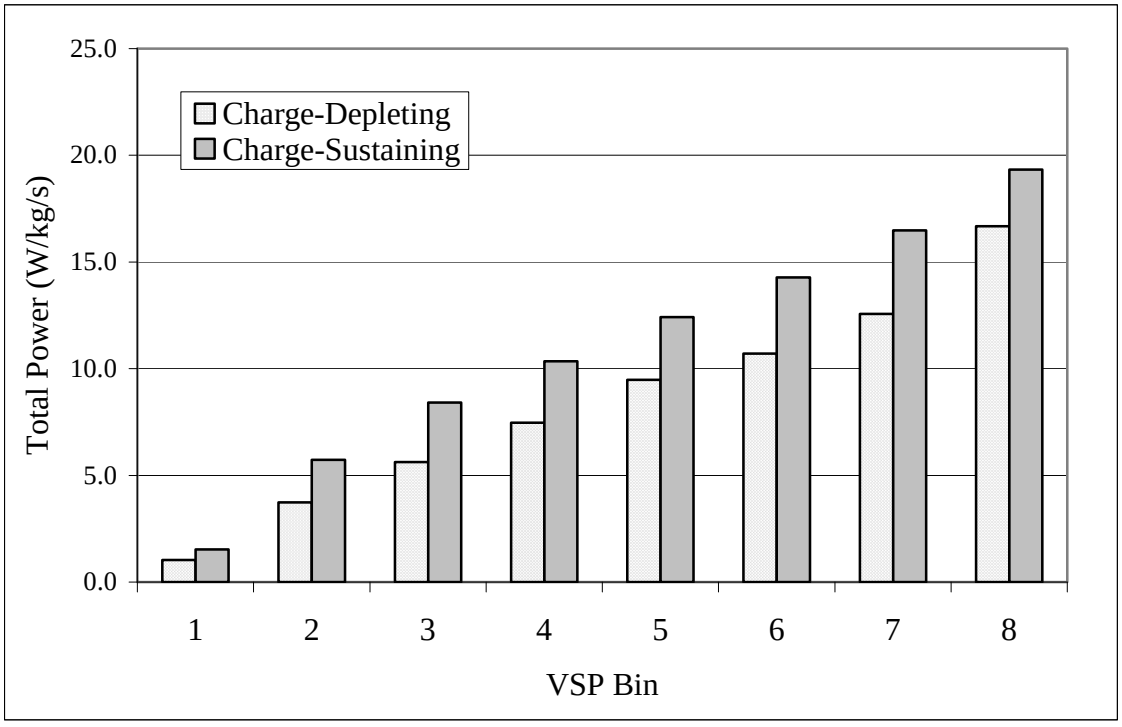

Figure 10.5: Total power output during hybrid operation according to operating mode by VSP bin.

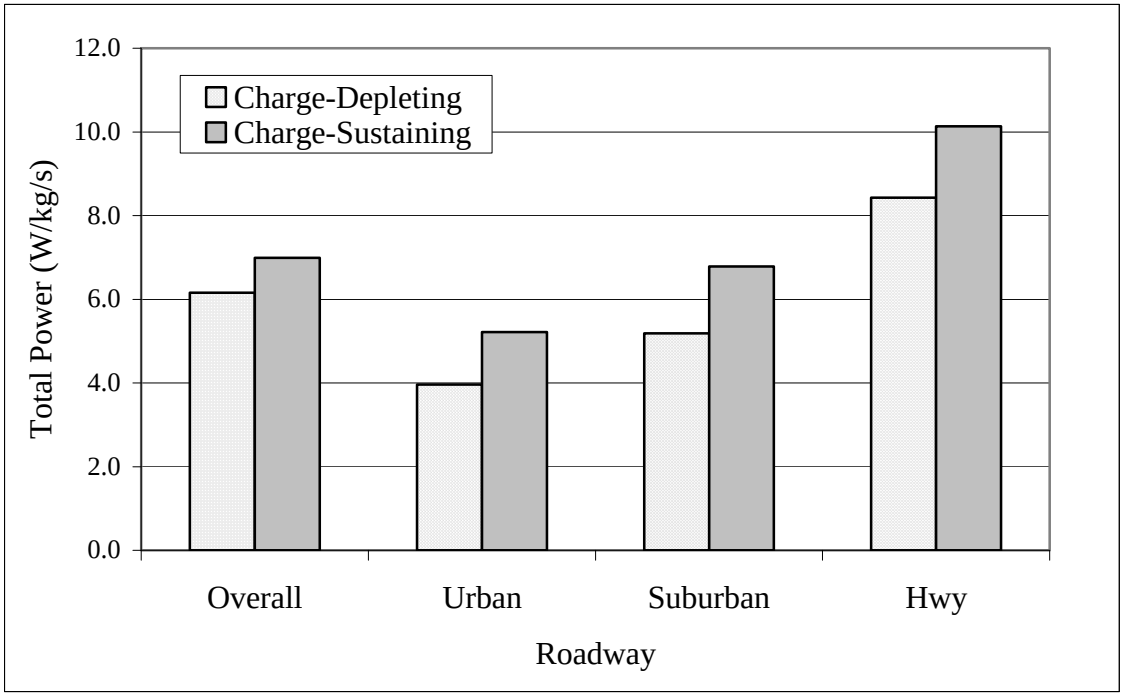

Figure 10.6: Total power output during hybrid operation according to operating mode by roadway type.

10.3.2 Emissions

Aside from carbon dioxide emissions (CO_2), all measured exhaust pollutants proved to be statistically significant responses to operating mode during the PHEV's hybrid driving (Table 10.9). Consistent with the overall operating mode analysis, even during the hybrid-operation focused analysis, the PHEV Sprinter's highest emissions of CO_2, NO and NO_2 occurred during charge-sustaining mode. As a direct product of the combustion reaction, the chemical and thermodynamic processes affecting CO_2 formation are in direct relation to the diesel ICE's operation and power output. Similarly, NO and NO_2 production, while not directly involved in the oxidation of diesel fuel to water and carbon dioxide, proliferates when nitrogen and unreacted oxygen in the air stream are subjected to the thermodynamic conditions created during normal ICE operation.

Consequently, CO_2, NO, and NO_2 emissions correlated strongly with both dICE power output and fuel use.

Carbon monoxide and hydrocarbon emissions did not trend with the dICE power output like CO_2 and NO, and NO_2. It was noted and discussed earlier that exhaust emissions of pollutants whose formation was most directly tied with transient ICE operation were actually higher during charge-depleting operation, when the ICE provided a proportionally lower amount of the PHEV Sprinter's power. This was also the case during the hybrid-focused analysis. Typically, cold starting an internal combustion engine and periods of immediate power demand will result in transient ICE functioning, where the inherent efficiency of steady state operation is lost in order to meet the immediate demands placed on the engine and vehicle. In this manner, the formation and emission of transient pollutants is not a function of fuel use or power output, but of irregular conditions outside of ICE steady-state operation. Figures 10.7 through 10.10 display CO and HC emissions during charge-depleting versus charge-sustaining mode under hybrid operation. Graphs displaying the relative emissions of the other monitored pollutants are provided in Appendix F.

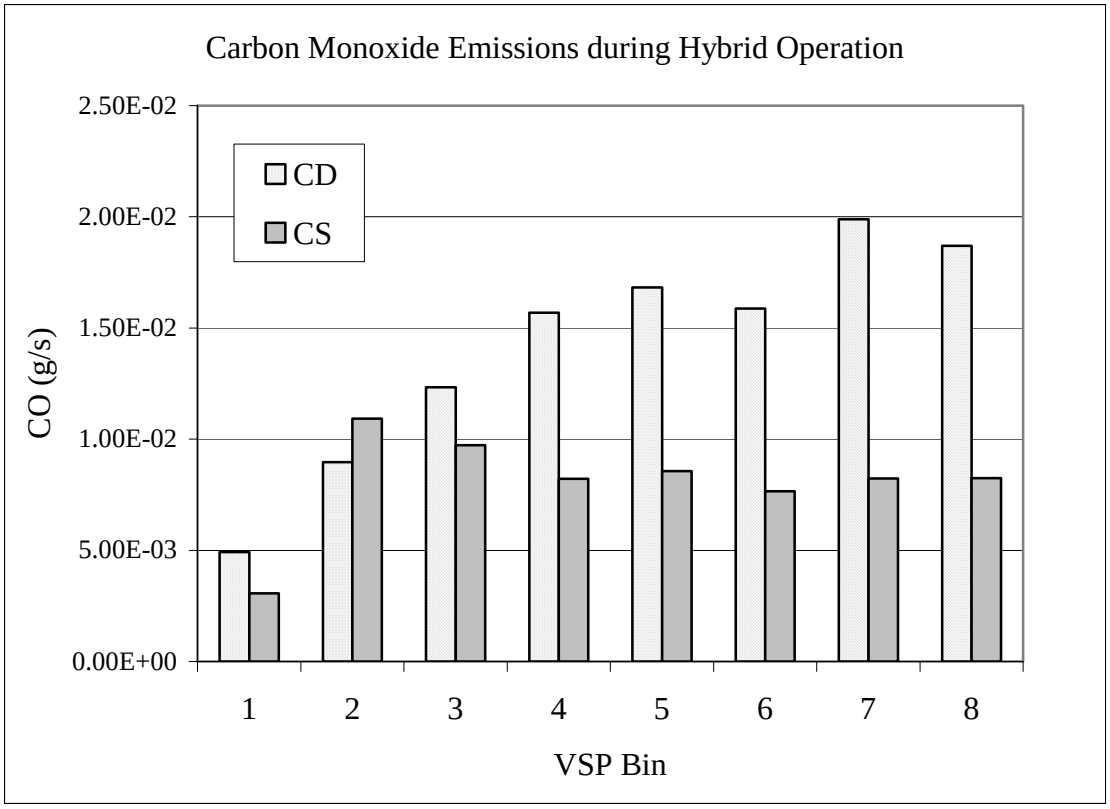

Figure 10.7: Carbon monoxide emissions according to operating mode by VSP bin, based on hybrid driving only.

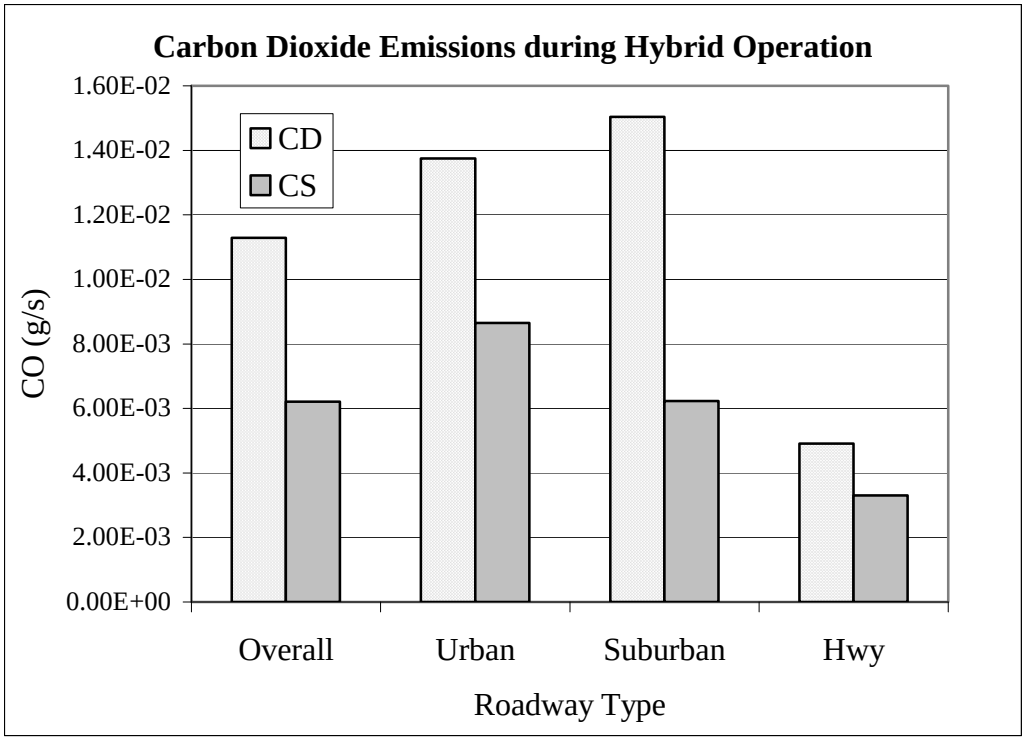

Figure 10.8: Carbon monoxide emissions according to operating mode by roadway type, based on hybrid driving only.

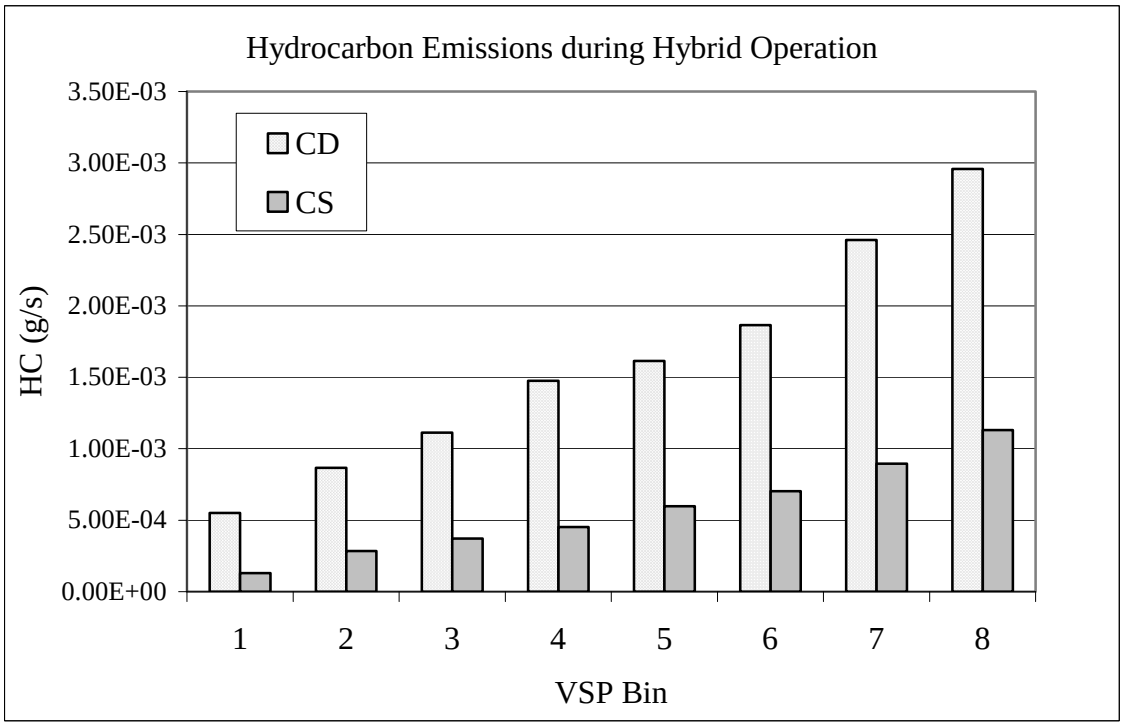

Figure 10.9: Hydrocarbon emissions according to operating mode by VSP bin, based on hybrid driving only.

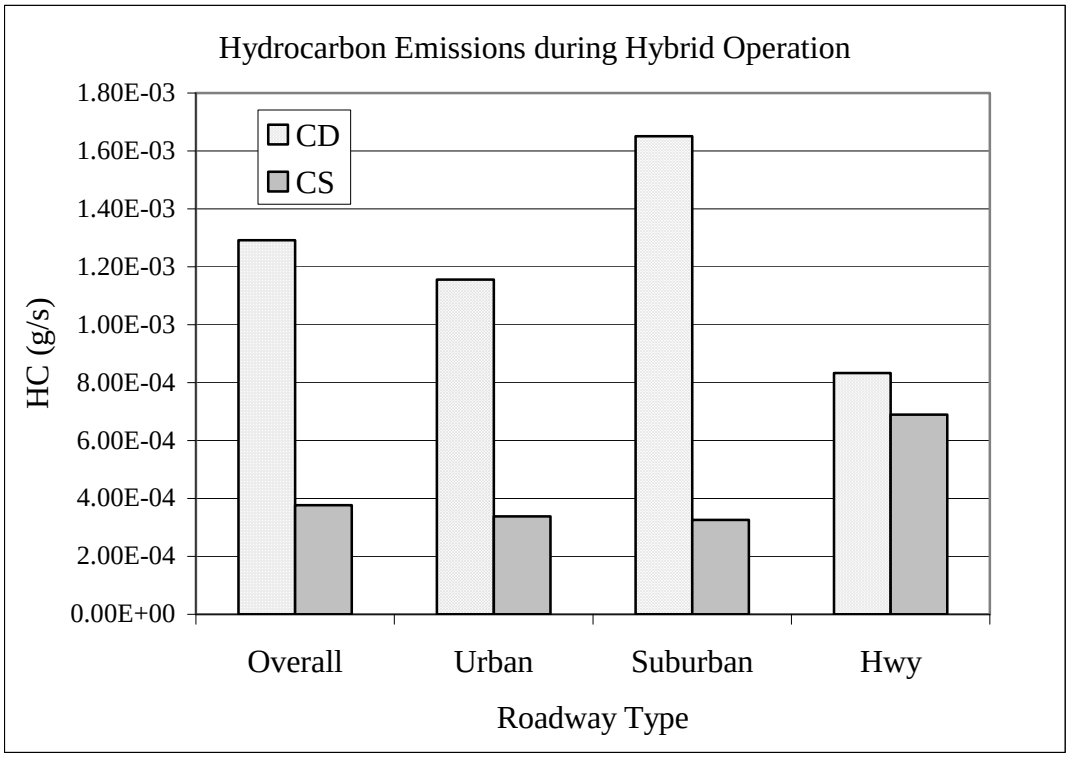

Figure 10.10: Hydrocarbon emissions according to operating mode by roadway type, based on hybrid driving only.

When the evaluation is based solely on hybrid operation, it is obvious that charge-depleting mode results in higher CO and HC emissions than charge-sustaining mode. The difference between the operating modes is magnified in the absence of electric-only data.

10.4 Transient Diesel ICE Assessment

10.4.1 Diesel ICE On/Off Cycling

Exhaust temperature data monitored and recorded by the Semtech system was used in the previous section as an assessment of possible transient dICE operation. The generalized analysis was based primarily on the results from the ANOVA and Kruskal-Wallis tests in addition to relative differences in the mean temperatures between the two operating modes. Without dissecting the data on the micro-scale level, the macro-scale analysis presented earlier only provided a gross means of estimating transient operation. Electric-only data contained in the operating mode analysis effectively diluted the exhaust temperature data by interjecting periods of time when the dICE was off, resulting in ambient temperature measurements for each second of reported exhaust temperature. This dilution was amplified during charge-depleting operation, when the PHEV Sprinter's electric-only operation was maximized. Based on the analytical efforts and scope of the operating mode analysis, it was not possible to discern the extent to which the charge-deleting mode's exhaust temperature data were artificially lowered. Continued investigation regarding the dICE's operation and tendency towards transient operation in the different operating modes will redirect the exhaust temperature analysis by focusing solely on the hybrid-driving data. Since the PHEV Sprinter's hybrid operation was defined by active dICE operation, there is no risk of biasing the analysis with the presence of electric-only data. Even with the analytical focus on hybrid operation, the PHEV's exhaust temperature remained a statistically significant response ($\alpha<0.025$) to the active operating mode (Tables 10.7 to 10.9). This gives verification to the fact that the diesel ICE behaved very differently according to active operating mode.

Figures 10.11 and 10.12 display the PHEV's exhaust temperature according to operating mode across the VSP bins and for the designated roadways.

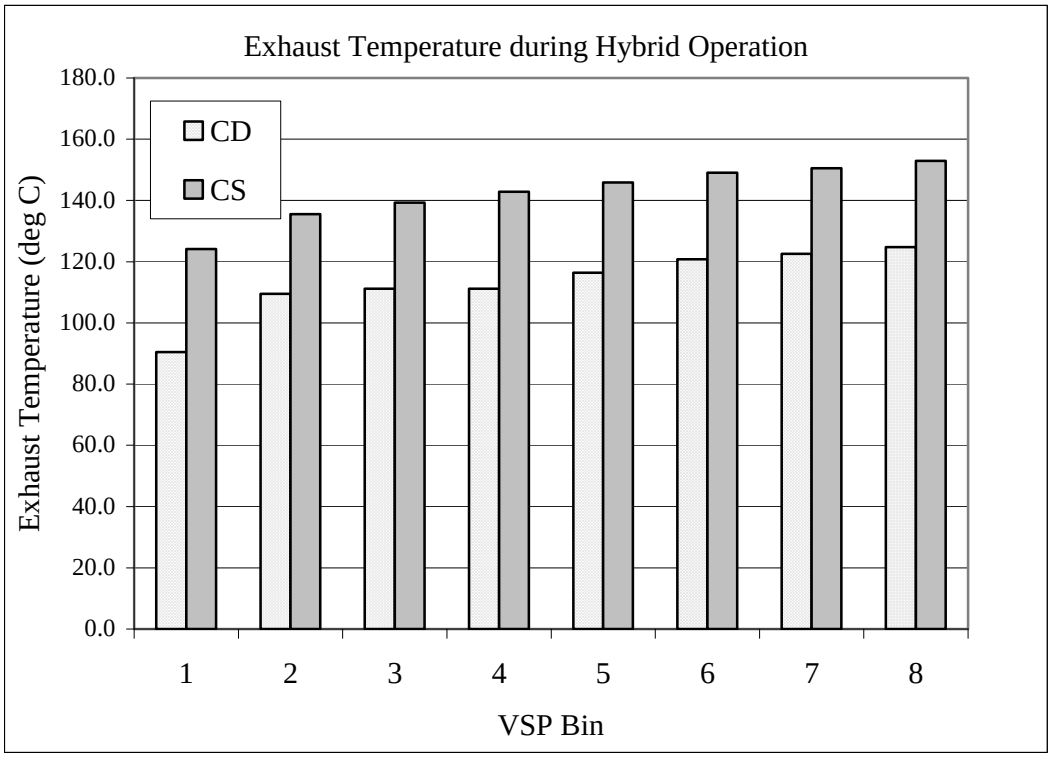

Figure 10.11: Exhaust temperature according to operating mode by VSP bin, based on hybrid driving only.

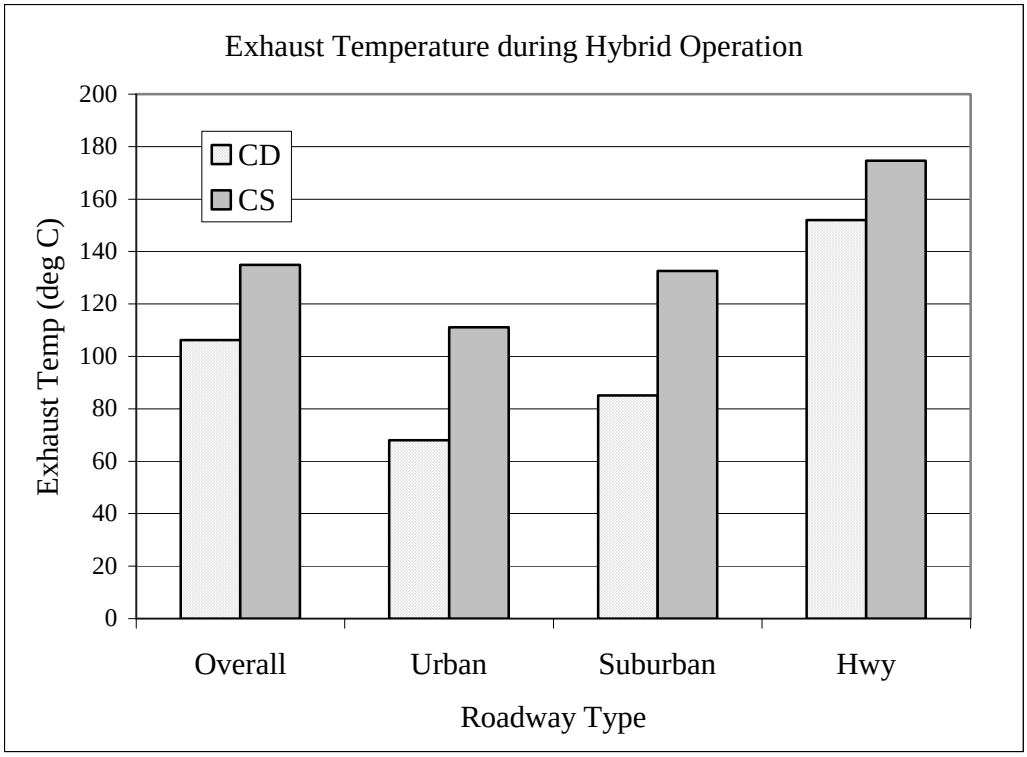

Figure 10.12: Exhaust temperature according to operating mode by roadway type, based on hybrid driving only.

When reported for hybrid driving only, the PHEV Sprinter's exhaust temperatures still remained consistently lower during charge-depleting operation compared with charge-sustaining mode. Within the PHEV context, the ICE is continually cycled on and off as the PHEV attempts to maximize its electric-only or zero-emissions road time. As a result of this, the ICE will experience a number of "cold starts" with the amount of time between the off/on cycle dictating the degree to which the start would be considered cold. Additionally, short on-to-off cycles will impede full ICE warm-up, resulting in lower average exhaust temperatures. Both situations (cold starts and operating prior to full warm up) will result in some degree of transient operation. A snapshot of typical charge-depleting operation is provided below. Extended periods of dICE shutdown are observed in the, nominally, 17minute (1,000 second) timeframe displayed in Figure 10.13.

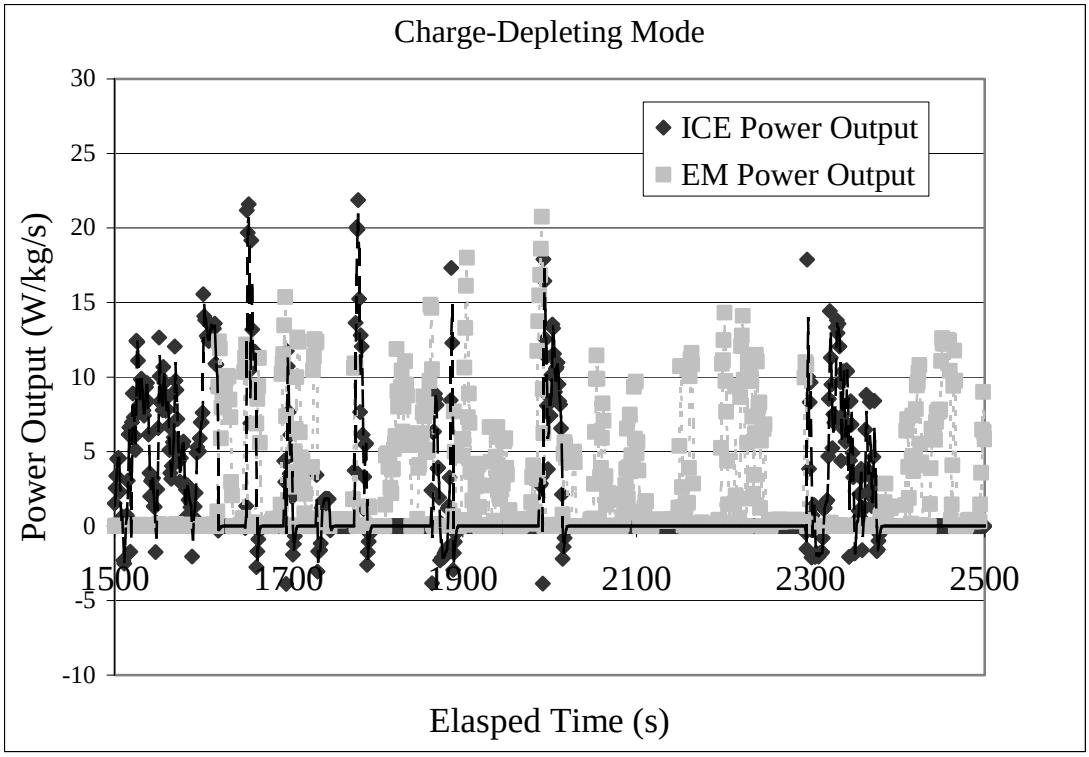

Figure 10.13: Sample of charge-depleting mode operation detailing the contiguous power demands on both the dICE and EM.

The statistical significance established between the operating modes during hybrid operation gives proof that the original differences found amid the PHEV Sprinter's two operating modes (Chapter 9) were due to more than just the prevalence of electric-only operation within the modes. In order to expound upon the difference in the dICE's functioning between the operating modes, the number of on/off cycles and average duration of each cycle for both power sources was assessed for each operating mode. Table 10.10 provides a complete summary of the I/O (on/off) cycles experienced by the PHEV's internal combustion engine for both modes of operation. Regardless of normalization basis (distance or time), charge-depleting operation resulted in the highest frequency of dICE on/off cycles when compared to charge-sustaining operation. The

following data were obtained from the entire set of data files selected for the VSP analysis and utilized for all subsequent investigations.

Table 10.10: Overall summary of ICE on/off cycling for each operating mode.

Charge-Depleting Mode:	
# I/O ICE Cycles CD:	123
Distance CD (km):	157.10
Time CD (min):	286.2
# CD I/O ICE Cycles/km:	0.783
# CD I/O ICE Cycles/min:	0.430
Charge-Sustaining Mode:	
# I/O ICE Cycles CS:	335
Distance CS (km):	482.88
Time CS (min):	913.6
# CS I/O ICE Cycles/km:	0.694
# CS I/O ICE Cycles/min:	0.367
% Difference betwee CD/CS distance:	12.1%
% Difference betwee CD/CS time:	15.9%

Table 10.10 gives data supporting the frequency of on/off cycles experienced by the dICE within each operating mode. However, the relative duration of off-time and the average length of time that the dICE remained off for each on/off cycle ultimately determined the degree of cold start and dICE warm-up experienced each time the engine came back online. According to both the calculated means and determined medians of dICE off time, it cannot be conclusively stated if one operating mode resulted in, on average, longer periods of dICE downtime compared to the other. While the parametric analysis suggests that charge-depleting operation resulted in longer periods of dICE shutdown based on the reported means, the non-parametric analysis indicates that charge-sustaining operation actually reported the longest durations of dICE shutdown. Based on

these analyses, it cannot be decisively determined if the operating modes were in fact different from one another with regards to the duration of ICE shutdown periods.

Table 10.11: Statistical analysis of the dICE's off time between starts according to operating mode.

Synopsis of time ICE off between I/O Cycle:	
Charge-Depleting Mean (seconds)	78.8
Charge-Sustaining Mean (seconds)	61.7
ANOVA p-value	0.053
Charge-Depleting Median (seconds)	35.0
Charge-Sustaining Median (seconds)	43.0
Kruskal-Wallis p-value	0.549

A dual histogram comparing the distributions of the dICE off time between the operating modes is provided in Figure 10.14. The majority of the instances in which the dICE was pulled offline were for relatively short periods of time. During charge-depleting operation, 44% of the times that the dICE was pulled off-line, it was for less than 30seconds with almost 70% of the periods of dICE disengagement occurring for less than 1minute. During charge-sustaining operation, the percentages were slightly less with 34% of the disengagements resulting in dICE stop times of 30seconds or less and 65% of the stop times lasting 1minute or less. The largest difference in dICE off time between the operating modes exists in the tails of each distribution. Charge-depleting mode experienced a relatively small number of extremely long periods of dICE shutdown that were not present during charge-sustaining operation. Charge-depleting operation also resulted in the highest frequency of long dICE shutdown times with 8.2% of the dICE's stop times resulting in the engine being offline for a period of 4mintues or greater, this percentage was only 1.8% during charge-sustaining mode.

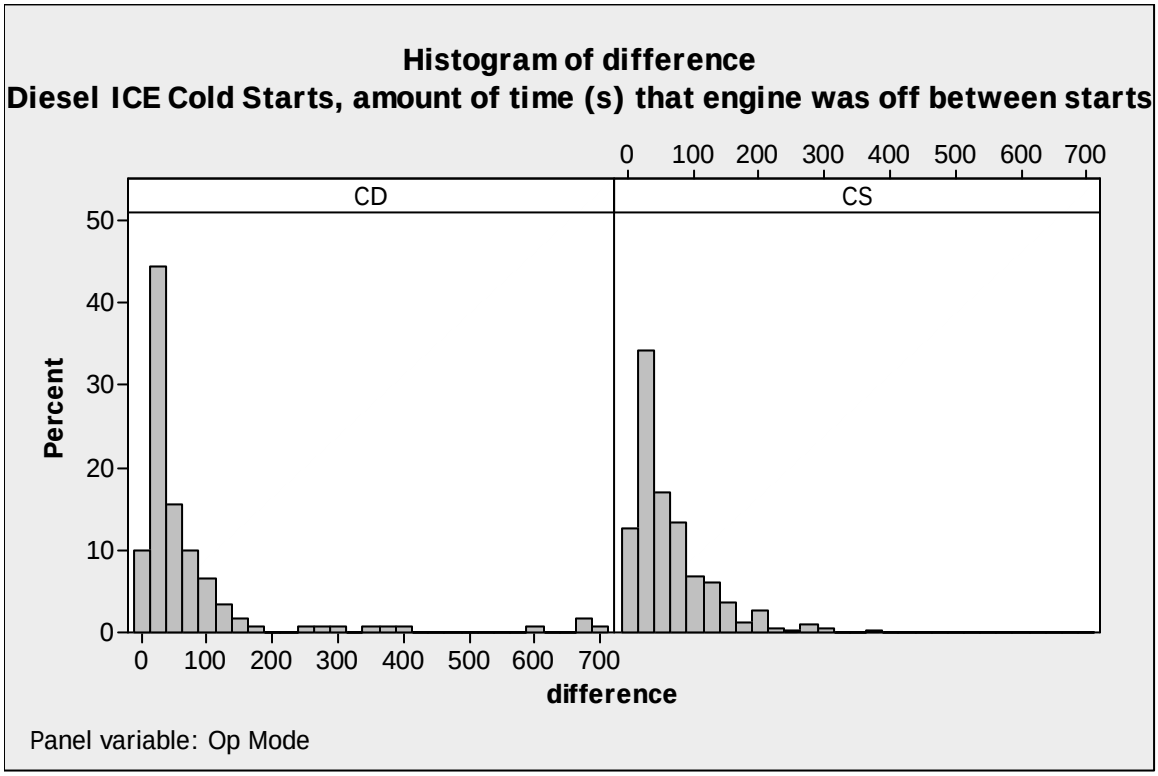

Figure 10.14: Relative distributions of dICE shutdown according to operating mode.

While the duration of dICE shutdown references the degree of cold start the engine was experiencing in each operating mode, the amount of time, on average, that the dICE remained running during each period of on time is reflective of the degree of warm-up achieved within each operating mode, again on average. Table 10.12 details the periods of time that the dICE remained engaged for each mode. In this case, the results of the statistical tests, parametric or nonparametric, are conclusive. Charge-sustaining operation resulted in longer durations of dICE operation between off times. Based on the calculated mean, charge-sustaining maintained dICE operation more than 66% longer than charge-depleting mode. This discrepancy is vastly more significant when focusing on the resulting median on-time between the modes with charge-sustaining mode

demonstrating dICE run times of almost eight times longer than charge-depleting mode. Histograms showing the relative distributions in dICE on-time or engagement between the operating modes are provided in Figure 10.15. During charge-depleting operation, dICE recruitment is short-lived and occurs as brief periods of engine start/stop cycling compared with charge-sustaining operation, which still cycles the ICE on and off, but tends to keep the internal combustion engine running for longer periods of time between being offline for electric-only driving.

Table 10.12: Summary of the dICE on time according to operating mode.

Synopsis of time ICE was running per I/O Cycle:	
Charge-Depleting Mean (seconds)	62.6
Charge-Sustaining Mean (seconds)	104.1
ANOVA p-value	0.000
Charge-Depleting Median (seconds)	10.0
Charge-Sustaining Median (seconds)	79.0
Kruskal-Wallis p-value	0.000

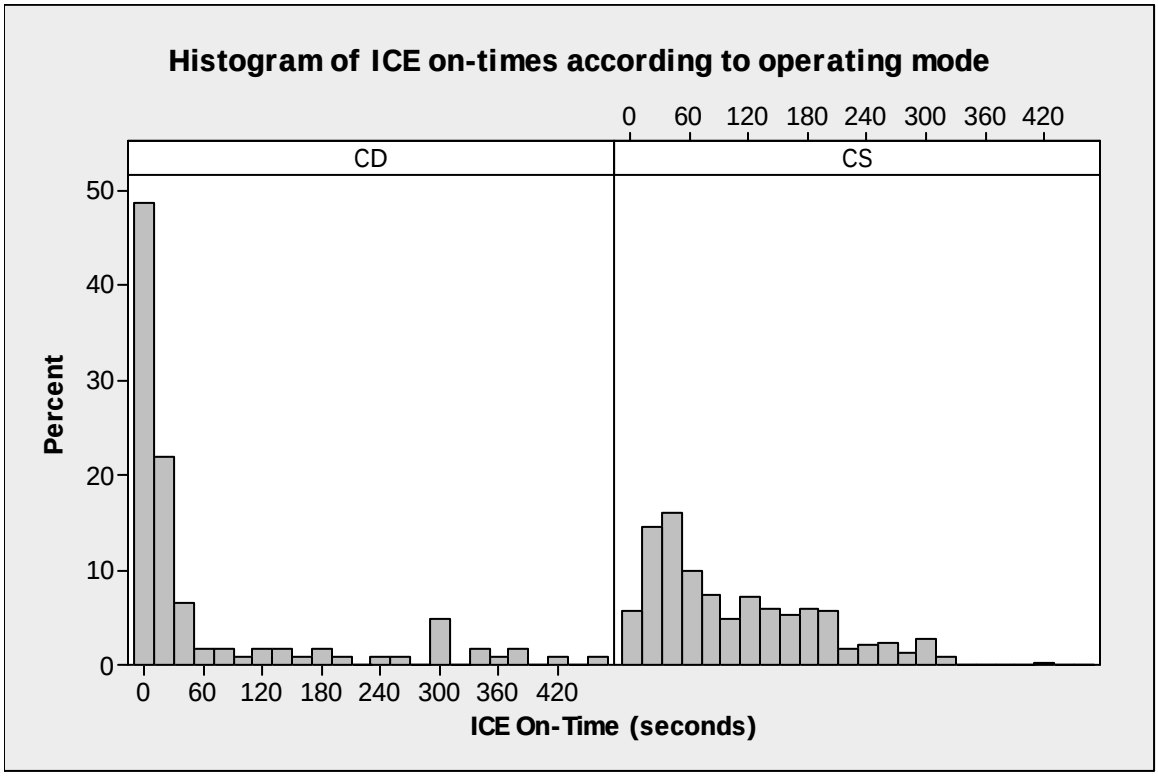

Figure 10.15: Relative distributions of ICE on time according to operating mode.

10.4.2 Direct Oxidation Catalyst Implications

Thus far, the relative high level of carbon monoxide (CO) and hydrocarbon (HC) emissions during charge-depleting operation has been attributed to transient dICE operation as indicated by depressed exhaust temperatures and increased on/off cycling with a higher propensity of cold starts. The PHEV Sprinter was equipped with a direct oxidation catalyst (DOC) employed for the primary purpose of reducing CO and HC levels in the PHEV's exhaust. DOCs do not operate effectively until fully warmed up. Since the DOC is brought to operating temperature through convective heating with the vehicle's exhaust flow, lower average exhaust temperatures are an indication of inefficient catalyst function. DOC-specific data were not made available, so it is not possible to discern the relative quantitative impacts that transient dICE operation and sub

par catalyst function had on CO and HC emissions. While the duration of time that the dICE was offline between periods of hybrid driving was not statistically significant according to operating mode, the amount of time that the dICE tended to remain operational before being pulled offline for electric-only operation was statistically significant between the operating modes. Charge-depleting operation consistently resulted in shorter periods of dICE run time, which, in turn, gave less opportunity for the dICE to fully warm up between periods of electric-only operation. This lack of warm up translates not only to the possibility of transient operation, but also to the likelihood that the DOC was less able to achieve full warm up during charge-depleting operation.

While the tendency towards cold starts, based on duration of electric-only operation, between the modes could not be statistically determined. Charge-depleting operation still resulted in more dICE on/off cycles than charge-sustaining operation. In effort to further elucidate the increased propensity of charge-depleting mode to result in higher emissions of CO and HC, snapshots of time comparing the relative emissions of CO and HC between the operating modes are provided in Figures 10.16 and 10.17. The magnitude of the emissions peaks between the modes is visually significant with charge-depleting operation resulting in significantly higher peaks of both CO and HC emissions.

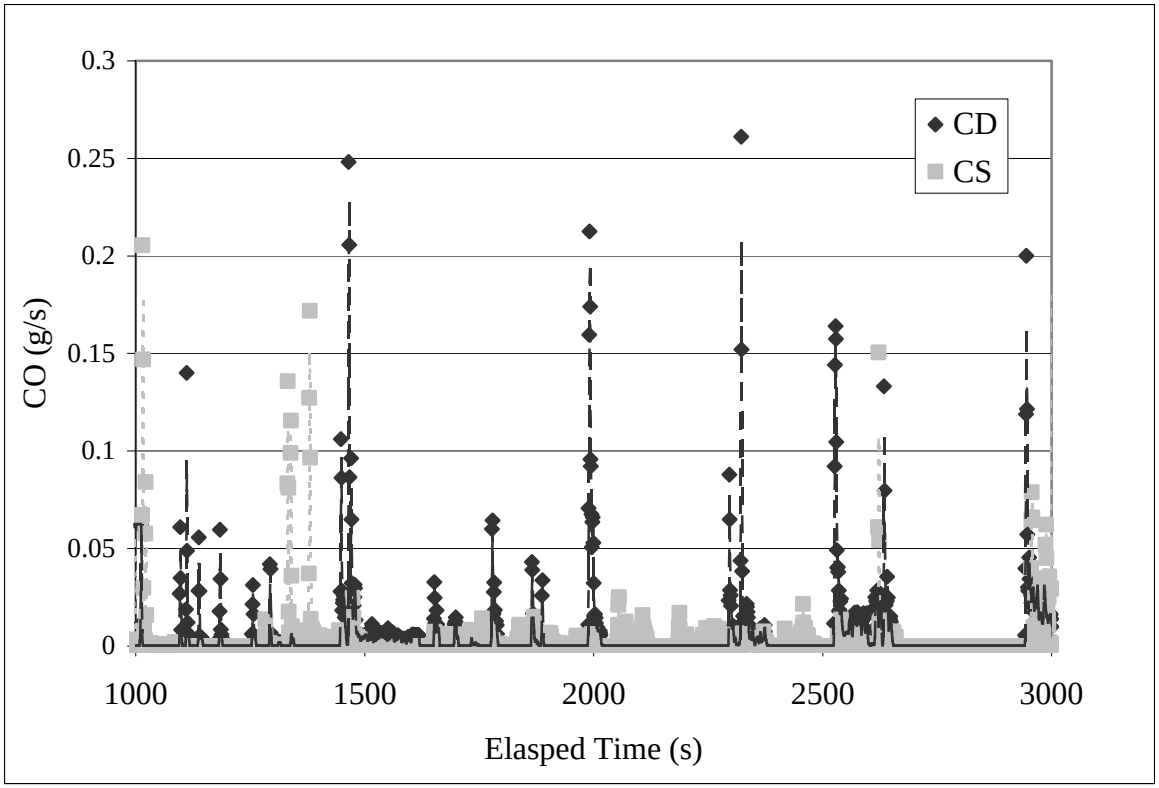

Figure 10.16: Carbon monoxide emissions according to operating mode for a snapshot of PHEV Sprinter on-road driving.

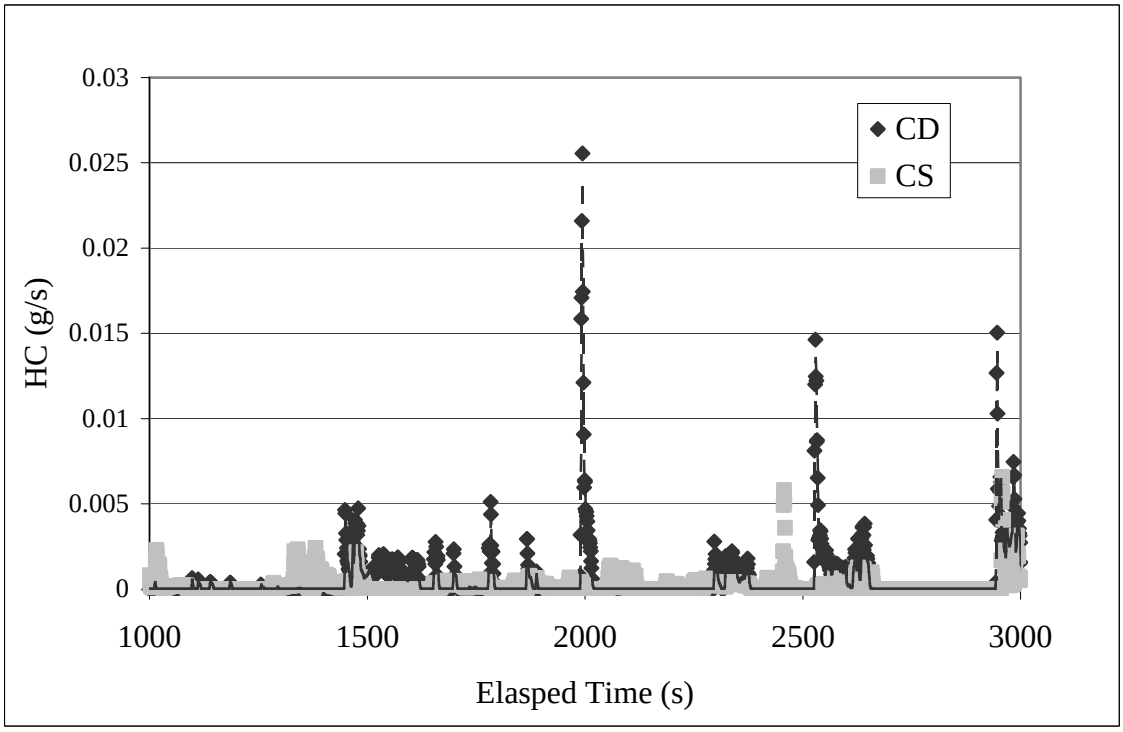

Figure 10.17: Hydrocarbon emissions according to operating mode for a snapshot of PHEV Sprinter on-road driving.

10.5 Concluding Remarks

No statistically significant relationship presented between the EM's use during electric-only operation and active operating mode, suggesting that the PHEV Sprinter operated under the same overarching control scheme for all electric-only driving regardless of the battery's state of charge. Changes in the PHEV Sprinter's control scheme were apparent when the PHEV's on-road data were filtered to investigate hybrid operation singly. During hybrid driving, defined by engagement of the dICE, the EM provided proportionally more power during charge-depleting mode compared with charge-sustaining operation, giving indication that the PHEV's level of electric-assist was a function of battery state of charge. The increase in EM recruitment during hybrid driving translated to total power output, with charge-depleting mode resulting in slightly more efficient on-road travel compared with charge-sustaining operation.

Conversely, during charge-sustaining operation, the dICE provided consistently more motive power than comparable on-road travel during charge-depleting operation. Even with electric-only driving removed from the dataset, emissions, dICE operation and power output, and exhaust temperature were conclusively statistically significant responses to operating mode, regardless of the basis for analysis (VSP bin, driving mode, or roadway type).

Similar to previous investigations, carbon dioxide, nitric oxide, and nitrogen dioxide emissions trended with the PHEV Sprinter's fuel use and dICE power output. However, both carbon monoxide and hydrocarbon emissions remained consistently higher during charge-depleting operation, despite lower overall power output. The potential for transient dICE operation during charge-depleting mode was first observed in

the reported exhaust temperatures, with charge-sustaining operation resulting in statistically significant higher overall exhaust temperatures. Low exhaust temperatures are suggestive of extensive periods of dICE disengagement and insufficient opportunity for the dICE to reach operating temperature when employed.

Investigation into the dICE's cycling during the different operating modes showed that during charge-depleting operation the dICE cycled on and off more frequently than during charge-sustaining operation. While the amount of shutdown time per cycle was not statistically significant according to operating mode, similar investigation regarding the amount of time, on average, that the dICE was engaged between off/on cycles was significantly higher during charge-sustaining operation. This suggests that while the amount of time for engine cool down may have not been statistically significant between the operating modes, the amount of time for engine warm-up was. Investigation of the dICE shutdown time histograms between the operating modes showed that charge-depleting operation resulted in instances where the dICE was shut down for extensive periods of time. Likewise, charge-depleting operation resulted in a high frequency of short time periods when the dICE was functioning, whereas charge-sustaining operation tended to keep the dICE engaged for longer durations once it was brought back on line.

Ultimately, while increasing electric-only capacity of the PHEV Sprinter makes certain efficiency gains, this increased efficiency does have some deleterious impacts on dICE operation. Based on emissions, carbon monoxide and hydrocarbon emissions are highest during the "most efficient" of the operating modes, charge-depleting. Charge-depleting operation results in the internal combustion engine being started more often (on the basis of time and distance), and it also results in less time for engine warm up.

Unfortunately, this study was not afforded comparable conventional and gasoline-based PHEV Sprinters for comparative purposes. There is no way to discern if the phenomenon reported here with regards to carbon monoxide and hydrocarbon emissions are specific to the diesel internal combustion engine or if they would translate to the gasoline-based PHEV Sprinters as well.

Chapter 11: Vocation Assessment (solo versus in-service transit driving)

11.1 Introduction and Background

One of the fundamental purposes of the Kansas City Transit Authority's participation in the Daimler/Chrysler Plug-in Sprinter proof of concept study was to showcase the PHEV Sprinter's suitability as applied to public transit service. As part of the Phase I Plug-in Hybrid Vehicle Proof of Concept study, the Kansas City slated PHEV Sprinter was the only participating vehicle placed into the public transit arena. The remaining Phase I prototypes were evaluated in more conventional service and delivery applications by their respective participating partners. In order to fully assess the Kansas City PHEV Sprinter's on-road operation, the demonstration study was designed in two phases, accounting for the different drive schemes under which the PHEV Sprinter van would be most readily employed: in-service transit simulation and civilian driving.

The Kansas City PHEV Sprinter was enabled to meet the demands imposed by on-road transit operation through a retrofit with additional seating, a hydraulic wheelchair lift, an electric side door, fare box, and additional radio communications. The weight of the retrofit resulted in a vehicle operating at or near its payload capacity while empty of passengers. In addition to payload concerns, insurance and passenger liability issues hindered the operator's ability to place the PHEV Sprinter into actual transit service during the on-road demonstration study's timeline. However, in efforts to meet the goals of the proof-of-concept trial period, the Kansas City PHEV Sprinter was placed into simulated transit scenarios serving as a chase vehicle by shadowing in-service KCATA buses. On-road emissions research has proven that the chase-vehicle study design is a

viable substitution for tracking and monitoring a specific vehicle's driving patterns and emissions (Yao et al., 2007 and Yu et al. 2008).

Operator observation early in the PHEV Sprinter demonstration study suggested that the driving patterns exhibited by transit bus operators could vary significantly from normal civilian driving patterns, even on the same roadways. Upon this observation, the demonstration study was expanded to collect on-road data representative of both transit operation (including passenger drop-off and pick-up stops and the requirement of adhering to a set schedule) and non-transit driving. Pre-selected routes were driven while shadowing an in-service KCATA transit bus, and the same routes were driven without transit interference in a more civilian manner. All previous investigations have been conducted using on-road data collected while the PHEV Sprinter was being driven as a regular passenger or delivery vehicle. As a result of the demonstration study's redesign, the PHEV Sprinter's transit operation can be evaluated in contrast with more conventional on-road driving patterns. While operator tendencies and driving behaviors have been shown to have a statistically significant impact on a vehicle's emissions (Frey et al., 2008), the mono-operator implementation of the PHEV Sprinter demonstration study gains statistical power due to the removal of inherent operator differences, but loses its ability to serve as a more universal representation of the PHEV's operation under all circumstances, including the influences of multiple drivers. As a result of this, the study design and final dataset are perfectly suited for providing a comparison of transit versus civilian service, however the civilian service in consideration may not be a perfect embodiment of all civilian-driving patterns present on the road today. Regular, non-transit driving scenarios were conducted with every effort put towards abiding by all

local traffic laws (speed limits, posted stop signs, stop lights, and traffic signals) and following the roadways' immediate traffic patterns and flow. Natural rates of acceleration and deceleration vary from driver to driver, so the PHEV Sprinter's final on-road dataset possesses a certain amount of operator-influenced bias. While immeasurable, its presence should be noted nonetheless.

For the remainder of this discussion, data collected while shadowing an in-service transit bus will be referred to as "follow" while the data collected under normal, civilian driving is cited as "solo." Of the previously discussed "routes" only the 109, 123, and 110 routes proved to be suitable for collecting transit-specific data. Due to the potentially confounding influence that auxiliary system use and ambient temperature played on the data, the criteria established for selecting data for the previous investigations were imposed for selecting sample runs collected while shadowing (following) a transit bus. The following discussion and analyses were limited to on-road data collected during moderate ambient temperatures (between 40˚F and 66˚F) without the use of auxiliary system (heater or air conditioning).

Only the 110 and 123 routes were shadowed as in-service transit routes during acceptable ambient temperature and auxiliary system use. Therefore the following discussion will be limited to solo and follow data obtained while operating these two routes. The 123 route covered only suburban roadways, with nominal posted speed limits of 35mph, occasional traffic lights, and minimal traffic densities. This route covered 6.0 miles of the Kansas City midtown area traveling in an east/west manner between the Union Station/Crown Center area and Blue Valley Park off of 23rd Street to the east. Conversely, the 110 route traveled in a north/south direction servicing both the Kansas

City urban core near the River Market area and the more suburban areas to the south. In total, the 110 route covered a distance of 5.9 miles between the River Market area (downtown) and the 44th and Brooklyn stop-over location (southern suburb). Neither route experienced periods of extremely high traffic density, and, compared with the other routes that composed the PHEV Sprinter Demonstration Study, both the 110 and 123 routes were relatively mild driving, low-pressure routes. Given the PHEV Sprinter's size and capacity restrictions, only lower ridership routes were deemed suitable options for Sprinter employment. Both the 110 and 123 routes serviced similar ridership demands with approximately 143 passengers per day (8.7passengers/hr) riding the 110 route and 168 passengers per day (8.3passengers/hr) using the 123. Figure 11.1 showcases the 110 and 123 routes.

All in-service transit routes possessed layover points where the bus would sit stationary for several minutes in order to serve as a driver respite and provide a time buffer allowing the bus to maintain a set and attainable schedule throughout the day. Even though these layover stops were part of the in-service transit scheduled routes, their inclusion would artificially lower the overall velocity, emissions, and power output data as reported on a time basis. In order to eliminate sources of bias, all set layover points were removed from the datasets, so that the final "follow" datasets included only on-road data collected while the transit bus was following a set route.

Figure 11.1: Map detailing the 110 and 123 routes selected for the solo versus follow comparison.

More that 13hours of transit-simulated, on-road data were collected from the 123 and 110 routes, representing both charge-sustaining and charge-depleting operation. Sample runs driven "solo" on the 123 and 110 routes were selected from the dataset used for all prior investigations in order to mitigate any noise and natural on-road fluctuations that exist between the individual sample routes (109 versus 110 versus 123 versus 12th Street). The final dataset for this analysis, inclusive of all follow and solo data represents over 25hours of on-road sampling collected from over 600km of driving distance. This provides sufficient representation of urban and suburban travel as well as charge-

sustaining operation versus charge-depleting operation allowing for multiple levels of analysis.

11.2 Road-Based Variables

11.2.1 Potential Time-of-Day Influences

During preliminary statistical investigation of the selected follow/solo dataset, unforeseen discrepancies were observed between charge-sustaining and charge-depleting operation within each operator scenario (solo or follow). While emissions and power scheme output were expected to vary according to active operating mode, on-road variables such as velocity and acceleration and deceleration rates should have been similar regardless of whether the PHEV Sprinter was running in charge-depleting or charge-sustaining mode. Despite this, the unanticipated differences in the on-road driving behaviors between the two operating modes proved to possess some degree of statistical significance. In order to assess the potential influence that active operating mode had on on-road driver behavior, the on-road data were subjected to ANOVA and Kruskal-Wallis statistical analyses. Similar to previous investigations, a strict $\alpha<0.025$ was set for all analyses of the continuous, second-by-second datasets.

Overall synopses of the statistical work performed comparing the on-road behaviors between the two operation modes are provided in the following tables. Regardless of operating mode, all "follow" data were collected while driving under the KCATA's set bus schedule. The "solo" data, however, were obtained under normal driving conditions without the imposition of maintaining a set schedule of passenger stops and drop-offs. Because of this, differences observed between the operating modes while shadowing a KCATA transit bus were less statistically meaningful and conclusive between the parametric and non-parametric test. Solo driving, however, presented a considerably different on-road experience between the two operating modes. Velocity

proved to be a statistically significant response to operating mode for all roadways assessed, and during suburban travel both acceleration and deceleration rates were significantly different between the PHEV's two operating modes.

Table 11.1: Statistical summary of on-road variables during follow driving according to active operating mode.

Follow: Charge-Depleting vs Charge-Sustaining

Variable:	All Roads	Suburban Roads	Urban Roads
Velocity (km/h)	y	Inc2	n
Acceleration (m/s^2)	Inc1	Inc1	Inc1
Deceleration (m/s^2)	y	y	n

Inc1: y anova, n kw
Inc2: n anova, y kw

Table 11.2: Statistical summary of on-road variables during solo driving according to active operating mode.

Solo: Charge-Depleting vs Charge-Sustaining

Variable:	All Roads	Suburban Roads	Urban Roads
Velocity (km/h)	y	y	y
Acceleration (m/s^2)	y	y	n
Deceleration (m/s^2)	y	y	n

Inc1: y anova, n kw
Inc2: n anova, y kw

A relatively fixed schedule for all sampling efforts was adhered to for the PHEV demonstration study. In order to avoid the influence of rush hour traffic, data collection efforts did not generally begin until after 9:30am each morning. Conversely, on-road sampling did not extend past 4:00pm each afternoon. Despite all attempts to avoid abnormally high-traffic scenarios, the nature of the PHEV power scheme design gave possibility to the presence of time-of-day influence on the final dataset. Since charge-depleting operation is defined by excess battery holding capacity, sampling during

charge-depleting mode could only occur immediately after the PHEV Sprinter was removed from its A/C power source each morning. As a result of this, the PHEV Sprinter only operated in charge-depleting mode during the first 1-2 sample runs each day. With an overnight charge required to re-establish charge-depleting battery levels, mid- and late-day charge-depleting operation was not feasible. Additionally, charge-sustaining operation, for the most part, only occurred during mid- and late-day sampling. This mandate of the PHEV Sprinter's design gave way to the potential for time-of-day influences despite all efforts made to avoid rush hour circumstances. Frey et al. (2003 and 2008) and Krishmamurthy and Gautam (2006) all reported time of day effects on vehicle emissions data during on-road collection campaigns.

During solo driving, the PHEV Sprinter experienced slower average velocities during charge-depleting operation, when the on-road sampling occurred early in the morning hours at the start of each sample day. This trend is consistent regardless of the roadway type being navigated, and proved to be statistically meaningful at an $\alpha<0.025$. Conversely, the act of shadowing a KCATA transit bus during the early day resulted in slightly higher average velocities. No statistically significant difference existed between charge-depleting and charge-sustaining operation with regards to traffic patterns, assessed by the frequency and duration of stops or total amount of time at zero velocity when following a transit bus. Maintaining a set schedule during transit simulation resulted in consistency between runs regardless of time of day, traffic density, or ridership numbers.

Figure 11.2 displays the mean velocities for solo and follow driving for each roadway type according to active operating mode. Consistent with the roadway analysis performed earlier, urban driving resulted in slower travel speeds, regardless of the solo or

follow driving designation. Despite unforeseen discrepancies between the operating modes (and, consequently, time of day), traveled roadway was a larger influence on the PHEV Sprinter's on-road velocity. While some differences in average velocity exist between charge-depleting and charge-sustaining operation, only the results from the solo-driven runs proved to be statistically significant to the $\alpha<0.025$ level. There was, effectively, no meaningful difference in average velocity between the operating modes while the PHEV Sprinter was shadowing an in-service KCATA transit bus. While subtle differences in mean velocity may present from one serviced run to another, the requirement of maintaining a fixed schedule, regardless of the time of day, resulted in relatively consistent on-road velocities for the follow data. Therefore, variations in traffic density and patterns throughout the day had limited impact on the velocity profiles for the data collected while the PHEV was following an in-service transit bus.

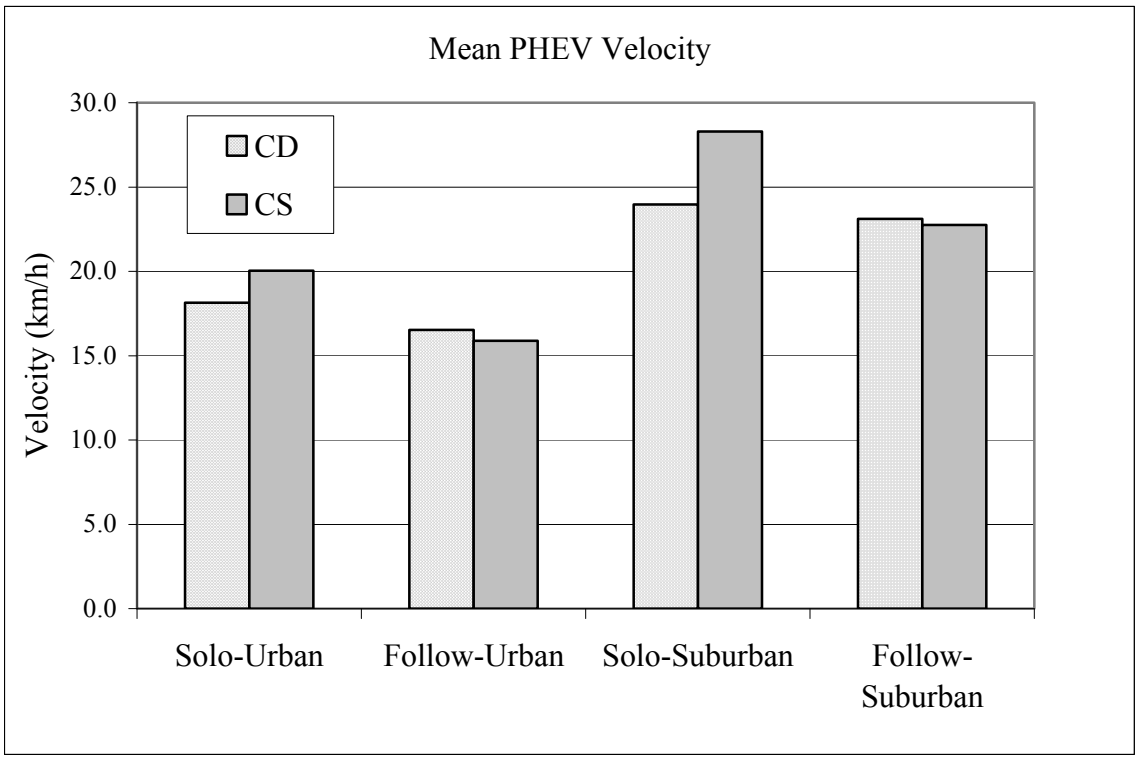

Figure 11.2: Mean velocities according to operating mode for both solo and follow driving.

While time of day influence is a viable explanation for the velocity differences between the operating modes, a similar analysis of the PHEV Sprinter's acceleration and deceleration rates appears less certain. Statistical analyses of acceleration and deceleration rates as a function of operating mode were less conclusive than the same tests for velocity; however, some discrepancies between the active operating modes do exist.

Despite the large differences in mean acceleration rates between the operating modes for all of the follow data, neither suburban nor urban acceleration demonstrated a conclusively statistically significant relationship to operating mode during the follow sample runs. High variances in acceleration rates between the operating modes negate the presence of statistical significance despite the large difference in calculated means, so

while the set level of significance was met for all Analyses of Variance (ANOVAs), the analyses universally failed the non-parametric Kruskal-Wallis tests. Acceleration rates during solo driving did not vary significantly according to operating mode while the PHEV Sprinter was navigating urban roadways, however, solo driving on suburban roads did exhibit a statistically meaningful relationship between acceleration rate and active operating mode. During solo driving scenarios, acceleration rates were highest while the PHEV Sprinter was in charge-sustaining operation. Even without conclusive statistical results, the tendency of acceleration rates to vary according to time of day does not present consistently between solo and follow driving, suggesting that overarching traffic patterns resulting from higher morning traffic densities cannot fully explain the discrepancies in on-road driving variables between the operating modes.

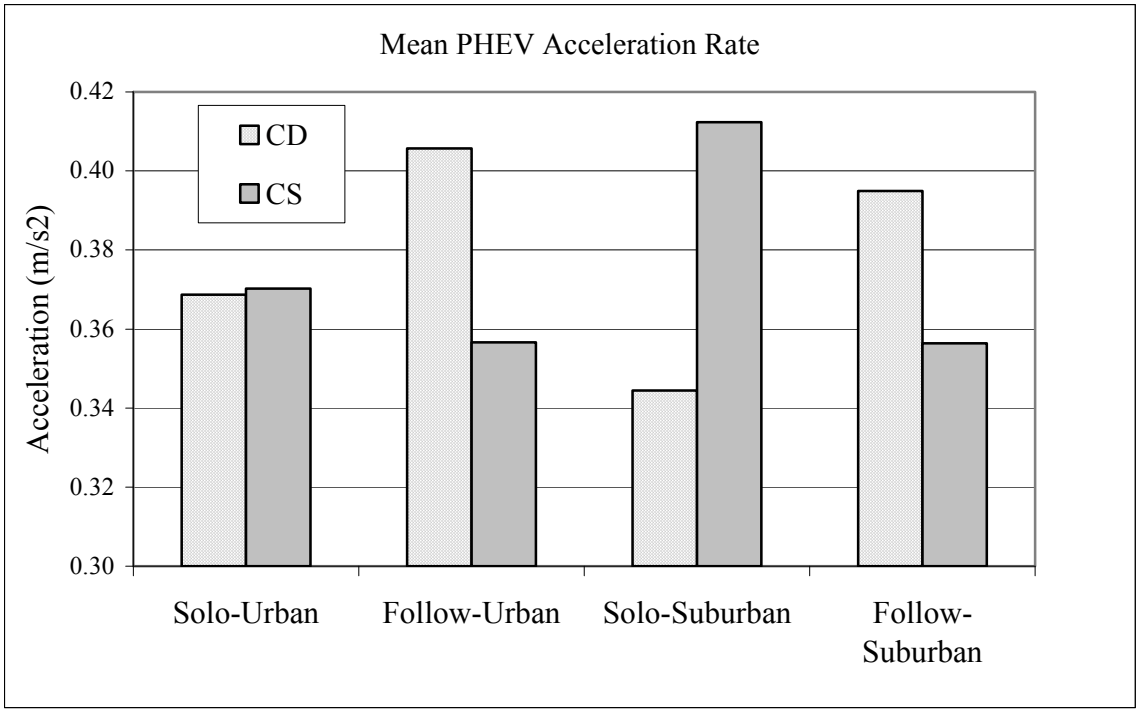

Figure 11.3: Mean acceleration rates according to operating mode for solo and follow driving.

Statistical analysis of deceleration rates between the operating modes exhibited slightly more conclusive results than the equivalent investigation of acceleration rates. Deceleration rate proved to be a statistically significant response to operating mode on suburban roads regardless of driving scheme (solo versus follow), but neither driving scheme proved meaningful to the set level of significance during urban travel. However, regardless of statistical validation, the PHEV Sprinter's mean deceleration rate was consistently lower during charge-sustaining operation compared with charge-depleting mode. This phenomenon may be attributable to variations in on-road driving profiles with varying traffic densities. However, it is also possible, in the case of both acceleration and deceleration rates, that the PHEV's active power scheme (charge-sustaining versus charge-depleting) may have resulted in unintended driver influence. Driver bias between electric-only operation and hybrid (or dICE-assisted driving) could have resulted in the different driving patterns exhibited between the operating modes, since electric only operation is significantly more prevalent during charge-depleting mode.

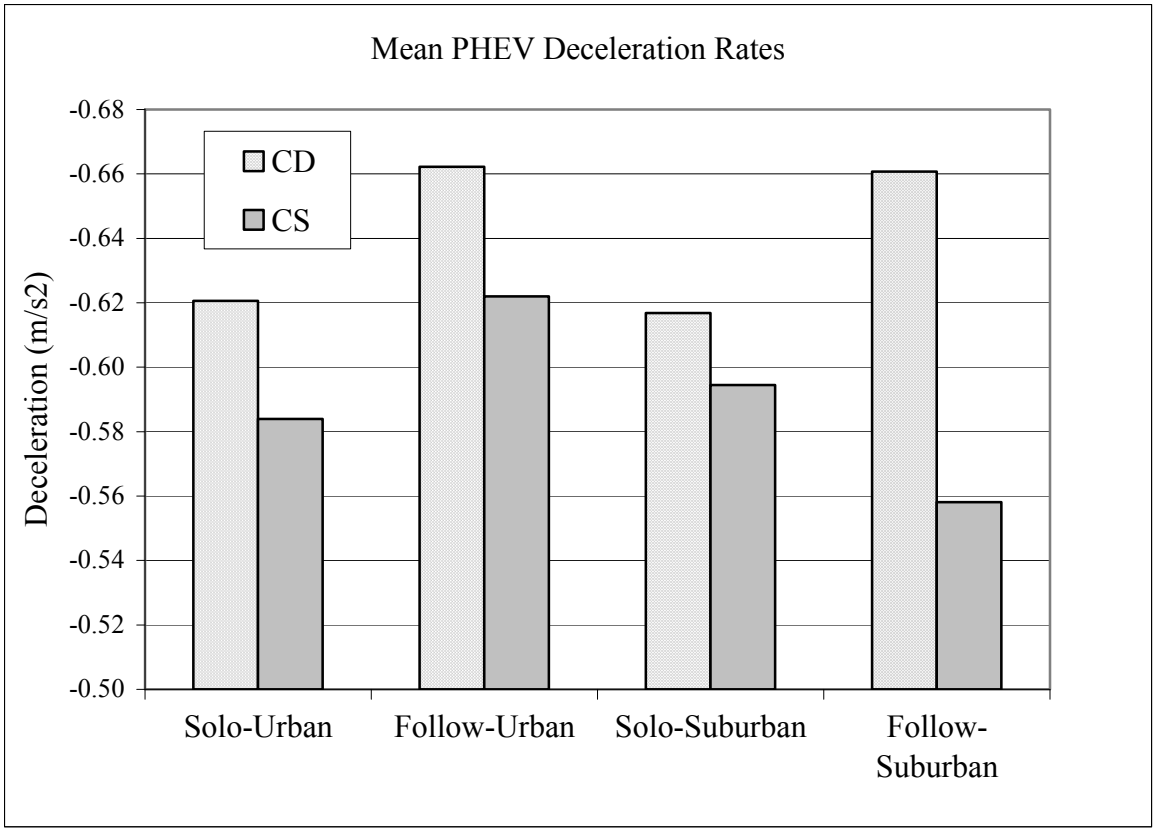

Figure 11.4: Mean deceleration rates according to operating mode for solo and follow driving.

In order to investigate the possibility of driver bias between the predominant PHEV power schemes, the data were segregated according to electric-only operation (as defined by a hybrid clutch position of 100%) and hybrid (dICE-assist or sole dICE powered) operation. Because solo and follow data were obtained under very different on-road situations, this investigation was conducted on each driving scheme separately.

Beginning with solo driving, the initial analysis focused on charge-depleting mode only, as this operating mode afforded the highest amount of electric-only on-road driving. Since statistical significance was not observed in acceleration and deceleration rates of urban roadway travel, suburban roads were the focus of the first statistical tests. During charge-depleting operation, solo driving on suburban roadways did not yield

significantly different ($\alpha<0.025$) deceleration rates according to power-scheme (electric-only versus hybrid operation). However, electric-only acceleration rates were significantly slower than those recorded during hybrid operation, when the dICE was providing at least a portion of the PHEV Sprinter's motive power (0.342m/s^2 compared with 0.386 m/s^2, respectively). When this analysis was expanded to include hybrid and electric-only data from both operating modes (charge-depleting and charge-sustaining), both deceleration and acceleration rates proved to be statistically meaningful responses to whether the PHEV was operating electric-only or in hybrid mode. The PHEV Sprinter's mean deceleration rates were calculated at -0.639m/s^2 for electric-only operation and –0.568 m/s^2 during hybrid operation. The relative difference between the measured acceleration rates, while still statistically significant, was less dramatic than the reported difference in deceleration rates (electric-only mean acceleration of 0.384 m/s^2 versus hybrid mean acceleration rate of 0.406 m/s^2). A third rendition of the statistical tests was preformed on the entire solo dataset, inclusive of both urban and suburban roadways. Again, both deceleration and acceleration rates proved to be statistically significant responses to power scheme with average deceleration rates of –0.633 m/s^2 and –0.572 m/s^2 for electric-only and hybrid operation, respectively. With respect to acceleration rates, the calculated mean values were 0.382 m/s^2 for electric-only operation and 0.401 m/s^2 during hybrid operation.

With acceleration and deceleration rates proving to be meaningful responses to power scheme regardless of the level of analysis (i.e. roadway type or according to active operating mode), it can be conclusively stated that the PHEV Sprinter's on-road driving behaviors, to a certain extent, were a function of active power scheme (electric-only or

hybrid operation). While time-of-day influences are still present, the driver's behavior with regards to the PHEV's acceleration and deceleration events is more closely attributable to the driver's reaction to the differences in the vehicle's behavior between electric-only and hybrid driving (during which the dICE was running). It is not possible to discern, however, if the driver's behaviors are the result of a psychological response to active power scheme or due to the mechanical differences in the PHEV Sprinter's operation between the two power schemes.

During electric-only operation, the PHEV Sprinter operated silently without transmission gearing. This quieter, smoother operation could have had a subtle, but measurable, impact on the driver's on-road assertiveness, resulting in slightly depressed acceleration rates. It is also possible that the electric-motor output during actual on-road operation while under a high payload, as was the Kansas City PHEV Sprinter, was slightly less capable of meeting the driver's acceleration demands, resulting in lower overall acceleration rates.

Similarly, inherent differences in the PHEV Sprinter's power scheme (electric-only versus hybrid) give plausible explanation to the variation in deceleration rates between the two schemes. During what is defined as hybrid operation in this case, the diesel ICE is continuously providing at least a portion of the PHEV's motive power. Due to limited engine speed ranges, internal combustion engines employ the use of transmission gearing in order to deliver drivetrain rotation speeds capable of meeting all on-road driving demands. With the turbo-charged diesel engine, some degree of engine braking occurred every time the throttle was disengaged. The enhanced deceleration resulting from increased backpressure through the turbo exhaust system may have

resulted in a lower reliance on the conventional friction braking system. While hybrid-electric vehicles are often equipped with computer simulated engine-braking responses, and regardless of whether or not one was employed on the PHEV Sprinter, more mild to no engine-braking effects during electric-only operation would require heavier reliance on the friction brakes in order to control the PHEV's deceleration rates. This increased use of friction braking during electric-only deceleration events (via the brake pedal) may logically justify the statistically more aggressive deceleration rates observed during electric-only operation.

A similar investigation of the follow data, where the PHEV Sprinter was being driven by the same operator, but under the influence of shadowing an in-service transit bus, inclusive of data from both operating modes, showed that acceleration rates were considerably less during electric-only operation compared with hybrid driving ($0.336 m/s^2$ versus $0.394 m/s^2$). The difference was less marked during charge-depleting operation ($0.374 m/s^2$ for electric-only and $0.436 m/s^2$ for hybrid driving), however charge-depleting operation occurred during the morning hours, when traffic densities were the highest. In these instances a lot of influencing factors relating not only to the PHEV Sprinter's inherent mechanical abilities or the driver's natural psychological bias were present including, but not limited to, time of day relationships.

The most significant conclusion to the above discussion is that statistical differences in on-road driving exist between the two operating modes. Some of these differences may be logical time-of-day influences, such as velocity, and others may be driver-imposed, such as acceleration and deceleration rates, but the fact still bears that

with regards to on-road variables, charge-depleting and charge-sustaining operation are not equivalent, and will be analyzed separately for the remainder of this objective.

11.2.2 Drive Scheme Effect

In order truly assess the impact that transit driving had on the PHEV Sprinter's emissions and operation, it was necessary to first evaluate the different on-road traits and behaviors that distinguish on-road transit service from solo or more civilian-based driving. Due to the inherent differences in on-road behavior between charge-depleting and charge-sustaining mode data, the operating modes will be investigated separately from one another in order to exclude the presence of confounding effects between operating mode on the transit service (follow) versus solo driving assessment.

When analyzed as a comprehensive dataset (inclusive of both roadways), charge-depleting operation resulted in statistically significant ($\alpha<0.025$) differences in on-road driving behaviors between following a transit bus and driving solo, with velocity, acceleration, and deceleration all proving to be statistically meaningful. The statistically comprehensive results achieved during the analysis of the complete, comprehensive dataset were maintained when the analysis was focused on suburban driving only. However, the significance in the on-road behaviors waned when the analysis was limited to urban roadways. While operating in and near the Kansas City urban core, neither acceleration nor deceleration rates proved to be statistically different between shadowing an in service transit bus (follow) and driving the same roads as a solo, independent driver.

Table 11.3: Statistical summary of driving-based variables during charge-depleting operation according to drive scheme (solo versus follow).

Variable:	All Roads	Suburban Roads	Urban Roads
Velocity (km/h)	y	y	y
Acceleration (m/s^2)	y	y	n
Deceleration (m/s^2)	y	y	n

Inc1: y anova, n kw
Inc2: n anova, y kw

During charge-sustaining operation, driving variables remained statistically significant responses to the PHEV Sprinter's driving scheme (follow or solo), however a couple instances exist where the statistical tests were inconclusive between the parametric and non-parametric analyses. With the exception of deceleration rates when analyzed as a comprehensive dataset, inclusive of both roadway types (failing the Kruskal-Wallis test), and acceleration rates on urban roadways (failing the ANOVA test), all driving behavior variables proved to be statistically meaningful ($\alpha<0.025$) for all levels of analysis.

Table 11.4: Statistical summary of driving-based variables during charge-sustaining operation according to drive scheme (solo versus follow).

Variable:	All Roads	Suburban Roads	Urban Roads
Velocity (km/h)	y	y	y
Acceleration (m/s^2)	y	y	Inc2
Deceleration (m/s^2)	Inc1	y	y

Inc1: y anova, n kw
Inc2: n anova, y kw

Velocity was consistently a meaningful response to driving scheme, regardless of operating mode or roadway travel. In all cases, solo driving resulted in higher on-road mean velocities than following a transit bus. In order to meet ridership demands, transit

service required both unscheduled and scheduled stops throughout each route. The presence of additional stops and increased stationary time will reduce the overall mean velocity. Stop profiles are evaluated in subsequent paragraphs, but it is important to consider the sources of potential deviation between solo and follow driving.

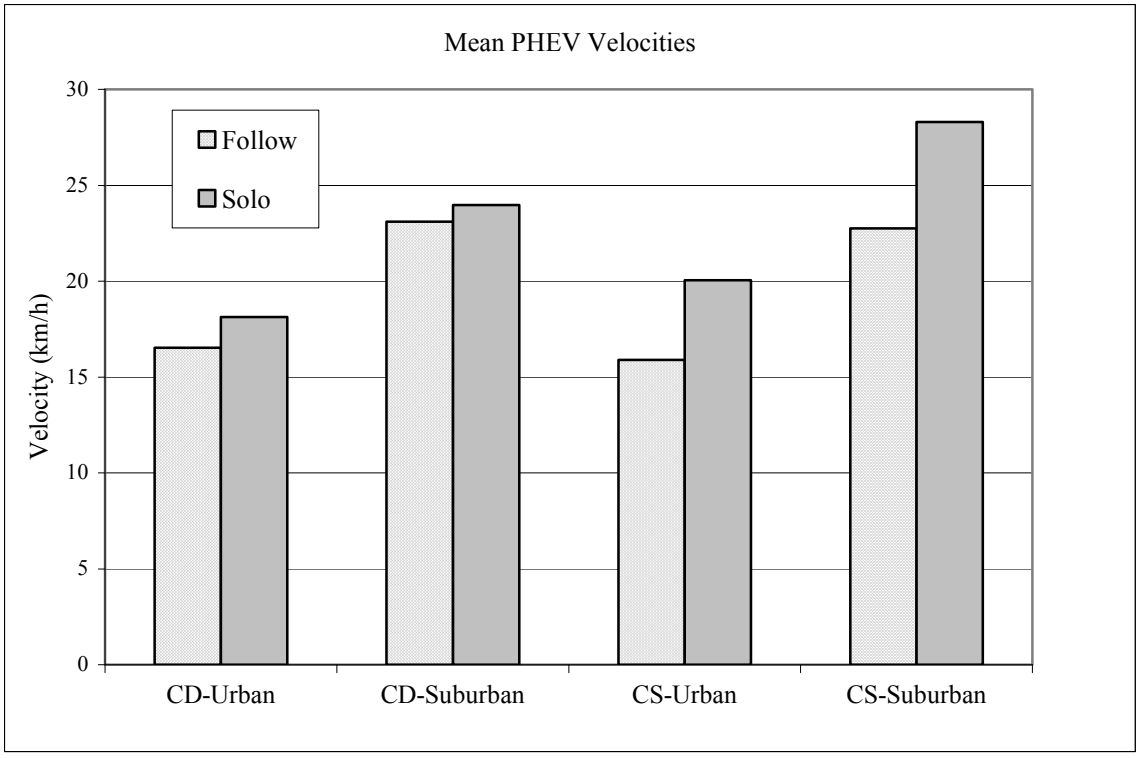

Figure 11.5: Mean velocities according to drive scheme for each operating mode.

While the presence of passenger-mandated stops during follow sampling presents a potential source of bias resulting in an artificially depressed velocity evaluation, redundant analysis of the data void of zero velocity data still shows that, regardless of roadway or operating mode, following a transit bus always resulted in statistically significantly lower travel speeds.

Similar to previous statistical efforts, ANOVA and Kruskal-Wallis tests were used to evaluate stop/traffic profiles between the two driving schemes (follow versus solo). The data used to complete this investigation was based on individual sample runs; therefore the required level for determining statistical significance was reduced slightly to $\alpha<0.05$ in accordance with past sample-run based analyses.

As mentioned previously, prior to all solo/follow investigations, data collected during layover periods between scheduled routes was removed from the follow dataset. In order to maintain a consistent and reproducible schedule for the day, each transit route was designed with a several minute layover period between the end of one route and the start of the subsequent route. In addition to allowing the bus to remain on its set schedule, the layover period also served as a regular respite for the bus drivers. Because this time is not reflective of actual transit driving, this stationary period was removed from all data prior to analysis.

Each sample route had subtle variations in duration and distance, so stop and stationary data were normalized according to both sample run distance and duration. During charge-depleting operation, no statistically significant difference existed between the stop profiles and amount of stationary time between follow and solo driving. Conversely, most of the calculated indicators used to describe the PHEV Sprinter's stop/start profile proved to be statistically significant responses to drive scheme during charge-sustaining operation (Table 11.6). Aside from the amount of time per individual stop during urban driving and the number of stops per run time during charge-sustaining suburban driving, all other measures met the alpha<0.05 for all ANOVA and Kruskal-Wallis analyses.

Table 11.5: Statistical summary of traffic profile variables according to drive scheme during charge-depleting operation.

Variable:	Urban	Suburban
Time/Stop (s)	n	n
# Stops/Distance	n	n
# Stops/Minute	n	n
% Time Stopped (V=0km/h)	n	n

Inc1: y anova, n kw
Inc2: n anova, y kw

Table 11.6: Statistical summary of traffic profile variables according to drive scheme during charge-sustaining operation.

Variable:	Urban	Suburban
Time/Stop (s)	n	y
# Stops/Distance	y	y
# Stops/Minute	y	n
% Time Stopped (V=0km/h)	y	y

Inc1: y anova, n kw
Inc2: n anova, y kw

Time-of-day influences may have contributed to the lack of statistical significance found for all charge-depleting analyses. Increased traffic density during the morning hours may have been a larger function of the PHEV Sprinter's stop profiles than the on-road activities related specifically to transit operation. Due to the lack of statistical significance found during charge-depleting mode, the following discussion will be limited to charge-sustaining operation.

All measures of stop time and frequency were higher during simulated transit driving, regardless of roadway type. Aside from the amount of elapsed time per stop during urban driving and the number of stops per run time during suburban driving, all tests met the specified level determining statistical significance ($\alpha<0.05$). As intuitively

expected, transit driving resulted in a higher frequency of stops (according to both a time and distance basis of normalization) and resulted in, on average, longer elapsed times during each stop. While it was originally expected that the increased stop time during follow driving could have been the source of the velocity differences between the driving-schemes, ANOVA and Kruskal-Wallis analysis of the entire charge-sustaining dataset void of all zero velocity data still showed velocity as a statistically significant response (p-value = 0.000 for both tests) to driving scheme with follow driving resulting in significantly lower velocities than solo driving.

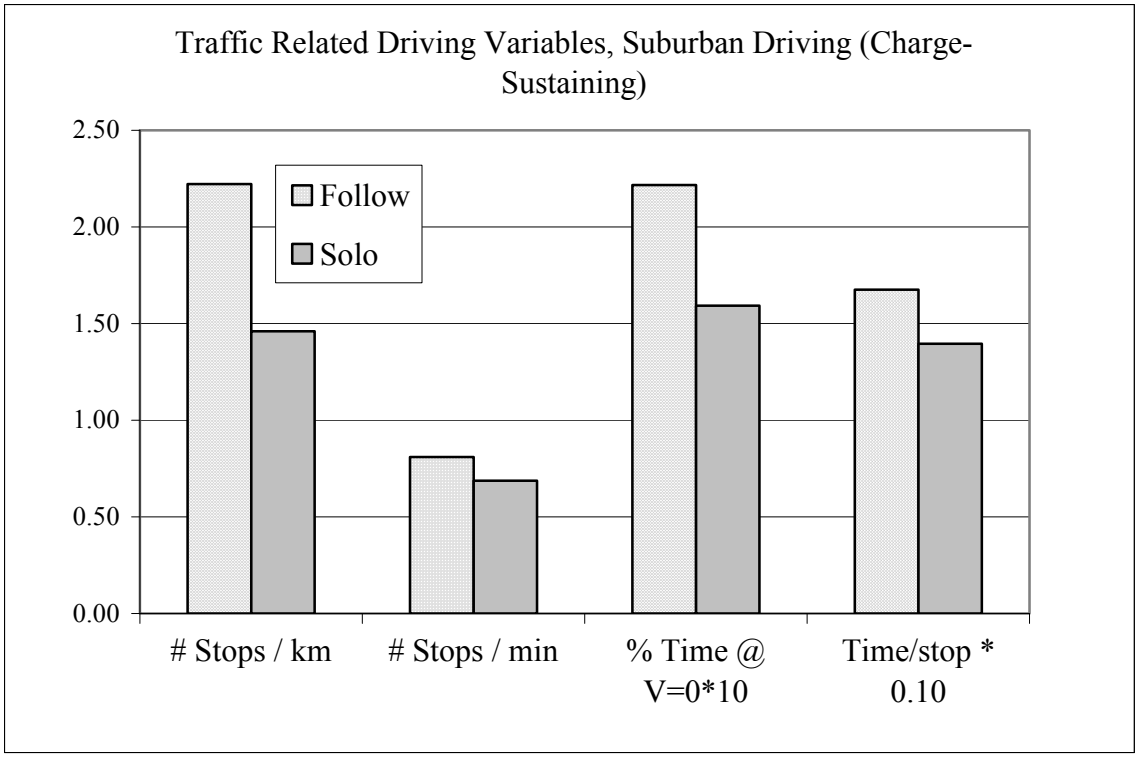

Figure 11.6: Stop profiles according to drive scheme during charge-sustaining operation on suburban roadways.

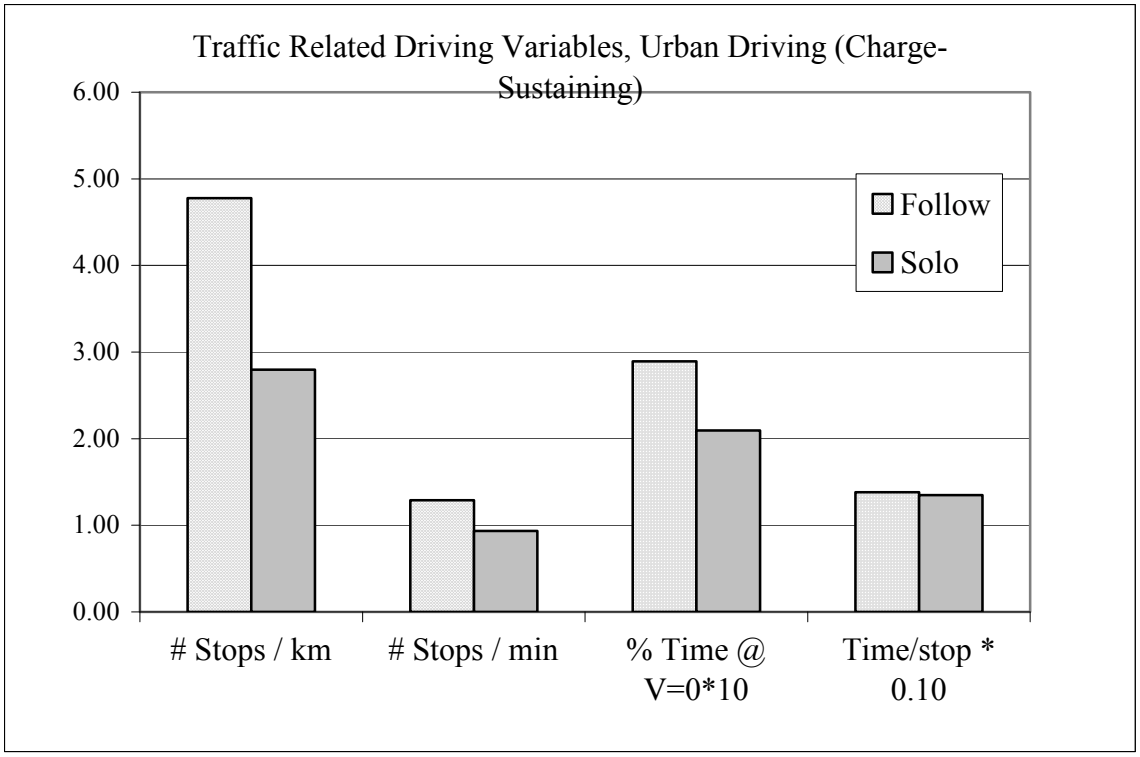

Figure 11.7: Stop profiles according to drive scheme during charge-sustaining operation on urban roadways.

Both acceleration and deceleration rates proved to be statistically significant responses to driving scheme depending on the roadway type being navigated. With regards to acceleration rates, urban travel did not yield statistically significant results according to drive scheme. Suburban travel, however, did present statistically meaningful relationships between acceleration rates and drive scheme for both operating modes. The relative relationship in acceleration rates between solo and follow driving varied according to the time-of-day (or consequently, active operating mode). Transit service (follow) resulted significantly higher acceleration rates from the PHEV Sprinter during charge-depleting operation. Since these rates occurred in the early morning, it is plausible that transit driving required slightly more aggressive driving profiles in order to maintain its set schedule during the morning hours, when roadways possessed higher

traffic densities. However, during charge-sustaining operation, during the late-morning and mid-afternoon hours, following transit buses resulted in more mild acceleration rates.

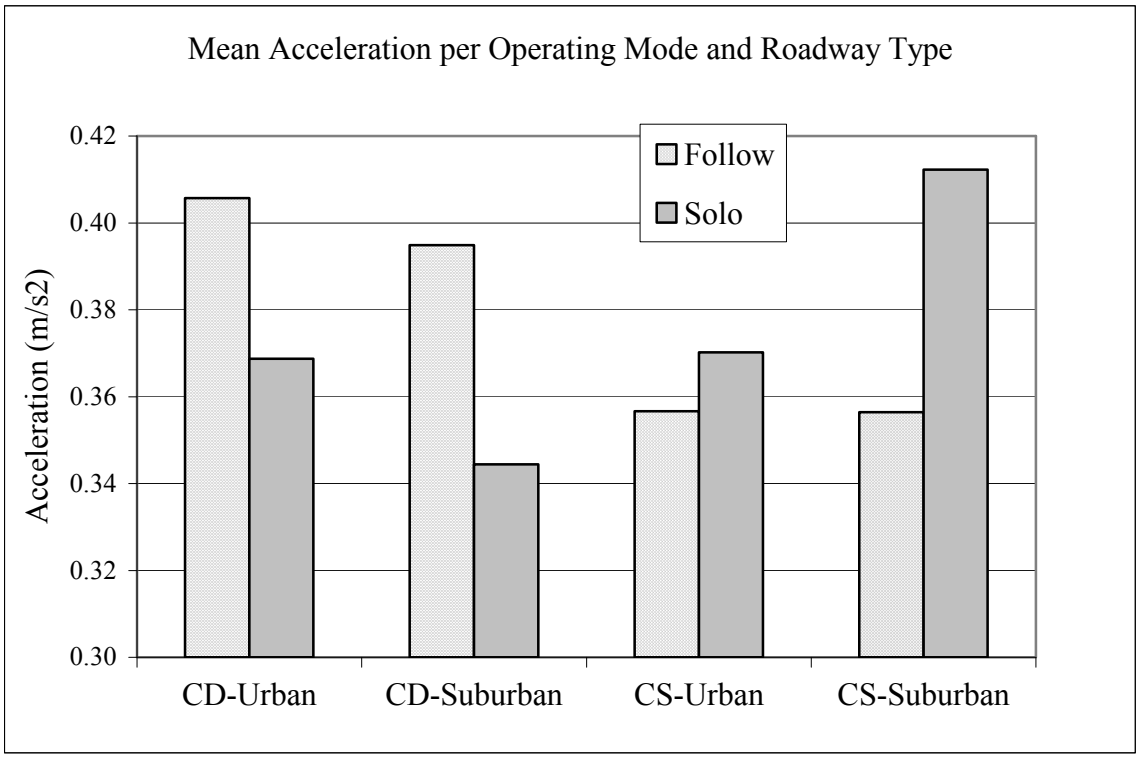

Figure 11.8: Acceleration rates by operating mode and roadway according to drive scheme.

Deceleration rates were generally more aggressive (more negative) while the PHEV Sprinter was shadowing a transit bus. In addition to adhering to a set schedule of passenger stops, transit operation also required that the bus make unscheduled, but still frequent, stops according to passenger demand. These stops were prompted by either passenger request to exit the bus or passenger presence at the stop location. Due to the demand-nature of these stops, it is not unreasonable that the stops were made with little notice to the bus driver, and therefore required more aggressive deceleration rates in order to manage each stop. In addition to providing a visual display of deceleration rates

according to drive scheme for each operating mode and traveled roadway, the following figure gives good illustration to the variation in deceleration rates between charge-sustaining and charge-depleting operation.

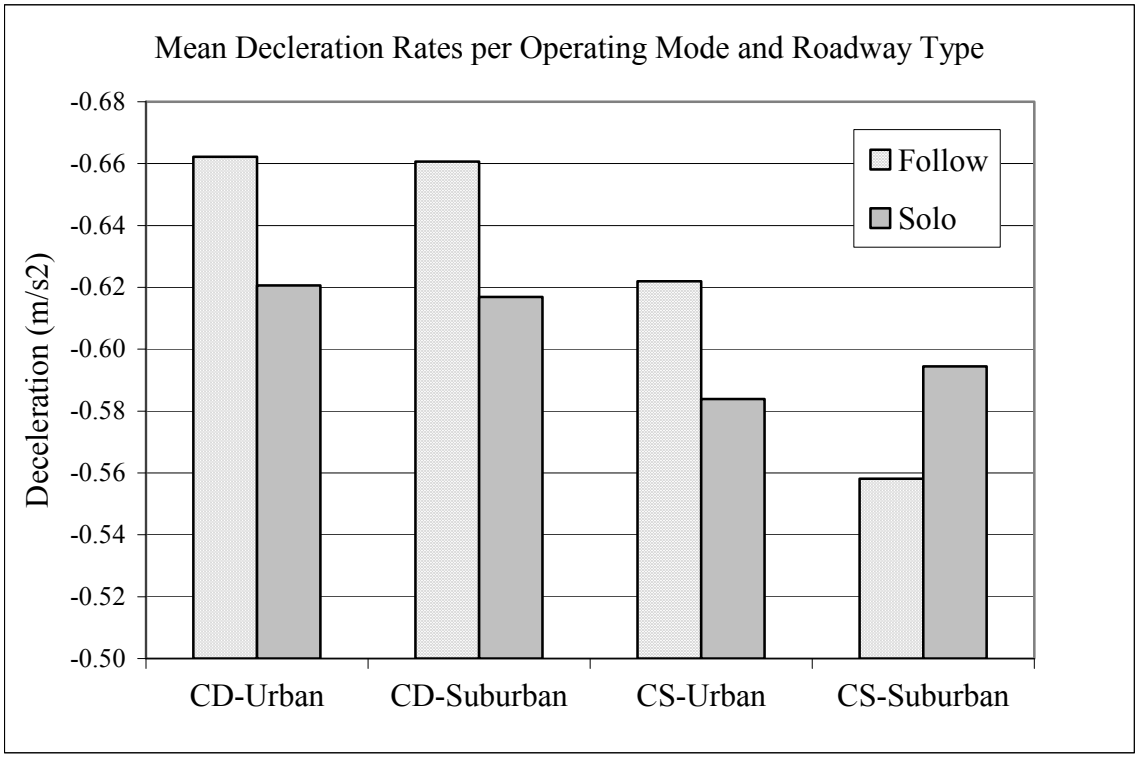

Figure 11.9: Deceleration rates by operating mode and roadway according to drive scheme.

11.3 Power Related Variables

The previous section gave statistical basis to the fact that the PHEV Sprinter's on-road experience differed according to driving scheme: following a transit bus as a chase vehicle or driving solo according to local traffic patterns and rules. Velocity, acceleration, deceleration, and stop profiles demonstrated statistically significant responses to driving scheme according to active operating mode.

In order to evoke discussion regarding the PHEV Sprinter's suitability as a transit-oriented vehicle, further investigation into the PHEV's power usage was conducted. Total power output as well as the output of the individual subsystems (diesel ICE and electric motor) was assessed using the statistical techniques identified and employed earlier. The set levels of significance were mandated according to the particular dataset being considered. All continuous data were required to meet a strict $\alpha<0.025$, while the sample-run based dataset met statistical significance with a slightly reduced constraint of $\alpha<0.05$.

Analysis of the data collected during charge-depleting mode showed few statistically valid responses between power output and driving scheme. An insufficient number of sample runs were collected while following a transit bus on urban roads during charge-depleting operation, so urban travel was excluded from the sample-run based analysis. Sufficient second-by-second data collected on urban roadways was available to justify statistical analysis of the continuous dataset's urban travel. Aside from power output from the diesel ICE and electrical recuperation rates during suburban travel, power output failed to demonstrate a meaningful response to driving scheme. During charge-depleting operation, the PHEV Sprinter's power usage remained statistically equivalent

regardless of whether the PHEV was following an in-service transit bus or being driven in a more civilian manner. This lack of power definition between follow and solo driving is somewhat surprising given the reported differences in velocity, acceleration and deceleration rates between the drive schemes during charge-depleting operation.

Table 11.7: Statistical summary of sample run-based dataset analysis of power output according to drive scheme, charge-depleting operation.

Variable:	All Roadways	Suburban Roads
ICE, W/kg/s	n	n
EM, W/kg/s	n	n
Total Wrk, W/kg/s	n	n
Recup, W/kg/s	n	n
Velocity, km/h	n	n

Inc1: y anova, n kw
Inc2: n anova, y kw

Table 11.8: Statistical summary of continuous dataset analyses of power output according to drive scheme, charge-depleting operation.

Charge-Depleting, Continuous Datset

Variable:	All Roadways	Suburban Roads	Urban Roads
VSP Ins, W/kg/s	Inc2	n	Inc2
dICE, W/kg/s	Inc2	y	Inc1
EM, W/kg/s	Inc1	Inc1	n
Total Wrk, W/kg/s	n	Inc2	Inc1
Recup, W/kg/s	Inc1	y	n

Inc1: y anova, n kw
Inc2: n anova, y kw

During charge-sustaining operation, the impact that drive scheme had on the PHEV Sprinter's power usage and output proved to be more statistically noteworthy. During suburban travel, all power-related variables, except EM power output, demonstrated a statistically significant response to the follow or solo drive scheme. Electric motor power output failed to conclusively meet the levels of statistical

significance for the Kruskal-Wallis analysis of the continuous dataset. Urban travel, however, was considerably less definite in its statistical viability. Contrary to suburban travel, none of the power output variables proved to be conclusively significant for either level of analysis (by sample run or on the continuous dataset) aside from the electric motor (EM) power output, which met the required levels of significance for both the sample-run based analysis as well as the continuous dataset.

Table 11.9: Statistical summary of sample-run based analyses of power output according to drive scheme, charge-sustaining operation.

Charge-Sustaining by Data File Means

Variable:	All Roadways	Suburban Roads
dICE, W/kg/s	y	y
EM, W/kg/s	y	y
Total Wrk, W/kg/s	y	y
Recup, W/kg/s	y	y

Inc1: y anova, n kw
Inc2: n anova, y kw

Table 11.10: Statistical summary of continuous dataset analyses of power output according to drive scheme, charge-sustaining operation.

Charge-Sustaining, Continuous Dataset

Variable:	All Roadways	Suburban Roads	Urban Roads
VSP Ins, W/kg/s	y	y	Inc2
dICE, W/kg/s	Inc1	y	Inc2
EM, W/kg/s	y	Inc1	y
Total Wrk, W/kg/s	y	y	Inc1
Recup, W/kg/s	y	y	Inc1

Inc1: y anova, n kw
Inc2: n anova, y kw

While differences in the mean total power output between the drive schemes are visually apparent in the following chart, only the charge-sustaining suburban travel

proved to be statistically significant, with solo driving requiring more total power output than following a transit bus. Figure 11.10 shows bold outlines for scenarios where statistical significance was achieved. Even without meeting the strict demands set on alpha for determining statistical significance, solo driving consistently required more total power output than shadowing an in service transit bus. This finding is contrary to the original expectations prior to initiating this investigation, where, based solely on driver observation, follow driving was suspected to be the more aggressive of the two drive schemes. The higher velocities and acceleration rates recorded during solo operation translated to higher overall power requirements.

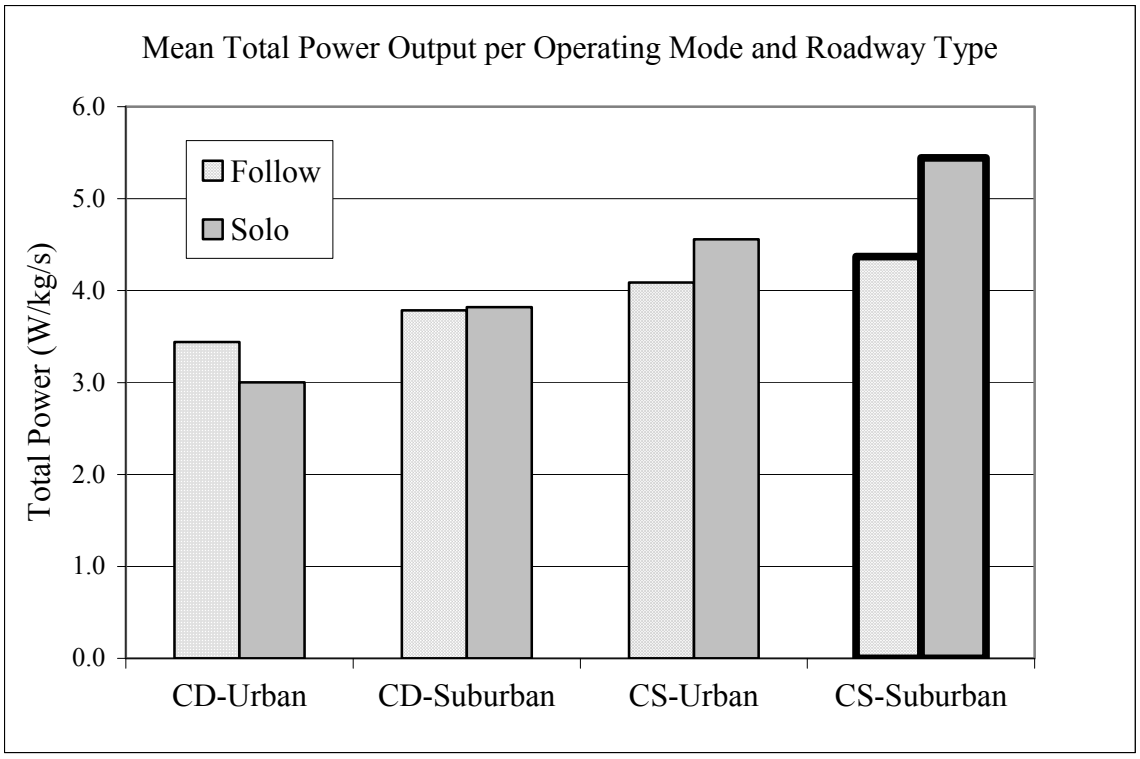

Figure 11.10: Total power output according to drive scheme.

Diesel ICE power output proved to be statistically inconclusive for all urban driving regardless of active operating mode. However, while driving suburban roadways, the PHEV Sprinter consistently required a higher rate of power output from the dICE for solo driving compared with following a transit bus. The PHEV's dICE recruitment has been shown to increase with increasing acceleration rates and on-road velocities, both of which where higher during solo driving. Contrary to the significance found when analyzing the dICE power output data, the electric motor (EM) did not prove to demonstrate a statistically significant response to drive scheme under any scenario except while navigating urban roadways during charge-sustaining operation. Similar to the both total power output and dICE power output, during charge-sustaining, suburban travel, solo driving required a stronger use of the EM compared to following a transit bus, however, not to a statistically significant level. Similar to Figure 11.10, relationships that demonstrated statistical significance are denoted with bold outlines in Figures 11.11 and 11.12.

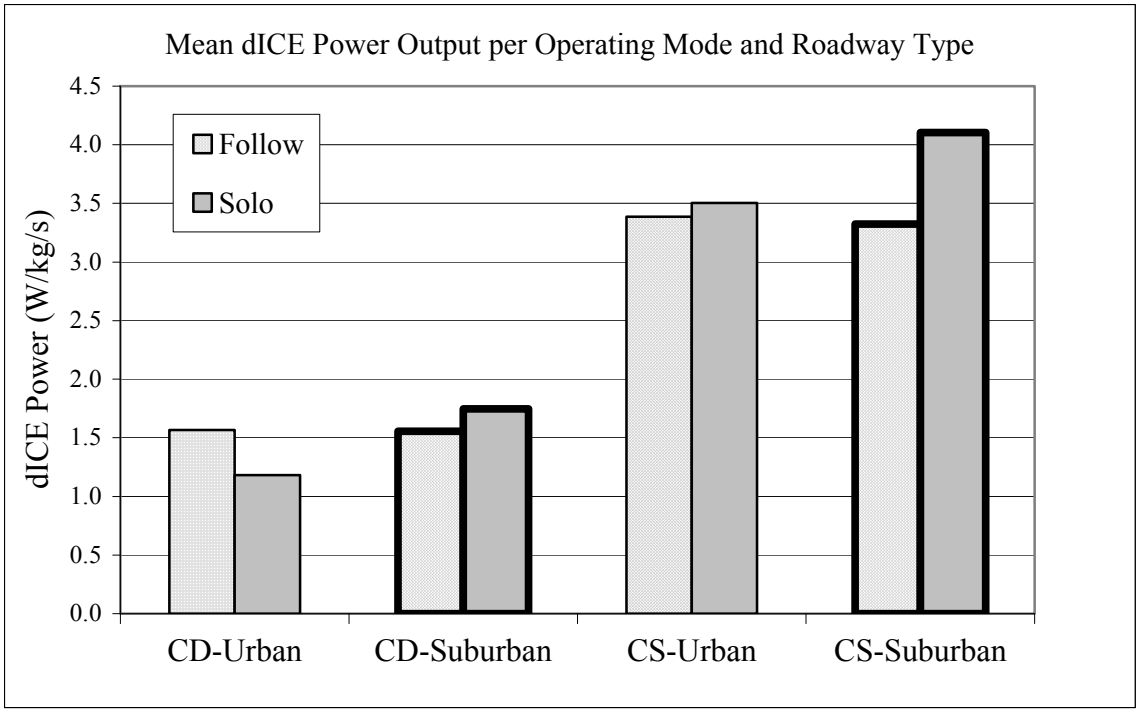

Figure 11.11: Diesel ICE power output according to drive scheme.

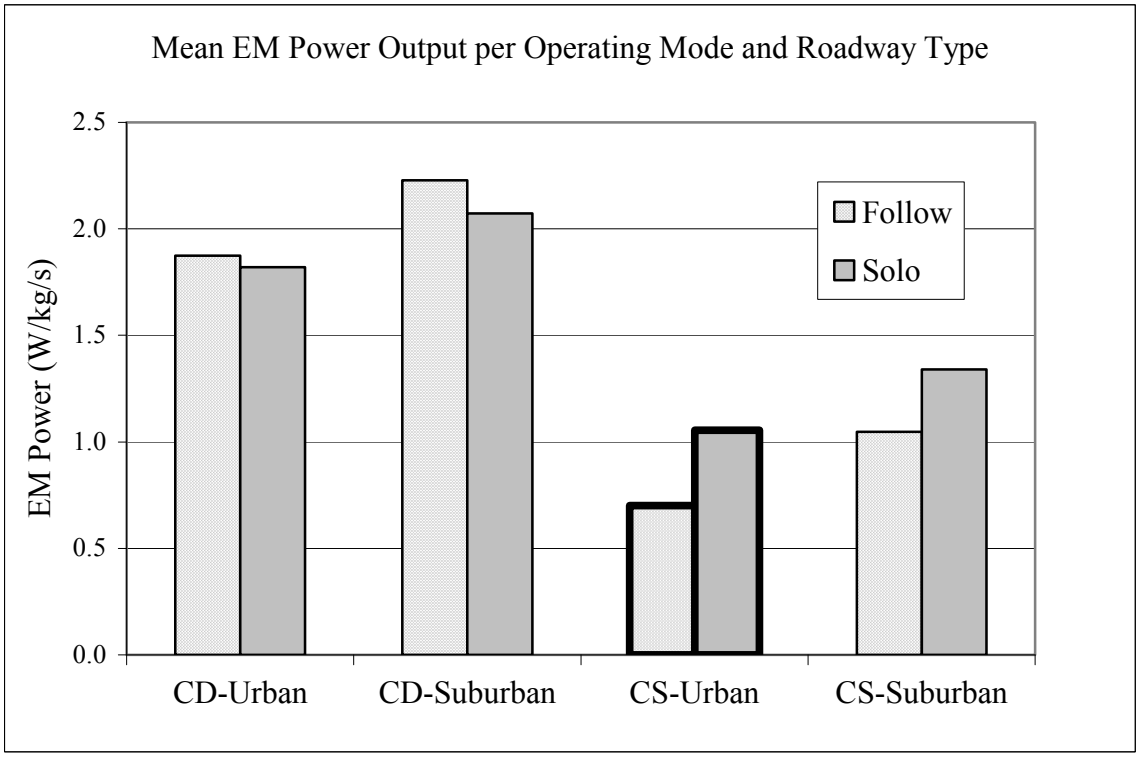

Figure 11.12: Electric motor power output according to drive scheme.

No statistically significant relationship was found between electrical recuperation rates and drive scheme for urban travel, regardless of active operating mode. However, during suburban travel, solo driving consistently resulted in higher rates of electrical recuperation compared with shadowing a transit bus. A large portion of the PHEV Sprinter's recuperation capacity occurs during deceleration events. Periods of strong deceleration require the use of friction braking over regenerative braking in the interest of on-road safety. However, more mild deceleration events result in better utilization of the PHEV's regenerative braking capabilities. As found and discussed earlier, charge-sustaining deceleration was less aggressive than that reported during charge-depleting operation, likely due to time-of-day influences associated with higher traffic density during the morning hours. Additionally, follow driving required significantly stronger (more quantitatively negative) deceleration events than solo driving. The impact that deceleration trends have on PHEV operation is mirrored in the respective recuperation rates between driving scheme and operating mode. During urban travel, recuperation rates did not yield conclusive statistical results as a function of driving scheme. However, recuperation rates observed while driving suburban roadways did prove to be statistically significant responses to drive scheme, with follow driving resulting in reduced recuperation rates, presumably in association with the more aggressive deceleration experienced while the PHEV shadowed in-service transit buses during suburban travel. Relationships that demonstrated statistical significance are denoted with bold outlines in Figure 11.13.

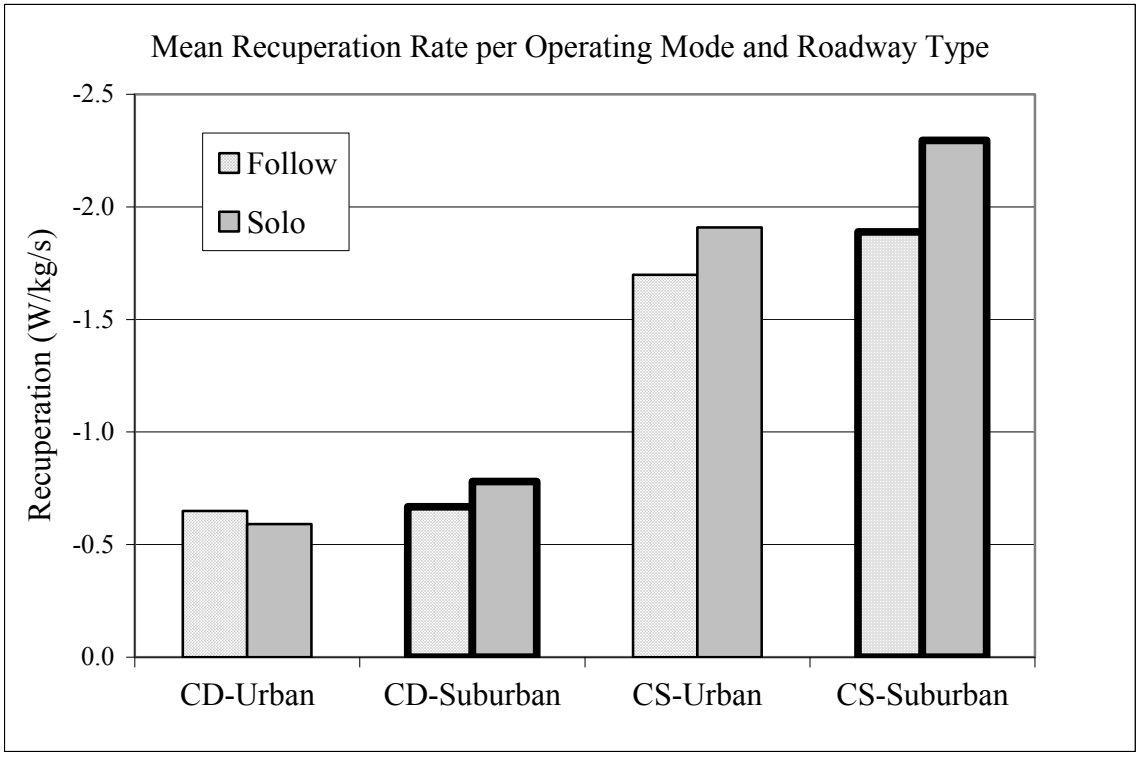

Figure 11.13: Recuperation rates according to drive scheme.

11.4 Pollutant Emissions

11.4.1 Charge-Depleting Mode

Pollutant emissions were investigated in the same manner used for the power and road-based variables assessments. All analyses were conducted in duplicate: first on the sample-run based dataset and again on the continuous, second-by-second dataset, with all analyses performed using both the parametric and nonparametric statistical tests. Levels of significance were maintained at $\alpha<0.025$ and $\alpha<0.05$ for the continuous and run-based analyses, respectively. Statistical analysis of charge-depleting mode, when applied to the continuous dataset, yielded a number of pollutant responses to drive scheme that met the required level of significance. Exhaust flowrate and temperature were analyzed on a continuous basis, giving additional, supportive information concerning the diesel ICE's function.

Table 11.11: Statistical summary of pollutant emission according to drive scheme during charge-depleting operation conducted on the sample run-based dataset.

Variable:	All Roadways	Suburban Roads
Fuel, gal/s	n	n
CO_2, g/s	n	n
CO, g/s	n	n
NOx, g/s	n	n
NO, g/s	n	n
NO_2, g/s	n	n
HC, g/s	n	n

Table 11.12: Statistical summary of pollutant emissions according to drive scheme during charge-depleting operation conducted on the continuous dataset.

Charge-Depleting, Continuous Datset

Variable:	All Roadways	Suburban Roads	Urban Roads
Fuel, gal/s	Inc2	Inc2	y
CO_2, g/s	Inc2	Inc2	y
CO, g/s	y	y	y
NOx, g/s	Inc2	y	y
NO, g/s	y	y	y
NO_2, g/s	Inc2*	y	y
HC, g/s	y	y	Inc2
Exhaust Flow, SCFM	y	Inc2	y
Exhaust Temp, C	y	y	y

Inc1: y anova, n kw
Inc2: n anova, y kw

While the sample run-based dataset failed to demonstrate statistical significance for any of the measured pollutants, analysis of the continuous dataset during urban travel yielded strong statistical significance for all pollutant emissions and related variables as a function of drive scheme. Whereas the results found during the power evaluation earlier showed weak statistical significance between the PHEV Sprinter's power output and drive scheme during charge-depleting, urban operation with only EM power output yielding statistical results that fell within the $\alpha<0.025$ required level of significance. However, where the actual power data failed to establish meaningful statistical validation comparing the demonstration study's drive schemes, the variables most strongly correlated to the PHEV's power usage (CO_2, NO, fuel usage, and exhaust conditions), did prove to be statistically significant during charge-depleting urban travel, with follow driving resulting in higher overall exhaust emissions and increased fuel use.

Hydrocarbon emissions demonstrated the least statistically significant response to drive scheme by failing to conclusively pass the levels of significance for both parametric and nonparametric analyses. While the response of hydrocarbon emissions to drive scheme failed to meet the ANOVA criteria ($\alpha<0.025$), CO emissions, also a marker of transient dICE operation, were significantly higher during follow driving. In previous sections, pollutant emissions resulting from more stable dICE operation have been shown to trend with power output and fuel use. With regards to the drive scheme investigation, these pollutants and variables demonstrated some level of statistical significance during urban travel, but the relative difference between solo and follow driving is markedly lower compared to past investigations.

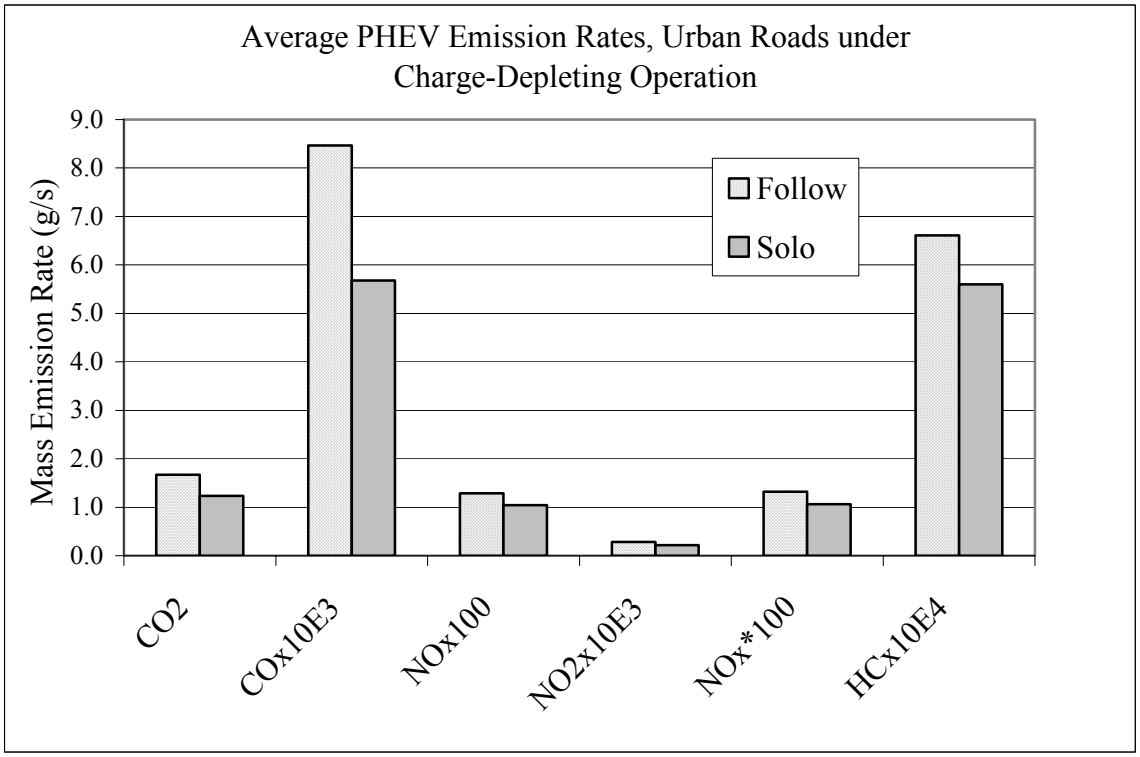

Figure 11.14: Pollutant emission rates during charge-depleting operation of urban roadways according to drive scheme.

Consistent with the pollutant emissions, urban driving during charge-depleting operation resulted in higher overall exhaust flowrates and temperatures during follow driving compared with solo driving. Trends in exhaust conditions proved to be statistically significant ($\alpha<0.025$). Higher average exhaust flowrates are indicative of overall increased dICE use (on a time basis) and/or higher overall demand during dICE function resulting from increased engine speeds. Engine exhaust temperatures are regulated by the engine cooling system, so an upper bound exists for all reported normal operating temperatures. Because of this, higher mean and median exhaust temperatures are a function of the dICE's state of warm-up. The reported trends suggest that the dICE tended to operate more warmed-up during urban, charge-depleting, follow driving compared with solo driving.

Table 11.13: Exhaust parameters during charge-depleting operation according to drive scheme.

	Road	Drive-Scheme	Median	Mean
Exhaust Flowrate (SCFM)	All	Follow	1.49	37.09
		Solo	1.07	34.08
	Urban	Follow	14.03	37.40
		Solo	1.04	28.07
Exhaust Temp (deg C)	All	Follow	53.5	55.2
		Solo	40.0	49.7
	Urban	Follow	61.0	59.8
		Solo	42.2	42.1

The ultimate difference in follow versus solo driving is based on the PHEV Sprinter's on-road driving behaviors (velocity, acceleration, and deceleration rates), tying the PHEV's on-road experience to its emissions provides the most comprehensive picture

of the true differences and implications in transit (follow) versus solo driving. Little statistical significance was found in the analyses of the driving variables between follow and solo driving during charge-depleting, urban travel. Only velocity proved to be statistically significant, with acceleration rates being statistically inconclusive between the parametric and nonparametric tests. When analyzed without the bias of zero velocity data, acceleration rate during charge-depleting urban travel became statistically conclusive, passing both the parametric and non-parametric tests (p-values=0.000). Regardless of the inclusion of zero velocity data, follow driving consistently resulted in higher overall acceleration rates. The previous analyses only addressed mean acceleration rates and did not assess the duration of time that the PHEV Sprinter may have been under acceleration within each drive scheme. Table 11.14 provides the relative amount of time that the PHEV was under acceleration between the two drive schemes during charge-depleting, urban travel. Acceleration was defined in two manners; initially, seconds of data collection where acceleration rates were greater than $0 m/s^2$ were used as an assessment of time under acceleration. As a second marker for determining acceleration events, the drive mode model presented earlier (Chapter 6) was employed here as well. The drive mode analysis required more stringent and aggressive criteria in order to define an acceleration event, and therefore, eliminated data where the PHEV Sprinter was under mild, naturally undulating periods of acceleration. During follow driving the PHEV was actually under periods of acceleration (as defined by acceleration$>0 m/s^2$) for a relatively shorter amount of time compared with solo driving. However, follow driving resulted in a higher proportion of acceleration events strong enough to be defined by the "Accel" drive mode. While the PHEV may have,

technically, spent relatively less time accelerating during urban, charge-depleting transit-simulated driving, its acceleration profile was more aggressive, and more aggressive for a proportionally larger amount of time than during solo driving. Since acceleration periods, specifically periods of strong acceleration, give cause to transient dICE operation, the relatively high carbon monoxide emissions during follow driving are suggestive of the vehicle's more aggressive driving profile.

Table 11.14: Relative prominence of acceleration events according to drive scheme during charge-depleting, urban travel.

Charge-Depleting:

Acceleration Basis	Roadway	Measure	Drive-Scheme	
			Follow	Solo
Acceleration Rates > 0m/s^2	All Roadways	Total Time (s)	13198	10050
		Time with Positive Acceleration (s)	9974	7436
		% Time at A>0m/s^2	**75.6%**	**74.0%**
	Urban	Total Time (s)	1599	1797
		Time with Positive Acceleration (s)	1161	1366
		% Time at A>0m/s^2	**72.6%**	**76.0%**
Driving Mode = Accel	All Roadways	Total Time (s)	13198	10050
		Time during Accel Mode (s)	2188	1562
		% Time during Accel Mode	**16.6%**	**15.5%**
	Urban	Total Time (s)	1599	1797
		Time during Accel Mode (s)	282	283
		% Time during Accel Mode	**17.6%**	**15.7%**

The PHEV's exhaust emissions proved to be a statistically significant response to drive scheme (follow versus solo driving) during urban driving. Aside from hydrocarbon emissions, which were statistically inconclusive, all measured pollutants and exhaust flowrate variables were consistently higher during follow driving. This finding falls in

accordance with the less-statistically meaningful power investigation, and reported on-road driving behaviors between the two driving schemes.

While the variables most closely associated with dICE power output failed to meet the required levels of significance for suburban travel (CO_2 and fuel use), those pollutants whose production and emission was related to transient dICE operation proved to be statistically meaningful responses to drive scheme for both suburban and urban travel (CO, NO_2, and HC). During travel on inherently faster traveling roadways (i.e. suburban), transit simulation resulted in lower overall emissions of NO and NO_2 than the solo-driven sample runs. Consistent with charge-depleting urban travel, more transient pollutants whose formation and emission is a function of non-steady state dICE operation, were still higher during transit-simulated driving (follow) while driving suburban roadways.

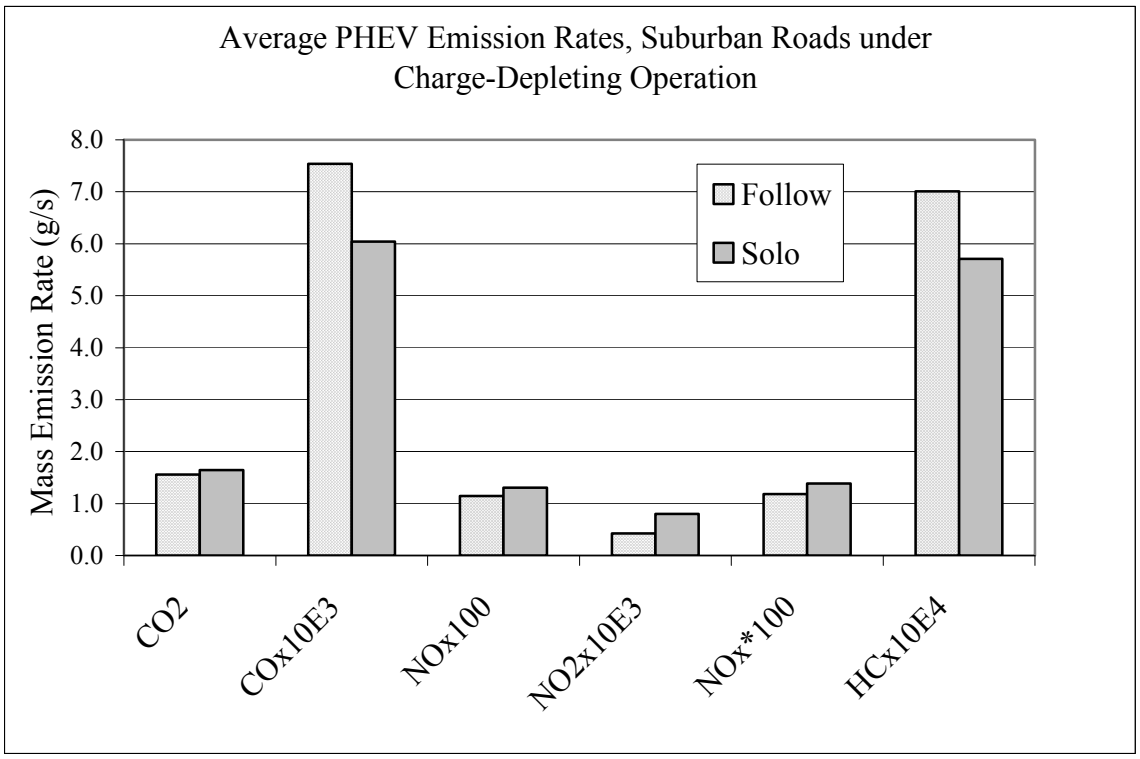

Figure 11.15: Pollutant emission rates during charge-depleting operation of suburban roadways according to drive scheme.

In order to provide additional insight into the dICE's operation between drive scheme, statistical analysis was extended to the exhaust flowrate and temperature data from the continuous dataset. While exhaust flow failed to provide conclusive statistical results, failing the ANOVA test, exhaust temperature proved to be a statistically significant response to drive scheme with transit-simulation resulting in considerably higher mean and median exhaust temperatures during suburban travel.

The power discussion earlier showed that solo driving on suburban roadways resulted in significantly higher dICE power output than follow driving. Because of this, it makes intuitive sense that the PHEV Sprinter would also have a higher emissions load during solo suburban driving, which is the case with respect to carbon dioxide (although not statistically conclusive), nitrogen oxide, and nitrogen dioxide. However, with regards

to carbon monoxide and hydrocarbon emissions, follow suburban driving well exceeded solo driving. Despite the relatively reduced dICE power output required by follow driving, the PHEV's measured exhaust temperatures were statistically higher during follow driving compared with solo driving. Coupled with power output trends, the elevated exhaust temperatures suggest that the dICE's operation may have been somewhat more aggressive when the PHEV was shadowing an in-service transit bus on suburban roadways.

Table 11.15: Exhaust parameters during charge-depleting, suburban travel according to drive scheme.

Charge-Depleting

	Road	Drive-Scheme	Median	Mean
Exhaust Flowrate (SCFM)	All	Follow	1.49	37.09
		Solo	1.07	34.08
	Suburban	Follow	1.43	37.04
		Solo	1.08	35.38
Exhaust Temp (deg C)	All	Follow	53.5	55.2
		Solo	40.0	49.7
	Suburban	Follow	51.7	54.5
		Solo	39.2	51.4

Expanding this discussion to the PHEV Sprinter's road-based variables, primarily velocity and acceleration, provides explanatory power to the seemingly incongruous exhaust emissions profiles between solo and follow driving of suburban roadways during charge-depleting operation. While stop profiles were not statistically different between solo and follow driving, all on-road variables (velocity, acceleration, and deceleration)

proved to be statistically significant responses to drive scheme. Solo driving resulted in higher average velocities, but following transit buses resulted in average acceleration rates that were almost 15% higher than solo driving. While the reported averages give an indication to which drive scheme generally had the higher rate of acceleration, it does not provide any insight into the relative proportion of the PHEV Sprinter's on-road time that was spent in periods of acceleration. Table 11.16 displays the relative amount of time that the PHEV Sprinter was under acceleration between solo and follow driving while navigating suburban roadways during charge-depleting operation. Regardless of the basis for establishing periods of acceleration (according to driving mode or acceleration rates greater than $0 m/s^2$), transit-simulated driving resulted in a higher proportion of time accelerating than solo driving. This difference is magnified when the driving mode model is used to differentiate periods of acceleration, indicating that not only was the PHEV under acceleration for more time during follow driving, but that these periods of acceleration were significantly more aggressive than those recorded during solo driving.

Table 11.16: Relative prominence of acceleration events according to drive scheme during charge-depleting, suburban travel.

Charge-Depleting:

Acceleration Basis	Roadway	Measure	Drive-Scheme	
			Follow	Solo
Acceleration Rates > 0m/s^2	All Roadways	Total Time (s)	13198	10050
		Time with Positive Acceleration (s)	9974	7436
		% Time at A>0m/s^2	**75.6%**	**74.0%**
	Suburban	Total Time (s)	11599	8253
		Time with Positive Acceleration (s)	8813	6070
		% Time at A>0m/s^2	**76.0%**	**73.5%**
Driving Mode = Accel	All Roadways	Total Time (s)	13198	10050
		Time during Accel Mode (s)	2188	1562
		% Time during Accel Mode	**16.6%**	**15.5%**
	Suburban	Total Time (s)	11599	8253
		Time during Accel Mode (s)	1906	1279
		% Time during Accel Mode	**16.4%**	**15.5%**

Since periods of strong acceleration place the dICE into a more transient state of operation, it is during these times that the more transient emissions occur. While increased dICE power demand during solo driving resulted in overall higher emissions of carbon dioxide and nitrogen dioxides, the stronger and more frequent periods of acceleration demanded by transit service resulted in significantly higher carbon monoxide and hydrocarbon exhaust emissions.

11.4.2 Charge-Sustaining Mode

Similar to the charge-depleting analysis, during charge-sustaining operation, the sample-run based investigation of urban roadways did not determine statistical significance for any of the variables investigated here. Suburban travel, however, did result in statistically significant responses between all variables except CO and HC, with

inconclusive NO_2 data failing the ANOVA test. When expanded to the continuous dataset, statistical significance was more universally achieved with all but CO emissions proving to be statistically significant responses to drive scheme during suburban travel, and CO, NO, and HC emissions showing statistically meaningful responses to drive scheme while the PHEV Sprinter navigated urban roadways. Exhaust conditions (flowrate and temperature) were included in the efforts conducted on the continuous dataset providing additional explanatory power into the PHEV's emissions profile for each driving scheme.

Table 11.17: Statistical summary of the pollutant emissions during charge-sustaining operation according to drive scheme for the sample-run based analyses.

Charge-Sustaining by Data File Means

Variable:	All Roadways	Suburban Roads	Urban Roads
Fuel, gal/s	y	y	n
CO_2, g/s	y	y	n
CO, g/s	n	n	n
NOx, g/s	y	y	n
NO, g/s	y	y	n
NO_2, g/s	n	Inc2	n
HC, g/s	n	n	n

Inc1: y anova, n kw
Inc2: n anova, y kw

Table 11.18: Statistical summary of pollutant emissions and related variables during charge-sustaining operation according to drive scheme for the analyses of the continuous dataset.

Charge-Sustaining, Continuous Dataset

Variable:	All Roadways	Suburban Roads	Urban Roads
Fuel, gal/s	y	y	Inc2
CO_2, g/s	y	y	Inc2
CO, g/s	y	Inc2	y
NOx, g/s	y	y	Inc2*
NO, g/s	y	y	y
NO_2, g/s	y	y	Inc2
HC, g/s	y	y	y
Exhaust Flow, SCFM	y	y	n
Exhaust Temp, C	y	y	y

Inc1: y anova, n kw
Inc2: n anova, y kw

As mentioned previously, pollutant emissions demonstrated the smallest response to drive scheme during charge-sustaining, urban travel compared with the other investigations. Variables closely tied with the dICE operation (CO_2 and fuel use) were the least statistically significant. As discussed earlier, however, the power analysis of charge-sustaining urban travel yielded no statistically meaningful response in power output according to drive scheme, regardless of the level of analysis (run-based or continuous datasets). Aside from EM power output, total power and the dICE power output showed no statistical difference between solo and follow driving, although the magnitude of the calculated means showed solo driving as the more power demanding drive scheme during urban, charge-sustaining operation.

Carbon monoxide, hydrocarbon, and nitrogen monoxide emissions, however, proved to be statistically significant responses to drive scheme, with solo driving resulting in higher levels of NO and HC emissions, while transit-simulated follow driving

produced the highest levels of CO emissions. Figure 11.16 displays the relative magnitude of the PHEV Sprinter's emissions during charge-sustaining, urban driving according to drive scheme.

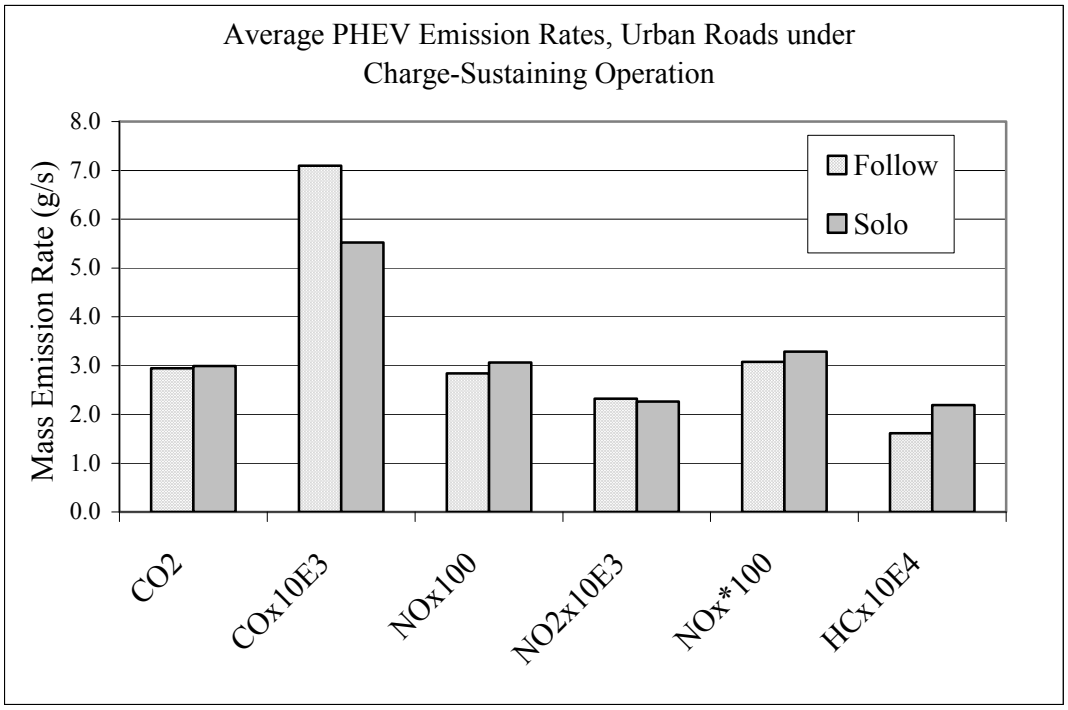

Figure 11.16: Pollutant emission rates during charge-sustaining operation of urban roadways according to drive scheme.

Table 11.19: Exhaust parameters during charge-sustaining, urban travel according to drive scheme.

	Road	Drive-Scheme	Median	Mean
Exhaust Flowrate (SCFM)	All	Follow	25.47	52.24
		Solo	26.76	61.34
	Urban	Follow	25.47	51.29
		Solo	25.66	53.18
Exhaust Temp (deg C)	All	Follow	119.0	108.4
		Solo	122.0	110.8
	Urban	Follow	120.5	111.4
		Solo	110.3	101.2

Some meaningful differences did present between charge-sustaining urban operation's on-road variables, with solo driving resulting in significantly higher velocities. However, acceleration rates did not vary significantly with drive scheme according to the initial investigation of the continuous dataset. Identical analyses of the continuous data void of zero velocity data, did, however, give conclusive statistical significance to the response of acceleration rate according to drive scheme, with transit-simulated driving resulting in more assertive (higher) acceleration rates compared to solo driving. In efforts to give reasonable justification to the response of CO, HC and NO emissions, on-road driving traits give a basis for cause and effect discussions. In this case, acceleration events provide the on-road performance demands most apt to result in transient dICE operation. Table 11.20 displays the relative proportions of the PHEV Sprinter's on-road time that was in periods of acceleration between the two driving schemes. Regardless of the method for defining a second of acceleration (positive acceleration rate or drive mode model), solo driving resulted in a larger proportion of its time in acceleration events. While transit-simulated driving resulted in more aggressive periods of acceleration, solo driving resulted in longer periods of acceleration.

Table 11.20: Relative prominence of acceleration events according to drive scheme during charge-sustaining, urban travel.

Acceleration Basis	Roadway	Measure	Drive-Scheme	
			Follow	Solo
Acceleration Rates > 0m/s^2	All Roadways	Total Time (s)	35594	32543
		Time with Positive Acceleration (s)	27789	27109
		% Time at A>0m/s^2	**78.1%**	**83.3%**
	Urban	Total Time (s)	7017	4344
		Time with Positive Acceleration (s)	5126	3466
		% Time at A>0m/s^2	**73.1%**	**79.8%**
Driving Mode = Accel	All Roadways	Total Time (s)	35594	32543
		Time during Accel Mode (s)	4912	5332
		% Time during Accel Mode	**13.8%**	**16.4%**
	Urban	Total Time (s)	7017	4344
		Time during Accel Mode (s)	1024	665
		% Time during Accel Mode	**14.6%**	**15.3%**

Traffic profiles were discussed earlier, with suburban, charge-sustaining operation showing statistically different traffic profile measures according to active drive scheme (follow versus solo). Follow driving consistently resulted in a higher frequency of stops and longer amount of on-road time at zero velocity. These findings are somewhat incongruous to the relative proportions of acceleration time found between the operating modes. However, since solo driving resulted in consistently and meaningfully higher average velocities, relatively longer periods of acceleration were required during solo driving in order to achieve its cruising velocity compared to follow driving. Based on the relative difference in hydrocarbon emissions, it is plausible that the duration of time under acceleration was a stronger factor in determining HC emissions than the overall rate of acceleration, giving cause to the statistically higher HC emission rates observed during solo driving. However, the significantly higher exhaust temperatures and more

aggressive acceleration events reported during transit-simulated driving could be the basis for high CO emissions during follow driving.

Regardless of the exact cause-and-effect pathways of pollutant formation, follow driving resulted in significantly higher CO emissions, producing over 27% more CO than solo driving on equivalent roadways. With transit service requiring an increased frequency of stops compared with solo driving, the PHEV Sprinter, under the follow drive scheme, transitioned from stop (zero velocity) to movement a significantly higher percentage of its on-road time than solo driving. This transition from stop to movement coupled with the overall higher acceleration rates may be the implicating factors resulting in the high carbon monoxide emissions and exhaust temperatures reported during follow driving.

Charge-sustaining, suburban driving yielded overall more statistically conclusive results regarding the PHEV Sprinter's on-road emissions. In most cases, statistical validity was supported by both the sample run-based and continuous dataset analyses. Aside from CO emissions, all measured pollutants proved to be statistically significant responses to drive scheme with solo driving resulting in universally higher exhaust emissions for all statistically meaningful constituents.

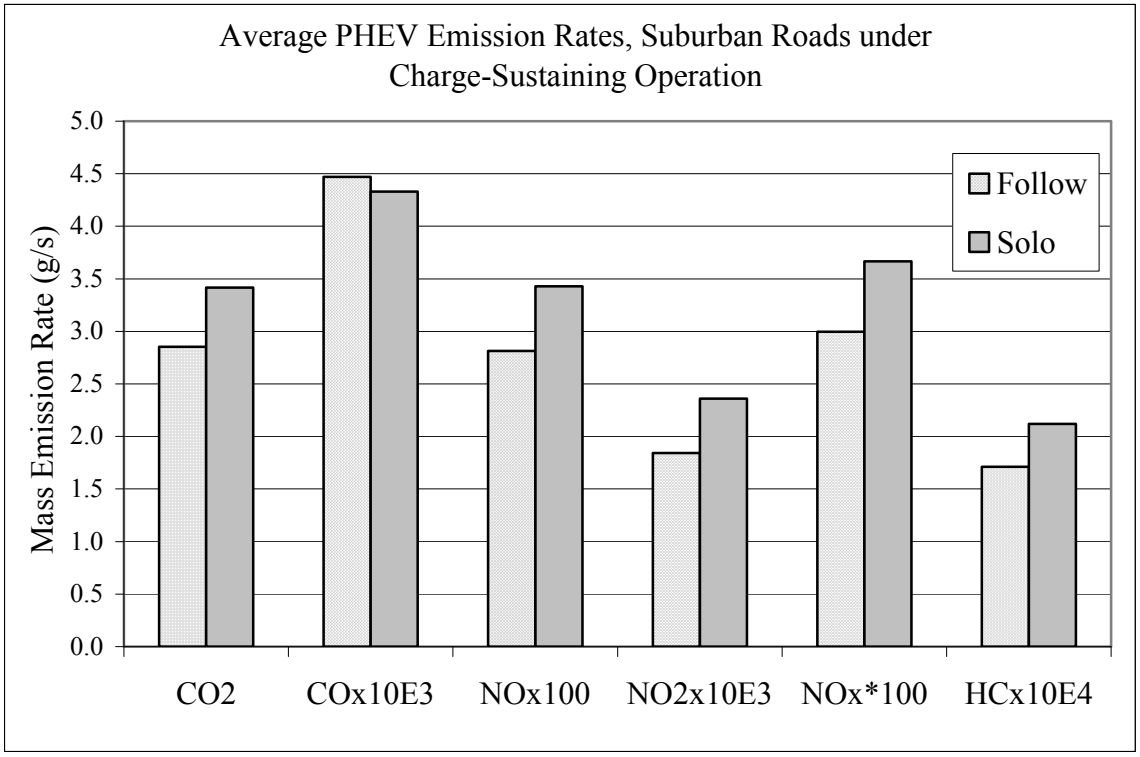

Figure 11.17: Pollutant emission rates during charge-sustaining operation of suburban roadways according to drive scheme.

Table 11.21: Exhaust parameters during charge-sustaining, suburban travel according to drive scheme.

	Road	Drive-Scheme	Median	Mean
Exhaust Flowrate (SCFM)	All	Follow	25.47	52.24
		Solo	26.76	61.34
	Suburban	Follow	25.46	52.48
		Solo	27.74	62.6
Exhaust Temp (deg C)	All	Follow	119.0	108.4
		Solo	122.0	110.8
	Suburban	Follow	118.4	107.6
		Solo	123.6	112.3

Despite the appearance that carbon monoxide emissions were higher during follow driving than solo driving, carbon monoxide emissions failed both statistical tests

in the sample run-based analysis, and did not meet the criteria for the parametric ANOVA test for the continuous dataset analysis. Charge-sustaining, suburban driving is the first category of the PHEV Sprinter's on-road operation where carbon monoxide emissions were not higher during transit-simulated follow driving to the set level of statistical significance ($\alpha<0.05$ for the sample-run based analysis and $\alpha<0.025$ for the continuous dataset).

As discussed earlier, aside from the Kruskal-Wallis analysis of the continuous dataset on EM power output, all power-related variables for charge-sustaining suburban travel demonstrated statistical significance according to drive scheme. Charge-sustaining solo driving of suburban roadways consistently produced and resulted in higher exhaust emissions. The PHEV Sprinter's exhaust emissions were mirrored in its power output, with solo driving requiring higher power output from the diesel ICE and from the overall subsystems combined. This increased power demand directly translates to the PHEV's increased emissions of CO_2, NO, and NOx during solo driving described here.

Similarly, the PHEV's on-road experience, as reported by velocity and acceleration profiles, gives explanatory cause to the relative levels of the transient exhaust pollutant emissions between solo and follow driving. Charge-sustaining suburban driving resulted in statistically meaningful differences in the PHEV's velocity, acceleration, and stop profiles between solo and transit-simulated driving. Several driving factors differentiated solo driving from follow driving; solo driving resulted in higher velocities and acceleration rates, with a proportionally higher percentage of the PHEV's on-road time spent in periods of acceleration (Table 11.22). Where solo driving exhibited more generally assertive on-road driving patterns, follow driving required a

higher frequency of stops with longer stop durations on average. While CO emissions did not prove to be statistically significant responses to drive scheme, HC and NO_2 (both, particularly HC, promoted by transient dICE function) emissions did exhibit statistically meaningful responses to drive scheme, with solo driving producing higher levels of both HC and NO_2 in the PHEV's exhaust. It was surmised earlier that more extensive acceleration profiles appeared to contribute to HC emissions, whereas increased instances where the vehicle was transitioning from stop to moving or periods of aggressive acceleration appeared to promote CO emissions. The relative difference in acceleration profiles between solo and follow driving here coupled with the significantly higher mass emissions of HC and NO_2, but not CO give additional support to this deduction.

Table 11.22: Relative prominence of acceleration events according to drive scheme during charge-sustaining, suburban travel.

Acceleration Basis	Roadway	Measure	Drive-Scheme	
			Follow	Solo
Acceleration Rates > 0m/s^2	**All Roadways**	Total Time (s)	35594	32543
		Time with Positive Acceleration (s)	27789	27109
		% Time at A>0m/s^2	**78.1%**	**83.3%**
	Suburban	Total Time (s)	28577	28199
		Time with Positive Acceleration (s)	22663	23643
		% Time at A>0m/s^2	**79.3%**	**83.8%**
Driving Mode = Accel	**All Roadways**	Total Time (s)	35594	32543
		Time during Accel Mode (s)	4912	5332
		% Time during Accel Mode	**13.8%**	**16.4%**
	Suburban	Total Time (s)	28577	28199
		Time during Accel Mode (s)	3888	4667
		% Time during Accel Mode	**13.6%**	**16.6%**

11.5 Concluding Remarks

One of the primary purposes of the Kansas City Plug-in Hybrid Electric Sprinter Demonstration Study was to provide a public transit platform to supplement the original Sprinter PHEV Proof of Concept study. However, limitations in available payload and liability issues prevented the Kansas City PHEV Sprinter from ever serving as a conventional transit bus. As a compromise to this, the PHEV shadowed an in-service transit vehicle serving as a chase-vehicle in order to simulate transit driving. Discrepancies between transit driving and normal, civilian driving became apparent early in the on-road sampling efforts, so the demonstration study was expanded to include civilian, or solo, driving of identical routes and roadways. Expanding the on-road investigation gave way to providing a basis for comparing and contrasting the difference in transit service from delivery or private driving and the implications that the differences might have on the PHEV Sprinter's operation and emissions.

Of the originally selected transit routes, only the 110 and 123 routes were sampled during conditions (ambient temperature and auxiliary system use) previously determined to eliminate sampling-based bias. While statistically significant differences did exist, when compared to previous investigations, the follow versus solo discussion presented the least statistically meaningful differences in the PHEV Sprinter's on-road experience, power usage, and emissions. Because of this, phenomenon not apparent in the original VSP, operating mode, or roadway-based analyses emerged. Despite efforts to avoid rush hour bias, time-of-day influence was still present to a small degree, resulting in different on-road behaviors between charge-depleting and charge-sustaining modes. Additionally, acceleration and deceleration rates proved to be statistically significant factors in

association with the PHEV's active power-scheme: electric-only operation versus hybrid driving. While it is uncertain whether the differences in the PHEV Sprinter's acceleration and deceleration profiles during electric-only operation were related to driver bias due to unintended psychological response to electric-only driving or if the PHEV Sprinter's mechanical abilities varied according to whether the diesel ICE was providing at least supplementary power, the differences in on-road variables were significant and noteworthy.

Despite the emergence of time-of-day and power-scheme influences, some statistically significant differences did exist between solo and follow driving in both the PHEV Sprinter's power usage (overall and between the subsystems) and resulting emissions. The differences were not universal with roadway and active operating mode (time-of-day) resulting in high power demands and emissions during follow driving under some conditions. Whereas, a different operating mode or roadway presented solo as the more power-demanding and emissions-producing drive scheme. Follow driving did, however, result in generally lower average velocities, traffic profiles with a higher frequency of stops and more time at zero velocity, and higher carbon monoxide emissions. Again, this investigation was limited to two KCATA transit routes servicing moderate ridership. The identical investigation, expanded to a transit route with higher ridership demands or servicing alternate roadways would likely result in more universal conclusions.

Chapter 12: Conclusions

Over the course of five months, the PHEV Sprinter underwent over 1,180miles of on-road testing resulting in the collection of over 81hours of second-by-second emissions and operating data. As the first production-based (versus retrofitted) plug-in hybrid vehicle to face on-road testing, the prototype Sprinter's initial evaluation placed the vehicle into a variety of different geographic and topographic situations throughout the Kansas City area. In order to meet the criteria of the proof of concept study, a sample network built around the KCATA's actively serviced public-transit routes was developed. The final study network of selected and developed routes resulted in PHEV evaluation while traveling over three distinct roadway types.

Given the considerable size of the final dataset, both with regard to the expanse of time over which the PHEV Sprinter was assessed in addition to the sizeable total distance that on-road testing occurred, several primary objectives were set forth from which to base the PHEV's demonstration study.

- **Vehicle Specific Power Analysis:** In line with current practices, it was important to verify whether or not the alternative plug-in hybrid drivetrain would deliver statistical viability when subjected to the VSP modal analysis that is currently used as a base for the EPA's top vehicle emission models.

- **Roadway Analysis:** The sample matrix was specifically developed to showcase the PHEV Sprinter's operation while navigating a variety of different on-road scenarios. In and around the Kansas City's metropolitan area, three primary roadway distinctions were observed: urban, suburban, and

highway. These designations provided a categorical method to assess the PHEV's on-road operation and emissions.

- **Operating Mode Assessment:** Plug-in capabilities coupled with petroleum/electric hybrid drive abilities distinguish PHEVs from hybrid electric vehicles and electric vehicles. Because it can operate from three different drivetrain configurations, PHEV operation occurs according to two primary operating modes: charge-depleting and charge-sustaining. The modal assessments from the first two objectives provide a strong framework form which to investigate the PHEV's operating modes.

- **Diesel Internal Combustion Engine:** The application of a diesel internal combustion engine to the plug-in hybrid drivetrain was a novel feature of the Kansas City-based PHEV Sprinter. It was one of only two proof of concept PHEV Sprinters employing diesel internal combustion engines (ICEs) for long-range driving. The application of diesel combustion was also unique compared to conventional hybrid vehicles in production at the time of testing. Because of this, the diesel engine's function and operation provided an additional facet to the demonstration study.

- **Drive-Scheme Evaluation:** Originally brought to Kansas City for testing as a transit vehicle, it was important to address the suitability of the PHEV Sprinter within the public transit arena. In order to accomplish this while still providing a dataset devoid of inherent bias present in transit operation, the PHEV Sprinter was tested according to two drive schemes: solo or civilian

driving and transit driving simulated by following an in-service transit bus. A comparison between the two drive-schemes provided the final platform for PHEV Sprinter assessment.

On-road testing spanned a period of 5months from September 2007 through January 2008, during which the ambient temperatures varied considerably. Additionally, although used as minimally as possible, occasional air conditioning and heater employment were required in order to maintain a basic level of operator comfort. While not a fundamental objective of the PHEV Sprinter's demonstration study, a rudimentary investigation into the impact that both ambient temperature and auxiliary system use had on the PHEV Sprinter's operation and emissions was necessary in order to mitigate potential bias in the final dataset selected for all primary objective analyses.

The final results from this basic analysis were not 100% inclusive of all exhaust pollutants or power output measures, but some relationship presented between auxiliary system use and the PHEV Sprinter's operation and resulting emissions. All measured pollutants, except for hydrocarbons, demonstrated higher exhaust levels when the air conditioning was operational. Since the data were not collected in a controlled environment, auxiliary system use was directly dependent upon ambient temperature, so the impacts of each could not be segregated.

Additionally, the diesel ICE showed a statistically significant response to air conditioning use, suggesting that the diesel ICE was recruited secondarily as an assist to the electric motor when the PHEV's systems required it.

As an interesting aside to the ambient temperature/auxiliary system assessment, it was noted that the two roadway links selected for this evaluation, which had originally been seen as equivalent, exhibited very different power demands on the PHEV Sprinter which resulted in significantly different exhaust emissions between the two links. The selected roadway links were of equivalent length, within close geographic proximity, had identically posted speed limits, and similar traffic patterns (aside from one rarely encumbering stoplight on 11th street). Despite these commonalities, the links resulted in different power and emissions profiles. This limits the possibility of developing a specific drive cycle, which can be traced and replicated like laboratory-based dynamometer drive cycles.

Vehicle Specific Power Modal Analysis:

Vehicle Specific Power, VSP, is a calculated proxy for simulating a vehicle's on-road power load based on the vehicle's physical characteristics, physical forces and resistances acting on the vehicle while moving, and on the vehicle's actual on-road driving. On a modal level, VSP has been employed for the development of current emission models. In order to maintain continuity with existing research and to assess the PHEV platform's suitability for application to existing models, the PHEV Sprinter data were subjected to VSP modal analysis. In addition to the VSP analysis, a second modal analysis was implemented. This second model is based on active driving mode, and provided a more intuitive basis for discussing the PHEV 's operation and emissions.

The VSP modal analysis used for the PHEV Sprinter was based on the heavy-duty vehicle VSP binning procedure developed by Frey (2008). According to this model, the

PHEV Sprinter's on-road emissions and operating data were segregated into eight discrete VSP bins based on VSP ranges. It was originally uncertain whether the PHEV's dual mode driving would provide statistically significant differences between the VSP bins. The presence of electric-only data at any point in the PHEV's operation results in not insignificant spans of zero-valued emissions, fuel use, and diesel internal combustion engine (dICE) power output data, making statistical continuity according to VSP questionable. Ultimately, all emissions and operating variables proved to be statistically significant responses to both VSP bin and active driving mode.

Segregating the PHEV Sprinter's relative power output between its subsystems according to VSP bin provided additional insight regarding the PHEV's overall control scheme and its response to immediate on-road loads. While the PHEV Sprinter's total power output and dICE power output both increased with increasing VSP bin (and, hence, increased on-road load), the electric motor (EM) showed a peak power output at VSP bin 6, with a continual decrease with increasing VSP during bins 7 through 8. These trends were maintained for both operating modes; however, the relative portion of the power output from the EM was significantly higher during charge-depleting operation. Similar to conventional heavy-duty vehicles, the PHEV Sprinter's emissions universally increased with increasing VSP bin.

The VSP modal model also gave basis for comparing the PHEV Sprinter's emissions loads to conventional ICE-driven vehicles. Unfortunately, data were not available for the equivalent weight class of vehicle as the PHEV Sprinter, however comparisons between heavier heavy-duty-diesel transit buses (HDDVs) and smaller passenger-based gasoline-powered vehicles could still be made. Ultimately, the PHEV

Sprinter experienced significantly reduced emissions and fuel consumption compared with heavy-duty-diesel transit buses. This trend applies to all measured pollutants except hydrocarbons, whose emission in the upper VSP bins was actually higher during the PHEV's charge-depleting operation than the HDDVs'.

An unexpected feature of the PHEV Sprinter's data was that within the discrete VSP bins, power output and emissions proved to be statistically significant responses to sample route. Given the nature of the VSP equation, homogeneity within the bins was expected. This phenomenon left some question regarding the PHEV's exact power scheme and subsystem recruitment. Rather than being dictated solely by immediate road load, it is suspected that historical driving tendencies and/or localized trends in topography might play a role in the PHEV Sprinter's power control algorithm. Regardless of the cause, the inter-route variability, while statistically significant, was minimal compared to the variability in power output and emissions between the VSP bins.

Roadway Analysis:

The study design designated three discrete roadway or facility types: urban, suburban, and highway. Urban driving was defined by proximity to Kansas City's urban core, a high frequency of traffic signals, and low posted speed limits. Suburban roadways served as transitions from the urban core into surrounding communities and neighborhoods. Suburban travel, generally, occurred at higher posted speed limits than urban driving with fewer driving interruptions from posted traffic signals or stop signs. Conversely, highway travel was void of all mandated traffic interruptions and was

conducted according to a consistently set 55mph speed limit. Analysis of road, driving, and traffic-based variables proved that the roadway designations represented statistically unique on-road experiences.

Roadway velocities imposed some interpretive bias on the final results with time-based analyses leading to different conclusions than distance-based analyses. While power output and emissions universally proved to be statistically significant responses to roadway type, when assessed on a time-basis, slower urban travel showed the highest efficiency, lowest emitting on-road operation, with highway driving demonstrating the least efficient, highest emitting mode of travel. The converse held true when the analysis was conducted on a distance basis.

According to roadway type, the PHEV Sprinter's power output and usage was more statistically robust during charge-sustaining operation, when the PHEV was operating in a more consistent manner with fewer periods of electric-only operation. During charge-depleting operation, however, EM power output became less definable according to roadway, particularly when the in-town based suburban and urban roads were compared against each other.

Except for the sample run-based analysis of nitrogen oxide (NO_2) and the in-town roadways analysis of NO_2 and hydrocarbon (HC) emissions, all measured pollutants emission and fuel use were statistically significant responses to roadway type. On a time basis, in accordance with power output, highway driving resulted in the highest levels (by a factor of two) of all emissions aside from NO_2 and carbon monoxide (CO), which remained low. With respect to in-town driving, suburban travel resulted in higher mass emissions of all pollutants except CO. Carbon monoxide emissions were consistently

high for all urban travel, regardless of unit basis. However, when the same analyses were applied to the distance-based data, highway driving resulted in the most fuel efficient, least polluting travel. On the other hand, distance-based urban driving proved to be the least fuel efficient, highest polluting roadway, demonstrating extremely high levels of CO emissions.

The roadway assessment of charge-depleting operation yielded statistically significant responses to power output, fuel use, and exhaust emissions according to roadway designation. However, despite excess battery capacity and increased electric-only operation, charge-depleting mode resulted in higher levels of both CO and HC emissions. Transient operation of the dICE during charge-depleting mode resulted in engine conditions that promoted the production of secondary pollutants.

Similar to the VSP analysis, statistically significant differences in traffic patterns and certain driving variables were observed between the different sample routes for a given roadway designation. Despite these differences, the route-influenced variations were much smaller than the differences found in the same variables between the roadway types.

Operating Mode Assessment:

With their varying drivetrain capabilities, plug-in hybrid vehicles operate within one of two primary operating modes: charge-depleting and charge-sustaining. During periods of excess stored battery capacity, the PHEV will preferentially use its EM in order to meet on-road driving demands, only employing the ICE as necessary. During this period (charge-depleting mode) the battery packs are continually being discharged as

the vehicle maximizes its electric-only drive potential. However, once the excess stored battery capacity has been depleted to a predetermined level of state of charge, the PHEV enters more conventional hybrid operation, using the EM and ICE together in order to meet the driver's demands. During this time (charge-sustaining operation) the PHEV works to maintain a set battery state of charge range, using the EM only as regenerative braking and electrical recuperation are able to increase the battery's stored capacity.

Initial reports from Daimler indicated that the PHEV Sprinter would achieve, nominally, 20miles of electric-only operation during charge-depleting mode. Preliminary investigation of the Kansas City PHEV, however, suggested that the PEHV Sprinter did not achieve the Daimler cited level of electric-only travel during charge-depleting operation. However, as expected, and inline with the PHEV's design and intent, charge-depleting mode did result in more electric-only operation than charge-sustaining mode, for all VSP bins and roadways (except highway). As road loads and power demands increased, the operating modes began to converge with respect to electric-only drive time. Similarly, as roadway average velocities increased the relative difference between electric-only range achieved during charge-depleting operation versus charge-sustaining operation diminished. During high velocity instances, such as highway driving, there was no distinguishable difference in eclectic-only drive distance between the two operating modes. At high travel velocities, the PHEV Sprinter preferentially utilized the dICE, regardless of state of battery charge.

All measures of power output (total, dICE, and EM) proved to be statistically significant responses to operating mode across all eight VSP bins and roadway types, except in the case of highway operation, where EM failed do show any distinction

between the two operating modes. As expected, charge-depleting driving resulted in more prominent use of the EM during all VSP bins and roadway types. However, the difference between the operating modes diminished with increasing average velocity according to roadway type and with increasing power load, measured by increasing VSP bin. Generally, EM use peaked around VSP bins 5 or 6 (mode dependent) and then tapered off with increasing VSP in bins 7 and 8. Charge-depleting mode demonstrated a prolonged plateau of EM power output through bins 5, 6, and 7 before a experiencing a large drop in bin 8.

One of the more interesting results found during this investigation comes in the way of total power output. Despite controlling for ambient temperature and auxiliary system use and verifying that on-road driving parameters velocity and acceleration were the same between the operating modes for different roadway types, the total power output was consistently higher during charge-sustaining operation when compared to equivalent use charge-depleting operation. Since electric motors are inherently more efficient than internal combustion engines, periods of PHEV Sprinter operation that experienced relatively high engagement of the EM actually witnessed lower total power output.

Emissions proved to be statistically significant responses to operating mode according to both roadway type and VSP bin. Fuel use and pollutant emissions most directly related to the combustion reaction trended with dICE power output, with charge-sustaining operation resulting in higher fuel requirements and increased emissions of carbon dioxide (CO_2) and NO_2. However, CO and HC exhaust levels are less correlated with the combustion process and more directly attributed to transient dICE operation. Since charge-depleting mode continually cycles the dICE on and off, it is not unexpected

that charge-depleting operation results in more transient dICE behavior, and, consequently, higher levels of CO and HC emissions. An investigation into the PHEV Sprinter's exhaust temperature supported this theory, which was given specific focus in the following section.

Diesel Internal Combustion Engine:

The proof-of-concept Phase I PHEV Sprinter study was one of the first studies presenting diesel hybrid electric vehicles. Additionally, the Kansas City PHEV Sprinter was one of only two diesel-based PHEV Sprinters placed on the road during the proof of concept testing. There are several operating characteristics regarding diesel ICE operation that may or may not be best suited to PHEV application. For example, in cold operating temperatures, it is possible that the diesel oxidation catalyst rarely reaches sufficient operating temperature to effectively control carbon monoxide and hydrocarbon emissions during high state of charge (SOC) operation (when the diesel engine is only used as needed). Heywood (1988) noted that during transient diesel operation, instances of increased emissions load were likely.

The variables dictating electric motor function during electric-only operation did not yield strong statistical significance between the two operating modes, suggesting that the EM, when functioning in an electric-only capacity, operated under the same general power control scheme within each operating mode. Charge depleting mode simply experienced more time in electric-only operation, but EM operation was consistent regardless of which mode it occurred. However, during hybrid driving, when the dICE was active, the EM provided proportionally more power during charge-depleting mode

than charge-sustaining mode, indicating that its ICE assist was greater with excess stored battery capacity. While electric-only driving remained independent of operating mode, the PHEV Sprinter's hybrid operation was a function of battery SOC and demonstrated a response to the PHEV's active operating mode.

The diesel ICE investigation was conducted on the dataset filtered for hybrid operation (all electric-only driving was removed). Based on the PHEV Sprinter's hybrid operation, emissions, dICE function, and exhaust temperature were conclusively statistically significant responses to the PHEV's active operating mode, regardless of basis of analysis (VSP bin, driving mode model, or roadway type). Charge-sustaining operation consistently required more dICE power than charge-depleting mode. As a result of this, charge-sustaining operation resulted in increased fuel use, CO_2, nitric oxide (NO), and NO_2 emissions (consistent with what was reported in previous sections).

Despite increased reliance on the dICE during charge-sustaining operation, CO and HC emissions remained significantly elevated during charge-depleting mode. Investigation into the dICE's cycling during the different operating modes showed that during charge-depleting operation the dICE cycled on and off more frequently than during charge-sustaining operation. While the amount of shutdown time per cycle was not statistically significant according to operating mode, a similar investigation regarding the amount of time, on average, that the dICE was engaged between off/on cycles was statistically significantly higher during charge-sustaining operation. This suggests that while the amount of time for engine cool down may have not been statistically significant between the operating modes, the amount of time for engine warm-up was. Investigation of the dICE shutdown time histograms between the operating modes showed that charge-

depleting operation resulted in a low frequency of instances where the dICE was shut down for extensive periods of time. Likewise, the histograms detailing the periods of time that the dICE was engaged show charge-depleting operation to have a high frequency of very short engagement times, whereas charge-sustaining operation tended to run dICE for longer periods of time once it was brought back on line. These observations indicate that during charge-depleting operation the dICE was started while cold and not given adequate run time before off cycles to warm up, giving ample opportunity for transient operation, and, hence, the formation of transient emissions.

Drive Scheme Evaluation:

The PHEV Sprinter was originally brought to Kansas City in order to test the PHEV concept in public transit operation. However, limitations in available payload and liability issues prevented the Kansas City PHEV Sprinter from ever serving as a conventional transit bus. In order to maintain the original intent of the study, the PHEV Sprinter was implemented as a chase vehicle that would follow select in-service KCATA transit buses to simulate transit operation. However, discrepancies between transit driving and normal, civilian driving became apparent early in the on-road sampling efforts, so the on-road data collection design was expanded to include civilian, or solo, driving of identical routes and roadways. The redesign gave means to developing the final, drive-scheme objective by providing a basis to compare and contrast the differences in transit service from delivery or private driving and the implications that those differences might have on the PHEV Sprinter's operation and emissions.

While statistically significant differences did exist between the drive-schemes, when compared to previous investigations, the follow versus solo discussion presented the least statistically meaningful differences in the PHEV Sprinter's on-road experience, power usage, and emissions. As a consequence of this and the reduced number of routes available for the drive-scheme investigation (110 and 123), phenomenon not apparent in the original VSP, operating mode, or roadway-based analyses emerged. Given the nature of PHEV charging, on-road sampling between the operating modes did have a time-of-day function, which resulted in different driving behaviors between the operating modes for solo driving in particular.

Ultimately, it was revealed that acceleration and deceleration rates were statistically significant factors according to the PHEV's active power-scheme: electric-only operation versus hybrid driving. While it is uncertain whether the differences in the PHEV Sprinter's acceleration and deceleration profiles during electric-only operation were related to driver bias due to unintended psychological response to electric-only driving or if the PHEV Sprinter's mechanical abilities varied according to whether the diesel ICE was providing at least supplementary power, the differences in on-road variables were significant and noteworthy.

Despite the emergence of time-of-day and power-scheme influences, some statistically significant differences did exist between solo and follow driving in both the PHEV Sprinter's power usage (overall and between the subsystems) and resulting emissions. The differences were not universal with roadway and active operating mode (time-of-day) resulting in high power demands and emissions during follow driving under some conditions. Whereas, a different operating mode or roadway presented solo

as the more power-demanding and emissions-producing drive-scheme. Follow driving did, however, result in generally lower average velocities, traffic profiles with a higher frequency of stops and more time at zero velocity, and higher carbon monoxide emissions. Again, this investigation was limited to two KCATA transit routes servicing moderate ridership. The identical investigation, expanded to a transit route with higher ridership demands or servicing alternate roadways would likely result in more universal conclusions.

Concluding Remarks:

The preceding document provides a detailed and comprehensive vantage point of a prototype, production-based plug-in hybrid vehicle built on Daimler's Sprinter chassis. Four PHEV Sprinters were developed by Daimler and included in the Phase I proof of concept testing, and each vehicle was unique from the others. Because of this, each PHEV Sprinter brought to the road represented prototype-level development and all of the nuances that accompany it. As a diesel-based PHEV, the Kansas City designated Sprinter was a novel vehicle, and its testing and analysis is representative of it as such. While some of the overarching trends and findings discussed here may inevitably translate to the plug-in hybrid vehicle market in general, they currently represent the behaviors and operation of one vehicle in its proof of concept testing phase.

References

Agar, B., Baetz, B. and Wilson, B. "Fuel Consumption, Emissions Estimation, and Emissions Cost Estimates Using Global Positioning Data." *Journal of the Air & Waste Management Association,* Vol. 57, pp.348-354, March 2007.

Alexander, M. and Duvall, M. "Plug-in Hybrid Electric Vehicle Data Collection and Analysis Plan." *Electric Power Research Institute Interim Report,* February 2007.

Argus Air Daily. "EPRI, GM agree to advance PHEVs." *Argus Air Daily,* Vol. 15, No. 140, July 22, 2008. www.argusmediagroup.com.

Baldauf, R., Gabele, P, Crews, W., Snow, R. and Cook, J. "Criteria and Air-Toxic Emissions from In-Use Automobiles in the National Low-Emission Vehicle Program." *Journal of the Air & Waste Management Association,* Vol. 55, pp. 1263-1268, September 2005.

Baldauf, R., Thoma, E., Hays, M., Shores, R., Kinsey, J., Gullet, B., Kimbrough, K., Isakov, V., Long, T., Snow, R., Khlystov, A., Weinstine, J., Chen, F., Seila, R., Olson, D., Gilmour, I., Cho, S., Waktins, N., Rowley, R. and Bang, J. "Traffic and Meteorological Impacts on Near-Road Air Quality: Summary of Methods and Trends from Raleigh Near-Road Study." *Journal of the Air & Waste Management Assocation,* Vol. 58, pp. 865-878, July 2008.

Barth, M., Younglove, T., Wenzel, T., Scora, G., An, F., Ross, M., and Norbeck, J. "Analysis of Modal Emissions from Diverse In-Use Vehicle Fleet." *Transportation Research Record.* Paper No. 97119, pp. 73-84, 1997.

BC Climate Exchange. "Hybrid Basics." *Hybrid Experience Report,* Nov. 2, 2008. http://www.hybridexperience.ca/Basics_Of_Hybrids.htm

Bishop, G. and Stedman, D. "A Decade of On-road Emissions Measurements." *Environmental Science and Technology,* Vol. 42, No. 5, pp. 1651-1656, 2008.

Bohn, T., Duoba, M., and Carlson, R. "In-Situe Torque Measurements in Hybrid Electric Vehicle Powertrains." *Paper No 276, Presented at International Electric Vehicle Symposium, (EVS-23), Anaheim, CA, 2007.*

Boughedaoui, M., Kerbachi, R. and Joumard, R. "On-Board Emission Measurement of High-Loaded Light-Duty Vehicles in Algeria." *Journal of the Air & Waste Management Association,* Vol. 58, pp. 45-54, January 2008.

Broderick, C., Dwyer, H., Farshchi, M., Harris, D.B. and King, F. Jr. "Effects of Engine Speed and Accessory Load on Idling Emissions from Heavy-Duty Diesel Truck Engines." *Journal of the Air & Waste Management Association,* Vol. 52, No. 9, pp-1026-1031, 2002.

Brown, J., King, F, Mitchel, W., Squier, W., Harris, B. and Kinsey, J. "On-Road Facility to Measure and Characterize Emissions from Heavy-Duty Diesel Vehicles." *Journal of the Air & Waste Management Association,* Vol. 52, pp.388-395, April 2002.

Cadle, S., Croes, B., Minassian, F., Natarajan, M., Tierney, E. and Lawson, D. "Real-World Vehicle Emissions: A Summary of the Thirteenth Coordinating Research Council On-Road Vehicle Emissions Workshop." *Journal of the Air & Waste Management Association,* Vol. 54, pp. 8-23, January 2004.

Cadle, S., Belian, T., Black, K., Minassain, F., Natarajan, M. Tierney, E. and Lawson, D. "Real-World Vehicle Emissions: A Summary of the 14th Coordinating Research Council On-Road Vehicle Emissions Workshop." *Journal of the Air & Waste Management Association,* Vol. 55, pp. 130-146, February 2005.

Cadle, S., Belian, T., Black, K., Carlock, M., Graze, R. Minassain, F., Murray, H.. Nam, E., Natarajan, M. and Lawson, D. "Real-World Vehicle Emissions: A Summary of the 15th Coordinating Research Council On-Road Vehicle Emissions Workshop." *Journal of the Air & Waste Management Association,* Vol. 56, pp. 121-136, February 2006.

Cadle, S., Ayala, A., Black, K., Fulper, C., Graze, R., Minassain, F., Murray, H., Natarajan, M., Tennant, C. and Lawson, D. "Real-World Vehicle Emissions: A Summary of the Sixteenth Coordinating Research Council On-Road Vehicle Emissions Workshop." *Journal of the Air & Waste Management Association,* Vol. 57, pp. 139-145, February 2007.

Cadle, S., Ayala, A., Black, K., Graze, R., Koupal, J., Minassian, F., Murray, H., Natarajan, M., Tennant, C. and Lawson, D. "Real-World Vehicle Emissions: A Summary of the Seventeenth Coordinating Research Council On-Road Vehicle Emissions Workshop." *Journal of the Air & Waste Management Association,* Vol. 58, pp. 3-11, January 2008.

Carlson, R., Duoba, M., Bohn, T., and Vyas, A. "Testing and Analysis of Three Plug-in Hybrid Electric Vehicles." *SAE International Technical Paper Series,* Paper No. 2007-01-0283, 2007.

Carlson, R., Lohse-Busch, H., Duoba, M., and Shidore, N. "Drive Cycle Fuel Consumption Variability of Plug-In Hybrid Electric Vehicles Due to Aggressive Driving." *SAE International Technical Paper Series,* Paper No. 2009-01-1335, 2009.

Chan, T., Ning, Z., Wang, J., Cheung, C., Leung, C. and Hung, W. "Gaseous and Particle Emission Factors from the Selected On-Road Petrol/Gasoline, Diesel, and

Liquefied Petroleum Gas Vehicles." *Energy & Fuels*, Vol. 21, pp.2710-2718, 2007.

Clark, N.N., Gajendran, P. and Kern, J.M., "A Predictive Tool for Emissions from Heavy-Duty Diesel Vehicles," *Environmental Science & Technology*, Vol. 37, No. 1, pp. 7-15, 2004.

Clayton, M. "A reality check on plug-in hybrids." *The Christian Science Monitor*, Sept. 25, 2006.

Coburn, T. "Mixed-Model Statistical Analysis of Fuel, Equipment, Mileage and Driving Schedule Effects on Particulate Matter Emissions from Heavy Diesel-Powered Vehicles." *Journal of the Air & Waste Management Association*, Vol. 54, pp.1151-1161, September 2004.

Cohen, J., Hammitt, J. and Levy, J. "Fuels for Urban Transit Buses: A Cost-Effectiveness Analysis." *Environmental Science and Technology*, Vol. 37, No. 8, pp.1477-1484, 2003.

Clark, N., Kern, J., Atkinson, C. and Nine, R. "Factors Affecting Heavy-Duty Diesel Vehicle Emissions." *Journal of the Air & Waste Management Association.*, Vol. 52, pp. 84-94, January, 2002.

Cocker, D., Shah, S., Johnson, K., Miller, J. and Norbeck, J. "Development and Application of a Mobile Laboratory for Measuring Emissions from Diesel Engines. 1. Regulated Gaseous Emissions." *Environmental Science and Technology*, Vol. 38, No. 7, pp. 2182-2189, 2004.

Collins, J., Shepherd, P, Durbin, T., Lents, J., Norbeck, J. and Barth, M. "Measurements of In-Use Emissions from Modern Vehicles Using an On-Board Measurement System." *Environmental Science and Technology*, Vol. 41, No. 18, pp. 6554-6561, 2007.

Cook, R., Touma, J., Fernandez, A., Brzezinski, D., Bailey, C., Scarbro, C., Thurman, J., Strum, M., Ensley, D. and Baldauf, R. "Impact of Underestimating the Effects of Cold Temperature on Motor Vehicle Start Emissions of Air Toxics in the United States." *Journal of the Air & Waste Management Association*, Vol. 57, pp. 1469-1479, December 2007.

Daimler. "Shaping Future Transportation: CleanDrive Technologies." http://www.daimler.com/dccom/, accessed October 25, 2008.

DaimlerChrysler. "DaimlerChrysler Tests Plug-in Hybrid Van – Daily Auto Insider." *Car and Driver*, www.caranddriver.com, March 28, 2007.

Darr, L., Buchanan, B., Jack, J., Lowell, D., and Shires, C. "Commercial Bus Emissions and Fuel Use: Idling Versus Urban Circulator." *Transportation Research Record: Journal of the Transportation Research Board.* No. 2011, pp. 57-67, 2007.

Department of Energy. Accessed October, 2011, http://energy.gov/.

DieselNet. Accessed May 2008, www.dieselnet.com.

Duoba, M., Carlson, R., and Bocci, D. "Calculating Results and Performance Parameters for PHEVs." *SAE International Technical Paper Series*, Paper No. 2009-01-1328, 2009.

Durbin, T., Johnson, K., Cocker, D., and Miller, J. "Evaluation and Comparison of Portable Emissions Measurement Systems and Federal Reference Methods for Emissions from a Back-Up Generator and a Diesel Truck Operated on a Chassis Dynamometer." *Environmental Science and Technology*, Vol. 41, No. 17, pp. 6199-6204, 2007.

Duvall, M. "Plug-In Hybrid Vehicles Technology Challenges." *ZEV Technology Symposium, California Air Resources Board*, September 25-27, 2006.

Electric Power Research Institute (EPRI). "The Power to Reduce CO_2 Emissions, The Full Portfolio." *Electric Power Research Institute,* August 2007.

Electric Power Research Institute (EPRI). "Environmental Assessment of Plug-In Hybrid Vehicles, Volume 1." *Electric Power Research Institute*, www.epri.com, 2007.

Electric Power Research Institute (EPRI). "Environmental Assessment of Plug-In Hybrid Vehicles, Volume 2." *Electric Power Research Institute*, www.epri.com, 2008.

Elgowainy, A., Burnham, A., Wang, M., Molburg, J., and Rousseau, A. "Well-To-Wheels Energy Use and Greenhouse Gas Emissions of Plug-In Hybrid Electric Vehicles." *SAE International Journal of Fuels and Lubricants*, Vol. 2, Iss. 1, pp. 627 - 644, 2009.

Ensfield, C. "On-Road Emissions Testing of 18 Tier 1 Passenger Cars and 17 Diesel-Powered Public Transport Buses." *Assessment and Standards Division, Office of Transportation and Air Quality (OTAQ), U.S. Environmental Protection Agency*, EPA420-R-02-030, 2002.

Environmental Protection Agency, www.epa.org.

Environmental Protection Agency. "In-Use Testing Program for Heavy-Duty Diesel Engines and Vehicles, Technical Support Document." *Assessment and Standards Division, Office of Transportation and Air Quality (OTAQ), U.S. Environmental Protection Agency,* EPA420-R-05-006, 2005.

European Commission Mobility & Transport. Accessed July, 2011, http://ec.europa.eu/transport/index_en.htm.

EU2005a. Commission Communication – "Implementing the Community Strategy to Reduce CO_2 Emissions from Cars: fifth annual communication on the effectiveness of the strategy." *Bulletin EU 6-2005, Environment (12/12).*

Fellah, M., Singh, G., Rousseau, A., Pagerit, S., Nam, E., and Hoffman, G. "Impact of Real-World Drive Cycles on PHEV Battery Requirements." *SAE International Technical Paper Series,* Paper No. 2009-01-1383, 2009.

Fleets and Fuels. "Fleets & Fuels: Electric Transportation is Considered Vital for Electricity to Fulfill Its Global Promise," *Fleets and Fuels,* September 6, 2004.

Fontaras, G. and Samaras, Z. "A quantitative analysis of the European Automakers' voluntary commitment to reduce CO_2 emissions from new passenger cars based on independent experimental data." *Energy Policy,* Vol. 35, pp.2239-2248, 2007.

Fontaras, G., Pistikopoulus, P. and Samaras, Z. "Experimental evaluation of hybrid vehicle fuel economy and pollutant emissions over real-world simulation driving cycles." *Atmospheric Environment,* Vol. 42, pp.4023-4035, 2008.

Frey, C., "Methodology for Developing Modal Emission Rates for EPA's Multi-Scale Motor Vehicle and Equipment Emission System," EPA420-R-02-027 October 2002 (Prepared for EPA by Computational Laboratory for Energy, Air and Risk, Department of Civil Engineering North Carolina State University, Raleigh, NC, EPA Contract No. PR-CI-02-10493.)

Frey, C., Annual, A. and Chen, J. "Recommended Strategy for On-Board Emission Data Analysis and Collection for the New Generation Model." *Office of Transportation and Air Quality, U.S. Environmental Protection Agency,* February, 2002.

Frey, C., Unla, A., Rouphail, N. and Colyar, J. "On-Road Measurement of Vehicle Tailpipe Emissions Using a Portable Instrument." *Journal of the Air & Waste Management Association,* Vol. 53, pp. 992-1002, August 2003.

Frey, C., Rouphail, N., and Zhai, H. "Speed- and Facility-Specific Emission Estimates for On-Road Light-Duty Vehicles on the Basis of Real-World Speed Profiles." *Transportation Research Record: Journal of the Transportation Research Board.* No. 1987, pp. 128-137, 2006.

Frey, C., Rouphail, N., Zhai, H., Farias, T. and Goncalves, G. "Comparing real-world fuel consumption for diesel- and hydrogen-fueled transit buses and implication for emissions." *Transportation Research Part D: Transport and Environment,* Vol. 12, Iss. 4, pp. 281-291, June 2007.

Frey, C., Zhang, K. and Rouphail, N. "Fuel Use and Emissions Comparisons for Alternative Routes, Time of Day, Road Grade, and Vehicles Based on In-Use Measurements." *Environmental Science and Technology,* Vol. 42, No. 7, pp.2483-2489, 2008.

Gardetto, E., Bagain, T. and Linder, J. "High-Mileage Study of On-Board Diagnostic Emissions." *Journal of the Air & Waste Management Association,* Vol. 55, pp. 1480-1486, October 2005.

Gonder, J. and Markel, T. "Energy management Strategies for Plug-in Hybrid Electric Vehicles." *SAE World Congress,* April 16-19, 2007. Technical Report NREL/CP-540-40970.

Green Car Congress. "DaimlerChrysler Ramps Up its Plug-In Sprinter Development Program." www.greencarcongress.com/2007/01/daimlerchrysler_1.html, January 19, 2007.

Granovskii, M., Dincer, I., and Rosen, M. "Economic and environmental comparison of conventional, hybrid, electric and hydrogen fuel cell vehicles." *Journal of Power Sources,* Vol. 159, pp. 1186-1193, 2006.

Hamilton, T. "$38.83 to power hybrid plug-in for 6 days." *The Toronto Star,* June 9, 2008.

Heywood, J.B., 1988; Internal Combustion Engine Fundamentals; McGraw-Hill, New York; ISBN 0-07-100499-8;

Hohl, C., Carter, R.E., Peltier, E., Lane, D.D. "Plug-In Hybrid Emissions Characterization and Demonstration Study, Final Report." Submitted to EPRI, Daimler, and Chrysler, July 2008.

Huai, Tao, Durbin, T., Younglove, T., Scora, G., Barth, M., and Norbeck, J. "Vehicle Specific Power Approach to Estimating On-Road NH3 Emissions from Light-Duty Vehicles." *Environmental Science & Technology,* Vol. 39, pp. 9595-9600, 2005.

Hung, W., Tong, H. and Chun-Shun, C. "A Modal Approach to Vehicle Emissions and Fuel Consumption Model Development." *Journal of the Air & Waste Management Association,* Vol. 55, pp. 1431-1440, October 2005.

IEEE. "The Smart Hybrid: Flip a switch and Daimler Chrysler's plug-in hybrid electric van will be become an electric vehicle," *IEEE Spectrum Online*.

Jarrett, R. and Clark, N.N., "Weighting of Parameters in Artificial Neural Network Prediction of Heavy-Duty Diesel Engine Emissions," *SAE Power train & Fluid*

Systems Conference, 2002 SAE Transactions: Journal of Fuels & Lubricants Vol. 111 pp. 1974-1983, 2003.

Jayasinghe, C.S. "Performance of Compact Mobile Emissions Monitoring System for Real-Time On-Board Emissions Measurement." Master of Science Thesis submitted to the Department of Mechanical and Aerospace Engineering, West Virginia University, 2007.

Jazcilevich, A., Garcia-Fragoso, A., Garcia Reynoso, A., Grutter, M., Diego-Ayala, U., Lents, J. and Davis, N. "A Vehicle Emissions System Using a Car Simulator and a Geographical Information System: Part 1-System Description and Testing." *Journal of the Air & Waste Management Association,* Vol. 57, pp. 1234-1240, October 2007.

Jimenez-Palacios, J. L. "Understanding and Quantifying Motor Vehicle Emissions with Vehicle Specific Power and TILDAS Remote Sensing," Doctor of Philosophy Thesis submitted to the Department of Mechanical Engineering, Massachusetts Institute of Technology, 1999.

Khan, S., Clark, N., Thomspon, G., Wayne, S., Guatam, M, Lyons, D. and Hawelti, D. "Idle Emissions from Heavy-Duty Diesel Vehicles: Review and Recent Data." *Journal of the Air & Waste Management Association,* Vol. 56, pp.1404-1419, October 2006.

Kitner-Meyer, M.; Schneider, K.; Pratt, R. "Impact Assessment of Plug-in Hybrid Vehicles on Electric utilities and Regional U.S. Power Grids, Part 1: Technical Analysis." *Electric Utility Environmental Conference, Tucson, AZ,* Jan. 21-24, 2007.

Kliesch, J. and Langer, T. "Plug-In Hybrids: an Environmental and Economic Performance Outlook." *American Council for an Energy-Efficient Economy,* Report No. T061, September 2006.

Kramer, T. "US HDDE Manufacturer Experience with In-Use Testing and PEMS Integration." *European Commission – Joint Research Centre, Real World Emissions Measurement,* Milan, Italy, March 19-21, 2007.

Krishnamurthy, M. and Guatam, M. "Modal analysis of in-use emission from heavy-duty diesel engines: on-board measurement." *Journal of Automobile Engineering,* Vol. 220, Part D, pp. 611-625, 2006.

Lambert, D., Vojtisek, M. and Wilson, J. "Evaluation of on road emissions from transit buses during revenue service." *US EPA 11th International Emission Inventory Conference – "Emission Inventories – Partnering for the Future,"* April 15-18, 2002.

Lloyd, A. and Cackette, T. "Diesel Engines: Environmental Impact and Control." *Journal of the Air & Waste Management Association,* Vol. 51, pp. 809-847, June 2001.

Lough, G., Christensen, C., Schauer, J., Tortorelli, J., Mani, E., Lawson, D., Clark, N. and Gabele, P. "Development of molecular marker source profiles for emissions from on-road gasoline and diesel vehicle fleets." *Journal of the Air & Waste Management Association,* Vol. 57, pp.1190-1199, October 2007.

Mathis, J. "Plug-in hybrid buses attract energy-minded officials," *Lawrence Journal World,* September 17, 2004.

Mazzoleni, C., Kuhns, H., Moosmuller, H., Keislar, R., Barber, P., Robinsom, N. and Watson, J. "On-Road Vehicle Particulate Matter and Gaseous Emission Distributions in Las Vegas, Nevada, Compared with Other Areas." *Journal of the Air & Waste Management Association,* Vol. 54, pp. 711-726, June 2004.

Miyasato, M. "South Coast AQMD Plug-in Sprinter Van Program." *ZEV Symposium, California Air Resources Board,* September 27, 2006.

Moawad, A., Singh, G., Hagspiel, S., Fellah, M., and Rousseau, A. "Impact of Real World Drive Cycles on PHEV Fuel Efficiency and Cost for Different Powertrain and Battery Characteristics." *Presented at International Electric Vehicle Symposium, (EVS-24), Stavanger, Norway, 2009.*

Morawska, L., Ristovski, Z., Johnson, G., Jayarante, E., and Mengersen, K. "Novel Method for On-Road Emission Factor Measurements Using a Plume Capture Trailer." *Environmental Science and Technology,* Vol. 41, No. 2, pp. 574-579, 2007.

Motavalli, J. "Hybrid Bans with a Power Cord; Dodge tests a small fleet of Sprinters for delivery." *New York Times,* October 20, 2006.

Muster, Tobias. "Fuel Savings Potential and Cost Considerations for US Class 8 Heavy Duty Trucks through Resistance Reductions and improved Propulsion Technologies until 2020." *Massachusetts Institute of Technology,* Energy Laboratory Publication # MIT_EL 00-001, May 2000.

Nam, E., and Giannelli, R. "Fuel Consumption Modeling of Conventional and Advanced Technology Vehicles in the Physical Emission Rate Estimator (PERE), Draft." *EPA420-P-05-001,* February 2005.

Nevius, T., and Tooney, R. "Improved PHEV Emission Measurements in a Chassis Dynamometer Test Cell." *SAE International Technical Paper Series,* Paper No. 2010-01-1925, 2010.

Nine, R.D., Clark, N.N., Gautam, M., Wayne, W.S., Thompson, G. and Lyons, D.W., "Emissions Trends for Heavy-Heavy Duty Trucks," *14th CRC On-Road Vehicle Emissions Workshop, San Diego, CA*, 2004.

Norbye, J.P. and Dunne, J. "…and a Commuter Car with Hybrid Drive." *Popular Science,* July 1969.

North, R.J. "Assessment of real-world pollutant emissions from a light-duty diesel vehicle." PhD Thesis submitted to the Center of Transport Studies, Department of Civil and Environmental Engineering, University of London, December 2006.

Northeast Advanced Vehicle Consortium (NAVC). "Hybrid-Electric Drive Heavy-Duty Vehicle Testing Project." *Defense Advanced Research Projects Agency*, NAV1098-PG009837, 2000.

Northeast Advanced Vehicle Consortium (NAVC). "Hybrid Transit Bus Certification Workgroup, Engine Certification Recommendations Report." NAVC0599-AVP009903, 2000.

Northeast Advanced Vehicle Consortium (NAVC). "Analysis of Electric Drive Technologies for Transit Applications: Battery-Electric, Hybrid-Electric, and Fuel Cells." *U.S. Department of Transportation, Federal Transit Administration*, FTA-MA-26-7100-05.1, 2005.

Nylund, N. and Erkkila, K., "Heavy-Duty Truck Emissions and Fuel Consumption Simulating Real-World Driving in Laboratory Conditions." *2005 DEER Conference,* Chicago, IL, August 21-25, 2005.

Parks, N. "Energy efficiency and the smart grid." *Environmental News, Environmental Science & Technology*, May 1, 2009, pp. 2999-3000.

Patil, R., Adornato, B., and Filipi, Z. "Impact of Naturalistic Driving Patterns on PHEV Performance and System Design." *SAE International Technical Paper Series,* Paper No. 2009-01-2715, 2009.

Pestrov, V.A. "Coast Down Method in Time-Distance Variables," SAE 9760408, 1997.

Plug In America. Accessed November, 2011, www.pluginamerica.org/ .

Plug-In Partners National Compagaign Kick-off, "To Mass Produce Flexible-Fuel Plug-in Hybrid Electric Vehicles," Washington D.C., January 2006.

Portmann, D. "Plug-In Hybrid Sprinter." *Plug-In 2008 Conference,* San Jose, CA, July 22, 2008.

Qiao, F., Yu, L., and Vojtisek-Lom, M. "On-Road Vehicle Emission and Activity Data Collection and Evaluation in Houston, Texas." *Transportation Research Record: Journal of the Transportation Research Board.* No. 1941, pp. 60-71, 2005.

Reynolds, C., and Kandlikar, M. "How hybrid-electric vehicles are different from conventional vehicles: the effect of weight and power on fuel consumption." *Environmental Research Letters,* No. 2 (2007) 014003, pp. 1-8.

Rousseau, A., Pagerit, S., Gao, D. "Plug-in Hybrid Electric Vehicle Control Strategy Parameter Optimization." *Presented at International Electric Vehicle Symposium, (EVS-23), Anaheim, CA, 2007.*

Rugh, J. "Proposal for a Vehicle Level Test Procedure to Measure Air Conditioning Fuel Use." *SAE International Technical Paper Series,* Paper No. 2010-01-0799, 2010.

Samaras, C. and Meisterling, K. "Life Cycle Assessment of Greenhouse Gas Emissions from Plug-In Hybrid Vehicles: Implications for Policy." *Environmental Science and Technology,* Vol. 42, No. 9, pp.3170-3176, 2008.

Sanna, L. "Driving the Solution-The Plug-in Hybrid Vehicle." *EPRI Journal,* Fall 2005.

Schifter, I., Diaz, L. and Lopez-Salinas, E. "A Predictive Model to Correlate Fuel Specifications with On-Road Vehicles Emissions in Mexico." *Environmental Science and Technology,* Vol. 40, No. 4, pp. 1270-1279, 2006.

Sensors, Inc. The Semtech User's Manual, 2006.

Sensors, Inc. Vehicle Exhaust FlowMeter, SEMTECH EFM User's Manual, 2006.

Sharer, P., Roussequ, A., Karbowski, D., and Pagerit, S. "Plug-in Hybrid Electric Vehicle Control Strategy: Comparison between EV and Charge-Depleting Options." *SAE International Technical Paper Series,* Paper No. 2008-01-0460, 2008.

Shidore, N., Bohn, T., Duoba, M., Lohse-Busch, H., and Sharer, P. "PHEV 'All electric range' and fuel economy in charge sustaining mode for low SOC operation of the jcs VL41M Li-ion battery using Battery HIL." *Presented at International Electric Vehicle Symposium, (EVS-23), Anaheim, CA, 2007.*

Shidore, N., Vyas, A., and Kwon, J. "Impact of Energy Management on the NPV Gasoline Savings of PHEVs." *SAE International Technical Paper Series,* Paper No. 2010-01-1236, 2010.

Shorter, J., Herndon, S., Zahniser, M., Nelson, D., Wormhoudt, J., Demerjian, K., and Kolb, C. "Real-Time Measurements of Nitrogen Oxide Emissions from In-Use

New York City Transit Buses Using a Chase Vehicle." *Environmental Science and Technology*, Vol. 39, No. 20, pp. 7991-8000, 2005.

Sioshansi, R., Denholm, P. "Emissions Impacts and Benefits of Plug-In Hybrid Electric Vehicles and Vehicle-to-Grid Services." *Environmental Science and Technology*, Vol. 43, No. 4, pp. 1199-1203, 2009.

Sioshansi, R., Denholm, P. "The Value of Plug-In Hybrid Electric Vehicles as Grid Resources." *The Energy Journal*, Vol. 31, No. 3, 2010.

Smith, D., Lohse-Busch, H., and Irick, D. "A Preliminary Investigation into the Mitigation of Plug-in Hybrid Vehicle Tailpipe Emissions Through Supervisory Control Methods." *SAE International Technical Paper Series*, Paper No. 2010-01-1266, 2010.

Society of Automotive Engineers. "Standard J1711: Recommended Practice for Measuring the Exhaust Emissions and Fuel Economy of Hybrid-Electric Vehicles, Including Plug-In Hybrid Vehicles." June, 2010.

Sonntag, D., Gao, H and Holmen, B. "Variability of Particle Number Emissions from Diesel and Hybrid Diesel-Electric Buses in Real Driving Conditions." *Environmental Science & Technology*, Vol. 42, No. 15, pp. 5637-5643, 2008.

Sonntag, D., Gao, H and Holmen, B. "Modeling On-Road Particle Number Emissions from a Hybrid Diesel-Electric Bus." *Transportation Research Record: Journal of the Transportation Research Board*, No. 2011, pp. 40-48, 2007.

Stephan, C. and Sullivan, J. "Environmental and Energy Implications of Plug-In Hybrid-Electric Vehicles." *Environmental Science and Technology*, Vol. 42, No. 4, pp.1185-1190, 2008.

Stockar, S., Tulpule, P., Marano, V., and Rizzoni, G. "Energy, Economical and Environmental Analysis of Plug-In Hybrid Electric Vehicles Based on Common Driving Cycles." *SAE International Journal of Engines*, Vol. 2, Iss. 2, pp. 467 – 476, 2009.

Stone, B. Jr., Mednick, A., Holloway, T., and Spak, S. "Mobile Source CO_2 Mitigation through Smart Growth Development and Vehicle Fleet Hybridization." *Environmental Science & Technology*, Vol. 43, No. 6, pp. 1704-1710, 2009.

Tate, E., Harpster, O., and Savagian, P. "The Electrification of the Automobile: From Conventional Hybrid, to Plug-in Hybrids, to Extended-Range Electric Vehicles." *SAE International Journal of Passenger Cars – Electronic and Electrical Systems*, Vol. 1, Iss. 1, pp. 156 – 166, 2008.

The California Cars Initiative. "How Carmakers are responding to the Plug-In Hybrid Opportunity." *International Humanities Center,* September 24, 2008. www.calcars.org

The California Cars Initiative, http://www.calcars.org/vehicles.html, accessed October 25, 2008.

Toth-Nagy, C., Conley, J., Jarrett, R., and Clark, N. "Further Validation of Artificial Neural-Network Based Emissions Simulation Models for Conventional and Hybrid Electric Vehicles." *Journal of the Air & Waste Management Association,* Vol. 56, pp. 898-910, July 2006.

Toyota Motor Corporation. "Series Parallel Hybrid System." *Hybrid Synergy Drive,* Oct. 30, 2008. http://www.hybridsynergydrive.com/en/series_parallel.html

Unal, A., Frey, C., and Rouphail, N. "Quantification of Highway Vehicle Emissions Hot Spots Based upon On-Board Measurements." *Journal of the Air & Waste Management Association,* Vol. 54, pp.130-140, February 2004.

U.S. Department of Energy. "Plug-In Hybrid Electric Vehicle Conversions." *Alternative Fuels and Advanced Vehicles Data Center* October 23, 2008. http://www.afdc.energy.gov/afdc/vehicles/plugin_hybrids_conversions.html

Vojtisek-Lom, M. and Wilson, P. "Real-World Emissions from Private Diesel Passenger Vehicles Running on Unrefined Waste Vegetable Oil." *14th Coordinating Research Council Workshop on On-Road Vehicle Emissions,* San Diego, CA, March 29-31, 2004.

Vyas, A., Santani, D., Duoba, M., Alexander, M. "Plug-In Hybrid Electric Vehicles: How Does One Determine Their Potential for Reducing U.S. Oil Dependence?" *Presented at International Electric Vehicle Symposium, (EVS-23), Anaheim, CA, 2007.*

Wayne, W. S., Clark, N. N., and Nine, R. D. "A Comparison of Emissions and Fuel Economy from Hybrid-Electric and Conventional-Drive Transit Buses," *Energy and Fuels,* 18(1), 257-270, 2004.

Yanowitz, J., McCormick, R. and Graboski, M. "In-Use Emissions from Heavy-Duty Diesel Vehicles." *Environmental Science and Technology,* Vol. 34, No. 5, pp.729-740, 2000.

Younglove, T., Scora, G. and Barth, M. "Designing On-Road Vehicle Test Programs for Effective Vehicle Emission Model Development." *Transportation Research Board (TRB) Paper No. 05-2770,* March 2005.

Yao, Z., Wang, Q., He, K., Huo, H., Ma, Y. and Zhang, Q. "Characteristics of Real-World Vehicular Emissions in Chinese Cities." *Journal of the Air & Waste Management Association,* Vol. 27, pp.1379-1386, November 2007.

Yu, L., Wang, Z., Qiao, F., and Qi, Y. "Approach to Development and Evaluation of Driving Cycles for Classified Roads Based on Vehicle Emission Characteristics." *Transportation Research Record: Journal of the Transportation Research Board,* No. 2058, pp. 58-67, 2008.

Zgheib, E., and Clodic, D. "CO_2 Emission and Energy Reduction Evaluations of Plug-in Hybrid Vehicles." *SAE International Technical Paper Series,* Paper No. 2009-01-1324, 2009.

Zhai, H., Frey, C. and Rouphail, N. "Speed- and Facility-Specific Emissions Estimates for Transit Buses based on Measured Speed Profiles." *Proceedings, Annual Meeting of the Air & Waste Management Association,* June 2006.

Zhai, H., Frey, C., and Rouphail, N. "A Vehicle-Specific Power Approach to Speed- and Facility-Specific Emissions Estimates for Diesel Transit Buses." *Environmental Science and Technology,* Vol. 41, No. 21, pp. 7985-7991, 2008.

Zhang, K. and Frey, C. "Road Grade Estimation for On-Road Vehicle Emissions Modeling Using Light Detection and Ranging Data." *Journal of the Air & Waste Management Association,* Vol. 56, pp. 777-788, June 2006.

Zhang, K. and Frey, C. "Evaluation of Response Time of a Portable System for In-Use Vehicle Tailpipe Emissions Measurement." *Environmental Science and Technology,* Vol. 42, No. 1, pp.221-227, 2008.

Zielinska, B., Sagebiel, J., McDonald, J., Whitney, K, Lawson, D. "Emission Rates and Comparative Chemical Composition from Selected In-Use Diesel and Gasoline-Fueled Vehicles." *Journal of the Air & Waste Management Association,* Vol. 54, pp.1138-1150, September 2004.

Appendix A: Summary table of all PHEV runs.

The following summary table provides cumulative data results for individual sample runs. Semtech-measured data were obtained from the Semtech summary information included by SensorTech-PC with every data file.

File names reference the actual file names in the digitally supplied databank. The route path references the exact roadway loop or portion of the sample route that was driven for each particular file. Partial or full runs refer to the KCATA transit routes, where partial runs did not result in a complete loop of the route, but only portion of the route. The entire route loop was completed for all full runs.

Brake horsepower emissions data were calculated for each individual sample run from the time-aligned dataset.

Table A-1: Summarized PHEV dataset according to sample run, sample information and route path.

Run Information						Sample Information		
Route	Date	Follow or Solo	Data File Name	Full or Partial Run	Route Path	Avg. Amb. Temp. (degC)	Run Time (s)	Distance Traveled (mi)
12st	9/24/2007	solo	Sept24_12TC&WBS1	full+	11th/Trst - QH - WB - VBloop - QH - Crystal Loop - 11thTrst	31.55	7305	27.013
109	9/11/2007	follow	Sept11_109WnrLpF1&2	full	109: Winner Loop (Wnr Lp - Dntwn - Wnr Lp)	25.35	2314	7.786
109	9/11/2007	follow	Sept11_109WnrLpF1&2	partial	109: Winner Loop (Wnr Lp - Dntwn (11th/Grand))	26.39	1771	4.098
109	9/11/2007	follow	Sept11_WnchstrLpF1&2 - run1	partial	109: Winchester (9th/VBrnt - Dntwn - 12th/Win)	29.18	1942	7.380
109	9/11/2007	follow	Sept11_WnchstrLpF1&2 - run2	full	109: Winchester (12th/Win - Dwntn - 12th/Win)	29.07	3197	9.061
109	9/11/2007	follow	Sept11_WnchstrLpF1&2 - run3	partial	109: Winchester (12th/Win - 9th/Paseo - KCATA)	28.15	1772	4.682
109	9/13/2007	follow	PHEV9-13-07B (run1)	full	109: Wnchstr Lp (9th/Hard - Dntn - Wnchstr Lp - 9th/hard)	30.02	1900	9.123
109	9/13/2007	follow	PHEV9-13-07B (run2)	full	109: Winner Loop (Wnr Lp - Dntwn - Wnr Lp)	30.49	1671	7.921
109	9/13/2007	follow	9/13: File D	partial	109: Winner Loop	32.26	2305	5.707
109	1/9/2008	solo	jan9_109S1	partial	11th/Char - 10th/Char - Winner Stop	4.00	542	3.230
109	1/9/2008	solo	jan9_109S2	full	Winner Loop - Dwntn - Winner Stop	4.33	1533	8.264
109	1/9/2008	solo	jan9_109S3	full	Winner Loop - Dwntn - Winner Stop	6.00	1458	7.822
109	1/9/2008	solo	jan9_109S4	full	Winner Loop - Dwntn - Winner Stop	7.08	1395	7.825
109	1/9/2008	solo	jan9_109s5	full	Winner Loop - Dwntn - Winner Stop	8.46	1471	7.832
109	1/9/2008	solo	jan9_109S6	partial	Winner Loop - 9th/Paseo - KCATA	8.35	945	4.227
109	1/9/2008	solo	jan9_109S7	full	Winner Loop - Dwntn - Winner Stop	6.92	1667	7.823
109	1/9/2008	solo	Jan9_109S8	partial	Winner Loop - Dwntn - 10th/Char	6.45	1087	4.941
109	8/19/2007	solo	PHEV8-19-07 (run1)	full	109: Both Loop (Wnr Lp - Dntwn - 12th/Wnchstr)	32.37	1668	8.586
109	8/19/2007	solo	PHEV8-19-07 (run2)	full	109: Winchester (12th/Wnchstr - Dntwn - 12th/Wnchstr)	31.78	1776	9.150
109	8/19/2007	solo	PHEV8-19-07 (run3)	full	109: Winchester (12th/Wnchstr - Dntwn - 12th/Wnchstr)	32.41	1657	9.770
109	8/19/2007	solo	PHEV8-19-07 (run4)	full	109: Winchester (12th/Wnchstr - Dntwn - 12th/Wnchstr)	31.65	1748	9.054
109	9/12/2007	solo	Sept12_109BothLpsS (run 2)	partial	109: Wnchstr (9th/Paseo - Wnchstr Lp - Dntwn - 10th/Grnd)	20.34	1596	8.174
109	9/12/2007	solo	Sept12_109BothLpsS (run 1)	full	109 Winner Lp: 9th/Paseo - Winner Lp - Dwntn - 9th/Paseo	20.15	1639	7.838
109	9/13/2007	solo	PHEV9-13-07B (run3)	partial	109: Winchester (9th/Hard - Dntwn - 9th/Hard - 12th/Wnchstr)	39.10	1487	7.798
109	9/10/2007	solo	Sept10_phev (run 1)	full	109 Wnchstr: 9th/Paseo - Wnchstr Lp - Dwtn - 9th/Paseo	22.09	1662	8.923
109	9/10/2007	solo	Sept10_phev (run 2)	partial	109 Wnchstr: 9th/Paseo - Wnchstr Lp - 9th/Norton	23.00	961	5.477
109	9/10/2007	solo	Sept10_phevB (Run 1)	full	109: Winner Loop (9th/Hard - Winner - Dwtn - 9th/hard)	24.77	2171	8.737
109	9/10/2007	solo	Sept10_phevB (run 2)	full	109: Wnchstr Lp (9th/Hard - Dntn - Wnchstr Lp - 9th/hard)	26.05	2541	9.153
110	12/5/2007	follow	dec5_110F1	full	RM - 44th/Brkln - RM	0.95	3299	11.583
110	12/5/2007	follow	dec5_110F2	partial	RM - 44th/Brkln - RM (lost bus at RM, caught at ?)	0.91	1439	6.038
110	12/5/2007	follow	dec5_110F2b	partial	44th/Brkln - 11th/Char	0.55	1785	4.460

Table A-1: continued.

Run Information						Sample Information		
Route	Date	Follow or Solo	Data File Name	Full or Partial Run	Route Path	Avg. Amb. Temp. (degC)	Run Time (s)	Distance Traveled (mi)
110	12/21/2007	follow	dec21_110F1	partial	11th/Char - RM - 44th/Brkln	7.41	2134	7.655
110	12/21/2007	follow	dec21_110F2	full	44th/Brkln - RM - 44th/Brkln	10.14	3216	11.791
110	12/21/2007	follow	dec21_110F3	full	44th/Brkln - RM - 44th/Brkln	12.94	3351	11.783
110	12/21/2007	follow	dec21_110F5	full	44th/Brkln - RM - 44th/Brkln	11.60	3468	11.774
110	12/21/2007	follow	dec21_110F6	partial	44th/Brkln - 11th/Char	11.00	1257	4.460
110	1/7/2008	follow	jan7_110F1	partial	11th/Char - RM - 44th/Brkln	18.43	2462	7.643
110	1/7/2008	follow	jan7_110F2	full	44th/Brkln - RM - 44th/Brkln	18.53	3264	11.873
110	1/7/2008	follow	jan7_110F3	full	44th/Brkln - RM - 44th/Brkln	18.94	3361	11.779
110	1/7/2008	follow	jan7_110F4	full	44th/Brkln - RM - 44th/Brkln	18.99	3513	11.774
110	1/7/2008	follow	jan7_110F5	full	44th/Brkln - RM - 44th/Brkln	15.19	3775	11.765
110	1/7/2008	follow	jan7_110F6	partial	44th/Brkln - 11th/Char	13.51	1178	4.450
110	9/24/2007	solo	Sept24_110S1	full	11thTrst - River Market - Brkln/44th - 11th/Trst	32.02	3223	12.178
110	11/29/2007	solo	nov29_110S1	full	11th/Char - RM - 44th/Brkln - 11th/Char	6.58	2968	14.199
110	11/29/2007	solo	nov29_110S2	full	11th/Char - RM - 44th/Brkln - 11th/Char	8.00	2580	12.135
110	11/29/2007	solo	Nov29_110S3	full	11th/Char - RM - 44th/Brkln - 11th/Char	9.74	2413	11.907
110	11/29/2007	solo	Nov29_110S4	full	11th/Char - RM - 44th/Brkln - 11th/Char	9.96	2622	12.690
110	12/20/2007	solo	dec20_110S1	partial	11th/Char - RM - 44th/Brkln	7.74	2062	7.685
110	12/20/2007	solo	dec20_110S2	full	44th/Brkln - RM - 44th/Brkln	8.57	2651	11.793
110	12/20/2007	solo	dec20_110S3	partial	44th/Brkln - RM - 10th/Paseo - KCATA	9.46	1950	8.330
110	12/20/2007	solo	dec20_110s4	partial	KCATA - 10th/Paseo - 44th/Brkln	13.63	1227	5.635
110	12/20/2007	solo	dec20_110s5	full	44th/Brkln - RM - 44th/Brkln	10.55	2844	12.259
110	12/20/2007	solo	dec20_110s6	full	44th/Brkln - RM - 44th/Brkln	10.55	2842	11.567
110	12/20/2007	solo	dec20_110s7	partial	44th/Brkln - 11th/Char	10.25	1010	4.440
110	12/21/2007	solo	dec21_110S4	partial	44th/Brkln - 11th/Paseo - KCATA	14.30	1427	3.742
110	12/21/2007	solo	dec21_110S5 mark 1	partial	KCATA - 44th/Brkln	16.70	781	3.751
110	12/21/2007	solo	dec21_110S5 mark 2	partial	44th/Brkln - 24th/Vine - 44th/Brkln	12.88	1229	5.718
123	11/20/2007	follow	phv_nov20_123F1	1.5routes	(solo 22nd/Frst to 19th/Trst) WB 19th/Trst - US - 19th/Trst - BVPark - 19th/Trst - US	20.79	5613	15.472
123	11/20/2007	follow	phv_nov20_123F2	full	US - BVPark - US	23.11	3156	11.858
123	11/20/2007	follow	phv_nov20_123F3	full	US - BVPark - US	24.16	3550	11.867
123	11/20/2007	follow	phv_nov20_123F4	full	US - BVPark - US	23.47	2779	10.408

Table A-1: continued.

Run Information						Sample Information		
Route	Date	Follow or Solo	Data File Name	Full or Partial Run	Route Path	Avg. Amb. Temp. (degC)	Run Time (s)	Distance Traveled (mi)
123	11/20/2007	follow	phv_nov20_123F5	partial	US - BVPark - 19thForest (dropped off route early)	24.00	2688	9.196
123	11/29/2007	follow	Nov29_123F1	partial	19th/Trst - Summit/23rd - Pershing - 19thTrst - 11th/Char	5.37	1678	4.474
123	12/4/2007	follow	dec4_123F2	full	US - BVPark - US	13.62	3378	11.877
123	12/4/2007	follow	dec4_123F3	full	US - BVPark - US	15.49	3373	11.852
123	12/4/2007	follow	dec4_123F4	parital	*US - BVPark - US*	16.45	782	2.373
123	12/5/2007	follow	dec5_123F1	partial	19th/Trst - Summit - CC - US	-1.00	1030	3.604
123	12/5/2007	follow	dec5_123F2	full	US - BVPark - US	-0.67	3298	11.900
123	12/5/2007	follow	dec5_123F3	full	US - BVPark - US	0.51	3378	11.891
123	12/5/2007	follow	dec5_123F4	full	US - BVPark - US	0.81	3434	11.977
123	9/24/2007	solo	Sept24_pseudo123S1	full	11th/Char - (123 w/o summit) cc/us - hard to bv condos	32.11	5834	14.421
123	11/19/2007	solo	nov19_123S1	full	22nd/Frst - 19th/Trst - US/CC - 23rd/Park - 22nd/Frst	24.15	3003	12.019
123	11/19/2007	solo	nov19_123S2	full	22nd/Frst - 19th/Trst - US/CC - 23rd/Park - 22nd/Frst - KCATA	25.25	4534	12.218
123	11/19/2007	solo	nov19_123S3	full	22nd/Frst - 19th/Trst - US/CC - 23rd/Park - 22nd/Frst	24.48	4264	12.454
123	11/26/2007	solo	Nov26_123S1	full	22nd/Tracy - 19th - US/CC (skip Summmit) - BVPark - US/CC	9.60	4572	15.495
123	11/19/2007	solo	nov19_123S4	full	22nd/Frst - 19th/Trst - US/CC - 23rd/Park - 22nd/Frst	22.60	3217	12.295
123	11/26/2007	solo	nov26_123S2	full	US - BVPark - US	11.16	3002	11.883
123	11/26/2007	solo	Nov26_123S3	full	US - BVPark - US	10.77	2867	11.888
123	11/26/2007	solo	Nov26_123S4	partial	US - BVPark - SWTfcWy/Summit - 20th/Frst	9.99	3197	11.742
123	11/28/2007	solo	Nov28_123S1	partial	19th/Trst - CC - US	10.26	991	3.595
123	11/28/2007	solo	Nov28_123S2	partial	US - BVPark -19th/Trst - 22nd/Tracy	8.64	2140	9.059
123	12/4/2007	solo	dec4_123S1	partial	19th/Trst - Summit - CC - US	13.59	1500	3.593
12T/C	10/19/2007	solo	oct19_12TCs1	full	11th/Char - QH - Truman/Crystal - 11th/Char	16.30	3473	10.907
12T/C	10/19/2007	solo	Oct19_12TCs2	full	11th/Char - QH - Truman/Crystal - 11th/Char	18.46	3306	10.901
12T/C	10/19/2007	solo	Oct19_12TCs3	full	11th/Char - QH - Truman/Crystal - 11th/Char	19.97	2864	10.897
12T/C	10/19/2007	solo	Oct19_12TCS4	full	11th/Char - QH - Truman/Crystal - 11th/Char	20.42	2837	10.895
12T/C	10/19/2007	solo	Oct19_12TCS5	full	11th/Char - QH - Truman/Crystal - 11th/Char	20.84	2775	10.891
12T/C	10/19/2007	solo	Oct19_12TCS6	full	11th/Char - QH - Truman/Crystal - 11th/Char	20.59	2682	10.902
12T/C	10/24/2007	solo	Oct24_12partial	partial	11th/Char - QH - KCATA	13.76	1546	4.010
12T/C	11/13/2007	solo	Nov13_12TC_Tst10	full	11th/Char - QH - Truman/Crystal - 11th/Char	19.41	2603	11.614
12T/C	11/13/2007	solo	Nov13_12TC_Tst11	full	11th/Char - QH - Truman/Crystal - 11th/Char	19.52	2601	11.616
12T/C	11/13/2007	solo	Nov13_12TC_tst14	full	11th/Char - QH - Truman/Crystal - 11th/Char	20.29	2520	11.621

Table A-1: continued.

Run Information						Sample Information		
Route	Date	Follow or Solo	Data File Name	Full or Partial Run	Route Path	Avg. Amb. Temp. (degC)	Run Time (s)	Distance Traveled (mi)
12T/C	11/13/2007	solo	Nov13_12TC_Tst15	full	11th/Char - QH - Truman/Crystal - 11th/Char	19.51	2420	11.637
12T/C	11/16/2007	solo	phev_nov16_12TCs1 phev_nov16_12TCs1a	full	11th/Char - QH - Truman/Crystal - 11th/Char	14.43	2797	11.168
12T/C	11/16/2007	solo	phev_nov16_12TCs2	full	11th/Char - QH - Truman/Crystal - 11th/Char	15.51	2579	11.299
12T/C	11/16/2007	solo	phev_nov16_12TCs3	full	11th/Char - QH - Truman/Crystal - 11th/Char	16.34	2596	10.898
12WB	1/6/2008	follow	jan6_12WBF1	partial	11/Char - WB - 24th/Hard	14.64	2648	8.990
12WB	1/6/2008	follow	jan6_12wbF2	partial	24th/Hard - WB - 12th/Paseo - KCATA	14.98	2842	9.317
12WB	1/6/2008	follow	jan6_12WBF3	partial	11th/Char - 12th/Char - 24th/Hardesty	16.00	1303	5.153
12WB	1/6/2008	na	jan6_12WBF4	na	NA (intended 24th/Hard - WB - 24th/Hard)	16.30	1320	6.488
12WB	10/18/2007	solo	Oct18_12WBS1	full	11thTrst - WB - 24thHardesty - 11th/Trst	19.08	3221	13.971
12WB	10/18/2007	solo	Oct18_12WBS2	full	11th/Char - WB - 24th/Hard - 11th/Char	20.94	5248	14.404
12WB	10/18/2007	solo	Oct18_12WBS3	full	11th/Char - WB - 24th/Hard - 11th/Char	20.66	2977	12.999
12WB	10/18/2007	solo	Oct18_12WBS4a & Oct18_12WBS4b	full	11th/Char - WB - 24th/Hard - 11th/Char	20.08	2975	13.153
12WB	11/16/2007	solo	phev_nov16_12WBs4	full	11th/Char - QH - WB - 24th/Hard - 11th/Char	16.63	3759	13.004
Hwy	11/28/2007	solo	Nov28_Hwy1	full	22nd/Tracy - 71S - 75thExit - 71N - PaseoExit - Tracy	12.04	1591	13.517
Hwy	11/28/2007	solo	Nov28_hwy2	full	Paseo/Tracy - 71S - 75thExit - 71N - Paseo/Tracy	12.00	1255	13.205
Hwy	11/28/2007	solo	Nov28_hwy3	full	Paseo/Tracy - 71S - 75thExit - 71N - Paseo/Tracy	12.00	1298	13.210
Hwy	11/28/2007	solo	Nov28_hwy4	full	Paseo/Tracy - 71S - 75thExit - 71N - Paseo/Tracy	12.00	1299	13.202
Hwy	11/28/2007	solo	NOv28_hwy5	full	Paseo/Tracy - 71S - 75thExit - 71N - Paseo/Tracy	11.64	1381	13.207
Hwy	11/29/2007	solo	Nov29_Hwy1	full	22nd/Tracy - 71S - 75thExit - 71N - PaseoExit - Tracy	10.14	1412	13.218
Hwy	1/9/2008	solo	jan9_hwy1	full	Tracy/21 - 71S - 75thExit - 71N - PaseoExit - Tracy	7.43	1330	13.216
Hwy	1/9/2008	solo	jan9_hwy2	full	Tracy/21 - 71S - 75thExit - 71N - PaseoExit - Tracy	7.00	1250	13.209
Hwy	1/9/2008	solo	jan9_hwy3	full	Tracy/21 - 71S - 75thExit - 71N - PaseoExit - Tracy	7.19	1310	13.208
Hwy	1/9/2008	solo	jan9_hwy4	full	Tracy/21 - 71S - 75thExit - 71N - PaseoExit - Tracy	7.00	1318	13.205
Hwy	1/9/2008	solo	jan9_hwy5	full	Tracy/21 - 71S - 75thExit - 71N - PaseoExit - Tracy	7.00	1331	13.212
Xfer	8/19/2007	solo	PHEV8-19-07 (XferA)	na	Xfer: KCATA - 9th/Paseo - Winner Lp	32.89	880	4.051
Xfer	10/18/2007	solo	Oct18_xferA	na	KCATA - 11th/Charolotte	22.41	596	1.008
Xfer	10/19/2007	solo	Oct19_xferA	na	11th/Char - KCATA	20.66	390	1.110
Xfer	10/19/2007	solo	oct19_xferB	na	KCATA - 11th/Charolotte	23.52	347	0.995
Xfer	11/13/2007	solo	Nov12_xfera_tst12_NODLM	na	11th/Char - KCATA	20.42	404	1.174

Table A-1: continued.

Run Information						Sample Information		
Route	Date	Follow or Solo	Data File Name	Full or Partial Run	Route Path	Avg. Amb. Temp. (degC)	Run Time (s)	Distance Traveled (mi)
Xfer	11/13/2007	solo	Nov13_xferb_tst13_NODLM	na	KCATA - 11th/Charolotte	22.62	296	1.040
Xfer	11/16/2007	solo	phev_nov16_xfera	na	11th/Char - KCATA	17.00	400	1.114
Xfer	11/16/2007	solo	phev_nov16_xferb	na	KCATA - 11th/Charolotte	19.26	383	0.982
Xfer	11/29/2007	solo	Nov29_xfer1	na	11th/Char - KCATA	9.00	301	1.092
Xfer	11/29/2007	solo	Nov29_xfer2	na	KCATA - 11th/Charolotte	10.84	290	0.997
Xfer	11/29/2007	solo	Nov29_xfer3 NO DLM	na	11th/Char - 22nd/Forest	10.00	385	1.971
xfer	12/5/2007	solo	dec5_xfer1	na	US - Main - 18th - pick up 110 route - RM	0.76	1033	3.283
Xfer	1/6/2008	solo	jan6_xfera	na	KCATA - 11th/Charolotte	17.48	276	1.005
Xfer	1/9/2008	solo	Jan9_xfera	na	KCATA - 22nd/Frst	9.37	380	1.199
Xfer	1/9/2008	solo	jan9_xferb	na	24th/Tracy - Trst - Winner Stop	7.00	845	4.549
Xfer	9/11/2007	solo	Sept11_WnchstrLpF1&2 -xfera	na	KCATA - 9th/Paseo - 9th/VanBrunt	33.15	857	3.511
Xfer	9/12/2007	solo	Sept12_109BothLpsS (XferA)	na	Xfer: KCATA - 9th/Paseo	22.29	358	1.027
Xfer	9/10/2007	solo	Sept10_phev (XferA)	na	KCATA - 9th/Woodland	23.86	519	1.959
Xfer	9/10/2007	solo	Sept10_phevB (xferB)	na	9th/Hrd - 9th/Paseo - 18th - KCATA	23.23	4614	3.482

Total:		291991	1181.6
Mean:	16.24	2163	8.75
Standard Deviation:	8.71	1259	4.40
Minimum:	-1.00	276	0.98
Maximum:	39.10	7305	27.01

Table A-2: Summarized PHEV dataset detailing sample run fuel usage, overall and brake horsepower-based emissions.

Run Information					Fuel Usage		Emissions Data (Overall)				Emissions Data (brake-hp basis)					
Route	Date	Follow or Solo	Data File Name	Full or Partial Run	Cons (gal)	Overall Economy (mpg)	CO_2 (g/mi)	CO (g/mi)	NOx (g/mi)	THC (g/mi)	CO_2 (g/bhp-hr)	CO (g/bhp-hr)	NO (g/bhp-hr)	NO_2 (g/bhp-hr)	NOx (g/bhp-hr)	THC (g/bhp-hr)
12st	9/24/2007	solo	Sept24_12TC&WBS1	full+	2.233	12.37	822.93	1.251	8.71	0.047	576.91	0.877	5.58	0.527	6.10	0.033
109	9/11/2007	follow	Sept11_109WnrLpF1&2	full	0.712	10.93	901.36	0.542	10.07	0.027	583.44	0.351	5.57	0.950	6.52	0.018
109	9/11/2007	follow	Sept11_109WnrLpF1&2	partial												
109	9/11/2007	follow	Sept11_WnchstrLpF1&2 - run1	partial	0.711	10.37	934.43	0.774	10.87	0.043	594.70	0.493	6.06	0.860	6.92	0.027
109	9/11/2007	follow	Sept11_WnchstrLpF1&2 - run2	full	0.982	9.22	1037.15	1.116	12.87	0.049	602.51	0.652	6.71	0.736	7.44	0.028
109	9/11/2007	follow	Sept11_WnchstrLpF1&2 - run3	partial	0.469	9.98	943.85	1.055	11.30	0.047	593.81	0.664	6.44	0.673	7.11	0.030
109	9/13/2007	follow	PHEV9-13-07B (run1)	full	0.701	13.01	729.76	0.762	8.34	0.029	584.35	0.608	6.01	0.646	6.66	0.023
109	9/13/2007	follow	PHEV9-13-07B (run2)	full	0.552	14.34	662.71	0.672	7.54	0.026	476.74	0.483	4.91	0.511	5.42	0.018
109	9/13/2007	follow	9/13: File D	partial	0.696	9.26	1100.42	1.039	13.41	0.081	605.96	0.572	6.94	0.449	7.38	0.045
109	1/9/2008	solo	jan9_109S1	partial	0.138	24.66	413.77	1.734	3.45	0.227	745.99	3.126	6.11	0.110	6.22	0.409
109	1/9/2008	solo	jan9_109S2	full	0.231	38.01	269.61	0.880	2.11	0.100	650.90	2.125	5.01	0.078	5.09	0.241
109	1/9/2008	solo	jan9_109S3	full	0.267	31.05	330.14	0.705	3.35	0.100	611.48	1.306	6.00	0.197	6.20	0.185
109	1/9/2008	solo	jan9_109S4	full	0.416	19.90	516.38	0.528	5.85	0.038	566.15	0.579	6.02	0.399	6.42	0.041
109	1/9/2008	solo	jan9_109s5	full	0.458	18.07	568.62	0.536	6.60	0.041	575.79	0.543	6.33	0.346	6.68	0.042
109	1/9/2008	solo	jan9_109S6	partial	0.303	14.84	692.56	1.005	7.57	0.042	568.40	0.825	5.94	0.278	6.22	0.035
109	1/9/2008	solo	jan9_109S7	full	0.494	16.79	612.82	0.479	6.89	0.050	577.46	0.451	6.30	0.189	6.49	0.047
109	1/9/2008	solo	Jan9_109S8	partial	0.319	16.56	620.86	0.830	6.98	0.039	578.79	0.773	6.29	0.221	6.51	0.036
109	8/19/2007	solo	PHEV8-19-07 (run1)	full	0.765	12.02	847.63	0.786	8.04	0.021	577.93	0.536	4.04	1.442	5.48	0.014
109	8/19/2007	solo	PHEV8-19-07 (run2)	full	0.740	13.09	778.39	0.959	7.14	0.015	577.78	0.712	3.96	1.336	5.30	0.011
109	8/19/2007	solo	PHEV8-19-07 (run3)	full	0.727	14.17	718.26	0.822	6.51	0.005	575.07	0.658	4.05	1.156	5.21	0.004
109	8/19/2007	solo	PHEV8-19-07 (run4)	full	0.687	13.79	739.45	0.859	7.00	0.003	573.51	0.666	4.21	1.216	5.43	0.002
109	9/12/2007	solo	Sept12_109BothLpsS (run 2)	partial	0.522	17.04	594.98	0.573	6.55	0.022	572.36	0.577	5.79	0.483	6.27	0.021
109	9/12/2007	solo	Sept12_109BothLpsS (run 1)	full	0.121	68.38	148.96	0.617	1.24	0.049	631.62	2.615	5.11	0.144	5.25	0.207
109	9/13/2007	solo	PHEV9-13-07B (run3)	partial												
109	9/10/2007	solo	Sept10_phev (run 1)	full	0.171	55.78	182.09	0.990	1.53	0.037	589.99	3.207	4.33	0.623	4.95	0.121
109	9/10/2007	solo	Sept10_phev (run 2)	partial	0.368	15.89	646.65	0.566	6.74	0.002	583.41	0.511	4.69	1.384	6.08	0.002
109	9/10/2007	solo	Sept10_phevB (Run 1)	full	0.737	12.85	778.77	0.980	8.59	0.022	588.15	0.740	5.56	0.928	6.49	0.017
109	9/10/2007	solo	Sept10_phevB (run 2)	full	0.826	11.48	890.16	0.595	9.22	0.008	590.29	0.394	5.14	0.970	6.11	0.005
110	12/5/2007	follow	dec5_110F1	full	0.877	13.96	737.44	1.026	7.96	0.057	585.86	0.815	6.07	0.250	6.32	0.045
110	12/5/2007	follow	dec5_110F2	partial	0.414	15.66	657.03	0.767	6.90	0.044	583.82	0.682	5.90	0.228	6.13	0.039
110	12/5/2007	follow	dec5_110F2b	partial	0.325	14.50	710.33	0.696	8.07	0.042	588.05	0.576	6.47	0.209	6.68	0.034

Table A-2: continued.

Run Information					Fuel Usage		Emissions Data (Overall)				Emissions Data (brake-hp basis)					
Route	Date	Follow or Solo	Data File Name	Full or Partial Run	Cons (gal)	Overall Economy (mpg)	CO_2 (g/mi)	CO (g/mi)	NOx (g/mi)	THC (g/mi)	CO_2 (g/bhp-hr)	CO (g/bhp-hr)	NO (g/bhp-hr)	NO_2 (g/bhp-hr)	NOx (g/bhp-hr)	THC (g/bhp-hr)
110	12/21/2007	follow	dec21_110F1	partial	0.290	27.88	365.26	2.435	2.59	0.233	665.82	4.439	4.60	0.122	4.72	0.425
110	12/21/2007	follow	dec21_110F2	full	0.630	19.85	516.03	1.222	5.20	0.078	592.68	1.403	5.53	0.441	5.97	0.089
110	12/21/2007	follow	dec21_110F3	full	0.907	13.75	746.42	0.870	8.02	0.024	580.92	0.677	5.78	0.468	6.24	0.018
110	12/21/2007	follow	dec21_110F5	full	0.799	15.63	656.55	1.338	7.03	0.021	590.22	1.202	5.99	0.329	6.32	0.019
110	12/21/2007	follow	dec21_110F6	partial	0.330	14.34	716.09	1.295	8.35	0.039	599.49	1.084	6.70	0.291	6.99	0.032
110	1/7/2008	follow	jan7_110F1	partial	0.229	33.90	299.51	1.690	2.26	0.162	669.22	3.776	4.97	0.072	5.04	0.362
110	1/7/2008	follow	jan7_110F2	full	0.850	14.79	690.99	1.869	6.60	0.068	595.92	1.612	4.93	0.765	5.69	0.058
110	1/7/2008	follow	jan7_110F3	full	0.907	13.76	744.62	1.152	7.61	0.027	591.44	0.915	5.53	0.514	6.04	0.022
110	1/7/2008	follow	jan7_110F4	full	0.930	13.43	760.58	1.734	7.93	0.036	598.81	1.365	5.87	0.371	6.24	0.028
110	1/7/2008	follow	jan7_110F5	full	0.966	12.93	792.68	1.189	8.52	0.060	601.95	0.903	6.17	0.291	6.47	0.046
110	1/7/2008	follow	jan7_110F6	partial	0.348	13.53	757.93	1.161	7.62	0.069	567.65	0.870	5.48	0.224	5.71	0.051
110	9/24/2007	solo	Sept24_110S1	full	1.091	11.67	871.77	1.212	9.15	0.057	571.88	0.795	5.68	0.323	6.00	0.038
110	11/29/2007	solo	nov29_110S1	full	0.644	23.36	440.07	0.757	4.55	0.063	593.11	1.020	5.69	0.437	6.13	0.085
110	11/29/2007	solo	nov29_110S2	full	0.803	15.98	643.81	0.608	7.48	0.048	575.32	0.543	6.26	0.422	6.68	0.042
110	11/29/2007	solo	Nov29_110S3	full	0.770	16.40	626.84	0.609	7.46	0.041	566.58	0.550	6.38	0.370	6.75	0.037
110	11/29/2007	solo	Nov29_110S4	full	0.837	15.93	645.27	0.611	7.11	0.028	566.54	0.536	5.95	0.295	6.24	0.025
110	12/20/2007	solo	dec20_110S1	partial	0.223	36.35	280.31	1.706	2.07	0.197	654.42	3.984	4.76	0.082	4.84	0.459
110	12/20/2007	solo	dec20_110S2	full	0.511	24.50	418.57	0.998	3.80	0.084	588.49	1.403	4.85	0.497	5.34	0.118
110	12/20/2007	solo	dec20_110S3	partial	0.593	14.92	687.99	0.889	7.32	0.028	582.95	0.753	5.55	0.650	6.20	0.023
110	12/20/2007	solo	dec20_110s4	partial	0.336	17.80	576.54	0.505	5.96	0.016	563.79	0.494	5.35	0.470	5.82	0.016
110	12/20/2007	solo	dec20_110s5	full	0.839	15.52	661.52	0.978	7.05	0.028	578.55	0.855	5.72	0.449	6.17	0.024
110	12/20/2007	solo	dec20_110s6	full	0.762	16.02	641.04	0.971	7.09	0.031	580.20	0.879	6.06	0.366	6.42	0.028
110	12/20/2007	solo	dec20_110s7	partial	0.337	13.96	735.88	0.889	7.99	0.038	571.36	0.690	5.95	0.255	6.21	0.029
110	12/21/2007	solo	dec21_110S4	partial	0.253	15.73	652.31	0.566	7.16	0.024	561.63	0.487	5.90	0.266	6.17	0.021
110	12/21/2007	solo	dec21_110S5 mark 1	partial	0.249	16.00	641.06	0.971	6.73	0.030	563.47	0.853	5.66	0.257	5.92	0.026
110	12/21/2007	solo	dec21_110S5 mark 2	partial	0.375	16.11	636.40	0.879	6.82	0.045	15.86	16.442	14.35	13.965	15.18	3.472
123	11/20/2007	follow	phv_nov20_123F1	1.5routes	0.961	17.05	599.27	1.727	5.15	0.090	606.60	1.747	4.34	0.865	5.21	0.091
123	11/20/2007	follow	phv_nov20_123F2	full	1.199	10.50	975.52	1.208	9.56	0.055	592.00	0.733	4.96	0.841	5.80	0.034
123	11/20/2007	follow	phv_nov20_123F3	full	1.106	11.45	893.42	1.365	8.85	0.044	590.31	0.902	5.23	0.619	5.85	0.029
123	11/20/2007	follow	phv_nov20_123F4	full	0.932	11.84	863.86	1.322	8.15	0.046	600.03	0.918	5.13	0.530	5.66	0.032

Table A-2: continued.

Run Information					Fuel Usage		Emissions Data (Overall)				Emissions Data (brake-hp basis)					
Route	Date	Follow or Solo	Data File Name	Full or Partial Run	Cons (gal)	Overall Economy (mpg)	CO_2 (g/mi)	CO (g/mi)	NOx (g/mi)	THC (g/mi)	CO_2 (g/bhp-hr)	CO (g/bhp-hr)	NO (g/bhp-hr)	NO_2 (g/bhp-hr)	NOx (g/bhp-hr)	THC (g/bhp-hr)
123	11/20/2007	follow	phv_nov20_123F5	partial	0.846	11.58	883.35	1.438	8.35	0.042	585.33	0.953	5.13	0.402	5.53	0.028
123	11/29/2007	follow	Nov29_123F1	partial	0.268	17.65	579.29	2.807	5.24	0.285	715.25	3.466	6.19	0.284	6.47	0.351
123	12/4/2007	follow	dec4_123F2	full	0.555	22.73	450.05	1.424	3.65	0.059	591.95	1.873	4.43	0.361	4.80	0.078
123	12/4/2007	follow	dec4_123F3	full	1.148	10.99	932.02	1.954	9.52	0.074	587.00	1.231	5.53	0.468	6.00	0.046
123	12/4/2007	follow	dec4_123F4	parital	0.209	11.99	853.81	2.075	8.97	0.047	555.11	1.349	5.55	0.279	5.83	0.030
123	12/5/2007	follow	dec5_123F1	partial	0.245	15.56	657.03	3.643	5.83	0.376	709.83	3.936	6.07	0.228	6.30	0.406
123	12/5/2007	follow	dec5_123F2	full	0.496	25.41	402.71	1.568	3.16	0.128	642.65	2.503	4.87	0.169	5.04	0.204
123	12/5/2007	follow	dec5_123F3	full	0.855	14.78	694.91	1.097	7.15	0.057	591.45	0.933	5.70	0.389	6.08	0.048
123	12/5/2007	follow	dec5_123F4	full	0.992	12.82	801.95	1.232	8.38	0.062	576.40	0.886	5.70	0.325	6.03	0.045
123	9/24/2007	solo	Sept24_pseudo123S1	full	1.444	10.56	964.91	1.173	10.03	0.064	587.73	0.714	5.73	0.373	6.11	0.039
123	11/19/2007	solo	nov19_123S1	full	0.396	32.34	314.43	1.508	2.46	0.096	631.14	3.027	4.52	0.420	4.94	0.193
123	11/19/2007	solo	nov19_123S2	full	1.056	12.27	833.65	1.199	8.80	0.036	585.86	0.843	4.86	1.322	6.19	0.025
123	11/19/2007	solo	nov19_123S3	full	1.101	12.52	817.32	0.985	8.63	0.035	585.84	0.706	5.24	0.945	6.19	0.025
123	11/26/2007	solo	Nov26_123S1	full	0.733	22.44	456.55	1.463	3.96	0.140	618.61	1.983	4.95	0.413	5.36	0.190
123	11/19/2007	solo	nov19_123S4	full	1.072	12.19	840.68	1.264	8.52	0.038	582.01	0.875	5.16	0.740	5.90	0.026
123	11/26/2007	solo	nov26_123S2	full	0.932	13.53	758.99	1.172	8.10	0.054	578.59	0.893	5.66	0.518	6.17	0.041
123	11/26/2007	solo	Nov26_123S3	full	0.923	13.68	750.90	0.905	7.93	0.046	573.59	0.692	5.65	0.406	6.06	0.035
123	11/26/2007	solo	Nov26_123S4	partial	0.917	13.66	751.21	1.174	7.73	0.049	570.13	0.891	5.54	0.328	5.87	0.037
123	11/28/2007	solo	Nov28_123S1	partial	0.255	14.85	690.95	1.357	7.34	0.066	584.96	1.149	5.97	0.249	6.22	0.056
123	11/28/2007	solo	Nov28_123S2	partial	0.701	13.69	750.08	1.354	7.49	0.081	568.23	1.026	5.36	0.315	5.67	0.062
123	12/4/2007	solo	dec4_123S1	partial	0.223	17.13	595.84	2.821	4.86	0.164	697.95	3.305	5.47	0.223	5.70	0.192
12T/C	10/19/2007	solo	oct19_12TCs1	full	0.796	14.51	706.55	0.953	7.25	0.039	579.23	0.782	5.39	0.557	5.94	0.032
12T/C	10/19/2007	solo	Oct19_12TCs2	full	0.775	14.91	687.47	0.971	7.79	0.026	579.35	0.818	5.89	0.672	6.56	0.022
12T/C	10/19/2007	solo	Oct19_12TCs3	full	0.800	14.42	710.56	1.019	7.93	0.033	573.57	0.823	5.92	0.478	6.40	0.027
12T/C	10/19/2007	solo	Oct19_12TCS4	full	0.834	13.77	743.93	1.158	8.56	0.027	579.73	0.903	6.14	0.533	6.67	0.021
12T/C	10/19/2007	solo	Oct19_12TCS5	full	0.851	13.58	754.05	1.072	8.55	0.031	574.05	0.816	6.04	0.467	6.51	0.024
12T/C	10/19/2007	solo	Oct19_12TCS6	full	0.813	14.34	714.15	0.958	7.96	0.031	570.68	0.766	5.89	0.466	6.36	0.025
12T/C	10/24/2007	solo	Oct24_12partial	partial	0.220	19.48	525.78	1.619	3.91	0.100	632.58	1.948	4.27	0.431	4.70	0.120
12T/C	11/13/2007	solo	Nov13_12TC_Tst10	full	0.228	50.91	200.37	0.835	1.59	0.090						
12T/C	11/13/2007	solo	Nov13_12TC_Tst11	full	0.561	20.72	495.24	0.547	5.45	0.038						
12T/C	11/13/2007	solo	Nov13_12TC_tst14	full	0.764	15.20	674.40	0.730	7.42	0.012						

Table A-2: continued.

Run Information					Fuel Usage		Emissions Data (Overall)				Emissions Data (brake-hp basis)					
Route	Date	Follow or Solo	Data File Name	Full or Partial Run	Cons (gal)	Overall Economy (mpg)	CO_2 (g/mi)	CO (g/mi)	NOx (g/mi)	THC (g/mi)	CO_2 (g/bhp-hr)	CO (g/bhp-hr)	NO (g/bhp-hr)	NO_2 (g/bhp-hr)	NOx (g/bhp-hr)	THC (g/bhp-hr)
12T/C	11/13/2007	solo	Nov13_12TC_Tst15	full	0.764	15.24	673.77	0.627	7.26	0.013						
12T/C	11/16/2007	solo	phev_nov16_12TCs1 phev_nov16_12TCs1a	full	0.679	17.44	588.24	0.865	6.56	0.069	592.70	0.871	5.81	0.793	6.61	0.069
12T/C	11/16/2007	solo	phev_nov16_12TCs2	full	0.777	15.62	657.98	0.744	7.44	0.032	568.26	0.643	5.50	0.921	6.42	0.028
12T/C	11/16/2007	solo	phev_nov16_12TCs3	full	0.723	15.98	642.26	0.736	7.38	0.027	574.13	0.658	5.80	0.796	6.59	0.024
12WB	1/6/2008	follow	jan6_12WBF1	partial	0.304	30.99	328.92	1.612	2.59	0.122	642.46	3.148	4.90	0.160	5.06	0.239
12WB	1/6/2008	follow	jan6_12wbF2	partial	0.573	17.36	589.83	1.516	5.97	0.043	598.92	1.540	5.26	0.804	6.06	0.043
12WB	1/6/2008	follow	jan6_12WBF3	partial	0.305	17.91	573.37	0.414	6.50	0.022	557.09	0.402	5.82	0.496	6.31	0.021
12WB	1/6/2008	na	jan6_12WBF4	na	0.424	16.41	625.06	0.632	6.71	0.026	560.13	0.566	5.52	0.496	6.02	0.023
12WB	10/18/2007	solo	Oct18_12WBS1	full												
12WB	10/18/2007	solo	Oct18_12WBS2	full							No EFM Data (no mass emissions)					
12WB	10/18/2007	solo	Oct18_12WBS3	full												
12WB	10/18/2007	solo	Oct18_12WBS4a & Oct18_12WBS4b	full												
12WB	11/16/2007	solo	phev_nov16_12WBs4	full	0.898	15.48	662.90	0.942	7.52	0.029	571.78	0.812	5.78	0.712	6.49	0.025
Hwy	11/28/2007	solo	Nov28_Hwy1	full	0.683	20.96	491.19	0.504	4.07	0.072	2379.30	2.441	18.41	1.290	19.70	0.350
Hwy	11/28/2007	solo	Nov28_hwy2	full	0.562	24.91	412.53	0.520	3.46	0.117	587.32	0.740	4.68	0.252	4.93	0.167
Hwy	11/28/2007	solo	Nov28_hwy3	full	0.568	24.65	417.67	0.349	3.47	0.052	584.19	0.488	4.59	0.263	4.85	0.073
Hwy	11/28/2007	solo	Nov28_hwy4	full	0.645	21.68	474.64	0.407	4.34	0.058	574.29	0.492	4.95	0.302	5.25	0.071
Hwy	11/28/2007	solo	NOv28_hwy5	full	0.664	21.05	489.03	0.369	4.70	0.043	570.19	0.431	5.16	0.313	5.48	0.050
Hwy	11/29/2007	solo	Nov29_Hwy1	full	0.768	18.15	568.03	0.203	5.76	0.034	562.33	0.201	5.46	0.235	5.70	0.034
Hwy	1/9/2008	solo	jan9_hwy1	full	0.749	18.68	551.43	0.226	5.48	0.042	573.79	0.235	5.43	0.275	5.71	0.044
Hwy	1/9/2008	solo	jan9_hwy2	full	0.651	21.48	479.53	0.194	4.52	0.046	572.60	0.232	5.29	0.109	5.40	0.055
Hwy	1/9/2008	solo	jan9_hwy3	full	0.706	19.81	519.47	0.389	4.89	0.099	565.91	0.423	5.24	0.088	5.32	0.108
Hwy	1/9/2008	solo	jan9_hwy4	full	0.709	19.67	523.29	0.423	4.84	0.104	570.00	0.460	5.21	0.064	5.27	0.113
Hwy	1/9/2008	solo	jan9_hwy5	full	0.708	19.75	521.46	0.347	5.06	0.083	561.79	0.374	5.38	0.077	5.45	0.089
Xfer	8/19/2007	solo	PHEV8-19-07 (XferA)	na	0.348	12.30	822.99	2.147	7.15	0.084	611.73	1.596	4.33	0.985	5.31	0.063
Xfer	10/18/2007	solo	Oct18_xferA	na												
Xfer	10/19/2007	solo	Oct19_xferA	na	0.067	17.45	585.81	1.765	6.34	0.028	588.20	1.772	5.90	0.462	6.37	0.029
Xfer	10/19/2007	solo	oct19_xferB	na	0.116	9.05	1130.36	2.239	12.36	0.066	565.53	1.120	5.78	0.407	6.18	0.033
Xfer	11/13/2007	solo	Nov12_xfera_tst12_NODLM	na	0.089	13.22	775.48	1.289	8.11	0.025						

Table A-2: continued.

Run Information				Full or Partial Run	Fuel Usage		Emissions Data (Overall)				Emissions Data (brake-hp basis)					
Route	Date	Follow or Solo	Data File Name		Cons (gal)	Overall Economy (mpg)	CO_2 (g/mi)	CO (g/mi)	NOx (g/mi)	THC (g/mi)	CO_2 (g/bhp-hr)	CO (g/bhp-hr)	NO (g/bhp-hr)	NO_2 (g/bhp-hr)	NOx (g/bhp-hr)	THC (g/bhp-hr)
Xfer	11/13/2007	solo	Nov13_xferb_tst13_NODLM	na	0.097	10.77	951.66	1.246	10.33	0.117						
Xfer	11/16/2007	solo	phev_nov16_xfera	na	0.068	17.38	590.73	1.276	6.30	0.022	557.06	1.203	5.47	0.471	5.94	0.021
Xfer	11/16/2007	solo	phev_nov16_xferb	na	0.109	9.60	1070.91	1.430	11.79	0.045	573.35	0.765	5.79	0.517	6.31	0.024
Xfer	11/29/2007	solo	Nov29_xfer1	na	0.077	15.23	675.64	0.518	7.55	0.021	559.13	0.429	5.76	0.489	6.25	0.017
Xfer	11/29/2007	solo	Nov29_xfer2	na	0.096	11.02	932.41	1.131	10.76	0.070	541.29	0.656	6.00	0.240	6.24	0.041
Xfer	11/29/2007	solo	Nov29_xfer3 NO DLM	na	0.154	12.81	802.34	0.847	7.94	0.029						
xfer	12/5/2007	solo	dec5_xfer1	na	0.290	11.95	861.27	1.261	9.77	0.094	580.84	0.850	6.35	0.236	6.59	0.064
Xfer	1/6/2008	solo	jan6_xfera	na	0.121	8.79	1166.79	2.440	12.96	0.008	575.79	1.204	5.86	0.540	6.40	0.004
Xfer	1/9/2008	solo	Jan9_xfera	na	0.122	10.45	982.77	1.807	10.84	0.092	566.31	1.041	5.95	0.298	6.25	0.053
Xfer	1/9/2008	solo	jan9_xferb	na	0.157	30.71	333.92	0.586	3.36	0.082	556.68	0.977	5.51	0.084	5.59	0.136
Xfer	9/11/2007	solo	Sept11_WnchstrLpF1&2 -xfera	na	0.204	17.18	572.35	1.019	6.35	0.065	571.45	1.029	6.02	0.424	6.45	0.064
Xfer	9/12/2007	solo	Sept12_109BothLpsS (XferA)	na	0.024	44.24	227.26	2.624	1.26	0.226	874.04	10.091	4.30	0.526	4.83	0.868
Xfer	9/10/2007	solo	Sept10_phev (XferA)	na	0.087	24.49	415.57	1.766	3.25	0.121	741.81	3.152	5.41	0.387	5.80	0.216
Xfer	9/10/2007	solo	Sept10_phevB (xferB)	na	0.347	11.13	917.26	0.777	9.44	0.008	586.12	0.497	5.09	0.940	6.03	0.005
				Total:	74.4	2268										
				Mean:	0.581	17.72	661.91	1.098	6.87	0.062	602.59	1.335	5.68	0.592	6.16	0.110
				Standard Deviation:	0.345	8.88	202.97	0.579	2.52	0.055	176.89	1.835	1.54	1.263	1.60	0.331
				Minimum:	0.024	8.79	148.96	0.194	1.24	0.002	15.86	0.201	3.96	0.064	4.70	0.002
				Maximum:	2.233	68.38	1166.79	3.643	13.41	0.376	2379.30	16.442	18.41	13.965	19.70	3.472

Table A-3: Summarized PHEV dataset detailing state of battery charge for each sample run.

Run Information					State of Battery Charge		
Route	Date	Follow or Solo	Data File Name	Full or Partial Run	Avg (%)	Max (%)	Min (%)
12st	9/24/2007	solo	Sept24_12TC&WBS1	full+	36.2	38.8	33.9
109	9/11/2007	follow	Sept11_109WnrLpF1&2	full	36.2	37.6	34.3
109	9/11/2007	follow	Sept11_109WnrLpF1&2	partial	36.0	38.0	34.4
109	9/11/2007	follow	Sept11_WnchstrLpF1&2 - run1	partial	35.8	37.5	33.8
109	9/11/2007	follow	Sept11_WnchstrLpF1&2 - run2	full	36.1	37.6	33.6
109	9/11/2007	follow	Sept11_WnchstrLpF1&2 - run3	partial	36.5	37.5	34.3
109	9/13/2007	follow	PHEV9-13-07B (run1)	full	36.1	38.5	34.2
109	9/13/2007	follow	PHEV9-13-07B (run2)	full	36.9	38.2	35.0
109	9/13/2007	follow	9/13: File D	partial	35.7	37.7	34.1
109	1/9/2008	solo	jan9_109S1	partial	86.0	90.0	84.7
109	1/9/2008	solo	jan9_109S2	full	70.8	84.7	56.4
109	1/9/2008	solo	jan9_109S3	full	42.6	56.4	34.2
109	1/9/2008	solo	jan9_109S4	full	36.5	39.5	34.4
109	1/9/2008	solo	jan9_109s5	full	36.7	38.8	34.4
109	1/9/2008	solo	jan9_109S6	partial	36.2	37.7	34.3
109	1/9/2008	solo	jan9_109S7	full	36.7	40.3	34.1
109	1/9/2008	solo	Jan9_109S8	partial	36.5	37.9	34.3
109	8/19/2007	solo	PHEV8-19-07 (run1)	full	36.1	37.6	34.1
109	8/19/2007	solo	PHEV8-19-07 (run2)	full	36.2	37.7	34.1
109	8/19/2007	solo	PHEV8-19-07 (run3)	full	36.3	37.6	34.0
109	8/19/2007	solo	PHEV8-19-07 (run4)	full	36.3	37.8	34.2
109	9/12/2007	solo	Sept12_109BothLpsS (run 2)	partial	36.4	38.1	34.1
109	9/12/2007	solo	Sept12_109BothLpsS (run 1)	full	56.6	76.6	35.8
109	9/13/2007	solo	PHEV9-13-07B (run3)	partial	36.7	36.2	36.7
109	9/10/2007	solo	Sept10_phev (run 1)	full	54.0	80.9	33.9
109	9/10/2007	solo	Sept10_phev (run 2)	partial	36.3	37.8	34.2
109	9/10/2007	solo	Sept10_phevB (Run 1)	full	35.9	38.5	34.2
109	9/10/2007	solo	Sept10_phevB (run 2)	full	36.2	37.9	34.2
110	12/5/2007	follow	dec5_110F1	full	36.7	38.8	34.2
110	12/5/2007	follow	dec5_110F2	partial	36.7	37.7	34.3
110	12/5/2007	follow	dec5_110F2b	partial	36.0	37.6	34.4
110	12/21/2007	follow	dec21_110F1	partial	77.8	91.0	56.1
110	12/21/2007	follow	dec21_110F2	full	38.9	56.1	34.1
110	12/21/2007	follow	dec21_110F3	full	36.5	38.2	34.1
110	12/21/2007	follow	dec21_110F5	full	36.3	37.7	34.2
110	12/21/2007	follow	dec21_110F6	partial	35.8	37.5	34.3
110	1/7/2008	follow	jan7_110F1	partial	74.5	89.6	49.7
110	1/7/2008	follow	jan7_110F2	full	37.2	49.6	34.1
110	1/7/2008	follow	jan7_110F3	full	36.2	37.6	34.1
110	1/7/2008	follow	jan7_110F4	full	36.3	37.6	34.1
110	1/7/2008	follow	jan7_110F5	full	36.2	37.8	34.1
110	1/7/2008	follow	jan7_110F6	partial	36.7	37.5	34.3
110	9/24/2007	solo	Sept24_110S1	full	36.0	37.9	34.0
110	11/29/2007	solo	nov29_110S1	full	46.7	68.1	35.2
110	11/29/2007	solo	nov29_110S2	full	36.4	38.0	34.2
110	11/29/2007	solo	Nov29_110S3	full	36.4	37.7	34.3
110	11/29/2007	solo	Nov29_110S4	full	36.4	38.3	34.1
110	12/20/2007	solo	dec20_110S1	partial	79.8	91.9	61.8
110	12/20/2007	solo	dec20_110S2	full	42.2	61.8	34.3

Table A-3: continued.

Run Information					State of Battery Charge		
Route	Date	Follow or Solo	Data File Name	Full or Partial Run	Avg (%)	Max (%)	Min (%)
110	12/20/2007	solo	dec20_110S3	partial	36.0	37.6	34.1
110	12/20/2007	solo	dec20_110s4	partial	36.3	38.0	34.3
110	12/20/2007	solo	dec20_110s5	full	36.2	37.8	34.2
110	12/20/2007	solo	dec20_110s6	full	36.0	37.8	34.0
110	12/20/2007	solo	dec20_110s7	partial	36.1	37.5	34.2
110	12/21/2007	solo	dec21_110S4	partial	36.6	37.6	33.9
110	12/21/2007	solo	dec21_110S5 mark 1	partial	36.6	38.1	34.4
110	12/21/2007	solo	dec21_110S5 mark 2	partial	36.2	37.8	34.1
123	11/20/2007	follow	phv_nov20_123F1	1.5routes	58.3	90.8	34.2
123	11/20/2007	follow	phv_nov20_123F2	full	36.4	37.8	33.6
123	11/20/2007	follow	phv_nov20_123F3	full	36.6	38.0	34.2
123	11/20/2007	follow	phv_nov20_123F4	full	36.7	38.1	34.3
123	11/20/2007	follow	phv_nov20_123F5	partial	36.6	37.9	34.0
123	11/29/2007	follow	Nov29_123F1	partial	79.5	87.6	68.1
123	12/4/2007	follow	dec4_123F2	full	51.7	78.4	35.0
123	12/4/2007	follow	dec4_123F3	full	37.0	38.3	34.7
123	12/4/2007	follow	dec4_123F4	parital	36.5	37.7	34.4
123	12/5/2007	follow	dec5_123F1	partial	88.8	91.9	83.8
123	12/5/2007	follow	dec5_123F2	full	60.7	83.8	41.6
123	12/5/2007	follow	dec5_123F3	full	37.1	41.9	34.2
123	12/5/2007	follow	dec5_123F4	full	36.8	38.1	34.4
123	9/24/2007	solo	Sept24_pseudo123S1	full	36.3	37.8	34.1
123	11/19/2007	solo	nov19_123S1	full	65.7	91.8	34.7
123	11/19/2007	solo	nov19_123S2	full	36.5	38.1	33.8
123	11/19/2007	solo	nov19_123S3	full	36.4	38.3	34.3
123	11/26/2007	solo	Nov26_123S1	full	57.9	85.9	34.2
123	11/19/2007	solo	nov19_123S4	full	36.6	38.3	34.1
123	11/26/2007	solo	nov26_123S2	full	36.9	38.5	34.4
123	11/26/2007	solo	Nov26_123S3	full	36.6	39.1	34.1
123	11/26/2007	solo	Nov26_123S4	partial	36.5	39.3	34.0
123	11/28/2007	solo	Nov28_123S1	partial	36.4	37.7	34.0
123	11/28/2007	solo	Nov28_123S2	partial	36.8	38.4	34.2
123	12/4/2007	solo	dec4_123S1	partial	84.7	91.9	78.4
12T/C	10/19/2007	solo	oct19_12TCs1	full	36.5	38.5	34.2
12T/C	10/19/2007	solo	Oct19_12TCs2	full	36.2	37.8	34.0
12T/C	10/19/2007	solo	Oct19_12TCs3	full	36.2	37.9	34.3
12T/C	10/19/2007	solo	Oct19_12TCS4	full	36.1	38.1	34.0
12T/C	10/19/2007	solo	Oct19_12TCS5	full	36.5	38.1	34.4
12T/C	10/19/2007	solo	Oct19_12TCS6	full	36.3	37.9	34.0
12T/C	10/24/2007	solo	Oct24_12partial	partial	83.6	90.7	73.5
12T/C	11/13/2007	solo	Nov13_12TC_Tst10	full			
12T/C	11/13/2007	solo	Nov13_12TC_Tst11	full			
12T/C	11/13/2007	solo	Nov13_12TC_tst14	full			
12T/C	11/13/2007	solo	Nov13_12TC_Tst15	full			
12T/C	11/16/2007	solo	phev_nov16_12TCs1 phev_nov16_12TCs1a	full	38.3	44.2	34.2
12T/C	11/16/2007	solo	phev_nov16_12TCs2	full	36.4	39.1	34.2
12T/C	11/16/2007	solo	phev_nov16_12TCs3	full	36.4	37.9	34.1
12WB	1/6/2008	follow	jan6_12WBF1	partial	74.4	92.6	50.5

Table A-3: continued.

Run Information					State of Battery Charge		
Route	Date	Follow or Solo	Data File Name	Full or Partial Run	Avg (%)	Max (%)	Min (%)
12WB	1/6/2008	follow	jan6_12wbF2	partial	38.0	50.4	34.4
12WB	1/6/2008	follow	jan6_12WBF3	partial	36.3	38.7	34.2
12WB	1/6/2008	na	jan6_12WBF4	na	37.3	39.0	35.6
12WB	10/18/2007	solo	Oct18_12WBS1	full	62.0	87.1	33.3
12WB	10/18/2007	solo	Oct18_12WBS2	full	36.2	37.8	33.9
12WB	10/18/2007	solo	Oct18_12WBS3	full	36.5	38.6	34.20
12WB	10/18/2007	solo	Oct18_12WBS4a & Oct18_12WBS4b	full	36.5	38.4	34.1
12WB	11/16/2007	solo	phev_nov16_12WBs4	full	36.4	38.6	34.2
Hwy	11/28/2007	solo	Nov28_Hwy1	full	82.7	88.3	76.4
Hwy	11/28/2007	solo	Nov28_hwy2	full	67.2	76.0	60.2
Hwy	11/28/2007	solo	Nov28_hwy3	full	53.7	60.2	48.4
Hwy	11/28/2007	solo	Nov28_hwy4	full	43.9	48.4	41.3
Hwy	11/28/2007	solo	NOv28_hwy5	full	42.5	44.6	38.1
Hwy	11/29/2007	solo	Nov29_Hwy1	full	41.6	44.5	34.9
Hwy	1/9/2008	solo	jan9_hwy1	full	41.9	44.6	34.5
Hwy	1/9/2008	solo	jan9_hwy2	full	43.1	44.7	39.0
Hwy	1/9/2008	solo	jan9_hwy3	full	42.5	44.7	37.5
Hwy	1/9/2008	solo	jan9_hwy4	full	42.8	44.6	39.8
Hwy	1/9/2008	solo	jan9_hwy5	full	42.2	44.5	39.4
Xfer	8/19/2007	solo	PHEV8-19-07 (XferA)	na	35.4	37.5	32.7
Xfer	10/18/2007	solo	Oct18_xferA	na	39.4	42.5	36.6
Xfer	10/19/2007	solo	Oct19_xferA	na	36.2	37.5	35.4
Xfer	10/19/2007	solo	oct19_xferB	na	35.5	36.6	34.0
Xfer	11/13/2007	solo	Nov12_xfera_tst12_NODLM	na			
Xfer	11/13/2007	solo	Nov13_xferb_tst13_NODLM	na			
Xfer	11/16/2007	solo	phev_nov16_xfera	na	36.0	37.2	34.2
Xfer	11/16/2007	solo	phev_nov16_xferb	na	36.6	37.6	34.9
Xfer	11/29/2007	solo	Nov29_xfer1	na	36.1	37.4	34.3
Xfer	11/29/2007	solo	Nov29_xfer2	na	36.4	37.5	34.9
Xfer	11/29/2007	solo	Nov29_xfer3 NO DLM	na			
xfer	12/5/2007	solo	dec5_xfer1	na	36.8	38.2	35.3
Xfer	1/6/2008	solo	jan6_xfera	na	35.9	37.4	34.4
Xfer	1/9/2008	solo	Jan9_xfera	na	36.3	37.7	34.2
Xfer	1/9/2008	solo	jan9_xferb	na	37.9	43.0	34.3
Xfer	9/11/2007	solo	Sept11_WnchstrLpF1&2 -xfera	na	38.1	44.8	34.2
Xfer	9/12/2007	solo	Sept12_109BothLpsS (XferA)	na	82.2	85.3	76.6
Xfer	9/10/2007	solo	Sept10_phev (XferA)	na	84.4	89.4	80.9
Xfer	9/10/2007	solo	Sept10_phevB (xferB)	na	36.0	37.5	34.2
				Total:			
				Mean:	43.3	48.1	38.4
				Standard Deviation:	14.2	18.6	11.4
				Minimum:	35.4	36.2	32.7
				Maximum:	88.8	92.6	84.7

Appendix B: Route maps and schedules for KCATA 109, 110, and 123 routes.

The following pages provide route maps and schedules for the KCATA transit routes designated as 109, 110, and 123. These schedules were current as of the time of PHEV Sprinter on-road sampling. The Kansas City Area Transit Authority provided all images (www.kcata.org).

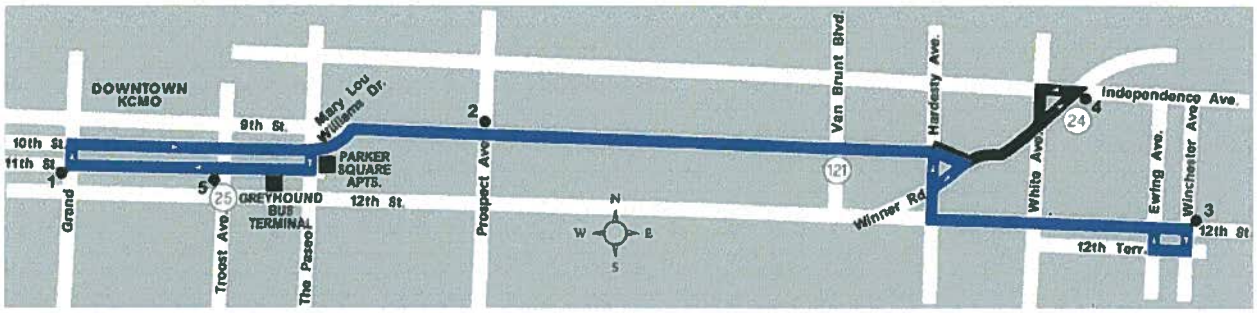

Figure B-1: Ninth Street (109) map, both Winner and Winchester loops (www.kcata.org).

Table B-1: Ninth Street (109) weekday schedule (www.kcata.org).

109-9th Street - *Monday through Friday*

Eastbound

	11th & Grand (1)	9th & Prospect (2)	12th & Winchester (3)	Independence Ave. & Winner Rd. (4)
AM	----	5:05	----	5:12
	----	5:21	5:30	----
	5:30	5:37	----	5:44
	5:50	5:58	6:08	----
	6:15	6:23	----	6:30
	6:40	6:48	6:58	----
	7:05	7:13	----	7:20
	7:30	7:38	7:49	----
	7:55	8:03	----	8:10
	8:20	8:28	8:39	----
	8:45	8:53	----	9:00
	9:10	9:18	9:28	----
	9:53	10:01	----	10:08
	10:30	10:38	----	10:45
	11:10	11:18	----	11:25
	11:50	11:58	----	12:05
PM	12:30	12:38	----	12:45
	1:10	1:18	1:27	----
	1:50	1:58	----	2:05
	2:30	2:38	2:48	----
	3:00	3:09	----	3:17
	3:25	3:34	----	3:42
	3:50	4:00	4:12	----
	4:15	4:25	----	4:34
	4:40	4:50	5:03	----
	5:05	5:15	----	5:24
	5:30	5:40	5:52	----
	5:50	5:59	----	6:07
	6:15	6:23	6:34	----
	6:40	6:48	----	6:56

Westbound

	Independence Ave. & Winner Rd. (4)	12th & Winchester (3)	9th & Prospect (2)	11th & Grand (1)
AM	5:15	----	5:23	5:30
	----	5:33	5:43	5:50
	5:58	----	6:06	6:15
	----	6:19	6:30	6:40
	6:47	----	6:55	7:05
	----	7:07	7:20	7:30
	7:37	----	7:45	7:55
	----	7:57	8:10	8:20
	8:29	----	8:37	8:45
	----	8:50	9:02	9:10
	9:19	----	9:27	9:35
	----	9:34	9:45	9:53
	10:14	----	10:22	10:30
	10:54	----	11:02	11:10
	11:34	----	11:42	11:50
PM	12:14	----	12:22	12:30
	12:54	----	1:02	1:10
	----	1:32	1:42	1:50
	2:14	----	2:22	2:30
	----	3:06	3:17	3:25
	3:34	----	3:42	3:50
	3:58	----	4:06	4:15
	----	4:20	4:31	4:40
	4:48	----	4:56	5:05
	----	5:10	5:21	5:30
	5:34	----	5:42	5:50
	----	5:56	6:07	6:15
	6:24	----	6:32	6:40
	----	6:39	6:49	----
	7:01	----	7:08	----

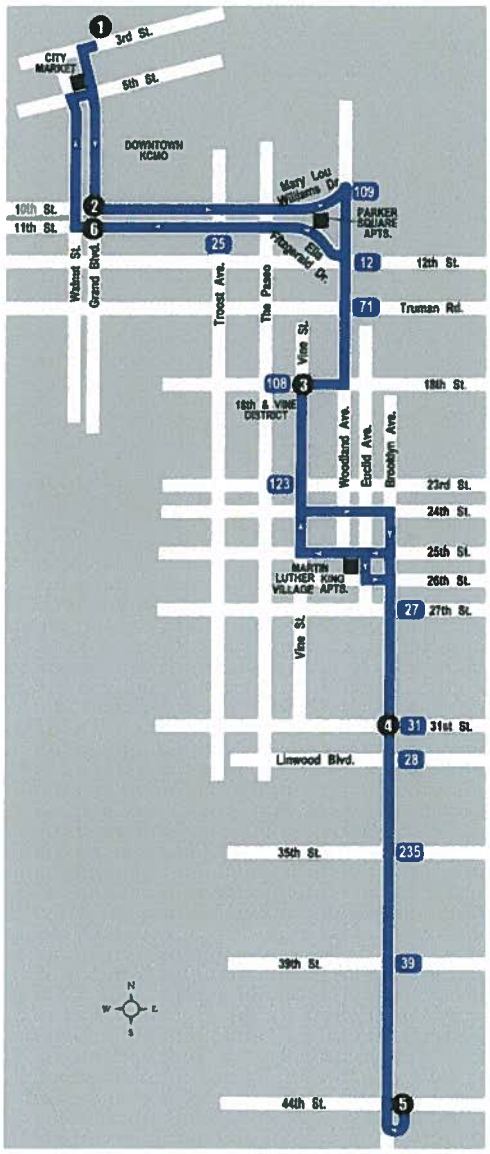

Figure B-2: 44th and Brooklyn (110) map (www.kcata.org).

Table B-2: Ninth Street (110) weekday schedule (www.kcata.org).

110-Woodland/Brooklyn - *Monday through Friday*

Southbound	3rd & Grand	10th & Grand	18th & Vine	31st & Brooklyn	44th & Brooklyn
	1	2	3	4	5
AM	----	----	4:54	5:01	5:07
	5:35	5:39	5:46	5:53	5:59
	6:31	6:36	6:44	6:51	6:57
	7:30	7:35	7:43	7:50	7:57
	8:30	8:35	8:43	8:50	8:57
	9:30	9:35	9:43	9:50	9:57
	10:30	10:35	10:43	10:50	10:57
	11:30	11:35	11:43	11:50	11:57
PM	12:30	12:35	12:44	12:51	12:58
	1:30	1:35	1:44	1:51	1:58
	2:30	2:35	2:44	2:51	2:58
	3:40	3:45	3:54	4:01	4:08
	4:45	4:50	4:59	5:06	5:13
	5:45	5:50	5:59	6:06	6:13
	6:45	6:50	6:58	7:05	7:11

Northbound	44th & Brooklyn	31st & Brooklyn	18th & Vine	11th & Grand	3rd & Grand
	5	4	3	6	1
AM	5:10	5:16	5:22	5:29	5:33
	6:03	6:10	6:17	6:25	6:30
	7:00	7:07	7:14	7:24	7:29
	8:02	8:08	8:15	8:24	8:29
	9:02	9:08	9:15	9:24	9:29
	10:02	10:08	10:15	10:24	10:29
	11:02	11:08	11:15	11:24	11:29
PM	12:02	12:08	12:15	12:24	12:29
	1:03	1:09	1:16	1:25	1:30
	2:03	2:09	2:16	2:25	2:30
	3:12	3:18	3:25	3:34	3:39
	4:12	4:18	4:25	4:34	4:39
	5:17	5:23	5:30	5:39	5:44
	6:17	6:23	6:29	6:37	6:42
	7:16	7:22	7:28	----	----

Figure B-3: 23rd Street (123) map (www.kcata.org).

Table B-3: 23rd Street (123) weekday schedule (www.kcata.org).

123-23rd Street - *Monday through Friday*

Westbound

	Legend	Park Tower	23rd & Prospect	19th & Troost	23rd & Summit	Pershing & Grand	Union Station
		1	2	3	4	5	6
AM		5:13	5:21	5:26	5:32	5:37	5:41
		5:48	5:56	6:01	6:07	6:12	6:16
		6:23	6:31	6:36	6:42	6:47	6:51
		6:58	7:08	7:13	7:21	7:26	7:30
		7:36	7:46	7:51	7:59	8:04	8:08
		8:11	8:21	8:26	8:34	8:39	8:43
		8:45	8:55	8:59	9:07	9:12	9:16
		9:20	9:30	9:34	9:42	9:47	9:51
		10:24	10:34	10:38	10:46	10:51	10:55
		11:29	11:39	11:43	11:51	11:56	12:00
PM		12:34	12:44	12:48	12:56	1:01	1:05
		1:39	1:49	1:53	2:01	2:06	2:10
		2:44	2:53	2:57	3:05	3:10	3:14
		3:49	3:58	4:02	4:10	4:15	4:19
		4:24	4:34	4:39	4:47	4:52	4:57
		4:59	5:09	5:14	4:22	5:27	5:32
		5:36	5:46	5:51	5:59	6:04	6:09
		6:10	6:20	6:25	6:33	6:38	6:43
		6:45	6:55	6:59	----	----	----

123-23rd Street - *Monday through Friday*

Eastbound

	Legend	Union Station	23rd & Summit	19th & Troost	23rd & Prospect	Park Tower
		6	4	3	2	1
AM		6:00	6:03	6:10	6:15	6:23
		6:35	6:38	6:45	6:50	6:58
		7:10	7:13	7:21	7:26	7:36
		7:45	7:48	7:56	8:01	8:11
		8:20	8:23	8:31	8:36	8:45
		8:55	8:58	9:06	9:11	9:20
		10:00	10:03	10:10	10:15	10:24
		11:05	11:08	11:15	11:20	11:29
PM		12:10	12:13	12:20	12:25	12:34
		1:15	1:18	1:25	1:30	1:39
		2:20	2:23	2:30	2:34	2:44
		3:25	3:28	3:35	3:39	3:49
		4:00	4:03	4:10	4:14	4:24
		4:35	4:38	4:45	4:49	4:59
		5:10	5:13	5:21	5:26	5:36
		5:45	5:48	5:56	6:01	6:10
		6:20	6:23	6:31	6:36	6:45
		6:55	6:58	7:05	----	----

Appendix C: Ambient Temperature and Auxiliary System Use.

The following pages provide data summaries for the sample run-based data used during the ambient temperature and auxiliary system use investigation. Complete, second-by-second data was submitted digitally. The file names included here reference the file names in the bulk data submission.

Table C-1: Compiled data for the 10th Street link, ambient conditions and velocity during no auxiliary system use, according to data file.

File	Route	Auxilliary System	Average Temp (F)	Average SOC*	Distance (m)	Velocity (km/h)			
						Average	Mean	Median	Max
JAN9_109S7	109	None	44	36.7	726.3	27.0	27.5	35.4	52.8
JAN9_109S5	109	None	47	37.4	719.4	41.1	41.2	46.0	51.3
JAN9_109S4	109	None	45	37.4	714.2	44.3	45.2	45.0	49.6
JAN9_109S8	109	None	44	34.6	573.0	35.0	35.8	45.1	51.1
NOV29_110S2	110	None	46	34.7	731.9	45.4	46.2	46.2	49.1
NOV29_110S3	110	None	50	35.4	735.4	49.0	49.9	49.1	57.3
NOV29_110S4	110	None	50	36.2	739.9	33.3	33.9	44.6	49.7

*SOC: State of Charge

Table C-2: Compiled emissions data for the 10th Street link, during no auxiliary system use, according to data file.

File	Route	Auxilliary System	Total Pollutant Emission per Distance Traveled (g/km)					
			CO_2	CO	NO	NO_2	NOx	HC
JAN9_109S7	109	None	500.3	0.254	5.811	0.238	6.049	0.02670
JAN9_109S5	109	None	212.6	0.072	2.743	0.158	2.901	0.00979
JAN9_109S4	109	None	132.1	0.082	1.319	0.117	1.436	0.00468
JAN9_109S8	109	None	47.5	0.100	0.453	0.038	0.491	0.00269
NOV29_110S2	110	None	206.1	0.110	2.028	0.229	2.258	0.00540
NOV29_110S3	110	None	37.2	0.039	0.262	0.051	0.313	0.00072
NOV29_110S4	110	None	0.0	0.000	0.000	0.000	0.000	0.00000

Table C-3: Compiled Total Power Output data for the 10th Street link, during no auxiliary system use, according to data file.

File	Route	Total Power			
		Total (W/kg/s)	Mean (W/kg/s)	Median (W/kg/s)	Max (W/kg/s)
JAN9_109S7	109	428.8	4.42	1.82	18.57
JAN9_109S5	109	233.5	3.49	0.00	17.20
JAN9_109S4	109	182.8	3.14	0.00	15.43
JAN9_109S8	109	117.0	1.98	1.14	11.11
NOV29_110S2	110	224.0	3.86	0.40	16.83
NOV29_110S3	110	181.3	3.36	0.89	11.94
NOV29_110S4	110	210.3	2.63	0.00	15.90

Table C-4: Compiled dICE Power Output data for the 10th Street link, during no auxiliary system use, according to data file.

File	Route	Internal Combustion Engine Power (W/kg/s)			
		Total (W/kg/s)	Mean (W/kg/s)	Median (W/kg/s)	Max (W/kg/s)
JAN9_109S7	109	428.8	4.42	1.82	18.57
JAN9_109S5	109	189.8	2.97	0.00	17.20
JAN9_109S4	109	121.2	2.09	0.00	15.43
JAN9_109S8	109	11.0	0.19	0.00	5.07
NOV29_110S2	110	167.9	2.90	0.10	16.83
NOV29_110S3	110	22.0	0.41	0.00	11.09
NOV29_110S4	110	0.0	0.00	0.00	0.00

Table C-5: Compiled EM Power Output data for the 10th Street link, during no auxiliary system use, according to data file.

File	Route	Electric Motor Power Total (W/kg/s)	Mean (W/kg/s)	Median (W/kg/s)	Max (W/kg/s)
JAN9_109S7	109	0.0	0.00	0.00	0.00
JAN9_109S5	109	33.7	0.53	0.00	12.14
JAN9_109S4	109	61.6	1.06	0.00	11.52
JAN9_109S8	109	106.0	1.80	0.00	11.11
NOV29_110S2	110	56.0	0.97	0.00	7.58
NOV29_110S3	110	159.3	2.95	0.07	11.94
NOV29_110S4	110	210.3	2.63	0.00	15.90

Table C-6: Compiled velocity and ambient conditions data for the 11th Street link, during no auxiliary system use, according to data file.

File	Route	Average Temp (F)	Average SOC*	Distance (m)	Velocity (km/h)			
					Average	Mean	Median	Max
Oct19_TCs1	12	61	34.7	257.4	35.6	34.3	41.6	43.4
phev_nov16_12TCs1	12	58	43.1	699.5	24.9	24.7	29.4	41.6
phev_nov16_12TCs2	12	60	35.5	701.8	28.4	28.4	32.7	47.6
phve_nov16_12TCs3	12	61	36.1	709.2	29.3	29.0	35.6	46.5
JAN9_109S4	109	45	37.6	729.8	41.1	41.3	41.5	53.6
JAN9_109S5	109	47	36.4	737.7	34.9	34.5	42.6	50.9
JAN9_109S7	109	44	36.2	736.2	24.5	24.7	29.7	50.1
JAN9_109S8	109	44	37.1	736.0	31.5	31.8	37.7	49.2
NOV29_110S2	110	46	35.6	666.7	24.5	24.5	29.2	43.6
NOV29_110S3	110	50	36.1	712.7	26.7	26.7	26.5	53.3
NOV29_110S4	110	50	35.7	715.2	20.3	20.3	19.3	47.9

*SOC: State of Charge

Table C-7: Compiled emissions data for the 11th Street link, during no auxiliary system use, according to data file.

File	Route	Auxilliary System	Total Pollutant Emission per Distance Traveled (g/km)					
			CO_2	CO	NO	NO_2	NOx	HC
Oct19_TCs1	12	None	214.7	1.368	1.489	0.008	1.498	0.14468
phev_nov16_12TCs1	12	None	442.6	1.635	3.396	0.119	3.515	0.18112
phev_nov16_12TCs2	12	None	0.0	0.000	0.000	0.000	0.000	0.00000
phve_nov16_12TCs3	12	None	267.8	0.490	2.045	0.175	2.220	0.01318
JAN9_109S4	109	None	490.3	0.157	4.709	0.256	4.964	0.03698
JAN9_109S5	109	None	473.6	0.331	4.578	0.194	4.772	0.06688
JAN9_109S7	109	None	665.7	0.268	6.952	0.200	7.153	0.03784
JAN9_109S8	109	None	458.4	0.210	4.672	0.087	4.758	0.02598
NOV29_110S2	110	None	80.6	0.086	0.667	0.041	0.708	0.00372
NOV29_110S3	110	None	389.9	0.707	3.475	0.110	3.585	0.03134
NOV29_110S4	110	None	374.1	0.288	3.345	0.180	3.525	0.01988

Table C8: Compiled Total Power Output data for the 11th Street link, during no auxiliary system use, according to data file.

File	Route	Total Power (W/kg/s)			
		Total	Mean	Median	Max
Oct19_TCs1	12	153.1	5.67	6.38	16.39
phev_nov16_12TCs1	12	429.8	4.21	1.97	19.86
phev_nov16_12TCs2	12	559.9	6.22	1.89	27.12
phve_nov16_12TCs3	12	452.1	5.14	1.57	23.39
JAN9_109S4	109	463.9	7.26	0.58	28.02
JAN9_109S5	109	571.2	7.42	3.81	23.79
JAN9_109S7	109	613.1	5.68	1.81	23.43
JAN9_109S8	109	557.2	6.63	2.25	23.67
NOV29_110S2	110	428.2	4.37	0.41	15.58
NOV29_110S3	110	541.4	5.64	0.39	27.90
NOV29_110S4	110	571.1	4.50	1.05	23.40

Table C-9: Compiled dICE Power Output data for the 11th Street link, during no auxiliary system use, according to data file.

File	Route	Internal Combustion Engine Power (W/kg/s)			
		Total	Mean	Median	Max
Oct19_TCs1	12	49.8	1.85	0.00	11.56
phev_nov16_12TCs1	12	298.1	2.92	0.00	18.25
phev_nov16_12TCs2	12	410.4	4.56	1.68	27.12
phve_nov16_12TCs3	12	243.4	2.77	0.00	23.39
JAN9_109S4	109	437.6	6.84	0.00	28.02
JAN9_109S5	109	430.6	2.97	0.00	23.79
JAN9_109S7	109	569.9	5.28	1.81	23.43
JAN9_109S8	109	420.4	5.01	0.00	23.68
NOV29_110S2	110	53.2	0.54	0.00	14.38
NOV29_110S3	110	333.5	3.47	0.00	27.90
NOV29_110S4	110	306.5	2.41	0.00	23.40

Table C-10: Compiled EM Power Output data for the 11th Street link, during no auxiliary system use, according to data file.

File	Route	Electric Motor Power (W/kg/s)			
		Total	Mean	Median	Max
Oct19_TCs1	12	103.2	3.82	0.00	16.39
phev_nov16_12TCs1	12	131.7	1.29	0.00	11.60
phev_nov16_12TCs2	12	149.5	1.66	0.00	19.30
phve_nov16_12TCs3	12	208.8	2.37	0.00	14.39
JAN9_109S4	109	26.3	0.42	0.00	6.08
JAN9_109S5	109	140.6	1.83	0.00	19.68
JAN9_109S7	109	43.2	0.40	0.00	11.39
JAN9_109S8	109	136.7	1.63	0.00	11.58
NOV29_110S2	110	375.0	3.83	0.38	15.58
NOV29_110S3	110	207.9	2.17	0.00	18.86
NOV29_110S4	110	264.6	2.08	0.00	17.09

Table C-11: Compiled ambient conditions and velocity data for the 10th Street link, with AC use, according to data file.

File	Route	Auxilliary System	Average Temp (F)	Average SOC*	Distance (m)	Velocity (km/h)			
						Average	Mean	Median	Max
110_Sep24S1	110	AC	90	36.0	721.3	26.8	27.2	41.0	52.0
109_Sep10Rn1	109	AC	77	36.8	726.1	38.4	39.1	46.0	53.7
109_Sep10Rn2	109	AC	79	36.5	724.3	16.1	16.4	8.1	48.4
109_Sep13Rn3	109	AC	102	37.2	733.7	50.8	51.7	51.7	56.5
109_Aug19S2	109	AC	89	34.8	726.8	18.4	18.7	7.2	53.7
109_Aug19S1	109	AC	90	35.9	732.5	26.9	27.3	38.4	51.6
109_Aug19S3	109	AC	90	37.1	732.9	45.5	46.2	45.2	51.9
109_Aug19S4	109	AC	89	36.0	725.1	43.5	44.3	48.3	53.3

*SOC: State of Charge

Table C-12: Compiled emissions data for the 10th Street link, with AC use, according to data file.

File	Route	Auxilliary System	Total Pollutant Emission per Distance Traveled (g/km)					
			CO_2	CO	NO	NO_2	NOx	HC
110_Sep24S1	110	AC	488.4	0.109	5.456	0.426	5.882	0.02842
109_Sep10Rn1	109	AC	99.4	0.000	1.113	0.150	1.263	0.00168
109_Sep10Rn2	109	AC	846.7	0.320	7.637	1.883	9.520	0.00489
109_Sep13Rn3	109	AC	0.0	0.000	0.000	0.000	0.000	0.00000
109_Aug19S2	109	AC	489.5	0.649	2.899	1.065	3.964	0.00665
109_Aug19S1	109	AC	522.0	0.340	3.576	1.442	5.018	0.01315
109_Aug19S3	109	AC	0.0	0.000	0.000	0.000	0.000	0.00000
109_Aug19S4	109	AC	379.2	0.375	2.703	0.772	3.475	0.00011

Table C-13: Compiled Total Power Output data for the 10th Street link, with AC use, according to data file.

File	Route	Total Power (W/kg/s)			
		Total	Mean	Median	Max
110_Sep24S1	110	399.1	4.12	1.89	14.49
109_Sep10Rn1	109	270.8	3.98	0.83	14.92
109_Sep10Rn2	109	691.5	4.27	1.88	20.04
109_Sep13Rn3	109	265.8	5.11	7.64	16.36
109_Aug19S2	109	557.3	3.93	1.78	25.40
109_Aug19S1	109	445.8	4.55	1.85	23.26
109_Aug19S3	109	113.3	1.95	0.00	11.45
109_Aug19S4	109	327.3	5.46	6.09	20.35

Table C-14: Compiled dICE Power Output data for the 10th Street link, with AC use, according to data file.

File	Route	Internal Combustion Engine Power (W/kg/s)			
		Total	Mean	Median	Max
110_Sep24S1	110	399.1	4.12	1.89	14.49
109_Sep10Rn1	109	94.8	1.39	0.00	14.66
109_Sep10Rn2	109	691.3	4.27	1.88	20.04
109_Sep13Rn3	109	265.8	5.11	7.64	16.36
109_Aug19S2	109	415.4	2.93	0.04	25.40
109_Aug19S1	109	445.7	4.55	1.85	23.53
109_Aug19S3	109	0.0	0.00	0.00	0.00
109_Aug19S4	109	327.3	5.46	6.09	20.35

Table C-15: Compiled EM Power Output data for the 10th Street link, with AC use, according to data file.

File	Route	Electric Motor Power (Wk/g/s)			
		Total	Mean	Median	Max
110_Sep24S1	110	0.0	0.00	0.00	0.00
109_Sep10Rn1	109	176.0	0.47	0.31	14.29
109_Sep10Rn2	109	0.2	0.00	0.00	0.06
109_Sep13Rn3	109	0.0	0.00	0.00	0.00
109_Aug19S2	109	141.9	1.00	0.00	16.86
109_Aug19S1	109	0.0	0.00	0.00	0.04
109_Aug19S3	109	113.3	1.95	0.00	11.45
109_Aug19S4	109	0.0	0.00	0.00	0.00

Table C-16: Compiled ambient conditions and velocity data for the 11th Street link, with AC use, according to data file.

File	Route	Auxilliary System	Average Temp (F)	Average SOC*	Distance (m)	Velocity (km/h)			
						Average	Mean	Median	Max
110_Sep24S1	110	AC	90	35.3	670.1	34.0	34.0	43.7	48.0
12_Oct19S6	12	AC	69	34.9	698.1	31.4	31.4	40.3	51.7
12_Oct19S5	12	AC	70	35.9	701.8	31.6	31.6	36.7	49.2
12_Oct19S4	12	AC	69	35.2	701.0	21.8	21.8	22.7	47.0
12_Oct19S3	12	AC	68	34.9	699.4	28.9	28.9	38.5	44.8
12_Sep24TC&WBB	12	AC	89	35.2	725.5	25.6	26.0	32.2	45.9
12_Sep24TC&WBA	12	AC	89	35.2	699.7	21.0	21.0	19.7	44.5
12_Oct19S2	12	AC	65	35.6	702.2	33.7	33.7	42.6	50.4
109_Sep10Rn1	109	AC	77	35.3	737.7	41.5	42.2	49.0	51.3
109_Sep10Rn2	109	AC	79	37.1	735.8	15.9	16.0	15.0	41.7
109_Sep13Rn3	109	AC	102	36.1	736.8	35.8	36.3	40.5	49.9
109_Sep12S2	109	AC	69	36.9	737.3	39.0	39.7	44.0	48.5
109_Aug19S2	109	AC	89	36.5	732.7	39.4	39.9	43.6	50.9
109_Aug19S1	109	AC	90	35.6	732.9	26.6	26.9	33.0	43.4
109_Aug19S3	109	AC	90	37.1	738.4	25.3	25.6	29.3	49.9
109_Aug19S4	109	AC	89	37.3	733.5	29.3	29.7	34.4	52.4

*SOC: State of Charge

Table C-17: Compiled emissions data for the 11th Street link, with AC use, according to data file.

File	Route	Auxilliary System	Total Pollutant Emission per Distance Traveled (g/km)					
			CO_2	CO	NO	NO_2	NOx	HC
110_Sep24S1	110	AC	165.4	0.808	1.252	0.021	1.272	0.05430
12_Oct19S6	12	AC	321.5	0.090	2.694	0.109	2.802	0.01591
12_Oct19S5	12	AC	363.9	0.174	3.260	0.146	3.405	0.01651
12_Oct19S4	12	AC	324.6	0.224	2.761	0.242	3.003	0.01090
12_Oct19S3	12	AC	544.9	0.653	5.295	0.129	5.424	0.03509
12_Sep24TC&WBB	12	AC	678.5	0.398	6.233	0.801	7.034	0.03256
12_Sep24TC&WBA	12	AC	668.1	3.080	5.084	0.189	5.273	0.09037
12_Oct19S2	12	AC	3.6	0.024	0.014	0.007	0.021	0.00036
109_Sep10Rn1	109	AC	34.4	0.013	0.099	0.014	0.114	0.00075
109_Sep10Rn2	109	AC	591.9	0.224	5.433	1.128	6.560	0.00574
109_Sep13Rn3	109	AC	0.0	0.000	0.000	0.000	0.000	0.00000
109_Sep12S2	109	AC	450.9	0.406	4.206	0.268	4.474	0.02976
109_Aug19S2	109	AC	607.4	0.437	4.217	1.163	5.380	0.01404
109_Aug19S1	109	AC	779.6	0.363	5.652	2.197	7.850	0.02204
109_Aug19S3	109	AC	818.4	0.637	5.906	1.921	7.827	0.01044
109_Aug19S4	109	AC	526.3	0.443	3.983	0.872	4.854	0.00549

Table C-18: Compiled Total Power Output data for the 11th Street link, with AC use, according to data file.

File	Route	Total Power (W/kg/s)			
		Total	Mean	Median	Max
110_Sep24S1	110	372.0	5.24	1.49	19.90
12_Oct19S6	12	443.0	5.54	0.51	28.36
12_Oct19S5	12	473.1	5.91	1.47	24.72
12_Oct19S4	12	479.6	4.14	0.46	26.17
12_Oct19S3	12	490.6	5.64	0.42	26.04
12_Sep24TC&WBB	12	630.1	6.18	1.89	25.66
12_Sep24TC&WBA	12	610.1	5.08	1.79	24.68
12_Oct19S2	12	329.7	4.40	0.44	18.74
109_Sep10Rn1	109	383.3	5.99	5.47	15.86
109_Sep10Rn2	109	607.9	3.64	1.87	19.50
109_Sep13Rn3	109	700.3	9.46	9.75	26.53
109_Sep12S2	109	529.1	7.78	6.00	26.67
109_Aug19S2	109	543.7	8.12	5.63	24.71
109_Aug19S1	109	668.2	6.75	5.90	22.51
109_Aug19S3	109	727.3	6.93	1.91	28.74
109_Aug19S4	109	615.7	6.84	1.75	23.68

Table C-19: Compiled dICE Power Output data for the 11th Street link, with AC use, according to data file.

File	Route	Internal Combustion Engine Power (W/kg/s)			
		Total	Mean	Median	Max
110_Sep24S1	110	113.8	1.60	0.00	14.46
12_Oct19S6	12	273.7	3.42	0.00	28.36
12_Oct19S5	12	316.8	3.96	0.00	24.72
12_Oct19S4	12	272.2	2.35	0.00	26.17
12_Oct19S3	12	474.0	5.45	0.00	26.04
12_Sep24TC&WBB	12	589.2	5.78	1.88	25.66
12_Sep24TC&WBA	12	513.4	4.28	1.40	24.68
12_Oct19S2	12	-13.4	-0.18	0.00	0.00
109_Sep10Rn1	109	40.9	0.64	0.00	14.02
109_Sep10Rn2	109	512.3	3.07	1.18	19.50
109_Sep13Rn3	109	583.5	7.88	6.55	23.55
109_Sep12S2	109	402.4	5.92	1.09	23.13
109_Aug19S2	109	543.7	8.12	5.63	24.71
109_Aug19S1	109	668.2	6.75	5.89	22.51
109_Aug19S3	109	727.2	6.93	1.91	28.74
109_Aug19S4	109	495.1	5.50	0.00	23.68

Table C-20: Compiled EM Power Output data for the 11th Street link, with AC use, according to data file.

File	Route	Electric Motor Power (W/kg/s)			
		Total	Mean	Median	Max
110_Sep24S1	110	258.8	3.64	0.00	16.41
12_Oct19S6	12	169.3	2.12	0.00	17.62
12_Oct19S5	12	156.2	1.95	0.00	16.67
12_Oct19S4	12	207.4	1.79	0.00	16.45
12_Oct19S3	12	16.6	0.19	0.00	3.45
12_Sep24TC&WBB	12	41.0	0.40	0.00	11.10
12_Sep24TC&WBA	12	96.7	0.81	0.00	9.24
12_Oct19S2	12	343.1	4.58	0.44	18.74
109_Sep10Rn1	109	342.4	5.35	3.62	12.77
109_Sep10Rn2	109	95.7	0.57	0.00	8.06
109_Sep13Rn3	109	116.8	1.58	0.00	18.45
109_Sep12S2	109	126.7	1.86	6.00	19.84
109_Aug19S2	109	0.0	0.00	0.00	0.00
109_Aug19S1	109	0.1	0.00	0.00	0.05
109_Aug19S3	109	0.2	0.00	0.00	0.05
109_Aug19S4	109	120.6	1.34	0.00	15.47

Table C-21: Compiled ambient conditions and velocity data for the 10th Street link, with heater use, according to data file.

File	Route	Auxilliary System	Average Temp (F)	Average SOC*	Distance (m)	Velocity (km/h) Average	Mean	Median	Max
110_DEC20S3	110	Htr	35.88	49.0	720.6	27.6	28.1	36.1	45.2
110_DEC20S5	110	Htr	34.854	51.0	709.7	41.9	42.6	47.3	53.4
110_DEC20S6	110	Htr	37.332	51.0	725.3	27.5	28.0	36.1	55.6

*SOC: State of Charge

Table C-22: Compiled emissions data for the 10th Street link, with AC use, according to data file.

File	Route	Auxilliary System	Total Pollutant Emission per Distance Traveled (g/km) CO_2	CO	NO	NO_2	NOx	HC
110_DEC20S3	110	Htr	0.0	0.000	0.000	0.001	0.001	0.00000
110_DEC20S5	110	Htr	0.0	0.001	0.000	0.000	0.000	0.00000
110_DEC20S6	110	Htr	181.3	0.061	2.121	0.146	2.268	0.00732

Table C-23: Compiled Total Power Output data for the 10th Street link, with AC use, according to data file.

File	Route	Total Power (W/kg/s) Total	Mean	Median	Max
110_DEC20S3	110	157.5	1.68	0.30	11.15
110_DEC20S5	110	185.4	3.04	0.00	17.16
110_DEC20S6	110	239.5	2.52	0.33	14.95

Table C-24: Compiled dICE Power Output data for the 10th Street link, with AC use, according to data file.

File	Route	Internal Combustion Engine Power (W/kg/s)			
		Total	Mean	Median	Max
110_DEC20S3	110	0.0	0.00	0.00	0.00
110_DEC20S5	110	0.0	0.00	0.00	0.00
110_DEC20S6	110	160.2	1.69	0.00	14.95

Table C-25: Compiled EM Power Output data for the 10th Street link, with AC use, according to data file.

File	Route	Electric Motor Power (W/kg/s)			
		Total	Mean	Median	Max
110_DEC20S3	110	157.5	1.68	0.30	11.15
110_DEC20S5	110	185.4	3.04	0.00	17.16
110_DEC20S6	110	79.4	2.03	0.00	12.49

Table C-26: Compiled ambient conditions and velocity data for the 11th Street link, with heater use, according to data file.

File	Route	Auxilliary System	Average Temp (F)	Average SOC*	Distance (m)	Velocity (km/h)			
						Average	Mean	Median	Max
110_DEC20S3	110	Htr	49	35.8	732.4	29.0	29.4	36.8	52.4
110_DEC20S5	110	Htr	51	36.7	728.1	30.5	30.9	36.8	52.2
110_DEC20S6	110	Htr	51	37.0	731.8	46.2	46.9	46.6	53.7

*SOC: State of Charge

Table C-27: Compiled emissions data for the 11th Street link, with heater use, according to data file.

File	Route	Auxilliary System	Total Pollutant Emission per Distance Traveled (g/km)					
			CO_2	CO	NO	NO_2	NOx	HC
110_DEC20S3	110	Htr	101.1	0.019	1.026	0.098	1.124	0.00601
110_DEC20S5	110	Htr	616.8	0.392	5.576	0.432	6.009	0.04240
110_DEC20S6	110	Htr	322.1	0.163	3.144	0.201	3.345	0.01626

Table C-28: Compiled Total Power Output data for the 11th Street link, with heater use, according to data file.

File	Route	Total Power (W/kg/s)			
		Total	Mean	Median	Max
110_DEC20S3	110	470.0	5.17	0.40	23.14
110_DEC20S5	110	674.2	7.84	4.97	25.26
110_DEC20S6	110	416.5	7.31	7.21	24.10

Table C-29: Compiled dICE Power Output data for the 11th Street link, with heater use, according to data file.

File	Route	Internal Combustion Engine Power (W/kg/s)			
		Total	Mean	Median	Max
110_DEC20S3	110	110.8	1.22	0.00	23.14
110_DEC20S5	110	556.8	6.48	1.46	24.69
110_DEC20S6	110	300.6	5.27	0.15	24.10

Table C-30: Compiled EM Power Output data for the 11th Street link, with heater use, according to data file.

File	Route	Electric Motor Power (W/kg/s)			
		Total	Mean	Median	Max
110_DEC20S3	110	359.2	3.95	0.36	16.45
110_DEC20S5	110	117.4	1.37	0.00	20.21
110_DEC20S6	110	115.9	2.03	0.00	12.49

Appendix D: Vehicle Specific Power Analysis

The following tables provide PHEV Sprinter descriptive data summarized according to VSP bin and driving mode as defined in Chapter 6. Statistical results achieved from ANOVA and Kruskal-Wallis analyses accompany their respective tables.

Table D-1: Descriptive statistics of dICE power output during charge-sustaining operation according to VSP Bin.

Internal Combustion Engine Power (W/kg/s)								
VSP Bin	N	Mean	St Dev	Min	1st Quart.	Median	3rd Quart.	Max
1	29028	0.832	2.720	-3.724	0.000	0.000	1.720	24.446
2	5406	3.528	4.938	-2.797	0.000	0.000	7.899	23.037
3	5071	5.452	5.784	-3.511	0.000	5.367	10.183	31.782
4	4563	6.968	6.318	-3.122	0.000	8.282	11.866	28.243
5	4149	8.246	7.087	-4.346	0.000	9.597	14.173	29.921
6	3408	9.376	7.771	-3.856	0.000	10.994	15.640	31.383
7	3434	11.972	8.196	-4.862	2.383	13.878	18.244	29.808
8	2956	16.367	8.473	-3.825	13.473	18.283	22.292	31.779
All	58015							
ANOVA, P-Value:		**0.0000**						
Kruskal-Wallis, P-Value:		**0.0000**						

Table D-2: Descriptive statistics of EM power output during charge-sustaining operation according to VSP Bin.

Electric Motor Power Output (W/kg/s)								
VSP Bin	N	Mean	St Dev	Min	1st Quart.	Median	3rd Quart.	Max
1	29028	0.240	1.023	0.000	0.000	0.000	0.024	19.303
2	5406	1.000	2.275	0.000	0.000	0.000	0.358	15.272
3	5071	1.602	3.033	0.000	0.000	0.000	2.089	16.046
4	4563	2.187	3.808	0.000	0.000	0.000	3.818	19.965
5	4149	3.062	4.753	0.000	0.000	0.000	7.093	21.522
6	3408	3.803	5.541	0.000	0.000	0.000	9.789	21.140
7	3434	3.539	6.008	0.000	0.000	0.000	8.018	21.228
8	2956	2.302	5.571	0.000	0.000	0.000	0.000	21.722
All	58015							
ANOVA, P-Value:		**0.0000**						
Kruskal-Wallis, P-Value:		**0.0000**						

Table D-3: Descriptive statistics of total power output during charge-sustaining operation according to VSP Bin.

Total Power Output (W/kg/s)								
VSP Bin	N	Mean	St Dev	Min	1st Quart.	Median	3rd Quart.	Max
1	29028	1.071	2.839	-3.724	0.000	0.339	1.797	24.446
2	5406	4.528	4.744	-2.797	0.164	3.693	8.386	23.037
3	5071	7.054	5.027	-3.511	3.117	7.587	10.576	31.782
4	4563	9.155	4.935	-2.925	6.244	9.563	12.220	28.243
5	4149	11.309	4.867	-3.033	8.787	11.185	14.556	31.968
6	3408	13.179	4.833	-2.346	10.520	12.949	16.158	31.383
7	3434	15.512	4.943	-2.758	12.430	15.246	18.917	33.935
8	2956	18.669	5.831	-1.754	15.474	18.983	22.746	33.659
All	58015							
ANOVA, P-Value:		**0.0000**						
Kruskal-Wallis, P-Value:		**0.0000**						

Table D-4: Descriptive statistics of fuel use during charge-sustaining operation according to VSP Bin.

Fuel (gal/s)								
VSP Bin	N	Mean	St Dev	Min	1st Quart.	Median	3rd Quart.	Max
1	29028	1.06E-04	2.10E-04	0.00E+00	0.00E+00	1.40E-05	1.61E-04	2.08E-03
2	5406	3.07E-04	3.68E-04	0.00E+00	0.00E+00	1.43E-04	5.69E-04	2.10E-03
3	5071	4.21E-04	4.21E-04	0.00E+00	1.00E-06	3.65E-04	7.38E-04	2.07E-03
4	4563	5.30E-04	4.68E-04	0.00E+00	1.00E-06	5.67E-04	8.65E-04	2.12E-03
5	4149	6.11E-04	5.16E-04	0.00E+00	1.00E-06	6.75E-04	1.01E-03	2.21E-03
6	3408	6.96E-04	5.69E-04	0.00E+00	7.00E-06	7.73E-04	1.14E-03	2.33E-03
7	3434	8.85E-04	6.11E-04	0.00E+00	2.90E-04	9.95E-04	1.34E-03	2.34E-03
8	2956	1.20E-03	6.30E-04	0.00E+00	8.93E-04	1.34E-03	1.67E-03	2.39E-03
All	58015							
ANOVA, P-Value:		**0.0000**						
Kruskal-Wallis, P-Value:		**0.0000**						

Table D-5: Descriptive statistics of carbon dioxide emissions during charge-sustaining operation according to VSP Bin.

		CO_2 (g/s)						
VSP Bin	N	Mean	St Dev	Min	1st Quart.	Median	3rd Quart.	Max
1	29028	1.082	2.167	0.000	0.000	0.067	1.661	21.436
2	5406	3.157	3.781	0.000	0.000	1.483	5.865	21.642
3	5071	4.328	4.327	0.000	0.000	3.760	7.601	21.121
4	4563	5.454	4.812	0.000	0.000	5.847	8.914	21.767
5	4149	6.289	5.306	0.000	0.000	6.956	10.433	22.714
6	3408	7.164	5.856	0.000	0.036	7.961	11.759	23.955
7	3434	9.116	6.291	0.000	3.026	10.258	13.827	24.115
8	2956	12.326	6.492	0.000	9.198	13.828	17.200	24.619
All	58015							
	ANOVA, P-Value:	**0.0000**						
	Kruskal-Wallis, P-Value:	**0.0000**						

Table D-6: Descriptive statistics of carbon monoxide emissions during charge-sustaining operation according to VSP Bin.

		CO (g/s)						
VSP Bin	N	Mean	St Dev	Min	1st Quart.	Median	3rd Quart.	Max
1	29028	1.72E-03	1.34E-02	0.00E+00	0.00E+00	1.00E-05	5.20E-04	5.28E-01
2	5406	6.42E-03	2.89E-02	0.00E+00	0.00E+00	3.30E-04	2.40E-03	3.51E-01
3	5071	6.31E-03	2.80E-02	0.00E+00	0.00E+00	9.20E-04	2.75E-03	4.26E-01
4	4563	5.38E-03	2.27E-02	0.00E+00	0.00E+00	1.46E-03	3.06E-03	3.98E-01
5	4149	5.71E-03	2.25E-02	0.00E+00	0.00E+00	1.74E-03	3.39E-03	4.24E-01
6	3408	5.45E-03	1.72E-02	0.00E+00	1.00E-05	2.01E-03	4.00E-03	2.88E-01
7	3434	6.68E-03	1.60E-02	0.00E+00	4.20E-04	2.88E-03	5.54E-03	2.15E-01
8	2956	9.04E-03	2.30E-02	0.00E+00	1.87E-03	3.91E-03	6.98E-03	3.18E-01
All	58015							
	ANOVA, P-Value:	**0.0000**						
	Kruskal-Wallis, P-Value:	**0.0000**						

Table D-7: Descriptive statistics of nitric oxide emissions during charge-sustaining operation according to VSP Bin.

	NO (g/s)							
VSP Bin	N	Mean	St Dev	Min	1st Quart.	Median	3rd Quart.	Max
1	29028	0.012	0.023	0.000	0.000	0.001	0.019	0.221
2	5406	0.031	0.039	0.000	0.000	0.015	0.054	0.241
3	5071	0.044	0.045	0.000	0.000	0.034	0.078	0.244
4	4563	0.055	0.050	0.000	0.000	0.053	0.097	0.222
5	4149	0.063	0.055	0.000	0.000	0.063	0.107	0.269
6	3408	0.070	0.060	0.000	0.000	0.072	0.118	0.257
7	3434	0.086	0.064	0.000	0.014	0.099	0.136	0.278
8	2956	0.112	0.065	0.000	0.063	0.128	0.164	0.265
All	58015							

ANOVA, P-Value: 0.0000
Kruskal-Wallis, P-Value: 0.0000

Table D-8: Descriptive statistics of nitrogen dioxide emissions during charge-sustaining operation according to VSP Bin.

	NO_2 (g/s)							
VSP Bin	N	Mean	St Dev	Min	1st Quart.	Median	3rd Quart.	Max
1	29028	1.34E-03	2.54E-03	0.00E+00	0.00E+00	2.70E-04	1.89E-03	4.00E-02
2	5406	2.61E-03	3.97E-03	0.00E+00	0.00E+00	1.16E-03	3.62E-03	4.30E-02
3	5071	3.06E-03	4.15E-03	0.00E+00	0.00E+00	1.67E-03	4.36E-03	3.19E-02
4	4563	3.56E-03	4.51E-03	0.00E+00	1.00E-05	2.24E-03	5.14E-03	4.25E-02
5	4149	3.55E-03	4.48E-03	0.00E+00	1.00E-05	2.19E-03	5.30E-03	5.48E-02
6	3408	3.57E-03	4.39E-03	0.00E+00	1.00E-05	2.23E-03	5.33E-03	4.14E-02
7	3434	4.09E-03	4.88E-03	0.00E+00	6.00E-05	2.76E-03	5.88E-03	4.10E-02
8	2956	4.78E-03	4.95E-03	0.00E+00	7.25E-04	3.52E-03	7.40E-03	3.86E-02
All	58015							

ANOVA, P-Value: 0.0000
Kruskal-Wallis, P-Value: 0.0000

Table D-9: Descriptive statistics of NOx emissions during charge-sustaining operation according to VSP Bin.

NOx (g/s)								
VSP Bin	N	Mean	St Dev	Min	1st Quart.	Median	3rd Quart.	Max
1	29028	0.0134	0.0245	0.0000	0.0000	0.0011	0.0224	0.2427
2	5406	0.0340	0.0419	0.0000	0.0000	0.0169	0.0576	0.2497
3	5071	0.0468	0.0479	0.0000	0.0000	0.0369	0.0833	0.2486
4	4563	0.0590	0.0534	0.0000	0.0000	0.0564	0.1029	0.2289
5	4149	0.0661	0.0581	0.0000	0.0000	0.0665	0.1130	0.2773
6	3408	0.0731	0.0633	0.0000	0.0002	0.0754	0.1238	0.2717
7	3434	0.0903	0.0666	0.0000	0.0146	0.1028	0.1419	0.2942
8	2956	0.1173	0.0676	0.0000	0.0675	0.1328	0.1688	0.2834
All	58015							

ANOVA, P-Value: 0.0000
Kruskal-Wallis, P-Value: 0.0000

Table D-10: Descriptive statistics of hydrocarbon emissions during charge-sustaining operation according to VSP Bin.

Hydrocarbon (g/s)								
VSP Bin	N	Mean	St Dev	Min	1st Quart.	Median	3rd Quart.	Max
1	29028	7.40E-05	1.57E-04	0.00E+00	0.00E+00	2.00E-05	8.00E-05	6.58E-03
2	5406	1.77E-04	2.66E-04	0.00E+00	0.00E+00	9.00E-05	2.70E-04	5.64E-03
3	5071	2.47E-04	3.17E-04	0.00E+00	0.00E+00	1.70E-04	3.70E-04	3.65E-03
4	4563	3.18E-04	4.12E-04	0.00E+00	0.00E+00	2.50E-04	4.70E-04	8.97E-03
5	4149	4.14E-04	7.66E-04	0.00E+00	0.00E+00	3.10E-04	5.60E-04	2.63E-02
6	3408	5.51E-04	1.23E-03	0.00E+00	1.00E-05	3.90E-04	6.50E-04	2.45E-02
7	3434	7.89E-04	1.74E-03	0.00E+00	1.60E-04	5.30E-04	8.30E-04	3.68E-02
8	2956	1.53E-03	4.16E-03	0.00E+00	4.50E-04	7.50E-04	1.18E-03	6.74E-02
All	58015							

ANOVA, P-Value: 0.0000
Kruskal-Wallis, P-Value: 0.0000

Table D-11: Descriptive statistics of dICE power output during charge-sustaining operation according to driving mode.

Internal Combustion Engine Power (W/kg/s)								
VSP Bin	N	Mean	St Dev	Min	1st Quart.	Median	3rd Quart.	Max
Accel	8232	8.809	9.190	-4.862	0.000	5.500	17.086	31.782
Cruise	33028	5.301	6.928	-4.346	0.000	0.588	10.620	30.914
Decel	7715	0.246	1.247	-2.556	-0.184	0.000	1.157	12.322
Idle	9040	0.977	1.166	-1.207	0.000	0.000	1.827	10.152
All	58015							
ANOVA, P-Value:		**0.0000**						
Kruskal-Wallis, P-Value:		**0.0000**						

Table D-12: Descriptive statistics of EM power output during charge-sustaining operation according to driving mode.

Electric Motor Power Output (W/kg/s)								
VSP Bin	N	Mean	St Dev	Min	1st Quart.	Median	3rd Quart.	Max
Accel	8232	4.747	6.044	0.000	0.000	0.028	10.776	21.722
Cruise	33028	1.006	2.746	0.000	0.000	0.000	0.000	21.087
Decel	7715	0.063	0.257	0.000	0.000	0.000	0.000	7.768
Idle	9040	0.253	0.675	0.000	0.000	0.070	0.354	13.399
All	58015							
ANOVA, P-Value:		**0.0000**						
Kruskal-Wallis, P-Value:		**0.0000**						

Table D-13: Descriptive statistics of dICE power output during charge-sustaining operation according to driving mode.

Total Power Output (W/kg/s)								
VSP Bin	N	Mean	St Dev	Min	1st Quart.	Median	3rd Quart.	Max
Accel	8232	13.555	6.591	-2.866	9.432	13.249	18.206	33.935
Cruise	33028	6.307	6.722	-3.724	0.000	5.845	11.081	33.659
Decel	7715	0.309	1.260	-2.556	-0.181	0.000	1.180	12.322
Idle	9040	1.230	1.149	-0.817	0.350	1.407	1.830	13.399
All	58015							
ANOVA, P-Value:		**0.0000**						
Kruskal-Wallis, P-Value:		**0.0000**						

Table D-14: Descriptive statistics of fuel use during charge-sustaining operation according to driving mode.

		Fuel (gal/s)						
VSP Bin	N	Mean	St Dev	Min	1st Quart.	Median	3rd Quart.	Max
Accel	8232	6.79E-04	6.90E-04	0.00E+00	0.00E+00	4.62E-04	1.31E-03	2.39E-03
Cruise	33028	4.20E-04	4.81E-04	0.00E+00	1.00E-06	1.84E-04	7.74E-04	2.32E-03
Decel	7715	4.90E-05	1.53E-04	0.00E+00	0.00E+00	1.00E-05	3.50E-05	2.12E-03
Idle	9040	1.03E-04	1.64E-04	0.00E+00	0.00E+00	1.00E-06	1.72E-04	1.98E-03
All	58015							

ANOVA, P-Value: 0.0000
Kruskal-Wallis, P-Value: 0.0000

Table D-15: Descriptive statistics of carbon dioxide emissions during charge-sustaining operation according to driving mode.

		CO_2 (g/s)						
VSP Bin	N	Mean	St Dev	Min	1st Quart.	Median	3rd Quart.	Max
Accel	8232	6.980	7.100	0.000	0.000	4.759	13.424	24.619
Cruise	33028	4.321	4.955	0.000	0.000	1.906	7.973	23.898
Decel	7715	0.493	1.581	0.000	0.000	0.032	0.366	21.767
Idle	9040	1.060	1.672	0.000	0.000	0.000	1.773	20.309
All	58015							

ANOVA, P-Value: 0.0000
Kruskal-Wallis, P-Value: 0.0000

Table D-16: Descriptive statistics of carbon monoxide emissions during charge-sustaining operation according to driving mode.

		CO (g/s)						
VSP Bin	N	Mean	St Dev	Min	1st Quart.	Median	3rd Quart.	Max
Accel	8232	1.17E-02	3.36E-02	0.00E+00	0.00E+00	2.18E-03	6.94E-03	4.24E-01
Cruise	33028	3.30E-03	1.59E-02	0.00E+00	0.00E+00	6.10E-04	2.62E-03	4.26E-01
Decel	7715	6.92E-04	4.60E-03	0.00E+00	0.00E+00	1.00E-05	5.00E-04	2.07E-01
Idle	9040	2.51E-03	1.97E-02	0.00E+00	0.00E+00	1.00E-05	4.00E-04	5.28E-01
All	58015							

ANOVA, P-Value: 0.0000
Kruskal-Wallis, P-Value: 0.0000

Table D-17: Descriptive statistics of nitric oxide emissions during charge-sustaining operation according to driving mode.

NO (g/s)								
VSP Bin	N	Mean	St Dev	Min	1st Quart.	Median	3rd Quart.	Max
Accel	8232	0.060	0.064	0.000	0.000	0.039	0.114	0.265
Cruise	33028	0.045	0.052	0.000	0.000	0.021	0.082	0.278
Decel	7715	0.005	0.015	0.000	0.000	0.000	0.003	0.207
Idle	9040	0.013	0.018	0.000	0.000	0.000	0.022	0.198
All	58015							

ANOVA, P-Value: 0.0000
Kruskal-Wallis, P-Value: 0.0000

Table D-18: Descriptive statistics of nitrogen dioxide emissions during charge-sustaining operation according to driving mode.

NO_2 (g/s)								
VSP Bin	N	Mean	St Dev	Min	1st Quart.	Median	3rd Quart.	Max
Accel	8232	3.92E-03	5.29E-03	0.00E+00	0.00E+00	1.99E-03	6.14E-03	5.48E-02
Cruise	33028	2.66E-03	3.73E-03	0.00E+00	1.00E-05	1.31E-03	3.77E-03	4.30E-02
Decel	7715	7.68E-04	2.14E-03	0.00E+00	0.00E+00	1.50E-04	5.10E-04	3.59E-02
Idle	9040	1.52E-03	2.54E-03	0.00E+00	0.00E+00	1.00E-05	2.44E-03	3.69E-02
All	58015							

ANOVA, P-Value: 0.0000
Kruskal-Wallis, P-Value: 0.0000

Table D-19: Descriptive statistics of NOx emissions during charge-sustaining operation according to driving mode.

NOx (g/s)								
VSP Bin	N	Mean	St Dev	Min	1st Quart.	Median	3rd Quart.	Max
Accel	8232	0.0637	0.0679	0.0000	0.0000	0.0436	0.1213	0.2834
Cruise	33028	0.0474	0.0544	0.0000	0.0000	0.0239	0.0873	0.2942
Decel	7715	0.0055	0.0169	0.0000	0.0000	0.0005	0.0031	0.2427
Idle	9040	0.0142	0.0202	0.0000	0.0000	0.0000	0.0242	0.2179
All	58015							

ANOVA, P-Value: 0.0000
Kruskal-Wallis, P-Value: 0.0000

Table D-20: Descriptive statistics of hydrocarbon emissions during charge-sustaining operation according to driving mode.

	Hydrocarbon (g/s)							
VSP Bin	N	Mean	St Dev	Min	1st Quart.	Median	3rd Quart.	Max
Accel	8232	6.24E-04	1.79E-03	0.00E+00	0.00E+00	2.80E-04	6.90E-04	3.83E-02
Cruise	33028	3.26E-04	1.23E-03	0.00E+00	0.00E+00	1.40E-04	4.10E-04	6.74E-02
Decel	7715	3.40E-05	9.40E-05	0.00E+00	0.00E+00	1.00E-05	4.00E-05	2.35E-03
Idle	9040	5.30E-05	1.00E-04	0.00E+00	0.00E+00	0.00E+00	7.00E-05	2.29E-03
All	58015							
ANOVA, P-Value:		**0.0000**						
Kruskal-Wallis, P-Value:		**0.0000**						

Table D-21: Descriptive statistics of dICE power output during charge-depleting operation according to VSP Bin.

Internal Combustion Engine Power (W/kg/s)								
VSP Bin	N	Mean	St Dev	Min	1st Quart.	Median	3rd Quart.	Max
1	9399	0.292	1.722	-5.041	0.000	0.000	0.000	24.271
2	1597	1.587	3.111	-5.028	0.000	0.000	2.581	24.793
3	1478	2.651	4.032	-4.397	0.000	0.000	5.077	24.876
4	1318	3.874	4.738	-3.306	0.000	1.937	7.129	22.119
5	1254	5.113	5.574	-4.112	0.000	4.348	9.652	23.360
6	1152	6.342	6.027	-3.587	0.000	7.088	11.378	22.800
7	1217	8.520	6.675	-4.264	0.000	10.308	13.730	25.758
8	1061	13.429	7.984	-4.617	9.105	15.055	19.300	31.808
All	18476							
ANOVA, P-Value:		**0.0000**						
Kruskal-Wallis, P-Value:		**0.0000**						

Table D-22: Descriptive statistics of EM power output during charge-depleting operation according to VSP Bin.

Electric Motor Power Output (W/kg/s)								
VSP Bin	N	Mean	St Dev	Min	1st Quart.	Median	3rd Quart.	Max
1	9399	0.402	1.245	0.000	0.000	0.000	0.403	15.045
2	1597	1.552	2.731	0.000	0.000	0.021	2.201	12.726
3	1478	2.459	3.591	0.000	0.000	0.041	4.489	15.068
4	1318	3.208	4.239	0.000	0.000	0.048	6.644	17.064
5	1254	4.017	5.108	0.000	0.000	0.049	9.034	20.407
6	1152	4.335	5.621	0.000	0.000	0.047	10.529	18.819
7	1217	4.367	6.528	0.000	0.000	0.028	11.041	21.456
8	1061	2.848	6.025	0.000	0.000	0.000	0.094	21.847
All	18476							
ANOVA, P-Value:		**0.0000**						
Kruskal-Wallis, P-Value:		**0.0000**						

Table D-23: Descriptive statistics of total power output during charge-depleting operation according to VSP Bin.

Total Power Output (W/kg/s)								
VSP Bin	N	Mean	St Dev	Min	1st Quart.	Median	3rd Quart.	Max
1	9399	0.693	2.080	-5.041	0.000	0.364	0.884	24.355
2	1597	3.139	3.522	-5.028	0.342	2.364	5.152	24.905
3	1478	5.110	4.071	-3.874	2.084	4.722	7.563	24.924
4	1318	7.082	4.031	-3.306	4.416	6.916	9.693	23.546
5	1254	9.131	4.265	-2.906	6.455	9.408	11.691	24.178
6	1152	10.676	3.955	-2.204	8.462	10.923	12.961	23.711
7	1217	12.887	4.672	-3.469	10.483	12.815	15.465	33.920
8	1061	16.278	5.669	-3.305	12.882	16.165	20.228	31.811
All	18476							
ANOVA, P-Value:		**0.0000**						
Kruskal-Wallis, P-Value:		**0.0000**						

Table D-24: Descriptive statistics of fuel use during charge-depleting operation according to VSP Bin.

Fuel (gal/s)								
VSP Bin	N	Mean	St Dev	Min	1st Quart.	Median	3rd Quart.	Max
1	9399	5.40E-05	1.29E-04	0.00E+00	0.00E+00	0.00E+00	3.40E-05	2.01E-03
2	1597	1.57E-04	2.39E-04	0.00E+00	0.00E+00	1.00E-06	2.62E-04	1.85E-03
3	1478	2.44E-04	3.12E-04	0.00E+00	0.00E+00	6.30E-05	4.38E-04	2.04E-03
4	1318	3.30E-04	3.70E-04	0.00E+00	0.00E+00	2.38E-04	5.85E-04	2.10E-03
5	1254	4.24E-04	4.26E-04	0.00E+00	0.00E+00	3.91E-04	7.62E-04	2.08E-03
6	1152	5.14E-04	4.63E-04	0.00E+00	0.00E+00	5.55E-04	9.06E-04	1.78E-03
7	1217	6.82E-04	5.02E-04	0.00E+00	1.07E-04	7.85E-04	1.05E-03	2.06E-03
8	1061	1.02E-03	5.80E-04	0.00E+00	6.91E-04	1.10E-03	1.44E-03	2.42E-03
All	18476							
ANOVA, P-Value:		**0.0000**						
Kruskal-Wallis, P-Value:		**0.0000**						

Table D-25: Descriptive statistics of carbon monoxide emissions during charge-depleting operation according to VSP Bin.

	CO_2 (g/s)							
VSP Bin	N	Mean	St Dev	Min	1st Quart.	Median	3rd Quart.	Max
1	9399	0.543	1.325	0.000	0.000	0.000	0.318	20.675
2	1597	1.617	2.456	0.000	0.000	0.001	2.714	19.046
3	1478	2.514	3.200	0.000	0.000	0.661	4.508	20.971
4	1318	3.394	3.801	0.000	0.000	2.445	6.023	20.929
5	1254	4.358	4.384	0.000	0.000	4.034	7.860	20.875
6	1152	5.289	4.769	0.000	0.000	5.719	9.325	18.369
7	1217	7.005	5.167	0.000	1.123	8.088	10.834	20.676
8	1061	10.517	5.981	0.000	7.104	11.328	14.753	24.842
All	18476							
ANOVA, P-Value:	**0.0000**							
Kruskal-Wallis, P-Value:	**0.0000**							

Table D-26: Descriptive statistics of carbon monoxide emissions during charge-depleting operation according to VSP Bin.

	CO (g/s)							
VSP Bin	N	Mean	St Dev	Min	1st Quart.	Median	3rd Quart.	Max
1	9399	1.59E-03	1.26E-02	0.00E+00	0.00E+00	1.00E-05	7.10E-04	5.29E-01
2	1597	3.53E-03	1.08E-02	0.00E+00	0.00E+00	2.00E-05	3.10E-03	2.32E-01
3	1478	6.13E-03	2.73E-02	0.00E+00	0.00E+00	5.10E-04	4.29E-03	4.83E-01
4	1318	8.10E-03	2.81E-02	0.00E+00	1.00E-05	1.77E-03	4.90E-03	4.06E-01
5	1254	9.25E-03	3.02E-02	0.00E+00	1.00E-05	2.56E-03	5.17E-03	4.48E-01
6	1152	9.73E-03	2.67E-02	0.00E+00	1.00E-05	3.04E-03	5.88E-03	3.90E-01
7	1217	1.66E-02	3.72E-02	0.00E+00	9.70E-04	4.04E-03	1.01E-02	4.14E-01
8	1061	2.10E-02	4.02E-02	0.00E+00	3.26E-03	6.12E-03	1.77E-02	4.56E-01
All	18476							
ANOVA, P-Value:	**0.0000**							
Kruskal-Wallis, P-Value:	**0.0000**							

Table D-27: Descriptive statistics of nitric oxide emissions during charge-depleting operation according to VSP Bin.

	NO (g/s)							
VSP Bin	N	Mean	St Dev	Min	1st Quart.	Median	3rd Quart.	Max
1	9399	0.005	0.011	0.000	0.000	0.000	0.003	0.181
2	1597	0.011	0.018	0.000	0.000	0.000	0.017	0.194
3	1478	0.018	0.025	0.000	0.000	0.004	0.029	0.196
4	1318	0.025	0.030	0.000	0.000	0.013	0.041	0.149
5	1254	0.034	0.038	0.000	0.000	0.022	0.061	0.240
6	1152	0.043	0.043	0.000	0.000	0.038	0.074	0.203
7	1217	0.057	0.048	0.000	0.002	0.059	0.096	0.242
8	1061	0.085	0.056	0.000	0.031	0.094	0.128	0.229
All	18476							

ANOVA, P-Value: 0.0000
Kruskal-Wallis, P-Value: 0.0000

Table D-28: Descriptive statistics of nitrogen dioxide emissions during charge-depleting operation according to VSP Bin.

	NO_2 (g/s)							
VSP Bin	N	Mean	St Dev	Min	1st Quart.	Median	3rd Quart.	Max
1	9399	4.32E-04	1.08E-03	0.00E+00	0.00E+00	0.00E+00	2.80E-04	2.03E-02
2	1597	1.01E-03	1.83E-03	0.00E+00	0.00E+00	1.00E-05	1.40E-03	1.43E-02
3	1478	1.33E-03	2.28E-03	0.00E+00	0.00E+00	1.40E-04	1.91E-03	2.43E-02
4	1318	1.52E-03	2.33E-03	0.00E+00	0.00E+00	3.75E-04	2.34E-03	2.72E-02
5	1254	1.93E-03	2.76E-03	0.00E+00	0.00E+00	7.65E-04	3.23E-03	2.97E-02
6	1152	2.21E-03	2.78E-03	0.00E+00	0.00E+00	9.50E-04	3.95E-03	1.92E-02
7	1217	2.66E-03	2.87E-03	0.00E+00	1.20E-04	1.64E-03	4.55E-03	2.12E-02
8	1061	3.02E-03	3.11E-03	0.00E+00	7.85E-04	2.13E-03	4.40E-03	2.35E-02
All	18476							

ANOVA, P-Value: 0.0000
Kruskal-Wallis, P-Value: 0.0000

Table D-29: Descriptive statistics of NOx emissions during charge-depleting operation according to VSP Bin.

NOx (g/s)								
VSP Bin	N	Mean	St Dev	Min	1st Quart.	Median	3rd Quart.	Max
1	9399	0.0054	0.0121	0.0000	0.0000	0.0000	0.0041	0.1862
2	1597	0.0121	0.0194	0.0000	0.0000	0.0000	0.0193	0.2033
3	1478	0.0193	0.0269	0.0000	0.0000	0.0048	0.0310	0.2104
4	1318	0.0262	0.0319	0.0000	0.0000	0.0148	0.0439	0.1568
5	1254	0.0360	0.0400	0.0000	0.0000	0.0257	0.0636	0.2469
6	1152	0.0447	0.0445	0.0000	0.0000	0.0410	0.0767	0.2130
7	1217	0.0597	0.0499	0.0000	0.0030	0.0626	0.0994	0.2486
8	1061	0.0883	0.0571	0.0000	0.0315	0.0979	0.1321	0.2358
All	18476							

ANOVA, P-Value: 0.0000
Kruskal-Wallis, P-Value: 0.0000

Table D-30: Descriptive statistics of hydrocarbon emissions during charge-depleting operation according to VSP Bin.

Hydrocarbon (g/s)								
VSP Bin	N	Mean	St Dev	Min	1st Quart.	Median	3rd Quart.	Max
1	9399	1.81E-04	4.54E-04	0.00E+00	0.00E+00	0.00E+00	1.50E-04	6.72E-03
2	1597	3.83E-04	7.44E-04	0.00E+00	0.00E+00	0.00E+00	4.70E-04	9.22E-03
3	1478	5.52E-04	1.05E-03	0.00E+00	0.00E+00	1.20E-04	6.70E-04	1.41E-02
4	1318	7.91E-04	1.70E-03	0.00E+00	0.00E+00	3.05E-04	8.30E-04	2.81E-02
5	1254	8.92E-04	1.88E-03	0.00E+00	0.00E+00	3.80E-04	9.10E-04	2.55E-02
6	1152	1.13E-03	2.40E-03	0.00E+00	0.00E+00	4.70E-04	1.14E-03	2.46E-02
7	1217	1.93E-03	4.11E-03	0.00E+00	1.15E-04	6.70E-04	1.72E-03	6.42E-02
8	1061	3.18E-03	6.12E-03	0.00E+00	5.80E-04	1.21E-03	2.86E-03	6.49E-02
All	18476							

ANOVA, P-Value: 0.0000
Kruskal-Wallis, P-Value: 0.0000

Table D-31: Descriptive statistics of dICE power output during charge-depleting operation according to driving mode.

Internal Combustion Engine Power (W/kg/s)								
VSP Bin	N	Mean	St Dev	Min	1st Quart.	Median	3rd Quart.	Max
Accel	2417	5.124	7.563	-4.617	0.000	0.000	10.225	31.808
Cruise	10500	3.684	5.722	-5.041	0.000	0.000	7.238	27.825
Decel	2212	0.025	0.963	-3.338	0.000	0.000	0.000	13.194
Idle	3347	0.452	0.868	-0.295	0.000	0.000	0.000	8.659
All	18476							
ANOVA, P-Value:	**0.0000**							
Kruskal-Wallis, P-Value:	**0.0000**							

Table D-32: Descriptive statistics of EM power output during charge-depleting operation according to driving mode.

Electric Motor Power Output (W/kg/s)								
VSP Bin	N	Mean	St Dev	Min	1st Quart.	Median	3rd Quart.	Max
Accel	2417	6.719	6.202	0.000	0.010	6.889	11.555	21.847
Cruise	10500	1.394	3.170	0.000	0.000	0.000	0.225	21.547
Decel	2212	0.112	0.313	0.000	0.000	0.000	0.084	7.768
Idle	3347	0.406	0.642	0.000	0.122	0.387	0.484	11.387
All	18476							
ANOVA, P-Value:	**0.0000**							
Kruskal-Wallis, P-Value:	**0.0000**							

Table D-33: Descriptive statistics of total power output during charge-depleting operation according to driving mode.

Total Power Output (W/kg/s)								
VSP Bin	N	Mean	St Dev	Min	1st Quart.	Median	3rd Quart.	Max
Accel	2417	11.843	5.982	-3.469	7.792	11.451	15.313	31.811
Cruise	10500	5.078	5.758	-5.041	0.000	3.631	9.207	33.920
Decel	2212	0.137	1.010	-3.338	0.000	0.000	0.397	13.194
Idle	3347	0.857	0.894	0.000	0.383	0.480	1.616	11.387
All	18476							
ANOVA, P-Value:	**0.0000**							
Kruskal-Wallis, P-Value:	**0.0000**							

Table D-34: Descriptive statistics of fuel use during charge-depleting operation according to driving mode.

		Fuel (gal/s)						
VSP Bin	N	Mean	St Dev	Min	1st Quart.	Median	3rd Quart.	Max
Accel	2417	4.33E-04	5.90E-04	0.00E+00	0.00E+00	9.00E-06	7.98E-04	2.42E-03
Cruise	10500	3.19E-04	4.15E-04	0.00E+00	0.00E+00	8.80E-05	5.78E-04	2.20E-03
Decel	2212	1.50E-05	4.30E-05	0.00E+00	0.00E+00	0.00E+00	1.10E-05	7.29E-04
Idle	3347	4.80E-05	9.20E-05	0.00E+00	0.00E+00	0.00E+00	3.00E-06	1.52E-03
All	18476							
ANOVA, P-Value:		**0.0000**						
Kruskal-Wallis, P-Value:		**0.0000**						

Table D-35: Descriptive statistics of carbon dioxide emissions during charge-depleting operation according to driving mode.

		CO_2 (g/s)						
VSP Bin	N	Mean	St Dev	Min	1st Quart.	Median	3rd Quart.	Max
Accel	2417	4.433	6.051	0.000	0.000	0.037	8.221	24.842
Cruise	10500	3.282	4.279	0.000	0.000	0.917	5.957	22.606
Decel	2212	0.138	0.445	0.000	0.000	0.000	0.036	7.472
Idle	3347	0.490	0.946	0.000	0.000	0.000	0.009	15.221
All	18476							
ANOVA, P-Value:		**0.0000**						
Kruskal-Wallis, P-Value:		**0.0000**						

Table D-36: Descriptive statistics of carbon monoxide emissions during charge-depleting operation according to driving mode.

		CO (g/s)						
VSP Bin	N	Mean	St Dev	Min	1st Quart.	Median	3rd Quart.	Max
Accel	2417	2.19E-02	5.31E-02	0.00E+00	0.00E+00	1.60E-04	1.82E-02	5.29E-01
Cruise	10500	4.61E-03	1.35E-02	0.00E+00	0.00E+00	1.19E-03	4.14E-03	2.48E-01
Decel	2212	4.45E-04	1.97E-03	0.00E+00	0.00E+00	1.00E-05	3.50E-04	7.12E-02
Idle	3347	9.75E-04	9.09E-03	0.00E+00	0.00E+00	1.00E-05	4.00E-05	2.95E-01
All	18476							
ANOVA, P-Value:		**0.0000**						
Kruskal-Wallis, P-Value:		**0.0000**						

Table D-37: Descriptive statistics of nitric oxide emissions during charge-depleting operation according to driving mode.

NO (g/s)								
VSP Bin	N	Mean	St Dev	Min	1st Quart.	Median	3rd Quart.	Max
Accel	2417	0.031	0.046	0.000	0.000	0.000	0.053	0.215
Cruise	10500	0.027	0.038	0.000	0.000	0.007	0.041	0.242
Decel	2212	0.001	0.004	0.000	0.000	0.000	0.000	0.072
Idle	3347	0.005	0.010	0.000	0.000	0.000	0.000	0.135
All	18476							
ANOVA, P-Value:		**0.0000**						
Kruskal-Wallis, P-Value:		**0.0000**						

Table D-38: Descriptive statistics of nitrogen dioxide emissions during charge-depleting operation according to driving mode.

NO_2 (g/s)								
VSP Bin	N	Mean	St Dev	Min	1st Quart.	Median	3rd Quart.	Max
Accel	2417	1.29E-03	2.83E-03	0.00E+00	0.00E+00	1.00E-05	1.34E-03	2.97E-02
Cruise	10500	1.59E-03	2.28E-03	0.00E+00	0.00E+00	4.50E-04	2.63E-03	2.72E-02
Decel	2212	1.35E-04	3.96E-04	0.00E+00	0.00E+00	0.00E+00	1.20E-04	5.80E-03
Idle	3347	2.73E-04	7.84E-04	0.00E+00	0.00E+00	0.00E+00	3.00E-05	1.03E-02
All	18476							
ANOVA, P-Value:		**0.0000**						
Kruskal-Wallis, P-Value:		**0.0000**						

Table D-39: Descriptive statistics of NOx emissions during charge-depleting operation according to driving mode.

NOx (g/s)								
VSP Bin	N	Mean	St Dev	Min	1st Quart.	Median	3rd Quart.	Max
Accel	2417	0.0319	0.0481	0.0000	0.0000	0.0002	0.0553	0.2289
Cruise	10500	0.0283	0.0398	0.0000	0.0000	0.0083	0.0437	0.2486
Decel	2212	0.0013	0.0040	0.0000	0.0000	0.0000	0.0006	0.0729
Idle	3347	0.0057	0.0108	0.0000	0.0000	0.0000	0.0002	0.1374
All	18476							
ANOVA, P-Value:		**0.0000**						
Kruskal-Wallis, P-Value:		**0.0000**						

Table D-40: Descriptive statistics of hydrocarbon emissions during charge-depleting operation according to driving mode.

	Hydrocarbon (g/s)							
VSP Bin	N	Mean	St Dev	Min	1st Quart.	Median	3rd Quart.	Max
Accel	2417	1.72E-03	3.83E-03	0.00E+00	0.00E+00	0.00E+00	1.81E-03	3.59E-02
Cruise	10500	7.22E-04	2.19E-03	0.00E+00	0.00E+00	2.50E-04	7.40E-04	6.49E-02
Decel	2212	8.60E-05	2.62E-04	0.00E+00	0.00E+00	0.00E+00	3.00E-05	4.81E-03
Idle	3347	1.17E-04	2.79E-04	0.00E+00	0.00E+00	0.00E+00	0.00E+00	3.93E-03
All	18476							
ANOVA, P-Value:		**0.0000**						
Kruskal-Wallis, P-Value:		**0.0000**						

Appendix E: Roadway Analysis

The following tables provide summarized descriptive statistics of PHEV Sprinter's on-road power, driving, and emissions variables segregated according to roadway type (urban, suburban, or highway), active operating mode during data collection (charge-depleting or charge-sustaining), and VSP bin (1 through 8).

Additional tables supplying sample-run based data are to follow. The file names referenced in the sample run-based tables correspond to the individual data files of continuous data provided in digital submission.

The following tables were created for the roadway analysis, but were used in subsequent analyses regarding the PHEV's different operating modes.

Table E-1: Descriptive statistics of PHEV Sprinter emissions data by VSP bin for Highway travel during charge-sustaining operation.

Variable	VSP Bin	Road Code	Total	N	N Missing	Mean	SE Mean	Std. Dev.	Minimum	Q1	Median	Q3	Maximum
Fuel (gal/s)	1	Hwy	1263	1263	0	1.91E-04	8.00E-06	2.67E-04	0.00E+00	5.00E-06	4.30E-05	2.84E-04	1.32E-03
	2	Hwy	440	440	0	5.20E-04	1.60E-05	3.26E-04	0.00E+00	2.89E-04	4.95E-04	7.52E-04	1.24E-03
	3	Hwy	545	545	0	6.39E-04	1.30E-05	3.11E-04	0.00E+00	4.32E-04	6.56E-04	8.80E-04	1.33E-03
	4	Hwy	541	541	0	7.21E-04	1.30E-05	2.99E-04	0.00E+00	5.48E-04	7.55E-04	9.18E-04	1.70E-03
	5	Hwy	618	618	0	8.06E-04	1.30E-05	3.26E-04	0.00E+00	6.83E-04	8.30E-04	9.97E-04	2.13E-03
	6	Hwy	586	586	0	8.76E-04	1.50E-05	3.66E-04	0.00E+00	7.43E-04	9.11E-04	1.07E-03	2.32E-03
	7	Hwy	678	678	0	9.97E-04	1.40E-05	3.58E-04	0.00E+00	8.71E-04	1.02E-03	1.16E-03	2.22E-03
	8	Hwy	618	618	0	1.29E-03	1.60E-05	4.00E-04	0.00E+00	1.07E-03	1.28E-03	1.53E-03	2.23E-03
CO_2 (g/s)	1	Hwy	1263	1263	0	1.95	0.08	2.77	0.00	0.01	0.46	2.95	13.58
	2	Hwy	440	440	0	5.37	0.16	3.36	0.00	2.99	5.12	7.76	12.81
	3	Hwy	545	545	0	6.60	0.14	3.21	0.00	4.46	6.77	9.07	13.73
	4	Hwy	541	541	0	7.44	0.13	3.08	0.00	5.66	7.79	9.48	17.47
	5	Hwy	618	618	0	8.31	0.14	3.36	0.00	7.05	8.56	10.29	21.92
	6	Hwy	586	586	0	9.04	0.16	3.77	0.00	7.66	9.40	10.99	23.90
	7	Hwy	678	678	0	10.28	0.14	3.69	0.00	8.98	10.50	11.96	22.87
	8	Hwy	618	618	0	13.28	0.17	4.13	0.00	10.99	13.20	15.79	22.96
CO (g/s)	1	Hwy	1263	1263	0	1.18E-03	5.80E-05	2.07E-03	0.00E+00	0.00E+00	1.20E-04	1.68E-03	2.12E-02
	2	Hwy	440	440	0	2.34E-03	9.20E-05	1.94E-03	0.00E+00	1.04E-03	2.05E-03	3.25E-03	1.08E-02
	3	Hwy	545	545	0	2.77E-03	1.77E-04	4.14E-03	0.00E+00	1.33E-03	2.31E-03	3.37E-03	6.54E-02
	4	Hwy	541	541	0	2.53E-03	7.70E-05	1.79E-03	0.00E+00	1.59E-03	2.33E-03	3.19E-03	1.65E-02
	5	Hwy	618	618	0	3.91E-03	7.30E-04	1.82E-02	0.00E+00	1.67E-03	2.45E-03	3.24E-03	4.24E-01
	6	Hwy	586	586	0	2.88E-03	1.50E-04	3.62E-03	0.00E+00	1.67E-03	2.45E-03	3.37E-03	4.96E-02
	7	Hwy	678	678	0	5.04E-03	5.06E-04	1.32E-02	0.00E+00	1.87E-03	2.75E-03	3.89E-03	1.50E-01
	8	Hwy	618	618	0	7.51E-03	8.51E-04	2.12E-02	0.00E+00	2.41E-03	3.70E-03	5.64E-03	2.95E-01
NO (g/s)	1	Hwy	1263	1263	0	0.017	0.001	0.024	0.000	0.000	0.005	0.027	0.143
	2	Hwy	440	440	0	0.043	0.002	0.033	0.000	0.020	0.036	0.060	0.145
	3	Hwy	545	545	0	0.055	0.002	0.035	0.000	0.031	0.049	0.077	0.149
	4	Hwy	541	541	0	0.066	0.002	0.036	0.000	0.043	0.061	0.090	0.200
	5	Hwy	618	618	0	0.077	0.002	0.038	0.000	0.055	0.076	0.103	0.217
	6	Hwy	586	586	0	0.089	0.002	0.044	0.000	0.065	0.091	0.116	0.233
	7	Hwy	678	678	0	0.104	0.002	0.043	0.000	0.086	0.108	0.128	0.249
	8	Hwy	618	618	0	0.135	0.002	0.046	0.000	0.114	0.138	0.166	0.260
NO_2 (g/s)	1	Hwy	1263	1263	0	1.19E-03	4.90E-05	1.74E-03	0.00E+00	0.00E+00	4.70E-04	1.83E-03	1.38E-02
	2	Hwy	440	440	0	2.26E-03	1.06E-04	2.23E-03	0.00E+00	7.80E-04	1.75E-03	2.87E-03	1.35E-02
	3	Hwy	545	545	0	2.70E-03	1.09E-04	2.55E-03	0.00E+00	9.75E-04	1.87E-03	3.68E-03	1.33E-02
	4	Hwy	541	541	0	2.80E-03	1.02E-04	2.38E-03	0.00E+00	1.25E-03	2.24E-03	3.62E-03	1.34E-02
	5	Hwy	618	618	0	2.99E-03	1.09E-04	2.72E-03	0.00E+00	9.10E-04	2.39E-03	3.98E-03	1.37E-02
	6	Hwy	586	586	0	3.02E-03	1.21E-04	2.94E-03	0.00E+00	9.68E-04	2.33E-03	4.01E-03	1.38E-02
	7	Hwy	678	678	0	2.70E-03	1.00E-04	2.61E-03	0.00E+00	8.00E-04	2.19E-03	3.82E-03	1.34E-02
	8	Hwy	618	618	0	2.64E-03	1.08E-04	2.69E-03	0.00E+00	5.95E-04	1.96E-03	3.75E-03	1.36E-02
NOx (g/s)	1	Hwy	1263	1263	0	0.018	0.001	0.025	0.000	0.000	0.006	0.029	0.155
	2	Hwy	440	440	0	0.045	0.002	0.034	0.000	0.021	0.038	0.063	0.159
	3	Hwy	545	545	0	0.058	0.002	0.037	0.000	0.033	0.051	0.081	0.160
	4	Hwy	541	541	0	0.069	0.002	0.037	0.000	0.045	0.063	0.094	0.209
	5	Hwy	618	618	0	0.080	0.002	0.040	0.000	0.056	0.079	0.107	0.221
	6	Hwy	586	586	0	0.092	0.002	0.045	0.000	0.066	0.094	0.120	0.235
	7	Hwy	678	678	0	0.107	0.002	0.044	0.000	0.088	0.111	0.131	0.256
	8	Hwy	618	618	0	0.137	0.002	0.047	0.000	0.116	0.142	0.168	0.267
HC (g/s)	1	Hwy	1263	1263	0	2.05E-04	6.00E-06	2.18E-04	0.00E+00	1.00E-05	1.40E-04	3.50E-04	1.05E-03
	2	Hwy	440	440	0	4.06E-04	1.20E-05	2.57E-04	0.00E+00	2.30E-04	3.90E-04	5.60E-04	2.38E-03
	3	Hwy	545	545	0	4.70E-04	1.10E-05	2.66E-04	0.00E+00	3.00E-04	4.60E-04	6.30E-04	2.97E-03
	4	Hwy	541	541	0	5.12E-04	1.20E-05	2.73E-04	0.00E+00	3.40E-04	4.90E-04	6.55E-04	2.20E-03
	5	Hwy	618	618	0	6.22E-04	3.30E-05	8.20E-04	0.00E+00	3.70E-04	5.20E-04	6.80E-04	1.13E-02
	6	Hwy	586	586	0	7.14E-04	4.90E-05	1.17E-03	0.00E+00	4.20E-04	5.60E-04	7.50E-04	1.83E-02
	7	Hwy	678	678	0	1.03E-03	8.70E-05	2.26E-03	0.00E+00	4.80E-04	6.90E-04	9.00E-04	3.68E-02

Table E-2: Descriptive statistics of PHEV Sprinter driving and road-based data by VSP bin for Highway travel during charge-sustaining operation.

Variable	VSP Bin	Road Code	Total	N	N Missing	Mean	SE Mean	Std. Dev.	Minimum	Q1	Median	Q3	Maximum
Velocity (km/h)	1	Hwy	1263	1263	0	59.8	0.9	30.4	0.0	43.2	72.1	84.9	93.1
	2	Hwy	440	440	0	76.2	0.9	18.8	1.5	72.2	84.2	87.3	92.2
	3	Hwy	545	545	0	78.3	0.7	16.3	0.9	74.0	84.8	87.5	93.4
	4	Hwy	541	541	0	79.1	0.6	14.2	1.1	75.0	84.8	87.4	93.0
	5	Hwy	618	618	0	77.6	0.6	14.3	8.1	73.3	82.9	86.3	91.7
	6	Hwy	586	586	0	77.3	0.6	13.6	13.7	73.1	82.6	86.3	91.9
	7	Hwy	678	678	0	76.3	0.6	14.4	15.8	72.9	81.2	85.9	91.7
	8	Hwy	618	618	0	76.9	0.5	12.4	17.0	71.0	81.0	85.9	91.4
Positive Accel (m/s^2)	1	Hwy	1263	274	989	0.049	0.007	0.123	0.000	0.000	0.000	0.059	1.267
	2	Hwy	440	208	232	0.132	0.013	0.184	0.000	0.035	0.065	0.121	1.330
	3	Hwy	545	279	266	0.160	0.015	0.247	0.001	0.039	0.094	0.161	2.197
	4	Hwy	541	286	255	0.170	0.013	0.227	0.000	0.048	0.121	0.193	1.943
	5	Hwy	618	333	285	0.242	0.018	0.324	0.000	0.066	0.140	0.252	2.262
	6	Hwy	586	349	237	0.233	0.015	0.284	0.000	0.058	0.152	0.269	1.982
	7	Hwy	678	507	171	0.257	0.015	0.331	0.001	0.056	0.130	0.292	2.046
	8	Hwy	618	595	23	0.289	0.012	0.289	0.005	0.113	0.190	0.366	2.465
Negative Accel (m/s^2)	1	Hwy	1263	989	274	-0.441	0.016	0.489	-3.429	-0.625	-0.229	-0.116	-0.002
	2	Hwy	440	232	208	-0.137	0.007	0.113	-0.514	-0.190	-0.103	-0.052	-0.001
	3	Hwy	545	266	279	-0.131	0.006	0.103	-0.430	-0.199	-0.106	-0.050	-0.001
	4	Hwy	541	255	286	-0.118	0.005	0.085	-0.394	-0.175	-0.105	-0.048	0.000
	5	Hwy	618	285	333	-0.098	0.004	0.068	-0.364	-0.142	-0.088	-0.043	-0.001
	6	Hwy	586	237	349	-0.077	0.004	0.061	-0.303	-0.108	-0.069	-0.026	0.000
	7	Hwy	678	171	507	-0.050	0.003	0.043	-0.186	-0.075	-0.040	-0.018	0.000
	8	Hwy	618	23	595	-0.048	0.010	0.046	-0.179	-0.075	-0.036	-0.009	-0.002
Positive Grade (%)	1	Hwy	1263	372	891	1.11%	0.12%	2.40%	0.00%	0.00%	0.00%	1.72%	22.79%
	2	Hwy	440	83	357	1.20%	0.13%	1.15%	0.00%	0.00%	0.98%	2.17%	4.54%
	3	Hwy	545	157	388	2.20%	0.55%	6.94%	0.00%	0.43%	1.33%	2.21%	83.94%
	4	Hwy	541	239	302	1.90%	0.57%	8.77%	0.00%	0.43%	1.25%	1.99%	135.98%
	5	Hwy	618	375	243	1.60%	0.06%	1.12%	0.00%	0.83%	1.63%	2.17%	8.84%
	6	Hwy	586	436	150	1.84%	0.05%	1.07%	0.00%	1.06%	1.80%	2.54%	5.89%
	7	Hwy	678	565	113	2.09%	0.05%	1.11%	0.00%	1.30%	2.11%	2.83%	6.32%
	8	Hwy	618	554	64	2.88%	0.08%	1.92%	0.00%	2.07%	2.75%	3.36%	36.40%
Negative Grade (%)	1	Hwy	1263	891	372	-2.88%	0.06%	1.66%	-18.49%	-3.38%	-2.80%	-1.91%	-0.40%
	2	Hwy	440	357	83	-2.26%	0.07%	1.32%	-15.04%	-2.88%	-2.17%	-1.33%	-0.40%
	3	Hwy	545	388	157	-1.93%	0.06%	1.11%	-9.10%	-2.54%	-1.69%	-1.20%	-0.40%
	4	Hwy	541	302	239	-1.65%	0.06%	0.98%	-5.74%	-2.35%	-1.62%	-0.83%	-0.40%
	5	Hwy	618	243	375	-1.72%	0.07%	1.12%	-5.52%	-2.44%	-1.37%	-0.83%	-0.40%
	6	Hwy	586	150	436	-1.66%	0.08%	1.03%	-4.91%	-2.27%	-1.42%	-0.84%	-0.39%
	7	Hwy	678	113	565	-1.69%	0.11%	1.14%	-4.74%	-2.50%	-1.32%	-0.83%	-0.40%
	8	Hwy	618	64	554	-1.61%	0.14%	1.09%	-4.91%	-2.27%	-1.30%	-0.79%	-0.41%

Table E-3: Descriptive statistics of PHEV Sprinter power data by VSP bin for Highway travel during charge-sustaining operation.

Variable	VSP Bin	Road Code	Total	N	N Missing	Mean	SE Mean	Std. Dev.	Minimum	Q1	Median	Q3	Maximum
Diesel ICE Power (W/kg/s)	1	Hwy	1263	1263	0	1.26	0.11	4.06	-2.89	-1.44	0.00	1.13	17.82
	2	Hwy	440	440	0	6.30	0.24	5.04	-2.40	0.84	6.81	10.18	18.85
	3	Hwy	545	545	0	8.26	0.20	4.58	-3.51	5.68	8.52	11.70	20.68
	4	Hwy	541	541	0	9.37	0.19	4.30	-2.46	7.61	9.46	12.07	22.62
	5	Hwy	618	618	0	10.52	0.17	4.32	-3.27	8.88	10.61	13.01	24.94
	6	Hwy	586	586	0	11.65	0.20	4.94	-0.48	9.83	11.91	14.14	27.14
	7	Hwy	678	678	0	13.26	0.19	5.06	-3.97	11.53	13.40	15.82	28.06
	8	Hwy	618	618	0	17.52	0.22	5.36	-3.83	14.64	17.81	20.84	30.91
Electric Motor Power (W/kg/s)	1	Hwy	1263	1263	0	0.11	0.01	0.53	0.00	0.00	0.00	0.00	10.45
	2	Hwy	440	440	0	0.27	0.06	1.23	0.00	0.00	0.00	0.00	11.60
	3	Hwy	545	545	0	0.37	0.07	1.67	0.00	0.00	0.00	0.00	14.19
	4	Hwy	541	541	0	0.39	0.07	1.72	0.00	0.00	0.00	0.00	12.47
	5	Hwy	618	618	0	0.81	0.12	2.92	0.00	0.00	0.00	0.00	15.17
	6	Hwy	586	586	0	1.14	0.15	3.64	0.00	0.00	0.00	0.00	15.27
	7	Hwy	678	678	0	1.20	0.15	4.02	0.00	0.00	0.00	0.00	18.89
	8	Hwy	618	618	0	0.80	0.15	3.66	0.00	0.00	0.00	0.00	21.67
Total Power (W/kg/s)	1	Hwy	1263	1263	0	1.37	0.11	4.06	-2.89	-1.44	0.18	1.31	17.82
	2	Hwy	440	440	0	6.57	0.23	4.86	-2.40	2.93	6.86	10.23	18.85
	3	Hwy	545	545	0	8.63	0.18	4.19	-3.51	6.26	8.70	11.79	20.68
	4	Hwy	541	541	0	9.76	0.16	3.77	-2.46	7.78	9.51	12.11	22.62
	5	Hwy	618	618	0	11.33	0.13	3.26	-0.71	9.36	10.99	13.16	24.94
	6	Hwy	586	586	0	12.80	0.14	3.45	1.80	10.54	12.29	14.41	27.14
	7	Hwy	678	678	0	14.47	0.14	3.60	1.00	12.21	13.73	16.06	33.94
	8	Hwy	618	618	0	18.32	0.17	4.27	1.23	15.11	18.21	21.10	30.98
Recup (W/kg/s)	1	Hwy	1263	1263	0	-2.182	0.060	2.115	-9.707	-2.911	-1.605	-1.115	0.000
	2	Hwy	440	440	0	-3.811	0.137	2.880	-12.952	-5.909	-2.804	-1.642	0.000
	3	Hwy	545	545	0	-3.950	0.120	2.804	-12.874	-5.747	-3.135	-1.806	0.000
	4	Hwy	541	541	0	-3.730	0.115	2.681	-11.744	-5.326	-3.123	-1.779	0.000
	5	Hwy	618	618	0	-3.156	0.105	2.610	-12.130	-4.419	-2.527	-1.332	0.000
	6	Hwy	586	586	0	-2.759	0.115	2.786	-12.989	-3.916	-1.809	-0.906	0.000
	7	Hwy	678	678	0	-2.300	0.101	2.628	-13.037	-3.071	-1.470	0.000	0.000
	8	Hwy	618	618	0	-1.564	0.097	2.418	-12.984	-2.203	-0.647	0.000	0.000

Table E-4: Descriptive statistics of PHEV Sprinter emissions data by VSP bin for Suburban travel during charge-sustaining operation.

	VSP Bin	Road Code	Total	N	N Missing	Mean	SE Mean	Std. Dev.	Minimum	Q1	Median	Q3	Maximum
Fuel (gal/s)	1	S	21714	21714	0	1.03E-04	1.00E-06	2.07E-04	0.00E+00	0.00E+00	1.40E-05	1.56E-04	2.02E-03
	2	S	4007	4007	0	2.94E-04	6.00E-06	3.70E-04	0.00E+00	0.00E+00	1.06E-04	5.66E-04	2.10E-03
	3	S	3643	3643	0	4.00E-04	7.00E-06	4.23E-04	0.00E+00	0.00E+00	2.96E-04	7.28E-04	2.07E-03
	4	S	3228	3228	0	5.05E-04	9.00E-06	4.83E-04	0.00E+00	1.00E-06	4.95E-04	8.39E-04	2.12E-03
	5	S	2799	2799	0	5.75E-04	1.00E-05	5.41E-04	0.00E+00	1.00E-06	5.64E-04	1.02E-03	2.26E-03
	6	S	2228	2228	0	6.55E-04	1.30E-05	6.10E-04	0.00E+00	1.00E-06	6.11E-04	1.19E-03	2.33E-03
	7	S	2150	2150	0	8.57E-04	1.50E-05	6.79E-04	0.00E+00	6.00E-06	9.75E-04	1.44E-03	2.34E-03
	8	S	1695	1695	0	1.22E-03	1.60E-05	6.71E-04	0.00E+00	8.03E-04	1.42E-03	1.73E-03	2.39E-03
CO_2 (g/s)	1	S	21714	21714	0	1.05	0.01	2.13	0.00	0.00	0.07	1.61	20.80
	2	S	4007	4007	0	3.02	0.06	3.80	0.00	0.00	1.11	5.83	21.64
	3	S	3643	3643	0	4.11	0.07	4.34	0.00	0.00	3.06	7.50	21.12
	4	S	3228	3228	0	5.20	0.09	4.97	0.00	0.00	5.11	8.65	21.77
	5	S	2799	2799	0	5.92	0.11	5.57	0.00	0.00	5.81	10.52	23.31
	6	S	2228	2228	0	6.74	0.13	6.28	0.00	0.00	6.30	12.30	23.96
	7	S	2150	2150	0	8.83	0.15	6.99	0.00	0.02	10.04	14.80	24.12
	8	S	1695	1695	0	12.59	0.17	6.92	0.00	8.28	14.58	17.86	24.62
CO (g/s)	1	S	21714	21714	0	1.75E-03	9.30E-05	1.37E-02	0.00E+00	0.00E+00	1.00E-05	5.20E-04	5.28E-01
	2	S	4007	4007	0	6.40E-03	4.50E-04	2.85E-02	0.00E+00	0.00E+00	1.60E-04	2.21E-03	3.51E-01
	3	S	3643	3643	0	6.46E-03	4.82E-04	2.91E-02	0.00E+00	0.00E+00	6.10E-04	2.59E-03	4.26E-01
	4	S	3228	3228	0	5.57E-03	4.17E-04	2.37E-02	0.00E+00	0.00E+00	1.14E-03	3.00E-03	3.98E-01
	5	S	2799	2799	0	5.94E-03	4.25E-04	2.25E-02	0.00E+00	0.00E+00	1.35E-03	3.49E-03	3.70E-01
	6	S	2228	2228	0	5.89E-03	3.82E-04	1.81E-02	0.00E+00	0.00E+00	1.78E-03	4.42E-03	2.88E-01
	7	S	2150	2150	0	6.77E-03	3.42E-04	1.59E-02	0.00E+00	1.00E-05	2.98E-03	6.31E-03	2.15E-01
	8	S	1695	1695	0	7.78E-03	4.31E-04	1.77E-02	0.00E+00	1.69E-03	4.08E-03	7.41E-03	3.18E-01
NO (g/s)	1	S	21714	21714	0	0.012	0.000	0.023	0.000	0.000	0.001	0.019	0.221
	2	S	4007	4007	0	0.031	0.001	0.040	0.000	0.000	0.011	0.056	0.241
	3	S	3643	3643	0	0.044	0.001	0.046	0.000	0.000	0.030	0.081	0.216
	4	S	3228	3228	0	0.055	0.001	0.053	0.000	0.000	0.050	0.100	0.222
	5	S	2799	2799	0	0.060	0.001	0.058	0.000	0.000	0.056	0.109	0.260
	6	S	2228	2228	0	0.065	0.001	0.064	0.000	0.000	0.058	0.120	0.257
	7	S	2150	2150	0	0.081	0.001	0.069	0.000	0.000	0.087	0.141	0.278
	8	S	1695	1695	0	0.111	0.002	0.069	0.000	0.049	0.127	0.166	0.265
NO_2 (g/s)	1	S	21714	21714	0	1.40E-03	1.80E-05	2.64E-03	0.00E+00	0.00E+00	3.00E-04	1.93E-03	4.00E-02
	2	S	4007	4007	0	2.78E-03	6.60E-05	4.17E-03	0.00E+00	0.00E+00	1.15E-03	3.92E-03	4.15E-02
	3	S	3643	3643	0	3.34E-03	7.40E-05	4.50E-03	0.00E+00	0.00E+00	1.86E-03	4.77E-03	3.19E-02
	4	S	3228	3228	0	3.88E-03	8.70E-05	4.93E-03	0.00E+00	0.00E+00	2.45E-03	5.66E-03	4.25E-02
	5	S	2799	2799	0	3.82E-03	9.30E-05	4.90E-03	0.00E+00	0.00E+00	2.33E-03	5.86E-03	5.48E-02
	6	S	2228	2228	0	3.86E-03	1.02E-04	4.81E-03	0.00E+00	0.00E+00	2.40E-03	6.01E-03	4.14E-02
	7	S	2150	2150	0	4.83E-03	1.19E-04	5.53E-03	0.00E+00	1.00E-05	3.37E-03	7.27E-03	4.10E-02
	8	S	1695	1695	0	6.43E-03	1.37E-04	5.66E-03	0.00E+00	2.10E-03	5.53E-03	9.10E-03	3.86E-02
NOx (g/s)	1	S	21714	21714	0	0.013	0.000	0.025	0.000	0.000	0.001	0.022	0.243
	2	S	4007	4007	0	0.034	0.001	0.043	0.000	0.000	0.013	0.060	0.250
	3	S	3643	3643	0	0.047	0.001	0.049	0.000	0.000	0.034	0.087	0.229
	4	S	3228	3228	0	0.059	0.001	0.056	0.000	0.000	0.055	0.107	0.235
	5	S	2799	2799	0	0.064	0.001	0.061	0.000	0.000	0.061	0.116	0.277
	6	S	2228	2228	0	0.069	0.001	0.067	0.000	0.000	0.062	0.128	0.272
	7	S	2150	2150	0	0.086	0.002	0.073	0.000	0.000	0.092	0.150	0.294
	8	S	1695	1695	0	0.117	0.002	0.072	0.000	0.054	0.135	0.175	0.283
HC (g/s)	1	S	21714	21714	0	6.70E-05	1.00E-06	1.46E-04	0.00E+00	0.00E+00	2.00E-05	8.00E-05	6.58E-03
	2	S	4007	4007	0	1.53E-04	4.00E-06	2.57E-04	0.00E+00	0.00E+00	6.00E-05	2.30E-04	5.64E-03
	3	S	3643	3643	0	2.13E-04	5.00E-06	3.05E-04	0.00E+00	0.00E+00	1.30E-04	3.10E-04	3.65E-03
	4	S	3228	3228	0	2.80E-04	7.00E-06	3.96E-04	0.00E+00	0.00E+00	2.00E-04	4.10E-04	8.97E-03
	5	S	2799	2799	0	3.69E-04	1.50E-05	7.88E-04	0.00E+00	0.00E+00	2.50E-04	5.00E-04	2.63E-02
	6	S	2228	2228	0	4.76E-04	2.40E-05	1.12E-03	0.00E+00	0.00E+00	2.90E-04	6.00E-04	2.39E-02
	7	S	2150	2150	0	6.66E-04	3.40E-05	1.60E-03	0.00E+00	0.00E+00	4.40E-04	7.53E-04	3.09E-02
	8	S	1695	1695	0	1.01E-03	4.90E-05	2.04E-03	0.00E+00	3.80E-04	6.80E-04	1.02E-03	3.04E-02

Table E-5: Descriptive statistics of PHEV Sprinter driving and road-based data by VSP bin for Suburban travel during charge-sustaining operation.

	VSP Bin	Road Code	Total	N	N Missing	Mean	SE Mean	Std. Dev.	Minimum	Q1	Median	Q3	Maximum
Velocity (km/h)	1	S	21714	21714	0	22.4	0.1	20.0	0.0	0.0	21.4	41.5	65.9
	2	S	4007	4007	0	35.0	0.3	16.9	0.0	19.3	40.9	49.0	62.3
	3	S	3643	3643	0	37.8	0.3	15.2	0.7	27.1	43.3	49.8	62.2
	4	S	3228	3228	0	38.0	0.3	14.2	1.4	27.5	43.0	49.2	65.6
	5	S	2799	2799	0	36.7	0.3	13.4	0.9	26.4	40.3	47.8	62.7
	6	S	2228	2228	0	35.6	0.3	12.2	2.8	25.7	37.3	46.2	60.7
	7	S	2150	2150	0	35.6	0.2	10.8	0.7	27.2	36.3	44.2	65.2
	8	S	1695	1695	0	38.0	0.2	9.3	1.0	32.1	38.3	45.2	62.8
Positive Accel (m/s^2)	1	S	21714	9246	12468	0.060	0.002	0.164	0.000	0.000	0.000	0.031	2.810
	2	S	4007	2119	1888	0.290	0.007	0.312	0.000	0.078	0.189	0.385	2.269
	3	S	3643	2525	1118	0.381	0.007	0.372	0.000	0.116	0.266	0.534	2.254
	4	S	3228	2472	756	0.492	0.009	0.448	0.000	0.156	0.350	0.708	2.705
	5	S	2799	2344	455	0.643	0.010	0.503	0.000	0.238	0.515	0.948	2.568
	6	S	2228	1981	247	0.755	0.012	0.522	0.000	0.314	0.691	1.102	2.533
	7	S	2150	2006	144	0.870	0.011	0.511	0.000	0.458	0.880	1.211	2.464
	8	S	1695	1605	90	0.898	0.013	0.518	0.000	0.483	0.873	1.272	2.825
Negative Accel (m/s^2)	1	S	21714	12465	9249	-0.690	0.005	0.503	-3.063	-1.077	-0.604	-0.245	0.000
	2	S	4007	1888	2119	-0.284	0.007	0.299	-2.052	-0.389	-0.184	-0.074	0.000
	3	S	3643	1118	2525	-0.220	0.007	0.236	-1.819	-0.298	-0.149	-0.060	0.000
	4	S	3228	756	2472	-0.168	0.006	0.164	-1.572	-0.232	-0.123	-0.054	0.000
	5	S	2799	455	2344	-0.159	0.007	0.158	-1.229	-0.218	-0.121	-0.050	0.000
	6	S	2228	247	1981	-0.152	0.009	0.142	-1.096	-0.215	-0.107	-0.054	0.000
	7	S	2150	144	2006	-0.151	0.013	0.154	-0.967	-0.193	-0.103	-0.052	0.000
	8	S	1695	90	1605	-0.171	0.017	0.164	-1.031	-0.285	-0.109	-0.045	-0.001
Positive Grade (%)	1	S	21714	11973	9741	2.27%	0.33%	36.12%	0.00%	0.00%	0.00%	1.56%	3389.74%
	2	S	4007	2095	1912	7.62%	3.76%	172.26%	0.00%	0.00%	1.61%	4.67%	7866.10%
	3	S	3643	2178	1465	3.51%	0.14%	6.44%	0.00%	0.00%	1.57%	3.92%	97.71%
	4	S	3228	2254	974	3.56%	0.14%	6.60%	0.00%	0.72%	2.07%	3.92%	103.74%
	5	S	2799	2017	782	3.93%	0.22%	9.64%	0.00%	0.93%	2.55%	4.59%	336.48%
	6	S	2228	1753	475	3.98%	0.14%	5.98%	0.00%	1.19%	2.94%	5.10%	101.43%
	7	S	2150	1765	385	4.58%	0.39%	16.23%	0.00%	1.23%	3.10%	5.76%	587.20%
	8	S	1695	1576	119	7.14%	0.48%	19.01%	0.00%	2.29%	4.96%	8.17%	580.78%
Negative Grade (%)	1	S	21714	9738	11976	-6.52%	0.20%	20.08%	-1505.58%	-6.89%	-4.26%	-2.31%	-0.15%
	2	S	4007	1912	2095	-3.02%	0.06%	2.60%	-21.57%	-3.96%	-2.28%	-1.36%	-0.33%
	3	S	3643	1465	2178	-2.76%	0.06%	2.14%	-17.88%	-3.74%	-2.15%	-1.33%	-0.32%
	4	S	3228	974	2254	-2.79%	0.06%	1.96%	-14.78%	-3.74%	-2.23%	-1.37%	-0.62%
	5	S	2799	782	2017	-2.78%	0.06%	1.75%	-12.65%	-3.79%	-2.31%	-1.45%	-0.59%
	6	S	2228	475	1753	-2.41%	0.06%	1.39%	-7.05%	-3.17%	-2.02%	-1.30%	-0.62%
	7	S	2150	385	1765	-2.19%	0.06%	1.15%	-7.36%	-2.83%	-1.92%	-1.28%	-0.70%
	8	S	1695	119	1576	-1.67%	0.08%	0.90%	-4.21%	-2.11%	-1.25%	-1.02%	-0.66%

Table E-6: Descriptive statistics of PHEV Sprinter power data by VSP bin for Suburban travel during charge-sustaining operation.

	VSP Bin	Road Code	Total	N	N Missing	Mean	SE Mean	Std. Dev.	Minimum	Q1	Median	Q3	Maximum
Diesel ICE Power (W/kg/s)	1	S	21714	21714	0	0.82	0.02	2.69	-2.85	0.00	0.00	1.71	24.45
	2	S	4007	4007	0	3.40	0.08	4.90	-2.76	0.00	0.00	8.04	23.04
	3	S	3643	3643	0	5.27	0.10	5.83	-3.50	0.00	3.93	10.11	31.78
	4	S	3228	3228	0	6.68	0.12	6.53	-3.05	0.00	7.95	11.85	28.24
	5	S	2799	2799	0	7.88	0.14	7.50	-4.35	0.00	8.94	14.64	29.92
	6	S	2228	2228	0	8.86	0.18	8.39	-3.86	0.00	9.91	16.45	27.94
	7	S	2150	2150	0	11.61	0.20	9.15	-4.86	0.00	14.42	19.45	29.75
	8	S	1695	1695	0	16.46	0.22	9.13	-3.51	13.16	18.84	23.24	31.78
Electric Motor Power (W/kg/s)	1	S	21714	21714	0	0.24	0.01	1.05	0.00	0.00	0.00	0.00	19.30
	2	S	4007	4007	0	1.04	0.04	2.31	0.00	0.00	0.00	0.52	15.36
	3	S	3643	3643	0	1.69	0.05	3.07	0.00	0.00	0.00	2.57	16.05
	4	S	3228	3228	0	2.44	0.07	3.94	0.00	0.00	0.00	4.85	19.96
	5	S	2799	2799	0	3.55	0.09	4.96	0.00	0.00	0.00	8.42	21.52
	6	S	2228	2228	0	4.60	0.12	5.77	0.00	0.00	0.00	10.81	21.14
	7	S	2150	2150	0	4.41	0.14	6.37	0.00	0.00	0.00	11.07	21.23
	8	S	1695	1695	0	2.86	0.15	6.02	0.00	0.00	0.00	0.02	21.65
Total Power (W/kg/s)	1	S	21714	21714	0	1.06	0.02	2.82	-2.85	0.00	0.33	1.80	24.45
	2	S	4007	4007	0	4.44	0.07	4.72	-2.76	0.10	3.35	8.46	23.04
	3	S	3643	3643	0	6.96	0.08	5.08	-3.05	2.81	7.64	10.48	31.78
	4	S	3228	3228	0	9.13	0.09	5.10	-2.92	5.93	9.64	12.22	28.24
	5	S	2799	2799	0	11.42	0.10	5.15	-2.87	8.68	11.32	14.98	31.97
	6	S	2228	2228	0	13.46	0.11	5.15	-2.25	10.53	13.35	17.01	27.94
	7	S	2150	2150	0	16.02	0.12	5.36	-2.16	12.55	16.12	19.97	30.19
	8	S	1695	1695	0	19.32	0.14	5.61	-1.75	16.16	19.52	23.45	31.78
Recup (W/kg/s)	1	S	21714	21714	0	-1.41	0.01	1.61	-12.69	-1.57	-1.31	0.00	0.58
	2	S	4007	4007	0	-2.39	0.04	2.78	-12.83	-4.63	-1.22	0.00	0.00
	3	S	3643	3643	0	-3.08	0.06	3.29	-12.87	-6.22	-1.47	0.00	0.00
	4	S	3228	3228	0	-3.42	0.06	3.59	-13.02	-6.69	-2.25	0.00	0.00
	5	S	2799	2799	0	-3.64	0.08	3.99	-13.08	-7.71	-2.00	0.00	0.00
	6	S	2228	2228	0	-3.59	0.09	4.23	-13.01	-7.72	0.00	0.00	0.00
	7	S	2150	2150	0	-3.97	0.10	4.38	-13.12	-8.10	-2.25	0.00	0.00
	8	S	1695	1695	0	-4.64	0.10	4.21	-13.10	-8.22	-4.54	0.00	0.00

Table E-7: Descriptive statistics of PHEV Sprinter emissions data by VSP bin for Urban travel during charge-sustaining operation.

	VSP Bin	Road Code	Total	N	N Missing	Mean	SE Mean	Std. Dev.	Minimum	Q1	Median	Q3	Maximum
Fuel (gal/s)	1	U	5832	5832	0	1.03E-04	3.00E-06	1.97E-04	0.00E+00	0.00E+00	1.30E-05	1.70E-04	2.08E-03
	2	U	752	752	0	2.73E-04	1.30E-05	3.47E-04	0.00E+00	0.00E+00	1.24E-04	4.33E-04	1.93E-03
	3	U	667	667	0	3.81E-04	1.70E-05	4.45E-04	0.00E+00	0.00E+00	2.15E-04	6.39E-04	1.84E-03
	4	U	602	602	0	4.78E-04	2.00E-05	4.79E-04	0.00E+00	0.00E+00	4.02E-04	8.90E-04	2.06E-03
	5	U	526	526	0	5.77E-04	2.30E-05	5.26E-04	0.00E+00	0.00E+00	5.53E-04	1.03E-03	1.96E-03
	6	U	358	358	0	6.50E-04	3.00E-05	5.60E-04	0.00E+00	5.00E-06	6.63E-04	1.13E-03	1.98E-03
	7	U	312	312	0	8.32E-04	3.50E-05	6.09E-04	0.00E+00	1.72E-04	9.96E-04	1.34E-03	2.17E-03
	8	U	276	276	0	7.30E-04	3.90E-05	6.43E-04	0.00E+00	2.30E-05	6.79E-04	1.34E-03	2.33E-03
CO_2 (g/s)	1	U	5832	5832	0	1.06	0.03	2.02	0.00	0.00	0.08	1.76	21.44
	2	U	752	752	0	2.79	0.13	3.55	0.00	0.00	1.29	4.44	19.90
	3	U	667	667	0	3.91	0.18	4.56	0.00	0.00	2.22	6.58	18.91
	4	U	602	602	0	4.91	0.20	4.92	0.00	0.00	4.12	9.15	21.13
	5	U	526	526	0	5.93	0.24	5.41	0.00	0.00	5.70	10.55	20.12
	6	U	358	358	0	6.68	0.31	5.77	0.00	0.01	6.83	11.62	20.38
	7	U	312	312	0	8.55	0.36	6.27	0.00	1.77	10.26	13.79	22.40
	8	U	276	276	0	7.50	0.40	6.62	0.00	0.19	7.01	13.71	24.05
CO (g/s)	1	U	5832	5832	0	1.92E-03	1.79E-04	1.36E-02	0.00E+00	0.00E+00	1.00E-05	5.80E-04	4.03E-01
	2	U	752	752	0	1.26E-02	1.53E-03	4.20E-02	0.00E+00	0.00E+00	4.00E-04	3.64E-03	3.33E-01
	3	U	667	667	0	9.77E-03	1.33E-03	3.42E-02	0.00E+00	0.00E+00	5.70E-04	3.72E-03	3.66E-01
	4	U	602	602	0	8.76E-03	1.18E-03	2.90E-02	0.00E+00	0.00E+00	1.23E-03	4.03E-03	2.84E-01
	5	U	526	526	0	8.85E-03	1.30E-03	2.98E-02	0.00E+00	0.00E+00	1.56E-03	5.06E-03	3.42E-01
	6	U	358	358	0	9.66E-03	1.42E-03	2.70E-02	0.00E+00	1.00E-05	2.26E-03	6.04E-03	2.65E-01
	7	U	312	312	0	1.51E-02	2.11E-03	3.73E-02	0.00E+00	3.80E-04	3.74E-03	1.11E-02	3.16E-01
	8	U	276	276	0	1.40E-02	2.00E-03	3.33E-02	0.00E+00	1.00E-05	2.75E-03	1.03E-02	2.27E-01
NO (g/s)	1	U	5832	5832	0	0.012	0.000	0.021	0.000	0.000	0.001	0.020	0.172
	2	U	752	752	0	0.028	0.001	0.036	0.000	0.000	0.015	0.045	0.236
	3	U	667	667	0	0.039	0.002	0.046	0.000	0.000	0.022	0.067	0.244
	4	U	602	602	0	0.049	0.002	0.050	0.000	0.000	0.040	0.087	0.219
	5	U	526	526	0	0.059	0.002	0.056	0.000	0.000	0.050	0.102	0.269
	6	U	358	358	0	0.062	0.003	0.057	0.000	0.000	0.055	0.113	0.210
	7	U	312	312	0	0.078	0.003	0.062	0.000	0.013	0.088	0.130	0.264
	8	U	276	276	0	0.067	0.004	0.065	0.000	0.001	0.052	0.120	0.221
NO_2 (g/s)	1	U	5832	5832	0	1.37E-03	3.20E-05	2.41E-03	0.00E+00	0.00E+00	2.60E-04	2.08E-03	3.35E-02
	2	U	752	752	0	2.73E-03	1.55E-04	4.26E-03	0.00E+00	0.00E+00	1.01E-03	3.83E-03	4.30E-02
	3	U	667	667	0	2.98E-03	1.63E-04	4.20E-03	0.00E+00	0.00E+00	1.47E-03	4.04E-03	3.15E-02
	4	U	602	602	0	3.22E-03	1.68E-04	4.12E-03	0.00E+00	0.00E+00	1.97E-03	4.87E-03	2.82E-02
	5	U	526	526	0	3.69E-03	1.97E-04	4.52E-03	0.00E+00	0.00E+00	2.41E-03	5.45E-03	3.18E-02
	6	U	358	358	0	4.04E-03	2.45E-04	4.63E-03	0.00E+00	1.80E-05	2.85E-03	6.03E-03	2.78E-02
	7	U	312	312	0	4.69E-03	2.74E-04	4.85E-03	0.00E+00	6.00E-04	3.84E-03	6.86E-03	4.02E-02
	8	U	276	276	0	4.27E-03	2.67E-04	4.43E-03	0.00E+00	3.55E-04	3.40E-03	6.61E-03	2.47E-02
NOx (g/s)	1	U	5832	5832	0	0.013	0.000	0.023	0.000	0.000	0.001	0.023	0.185
	2	U	752	752	0	0.031	0.001	0.039	0.000	0.000	0.017	0.050	0.240
	3	U	667	667	0	0.042	0.002	0.048	0.000	0.000	0.025	0.071	0.249
	4	U	602	602	0	0.052	0.002	0.053	0.000	0.000	0.044	0.091	0.224
	5	U	526	526	0	0.062	0.003	0.059	0.000	0.000	0.054	0.108	0.277
	6	U	358	358	0	0.066	0.003	0.060	0.000	0.000	0.059	0.118	0.218
	7	U	312	312	0	0.082	0.004	0.065	0.000	0.016	0.092	0.135	0.277
	8	U	276	276	0	0.071	0.004	0.067	0.000	0.001	0.057	0.128	0.228
HC (g/s)	1	U	5832	5832	0	8.50E-05	2.00E-06	1.76E-04	0.00E+00	0.00E+00	2.00E-05	9.00E-05	3.00E-03
	2	U	752	752	0	2.14E-04	1.40E-05	3.88E-04	0.00E+00	0.00E+00	8.00E-05	2.70E-04	4.54E-03
	3	U	667	667	0	2.71E-04	1.60E-05	4.25E-04	0.00E+00	0.00E+00	1.20E-04	3.60E-04	3.34E-03
	4	U	602	602	0	3.20E-04	2.20E-05	5.31E-04	0.00E+00	0.00E+00	2.10E-04	4.30E-04	7.60E-03
	5	U	526	526	0	4.18E-04	2.80E-05	6.40E-04	0.00E+00	0.00E+00	2.80E-04	5.50E-04	7.94E-03
	6	U	358	358	0	5.09E-04	4.20E-05	7.88E-04	0.00E+00	0.00E+00	3.15E-04	6.00E-04	6.03E-03
	7	U	312	312	0	9.35E-04	1.37E-04	2.42E-03	0.00E+00	8.00E-05	4.85E-04	8.28E-04	3.10E-02
	8	U	276	276	0	9.14E-04	1.55E-04	2.57E-03	0.00E+00	2.00E-05	3.10E-04	7.90E-04	2.94E-02

Table E-8: Descriptive statistics of PHEV Sprinter driving and road-based data by VSP bin for Urban travel during charge-sustaining operation.

	VSP Bin	Road Code	Total	N	N Missing	Mean	SE Mean	Std. Dev.	Minimum	Q1	Median	Q3	Maximum
Velocity (km/h)	1	U	5832	5832	0	12.3	0.2	14.1	0.0	0.0	6.2	23.7	54.6
	2	U	752	752	0	22.3	0.5	12.7	0.0	11.5	22.3	33.0	49.3
	3	U	667	667	0	26.2	0.5	11.8	0.0	16.8	27.7	35.0	49.9
	4	U	602	602	0	27.6	0.4	10.4	2.7	20.2	28.3	35.7	49.7
	5	U	526	526	0	28.4	0.5	10.8	0.0	20.7	30.0	36.7	53.7
	6	U	358	358	0	28.1	0.5	10.1	0.4	21.1	28.1	35.8	51.7
	7	U	312	312	0	29.1	0.5	8.8	2.7	23.1	29.2	34.8	51.1
	8	U	276	276	0	29.9	0.6	10.3	0.0	24.5	31.6	37.2	48.5
Positive Accel (m/s^2)	1	U	5832	3291	2541	0.073	0.003	0.196	0.000	0.000	0.000	0.000	2.146
	2	U	752	494	258	0.393	0.017	0.374	0.000	0.100	0.269	0.579	2.240
	3	U	667	494	173	0.477	0.018	0.394	0.000	0.180	0.383	0.675	2.424
	4	U	602	483	119	0.600	0.020	0.430	0.015	0.267	0.501	0.836	2.202
	5	U	526	454	72	0.664	0.024	0.518	0.000	0.230	0.561	0.935	2.540
	6	U	358	332	26	0.755	0.029	0.528	0.002	0.323	0.646	1.094	2.369
	7	U	312	293	19	0.822	0.031	0.533	0.005	0.353	0.754	1.207	2.286
	8	U	276	236	40	0.683	0.030	0.456	0.003	0.303	0.596	1.005	2.388
Negative Accel (m/s^2)	1	U	5832	2541	3291	-0.644	0.009	0.463	-2.487	-0.978	-0.577	-0.245	0.000
	2	U	752	258	494	-0.324	0.020	0.325	-1.483	-0.462	-0.203	-0.076	0.000
	3	U	667	173	494	-0.221	0.017	0.221	-1.333	-0.313	-0.160	-0.067	-0.001
	4	U	602	119	483	-0.219	0.023	0.246	-1.279	-0.294	-0.132	-0.051	-0.001
	5	U	526	72	454	-0.201	0.022	0.185	-0.889	-0.258	-0.159	-0.069	-0.001
	6	U	358	26	332	-0.214	0.040	0.203	-0.923	-0.310	-0.179	-0.067	-0.002
	7	U	312	19	293	-0.369	0.077	0.337	-1.082	-0.666	-0.262	-0.076	-0.001
	8	U	276	40	236	-0.322	0.057	0.360	-1.312	-0.550	-0.161	-0.055	-0.001
Positive Grade (%)	1	U	5832	3409	2423	52.40%	50.20%	2930.00%	0.00%	0.00%	0.00%	0.00%	171042.00%
	2	U	752	421	331	6.33%	2.62%	53.80%	0.00%	0.00%	1.01%	4.49%	1035.01%
	3	U	667	452	215	3.79%	0.31%	6.68%	0.00%	0.00%	1.74%	4.68%	53.46%
	4	U	602	439	163	4.61%	0.40%	8.40%	0.00%	0.79%	2.46%	5.07%	87.03%
	5	U	526	443	83	6.74%	0.88%	18.46%	0.00%	1.55%	3.72%	6.64%	330.76%
	6	U	358	311	47	12.72%	3.89%	68.58%	0.00%	2.05%	4.28%	7.25%	1019.62%
	7	U	312	298	14	7.66%	0.79%	13.56%	0.00%	2.56%	5.65%	8.67%	171.49%
	8	U	276	276	0	705.00%	671.00%	11152.00%	0.00%	8.00%	12.00%	30.00%	185296.00%
Negative Grade (%)	1	U	5832	2423	3409	-10.43%	0.68%	33.30%	-1178.40%	-9.87%	-5.76%	-3.11%	-0.07%
	2	U	752	331	421	-4.39%	0.19%	3.50%	-20.10%	-6.02%	-3.65%	-1.81%	-0.03%
	3	U	667	215	452	-3.50%	0.19%	2.73%	-16.50%	-4.47%	-2.65%	-1.67%	-0.09%
	4	U	602	163	439	-2.90%	0.16%	2.02%	-11.77%	-3.65%	-2.42%	-1.39%	0.00%
	5	U	526	83	443	-2.60%	0.19%	1.68%	-8.31%	-3.57%	-2.21%	-1.28%	-0.01%
	6	U	358	47	311	-2.16%	0.25%	1.69%	-7.21%	-3.28%	-1.69%	-1.05%	-0.10%
	7	U	312	14	298	-2.11%	0.32%	1.20%	-4.33%	-2.97%	-2.07%	-1.18%	-0.28%
	8	U	276	0	276	*	*	*	*	*	*	*	*

Table E-9: Descriptive statistics of PHEV Sprinter power data by VSP bin for Urban travel during charge-sustaining operation.

	VSP Bin	Road Code	Total	N	N Missing	Mean	SE Mean	Std. Dev.	Minimum	Q1	Median	Q3	Maximum
Diesel ICE Power (W/kg/s)	1	U	5832	5832	0	0.83	0.03	2.15	-3.18	0.00	0.00	1.81	21.15
	2	U	752	752	0	2.79	0.16	4.41	-3.81	0.00	0.00	5.06	19.15
	3	U	667	667	0	4.45	0.21	5.52	-2.75	0.00	1.50	8.30	20.87
	4	U	602	602	0	6.18	0.25	6.21	-2.21	0.00	7.08	11.27	22.51
	5	U	526	526	0	7.62	0.30	6.87	-2.82	0.00	9.58	12.52	23.40
	6	U	358	358	0	9.01	0.39	7.35	-2.35	0.00	12.05	13.70	31.38
	7	U	312	312	0	11.91	0.42	7.36	-3.44	3.40	14.45	16.27	29.81
	8	U	276	276	0	12.25	0.54	9.00	-1.72	1.39	15.97	18.99	31.63
Electric Motor Power (W/kg/s)	1	U	5832	5832	0	0.26	0.01	0.87	0.00	0.00	0.00	0.32	12.74
	2	U	752	752	0	1.29	0.09	2.46	0.00	0.00	0.00	1.24	12.48
	3	U	667	667	0	2.04	0.13	3.26	0.00	0.00	0.00	4.50	14.71
	4	U	602	602	0	2.67	0.17	4.08	0.00	0.00	0.00	6.16	15.82
	5	U	526	526	0	3.15	0.20	4.64	0.00	0.00	0.00	7.76	16.47
	6	U	358	358	0	3.25	0.28	5.22	0.00	0.00	0.00	7.83	17.38
	7	U	312	312	0	2.74	0.31	5.43	0.00	0.00	0.00	0.06	21.61
	8	U	276	276	0	1.82	0.28	4.71	0.00	0.00	0.00	0.00	20.10
Total Power (W/kg/s)	1	U	5832	5832	0	1.10	0.03	2.22	-3.16	0.00	0.44	1.82	21.15
	2	U	752	752	0	4.07	0.16	4.27	-2.80	0.30	3.93	5.76	19.15
	3	U	667	667	0	6.49	0.19	4.77	-2.44	3.18	6.43	9.48	20.87
	4	U	602	602	0	8.85	0.20	4.79	-2.21	6.70	9.09	11.86	22.51
	5	U	526	526	0	10.76	0.21	4.70	-2.82	8.84	10.72	13.32	23.40
	6	U	358	358	0	12.26	0.26	4.89	-2.35	10.88	12.65	14.05	31.38
	7	U	312	312	0	14.65	0.27	4.70	-2.76	13.42	14.96	16.48	29.81
	8	U	276	276	0	14.06	0.48	7.98	-1.72	8.71	17.01	19.59	31.63
Recup (W/kg/s)	1	U	5832	5832	0	-1.04	0.02	1.26	-10.96	-1.53	-1.10	0.00	0.00
	2	U	752	752	0	-1.59	0.09	2.33	-11.35	-1.99	-0.66	0.00	0.00
	3	U	667	667	0	-2.18	0.12	2.97	-11.73	-4.21	-0.54	0.00	0.00
	4	U	602	602	0	-2.72	0.14	3.41	-12.21	-5.67	0.00	0.00	0.00
	5	U	526	526	0	-3.12	0.16	3.71	-11.64	-6.58	0.00	0.00	0.13
	6	U	358	358	0	-3.39	0.21	4.03	-12.86	-7.61	-0.30	0.00	0.00
	7	U	312	312	0	-3.72	0.23	4.01	-12.93	-8.05	-1.77	0.00	0.00
	8	U	276	276	0	-4.30	0.25	4.07	-12.85	-8.13	-3.70	0.00	0.00

Table E-10: Descriptive statistics of PHEV Sprinter emissions data by VSP bin for Highway travel during charge-depleting operation.

Variable	VSP Bin	Rd Code	N	Mean	Std. Dev.	Median	Minimum	Maximum
Fuel (gal/s)	1	Hwy	1263	1.91E-04	2.67E-04	4.30E-05	0.00E+00	1.32E-03
	2	Hwy	440	5.20E-04	3.26E-04	4.95E-04	0.00E+00	1.24E-03
	3	Hwy	545	6.39E-04	3.11E-04	6.56E-04	0.00E+00	1.33E-03
	4	Hwy	541	7.21E-04	2.99E-04	7.55E-04	0.00E+00	1.70E-03
	5	Hwy	618	8.06E-04	3.26E-04	8.30E-04	0.00E+00	2.13E-03
	6	Hwy	586	8.76E-04	3.66E-04	9.11E-04	0.00E+00	2.32E-03
	7	Hwy	678	9.97E-04	3.58E-04	1.02E-03	0.00E+00	2.22E-03
	8	Hwy	618	1.29E-03	4.00E-04	1.28E-03	0.00E+00	2.23E-03
CO_2 (g/s)	1	Hwy	1263	1.95	2.77	0.46	0.00	13.58
	2	Hwy	440	5.37	3.36	5.12	0.00	12.81
	3	Hwy	545	6.60	3.21	6.77	0.00	13.73
	4	Hwy	541	7.44	3.08	7.79	0.00	17.47
	5	Hwy	618	8.31	3.36	8.56	0.00	21.92
	6	Hwy	586	9.04	3.77	9.40	0.00	23.90
	7	Hwy	678	10.28	3.69	10.50	0.00	22.87
	8	Hwy	618	13.28	4.13	13.20	0.00	22.96
CO (g/s)	1	Hwy	1263	1.18E-03	2.07E-03	1.20E-04	0.00E+00	2.12E-02
	2	Hwy	440	2.34E-03	1.94E-03	2.05E-03	0.00E+00	1.08E-02
	3	Hwy	545	2.77E-03	4.14E-03	2.31E-03	0.00E+00	6.54E-02
	4	Hwy	541	2.53E-03	1.79E-03	2.33E-03	0.00E+00	1.65E-02
	5	Hwy	618	3.91E-03	1.82E-02	2.45E-03	0.00E+00	4.24E-01
	6	Hwy	586	2.88E-03	3.62E-03	2.45E-03	0.00E+00	4.96E-02
	7	Hwy	678	5.04E-03	1.32E-02	2.75E-03	0.00E+00	1.50E-01
	8	Hwy	618	7.51E-03	2.12E-02	3.70E-03	0.00E+00	2.95E-01
NO (g/s)	1	Hwy	1263	0.017	0.024	0.005	0.000	0.143
	2	Hwy	440	0.043	0.033	0.036	0.000	0.145
	3	Hwy	545	0.055	0.035	0.049	0.000	0.149
	4	Hwy	541	0.066	0.036	0.061	0.000	0.200
	5	Hwy	618	0.077	0.038	0.076	0.000	0.217
	6	Hwy	586	0.089	0.044	0.091	0.000	0.233
	7	Hwy	678	0.104	0.043	0.108	0.000	0.249
	8	Hwy	618	0.135	0.046	0.138	0.000	0.260
NO_2 (g/s)	1	Hwy	1263	1.19E-03	1.74E-03	4.70E-04	0.00E+00	1.38E-02
	2	Hwy	440	2.26E-03	2.23E-03	1.75E-03	0.00E+00	1.35E-02
	3	Hwy	545	2.70E-03	2.55E-03	1.87E-03	0.00E+00	1.33E-02
	4	Hwy	541	2.80E-03	2.38E-03	2.24E-03	0.00E+00	1.34E-02
	5	Hwy	618	2.99E-03	2.72E-03	2.39E-03	0.00E+00	1.37E-02
	6	Hwy	586	3.02E-03	2.94E-03	2.33E-03	0.00E+00	1.38E-02
	7	Hwy	678	2.70E-03	2.61E-03	2.19E-03	0.00E+00	1.34E-02
	8	Hwy	618	2.64E-03	2.69E-03	1.96E-03	0.00E+00	1.36E-02
NOx (g/s)	1	Hwy	1263	0.018	0.025	0.006	0.000	0.155
	2	Hwy	440	0.045	0.034	0.038	0.000	0.159
	3	Hwy	545	0.058	0.037	0.051	0.000	0.160
	4	Hwy	541	0.069	0.037	0.063	0.000	0.209
	5	Hwy	618	0.080	0.040	0.079	0.000	0.221
	6	Hwy	586	0.092	0.045	0.094	0.000	0.235
	7	Hwy	678	0.107	0.044	0.111	0.000	0.256
	8	Hwy	618	0.137	0.047	0.142	0.000	0.267
HC (g/s)	1	Hwy	1263	2.05E-04	2.18E-04	1.40E-04	0.00E+00	1.05E-03
	2	Hwy	440	4.06E-04	2.57E-04	3.90E-04	0.00E+00	2.38E-03
	3	Hwy	545	4.70E-04	2.66E-04	4.60E-04	0.00E+00	2.97E-03
	4	Hwy	541	5.12E-04	2.73E-04	4.90E-04	0.00E+00	2.20E-03
	5	Hwy	618	6.22E-04	8.20E-04	5.20E-04	0.00E+00	1.13E-02
	6	Hwy	586	7.14E-04	1.17E-03	5.60E-04	0.00E+00	1.83E-02
	7	Hwy	678	1.03E-03	2.26E-03	6.90E-04	0.00E+00	3.68E-02

Table E-11: Descriptive statistics of PHEV Sprinter road-based and driving data by VSP bin for Highway travel during charge-depleting operation.

Variable	VSP Bin	Rd Code	N	Mean	Std. Dev.	Median	Minimum	Maximum
Velocity (km/h)	1	Hwy	1263	59.8	30.4	72.1	0.0	93.1
	2	Hwy	440	76.2	18.8	84.2	1.5	92.2
	3	Hwy	545	78.3	16.3	84.8	0.9	93.4
	4	Hwy	541	79.1	14.2	84.8	1.1	93.0
	5	Hwy	618	77.6	14.3	82.9	8.1	91.7
	6	Hwy	586	77.3	13.6	82.6	13.7	91.9
	7	Hwy	678	76.3	14.4	81.2	15.8	91.7
	8	Hwy	618	76.9	12.4	81.0	17.0	91.4
Positive Accel (m/s^2)	1	Hwy	274	0.049	0.123	0.000	0.000	1.267
	2	Hwy	208	0.132	0.184	0.065	0.000	1.330
	3	Hwy	279	0.160	0.247	0.094	0.001	2.197
	4	Hwy	286	0.170	0.227	0.121	0.000	1.943
	5	Hwy	333	0.242	0.324	0.140	0.000	2.262
	6	Hwy	349	0.233	0.284	0.152	0.000	1.982
	7	Hwy	507	0.257	0.331	0.130	0.001	2.046
	8	Hwy	595	0.289	0.289	0.190	0.005	2.465
Negative Accel (m/s^2)	1	Hwy	989	-0.441	0.489	-0.229	-3.429	-0.002
	2	Hwy	232	-0.137	0.113	-0.103	-0.514	-0.001
	3	Hwy	266	-0.131	0.103	-0.106	-0.430	-0.001
	4	Hwy	255	-0.118	0.085	-0.105	-0.394	0.000
	5	Hwy	285	-0.098	0.068	-0.088	-0.364	-0.001
	6	Hwy	237	-0.077	0.061	-0.069	-0.303	0.000
	7	Hwy	171	-0.050	0.043	-0.040	-0.186	0.000
	8	Hwy	23	-0.048	0.046	-0.036	-0.179	-0.002
Positive Grade (%)	1	Hwy	372	1.11%	2.40%	0.00%	0.00%	22.79%
	2	Hwy	83	1.20%	1.15%	0.98%	0.00%	4.54%
	3	Hwy	157	2.20%	6.94%	1.33%	0.00%	83.94%
	4	Hwy	239	1.90%	8.77%	1.25%	0.00%	135.98%
	5	Hwy	375	1.60%	1.12%	1.63%	0.00%	8.84%
	6	Hwy	436	1.84%	1.07%	1.80%	0.00%	5.89%
	7	Hwy	565	2.09%	1.11%	2.11%	0.00%	6.32%
	8	Hwy	554	2.88%	1.92%	2.75%	0.00%	36.40%
Negative Grade (%)	1	Hwy	891	-2.88%	1.66%	-2.80%	-18.49%	-0.40%
	2	Hwy	357	-2.26%	1.32%	-2.17%	-15.04%	-0.40%
	3	Hwy	388	-1.93%	1.11%	-1.69%	-9.10%	-0.40%
	4	Hwy	302	-1.65%	0.98%	-1.62%	-5.74%	-0.40%
	5	Hwy	243	-1.72%	1.12%	-1.37%	-5.52%	-0.40%
	6	Hwy	150	-1.66%	1.03%	-1.42%	-4.91%	-0.39%
	7	Hwy	113	-1.69%	1.14%	-1.32%	-4.74%	-0.40%
	8	Hwy	64	-1.61%	1.09%	-1.30%	-4.91%	-0.41%

Table E-12: Descriptive statistics of PHEV Sprinter power data by VSP bin for Highway travel during charge-depleting operation.

Variable	VSP Bin	Rd Code	N	Mean	Std. Dev.	Median	Minimum	Maximum
Diesel ICE Power (W/kg/s)	1	Hwy	1263	1.26	4.06	0.00	-2.89	17.82
	2	Hwy	440	6.30	5.04	6.81	-2.40	18.85
	3	Hwy	545	8.26	4.58	8.52	-3.51	20.68
	4	Hwy	541	9.37	4.30	9.46	-2.46	22.62
	5	Hwy	618	10.52	4.32	10.61	-3.27	24.94
	6	Hwy	586	11.65	4.94	11.91	-0.48	27.14
	7	Hwy	678	13.26	5.06	13.40	-3.97	28.06
	8	Hwy	618	17.52	5.36	17.81	-3.83	30.91
Electric Motor Power (W/kg/s)	1	Hwy	1263	0.11	0.53	0.00	0.00	10.45
	2	Hwy	440	0.27	1.23	0.00	0.00	11.60
	3	Hwy	545	0.37	1.67	0.00	0.00	14.19
	4	Hwy	541	0.39	1.72	0.00	0.00	12.47
	5	Hwy	618	0.81	2.92	0.00	0.00	15.17
	6	Hwy	586	1.14	3.64	0.00	0.00	15.27
	7	Hwy	678	1.20	4.02	0.00	0.00	18.89
	8	Hwy	618	0.80	3.66	0.00	0.00	21.67
Total Power (W/kg/s)	1	Hwy	1263	1.37	4.06	0.18	-2.89	17.82
	2	Hwy	440	6.57	4.86	6.86	-2.40	18.85
	3	Hwy	545	8.63	4.19	8.70	-3.51	20.68
	4	Hwy	541	9.76	3.77	9.51	-2.46	22.62
	5	Hwy	618	11.33	3.26	10.99	-0.71	24.94
	6	Hwy	586	12.80	3.45	12.29	1.80	27.14
	7	Hwy	678	14.47	3.60	13.73	1.00	33.94
	8	Hwy	618	18.32	4.27	18.21	1.23	30.98
Recup (W/kg/s)	1	Hwy	1263	-2.182	2.115	-1.605	-9.707	0.000
	2	Hwy	440	-3.811	2.880	-2.804	-12.952	0.000
	3	Hwy	545	-3.950	2.804	-3.135	-12.874	0.000
	4	Hwy	541	-3.730	2.681	-3.123	-11.744	0.000
	5	Hwy	618	-3.156	2.610	-2.527	-12.130	0.000
	6	Hwy	586	-2.759	2.786	-1.809	-12.989	0.000
	7	Hwy	678	-2.300	2.628	-1.470	-13.037	0.000
	8	Hwy	618	-1.564	2.418	-0.647	-12.984	0.000

Table E-13: Descriptive statistics of PHEV Sprinter emissions data by VSP bin for Suburban travel during charge-depleting operation.

Variable	VSP Bin	Rd Code	N	Mean	Std. Dev.	Median	Minimum	Maximum
Fuel (gal/s)	1	S	21714	1.03E-04	2.07E-04	1.40E-05	0.00E+00	2.02E-03
	2	S	4007	2.94E-04	3.70E-04	1.06E-04	0.00E+00	2.10E-03
	3	S	3643	4.00E-04	4.23E-04	2.96E-04	0.00E+00	2.07E-03
	4	S	3228	5.05E-04	4.83E-04	4.95E-04	0.00E+00	2.12E-03
	5	S	2799	5.75E-04	5.41E-04	5.64E-04	0.00E+00	2.26E-03
	6	S	2228	6.55E-04	6.10E-04	6.11E-04	0.00E+00	2.33E-03
	7	S	2150	8.57E-04	6.79E-04	9.75E-04	0.00E+00	2.34E-03
	8	S	1695	1.22E-03	6.71E-04	1.42E-03	0.00E+00	2.39E-03
CO_2 (g/s)	1	S	21714	1.05	2.13	0.07	0.00	20.80
	2	S	4007	3.02	3.80	1.11	0.00	21.64
	3	S	3643	4.11	4.34	3.06	0.00	21.12
	4	S	3228	5.20	4.97	5.11	0.00	21.77
	5	S	2799	5.92	5.57	5.81	0.00	23.31
	6	S	2228	6.74	6.28	6.30	0.00	23.96
	7	S	2150	8.83	6.99	10.04	0.00	24.12
	8	S	1695	12.59	6.92	14.58	0.00	24.62
CO (g/s)	1	S	21714	1.75E-03	1.37E-02	1.00E-05	0.00E+00	5.28E-01
	2	S	4007	6.40E-03	2.85E-02	1.60E-04	0.00E+00	3.51E-01
	3	S	3643	6.46E-03	2.91E-02	6.10E-04	0.00E+00	4.26E-01
	4	S	3228	5.57E-03	2.37E-02	1.14E-03	0.00E+00	3.98E-01
	5	S	2799	5.94E-03	2.25E-02	1.35E-03	0.00E+00	3.70E-01
	6	S	2228	5.89E-03	1.81E-02	1.78E-03	0.00E+00	2.88E-01
	7	S	2150	6.77E-03	1.59E-02	2.98E-03	0.00E+00	2.15E-01
	8	S	1695	7.78E-03	1.77E-02	4.08E-03	0.00E+00	3.18E-01
NO (g/s)	1	S	21714	0.012	0.023	0.001	0.000	0.221
	2	S	4007	0.031	0.040	0.011	0.000	0.241
	3	S	3643	0.044	0.046	0.030	0.000	0.216
	4	S	3228	0.055	0.053	0.050	0.000	0.222
	5	S	2799	0.060	0.058	0.056	0.000	0.260
	6	S	2228	0.065	0.064	0.058	0.000	0.257
	7	S	2150	0.081	0.069	0.087	0.000	0.278
	8	S	1695	0.111	0.069	0.127	0.000	0.265
NO_2 (g/s)	1	S	21714	1.40E-03	2.64E-03	3.00E-04	0.00E+00	4.00E-02
	2	S	4007	2.78E-03	4.17E-03	1.15E-03	0.00E+00	4.15E-02
	3	S	3643	3.34E-03	4.50E-03	1.86E-03	0.00E+00	3.19E-02
	4	S	3228	3.88E-03	4.93E-03	2.45E-03	0.00E+00	4.25E-02
	5	S	2799	3.82E-03	4.90E-03	2.33E-03	0.00E+00	5.48E-02
	6	S	2228	3.86E-03	4.81E-03	2.40E-03	0.00E+00	4.14E-02
	7	S	2150	4.83E-03	5.53E-03	3.37E-03	0.00E+00	4.10E-02
	8	S	1695	6.43E-03	5.66E-03	5.53E-03	0.00E+00	3.86E-02
NOx (g/s)	1	S	21714	0.013	0.025	0.001	0.000	0.243
	2	S	4007	0.034	0.043	0.013	0.000	0.250
	3	S	3643	0.047	0.049	0.034	0.000	0.229
	4	S	3228	0.059	0.056	0.055	0.000	0.235
	5	S	2799	0.064	0.061	0.061	0.000	0.277
	6	S	2228	0.069	0.067	0.062	0.000	0.272
	7	S	2150	0.086	0.073	0.092	0.000	0.294
	8	S	1695	0.117	0.072	0.135	0.000	0.283
HC (g/s)	1	S	21714	6.70E-05	1.46E-04	2.00E-05	0.00E+00	6.58E-03
	2	S	4007	1.53E-04	2.57E-04	6.00E-05	0.00E+00	5.64E-03
	3	S	3643	2.13E-04	3.05E-04	1.30E-04	0.00E+00	3.65E-03
	4	S	3228	2.80E-04	3.96E-04	2.00E-04	0.00E+00	8.97E-03
	5	S	2799	3.69E-04	7.88E-04	2.50E-04	0.00E+00	2.63E-02
	6	S	2228	4.76E-04	1.12E-03	2.90E-04	0.00E+00	2.39E-02
	7	S	2150	6.66E-04	1.60E-03	4.40E-04	0.00E+00	3.09E-02
	8	S	1695	1.01E-03	2.04E-03	6.80E-04	0.00E+00	3.04E-02

Table E-14: Descriptive statistics of PHEV Sprinter driving and road-based data by VSP bin for Suburban travel during charge-depleting operation.

Variable	VSP Bin	Rd Code	N	Mean	Std. Dev.	Median	Minimum	Maximum
Velocity (km/h)	1	S	21714	22.4	20.0	21.4	0.0	65.9
	2	S	4007	35.0	16.9	40.9	0.0	62.3
	3	S	3643	37.8	15.2	43.3	0.7	62.2
	4	S	3228	38.0	14.2	43.0	1.4	65.6
	5	S	2799	36.7	13.4	40.3	0.9	62.7
	6	S	2228	35.6	12.2	37.3	2.8	60.7
	7	S	2150	35.6	10.8	36.3	0.7	65.2
	8	S	1695	38.0	9.3	38.3	1.0	62.8
Positive Accel (m/s^2)	1	S	9246	0.060	0.164	0.000	0.000	2.810
	2	S	2119	0.290	0.312	0.189	0.000	2.269
	3	S	2525	0.381	0.372	0.266	0.000	2.254
	4	S	2472	0.492	0.448	0.350	0.000	2.705
	5	S	2344	0.643	0.503	0.515	0.000	2.568
	6	S	1981	0.755	0.522	0.691	0.000	2.533
	7	S	2006	0.870	0.511	0.880	0.000	2.464
	8	S	1605	0.898	0.518	0.873	0.000	2.825
Negative Accel (m/s^2)	1	S	12465	-0.690	0.503	-0.604	-3.063	0.000
	2	S	1888	-0.284	0.299	-0.184	-2.052	0.000
	3	S	1118	-0.220	0.236	-0.149	-1.819	0.000
	4	S	756	-0.168	0.164	-0.123	-1.572	0.000
	5	S	455	-0.159	0.158	-0.121	-1.229	0.000
	6	S	247	-0.152	0.142	-0.107	-1.096	0.000
	7	S	144	-0.151	0.154	-0.103	-0.967	0.000
	8	S	90	-0.171	0.164	-0.109	-1.031	-0.001
Positive Grade (%)	1	S	11973	2.27%	36.12%	0.00%	0.00%	3389.74%
	2	S	2095	7.62%	172.26%	1.61%	0.00%	7866.10%
	3	S	2178	3.51%	6.44%	1.57%	0.00%	97.71%
	4	S	2254	3.56%	6.60%	2.07%	0.00%	103.74%
	5	S	2017	3.93%	9.64%	2.55%	0.00%	336.48%
	6	S	1753	3.98%	5.98%	2.94%	0.00%	101.43%
	7	S	1765	4.58%	16.23%	3.10%	0.00%	587.20%
	8	S	1576	7.14%	19.01%	4.96%	0.00%	580.78%
Negative Grade (%)	1	S	9738	-6.52%	20.08%	-4.26%	-1505.58%	-0.15%
	2	S	1912	-3.02%	2.60%	-2.28%	-21.57%	-0.33%
	3	S	1465	-2.76%	2.14%	-2.15%	-17.88%	-0.32%
	4	S	974	-2.79%	1.96%	-2.23%	-14.78%	-0.62%
	5	S	782	-2.78%	1.75%	-2.31%	-12.65%	-0.59%
	6	S	475	-2.41%	1.39%	-2.02%	-7.05%	-0.62%
	7	S	385	-2.19%	1.15%	-1.92%	-7.36%	-0.70%
	8	S	119	-1.67%	0.90%	-1.25%	-4.21%	-0.66%

Table E-15: Descriptive statistics of PHEV Sprinter power data by VSP bin for Suburban travel during charge-depleting operation.

Variable	VSP Bin	Rd Code	N	Mean	Std. Dev.	Median	Minimum	Maximum
Diesel ICE Power (W/kg/s)	1	S	21714	0.82	2.69	0.00	-2.85	24.45
	2	S	4007	3.40	4.90	0.00	-2.76	23.04
	3	S	3643	5.27	5.83	3.93	-3.50	31.78
	4	S	3228	6.68	6.53	7.95	-3.05	28.24
	5	S	2799	7.88	7.50	8.94	-4.35	29.92
	6	S	2228	8.86	8.39	9.91	-3.86	27.94
	7	S	2150	11.61	9.15	14.42	-4.86	29.75
	8	S	1695	16.46	9.13	18.84	-3.51	31.78
Electric Motor Power (W/kg/s)	1	S	21714	0.24	1.05	0.00	0.00	19.30
	2	S	4007	1.04	2.31	0.00	0.00	15.36
	3	S	3643	1.69	3.07	0.00	0.00	16.05
	4	S	3228	2.44	3.94	0.00	0.00	19.96
	5	S	2799	3.55	4.96	0.00	0.00	21.52
	6	S	2228	4.60	5.77	0.00	0.00	21.14
	7	S	2150	4.41	6.37	0.00	0.00	21.23
	8	S	1695	2.86	6.02	0.00	0.00	21.65
Total Power (W/kg/s)	1	S	21714	1.06	2.82	0.33	-2.85	24.45
	2	S	4007	4.44	4.72	3.35	-2.76	23.04
	3	S	3643	6.96	5.08	7.64	-3.05	31.78
	4	S	3228	9.13	5.10	9.64	-2.92	28.24
	5	S	2799	11.42	5.15	11.32	-2.87	31.97
	6	S	2228	13.46	5.15	13.35	-2.25	27.94
	7	S	2150	16.02	5.36	16.12	-2.16	30.19
	8	S	1695	19.32	5.61	19.52	-1.75	31.78
Recup (W/kg/s)	1	S	21714	-1.408	1.614	-1.314	-12.690	0.580
	2	S	4007	-2.387	2.776	-1.219	-12.832	0.000
	3	S	3643	-3.075	3.289	-1.470	-12.866	0.000
	4	S	3228	-3.416	3.593	-2.254	-13.022	0.000
	5	S	2799	-3.640	3.989	-1.999	-13.078	0.000
	6	S	2228	-3.595	4.235	0.000	-13.010	0.000
	7	S	2150	-3.966	4.379	-2.245	-13.116	0.000
	8	S	1695	-4.638	4.212	-4.544	-13.098	0.000

Table E-16: Descriptive statistics of PHEV Sprinter emissions data by VSP bin for Urban travel during charge-depleting operation.

Variable	VSP Bin	Rd Code	N	Mean	Std. Dev.	Median	Minimum	Maximum
Fuel (gal/s)	1	U	5832	1.03E-04	1.97E-04	1.30E-05	0.00E+00	2.08E-03
	2	U	752	2.73E-04	3.47E-04	1.24E-04	0.00E+00	1.93E-03
	3	U	667	3.81E-04	4.45E-04	2.15E-04	0.00E+00	1.84E-03
	4	U	602	4.78E-04	4.79E-04	4.02E-04	0.00E+00	2.06E-03
	5	U	526	5.77E-04	5.26E-04	5.53E-04	0.00E+00	1.96E-03
	6	U	358	6.50E-04	5.60E-04	6.63E-04	0.00E+00	1.98E-03
	7	U	312	8.32E-04	6.09E-04	9.96E-04	0.00E+00	2.17E-03
	8	U	276	7.30E-04	6.43E-04	6.79E-04	0.00E+00	2.33E-03
CO_2 (g/s)	1	U	5832	1.06	2.02	0.08	0.00	21.44
	2	U	752	2.79	3.55	1.29	0.00	19.90
	3	U	667	3.91	4.56	2.22	0.00	18.91
	4	U	602	4.91	4.92	4.12	0.00	21.13
	5	U	526	5.93	5.41	5.70	0.00	20.12
	6	U	358	6.68	5.77	6.83	0.00	20.38
	7	U	312	8.55	6.27	10.26	0.00	22.40
	8	U	276	7.50	6.62	7.01	0.00	24.05
CO (g/s)	1	U	5832	1.92E-03	1.36E-02	1.00E-05	0.00E+00	4.03E-01
	2	U	752	1.26E-02	4.20E-02	4.00E-04	0.00E+00	3.33E-01
	3	U	667	9.77E-03	3.42E-02	5.70E-04	0.00E+00	3.66E-01
	4	U	602	8.76E-03	2.90E-02	1.23E-03	0.00E+00	2.84E-01
	5	U	526	8.85E-03	2.98E-02	1.56E-03	0.00E+00	3.42E-01
	6	U	358	9.66E-03	2.70E-02	2.26E-03	0.00E+00	2.65E-01
	7	U	312	1.51E-02	3.73E-02	3.74E-03	0.00E+00	3.16E-01
	8	U	276	1.40E-02	3.33E-02	2.75E-03	0.00E+00	2.27E-01
NO (g/s)	1	U	5832	0.012	0.021	0.001	0.000	0.172
	2	U	752	0.028	0.036	0.015	0.000	0.236
	3	U	667	0.039	0.046	0.022	0.000	0.244
	4	U	602	0.049	0.050	0.040	0.000	0.219
	5	U	526	0.059	0.056	0.050	0.000	0.269
	6	U	358	0.062	0.057	0.055	0.000	0.210
	7	U	312	0.078	0.062	0.088	0.000	0.264
	8	U	276	0.067	0.065	0.052	0.000	0.221
NO_2 (g/s)	1	U	5832	1.37E-03	2.41E-03	2.60E-04	0.00E+00	3.35E-02
	2	U	752	2.73E-03	4.26E-03	1.01E-03	0.00E+00	4.30E-02
	3	U	667	2.98E-03	4.20E-03	1.47E-03	0.00E+00	3.15E-02
	4	U	602	3.22E-03	4.12E-03	1.97E-03	0.00E+00	2.82E-02
	5	U	526	3.69E-03	4.52E-03	2.41E-03	0.00E+00	3.18E-02
	6	U	358	4.04E-03	4.63E-03	2.85E-03	0.00E+00	2.78E-02
	7	U	312	4.69E-03	4.85E-03	3.84E-03	0.00E+00	4.02E-02
	8	U	276	4.27E-03	4.43E-03	3.40E-03	0.00E+00	2.47E-02
NOx (g/s)	1	U	5832	0.013	0.023	0.001	0.000	0.185
	2	U	752	0.031	0.039	0.017	0.000	0.240
	3	U	667	0.042	0.048	0.025	0.000	0.249
	4	U	602	0.052	0.053	0.044	0.000	0.224
	5	U	526	0.062	0.059	0.054	0.000	0.277
	6	U	358	0.066	0.060	0.059	0.000	0.218
	7	U	312	0.082	0.065	0.092	0.000	0.277
	8	U	276	0.071	0.067	0.057	0.000	0.228
HC (g/s)	1	U	5832	8.50E-05	1.76E-04	2.00E-05	0.00E+00	3.00E-03
	2	U	752	2.14E-04	3.88E-04	8.00E-05	0.00E+00	4.54E-03
	3	U	667	2.71E-04	4.25E-04	1.20E-04	0.00E+00	3.34E-03
	4	U	602	3.20E-04	5.31E-04	2.10E-04	0.00E+00	7.60E-03
	5	U	526	4.18E-04	6.40E-04	2.80E-04	0.00E+00	7.94E-03
	6	U	358	5.09E-04	7.88E-04	3.15E-04	0.00E+00	6.03E-03
	7	U	312	9.35E-04	2.42E-03	4.85E-04	0.00E+00	3.10E-02
	8	U	276	9.14E-04	2.57E-03	3.10E-04	0.00E+00	2.94E-02

Table E-17: Descriptive statistics of PHEV Sprinter road-based and driving data by VSP bin for Urban travel during charge-depleting operation.

Variable	VSP Bin	Rd Code	N	Mean	Std. Dev.	Median	Minimum	Maximum
Velocity (km/h)	1	U	5832	12.3	14.1	6.2	0.0	54.6
	2	U	752	22.3	12.7	22.3	0.0	49.3
	3	U	667	26.2	11.8	27.7	0.0	49.9
	4	U	602	27.6	10.4	28.3	2.7	49.7
	5	U	526	28.4	10.8	30.0	0.0	53.7
	6	U	358	28.1	10.1	28.1	0.4	51.7
	7	U	312	29.1	8.8	29.2	2.7	51.1
	8	U	276	29.9	10.3	31.6	0.0	48.5
Positive Accel (m/s^2)	1	U	3291	0.073	0.196	0.000	0.000	2.146
	2	U	494	0.393	0.374	0.269	0.000	2.240
	3	U	494	0.477	0.394	0.383	0.000	2.424
	4	U	483	0.600	0.430	0.501	0.015	2.202
	5	U	454	0.664	0.518	0.561	0.000	2.540
	6	U	332	0.755	0.528	0.646	0.002	2.369
	7	U	293	0.822	0.533	0.754	0.005	2.286
	8	U	236	0.683	0.456	0.596	0.003	2.388
Negative Accel (m/s^2)	1	U	2541	-0.644	0.463	-0.577	-2.487	0.000
	2	U	258	-0.324	0.325	-0.203	-1.483	0.000
	3	U	173	-0.221	0.221	-0.160	-1.333	-0.001
	4	U	119	-0.219	0.246	-0.132	-1.279	-0.001
	5	U	72	-0.201	0.185	-0.159	-0.889	-0.001
	6	U	26	-0.214	0.203	-0.179	-0.923	-0.002
	7	U	19	-0.369	0.337	-0.262	-1.082	-0.001
	8	U	40	-0.322	0.360	-0.161	-1.312	-0.001
Positive Grade (%)	1	U	3409	52.40%	2930.00%	0.00%	0.00%	171042.00%
	2	U	421	6.33%	53.80%	1.01%	0.00%	1035.01%
	3	U	452	3.79%	6.68%	1.74%	0.00%	53.46%
	4	U	439	4.61%	8.40%	2.46%	0.00%	87.03%
	5	U	443	6.74%	18.46%	3.72%	0.00%	330.76%
	6	U	311	12.72%	68.58%	4.28%	0.00%	1019.62%
	7	U	298	7.66%	13.56%	5.65%	0.00%	171.49%
	8	U	276	705.00%	11152.00%	12.00%	0.00%	185296.00%
Negative Grade (%)	1	U	2423	-10.43%	33.30%	-5.76%	-1178.40%	-0.07%
	2	U	331	-4.39%	3.50%	-3.65%	-20.10%	-0.03%
	3	U	215	-3.50%	2.73%	-2.65%	-16.50%	-0.09%
	4	U	163	-2.90%	2.02%	-2.42%	-11.77%	0.00%
	5	U	83	-2.60%	1.68%	-2.21%	-8.31%	-0.01%
	6	U	47	-2.16%	1.69%	-1.69%	-7.21%	-0.10%
	7	U	14	-2.11%	1.20%	-2.07%	-4.33%	-0.28%
	8	U	0	*	*	*	*	*

Table E-18: Descriptive statistics of PHEV Sprinter power data by VSP bin for Urban travel during charge-depleting operation.

Variable	VSP Bin	Rd Code	N	Mean	Std. Dev.	Median	Minimum	Maximum
Diesel ICE Power (W/kg/s)	1	U	5832	0.83	2.15	0.00	-3.18	21.15
	2	U	752	2.79	4.41	0.00	-3.81	19.15
	3	U	667	4.45	5.52	1.50	-2.75	20.87
	4	U	602	6.18	6.21	7.08	-2.21	22.51
	5	U	526	7.62	6.87	9.58	-2.82	23.40
	6	U	358	9.01	7.35	12.05	-2.35	31.38
	7	U	312	11.91	7.36	14.45	-3.44	29.81
	8	U	276	12.25	9.00	15.97	-1.72	31.63
Electric Motor Power (W/kg/s)	1	U	5832	0.26	0.87	0.00	0.00	12.74
	2	U	752	1.29	2.46	0.00	0.00	12.48
	3	U	667	2.04	3.26	0.00	0.00	14.71
	4	U	602	2.67	4.08	0.00	0.00	15.82
	5	U	526	3.15	4.64	0.00	0.00	16.47
	6	U	358	3.25	5.22	0.00	0.00	17.38
	7	U	312	2.74	5.43	0.00	0.00	21.61
	8	U	276	1.82	4.71	0.00	0.00	20.10
Total Power (W/kg/s)	1	U	5832	1.10	2.22	0.44	-3.16	21.15
	2	U	752	4.07	4.27	3.93	-2.80	19.15
	3	U	667	6.49	4.77	6.43	-2.44	20.87
	4	U	602	8.85	4.79	9.09	-2.21	22.51
	5	U	526	10.76	4.70	10.72	-2.82	23.40
	6	U	358	12.26	4.89	12.65	-2.35	31.38
	7	U	312	14.65	4.70	14.96	-2.76	29.81
	8	U	276	14.06	7.98	17.01	-1.72	31.63
Recup (W/kg/s)	1	U	5832	-1.043	1.263	-1.103	-10.964	0.000
	2	U	752	-1.590	2.330	-0.664	-11.351	0.000
	3	U	667	-2.178	2.968	-0.543	-11.732	0.000
	4	U	602	-2.721	3.412	0.000	-12.212	0.000
	5	U	526	-3.121	3.705	0.000	-11.638	0.127
	6	U	358	-3.392	4.033	-0.296	-12.860	0.000
	7	U	312	-3.721	4.007	-1.765	-12.932	0.000
	8	U	276	-4.303	4.067	-3.700	-12.854	0.000

Table E-19: PHEV Sprinter fuel use, CO_2, CO, and HC data by sample run file during charge-sustaining highway driving.

Road Code	Route	File Name	N	Fuel Rate (gal/s)		CO_2 (g/s)		CO (g/s)		HC (g/s)	
				Mean	StDev	Mean	StDev	Mean	StDev	Mean	StDev
Hwy	Highway	Eight	851	6.38E-04	4.50E-04	6.572	4.648	0.0026	0.0071	6.06E-04	6.92E-04
Hwy	Highway	Five	832	6.01E-04	4.66E-04	6.185	4.812	0.0043	0.0089	4.19E-04	1.16E-03
Hwy	Highway	Nine	876	6.57E-04	4.97E-04	6.764	5.134	0.0035	0.0131	8.99E-04	2.40E-03
Hwy	Highway	Seven	791	7.66E-04	4.79E-04	7.890	4.946	0.0030	0.0186	5.43E-04	3.61E-04
Hwy	Highway	Six	693	7.49E-04	4.69E-04	7.724	4.839	0.0024	0.0033	3.78E-04	2.37E-04
Hwy	Highway	Ten	1246	7.63E-04	4.78E-04	7.860	4.936	0.0038	0.0090	8.07E-04	9.94E-04

Table E-20: PHEV Sprinter fuel use, CO_2, CO, and HC data by sample run file during charge-sustaining suburban driving.

Road Code	Route	File Name	N	Fuel Rate (gal/s)		CO_2 (g/s)		CO (g/s)		HC (g/s)	
				Mean	StDev	Mean	StDev	Mean	StDev	Mean	StDev
S	109	JAN9_S3	522	3.08E-04	4.03E-04	3.155	4.154	0.0049	0.0163	5.32E-04	7.06E-04
S	109	JAN9_S4	1015	3.26E-04	4.65E-04	3.355	4.791	0.0027	0.0141	2.52E-04	4.32E-04
S	109	JAN9_s5	1137	3.31E-04	4.60E-04	3.396	4.744	0.0030	0.0141	2.51E-04	4.10E-04
S	109	JAN9_S6	866	3.49E-04	4.99E-04	3.589	5.131	0.0052	0.0228	2.19E-04	3.12E-04
S	109	JAN9_S7	1325	3.22E-04	4.63E-04	3.312	4.769	0.0026	0.0094	2.82E-04	4.39E-04
S	109	JAN9_S8	775	3.34E-04	4.67E-04	3.437	4.809	0.0036	0.0163	2.17E-04	2.97E-04
S	110	DEC20_S2	924	3.02E-04	4.65E-04	3.102	4.791	0.0044	0.0172	2.27E-04	3.25E-04
S	110	DEC20_S3	1181	3.21E-04	4.75E-04	3.299	4.890	0.0036	0.0182	1.49E-04	2.49E-04
S	110	DEC20_S4	1094	3.07E-04	4.92E-04	3.151	5.066	0.0028	0.0148	8.80E-05	2.60E-04
S	110	DEC20_S5	1982	3.26E-04	4.93E-04	3.344	5.067	0.0046	0.0229	1.41E-04	2.52E-04
S	110	DEC20_S6	1899	3.00E-04	4.54E-04	3.081	4.668	0.0041	0.0198	1.48E-04	2.28E-04
S	110	Dec20_S7	882	3.82E-04	5.14E-04	3.922	5.292	0.0047	0.0228	2.01E-04	3.16E-04
S	110	DEC21_S4	678	3.73E-04	5.03E-04	3.829	5.171	0.0033	0.0203	1.40E-04	5.79E-04
S	110	Dec21_S5, M1	742	3.34E-04	5.08E-04	3.427	5.216	0.0052	0.0298	1.61E-04	4.00E-04
S	110	DEC21_S5, M2	1154	3.24E-04	4.76E-04	3.325	4.891	0.0046	0.0234	2.34E-04	1.19E-03
S	110	NOV29_S1	1101	3.54E-04	5.07E-04	3.641	5.231	0.0041	0.0177	1.84E-04	5.97E-04
S	110	NOV29_S2	1779	3.44E-04	4.97E-04	3.542	5.123	0.0026	0.0103	2.61E-04	1.15E-03
S	110	NOV29_S3	1782	3.33E-04	4.75E-04	3.427	4.900	0.0026	0.0135	2.40E-04	1.33E-03
S	110	NOV29_S4	1902	3.36E-04	4.87E-04	3.454	5.020	0.0029	0.0128	1.49E-04	2.24E-04
S	123	NOV26_S2	2721	3.42E-04	5.16E-04	3.516	5.314	0.0054	0.0265	2.49E-04	5.10E-04
S	123	NOV26_S3	2666	3.46E-04	5.16E-04	3.552	5.317	0.0043	0.0230	2.16E-04	5.52E-04
S	123	NOV26_S4	2759	3.31E-04	5.01E-04	3.402	5.162	0.0053	0.0263	2.21E-04	3.53E-04
S	123	NOV28_S1	924	2.76E-04	4.40E-04	2.836	4.521	0.0056	0.0257	2.70E-04	5.70E-04
S	123	Nov28_S2	2029	3.46E-04	5.42E-04	3.548	5.585	0.0064	0.0266	3.84E-04	1.48E-03
S	12T/C	Nov16_S1,1a	1568	3.33E-04	4.75E-04	3.419	4.901	0.0027	0.0104	2.84E-04	6.67E-04
S	12T/C	Nov16_S2	1551	3.40E-04	5.02E-04	3.497	5.172	0.0028	0.0138	1.63E-04	3.08E-04
S	12T/C	Nov16_s3	1503	3.53E-04	4.76E-04	3.619	4.903	0.0030	0.0123	1.43E-04	2.03E-04
S	12T/C	Oct19_S1	1736	3.25E-04	5.15E-04	3.340	5.295	0.0029	0.0103	1.09E-04	3.41E-04

Table E-21: PHEV Sprinter fuel use, CO_2, CO, and HC data by sample run file during charge-sustaining urban driving.

Road Code	Route	File Name	N	Fuel Rate (gal/s)		CO_2 (g/s)		CO (g/s)		HC (g/s)	
				Mean	StDev	Mean	StDev	Mean	StDev	Mean	StDev
U	109	JAN9_S3	61	0.00E+00	0.00E+00	0.000	0.000	0.0000	0.0000	0.00E+00	0.00E+00
U	109	JAN9_S4	313	2.65E-04	4.28E-04	2.724	4.403	0.0052	0.0315	1.78E-04	3.44E-04
U	109	JAN9_s5	283	2.91E-04	4.31E-04	2.998	4.436	0.0037	0.0172	1.92E-04	3.38E-04
U	109	JAN9_S7	280	2.36E-04	3.81E-04	2.428	3.921	0.0021	0.0076	1.49E-04	2.19E-04
U	109	JAN9_S8	269	2.17E-04	3.16E-04	2.226	3.243	0.0059	0.0241	1.32E-04	1.99E-04
U	110	DEC20_S2	321	3.59E-04	5.17E-04	3.679	5.309	0.0121	0.0324	1.21E-03	3.23E-03
U	110	DEC20_S3	658	3.22E-04	4.26E-04	3.307	4.385	0.0054	0.0244	1.05E-04	1.53E-04
U	110	DEC20_S5	743	2.60E-04	4.03E-04	2.672	4.147	0.0049	0.0233	1.10E-04	1.79E-04
U	110	DEC20_S6	709	2.60E-04	4.27E-04	2.667	4.386	0.0058	0.0302	1.29E-04	2.24E-04
U	110	NOV29_S2	739	2.57E-04	3.96E-04	2.640	4.075	0.0042	0.0206	1.95E-04	2.85E-04
U	110	NOV29_S3	582	3.00E-04	4.51E-04	3.086	4.646	0.0053	0.0233	1.49E-04	2.18E-04
U	110	NOV29_S4	592	3.31E-04	4.88E-04	3.408	5.027	0.0043	0.0215	1.54E-04	2.35E-04
U	12T/C	Nov16_S1,1a	1150	1.36E-04	3.06E-04	1.397	3.132	0.0052	0.0254	3.23E-04	8.35E-04
U	12T/C	Nov16_S2	855	2.44E-04	3.94E-04	2.508	4.049	0.0051	0.0220	1.37E-04	2.37E-04
U	12T/C	Nov16_s3	877	2.20E-04	3.81E-04	2.256	3.915	0.0046	0.0209	1.07E-04	1.98E-04
U	12T/C	Oct19_S1	893	2.59E-04	3.62E-04	2.653	3.715	0.0067	0.0249	2.87E-04	4.98E-04

Table E-22: PHEV Sprinter NO, NO_2 and NOx data by sample run file during charge-sustaining highway driving.

Road Code	Route	File Name	N	NO (g/s)		NO_2 (g/s)		NOx (g/s)	
				Mean	StDev	Mean	StDev	Mean	StDev
Hwy	Highway	Eight	851	0.061	0.050	1.37E-03	1.20E-03	0.063	0.051
Hwy	Highway	Five	832	0.056	0.049	3.44E-03	2.32E-03	0.060	0.050
Hwy	Highway	Nine	876	0.063	0.054	1.21E-03	1.14E-03	0.064	0.055
Hwy	Highway	Seven	791	0.076	0.055	4.26E-03	3.59E-03	0.081	0.057
Hwy	Highway	Six	693	0.077	0.053	3.75E-03	3.04E-03	0.081	0.055
Hwy	Highway	Ten	1246	0.074	0.053	1.21E-03	1.12E-03	0.075	0.053

Table E-23: PHEV Sprinter NO, NO_2 and NOx data by sample run file during charge-sustaining suburban driving.

Road Code	Route	File Name	N	NO (g/s)		NO_2 (g/s)		NOx (g/s)	
				Mean	StDev	Mean	StDev	Mean	StDev
S	109	JAN9_S3	522	0.034	0.045	1.32E-03	1.58E-03	0.036	0.047
S	109	JAN9_S4	1015	0.035	0.050	2.36E-03	3.15E-03	0.038	0.053
S	109	JAN9_s5	1137	0.038	0.052	2.09E-03	2.76E-03	0.040	0.054
S	109	JAN9_S6	866	0.037	0.051	1.74E-03	2.12E-03	0.039	0.052
S	109	JAN9_S7	1325	0.036	0.050	1.11E-03	1.49E-03	0.037	0.052
S	109	JAN9_S8	775	0.038	0.052	1.22E-03	1.54E-03	0.039	0.053
S	110	DEC20_S2	924	0.027	0.040	4.06E-03	5.59E-03	0.031	0.045
S	110	DEC20_S3	1181	0.032	0.047	3.54E-03	4.89E-03	0.036	0.051
S	110	DEC20_S4	1094	0.030	0.047	2.63E-03	4.10E-03	0.033	0.050
S	110	DEC20_S5	1982	0.033	0.050	2.49E-03	3.45E-03	0.036	0.052
S	110	DEC20_S6	1899	0.032	0.048	1.91E-03	2.42E-03	0.034	0.050
S	110	Dec20_S7	882	0.041	0.054	1.75E-03	2.14E-03	0.043	0.055
S	110	DEC21_S4	678	0.040	0.053	1.82E-03	2.61E-03	0.042	0.054
S	110	Dec21_S5, M1	742	0.034	0.052	1.56E-03	2.27E-03	0.036	0.053
S	110	DEC21_S5, M2	1154	0.034	0.050	1.53E-03	1.92E-03	0.036	0.051
S	110	NOV29_S1	1101	0.036	0.050	3.60E-03	4.55E-03	0.039	0.054
S	110	NOV29_S2	1779	0.038	0.055	2.59E-03	3.61E-03	0.041	0.058
S	110	NOV29_S3	1782	0.039	0.055	2.19E-03	3.06E-03	0.041	0.057
S	110	NOV29_S4	1902	0.036	0.051	1.73E-03	2.51E-03	0.038	0.052
S	123	NOV26_S2	2721	0.034	0.050	3.15E-03	4.46E-03	0.038	0.054
S	123	NOV26_S3	2666	0.035	0.050	2.51E-03	3.52E-03	0.037	0.053
S	123	NOV26_S4	2759	0.033	0.049	1.93E-03	2.75E-03	0.035	0.051
S	123	NOV28_S1	924	0.029	0.045	1.21E-03	1.75E-03	0.030	0.046
S	123	Nov28_S2	2029	0.033	0.051	1.97E-03	3.17E-03	0.035	0.053
S	12T/C	Nov16_S1,1a	1568	0.034	0.048	5.41E-03	7.28E-03	0.039	0.055
S	12T/C	Nov16_S2	1551	0.034	0.049	5.55E-03	7.32E-03	0.039	0.055
S	12T/C	Nov16_s3	1503	0.037	0.050	5.11E-03	6.37E-03	0.042	0.055
S	12T/C	Oct19_S1	1736	0.031	0.049	3.41E-03	4.84E-03	0.034	0.054

Table E-24: PHEV Sprinter NO, NO_2 and NOx data by sample run file during charge-sustaining urban driving.

Road Code	Route	File Name	N	NO (g/s)		NO_2 (g/s)		NOx (g/s)	
				Mean	StDev	Mean	StDev	Mean	StDev
U	109	JAN9_S3	61	0.000	0.000	0.00E+00	0.00E+00	0.000	0.000
U	109	JAN9_S4	313	0.029	0.048	1.92E-03	2.84E-03	0.031	0.051
U	109	JAN9_s5	283	0.030	0.042	1.59E-03	1.73E-03	0.032	0.043
U	109	JAN9_S7	280	0.027	0.044	6.74E-04	1.01E-03	0.027	0.044
U	109	JAN9_S8	269	0.023	0.030	1.10E-03	1.17E-03	0.025	0.031
U	110	DEC20_S2	321	0.031	0.047	1.39E-03	2.36E-03	0.033	0.048
U	110	DEC20_S3	658	0.030	0.040	3.91E-03	3.81E-03	0.034	0.043
U	110	DEC20_S5	743	0.026	0.038	2.35E-03	3.02E-03	0.028	0.041
U	110	DEC20_S6	709	0.028	0.045	1.73E-03	2.47E-03	0.030	0.048
U	110	NOV29_S2	739	0.030	0.044	1.94E-03	2.85E-03	0.032	0.046
U	110	NOV29_S3	582	0.034	0.049	2.12E-03	3.18E-03	0.036	0.051
U	110	NOV29_S4	592	0.037	0.053	1.95E-03	2.83E-03	0.039	0.055
U	12T/C	Nov16_S1,1a	1150	0.013	0.028	7.29E-04	1.54E-03	0.014	0.029
U	12T/C	Nov16_S2	855	0.025	0.038	3.80E-03	5.34E-03	0.028	0.043
U	12T/C	Nov16_s3	877	0.022	0.037	2.98E-03	5.14E-03	0.025	0.041
U	12T/C	Oct19_S1	893	0.025	0.034	2.16E-03	3.16E-03	0.027	0.036

Table E-25: PHEV Sprinter velocity and power data by sample run file during charge-sustaining highway and urban driving.

Road Code	Route	File Name	N	Velocity (km/h)		ICE Power (W/kg/s)		EM Power (W/kg/s)		Tot. Power (W/kg/s)		Recuperation (W/kg/s)	
				Mean	StDev	Mean	StDev	Mean	StDev	Mean	StDev	Mean	StDev
Hwy	Highway	Eight	851	70.4	22.3	8.07	6.51	0.78	3.02	8.86	6.32	-2.16	2.22
Hwy	Highway	Five	832	72.0	19.6	7.53	6.86	0.77	3.00	8.30	6.82	-2.52	2.64
Hwy	Highway	Nine	876	70.8	22.7	8.39	7.23	0.70	2.82	9.09	7.07	-2.61	2.67
Hwy	Highway	Seven	791	74.5	18.1	9.74	6.93	0.39	2.21	10.13	6.78	-3.06	2.95
Hwy	Highway	Six	693	73.1	22.7	9.70	6.83	0.41	2.15	10.12	6.59	-3.53	3.07
Hwy	Highway	Ten	1246	76.8	20.2	9.77	6.98	0.51	2.52	10.28	6.77	-2.89	2.42
U	109	JAN9_S3	61	38.3	6.4	0.00	0.00	4.71	3.94	4.71	3.94	-0.29	0.64
U	109	JAN9_S4	313	16.9	16.6	3.33	5.73	1.17	3.18	4.51	6.10	-1.83	2.99
U	109	JAN9_s5	283	18.5	17.3	3.60	5.78	1.11	3.27	4.70	6.13	-2.06	2.63
U	109	JAN9_S7	280	18.7	14.3	2.92	5.09	1.38	3.04	4.30	5.21	-1.69	2.74
U	109	JAN9_S8	269	19.5	15.1	2.49	4.29	1.39	2.91	3.87	4.51	-1.26	1.69
U	110	DEC20_S2	321	21.9	14.2	4.24	6.96	1.83	4.18	6.07	7.24	-2.04	3.05
U	110	DEC20_S3	658	20.2	15.1	3.71	5.92	0.92	2.77	4.64	6.05	-2.06	2.60
U	110	DEC20_S5	743	18.7	14.1	3.07	5.38	1.07	2.77	4.14	5.51	-1.67	2.47
U	110	DEC20_S6	709	18.7	15.6	3.14	5.62	0.98	2.88	4.11	5.85	-1.70	2.51
U	110	NOV29_S2	739	17.9	14.4	3.11	5.34	0.98	2.84	4.10	5.51	-1.90	2.49
U	110	NOV29_S3	582	22.7	15.3	3.71	6.08	1.09	2.66	4.80	5.99	-1.97	2.77
U	110	NOV29_S4	592	22.3	14.6	4.15	6.61	0.90	2.43	5.05	6.52	-2.17	2.93
U	12T/C	Nov16_S1,1a	1150	11.4	12.1	1.44	3.80	1.14	2.94	2.59	4.50	-0.85	1.50
U	12T/C	Nov16_S2	855	18.1	15.9	3.16	5.76	0.88	2.68	4.03	5.91	-1.78	2.50
U	12T/C	Nov16_s3	877	14.8	13.5	2.56	5.07	0.78	2.36	3.35	5.22	-1.51	2.44
U	12T/C	Oct19_S1	893	14.6	13.0	2.90	4.76	0.65	1.92	3.55	4.77	-1.64	2.28

Table E-26: PHEV Sprinter velocity and power data by sample run file during charge-sustaining suburban driving.

Road Code	Route	File Name	N	Velocity (km/h)		ICE Power (W/kg/s)		EM Power (W/kg/s)		Tot. Power (W/kg/s)		Recuperation (W/kg/s)	
				Mean	StDev	Mean	StDev	Mean	StDev	Mean	StDev	Mean	StDev
S	109	JAN9_S3	522	35.1	19.1	3.60	5.71	1.09	3.11	4.69	5.88	-2.63	2.89
S	109	JAN9_S4	1015	39.5	16.3	4.07	6.58	1.66	3.73	5.73	6.65	-2.57	3.06
S	109	JAN9_s5	1137	35.3	18.4	4.05	6.36	1.40	3.42	5.46	6.42	-2.40	2.87
S	109	JAN9_S6	866	28.3	18.9	4.38	6.82	1.24	3.15	5.62	6.80	-2.46	3.13
S	109	JAN9_S7	1325	30.3	21.5	3.98	6.41	1.17	3.19	5.14	6.51	-2.38	3.00
S	109	JAN9_S8	775	30.2	18.5	4.15	6.41	1.55	3.44	5.70	6.43	-2.31	2.99
S	110	DEC20_S2	924	31.1	17.1	3.61	6.46	1.32	3.40	4.94	6.68	-2.23	2.88
S	110	DEC20_S3	1181	29.6	17.4	3.97	6.42	1.44	3.51	5.41	6.52	-2.32	2.97
S	110	DEC20_S4	1094	29.8	16.7	3.81	6.88	1.58	3.56	5.39	7.02	-2.31	3.05
S	110	DEC20_S5	1982	28.8	18.5	4.05	6.71	1.22	3.14	5.27	6.76	-2.24	3.01
S	110	DEC20_S6	1899	28.3	19.6	3.72	6.17	1.29	3.25	5.01	6.29	-2.17	2.88
S	110	Dec20_S7	882	29.2	17.3	4.76	6.99	1.30	3.31	6.06	6.93	-2.61	3.24
S	110	DEC21_S4	678	32.0	18.3	4.71	6.97	1.61	3.94	6.31	7.10	-2.67	3.17
S	110	Dec21_S5, M1	742	29.3	20.0	4.25	6.95	1.21	3.05	5.45	6.99	-2.19	3.11
S	110	DEC21_S5, M2	1154	28.7	17.3	3.96	6.64	1.43	3.79	5.39	6.98	-2.40	2.92
S	110	NOV29_S1	1101	32.8	18.6	4.37	6.99	1.41	3.42	5.78	7.04	-2.41	3.18
S	110	NOV29_S2	1779	32.1	17.5	4.26	6.84	1.58	3.82	5.84	6.98	-2.52	3.15
S	110	NOV29_S3	1782	31.3	19.0	4.18	6.59	1.48	3.67	5.66	6.72	-2.51	3.11
S	110	NOV29_S4	1902	31.7	17.7	4.19	6.75	1.61	3.74	5.80	6.84	-2.46	3.17
S	123	NOV26_S2	2721	25.3	19.5	4.16	7.06	1.22	3.40	5.38	7.25	-2.14	2.83
S	123	NOV26_S3	2666	25.8	19.0	4.24	7.13	1.17	3.32	5.41	7.26	-2.23	2.86
S	123	NOV26_S4	2759	24.7	18.4	4.05	7.05	1.17	3.26	5.22	7.22	-2.09	2.83
S	123	NOV28_S1	924	22.5	17.6	3.33	5.87	1.11	3.16	4.44	6.15	-2.03	2.65
S	123	Nov28_S2	2029	25.9	18.2	4.26	7.52	1.35	3.63	5.61	7.79	-2.27	3.11
S	12T/C	Nov16_S1,1a	1568	32.9	19.4	4.02	6.56	1.45	3.72	5.47	6.78	-2.51	3.03
S	12T/C	Nov16_S2	1551	32.1	18.7	4.52	6.91	1.46	3.72	5.98	7.01	-2.61	3.06
S	12T/C	Nov16_s3	1503	33.4	18.5	4.38	6.66	1.14	3.05	5.51	6.65	-2.46	2.92
S	12T/C	Oct19_S1	1736	28.9	19.3	4.09	7.12	1.47	3.67	5.56	7.31	-2.26	3.08

Table E-27: PHEV Sprinter fuel use, CO_2, CO, and HC data by sample run file during charge-depleting operation.

Road Code	Route	File Name	N	Fuel Rate (gal/s)		CO_2 (g/s)		CO (g/s)		HC (g/s)	
				Mean	StDev	Mean	StDev	Mean	StDev	Mean	StDev
Hwy	Highway	Four	815	6.40E-04	4.32E-04	6.585	4.457	0.0044	0.0102	6.15E-04	1.42E-03
Hwy	Highway	One	827	6.10E-04	4.79E-04	6.279	4.929	0.0059	0.0240	9.07E-04	1.50E-03
Hwy	Highway	Three	747	5.72E-04	4.65E-04	5.896	4.797	0.0039	0.0061	6.26E-04	6.46E-04
Hwy	Highway	Two	615	6.07E-04	4.17E-04	6.251	4.302	0.0052	0.0165	1.02E-03	2.58E-03
S	109	Jan9_109S1	479	2.84E-04	3.28E-04	2.899	3.379	0.0123	0.0228	1.60E-03	1.74E-03
S	109	Jan9_S2	1183	1.72E-04	3.28E-04	1.765	3.379	0.0056	0.0191	6.90E-04	1.82E-03
S	109	JAN9_S3	614	1.70E-04	2.94E-04	1.749	3.023	0.0054	0.0175	8.98E-04	2.10E-03
S	110	DEC20_S1	1014	1.00E-04	2.67E-04	1.015	2.733	0.0068	0.0233	8.81E-04	3.09E-03
S	110	DEC20_S2	868	1.19E-04	3.23E-04	1.217	3.313	0.0050	0.0202	5.01E-04	1.48E-03
S	110	NOV29_S1	1085	1.55E-04	3.83E-04	1.591	3.947	0.0035	0.0139	4.19E-04	1.86E-03
S	123	Dec4_S1	1294	1.72E-04	3.61E-04	1.756	3.679	0.0083	0.0420	4.82E-04	1.31E-03
S	123	NOV26_S1	3992	1.83E-04	3.73E-04	1.879	3.834	0.0060	0.0246	5.77E-04	1.99E-03
S	12T/C	Oct24_partial	344	1.76E-04	3.63E-04	1.801	3.727	0.0063	0.0207	4.29E-04	1.54E-03
U	109	Jan9_S2	301	9.00E-05	2.55E-04	0.921	2.619	0.0036	0.0191	1.97E-04	5.28E-04
U	109	JAN9_S3	185	0.00E+00	0.00E+00	0.000	0.000	0.0000	0.0000	0.00E+00	0.00E+00
U	110	DEC20_S1	793	1.53E-04	2.97E-04	1.567	3.035	0.0087	0.0326	8.83E-04	2.33E-03
U	110	DEC20_S2	341	2.60E-05	1.49E-04	0.271	1.534	0.0006	0.0039	4.80E-05	2.48E-04
U	110	NOV29_S1	663	1.30E-04	2.91E-04	1.328	2.983	0.0047	0.0195	4.36E-04	9.59E-04
U	12T/C	Oct24_partial	1009	1.58E-04	3.12E-04	1.618	3.205	0.0047	0.0153	2.78E-04	6.10E-04

Table E-28: PHEV Sprinter NO, NO_2 and NOx data by sample run file during charge-depleting operation.

Road Code	Route	File Name	N	NO (g/s)		NO_2 (g/s)		NOx (g/s)	
				Mean	StDev	Mean	StDev	Mean	StDev
Hwy	Highway	Four	815	0.057	0.045	3.70E-03	2.11E-03	0.061	0.046
Hwy	Highway	One	827	0.049	0.045	3.69E-03	2.78E-03	0.053	0.046
Hwy	Highway	Three	747	0.046	0.043	2.34E-03	1.64E-03	0.049	0.044
Hwy	Highway	Two	615	0.050	0.044	2.83E-03	1.99E-03	0.053	0.044
S	109	Jan9_109S1	479	0.024	0.030	4.21E-04	1.02E-03	0.024	0.031
S	109	Jan9_S2	1183	0.014	0.028	2.17E-04	4.78E-04	0.014	0.028
S	109	JAN9_S3	614	0.014	0.026	2.69E-04	5.17E-04	0.015	0.027
S	110	DEC20_S1	1014	0.006	0.019	1.18E-04	4.14E-04	0.007	0.019
S	110	DEC20_S2	868	0.008	0.024	1.29E-04	4.61E-04	0.008	0.024
S	110	NOV29_S1	1085	0.015	0.040	6.23E-04	1.57E-03	0.016	0.041
S	123	Dec4_S1	1294	0.014	0.028	5.59E-04	1.09E-03	0.014	0.029
S	123	NOV26_S1	3992	0.015	0.030	1.25E-03	2.73E-03	0.016	0.032
S	12T/C	Oct24_partial	344	0.011	0.024	1.27E-03	2.45E-03	0.013	0.026
U	109	Jan9_S2	301	0.007	0.021	8.60E-05	2.98E-04	0.007	0.022
U	109	JAN9_S3	185	0.000	0.000	0.00E+00	1.00E-06	0.000	0.000
U	110	DEC20_S1	793	0.013	0.023	2.10E-04	3.67E-04	0.013	0.023
U	110	DEC20_S2	341	0.002	0.015	3.40E-05	2.10E-04	0.003	0.016
U	110	NOV29_S1	663	0.012	0.026	3.25E-04	7.13E-04	0.012	0.026
U	12T/C	Oct24_partial	1009	0.011	0.021	1.09E-03	2.32E-03	0.012	0.023

Table E-29: PHEV Sprinter velocity and acceleration data by sample run file during charge-depleting operation.

Road Code	Route	File Name	N	Velocity (km/h)		Positive Accel (m/s^2)		Negative Accel (m/s^2)	
				Mean	StDev	Mean	StDev	Mean	StDev
Hwy	Highway	Four	815	75.2	18.1	0.21	0.29	-0.22	0.30
Hwy	Highway	One	827	68.8	26.2	0.23	0.37	-0.31	0.37
Hwy	Highway	Three	747	73.8	20.2	0.21	0.28	-0.19	0.32
Hwy	Highway	Two	615	76.9	18.4	0.24	0.34	-0.22	0.33
S	109	Jan9_109S1	479	39.1	16.3	0.37	0.40	-0.45	0.44
S	109	Jan9_S2	1183	35.9	18.2	0.33	0.42	-0.47	0.49
S	109	JAN9_S3	614	35.1	16.6	0.44	0.45	-0.47	0.44
S	110	DEC20_S1	1014	30.9	16.9	0.43	0.45	-0.56	0.48
S	110	DEC20_S2	868	30.4	19.1	0.39	0.49	-0.56	0.49
S	110	NOV29_S1	1085	30.4	18.7	0.40	0.45	-0.59	0.54
S	123	Dec4_S1	1294	13.4	17.0	0.23	0.48	-0.76	0.55
S	123	NOV26_S1	3992	22.5	18.6	0.35	0.48	-0.63	0.50
S	12T/C	Oct24_partia	344	30.5	16.3	0.51	0.41	-0.58	0.48
U	109	Jan9_S2	301	17.9	14.2	0.36	0.48	-0.47	0.37
U	109	JAN9_S3	185	16.9	12.6	0.36	0.42	-0.48	0.44
U	110	DEC20_S1	793	16.7	14.1	0.38	0.50	-0.66	0.49
U	110	DEC20_S2	341	18.2	13.3	0.35	0.47	-0.56	0.42
U	110	NOV29_S1	663	19.9	14.8	0.37	0.48	-0.60	0.48
U	12T/C	Oct24_partia	1009	12.6	12.8	0.26	0.42	-0.62	0.46

Table E-30: PHEV Sprinter power data by sample run file during charge-depleting operation.

Road Code	Route	File Name	N	ICE Power (W/kg/s)		EM Power (W/kg/s)		Tot. Power (W/kg/s)		Recuperation (W/kg/s)	
				Mean	StDev	Mean	StDev	Mean	StDev	Mean	StDev
Hwy	Highway	Four	815	8.01	6.43	0.38	2.15	8.39	6.37	-1.32	1.75
Hwy	Highway	One	827	7.23	6.39	0.16	1.28	7.39	6.43	-0.30	0.82
Hwy	Highway	Three	747	7.11	6.86	0.73	2.88	7.84	6.79	-0.27	0.67
Hwy	Highway	Two	615	7.47	6.04	0.78	3.42	8.25	6.21	-0.26	0.78
S	109	Jan9_109S1	479	2.39	4.08	0.96	2.82	3.35	4.50	-0.49	0.81
S	109	Jan9_S2	1183	1.81	4.14	2.20	3.96	4.01	5.11	-0.47	1.01
S	109	JAN9_S3	614	1.76	3.71	2.87	4.83	4.63	5.27	-0.52	1.08
S	110	DEC20_S1	1014	1.06	3.56	2.59	4.46	3.66	5.52	-0.55	1.00
S	110	DEC20_S2	868	1.38	4.19	3.12	4.55	4.50	5.57	-0.58	1.26
S	110	NOV29_S1	1085	1.80	5.02	3.00	4.60	4.80	6.07	-1.06	2.27
S	123	Dec4_S1	1294	1.62	4.20	0.88	2.35	2.50	4.55	-0.44	0.85
S	123	NOV26_S1	3992	2.03	4.92	1.85	4.02	3.87	5.90	-0.92	1.62
S	12T/C	Oct24_partia	344	2.01	4.94	2.18	3.88	4.19	5.64	-0.74	1.28
U	109	Jan9_S2	301	0.94	3.07	2.05	3.55	2.99	4.25	-0.24	0.59
U	109	JAN9_S3	185	0.00	0.00	2.89	4.24	2.89	4.24	-0.24	0.63
U	110	DEC20_S1	793	1.49	3.76	1.81	3.74	3.30	4.99	-0.64	0.93
U	110	DEC20_S2	341	0.31	1.84	1.69	3.28	2.00	3.66	-0.49	0.95
U	110	NOV29_S1	663	1.27	3.45	1.90	3.60	3.16	4.46	-0.59	0.93
U	12T/C	Oct24_partia	1009	1.66	4.15	1.26	2.92	2.92	4.75	-0.35	0.66

The following correlation tables were developed for each roadway type and evaluated according to the criteria set below. The following correlation tables include stylized type identifying the extent of correlation, when one justified. Correlation coefficients corresponding to moderately positive correlations and stronger are provided in **bold** typeface.

Table E-31: Parameters for assessing correlation coefficients.

	Pearson Correlation Coefficient Range	**Corresponding R^2 Range**
Very High Positive Correlation	0.90 - 1.00	0.81 - 1.00
Good Positive Correlation	0.70 - 0.89	0.49 - 0.80
Moderate Positive Correlation	0.50 - 0.69	0.25 - 0.48
Weak Positive Correlation	0.30 - 0.49	0.09 - 0.24
Negligible Correlation	-0.29 - 0.29	0.00 - 0.08
Weak Negative Correlation	-0.30 - -0.49	0.09 - 0.24
Moderate Negative Correlation	-0.5 - -0.69	0.25 - 0.48
Good Negative Correlation	-0.70 - -0.89	0.49 - 0.80
Very High Negative Correlation	-0.90 - -1.00	0.81 - 1.00

Table E-32: Correlation results for charge-sustaining highway driving.

	Exhaust Temp (C)	Fuel (gal/s)	CO_2 (g/s)	CO (g/s)	NO (g/s)	NO_2 (g/s)	NOx (g/s)	HC (g/s)	Velocity (km/hr)	Accel (m/s^2)	Grade (%)	VSP Inst (W/kg/s)	ICE Pwr (W/kg/s)	EM Pwr (W/kg/s)	Total Pwr (W/kg/s)	Recup (W/kg/s)
Fuel (gal/s)	0.387															
	0.000															
CO_2 (g/s)	0.388	1.000														
	0.000	0.000														
CO (g/s)	-0.194	0.179	0.176													
	0.000	0.000	0.000													
NO (g/s)	0.378	**0.957**	**0.957**	0.085												
	0.000	0.000	0.000	0.006												
NO_2 (g/s)	**0.547**	0.425	0.426	-0.016	0.454											
	0.000	0.000	0.000	0.597	0.000											
NOx (g/s)	0.396	**0.956**	**0.956**	0.082	**0.999**	0.492										
	0.000	0.000	0.000	0.007	0.000	0.000										
HC (g/s)	-0.097	0.391	0.389	**0.672**	0.308	-0.042	0.299									
	0.002	0.000	0.000	0.000	0.000	0.173	0.000									
Velocity (km/hr)	**0.765**	**0.502**	**0.503**	-0.072	0.456	0.379	0.464	0.085								
	0.000	0.000	0.000	0.018	0.000	0.000	0.000	0.005								
Accel (m/s^2)	-0.279	0.309	0.309	0.315	0.249	0.065	0.247	0.258	0.020							
	0.000	0.000	0.000	0.000	0.000	0.036	0.000	0.000	0.525							
Grade (%)	0.037	0.417	0.417	0.050	0.454	0.090	0.448	0.098	-0.039	-0.091						
	0.228	0.000	0.000	0.105	0.000	0.003	0.000	0.001	0.200	0.003						
VSP Inst (W/kg/s)	0.057	**0.772**	**0.773**	0.198	**0.750**	0.234	**0.744**	0.329	0.260	**0.601**	**0.529**					
	0.063	0.000	0.000	0.000	0.000	0.000	0.000	0.000	0.000	0.000	0.000					
ICE Pwr (W/kg/s)	0.362	**0.988**	**0.988**	0.140	**0.958**	0.417	**0.956**	0.372	0.468	0.308	0.434	**0.785**				
	0.000	0.000	0.000	0.000	0.000	0.000	0.000	0.000	0.000	0.000	0.000	0.000				
EM Pwr (W/kg/s)	**-0.660**	-0.270	-0.271	0.254	-0.289	-0.224	-0.293	0.123	-0.376	0.445	-0.078	0.130	-0.260			
	0.000	0.000	0.000	0.000	0.000	0.000	0.000	0.000	0.000	0.000	0.011	0.000	0.000			
Total Pwr (W/kg/s)	0.115	**0.910**	**0.910**	0.243	**0.872**	0.341	**0.869**	0.431	0.335	0.490	0.416	**0.857**	**0.927**	0.122		
	0.000	0.000	0.000	0.000	0.000	0.000	0.000	0.000	0.000	0.000	0.000	0.000	0.000	0.000		
Recup (W/kg/s)	-0.371	-0.318	-0.318	0.027	-0.300	-0.419	-0.314	-0.086	-0.380	0.036	0.211	0.088	-0.322	0.254	-0.232	
	0.000	0.000	0.000	0.378	0.000	0.000	0.000	0.005	0.000	0.239	0.000	0.004	0.000	0.000	0.000	
SOC (%)	0.120	-0.498	**-0.497**	-0.277	**-0.522**	-0.363	**-0.528**	-0.339	-0.028	-0.370	-0.071	-0.339	**-0.510**	-0.172	**-0.591**	**0.511**
	0.000	0.000	0.000	0.000	0.000	0.000	0.000	0.000	0.355	0.000	0.021	0.000	0.000	0.000	0.000	0.000

Table E-33: Correlation results for charge-sustaining suburban driving.

	Exhaust Temp C)	Fuel (gal/s)	CO_2 (g/s)	CO (g/s)	NO (g/s)	NO_2 (g/s)	NOx (g/s)	HC (g/s)	Velocity (km/hr)	Accel (m/s^2)	Grade (%)	VSP Inst (W/kg/s)	ICE Pwr (W/kg/s)	EM Pwr (W/kg/s)	Total Pwr (W/kg/s)	Recup (W/kg/s)
Fuel (gal/s)	0.476															
	0.000															
CO_2 (g/s)	0.475	**1.000**														
	0.000	0.000														
CO (g/s)	0.081	0.348	0.344													
	0.000	0.000	0.000													
NO (g/s)	**0.504**	**0.952**	**0.952**	0.266												
	0.000	0.000	0.000	0.000												
NO_2 (g/s)	**0.503**	**0.704**	**0.704**	0.272	**0.706**											
	0.000	0.000	0.000	0.000	0.000											
NOx (g/s)	**0.514**	**0.953**	**0.953**	0.272	**0.998**	**0.744**										
	0.000	0.000	0.000	0.000	0.000	0.000										
HC (g/s)	0.179	0.461	0.460	0.321	0.394	0.215	0.388									
	0.000	0.000	0.000	0.000	0.000	0.000	0.000									
Velocity (km/hr)	0.301	0.249	0.249	-0.129	0.285	0.148	0.280	0.132								
	0.000	0.000	0.000	0.000	0.000	0.000	0.000	0.000								
Accel (m/s^2)	-0.016	0.418	0.418	0.255	0.350	0.272	0.351	0.225	0.056							
	0.145	0.000	0.000	0.000	0.000	0.000	0.000	0.000	0.000							
Grade (%)	0.031	0.053	0.053	0.043	0.053	0.066	0.055	0.023	-0.033	0.005						
	0.005	0.000	0.000	0.000	0.000	0.000	0.000	0.036	0.003	0.644						
VSP Inst (W/kg/s)	0.140	**0.605**	**0.606**	0.171	**0.562**	0.369	**0.559**	0.332	0.134	**0.711**	0.124					
	0.000	0.000	0.000	0.000	0.000	0.000	0.000	0.000	0.000	0.000	0.000					
ICE Pwr (W/kg/s)	0.427	**0.938**	**0.939**	0.258	**0.900**	**0.595**	**0.896**	0.434	0.286	0.415	0.052	**0.633**				
	0.000	0.000	0.000	0.000	0.000	0.000	0.000	0.000	0.000	0.000	0.000	0.000				
EM Pwr (W/kg/s)	-0.275	-0.221	-0.221	-0.066	-0.269	-0.223	-0.271	0.008	0.048	0.396	0.008	0.372	-0.225			
	0.000	0.000	0.000	0.000	0.000	0.000	0.000	0.474	0.000	0.000	0.451	0.000	0.000			
Total Pwr (W/kg/s)	0.284	**0.815**	**0.815**	0.222	**0.754**	0.475	**0.748**	0.432	0.306	**0.607**	0.055	**0.810**	**0.874**	0.277		
	0.000	0.000	0.000	0.000	0.000	0.000	0.000	0.000	0.000	0.000	0.000	0.000	0.000	0.000		
Recup (W/kg/s)	-0.478	**-0.722**	**-0.722**	-0.045	**-0.743**	-0.432	**-0.735**	-0.315	-0.466	-0.138	-0.013	-0.325	**-0.807**	0.348	**-0.622**	
	0.000	0.000	0.000	0.000	0.000	0.000	0.000	0.000	0.000	0.000	0.241	0.000	0.000	0.000	0.000	
SOC (%)	0.330	0.007	0.007	-0.076	0.034	0.116	0.041	-0.026	0.025	-0.060	-0.006	-0.029	-0.005	-0.070	-0.040	0.004
	0.000	0.537	0.508	0.000	0.002	0.000	0.000	0.022	0.023	0.000	0.606	0.009	0.627	0.000	0.000	0.725

Table E-34: Correlation results for charge-sustaining urban driving.

	Exhaust Temp (C)	Fuel (gal/s)	CO_2 (g/s)	CO (g/s)	NO (g/s)	NO_2 (g/s)	NOx (g/s)	HC (g/s)	Velocity (km/hr)	Accel (m/s^2)	Grade (%)	VSP Inst (W/kg/s)	ICE Pwr (W/kg/s)	EM Pwr (W/kg/s)	Total Pwr (W/kg/s)	Recup (W/kg/s)
Fuel (gal/s)	0.482															
	0.000															
CO_2 (g/s)	0.482	**1.000**														
	0.000	0.000														
CO (g/s)	0.111	0.448	0.443													
	0.000	0.000	0.000													
NO (g/s)	**0.507**	**0.960**	**0.961**	0.373												
	0.000	0.000	0.000	0.000												
NO_2 (g/s)	**0.543**	**0.704**	**0.704**	0.328	**0.686**											
	0.000	0.000	0.000	0.000	0.000											
NOx (g/s)	**0.522**	**0.962**	**0.963**	0.378	**0.998**	**0.727**										
	0.000	0.000	0.000	0.000	0.000	0.000										
HC (g/s)	0.102	0.436	0.435	0.376	0.376	0.144	0.366									
	0.000	0.000	0.000	0.000	0.000	0.000	0.000									
Velocity (km/hr)	0.256	0.332	0.333	-0.004	0.341	0.152	0.333	0.163								
	0.000	0.000	0.000	0.855	0.000	0.000	0.000	0.000								
Accel (m/s^2)	-0.013	0.386	0.386	0.277	0.340	0.278	0.343	0.179	0.074							
	0.566	0.000	0.000	0.000	0.000	0.000	0.000	0.000	0.001							
Grade (%)	0.020	-0.002	-0.002	0.000	0.003	-0.004	0.002	-0.002	-0.028	0.000						
	0.384	0.940	0.941	0.986	0.902	0.852	0.919	0.920	0.223	0.994						
VSP Inst (W/kg/s)	0.169	0.424	0.424	0.180	0.400	0.256	0.398	0.233	0.230	0.489	0.043					
	0.000	0.000	0.000	0.000	0.000	0.000	0.000	0.000	0.000	0.000	0.061					
ICE Pwr (W/kg/s)	0.415	**0.887**	**0.888**	0.336	**0.857**	**0.547**	**0.853**	0.382	0.359	0.394	-0.006	**0.504**				
	0.000	0.000	0.000	0.000	0.000	0.000	0.000	0.000	0.000	0.000	0.812	0.000				
EM Pwr (W/kg/s)	-0.260	-0.199	-0.199	-0.062	-0.226	-0.190	-0.228	0.021	0.168	0.354	-0.010	0.250	-0.217			
	0.000	0.000	0.000	0.008	0.000	0.000	0.000	0.358	0.000	0.000	0.674	0.000	0.000			
Total Pwr (W/kg/s)	0.280	**0.774**	**0.775**	0.300	**0.731**	0.444	**0.725**	0.386	0.436	**0.562**	-0.010	**0.620**	**0.876**	0.281		
	0.000	0.000	0.000	0.000	0.000	0.000	0.000	0.000	0.000	0.000	0.659	0.000	0.000	0.000		
Recup (W/kg/s)	-0.438	**-0.677**	**-0.678**	-0.104	**-0.695**	-0.365	**-0.685**	-0.266	-0.491	-0.067	0.004	-0.309	**-0.792**	0.289	**-0.636**	
	0.000	0.000	0.000	0.000	0.000	0.000	0.000	0.000	0.000	0.004	0.851	0.000	0.000	0.000	0.000	
SOC (%)	-0.082	-0.104	-0.103	-0.077	-0.096	-0.080	-0.097	0.012	-0.166	-0.031	0.006	-0.081	-0.116	-0.061	-0.144	0.143
	0.000	0.000	0.000	0.001	0.000	0.001	0.000	0.611	0.000	0.177	0.788	0.000	0.000	0.008	0.000	0.000

Table E-35: Correlation results for charge-depleting highway driving.

	Exhaust Temp (C)	Fuel (gal/s)	CO_2 (g/s)	CO (g/s)	NO (g/s)	NO_2 (g/s)	NOx (g/s)	HC (g/s)	Velocity (km/hr)	Accel (m/s^2)	Grade (%)	VSP Inst (W/kg/s)	ICE Pwr (W/kg/s)	EM Pwr (W/kg/s)	Total Pwr (W/kg/s)	Recup (W/kg/s)
Fuel (gal/s)	0.243															
	0.000															
CO_2 (g/s)	0.245	**1.000**														
	0.000	0.000														
CO (g/s)	-0.291	0.278	0.273													
	0.000	0.000	0.000													
NO (g/s)	0.256	**0.945**	**0.945**	0.170												
	0.000	0.000	0.000	0.000												
NO_2 (g/s)	**0.643**	**0.508**	**0.510**	-0.032	0.489											
	0.000	0.000	0.000	0.433	0.000											
NOx (g/s)	0.282	**0.947**	**0.947**	0.164	**0.999**	**0.527**										
	0.000	0.000	0.000	0.000	0.000	0.000										
HC (g/s)	-0.267	0.403	0.399	**0.798**	0.288	-0.057	0.278									
	0.000	0.000	0.000	0.000	0.000	0.161	0.000									
Velocity (km/hr)	**0.757**	0.386	0.388	-0.153	0.336	**0.556**	0.355	-0.035								
	0.000	0.000	0.000	0.000	0.000	0.000	0.000	0.389								
Accel (m/s^2)	-0.224	0.389	0.388	0.424	0.289	0.115	0.288	0.383	0.041							
	0.000	0.000	0.000	0.000	0.000	0.005	0.000	0.000	0.320							
Grade (%)	0.102	**0.554**	**0.555**	0.017	**0.614**	0.306	**0.613**	0.105	0.068	0.007						
	0.012	0.000	0.000	0.686	0.000	0.000	0.000	0.010	0.095	0.871						
VSP Inst (W/kg/s)	0.098	**0.847**	**0.848**	0.233	**0.818**	0.450	**0.820**	0.349	0.255	**0.606**	**0.619**					
	0.016	0.000	0.000	0.000	0.000	0.000	0.000	0.000	0.000	0.000	0.000					
ICE Pwr (W/kg/s)	0.240	**0.987**	**0.988**	0.228	**0.944**	0.483	**0.944**	0.368	0.353	0.378	**0.567**	**0.858**				
	0.000	0.000	0.000	0.000	0.000	0.000	0.000	0.000	0.000	0.000	0.000	0.000				
EM Pwr (W/kg/s)	**-0.522**	-0.174	-0.175	0.244	-0.201	-0.265	-0.209	0.193	-0.354	**0.498**	-0.067	0.140	-0.161			
	0.000	0.000	0.000	0.000	0.000	0.000	0.000	0.000	0.000	0.000	0.098	0.001	0.000			
Total Pwr (W/kg/s)	0.041	**0.911**	**0.911**	0.317	**0.858**	0.378	**0.855**	0.436	0.217	**0.562**	**0.536**	**0.901**	**0.929**	0.216		
	0.316	0.000	0.000	0.000	0.000	0.000	0.000	0.000	0.000	0.000	0.000	0.000	0.000	0.000		
Recup (W/kg/s)	-0.166	0.272	0.274	0.086	0.204	0.083	0.203	0.160	0.066	0.306	0.204	0.451	0.276	0.104	0.312	
	0.000	0.000	0.000	0.035	0.000	0.043	0.000	0.000	0.107	0.000	0.000	0.000	0.000	0.011	0.000	
SOC (%)	-0.293	-0.011	-0.011	0.080	-0.052	0.022	-0.049	0.125	-0.129	-0.037	-0.004	-0.053	-0.038	-0.033	-0.050	0.316
	0.000	0.794	0.792	0.049	0.205	0.584	0.227	0.002	0.002	0.371	0.921	0.192	0.348	0.422	0.219	0.000

Table E-36: Correlation results for charge-depleting suburban driving.

	Exhaust Temp (C)	Fuel (gal/s)	CO_2 (g/s)	CO (g/s)	NO (g/s)	NO_2 (g/s)	NOx (g/s)	HC (g/s)	Velocity (km/hr)	Accel (m/s^2)	Grade (%)	VSP Inst (W/kg/s)	ICE Pwr (W/kg/s)	EM Pwr (W/kg/s)	Total Pwr (W/kg/s)	Recup (W/kg/s)
Fuel (gal/s)	0.491															
	0.000															
CO_2 (g/s)	0.491	**1.000**														
	0.000	0.000														
CO (g/s)	0.137	**0.549**	**0.542**													
	0.000	0.000	0.000													
NO (g/s)	**0.508**	**0.946**	**0.947**	0.434												
	0.000	0.000	0.000	0.000												
NO_2 (g/s)	**0.568**	**0.617**	**0.618**	0.230	**0.640**											
	0.000	0.000	0.000	0.000	0.000											
NOx (g/s)	**0.523**	**0.946**	**0.946**	0.430	**0.999**	**0.676**										
	0.000	0.000	0.000	0.000	0.000	0.000										
HC (g/s)	0.188	**0.581**	**0.577**	**0.706**	0.443	0.174	0.436									
	0.000	0.000	0.000	0.000	0.000	0.000	0.000									
Velocity (km/hr)	0.238	0.209	0.209	0.059	0.183	0.074	0.180	0.205								
	0.000	0.000	0.000	0.006	0.000	0.001	0.000	0.000								
Accel (m/s^2)	-0.001	0.360	0.359	0.329	0.304	0.198	0.304	0.238	0.050							
	0.967	0.000	0.000	0.000	0.000	0.000	0.000	0.000	0.020							
Grade (%)	0.027	0.044	0.043	0.127	0.044	0.009	0.043	0.015	-0.022	0.012						
	0.216	0.038	0.043	0.000	0.038	0.673	0.044	0.489	0.304	0.585						
VSP Inst (W/kg/s)	0.135	**0.537**	**0.538**	0.335	0.477	0.263	0.474	0.396	0.148	**0.723**	0.062					
	0.000	0.000	0.000	0.000	0.000	0.000	0.000	0.000	0.000	0.000	0.004					
ICE Pwr (W/kg/s)	0.453	**0.975**	**0.976**	0.474	**0.917**	**0.612**	**0.917**	**0.531**	0.179	0.352	0.026	**0.549**				
	0.000	0.000	0.000	0.000	0.000	0.000	0.000	0.000	0.000	0.000	0.226	0.000				
EM Pwr (W/kg/s)	-0.221	-0.166	-0.167	0.075	-0.223	-0.172	-0.225	0.037	0.158	0.490	0.000	0.495	-0.146			
	0.000	0.000	0.000	0.000	0.000	0.000	0.000	0.082	0.000	0.000	0.987	0.000	0.000			
Total Pwr (W/kg/s)	0.203	**0.663**	**0.663**	0.435	**0.575**	0.367	**0.574**	0.454	0.259	**0.638**	0.021	**0.800**	**0.698**	**0.607**		
	0.000	0.000	0.000	0.000	0.000	0.000	0.000	0.000	0.000	0.000	0.337	0.000	0.000	0.000		
Recup (W/kg/s)	-0.366	-0.247	-0.248	0.031	-0.340	-0.387	-0.350	0.013	-0.160	0.188	-0.004	0.211	-0.267	0.292	-0.003	
	0.000	0.000	0.000	0.144	0.000	0.000	0.000	0.534	0.000	0.000	0.853	0.000	0.000	0.000	0.895	
SOC (%)	-0.199	-0.032	-0.033	0.057	-0.064	-0.215	-0.075	0.062	-0.131	0.007	0.024	-0.046	-0.073	-0.111	-0.139	0.271
	0.000	0.140	0.130	0.008	0.003	0.000	0.000	0.004	0.000	0.742	0.256	0.033	0.001	0.000	0.000	0.000

Table E-37: Correlation results for charge-depleting urban driving.

	Exhaust Temp (C)	Fuel (gal/s)	CO_2 (g/s)	CO (g/s)	NO (g/s)	NO_2 (g/s)	NOx (g/s)	HC (g/s)	Velocity (km/hr)	Accel (m/s^2)	Grade (%)	VSP Inst (W/kg/s)	ICE Pwr (W/kg/s)	EM Pwr (W/kg/s)	Total Pwr (W/kg/s)	Recup (W/kg/s)
Fuel (gal/s)	0.460															
	0.000															
CO_2 (g/s)	0.461	**1.000**														
	0.000	0.000														
CO (g/s)	0.233	**0.711**	**0.706**													
	0.000	0.000	0.000													
NO (g/s)	0.460	**0.945**	**0.945**	**0.693**												
	0.000	0.000	0.000	0.000												
NO_2 (g/s)	0.451	**0.591**	**0.592**	0.289	**0.505**											
	0.000	0.000	0.000	0.000	0.000											
NOx (g/s)	0.472	**0.951**	**0.950**	**0.688**	**0.999**	**0.550**										
	0.000	0.000	0.000	0.000	0.000	0.000										
HC (g/s)	0.301	**0.598**	**0.595**	**0.687**	**0.559**	0.148	**0.550**									
	0.000	0.000	0.000	0.000	0.000	0.000	0.000									
Velocity (km/hr)	0.129	0.158	0.158	0.085	0.101	0.056	0.102	0.224								
	0.001	0.000	0.000	0.030	0.009	0.149	0.009	0.000								
Accel (m/s^2)	0.020	0.427	0.427	0.384	0.393	0.259	0.396	0.245	0.078							
	0.610	0.000	0.000	0.000	0.000	0.000	0.000	0.000	0.046							
Grade (%)	-0.038	0.020	0.020	0.034	-0.007	0.005	-0.006	0.018	0.039	0.052						
	0.328	0.600	0.604	0.382	0.867	0.889	0.878	0.651	0.324	0.179						
VSP Inst (W/kg/s)	0.078	0.377	0.377	0.298	0.334	0.185	0.334	0.284	0.198	**0.581**	0.201					
	0.046	0.000	0.000	0.000	0.000	0.000	0.000	0.000	0.000	0.000	0.000					
ICE Pwr (W/kg/s)	0.414	**0.969**	**0.969**	**0.646**	**0.892**	**0.606**	**0.900**	**0.537**	0.134	0.432	0.029	0.400				
	0.000	0.000	0.000	0.000	0.000	0.000	0.000	0.000	0.001	0.000	0.450	0.000				
EM Pwr (W/kg/s)	-0.190	-0.144	-0.144	-0.014	-0.207	-0.092	-0.206	-0.032	0.195	0.486	0.086	0.479	-0.103			
	0.000	0.000	0.000	0.717	0.000	0.019	0.000	0.408	0.000	0.000	0.027	0.000	0.008			
Total Pwr (W/kg/s)	0.172	**0.625**	**0.625**	0.477	**0.520**	0.390	**0.527**	0.382	0.245	**0.685**	0.086	**0.656**	**0.679**	**0.661**		
	0.000	0.000	0.000	0.000	0.000	0.000	0.000	0.000	0.000	0.000	0.028	0.000	0.000	0.000		
Recup (W/kg/s)	-0.170	0.039	0.039	0.060	-0.035	0.014	-0.033	0.022	-0.156	0.333	0.091	0.300	0.087	0.335	0.314	
	0.000	0.323	0.313	0.121	0.374	0.715	0.402	0.581	0.000	0.000	0.019	0.000	0.025	0.000	0.000	
SOC (%)	**0.585**	0.198	0.197	0.139	0.183	0.204	0.190	0.161	-0.116	-0.002	0.024	-0.037	0.162	-0.113	0.038	-0.069
	0.000	0.000	0.000	0.000	0.000	0.000	0.000	0.000	0.003	0.969	0.535	0.340	0.000	0.004	0.326	0.079

Appendix F: Diesel Internal Combustion Engine Assessment

The following tables summarize the PHEV Sprinter's hybrid-only operation according to VSP bin and Roadway type.

Table F-1: Descriptive statistics summary for PHEV hybrid operation's emissions according to VSP bin during charge-depleting operation.

Variable	OP Mode	VSP Bin	N	Mean	Std. Dev.	Minimum	Q1	Median	Q3	Maximum
CO_2 (g/s)	CD	1	3020	1.68	1.87	0.01	0.40	1.65	1.98	20.68
		2	660	3.69	2.57	0.06	1.97	3.09	5.06	19.05
		3	688	5.08	2.87	0.08	3.03	4.63	6.70	20.97
		4	636	6.45	3.02	0.10	4.44	5.93	8.00	20.93
		5	605	7.75	3.21	0.20	5.49	7.54	9.70	20.88
		6	556	8.64	3.11	0.35	6.72	8.70	10.50	18.37
		7	692	9.91	3.52	0.05	7.84	9.83	11.93	20.68
		8	723	12.88	4.01	1.15	10.27	12.38	15.74	24.84
CO (g/s)	CD	1	3020	4.93E-03	2.18E-02	0.00E+00	7.60E-04	1.35E-03	3.09E-03	5.29E-01
		2	660	8.97E-03	1.77E-02	0.00E+00	2.16E-03	3.84E-03	8.46E-03	2.32E-01
		3	688	1.23E-02	3.73E-02	0.00E+00	2.73E-03	4.46E-03	1.00E-02	4.83E-01
		4	636	1.57E-02	3.80E-02	0.00E+00	2.84E-03	4.62E-03	1.25E-02	4.06E-01
		5	605	1.68E-02	4.04E-02	0.00E+00	3.15E-03	4.72E-03	1.18E-02	4.48E-01
		6	556	1.59E-02	3.35E-02	0.00E+00	3.24E-03	4.85E-03	1.13E-02	3.90E-01
		7	692	1.99E-02	4.06E-02	0.00E+00	3.44E-03	5.07E-03	1.45E-02	4.14E-01
		8	723	1.87E-02	3.22E-02	7.20E-04	4.00E-03	7.21E-03	1.89E-02	4.56E-01
NO (g/s)	CD	1	3020	0.016	0.016	0.000	0.004	0.015	0.021	0.181
		2	660	0.026	0.021	0.000	0.012	0.020	0.034	0.194
		3	688	0.036	0.026	0.000	0.019	0.030	0.047	0.196
		4	636	0.047	0.028	0.000	0.027	0.040	0.060	0.149
		5	605	0.061	0.033	0.000	0.037	0.057	0.079	0.240
		6	556	0.070	0.034	0.003	0.046	0.067	0.092	0.170
		7	692	0.081	0.038	0.001	0.055	0.080	0.106	0.242
		8	723	0.107	0.042	0.004	0.080	0.109	0.136	0.229
NO_2 (g/s)	CD	1	3020	1.27E-03	1.57E-03	0.00E+00	2.70E-04	5.40E-04	1.94E-03	2.03E-02
		2	660	2.24E-03	2.27E-03	0.00E+00	5.62E-04	1.60E-03	3.15E-03	1.43E-02
		3	688	2.61E-03	2.73E-03	0.00E+00	7.13E-04	1.88E-03	3.46E-03	2.43E-02
		4	636	2.78E-03	2.62E-03	0.00E+00	9.03E-04	2.11E-03	4.00E-03	2.72E-02
		5	605	3.39E-03	3.17E-03	0.00E+00	1.21E-03	2.69E-03	4.80E-03	2.97E-02
		6	556	3.60E-03	2.97E-03	0.00E+00	1.23E-03	2.94E-03	5.28E-03	1.92E-02
		7	692	3.83E-03	2.96E-03	0.00E+00	1.43E-03	3.39E-03	5.48E-03	2.12E-02
		8	723	3.79E-03	3.25E-03	0.00E+00	1.53E-03	2.93E-03	5.40E-03	2.35E-02
NOx (g/s)	CD	1	3020	0.017	0.016	0.000	0.005	0.017	0.022	0.186
		2	660	0.028	0.022	0.000	0.014	0.022	0.037	0.203
		3	688	0.039	0.027	0.000	0.021	0.032	0.050	0.210
		4	636	0.049	0.029	0.001	0.029	0.043	0.064	0.157
		5	605	0.064	0.035	0.000	0.040	0.059	0.083	0.247
		6	556	0.074	0.035	0.004	0.050	0.071	0.097	0.180
		7	692	0.085	0.039	0.001	0.059	0.085	0.110	0.249
		8	723	0.111	0.043	0.004	0.084	0.113	0.139	0.236
HC (g/s)	CD	1	3020	5.51E-04	6.47E-04	0.00E+00	1.50E-04	3.50E-04	6.80E-04	6.72E-03
		2	660	8.66E-04	8.99E-04	0.00E+00	3.20E-04	5.70E-04	1.15E-03	9.22E-03
		3	688	1.11E-03	1.24E-03	0.00E+00	3.90E-04	7.15E-04	1.45E-03	1.41E-02
		4	636	1.48E-03	1.90E-03	1.00E-05	4.60E-04	7.90E-04	1.84E-03	2.02E-02
		5	605	1.61E-03	2.23E-03	0.00E+00	4.90E-04	8.20E-04	1.98E-03	2.55E-02
		6	556	1.87E-03	2.68E-03	0.00E+00	5.40E-04	8.40E-04	2.12E-03	2.36E-02
		7	692	2.46E-03	3.99E-03	4.00E-05	5.60E-04	8.40E-04	2.71E-03	2.92E-02

Table F-2: Descriptive statistics summary for PHEV hybrid operation's power output and exhaust conditions according to VSP bin during charge-depleting operation.

Variable	OP Mode	VSP Bin	N	Mean	Std. Dev.	Minimum	Q1	Median	Q3	Maximum
Exhaust Temp (deg C)	CD	1	3020	90.5	40.2	19.4	59.9	78.2	123.4	189.4
		2	660	109.5	42.3	20.3	70.7	109.2	148.6	188.4
		3	688	111.2	43.3	21.0	72.5	114.3	150.4	189.8
		4	636	111.1	43.8	14.8	71.9	109.8	149.9	190.4
		5	605	116.4	43.7	14.3	76.4	126.0	153.2	190.3
		6	556	120.8	42.7	10.9	83.7	131.7	155.7	190.3
		7	692	122.6	44.7	13.7	81.8	138.3	160.4	190.4
		8	723	124.7	40.9	22.2	93.0	132.9	159.0	190.4
Diesel ICE Power (W/kg/s)	CD	1	3020	1.03	2.85	-5.04	-1.39	1.53	1.83	24.27
		2	660	3.69	3.77	-5.03	1.30	3.21	6.13	24.79
		3	688	5.43	4.25	-4.40	2.70	5.19	7.87	24.88
		4	636	7.34	4.11	-3.31	4.77	6.95	9.62	22.12
		5	605	9.17	4.43	-4.11	6.36	9.30	11.81	23.36
		6	556	10.46	4.21	-2.67	8.09	10.24	12.80	22.80
		7	692	12.24	4.62	-4.26	9.92	12.37	14.89	25.76
		8	723	16.47	5.27	-3.93	13.40	16.32	19.91	31.81
Electric Motor Power (W/kg/s)	CD	1	3020	0.01	0.27	0.00	0.00	0.00	0.00	11.01
		2	660	0.05	0.36	0.00	0.00	0.00	0.00	5.54
		3	688	0.20	1.35	0.00	0.00	0.00	0.02	14.63
		4	636	0.12	1.03	0.00	0.00	0.00	0.02	12.53
		5	605	0.30	1.75	0.00	0.00	0.00	0.03	14.72
		6	556	0.25	1.67	0.00	0.00	0.00	0.03	15.08
		7	692	0.33	1.81	0.00	0.00	0.00	0.04	14.93
		8	723	0.21	1.42	0.00	0.00	0.00	0.03	16.18
Total Power (W/kg/s)	CD	1	3020	1.04	2.88	-5.04	-1.39	1.53	1.83	24.36
		2	660	3.73	3.81	-5.03	1.32	3.22	6.14	24.91
		3	688	5.63	4.25	-3.87	2.90	5.37	8.02	24.92
		4	636	7.47	4.08	-3.31	4.87	7.06	9.66	23.55
		5	605	9.48	4.34	-2.91	6.45	9.44	11.88	24.18
		6	556	10.71	4.05	-2.20	8.22	10.37	12.97	22.82
		7	692	12.57	4.46	-3.47	10.09	12.50	15.11	33.92
		8	723	16.67	5.03	-3.31	13.48	16.43	20.11	31.81

Table F-3: Descriptive statistics summary for PHEV hybrid operation's emissions according to VSP bin during charge-sustaining operation.

Variable	OP Mode	VSP Bin	N	Mean	Std. Dev.	Minimum	Q1	Median	Q3	Maximum
CO_2 (g/s)	CS	1	16067	1.82	2.41	0.00	0.19	1.39	1.82	21.44
		2	3239	4.95	3.66	0.00	1.79	4.45	7.40	21.64
		3	3181	6.53	3.73	0.00	3.89	6.67	8.65	21.12
		4	2936	7.94	3.83	0.00	5.65	7.84	10.26	21.77
		5	2618	9.19	3.99	0.00	6.78	8.98	11.76	23.31
		6	2082	10.52	4.25	0.00	7.93	10.49	13.33	23.96
		7	2276	12.18	4.46	0.00	9.56	12.19	15.24	24.12
		8	2148	14.30	4.79	0.00	11.79	14.77	17.70	24.62
CO (g/s)	CS	1	16067	3.06E-03	1.77E-02	0.00E+00	1.40E-04	4.90E-04	1.05E-03	5.28E-01
		2	3239	1.09E-02	3.69E-02	0.00E+00	5.10E-04	1.86E-03	3.96E-03	3.51E-01
		3	3181	9.74E-03	3.44E-02	0.00E+00	9.45E-04	2.15E-03	3.82E-03	4.26E-01
		4	2936	8.22E-03	2.78E-02	0.00E+00	1.27E-03	2.39E-03	4.04E-03	3.98E-01
		5	2618	8.57E-03	2.76E-02	0.00E+00	1.52E-03	2.66E-03	4.58E-03	4.24E-01
		6	2082	7.66E-03	2.04E-02	0.00E+00	1.77E-03	2.95E-03	5.04E-03	2.88E-01
		7	2276	8.24E-03	1.94E-02	0.00E+00	2.14E-03	3.69E-03	6.61E-03	3.16E-01
		8	2148	8.25E-03	1.90E-02	0.00E+00	2.52E-03	4.41E-03	7.12E-03	3.18E-01
NO (g/s)	CS	1	16067	0.020	0.025	0.000	0.002	0.017	0.024	0.221
		2	3239	0.049	0.039	0.000	0.018	0.042	0.075	0.241
		3	3181	0.066	0.040	0.000	0.036	0.064	0.096	0.244
		4	2936	0.081	0.041	0.000	0.051	0.081	0.109	0.222
		5	2618	0.092	0.043	0.000	0.061	0.092	0.122	0.269
		6	2082	0.103	0.046	0.000	0.070	0.104	0.135	0.257
		7	2276	0.116	0.047	0.000	0.088	0.119	0.148	0.278
		8	2148	0.132	0.051	0.000	0.105	0.139	0.170	0.265
NO_2 (g/s)	CS	1	16067	2.24E-03	2.64E-03	0.00E+00	5.20E-04	1.58E-03	2.97E-03	3.99E-02
		2	3239	4.06E-03	4.14E-03	0.00E+00	1.38E-03	2.87E-03	5.34E-03	4.30E-02
		3	3181	4.70E-03	4.37E-03	0.00E+00	1.79E-03	3.43E-03	6.08E-03	3.19E-02
		4	2936	5.27E-03	4.66E-03	0.00E+00	2.21E-03	3.91E-03	6.78E-03	4.25E-02
		5	2618	5.27E-03	4.60E-03	0.00E+00	2.20E-03	3.96E-03	6.88E-03	5.48E-02
		6	2082	5.45E-03	4.55E-03	0.00E+00	2.33E-03	4.18E-03	7.30E-03	4.14E-02
		7	2276	5.84E-03	5.11E-03	0.00E+00	2.51E-03	4.37E-03	7.86E-03	4.10E-02
		8	2148	6.11E-03	5.09E-03	0.00E+00	2.35E-03	5.08E-03	8.59E-03	3.86E-02
NOx (g/s)	CS	1	16067	0.023	0.026	0.000	0.003	0.019	0.026	0.229
		2	3239	0.053	0.041	0.000	0.020	0.046	0.080	0.250
		3	3181	0.071	0.042	0.000	0.038	0.068	0.103	0.249
		4	2936	0.086	0.043	0.000	0.054	0.087	0.117	0.235
		5	2618	0.097	0.045	0.000	0.065	0.097	0.128	0.277
		6	2082	0.109	0.048	0.000	0.075	0.109	0.142	0.272
		7	2276	0.122	0.049	0.000	0.092	0.126	0.156	0.294
		8	2148	0.138	0.053	0.000	0.110	0.145	0.177	0.283
HC (g/s)	CS	1	16067	1.30E-04	1.90E-04	0.00E+00	3.00E-05	7.00E-05	1.60E-04	6.58E-03
		2	3239	2.85E-04	3.21E-04	0.00E+00	1.00E-04	2.10E-04	3.80E-04	5.64E-03
		3	3181	3.72E-04	3.45E-04	0.00E+00	1.70E-04	2.90E-04	4.80E-04	3.65E-03
		4	2936	4.52E-04	4.20E-04	0.00E+00	2.30E-04	3.70E-04	5.70E-04	8.97E-03
		5	2618	5.99E-04	8.93E-04	0.00E+00	2.90E-04	4.60E-04	6.70E-04	2.63E-02
		6	2082	7.03E-04	1.03E-03	0.00E+00	3.60E-04	5.30E-04	7.80E-04	2.39E-02
		7	2276	8.96E-04	1.70E-03	0.00E+00	4.30E-04	6.30E-04	9.00E-04	3.68E-02
		8	2148	1.13E-03	1.85E-03	0.00E+00	5.30E-04	7.90E-04	1.12E-03	3.04E-02

Table F-4: Descriptive statistics summary for PHEV hybrid operation's power output and exhaust conditions according to VSP bin during charge-sustaining operation.

Variable	OP Mode	VSP Bin	N	Mean	Std. Dev.	Minimum	Q1	Median	Q3	Maximum
Exhaust Temp (deg C)	CS	1	16067	124.2	33.0	17.6	107.1	127.2	146.1	214.4
		2	3239	135.5	34.3	17.8	119.5	138.6	159.0	214.6
		3	3181	139.3	36.0	17.5	123.5	144.0	164.1	215.0
		4	2936	142.9	34.9	16.4	127.0	147.6	166.7	214.7
		5	2618	145.9	35.1	18.3	127.9	151.0	171.4	213.1
		6	2082	149.0	33.5	18.7	131.5	153.6	173.6	214.7
		7	2276	150.5	33.4	18.7	132.8	157.3	174.2	213.4
		8	2148	153.0	31.7	17.3	137.5	159.1	175.0	209.0
Diesel ICE Power (W/kg/s)	CS	1	16067	1.52	3.42	-3.18	-1.27	1.43	1.85	24.45
		2	3239	5.72	5.14	-3.81	0.72	6.54	9.51	23.04
		3	3181	8.38	5.12	-3.50	6.01	9.17	11.49	31.78
		4	2936	10.31	4.97	-3.05	8.22	10.47	13.42	28.24
		5	2618	12.30	5.05	-4.35	9.62	12.32	15.72	29.92
		6	2082	14.05	5.26	-3.86	11.20	14.08	17.50	31.38
		7	2276	16.25	5.15	-4.18	13.21	16.14	19.83	29.81
		8	2148	19.26	5.46	-1.75	16.27	19.31	23.05	31.78
Electric Motor Power (W/kg/s)	CS	1	16067	0.00	0.18	0.00	0.00	0.00	0.00	15.15
		2	3239	0.01	0.37	0.00	0.00	0.00	0.00	15.27
		3	3181	0.04	0.55	0.00	0.00	0.00	0.00	14.20
		4	2936	0.05	0.66	0.00	0.00	0.00	0.00	13.97
		5	2618	0.12	1.12	0.00	0.00	0.00	0.00	14.24
		6	2082	0.23	1.58	0.00	0.00	0.00	0.00	15.02
		7	2276	0.23	1.62	0.00	0.00	0.00	0.00	16.97
		8	2148	0.07	0.87	0.00	0.00	0.00	0.00	17.11
Total Power (W/kg/s)	CS	1	16067	1.53	3.42	-3.16	-1.27	1.43	1.85	24.45
		2	3239	5.73	5.13	-2.80	0.76	6.55	9.52	23.04
		3	3181	8.42	5.08	-3.05	6.05	9.18	11.52	31.78
		4	2936	10.35	4.94	-2.93	8.25	10.51	13.44	28.24
		5	2618	12.42	4.91	-2.87	9.66	12.36	15.73	31.97
		6	2082	14.28	4.99	-2.35	11.38	14.17	17.54	31.38
		7	2276	16.48	4.88	-2.76	13.35	16.20	19.97	33.94
		8	2148	19.34	5.39	-1.75	16.32	19.35	23.07	31.78

Table F-5: Descriptive statistics summary for PHEV hybrid operation's emissions according to roadway type during charge-depleting operation.

Variable	Op Mode	Road Code	N	Mean	Std. Dev.	Minimum	Q1	Median	Q3	Maximum
CO_2 (g/s)	CD	Overall	7580	5.38	4.68	0.01	1.77	3.97	8.52	24.84
		Urban	1077.00	3.71	4.01	0.02	1.25	1.90	5.13	20.68
		Suburban	3832	4.71	4.74	0.01	1.38	2.48	7.43	23.88
		Hwy	2671	7.01	4.38	0.01	3.56	6.87	9.88	24.84
CO (g/s)	CD	Overall	7580	1.13E-02	3.10E-02	0.00E+00	1.48E-03	3.50E-03	7.94E-03	5.29E-01
		Urban	1077	1.38E-02	3.36E-02	0.00E+00	9.30E-04	2.97E-03	1.09E-02	4.44E-01
		Suburban	3832	1.50E-02	3.72E-02	0.00E+00	1.34E-03	4.51E-03	1.28E-02	5.29E-01
		Hwy	2671	4.91E-03	1.48E-02	0.00E+00	2.10E-03	3.20E-03	4.45E-03	3.85E-01
NO (g/s)	CD	Overall	7580	0.043	0.041	0.000	0.014	0.026	0.065	0.242
		Urban	1077	0.029	0.030	0.000	0.010	0.020	0.038	0.171
		Suburban	3832	0.038	0.039	0.000	0.011	0.021	0.054	0.242
		Hwy	2671	0.057	0.043	0.000	0.022	0.047	0.088	0.191
NO_2 (g/s)	CD	Overall	7580	2.42E-03	2.65E-03	0.00E+00	4.60E-04	1.60E-03	3.51E-03	2.97E-02
		Urban	1077	1.30E-03	2.20E-03	0.00E+00	2.70E-04	5.10E-04	1.25E-03	1.86E-02
		Suburban	3832	1.93E-03	2.82E-03	0.00E+00	3.00E-04	9.00E-04	2.46E-03	2.97E-02
		Hwy	2671	3.57E-03	2.11E-03	8.00E-05	1.91E-03	3.24E-03	4.85E-03	1.35E-02
NOx (g/s)	CD	Overall	7580	0.046	0.042	0.000	0.016	0.028	0.068	0.249
		Urban	1077	0.031	0.031	0.000	0.011	0.021	0.040	0.174
		Suburban	3832	0.039	0.041	0.000	0.013	0.023	0.057	0.249
		Hwy	2671	0.061	0.044	0.000	0.025	0.051	0.093	0.194
HC (g/s)	CD	Overall	7580	1.29E-03	2.35E-03	0.00E+00	3.30E-04	6.10E-04	1.36E-03	3.59E-02
		Urban	1077	1.16E-03	1.85E-03	0.00E+00	2.90E-04	6.00E-04	1.36E-03	2.55E-02
		Suburban	3832	1.65E-03	2.87E-03	0.00E+00	2.60E-04	8.00E-04	1.92E-03	3.59E-02
		Hwy	2671	8.33E-04	1.45E-03	0.00E+00	3.70E-04	5.40E-04	7.70E-04	2.85E-02
Exhaust Temp (deg C)	CD	Overall	7580	106.3	44.1	10.9	67.7	100.8	148.4	190.4
		Urban	1077	68.0	13.5	14.3	59.1	66.8	76.3	116.4
		Suburban	3832	85.1	33.2	10.9	62.1	81.1	107.6	182.4
		Hwy	2671	152.0	23.2	28.9	144.2	153.1	165.2	190.4
Diesel ICE Power (W/kg/s)	CD	Overall	7580	6.03	6.46	-5.04	1.50	4.46	8.27	99.52
		Urban	1077	3.79	5.32	-3.34	1.15	1.71	5.67	24.88
		Suburban	3832	5.02	6.40	-5.04	0.95	1.90	9.09	29.55
		Hwy	2671	8.37	6.27	-3.12	4.00	8.28	0.00	0.03
Electric Motor Power (W/kg/s)	CD	Overall	7580	0.13	1.12	0.00	0.00	0.00	0.00	16.18
		Urban	1077	0.17	1.23	0.00	0.00	0.00	0.00	12.53
		Suburban	3832	0.17	1.27	0.00	0.00	0.00	0.00	16.18
		Hwy	2671	0.06	0.77	0.00	0.00	0.00	0.01	15.08
Total Power (W/kg/s)	CD	Overall	7580	6.15	6.51	-5.04	1.56	4.63	10.66	33.92
		Urban	1077	3.96	5.46	-3.34	1.17	1.72	5.97	24.92
		Suburban	3832	5.19	6.48	-5.04	1.07	1.98	9.40	33.92
		Hwy	2671	8.43	6.28	-3.12	4.08	8.35	12.40	31.81

Table F-6: Descriptive statistics summary for PHEV hybrid operation's emissions according to roadway type during charge-sustaining operation.

Variable	Op Mode	Road Code	N	Mean	Std. Dev.	Minimum	Q1	Median	Q3	Maximum
CO_2 (g/s)	CS	Overall	34547	5.61	5.36	0.00	1.16	3.78	9.21	24.62
		Urban	5373.00	4.27	4.63	0.00	1.10	1.83	6.76	24.05
		Suburban	24517	5.42	5.51	0.00	0.89	3.05	8.72	24.62
		Hwy	4653	8.14	4.49	0.00	4.99	8.50	10.93	23.90
CO (g/s)	CS	Overall	34547	6.21E-03	2.42E-02	0.00E+00	3.70E-04	1.30E-03	3.47E-03	5.28E-01
		Urban	5373	8.65E-03	3.04E-02	0.00E+00	3.80E-04	8.50E-04	3.59E-03	4.03E-01
		Suburban	24517	6.23E-03	2.46E-02	0.00E+00	2.80E-04	1.09E-03	3.36E-03	5.28E-01
		Hwy	4653	3.31E-03	9.48E-03	0.00E+00	1.49E-03	2.43E-03	3.62E-03	4.24E-01
NO (g/s)	CS	Overall	34547	0.056	0.053	0.000	0.013	0.037	0.095	0.278
		Urban	5373	0.043	0.045	0.000	0.012	0.023	0.064	0.269
		Suburban	24517	0.055	0.054	0.000	0.010	0.033	0.094	0.278
		Hwy	4653	0.077	0.050	0.000	0.037	0.073	0.113	0.260
NO_2 (g/s)	CS	Overall	34547	3.80E-03	4.12E-03	0.00E+00	1.05E-03	2.57E-03	4.95E-03	5.48E-02
		Urban	5373	3.40E-03	3.57E-03	0.00E+00	9.45E-04	2.40E-03	4.46E-03	4.30E-02
		Suburban	24517	4.09E-03	4.42E-03	0.00E+00	1.11E-03	2.73E-03	5.42E-03	5.48E-02
		Hwy	4653	2.70E-03	2.53E-03	0.00E+00	9.40E-04	2.02E-03	3.63E-03	1.38E-02
NOx (g/s)	CS	Overall	34547	0.060	0.055	0.000	0.015	0.040	0.101	0.294
		Urban	5373	0.046	0.047	0.000	0.014	0.025	0.068	0.277
		Suburban	24517	0.059	0.057	0.000	0.012	0.036	0.101	0.294
		Hwy	4653	0.080	0.051	0.000	0.039	0.075	0.116	0.267
HC (g/s)	CS	Overall	34547	3.77E-04	8.20E-04	0.00E+00	6.00E-05	2.10E-04	4.80E-04	3.68E-02
		Urban	5373	3.38E-04	7.37E-04	0.00E+00	5.00E-05	1.50E-04	4.00E-04	2.94E-02
		Suburban	24517	3.26E-04	7.37E-04	0.00E+00	6.00E-05	1.60E-04	4.10E-04	3.09E-02
		Hwy	4653	6.90E-04	1.18E-03	0.00E+00	3.50E-04	5.20E-04	7.40E-04	3.68E-02
Exhaust Temp (deg C)	CS	Overall	34547	134.9	35.4	16.4	116.0	137.7	160.3	215.0
		Urban	5373	111.1	32.5	24.5	92.1	115.4	134.2	184.7
		Suburban	24517	132.6	32.3	16.4	117.2	136.2	154.6	204.9
		Hwy	4653	174.6	18.6	51.7	165.5	176.6	185.4	215.0
Diesel ICE Power (W/kg/s)	CS	Overall	34547	6.94	7.41	-4.35	0.92	5.47	12.31	31.78
		Urban	5373	5.19	6.32	-3.81	1.24	1.86	9.90	31.63
		Suburban	24517	6.72	7.61	-4.35	0.37	3.91	12.00	31.78
		Hwy	4653	10.10	6.56	-3.30	6.73	10.76	14.16	30.91
Electric Motor Power (W/kg/s)	CS	Overall	34547	0.1	0.7	0.0	0.0	0.0	0.0	17.1
		Urban	5373	0.03	0.52	0.00	0.00	0.00	0.00	13.82
		Suburban	24517	0.06	0.81	0.00	0.00	0.00	0.00	17.11
		Hwy	4653	0.03	0.61	0.00	0.00	0.00	0.00	15.39
Total Power (W/kg/s)	CS	Overall	34547	6.99	7.42	-3.16	0.98	5.62	12.35	33.94
		Urban	5373	5.22	6.33	-3.16	1.25	1.87	9.95	31.63
		Suburban	24517	6.78	7.62	-3.05	0.42	4.18	12.07	31.97
		Hwy	4653	10.13	6.56	-2.89	6.74	10.77	14.19	33.94

Appendix G: PHEV Vocation Analysis (follow vs. solo driving)

The PHEV Sprinter's emissions, power output, exhaust conditions, and on-road variables are summarized by operating mode (charge-depleting or charge-sustaining), roadway type (urban or suburban) and driving scheme (follow or solo) in the first group of tables (G-1 through G-5).

The PHEV Sprinter's time stopped profiles according to drive scheme are detailed in table G-6.

The final grouping of Appendix G tables provides the summarized sample run-based on-road PHEV data used for Chapter 11's analyses. The file names referenced here correspond to the data file names found in the continuous dataset's digital submission.

Table G-1: Summarized PHEV Sprinter emissions (CO_2, CO, and HC) according to roadway type for follow and solo driving during both charge-sustaining and charge-depleting operation.

Operating Mode	Solo / Follow	Roadway	N	Carbon Dioxide, g/s		Carbon Monoxide, g/s		Hydrocarbon, g/s	
				Mean	Std. Deviation	Mean	Std. Deviation	Mean	Std. Deviation
CD	Follow	All	13198	1.57	3.57	7.65E-03	2.86E-02	6.96E-04	2.36E-03
CD	Follow	Urban	1599	1.67	3.49	8.46E-03	2.92E-02	6.61E-04	1.38E-03
CD	Follow	Suburban	11599	1.56	3.58	7.54E-03	2.86E-02	7.01E-04	2.46E-03
CD	Solo	All	10050	1.57	3.54	5.98E-03	2.63E-02	5.69E-04	1.96E-03
CD	Solo	Urban	1797	1.23	2.83	5.68E-03	2.49E-02	5.60E-04	1.69E-03
CD	Solo	Suburban	8253	1.65	3.67	6.04E-03	2.66E-02	5.71E-04	2.01E-03
CS	Follow	All	35594	2.87	4.53	4.99E-03	2.42E-02	1.69E-04	3.99E-04
CS	Follow	Urban	7017	2.95	4.24	7.10E-03	2.91E-02	1.61E-04	2.75E-04
CS	Follow	Suburban	28577	2.85	4.60	4.47E-03	2.28E-02	1.71E-04	4.24E-04
CS	Solo	All	32543	3.36	5.04	4.49E-03	2.21E-02	2.13E-04	7.67E-04
CS	Solo	Urban	4344	2.99	4.51	5.52E-03	2.49E-02	2.19E-04	9.46E-04
CS	Solo	Suburban	28199	3.42	5.11	4.33E-03	2.16E-02	2.12E-04	7.36E-04

Table G-2: Summarized PHEV Sprinter emissions (NO_2, NO, and NOx) according to roadway type for follow and solo driving during both charge-sustaining and charge-depleting operation.

Operating Mode	Solo / Follow	Roadway	N	Nitrogen Monoxide, g/s		Nitrogen Dioxide, g/s		NOx, g/s	
				Mean	Std. Deviation	Mean	Std. Deviation	Mean	Std. Deviation
CD	Follow	All	13198	0.012	0.026	4.10E-04	9.40E-04	0.012	0.026
CD	Follow	Urban	1599	0.013	0.025	2.84E-04	5.09E-04	0.013	0.026
CD	Follow	Suburban	11599	0.011	0.026	4.27E-04	9.83E-04	0.012	0.027
CD	Solo	All	10050	0.013	0.029	6.99E-04	1.92E-03	0.013	0.030
CD	Solo	Urban	1797	0.010	0.023	2.19E-04	5.16E-04	0.011	0.024
CD	Solo	Suburban	8253	0.013	0.030	8.03E-04	2.09E-03	0.014	0.031
CS	Follow	All	35594	0.028	0.043	1.94E-03	2.89E-03	0.030	0.045
CS	Follow	Urban	7017	0.028	0.038	2.32E-03	3.06E-03	0.031	0.040
CS	Follow	Suburban	28577	0.028	0.044	1.84E-03	2.84E-03	0.030	0.046
CS	Solo	All	32543	0.034	0.050	2.35E-03	3.45E-03	0.036	0.052
CS	Solo	Urban	4344	0.031	0.045	2.26E-03	3.09E-03	0.033	0.047
CS	Solo	Suburban	28199	0.034	0.050	2.36E-03	3.50E-03	0.037	0.053

Table G-3: Summarized PHEV Sprinter power output according to roadway type for follow and solo driving during both charge-sustaining and charge-depleting operation.

Operating Mode	Solo / Follow	Roadway	N	ICE Power, W/kg/s		EM Power, W/kg/s		Total Power, W/kg/s		Recuperation, W/kg/s	
				Mean	Std. Deviation	Mean	Std. Deviation	Mean	Std. Deviation	Mean	Std. Deviation
CD	Follow	All	13198	1.56	4.52	2.19	4.22	3.74	5.82	-0.666	1.203
CD	Follow	Urban	1599	1.57	4.26	1.88	4.00	3.44	5.47	-0.650	0.997
CD	Follow	Suburban	11599	1.56	4.56	2.23	4.25	3.78	5.86	-0.669	1.229
CD	Solo	All	10050	1.65	4.43	2.03	4.00	3.67	5.52	-0.747	1.461
CD	Solo	Urban	1797	1.18	3.39	1.82	3.60	3.00	4.59	-0.591	0.934
CD	Solo	Suburban	8253	1.75	4.61	2.07	4.07	3.82	5.69	-0.781	1.550
CS	Follow	All	35594	3.34	5.98	0.98	2.82	4.32	6.16	-1.851	2.561
CS	Follow	Urban	7017	3.39	5.56	0.70	2.45	4.09	5.71	-1.698	2.311
CS	Follow	Suburban	28577	3.32	6.08	1.05	2.90	4.37	6.26	-1.889	2.618
CS	Solo	All	32543	4.02	6.73	1.30	3.39	5.33	6.88	-2.244	2.953
CS	Solo	Urban	4344	3.50	5.91	1.05	2.88	4.56	6.02	-1.908	2.658
CS	Solo	Suburban	28199	4.10	6.84	1.34	3.46	5.44	6.99	-2.295	2.992

Table G-4: Summarized PHEV Sprinter fuel and exhaust variables according to roadway type for follow and solo driving during both charge-sustaining and charge-depleting operation.

Operating Mode	Solo / Follow	Roadway	N	Fuel, gal/s		Exhaust Flow, SCFM		Exhaust Temp, C	
				Mean	Std. Deviation	Mean	Std. Deviation	Mean	Std. Deviation
CD	Follow	All	13198	1.54E-04	3.49E-04	37.1	64.4	55.2	30.8
CD	Follow	Urban	1599	1.64E-04	3.42E-04	37.4	60.9	59.8	19.6
CD	Follow	Suburban	11599	1.52E-04	3.49E-04	37.0	64.8	54.5	31.9
CD	Solo	All	10050	1.54E-04	3.45E-04	34.1	61.9	49.7	39.1
CD	Solo	Urban	1797	1.21E-04	2.77E-04	28.1	51.8	42.1	25.5
CD	Solo	Suburban	8253	1.61E-04	3.57E-04	35.4	63.8	51.4	41.3
CS	Follow	All	35594	2.80E-04	4.41E-04	52.2	65.5	108.4	44.3
CS	Follow	Urban	7017	2.87E-04	4.13E-04	51.3	60.1	111.4	41.5
CS	Follow	Suburban	28577	2.78E-04	4.48E-04	52.5	66.7	107.6	44.9
CS	Solo	All	32543	3.27E-04	4.89E-04	61.3	73.5	110.8	46.0
CS	Solo	Urban	4344	2.91E-04	4.38E-04	53.2	65.9	101.2	44.6
CS	Solo	Suburban	28199	3.33E-04	4.96E-04	62.6	74.6	112.3	46.0

Table G-5: Summarized PHEV Sprinter road-based variables according to roadway type for follow and solo driving during both charge-sustaining and charge-depleting operation.

Operating Mode	Solo / Follow	Roadway	N	Velocity		Acceleration		Deceleration	
				Mean	Std. Deviation	Mean	Std. Deviation	Mean	Std. Deviation
CD	Follow	All	13198	22.3	18.1	0.396	0.517	-0.661	0.528
CD	Follow	Urban	1599	16.5	14.6	0.406	0.524	-0.662	0.477
CD	Follow	Suburban	11599	23.1	18.4	0.395	0.515	-0.661	0.535
CD	Solo	All	10050	22.9	18.5	0.349	0.479	-0.618	0.505
CD	Solo	Urban	1797	18.1	14.3	0.369	0.486	-0.621	0.472
CD	Solo	Suburban	8253	24.0	19.1	0.344	0.477	-0.617	0.513
CS	Follow	All	35594	21.4	16.7	0.356	0.472	-0.570	0.469
CS	Follow	Urban	7017	15.9	14.0	0.357	0.481	-0.622	0.467
CS	Follow	Suburban	28577	22.8	17.1	0.356	0.470	-0.558	0.469
CS	Solo	All	32543	27.2	18.4	0.406	0.495	-0.593	0.503
CS	Solo	Urban	4344	20.0	14.9	0.370	0.463	-0.584	0.469
CS	Solo	Suburban	28199	28.3	18.6	0.412	0.499	-0.594	0.507

Table G-6: Summarized PHEV Sprinter stop profiles according to roadway type for follow and solo driving during both charge-sustaining and charge-depleting operation.

Operating Mode	Follow / Solo	Road	Time/Stop	# Stops / km	# Stops / min	% Time @ V=0
CD	Follow	Urban	15.4	4.22	1.17	29.3%
		Suburban	18.5	2.02	0.78	23.8%
	Solo	Urban	13.2	3.81	1.16	25.2%
		Suburban	21.5	1.81	0.68	25.2%
CS	Follow	Urban	13.8	4.78	1.29	28.9%
		Suburban	16.7	2.22	0.81	22.2%
	Solo	Urban	13.5	2.80	0.93	21.0%
		Suburban	14.0	1.46	0.69	15.9%

Table G-7: Mean values of PHEV Sprinter fuel rate, CO_2, CO, and HC emissions according to sample data file.

Follow / Solo	Operating Mode	Road Code	Route	File Name	N	Fuel Rate (gal/s)	CO_2 (g/s)	CO (g/s)	HC (g/s)
Solo	CD	S	110	DEC20_S1	1014	1.00E-04	1.015	0.0068	8.81E-04
Solo	CD	S	110	DEC20_S2	868	1.19E-04	1.217	0.0050	5.01E-04
Solo	CD	S	110	NOV29_S1	1085	1.55E-04	1.591	0.0035	4.19E-04
Solo	CD	S	123	Dec4_S1	1294	1.72E-04	1.756	0.0083	4.82E-04
Solo	CD	S	123	NOV26_S1	3992	1.83E-04	1.879	0.0060	5.77E-04
Solo	CD	U	110	DEC20_S1	793	1.53E-04	1.567	0.0087	8.83E-04
Solo	CD	U	110	DEC20_S2	341	2.60E-05	0.271	0.0006	4.80E-05
Solo	CD	U	110	NOV29_S1	663	1.30E-04	1.328	0.0047	4.36E-04
Follow	CD	S	110	DEC21_110F1	1065	1.21E-04	1.229	0.0103	1.19E-03
Follow	CD	S	110	DEC21_110F2	687	7.20E-05	0.729	0.0057	6.63E-04
Follow	CD	S	123	DEC4_123F2	2178	1.42E-04	1.451	0.0052	3.08E-04
Follow	CD	S	123	DEC5_123F1	950	2.58E-04	2.638	0.0146	1.51E-03
Follow	CD	S	123	DEC5_123F2	2944	1.68E-04	1.724	0.0067	5.46E-04
Follow	CD	S	123	DEC5_123F3	377	2.45E-04	2.522	0.0051	3.56E-04
Follow	CD	S	110	JAN7_110F2	356	1.37E-04	1.390	0.0113	1.10E-03
Follow	CD	S	110	JAN7_F1	1426	9.00E-05	0.914	0.0059	5.74E-04
Follow	CD	S	123	NOV29_123F1	1616	1.66E-04	1.696	0.0082	8.34E-04
Follow	CD	U	110	DEC21_110F1	788	2.04E-04	2.086	0.0111	7.83E-04
Follow	CD	U	110	JAN7_F1	811	1.24E-04	1.263	0.0059	5.43E-04

Table G-8: Mean values of PHEV Sprinter NO_2, NO, and NOx emissions according to sample data file during charge-depleting operation.

Follow / Solo	Operating Mode	Road Code	Route	File Name	N	NO (g/s)	NO_2 (g/s)	NOx (g/s)
Solo	CD	S	110	DEC20_S1	1014	0.006	1.18E-04	0.007
Solo	CD	S	110	DEC20_S2	868	0.008	1.29E-04	0.008
Solo	CD	S	110	NOV29_S1	1085	0.015	6.23E-04	0.016
Solo	CD	S	123	Dec4_S1	1294	0.014	5.59E-04	0.014
Solo	CD	S	123	NOV26_S1	3992	0.015	1.25E-03	0.016
Solo	CD	U	110	DEC20_S1	793	0.013	2.10E-04	0.013
Solo	CD	U	110	DEC20_S2	341	0.002	3.40E-05	0.003
Solo	CD	U	110	NOV29_S1	663	0.012	3.25E-04	0.012
Follow	CD	S	110	DEC21_110F1	1065	0.007	2.01E-04	0.008
Follow	CD	S	110	DEC21_110F2	687	0.004	7.00E-05	0.004
Follow	CD	S	123	DEC4_123F2	2178	0.009	4.79E-04	0.010
Follow	CD	S	123	DEC5_123F1	950	0.023	8.47E-04	0.023
Follow	CD	S	123	DEC5_123F2	2944	0.013	4.54E-04	0.014
Follow	CD	S	123	DEC5_123F3	377	0.019	5.32E-04	0.020
Follow	CD	S	110	JAN7_110F2	356	0.007	2.75E-04	0.007
Follow	CD	S	110	JAN7_F1	1426	0.006	8.70E-05	0.007
Follow	CD	S	123	NOV29_123F1	1616	0.015	6.74E-04	0.015
Follow	CD	U	110	DEC21_110F1	788	0.016	4.15E-04	0.016
Follow	CD	U	110	JAN7_F1	811	0.010	1.57E-04	0.010

Table G-9: Mean values of PHEV Sprinter velocity and power output according to sample data file during charge-depleting operation.

Follow / Solo	Operating Mode	Road Code	Route	File Name	N	Velocity (km/h)	ICE Power (W/kg/s)	EM Power (W/kg/s)	Tot. Power (W/kg/s)	Recuperation (W/kg/s)
Solo	CD	S	110	DEC20_S1	1014	30.9	1.06	2.59	3.66	-0.55
Solo	CD	S	110	DEC20_S2	868	30.4	1.38	3.12	4.50	-0.58
Solo	CD	S	110	NOV29_S1	1085	30.4	1.80	3.00	4.80	-1.06
Solo	CD	S	123	Dec4_S1	1294	13.4	1.62	0.88	2.50	-0.44
Solo	CD	S	123	NOV26_S1	3992	22.5	2.03	1.85	3.87	-0.92
Solo	CD	U	110	DEC20_S1	793	16.7	1.49	1.81	3.30	-0.64
Solo	CD	U	110	DEC20_S2	341	18.2	0.31	1.69	2.00	-0.49
Solo	CD	U	110	NOV29_S1	663	19.9	1.27	1.90	3.16	-0.59
Follow	CD	S	110	DEC21_110F1	1065	29.2	1.26	2.99	4.25	-0.55
Follow	CD	S	110	DEC21_110F2	687	28.0	0.76	3.35	4.11	-0.47
Follow	CD	S	123	DEC4_123F2	2178	23.8	1.60	2.40	4.00	-0.68
Follow	CD	S	123	DEC5_123F1	950	22.0	2.39	1.24	3.63	-0.85
Follow	CD	S	123	DEC5_123F2	2944	23.4	1.69	1.92	3.61	-0.71
Follow	CD	S	123	DEC5_123F3	377	23.0	2.76	1.82	4.58	-1.37
Follow	CD	S	110	JAN7_110F2	356	29.0	1.64	3.93	5.56	-0.43
Follow	CD	S	110	JAN7_F1	1426	21.8	0.91	2.48	3.39	-0.52
Follow	CD	S	123	NOV29_123F1	1616	16.0	1.57	1.65	3.22	-0.66
Follow	CD	U	110	DEC21_110F1	788	16.8	1.95	1.77	3.72	-0.74
Follow	CD	U	110	JAN7_F1	811	16.3	1.19	1.98	3.17	-0.56

Table G-10: Mean values of PHEV Sprinter fuel rate, CO_2, CO, and HC emissions according to sample data file during solo driving and charge-sustaining operation.

Follow / Solo	Operating Mode	Road Code	Route	File Name	N	Fuel Rate (gal/s)	CO_2 (g/s)	CO (g/s)	HC (g/s)
Solo	CS	S	110	DEC20_S2	924	3.02E-04	3.102	0.0044	2.27E-04
Solo	CS	S	110	DEC20_S3	1181	3.21E-04	3.299	0.0036	1.49E-04
Solo	CS	S	110	DEC20_S4	1094	3.07E-04	3.151	0.0028	8.80E-05
Solo	CS	S	110	DEC20_S5	1982	3.26E-04	3.344	0.0046	1.41E-04
Solo	CS	S	110	DEC20_S6	1899	3.00E-04	3.081	0.0041	1.48E-04
Solo	CS	S	110	Dec20_S7	882	3.82E-04	3.922	0.0047	2.01E-04
Solo	CS	S	110	DEC21_S4	678	3.73E-04	3.829	0.0033	1.40E-04
Solo	CS	S	110	Dec21_S5, M1	742	3.34E-04	3.427	0.0052	1.61E-04
Solo	CS	S	110	DEC21_S5, M2	1154	3.24E-04	3.325	0.0046	2.34E-04
Solo	CS	S	110	NOV29_S1	1101	3.54E-04	3.641	0.0041	1.84E-04
Solo	CS	S	110	NOV29_S2	1779	3.44E-04	3.542	0.0026	2.61E-04
Solo	CS	S	110	NOV29_S3	1782	3.33E-04	3.427	0.0026	2.40E-04
Solo	CS	S	110	NOV29_S4	1902	3.36E-04	3.454	0.0029	1.49E-04
Solo	CS	S	123	NOV26_S2	2721	3.42E-04	3.516	0.0054	2.49E-04
Solo	CS	S	123	NOV26_S3	2666	3.46E-04	3.552	0.0043	2.16E-04
Solo	CS	S	123	NOV26_S4	2759	3.31E-04	3.402	0.0053	2.21E-04
Solo	CS	S	123	NOV28_S1	924	2.76E-04	2.836	0.0056	2.70E-04
Solo	CS	S	123	Nov28_S2	2029	3.46E-04	3.548	0.0064	3.84E-04
Solo	CS	U	110	DEC20_S2	321	3.59E-04	3.679	0.0121	1.21E-03
Solo	CS	U	110	DEC20_S3	658	3.22E-04	3.307	0.0054	1.05E-04
Solo	CS	U	110	DEC20_S5	743	2.60E-04	2.672	0.0049	1.10E-04
Solo	CS	U	110	DEC20_S6	709	2.60E-04	2.667	0.0058	1.29E-04
Solo	CS	U	110	NOV29_S2	739	2.57E-04	2.640	0.0042	1.95E-04
Solo	CS	U	110	NOV29_S3	582	3.00E-04	3.086	0.0053	1.49E-04
Solo	CS	U	110	NOV29_S4	592	3.31E-04	3.408	0.0043	1.54E-04

Table G-11: Mean values of PHEV Sprinter NO_2, NO, and NOx emissions according to sample data file during solo driving and charge-sustaining operation.

Follow / Solo	Operating Mode	Road Code	Route	File Name	N	NO (g/s)	NO_2 (g/s)	NOx (g/s)
Solo	CS	S	110	DEC20_S2	924	0.027	4.06E-03	0.031
Solo	CS	S	110	DEC20_S3	1181	0.032	3.54E-03	0.036
Solo	CS	S	110	DEC20_S4	1094	0.030	2.63E-03	0.033
Solo	CS	S	110	DEC20_S5	1982	0.033	2.49E-03	0.036
Solo	CS	S	110	DEC20_S6	1899	0.032	1.91E-03	0.034
Solo	CS	S	110	Dec20_S7	882	0.041	1.75E-03	0.043
Solo	CS	S	110	DEC21_S4	678	0.040	1.82E-03	0.042
Solo	CS	S	110	Dec21_S5, M1	742	0.034	1.56E-03	0.036
Solo	CS	S	110	DEC21_S5, M2	1154	0.034	1.53E-03	0.036
Solo	CS	S	110	NOV29_S1	1101	0.036	3.60E-03	0.039
Solo	CS	S	110	NOV29_S2	1779	0.038	2.59E-03	0.041
Solo	CS	S	110	NOV29_S3	1782	0.039	2.19E-03	0.041
Solo	CS	S	110	NOV29_S4	1902	0.036	1.73E-03	0.038
Solo	CS	S	123	NOV26_S2	2721	0.034	3.15E-03	0.038
Solo	CS	S	123	NOV26_S3	2666	0.035	2.51E-03	0.037
Solo	CS	S	123	NOV26_S4	2759	0.033	1.93E-03	0.035
Solo	CS	S	123	NOV28_S1	924	0.029	1.21E-03	0.030
Solo	CS	S	123	Nov28_S2	2029	0.033	1.97E-03	0.035
Solo	CS	U	110	DEC20_S2	321	0.031	1.39E-03	0.033
Solo	CS	U	110	DEC20_S3	658	0.030	3.91E-03	0.034
Solo	CS	U	110	DEC20_S5	743	0.026	2.35E-03	0.028
Solo	CS	U	110	DEC20_S6	709	0.028	1.73E-03	0.030
Solo	CS	U	110	NOV29_S2	739	0.030	1.94E-03	0.032
Solo	CS	U	110	NOV29_S3	582	0.034	2.12E-03	0.036
Solo	CS	U	110	NOV29_S4	592	0.037	1.95E-03	0.039

Table G-12: Mean values of PHEV Sprinter velocity and power output according to sample data file during solo driving and charge-sustaining operation.

Follow / Solo	Operating Mode	Road Code	Route	File Name	N	Velocity (km/h)	ICE Power (W/kg/s)	EM Power (W/kg/s)	Tot. Power (W/kg/s)	Recuperation (W/kg/s)
Solo	CS	S	110	DEC20_S2	924	31.1	3.61	1.32	4.94	-2.23
Solo	CS	S	110	DEC20_S3	1181	29.6	3.97	1.44	5.41	-2.32
Solo	CS	S	110	DEC20_S4	1094	29.8	3.81	1.58	5.39	-2.31
Solo	CS	S	110	DEC20_S5	1982	28.8	4.05	1.22	5.27	-2.24
Solo	CS	S	110	DEC20_S6	1899	28.3	3.72	1.29	5.01	-2.17
Solo	CS	S	110	Dec20_S7	882	29.2	4.76	1.30	6.06	-2.61
Solo	CS	S	110	DEC21_S4	678	32.0	4.71	1.61	6.31	-2.67
Solo	CS	S	110	Dec21_S5, M1	742	29.3	4.25	1.21	5.45	-2.19
Solo	CS	S	110	DEC21_S5, M2	1154	28.7	3.96	1.43	5.39	-2.40
Solo	CS	S	110	NOV29_S1	1101	32.8	4.37	1.41	5.78	-2.41
Solo	CS	S	110	NOV29_S2	1779	32.1	4.26	1.58	5.84	-2.52
Solo	CS	S	110	NOV29_S3	1782	31.3	4.18	1.48	5.66	-2.51
Solo	CS	S	110	NOV29_S4	1902	31.7	4.19	1.61	5.80	-2.46
Solo	CS	S	123	NOV26_S2	2721	25.3	4.16	1.22	5.38	-2.14
Solo	CS	S	123	NOV26_S3	2666	25.8	4.24	1.17	5.41	-2.23
Solo	CS	S	123	NOV26_S4	2759	24.7	4.05	1.17	5.22	-2.09
Solo	CS	S	123	NOV28_S1	924	22.5	3.33	1.11	4.44	-2.03
Solo	CS	S	123	Nov28_S2	2029	25.9	4.26	1.35	5.61	-2.27
Solo	CS	U	110	DEC20_S2	321	21.9	4.24	1.83	6.07	-2.04
Solo	CS	U	110	DEC20_S3	658	20.2	3.71	0.92	4.64	-2.06
Solo	CS	U	110	DEC20_S5	743	18.7	3.07	1.07	4.14	-1.67
Solo	CS	U	110	DEC20_S6	709	18.7	3.14	0.98	4.11	-1.70
Solo	CS	U	110	NOV29_S2	739	17.9	3.11	0.98	4.10	-1.90
Solo	CS	U	110	NOV29_S3	582	22.7	3.71	1.09	4.80	-1.97
Solo	CS	U	110	NOV29_S4	592	22.3	4.15	0.90	5.05	-2.17

Table G-13: Mean values of PHEV Sprinter fuel use, CO_2, CO, and HC emissions according to sample data file during follow driving and charge-sustaining operation.

Follow / Solo	Operating Mode	Road Code	Route	File Name	N	Fuel Rate (gal/s)	CO_2 (g/s)	CO (g/s)	HC (g/s)
Follow	CS	S	110	DEC21_110F2	1488	2.31E-04	2.366	0.0037	1.85E-04
Follow	CS	S	110	DEC21_F3	2190	3.18E-04	3.267	0.0039	1.13E-04
Follow	CS	S	110	DEC21_F5	2546	2.30E-04	2.366	0.0041	7.80E-05
Follow	CS	S	110	DEC21_F6	1155	2.77E-04	2.841	0.0052	1.54E-04
Follow	CS	S	123	DEC4_123F2	896	2.75E-04	2.814	0.0074	8.80E-05
Follow	CS	S	123	DEC4_123F4	769	2.71E-04	2.771	0.0068	1.52E-04
Follow	CS	S	110	DEC5_110F2	1138	2.51E-04	2.579	0.0029	1.78E-04
Follow	CS	S	123	DEC5_123F3	2689	2.78E-04	2.860	0.0044	2.14E-04
Follow	CS	S	123	DEC5_123F4	3221	3.08E-04	3.163	0.0049	2.45E-04
Follow	CS	S	110	DEC5_F1	2108	2.85E-04	2.932	0.0037	2.11E-04
Follow	CS	S	110	JAN7_110F2	1950	2.85E-04	2.914	0.0061	1.76E-04
Follow	CS	S	110	JAN7_110F3	2377	2.78E-04	2.845	0.0034	1.00E-04
Follow	CS	S	110	JAN7_110F4	2333	2.82E-04	2.881	0.0056	1.39E-04
Follow	CS	S	110	JAN7_110F5	2566	2.75E-04	2.817	0.0032	2.18E-04
Follow	CS	S	110	JAN7_110F6	1151	3.01E-04	3.089	0.0047	2.80E-04
Follow	CS	U	110	DEC21_110F2	803	2.72E-04	2.793	0.0073	2.70E-04
Follow	CS	U	110	DEC21_F3	798	2.63E-04	2.703	0.0029	5.80E-05
Follow	CS	U	110	DEC21_F5	895	2.37E-04	2.425	0.0071	7.50E-05
Follow	CS	U	110	DEC5_110F2	294	4.34E-04	4.478	0.0055	2.70E-04
Follow	CS	U	110	DEC5_F1	808	3.07E-04	3.159	0.0058	2.43E-04
Follow	CS	U	110	JAN7_110F2	945	2.60E-04	2.657	0.0080	1.20E-04
Follow	CS	U	110	JAN7_110F3	701	3.44E-04	3.523	0.0089	1.42E-04
Follow	CS	U	110	JAN7_110F4	858	2.96E-04	3.022	0.0101	1.39E-04
Follow	CS	U	110	JAN7_110F5	915	2.85E-04	2.916	0.0072	2.11E-04

Table G-14: Mean values of PHEV Sprinter NO_2, NO, and HC emissions according to sample data file during follow driving and charge-sustaining operation.

Follow / Solo	Operating Mode	Road Code	Route	File Name	N	NO (g/s)	NO_2 (g/s)	NOx (g/s)
Follow	CS	S	110	DEC21_110F2	1488	0.023	1.76E-03	0.025
Follow	CS	S	110	DEC21_F3	2190	0.032	2.55E-03	0.035
Follow	CS	S	110	DEC21_F5	2546	0.024	1.26E-03	0.026
Follow	CS	S	110	DEC21_F6	1155	0.032	1.32E-03	0.033
Follow	CS	S	123	DEC4_123F2	896	0.026	2.70E-03	0.028
Follow	CS	S	123	DEC4_123F4	769	0.028	1.38E-03	0.029
Follow	CS	S	110	DEC5_110F2	1138	0.027	1.10E-03	0.028
Follow	CS	S	123	DEC5_123F3	2689	0.028	1.97E-03	0.030
Follow	CS	S	123	DEC5_123F4	3221	0.031	1.78E-03	0.033
Follow	CS	S	110	DEC5_F1	2108	0.029	1.16E-03	0.031
Follow	CS	S	110	JAN7_110F2	1950	0.025	3.59E-03	0.029
Follow	CS	S	110	JAN7_110F3	2377	0.027	2.47E-03	0.029
Follow	CS	S	110	JAN7_110F4	2333	0.028	1.65E-03	0.030
Follow	CS	S	110	JAN7_110F5	2566	0.029	1.33E-03	0.030
Follow	CS	S	110	JAN7_110F6	1151	0.030	1.21E-03	0.031
Follow	CS	U	110	DEC21_110F2	803	0.026	2.41E-03	0.028
Follow	CS	U	110	DEC21_F3	798	0.027	2.40E-03	0.030
Follow	CS	U	110	DEC21_F5	895	0.024	1.53E-03	0.025
Follow	CS	U	110	DEC5_110F2	294	0.043	1.38E-03	0.044
Follow	CS	U	110	DEC5_F1	808	0.034	1.57E-03	0.035
Follow	CS	U	110	JAN7_110F2	945	0.022	4.28E-03	0.026
Follow	CS	U	110	JAN7_110F3	701	0.032	3.05E-03	0.035
Follow	CS	U	110	JAN7_110F4	858	0.030	2.15E-03	0.032
Follow	CS	U	110	JAN7_110F5	915	0.029	1.50E-03	0.031

Table G-15: Mean values of PHEV Sprinter velocity and power output according to sample data file during follow driving and charge-sustaining operation.

Follow / Solo	Operating Mode	Road Code	Route	File Name	N	Velocity (km/h)	ICE Power (W/kg/s)	EM Power (W/kg/s)	Tot. Power (W/kg/s)	Recuperation (W/kg/s)
Follow	CS	S	110	DEC21_110F2	1488	24.1	2.70	1.18	3.88	-1.80
Follow	CS	S	110	DEC21_F3	2190	25.1	3.87	1.14	5.01	-2.12
Follow	CS	S	110	DEC21_F5	2546	21.6	2.77	0.89	3.66	-1.66
Follow	CS	S	110	DEC21_F6	1155	22.4	3.33	1.00	4.34	-1.98
Follow	CS	S	123	DEC4_123F2	896	18.9	3.17	1.01	4.18	-1.71
Follow	CS	S	123	DEC4_123F4	769	17.9	3.39	0.77	4.17	-1.80
Follow	CS	S	110	DEC5_110F2	1138	25.1	2.88	1.17	4.05	-2.04
Follow	CS	S	123	DEC5_123F3	2689	22.4	3.26	1.16	4.43	-2.00
Follow	CS	S	123	DEC5_123F4	3221	21.5	3.70	1.07	4.77	-1.98
Follow	CS	S	110	DEC5_F1	2108	25.6	3.54	1.30	4.84	-1.92
Follow	CS	S	110	JAN7_110F2	1950	23.2	3.36	0.91	4.27	-1.78
Follow	CS	S	110	JAN7_110F3	2377	23.1	3.31	0.97	4.28	-1.81
Follow	CS	S	110	JAN7_110F4	2333	23.6	3.34	0.96	4.30	-1.85
Follow	CS	S	110	JAN7_110F5	2566	21.4	3.24	0.95	4.19	-1.85
Follow	CS	S	110	JAN7_110F6	1151	22.4	3.66	1.16	4.82	-1.99
Follow	CS	U	110	DEC21_110F2	803	16.5	3.23	0.94	4.18	-1.74
Follow	CS	U	110	DEC21_F3	798	16.6	3.17	0.96	4.13	-1.54
Follow	CS	U	110	DEC21_F5	895	14.8	2.77	0.83	3.60	-1.40
Follow	CS	U	110	DEC5_110F2	294	22.0	5.49	1.37	6.86	-2.34
Follow	CS	U	110	DEC5_F1	808	16.2	3.60	0.84	4.45	-1.95
Follow	CS	U	110	JAN7_110F2	945	14.0	3.03	0.61	3.64	-1.54
Follow	CS	U	110	JAN7_110F3	701	17.8	4.23	0.31	4.54	-1.88
Follow	CS	U	110	JAN7_110F4	858	15.4	3.30	0.46	3.75	-1.69
Follow	CS	U	110	JAN7_110F5	915	14.5	3.24	0.42	3.67	-1.69